ADVANCES IN HUMAN IMMUNE SYSTEM (HIS) MOUSE MODELS FOR STUDYING HUMAN HEMATOPOIESIS AND CANCER IMMUNOTHERAPY

EDITED BY: Yasuyuki Saito, Alexandre P. A. Theocharides and Tim Willinger

PUBLISHED IN: Frontiers in Immunology and Frontiers in Oncology

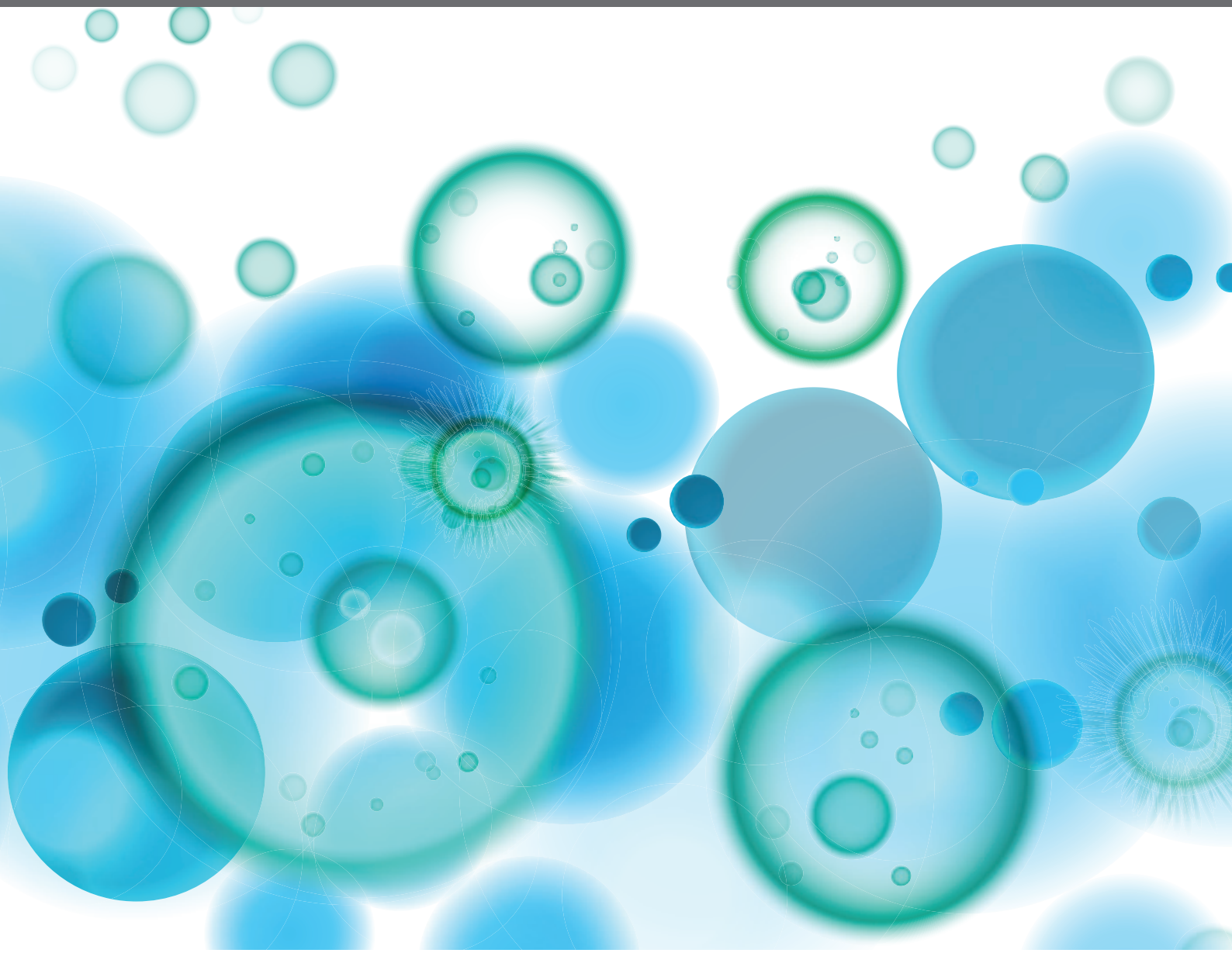

frontiers Research Topics

Frontiers eBook Copyright Statement

The copyright in the text of individual articles in this eBook is the property of their respective authors or their respective institutions or funders. The copyright in graphics and images within each article may be subject to copyright of other parties. In both cases this is subject to a license granted to Frontiers.

The compilation of articles constituting this eBook is the property of Frontiers.

Each article within this eBook, and the eBook itself, are published under the most recent version of the Creative Commons CC-BY licence. The version current at the date of publication of this eBook is CC-BY 4.0. If the CC-BY licence is updated, the licence granted by Frontiers is automatically updated to the new version.

When exercising any right under the CC-BY licence, Frontiers must be attributed as the original publisher of the article or eBook, as applicable.

Authors have the responsibility of ensuring that any graphics or other materials which are the property of others may be included in the CC-BY licence, but this should be checked before relying on the CC-BY licence to reproduce those materials. Any copyright notices relating to those materials must be complied with.

Copyright and source acknowledgement notices may not be removed and must be displayed in any copy, derivative work or partial copy which includes the elements in question.

All copyright, and all rights therein, are protected by national and international copyright laws. The above represents a summary only. For further information please read Frontiers' Conditions for Website Use and Copyright Statement, and the applicable CC-BY licence.

ISSN 1664-8714
ISBN 978-2-88974-318-6
DOI 10.3389/978-2-88974-318-6

About Frontiers

Frontiers is more than just an open-access publisher of scholarly articles: it is a pioneering approach to the world of academia, radically improving the way scholarly research is managed. The grand vision of Frontiers is a world where all people have an equal opportunity to seek, share and generate knowledge. Frontiers provides immediate and permanent online open access to all its publications, but this alone is not enough to realize our grand goals.

Frontiers Journal Series

The Frontiers Journal Series is a multi-tier and interdisciplinary set of open-access, online journals, promising a paradigm shift from the current review, selection and dissemination processes in academic publishing. All Frontiers journals are driven by researchers for researchers; therefore, they constitute a service to the scholarly community. At the same time, the Frontiers Journal Series operates on a revolutionary invention, the tiered publishing system, initially addressing specific communities of scholars, and gradually climbing up to broader public understanding, thus serving the interests of the lay society, too.

Dedication to Quality

Each Frontiers article is a landmark of the highest quality, thanks to genuinely collaborative interactions between authors and review editors, who include some of the world's best academicians. Research must be certified by peers before entering a stream of knowledge that may eventually reach the public - and shape society; therefore, Frontiers only applies the most rigorous and unbiased reviews.
Frontiers revolutionizes research publishing by freely delivering the most outstanding research, evaluated with no bias from both the academic and social point of view. By applying the most advanced information technologies, Frontiers is catapulting scholarly publishing into a new generation.

What are Frontiers Research Topics?

Frontiers Research Topics are very popular trademarks of the Frontiers Journals Series: they are collections of at least ten articles, all centered on a particular subject. With their unique mix of varied contributions from Original Research to Review Articles, Frontiers Research Topics unify the most influential researchers, the latest key findings and historical advances in a hot research area! Find out more on how to host your own Frontiers Research Topic or contribute to one as an author by contacting the Frontiers Editorial Office: frontiersin.org/about/contact

ADVANCES IN HUMAN IMMUNE SYSTEM (HIS) MOUSE MODELS FOR STUDYING HUMAN HEMATOPOIESIS AND CANCER IMMUNOTHERAPY

Topic Editors:
Yasuyuki Saito, Kobe University, Japan
Alexandre P. A. Theocharides, University Hospital Zürich, Switzerland
Tim Willinger, Karolinska Institutet (KI), Sweden

Topic Editor Prof. Aimin Xu receives financial support from Servier Laboratories. The other Topic Editors declare no competing interests with regards to the Research Topic theme.

Citation: Saito, Y., Theocharides, A. P. A., Willinger, T., eds. (2022). Advances in Human Immune System (HIS) Mouse Models for Studying Human Hematopoiesis and Cancer Immunotherapy. Lausanne: Frontiers Media SA. doi: 10.3389/978-2-88974-318-6

Table of Contents

05 ***Editorial: Advances in Human Immune System Mouse Models for Studying Human Hematopoiesis and Cancer Immunotherapy***
Yasuyuki Saito, Tim Willinger and Alexandre P. A. Theocharides

08 ***The Tumor Milieu Promotes Functional Human Tumor-Resident Plasmacytoid Dendritic Cells in Humanized Mouse Models***
Ilona-Petra Maser, Sabine Hoves, Christa Bayer, Gordon Heidkamp, Falk Nimmerjahn, Jan Eckmann and Carola H. Ries

25 ***Probing Reconstituted Human Immune Systems in Mice With Oncogenic γ-Herpesvirus Infections***
Christian Münz

33 ***Improved Detection of* in vivo *Human NK Cell-Mediated Antibody-Dependent Cellular Cytotoxicity Using a Novel NOG-FcγR-Deficient Human IL-15 Transgenic Mouse***
Ikumi Katano, Ryoji Ito, Kenji Kawai and Takeshi Takahashi

42 ***Human Immune System Mice With Autologous Tumor for Modeling Cancer Immunotherapies***
Liguang Sun, Chun-Hui Jin, Shulian Tan, Wentao Liu and Yong-Guang Yang

49 ***Humanized Mouse as a Tool to Predict Immunotoxicity of Human Biologics***
Kylie Su Mei Yong, Zhisheng Her, Sue Yee Tan, Wilson Wei Sheng Tan, Min Liu, Fritz Lai, Shi Min Heng, Yong Fan, Kenneth Tou En Chang, Cheng-I Wang, Jerry Kok Yen Chan, Jianzhu Chen and Qingfeng Chen

62 ***Different Human Immune Lineage Compositions Are Generated in Non-Conditioned NBSGW Mice Depending on HSPC Source***
Nicholas J. Hess, Payton N. Lindner, Jessica Vazquez, Samuel Grindel, Amy W. Hudson, Aleksandar K. Stanic, Akihiro Ikeda, Peiman Hematti and Jenny E. Gumperz

73 ***PD-1 Blockade Aggravates Epstein–Barr Virus$^+$ Post-Transplant Lymphoproliferative Disorder in Humanized Mice Resulting in Central Nervous System Involvement and CD4$^+$ T Cell Dysregulations***
Valery Volk, Sebastian J. Theobald, Simon Danisch, Sahamoddin Khailaie, Maja Kalbarczyk, Andreas Schneider, Julia Bialek-Waldmann, Nicole Krönke, Yun Deng, Britta Eiz-Vesper, Anna Christina Dragon, Constantin von Kaisenberg, Stefan Lienenklaus, Andre Bleich, James Keck, Michael Meyer-Hermann, Frank Klawonn, Wolfgang Hammerschmidt, Henri-Jacques Delecluse, Christian Münz, Friedrich Feuerhake and Renata Stripecke

93 ***Advances in Human Immune System Mouse Models for Studying Human Hematopoiesis and Cancer Immunotherapy***
Syed A. Mian, Fernando Anjos-Afonso and Dominique Bonnet

109 ***Advances in Human Immune System Mouse Models for Personalized Treg-Based Immunotherapies***
Isabelle Serr, Maria Kral, Martin G. Scherm and Carolin Daniel

117 ***Building the Next Generation of Humanized Hemato-Lymphoid System Mice***
Tijana Martinov, Kelly M. McKenna, Wei Hong Tan, Emily J. Collins, Allie R. Kehret, Jonathan D. Linton, Tayla M. Olsen, Nour Shobaki and Anthony Rongvaux

134 ***An Antibody-Drug Conjugate That Selectively Targets Human Monocyte Progenitors for Anti-Cancer Therapy***
Yuta Izumi, Masashi Kanayama, Zhongchuzi Shen, Masayuki Kai, Shunsuke Kawamura, Megumi Akiyama, Masahide Yamamoto, Toshikage Nagao, Keigo Okada, Norihiko Kawamata, Shigeo Toyota and Toshiaki Ohteki

149 ***Development of LT-HSC-Reconstituted Non-Irradiated NBSGW Mice for the Study of Human Hematopoiesis* In Vivo**
George Adigbli, Peng Hua, Masateru Uchiyama, Irene Roberts, Joanna Hester, Suzanne M. Watt and Fadi Issa

164 ***Testing Cancer Immunotherapy in a Human Immune System Mouse Model: Correlating Treatment Responses to Human Chimerism, Therapeutic Variables and Immune Cell Phenotypes***
Juan A. Marín-Jiménez, Anna Capasso, Matthew S. Lewis, Stacey M. Bagby, Sarah J. Hartman, Jeremy Shulman, Natalie M. Navarro, Hui Yu, Chris J. Rivard, Xiaoguang Wang, Jessica C. Barkow, Degui Geng, Adwitiya Kar, Ashley Yingst, Dejene M. Tufa, James T. Dolan, Patrick J. Blatchford, Brian M. Freed, Raul M. Torres, Eduardo Davila, Jill E. Slansky, Roberta Pelanda, S. Gail Eckhardt, Wells A. Messersmith, Jennifer R. Diamond, Christopher H. Lieu, Michael R. Verneris, Jing H. Wang, Katja Kiseljak-Vassiliades, Todd M. Pitts and Julie Lang

190 ***Inhibition of LDH-A by Oxamate Enhances the Efficacy of Anti-PD-1 Treatment in an NSCLC Humanized Mouse Model***
Tianyun Qiao, Yanlu Xiong, Yangbo Feng, Wenwen Guo, Yongsheng Zhou, Jinbo Zhao, Tao Jiang, Changhong Shi and Yong Han

202 ***Fit-For-All iPSC-Derived Cell Therapies and Their Evaluation in Humanized Mice With NK Cell Immunity***
Charlotte Flahou, Tatsuya Morishima, Hitoshi Takizawa and Naoshi Sugimoto

216 ***PD-1 Inhibition Enhances Blinatumomab Response in a UCB/PDX Model of Relapsed Pediatric B-Cell Acute Lymphoblastic Leukemia***
Mark Wunderlich, Nicole Manning, Christina Sexton, Eric O'Brien, Luke Byerly, Cody Stillwell, John P. Perentesis, James C. Mulloy and Benjamin Mizukawa

223 ***Humanized Mouse Models for the Advancement of Innate Lymphoid Cell-Based Cancer Immunotherapies***
Nina B. Horowitz, Imran Mohammad, Uriel Y. Moreno-Nieves, Ievgen Koliesnik, Quan Tran and John B. Sunwoo

238 ***Current Perspectives on the Role of TNF in Hematopoiesis Using Mice With Humanization of TNF/LT System***
Violetta S. Gogoleva, Kamar-Sulu N. Atretkhany, Arina P. Dygay, Taisiya R. Yurakova, Marina S. Drutskaya and Sergei A. Nedospasov

frontiers in Immunology

EDITORIAL
published: 23 December 2021
doi: 10.3389/fimmu.2021.829644

Editorial: Advances in Human Immune System Mouse Models for Studying Human Hematopoiesis and Cancer Immunotherapy

Yasuyuki Saito[1]*, *Tim Willinger*[2] *and Alexandre P. A. Theocharides*[3]

[1] Division of Molecular and Cellular Signaling, Department of Biochemistry and Molecular Biology, Kobe University Graduate School of Medicine, Kobe, Japan, [2] Center for Infectious Medicine, Department of Medicine Huddinge, Karolinska University Hospital, Karolinska Institutet, Stockholm, Sweden, [3] Department of Medical Oncology and Hematology, University of Zurich and University Hospital Zurich, Zurich, Switzerland

Keywords: humanized mouse, hematopoiesis, cancer immunotherapy, human immunology, translational research

Editorial on the Research Topic

Advances in Human Immune System (HIS) Mouse Models for Studying Human Hematopoiesis and Cancer Immunotherapy

OPEN ACCESS

Edited and reviewed by:
Catherine Sautes-Fridman, INSERM U1138 Centre de Recherche des Cordeliers (CRC), France

***Correspondence:**
Yasuyuki Saito
ysaito@med.kobe-u.ac.jp

Specialty section:
This article was submitted to Cancer Immunity and Immunotherapy, a section of the journal Frontiers in Immunology

Received: *06 December 2021*
Accepted: *08 December 2021*
Published: *23 December 2021*

Citation:
Saito Y, Willinger T and Theocharides APA (2021) Editorial: Advances in Human Immune System Mouse Models for Studying Human Hematopoiesis and Cancer Immunotherapy. Front. Immunol. 12:829644. doi: 10.3389/fimmu.2021.829644

INTRODUCTION

Gaining knowledge of human physiology and pathophysiology is often hampered by restricted access to human tissues or limited to performing *in vitro* assays. Furthermore, the development of novel therapeutics for cancer immunotherapy, autoimmune- and inflammatory diseases is tightly restricted by the use of human samples before moving to clinical trials, which is generally slow and costly. Human Immune System (HIS) mice - immunodeficient mice reconstituted with a human immune system – offer the unique opportunity to comprehensively study human hematopoiesis, infectious diseases, autoimmunity, and anti-tumor immunity *in vivo*. Recent progress in HIS mouse models, in which recipient immunodeficient mice carry several gene mutations or express human cytokines and self-recognition molecules, have improved human hematopoietic stem and progenitor cell (HSPC) engraftment as well as functional immune cell development in primary and secondary lymphoid tissues.

The articles in this Research Topic describe the latest developments in the field and indicate future directions to further improve HIS models and to apply them for more precisely characterizing human hematopoiesis as well as the human immune response against cancer.

RECENT PROGRESS IN HIS MOUSE MODELS

Human cell lines and organoids have proven to be particularly useful for *in vitro* high-throughput screens or gain/loss of function library studies in order to identify novel therapeutic targets for human diseases. The advantage of *in vivo* models is the more faithful recapitulation of human disease. Xenograft models support the development of human disease, the assessment of patient heterogeneity, and the investigation of the human immune system *in vivo*. They also allow the preclinical testing of novel therapeutic approaches.

In the presented series of articles, we aimed at covering the most recent development in the field of HIS mouse models with a particular focus on the application of immunotherapies. The review by Martinov et al. provides up-to-date information on current mouse models that have a humanized hemato-lymphoid system. The authors discuss the underlying principles of these models and point out outstanding challenges to build the next generation of mice with a human hematopoietic and immune system. Importantly, this review also provides guidance on how to identify humanized mouse models suited for specific research investigations. In another review, Mian et al. focus on humanized mouse models to investigate cancer immunotherapy by first giving an overview of recently developed models. In particular, they discuss challenges related to the development of specific human immune cell types and link the assessment of cancer immunotherapies with specific humanized mouse models for preclinical *in vivo* testing.

NOVEL APPROACHES TO IMPROVE HUMAN HEMATOPOIESIS IN MICE

Hematopoiesis occurs primarily in the bone marrow, where the hematopoietic stem and progenitor cell (HSPC) undergo expansion and multilineage differentiation. This process is regulated by a specific microenvironment called the hematopoietic stem cell niche. To establish HIS mice, opening the niche by, e.g., sub-lethal irradiation, is required for the stable engraftment of human HSPCs in the physical space. Mice engineered to carry a mutation in the *Kit* gene allow the engraftment of human HSPCs without irradiation due to the reduced competition of human HSPCs with mouse HSPCs for niche space. Hess et al. investigated the engraftment potential of various hematopoietic stem cell sources in non-irradiated NOD.B6 *scid* $Il2rg^{-/-}Kit^{W41/W41}$ (NBSGW) mice, which carry a hypomorphic mutation of the *KIT* gene. They show that the human engraftment level in mice transplanted with mobilized adult peripheral blood stem cells is significantly higher than in mice transplanted with human cord blood or bone marrow. The different HSPC sources also yielded different hematopoietic lineage engraftment patterns. However, the transplanted human cells lost the long-term engraftment potential *in vivo*. Adigbli et al. also used non-irradiated NBSGW mice, demonstrating engraftment of multiple human lymphoid and myeloid cell lineages after transplantation with CD133+ HSPCs. Moreover, NBSGW mice supported the development of human red blood cells when endogenous mouse macrophages were removed. Combined, the two studies provide useful information on the utility of the NBSGW mouse model for studying human hematopoiesis *in vivo*.

NOVEL TUMOR-BEARING MOUSE MODELS TO EVALUATE THE INTERACTION BETWEEN HUMAN TUMORS AND IMMUNE CELLS

Immune checkpoint inhibitors (ICI) are widely used in the treatment of solid tumors. However, a preclinical model to evaluate the anti-effect of ICI has not been established yet. In the methods paper published by Marín-Jiménez et al., the authors provide a very detailed description of their extensive experience with testing immunotherapies in human cord blood-derived Balb/c $Rag2^{-/-}Il2rg^{-/-}Sirpa^{NOD}$ mice. They investigated the response to ICI in various human solid tumors. Their work demonstrates that patient-derived xenografts are suited to investigate immunotherapies based on T-cell responses and constitutes an important resource for the development of preclinical models. Along these lines, Wunderlich et al. developed a preclinical model for pediatric and adolescents and young adults refractory B lymphoblastic leukemia (B-ALL) using NOD *scid* $Il2rg^{-/-}$ (NSG)-hSCF/IL3/GM-CSF^{Tg} or NOD $Rag1^{-/-}Il2rg^{-/-}$ (NRG)-hSCF/IL3/GM-CSF^{Tg} mice. Mice were "pre-engrafted" with human cord blood in order to generate functional effector T-cells. They confirmed the clinical efficacy of blinatumomab and also showed that interestingly the application of pembrolizumab reduced the B-ALL burden. Importantly, mice which were not pre-engrafted with human T-cells were unresponsive to treatment. Finally, they observed a synergistic effect of the combined treatment with blinatumomab and pembrolizumab. The combination led to an increased number of mice which lacked minimal residual disease and to prolonged survival supporting further investigation of this dual immunotherapeutic approach. Similarly, Qiao et al. developed a human tumor cell-line derived xenograft model for non-small cell lung cancer in order to test ICI. For this purpose, human PBMCs were transplanted before the tumor injection. They could show that the lactate dehydrogenase inhibitor oxamate and pembrolizumab act synergistically against tumor cells by increasing the number of CD8+ T-cells that infiltrate the tumor microenvironment.

Volk et al. used a model to mimic Epstein Baar virus (EBV)-associated post-transplant lymphoproliferative disorder (EBV-PTLD) by the infection of fully humanized NRG mice with EBV. They demonstrated that pembrolizumab induced expansion of EBV-positive tumor cells and infiltration of EBV-positive tumor cells into the central nervous system. This result is likely due to the emergence of dysfunctional T cells and may reflect clinical observations with spreading of EBV after ICI treatment.

IMMUNE CELL-SPECIFIC ANTI-TUMOR RESPONSES USING HIS MOUSE MODELS

The technical advances in the generation of humanized mice allow today to specifically investigate human immune cells *in vivo*. In the mini-review paper by Sun et al., the authors summarize recent advances with HIS mice that carry autologous tumor cells. They specifically focus on BLT humanized mice engrafted with human fetal liver CD34+ cells transduced with a MLL-AF9-GFP retrovirus to assess the response to immunotherapies in human leukemia, in particular anti-CD19 CAR T-cells.

In their original article, Katano et al. report the generation of human IL-15 transgenic NOD/Shi-*scid*/IL-2$R\gamma^{null}$ (NOG) mice, which lack the mouse Fcγ receptor and consequently do not produce antibody-dependent cellular cytotoxicity (ADCC). This allowed the authors to specifically examine the contribution of human NK cell-mediated ADCC to anti-tumor responses.

Therefore, this new model may prove useful for the preclinical testing of antibody-based approaches known to induce ADCC.

Maser et al. studied the anti-tumor effect of plasmacytoid dendritic cells (pDCs) in NOG-hIL3/GM-CSF^{Tg} mice, which supported the development of human pDCs. In certain tumor models, pDCs were recruited to tumors growing in mice. These intratumoral pDCs were functional as they produced type I interferon (IFN) in response to Toll-like receptor stimulation, which may prove beneficial for promoting NK cell-mediated anti-tumor activity.

Based on the identification of human monocyte-restricted progenitors, Izumi et al. investigated the effect of an anti-CD64 dimeric antibody conjugated with pyrrolobenzodiazepine (dPBD) *in vivo* in NOG mice. They showed that the anti-CD64-dPBD antibody selectively depleted monocyte progenitors without affecting the mature compartment. This compound also prevented the development of chronic myelomonocytic leukemia in mice, a disease with high therapeutic need. Finally, they extended their work to solid tumors and showed that the anti-CD64-dPBD antibody led to tumor growth regression by eliminating the tumor-associated macrophage population.

The review by Serr et al. summarizes the possible use of HIS mice to investigate and develop immunotherapies based on regulatory T-cells (Tregs). Tregs are known to facilitate tumor growth. The authors propose to use Treg inhibition to enhance anti-tumor responses in personalized humanized mouse models that are reconstituted with the patient's immune system and tumor cells.

Standard immunodeficient mice weakly support the development of human innate lymphoid cells (ILCs), in particular human NK-cells. Recent progress in the generation of humanized immunodeficient animals, in particular models that produce human IL-15, led to the development of human ILCs *in vivo*. In the review by Horowitz et al., the authors present humanized mouse models that can be used to study ILCs and potential therapeutic approaches that employ human ILCs against cancer. This review provides an excellent overview about the development of ILC-based cancer immunotherapy.

UNIQUE APPLICATIONS FOR SPECIFIC RESEARCH QUESTIONS USING HIS MICE

Flahou et al. review the use of HIS mice in the context of induced pluripotent stem cells (iPSC)-derived therapies for tissue regeneration. Here the authors suggest using humanized mouse models that develop human NK cells to evaluate the immunogenicity and rejection of transplanted iPSCs and their progeny. This could help to develop HLA-engineered iPSC-derived cells for universal clinical use.

Tumor necrosis factor (TNF) is a pro-inflammatory cytokine that controls inflammation. TNF inhibitors have been widely used in the clinic to treat autoimmune or inflammatory diseases. Gogoleva et al. review several humanized mouse models, which express human TNF in order to study human autoimmune diseases and the effect of TNF inhibitors on hematopoiesis *in vivo*.

Human γ-herpesviruses such as Epstein Barr virus (EBV) and Kaposi sarcoma-associated herpesvirus (KSHV) can induce lymphoproliferative diseases in humans. The immune response against γ-herpesviruses has been largely recapitulated in humanized mouse models. The review article by Münz focuses on the evaluation of immune responses to control pathologies induced by human γ-herpesviruses in humanized mouse models and discusses strategies for developing vaccines.

Furthermore, Yong et al. tested two different immunotherapeutics, including human interleukin-2 (Proleukin) and the anti-CD3 monoclonal antibody OKT3, in a humanized NSG model. Administration of Proleukin to humanized mice resulted in an increase of several pro-inflammatory cytokines and chemokines. Likewise, the use of OKT3 treatment in their model led to T-cell depletion along with an increase in several pro-inflammatory cytokines. This indicates that the presented models can reproduce the effect of these immunotherapeutics observed in patients.

CONCLUSION

This Research Topic shows the usefulness of HIS mouse models in translational research related to several important human diseases and we are looking forward to future developments in this exciting research area.

AUTHOR CONTRIBUTIONS

All authors listed have made a substantial, direct, and intellectual contribution to the work, and approved it for publication. All authors contributed equally to the work.

FUNDING

YS is supported by a Grant-in-Aid for Challenging Exploratory Research (20K21547) from the Ministry of Education, Culture, Sports, Science and Technology of Japan. TW is supported by a faculty-funded career position at Karolinska Institutet (2-1060/2018). APAT is supported by the Professor Dr. Max Cloëtta Foundation and the Swiss Cancer Research grant KFS-4875-08-2019.

Conflict of Interest: The authors declare that the research was conducted in the absence of any commercial or financial relationships that could be construed as a potential conflict of interest.

Publisher's Note: All claims expressed in this article are solely those of the authors and do not necessarily represent those of their affiliated organizations, or those of the publisher, the editors and the reviewers. Any product that may be evaluated in this article, or claim that may be made by its manufacturer, is not guaranteed or endorsed by the publisher.

Copyright © 2021 Saito, Willinger and Theocharides. This is an open-access article distributed under the terms of the Creative Commons Attribution License (CC BY). The use, distribution or reproduction in other forums is permitted, provided the original author(s) and the copyright owner(s) are credited and that the original publication in this journal is cited, in accordance with accepted academic practice. No use, distribution or reproduction is permitted which does not comply with these terms.

frontiers in Immunology

ORIGINAL RESEARCH
published: 08 September 2020
doi: 10.3389/fimmu.2020.02082

The Tumor Milieu Promotes Functional Human Tumor-Resident Plasmacytoid Dendritic Cells in Humanized Mouse Models

Ilona-Petra Maser[1], Sabine Hoves[1], Christa Bayer[1], Gordon Heidkamp[1], Falk Nimmerjahn[2], Jan Eckmann[1] and Carola H. Ries[1,3]**

[1] Roche Pharma Research and Early Development, Discovery Oncology, Roche Innovation Center Munich, Penzberg, Germany, [2] FAU Erlangen, Division of Genetics, Department of Biology, University of Erlangen-Nuremberg, Erlangen, Germany, [3] Dr. Carola Ries Consulting, Penzberg, Germany

OPEN ACCESS

Edited by:
Tim Willinger,
Karolinska Institutet, Sweden

Reviewed by:
Nobuyuki Onai,
Kanazawa Medical University, Japan
Lishan Su,
The University of North Carolina at Chapel Hill, United States

***Correspondence:**
Jan Eckmann
jan.eckmann@roche.com
Carola H. Ries
riescarola@gmx.de

Specialty section:
This article was submitted to Cancer Immunity and Immunotherapy, a section of the journal Frontiers in Immunology

Received: 05 March 2020
Accepted: 30 July 2020
Published: 08 September 2020

Citation:
Maser I-P, Hoves S, Bayer C, Heidkamp G, Nimmerjahn F, Eckmann J and Ries CH (2020) The Tumor Milieu Promotes Functional Human Tumor-Resident Plasmacytoid Dendritic Cells in Humanized Mouse Models. Front. Immunol. 11:2082. doi: 10.3389/fimmu.2020.02082

Particular interest to harness the innate immune system for cancer immunotherapy is fueled by limitations of immune checkpoint blockade. Plasmacytoid dendritic cells (pDC) are detected in a variety of solid tumors and correlate with poor clinical outcome. Release of type I interferons in response to toll-like-receptor (TLR)7 and TLR9 activation is the pDC hallmark. Mouse and human pDC differ substantially in their biology concerning surface marker expression and cytokine production. Here, we employed humanized mouse models (HIS) to study pDC function. We performed a comprehensive characterization of transgenic, myeloid-enhanced mouse strains (NOG-EXL and NSG-SGM3) expressing human interleukin-3 (hIL-3) and granulocyte-macrophage colony stimulating factor (GM-CSF) using identical humanization protocols. Only in HIS-NOG-EXL mice sufficient pDC infiltration was detectable. Therefore, we selected this strain for subsequent tumor studies. We analyzed pDC frequency in peripheral blood and tumors by comparing HIS-NOG-EXL with HIS-NOG mice bearing three different ovarian and breast tumors. Despite the substantially increased pDC numbers in peripheral blood of HIS-NOG-EXL mice, we detected TLR7/8 agonist responsive and thus functional pDCs only in certain tumor models independent of the mouse strain employed. However, HIS-NOG-EXL mice showed in general a superior humanization phenotype characterized by reconstitution of different myeloid subsets, NK cells and B cells producing physiologic IgG levels. Hence, we provide first evidence that the tumor milieu but not genetically introduced cytokines defines intratumoral (i.t.) frequencies of the rare pDC subset. This study provides model systems to investigate *in vivo* pro- and anti-tumoral human pDC functions.

Keywords: humanized mice, myeloid-enhanced mice, plasmacytoid dendritic cells (pDC), cancer immunotherapy, human pDC targeting, TLR agonists

INTRODUCTION

Efforts to harness the innate immune system for cancer therapy have mainly been focused on macrophages and dendritic cells (DCs). Macrophages are attractive to drug developers because of their abundance in the tumor microenvironment (TME) (1), while the rare dendritic cells are able to present tumor antigen and direct T cell responses (2). Human DCs are classified into three subtypes: Classical CD1c$^+$ DCs (cDC2), cross-presenting CD141$^+$ DCs (cDC1) and plasmacytoid CD303$^+$ DCs (pDC) (3–5). Whereas cDC2 cells play an important role in the stimulation of Th2 and Th17 responses against extracellular pathogens, the cDC1 subset takes up dead cells via CLEC9A and is mainly known to cross-present peptides via MHC class 1 to CD8$^+$ T cells (3). The very rare pDCs are capable to produce abundant amounts of all type I interferons in response to stimulation with TLR7 and 9. Hence, they contribute to antiviral immunity (6). While the role of pDCs in chronic viral infections such as HIV or Hepatitis B is well validated (7, 8), their pathogenic role in cancer is less clear. pDCs are detected in a variety of different solid tumors, especially in melanoma, ovarian and breast cancer (5, 9–13). Interestingly, despite their low abundance compared to tumor-associated macrophages (TAMs) or tumor infiltrating lymphocytes, pDC infiltration correlates with poor clinical outcome, likely due to the induction of suppressive immune cells (5, 10–13). However, TLR stimulation of pDCs *in vitro* results in killing of human tumor cells (14). Treatment of in-transit metastases with the TLR7/8 agonist Imiquimod in one melanoma patient showed clinical benefit through pDC activation (15). Therefore, pDCs represent an attractive therapeutic target as restoring their IFN-I-producing function is expected to not only stimulate other immune cells and directly kill tumor cells, but also to reduce the suppressive function of T regulatory cells (Tregs) (12, 13).

The low numbers of these potent cells has hampered development of pDC-targeting strategies, due to the challenging experimental manipulation. Additionally, mouse and human pDCs differ in their biology (8). Mouse pDCs produce high amounts of IL-12, whereas in humans cDCs are the major source for IL-12. Furthermore, TLR7 and TLR9 co-expression is restricted to human pDCs and B cells (8). Functional human pDCs have been successfully reconstituted in different humanized mouse strains and enabled analysis of pDC functionality in virology, autoimmune diseases and in melanoma (13, 15–18).

However, the generation of mice with a human immune system (HIS) represents a quite complex, multi-step process, where experimental parameters for each step can vary between different labs. Immune deficient mice have to be engrafted with human hematopoietic stem cells that requires a pre-conditioning regimen to delete the mouse hematopoietic stem cells (19). As a consequence, humanization protocols deviate in the use of newborn or adult mice, the source of the human cells [hematopoietic stem cells (HSC), fetal liver cells, or peripheral blood mononuclear cells (PBMC) as donor cells], different injections methods as well as irradiation or chemotherapy for pre-conditioning (20, 21). Also animal housing and diet influencing the microbiota have been reported to impact human engraftment quality and quantity (22–25).

Despite the tedious generation process, humanized mice are regularly used as they offer an *in vivo* test system to investigate the heterotypic cross-talk between human tumor cells and human immune cells or to evaluate therapeutic candidates that lack mouse cross-reactivity (19, 26). Although most commonly used HIS mouse models such as HIS-BRG, HIS-NOG or HIS-NSG mice were shown to sufficiently reflect human lymphoid (particularly T and B cell) development, they suffer from some critical limitations. These include impaired lymph node (LN) development, minimal antigen-specific IgG antibody production and lack of antigen-specific human T cell responses (27). Consistently, conventional HIS-mice poorly reconstitute human innate immune cells such as myeloid cells and NK cells, which is attributed to the lack of mouse cytokine cross-reactivity for critical cytokines e.g., IL-3, IL-15, GM-CSF, or M-CSF (28). To overcome this hurdle, transgenic mouse strains were designed to express human IL-3 and GM-CSF, referred to as NOG-EXL and NSG-SGM3 mice (29, 30).

Xenografted human tumors can provide a human cytokine milieu that shapes the functional activity as well as the frequency of tumor-associated myeloid cells. Therefore, we investigated the relative contributions of transgenic and tumor-derived cytokines to myeloid cell and, in particular, pDC reconstitution in both myeloid-enhanced and conventional HIS-models. Importantly, we used identical humanization protocols for all mouse strains, even identical stem cell donors that were pre-selected for high stem cell yield and thus sufficient for all 3 strains. Using two different ovarian tumors and one breast cancer patient derived xenograft (PDX), we identified specific tumors that are capable to generate functional, TLR agonist-responsive pDCs, which do not rely on cytokine expression in transgenic mice nor high pDC numbers in the periphery.

MATERIALS AND METHODS

Ethics Statement

All animal experiments were performed according to the national institutes of health guidelines for the care and use of laboratory animals and European Union directives and guidelines and were approved by the local ethics committees (Regierung von Oberbayern, Munich, Germany).

Animal Models

Female NOD.Cg-Prkdcscid Il2rgtm1SugTg(SV40/HTLV-IL3,CSF2)10-7Jic/JicTac transgenic mice (NOG-EXL) and non-transgenic NOD.Cg-Prkdcscid Il2rgtm1Sug/JicTac (NOG) mice were purchased from Taconic bioscience (4–5 weeks). Female NOD.Cg-Prkdcscid Il2rgtm1Wjl Tg(CMV-IL3,CSF2,KITLG)1Eav/MloySzJ (NSG-SGM3) were acquired from the Jackson laboratory at the same age. All mouse strains were kept according to the applicable animal protection law in a specific pathogen free (SPF) area. Mice were closely monitored for body weight and general conditions.

Generation of Humanized Mice

Humanized mice were generated through preconditioning with a chemotherapeutic agent. 15 mg/kg of Busulfan (Busilvex®,Pierre Faber) diluted in 0.9% Saline (Braun) was injected intraperitoneally (i.p.). Twenty-four hours later 10^5 human $CD34^+$ umbilical cord blood-derived HSC (Stem Cell Technologies/Allcells) in 100 μl phosphate-buffered saline (PBS) were transplanted into the mice via intra-venous (i.v.) tail vein injection. Same HSC donors were used and mice were randomized for individual donors.

Tumor Models

The human ovarian carcinoma cell line OVCAR-5 was purchased from the National Cancer Institute (Cat. Nr. 0507676). The cell line SK-OV-3 is an internal cell line, which was tested and authenticated to be SK-OV-3 after a full match with the reference databases of ATCC, JCRB, RIKEN, KCLB, and DSMZ. All cell lines were confirmed to be free of murine pathogens and murine viruses (Biomedical diagnostics, Hannover, Germany). To generate human xenograft tumors 3×10^6 OVCAR-5 or 5×10^6 SK-OV-3 tumor cells were injected in 100 μl PBS into the right flank of isoflurane anesthetized humanized mice. The human breast cancer patient-derived xenograft BC_038, a triple negative breast cancer, was obtained from Oncotest and transplanted into non-humanized NOG mice for three rounds *in vivo* before use in this study. Tumor fragments were digested with Collagenase D and DNase I (Roche), counted and injected into the mammary fat pad of humanized mice. Tumor growth was monitored twice a week by perpendicular caliper measurement and tumor volume was calculated using the following formula: $\text{volume} = 0.5 \times \text{length}^2 \times \text{width}$.

TLR Treatment *in vivo*

TLR9 agonist CpG-A (ODN 2216) and TLR7/8 agonist R848 were purchased from InvivoGen. Agonists were diluted with sterile endotoxin free water. Humanized mice were treated with 35 μg/mouse via i.p. or intra tumoral (i.t.) injection. Mice injected with sterile endotoxin containing water served as control.

Isolation of Human pDCs and *in vitro* Stimulation

Bone marrow (BM)-derived cells as well as splenocytes from humanized mice were pooled from up to ten individual mice to isolate pDCs using a customized isolation kit according to manufacturer's instructions (Stemcell Technologies). Briefly, cells were incubated with normal rat serum, pDC isolation cocktail, biotin and RapidSpheres™. Subsequently, cells were placed in a magnet from Stemcell technologies and the flow-through was collected. Purity of the enriched, untouched pDCs was usually 70%. Human $CD303^+$ $CD123^+$ cells were used for *in vitro* stimulation using 0.25 μg/μl of TLR agonists for 3 h followed by supernatant collection for cytokine analysis. Splenocytes from all humanized mouse strains did not contain sufficient numbers of pDC required for functional assays.

Protein Analysis

Cytokine levels in serum and tumor lysates from humanized mice were measured using the Bio-Plex system with Bio-Plex human cytokine 48 or 17-Plex kit as well as single analysis for IFN-α2 according to manufacturer's protocol (Bio-Rad). Chemokine levels in serum and tumor lysates from humanized mice were measured using the Bio-Plex system with human chemokine 40-Plex kit (Bio-Rad). Human and murine FLT3-L were measured by specific ELISA assays (R&D systems).

Immunoassay for Human-Specific IgG Antibodies

IgG antibodies serum levels of humanized mice were determined by immunoassay (31). Briefly, anti-human Fcγ-pan R10Z8E9 was digoxigenylated and subsequently biotinylated MAB anti-human Fcγ-pan R10Z8E9 was bound to streptavidin-coated microtiter plates at a concentration of 0.5 μg/mL. After incubation for 1 h the unbound antibody was removed by washing. Samples and standards were pre-incubated with 0.05 μg/mL of digoxigenylated MAB anti-human Fcγ-pan R10Z8E9 for 1 h. Afterwords, the mixture was added to wells of microtiter plates coated with the biotinylated anti-human IgG antibodies and incubated for 1 h. After washing, a polyclonal anti-digoxigenin-horseradish peroxidase conjugate (Roche, cat. no. 11633716001) was used to detect the bound digoxigenylated MAB anti-human Fcγ-pan R10Z8E9. A dilution of 50 mU was incubated for 1 h. The HRP of the antibody–enzyme conjugates catalyzed the color reaction of ABTS substrate. A Tecan plate reader at 405 nm wavelength measured the signal at 490 nm.

Tissue Preparation, Antibodies and Flow Cytometry

Peripheral blood samples were collected into EDTA-coated tubes from the facial vein using lancets. In brief, 20 μl aliquots of whole blood were first lysed with 1X RBC Lysis-buffer (Invitrogen) and washed with MACS running buffer (Miltenyi), before applying the antibodies. Blood leukocytes were tested for human CD45, CD3, CD33, CD14, CD16, CD56, and CD19 (REAfinity/Miltenyi). Live/dead exclusion was performed by propidium iodide (Miltenyi). Eight-color flow cytometry analyses were performed on Miltenyi MACS Quant 10.

The tumor was cut into small pieces using two scalpels. Additionally, tumor mass was simultaneously homogenized in C-tubes by gentleMACS Dissociator from Miltenyi and incubated with Collagenase D and DNase I (Roche). Tumor, BM and spleen were filtered through a combination of filters (100, 70, and 30 μm; Miltenyi) and lysed before samples were blocked for unspecific binding with mouse and human Fc blocking antibodies (Biolegend/Miltenyi). For intracellular staining, cells were fixed for 20 min and permeabilized (Invitrogen) prior to adding the intracellular antibodies for another 20 min.

Splenocytes, BM and tumor samples were tested in different panels for human CD1c, CD3, CD4, CD8, CD11b, CD11c, CD14, CD16, CD19, CD25, CD33, CD40, CD45, CD45RA, CD56, CD62L, CD66b, CD68, CD69, CD83, CD86, CD123, CD141, CD163, CD204, CD206, CD279, CD303, CLEC9A,

FOXP3, HLA-DR, and Nkp46 in 18-color combinations (see also **Supplementary Table 1**). Live/dead staining was performed with fixable ZOMBIE^{TM} UV dye (BioLegend). Antibodies and isotype controls were obtained from BD Bioscience or BioLegend. Eighteen-color flow cytometry analyses were performed on a BD Fortessa device. FCS files were analyzed by FlowJo (Version 10).

Statistical Analysis

Statistical analyses were performed using Prism 7.0 software (GraphPad Software). Normally distributed data were expressed as mean ± standard error of the means (SEM) unless noted otherwise. Nonparametric data was expressed as median ± interquatile range (IQR) and is indicated in the figure legend as such. The student *t*-test was used to compare normally distributed two-group data. Ordinary one-way ANOVA with Tukey multiple comparison or Kruskal-Wallis ANOVA with Dunn's multiple comparison were performed, if more than two groups were analyzed. Survival curve analysis was achieved using the log-rank (Mantel-Cox) and Gehan-Breslow-Wilcoxon tests. Individual data points are shown if $n < 5$. Each dot represents an individual mouse or analyzed sample. Statistical tests used are indicated in the figure legends.

RESULTS

Characterization of Humanized NOG and Myeloid Enhanced Mice

To delineate the contribution of transgene and tumor-derived cytokines to DC development in humanized mice, we first performed a detailed characterization of different myeloid enhanced transgenic mouse strains. For humanization NOG, NOG-EXL and SGM3 mice were pretreated with Busulfan and injected i.v. with human CD34$^+$ hematopoietic stem cells (HSCs) at 5–6 weeks of age. Body weight was monitored and humanization status was determined in peripheral blood in 2-week intervals (**Figure 1A**). Even though all mouse strains were humanized using the same protocol, differences in body weight and survival were observed (**Figures 1B,C**). HIS-NSG-SGM3 showed significantly increased body weight throughout the study accompanied by decreased overall survival compared to HIS-NOG and HIS-NOG-EXL mice. We detected a high proportion of human CD45$^+$ immune cells in LNs of HIS-NOG-EXL and HIS-NSG-SGM3 (**Figure 1D**) in contrast to the HIS-NOG control strain. Therefore, we omitted LN analysis from the latter due to the low humanization level < 25%. Anatomically, only myeloid enhanced mice showed robust axial LN development with HIS-NOG-EXL mice having the largest LNs (**Figure 1E**, **Supplementary Figure 1A**). LN immune cell analysis revealed a large T cell population in the transgenic mice, with CD4$^+$ T cells being the predominant subset with over 50% (**Figure 1D**).

One limitation of conventional HIS models is the lack of antibody class switch. Remarkably, myeloid-enhanced HIS mice and here in particular HIS-NOG-EXL mice, showed consistently high levels of total human IgG 16 weeks after humanization (**Figure 1F**). These levels are comparable with the increased IgG levels of NSG-SGM3 BLT compared to NSG mice and mCD47/BALB-HIS mice and even 2-fold higher than in IL-6 knock-in mice or as in specifically developed BRGST mice (27, 32–34). Furthermore, IgG was detectable from week 10 onward albeit at lower concentration (**Supplementary Figure 1B**).

Thymus size (**Supplementary Figure 1C**) as well as human CD45$^+$ levels (**Figure 1G**) were comparable across all strains. Yet again, transgenic mice presented an increased T/B cell ratio. Remarkably, HIS-NOG mice showed a high number of thymic B cells. Since this strain displays in general poor B cell differentiation, manifested in a lack of Ig class switching and absence of serum IgG, we hypothesize that immature B cell precursors may partially accumulate in the thymus.

CD4$^+$ T cell frequencies were comparable, while transgenic strains had higher CD8$^+$ and lower double positive frequency compared to HIS-NOG (**Figure 1G**). Splenomegaly was observed in both myeloid enhanced mouse strains compared to HIS-NOG (**Figure 1H**, **Supplementary Figure 1D**) that matched in size with other immune competent mouse strains. However, hepatosplenomegaly was exclusively detected in HIS-NSG-SGM3 mice (**Supplementary Figures 1E,F**), confirming published data (35, 36). Together, our data imply that IL-3 and GM-CSF transgene expression favor CD8$^+$ T cell reconstitution and antibody class switch associated with improved LN and thymus development.

Myeloid Enhanced HIS Mice Demonstrate Superior Overall Human Immune Cell Reconstitution

Next, we evaluated the general human immune cell engraftment in peripheral blood of different HIS models by flow cytometry (**Supplementary Figure 2A**). Whereas, lymphoid and myeloid cell distribution was comparable in blood of HIS-NOG-EXL, B and T cells dominated in HIS-NOG and HIS-NSG-SGM3, respectively (**Figure 2A**). Amongst the different strains tested, we found that HIS-NOG-EXL mice most closely mimic the human immune cell composition 16 weeks after reconstitution (**Figure 2A**). The transgene expression led to significantly improved CD33$^+$ myeloid reconstitution particularly in HIS-NOG-EXL mice (**Figure 2B**, **Supplementary Figures 2B,C**). Additionally, we observed marked differences in the monocytic lineage between humanized mice and human blood characterized by CD14 and CD16 expression. Classical CD14$^+$CD16$^-$ monocytes were present in blood of all HIS strains, intermediate CD14$^+$CD16^{dim} and non-classical CD14$^-$/CD16$^+$ monocytes were barely detectable (**Figures 2C,D**). Contrary to human blood, where classical monocytes are the dominant population, humanized mice underrepresent this population at the expense of a high frequency of immature CD33$^+$ cells lacking monocyte markers. This phenomenon might be attributed to the missing M-CSF crucial for monocyte/macrophage differentiation (28).

White blood cell composition in HIS mice is known to change over time (29, 30). Humanization was maintained as HIS-NOG-EXL and HIS-NSG-SGM3 displayed significantly higher overall engraftment levels when compared to HIS-NOG (**Figure 2E**). In contrast, individual immune cell subsets followed different kinetics. Whereas, CD3$^+$ T cells slightly increased, CD19$^+$ B cells declined over time. Myeloid enhanced HIS

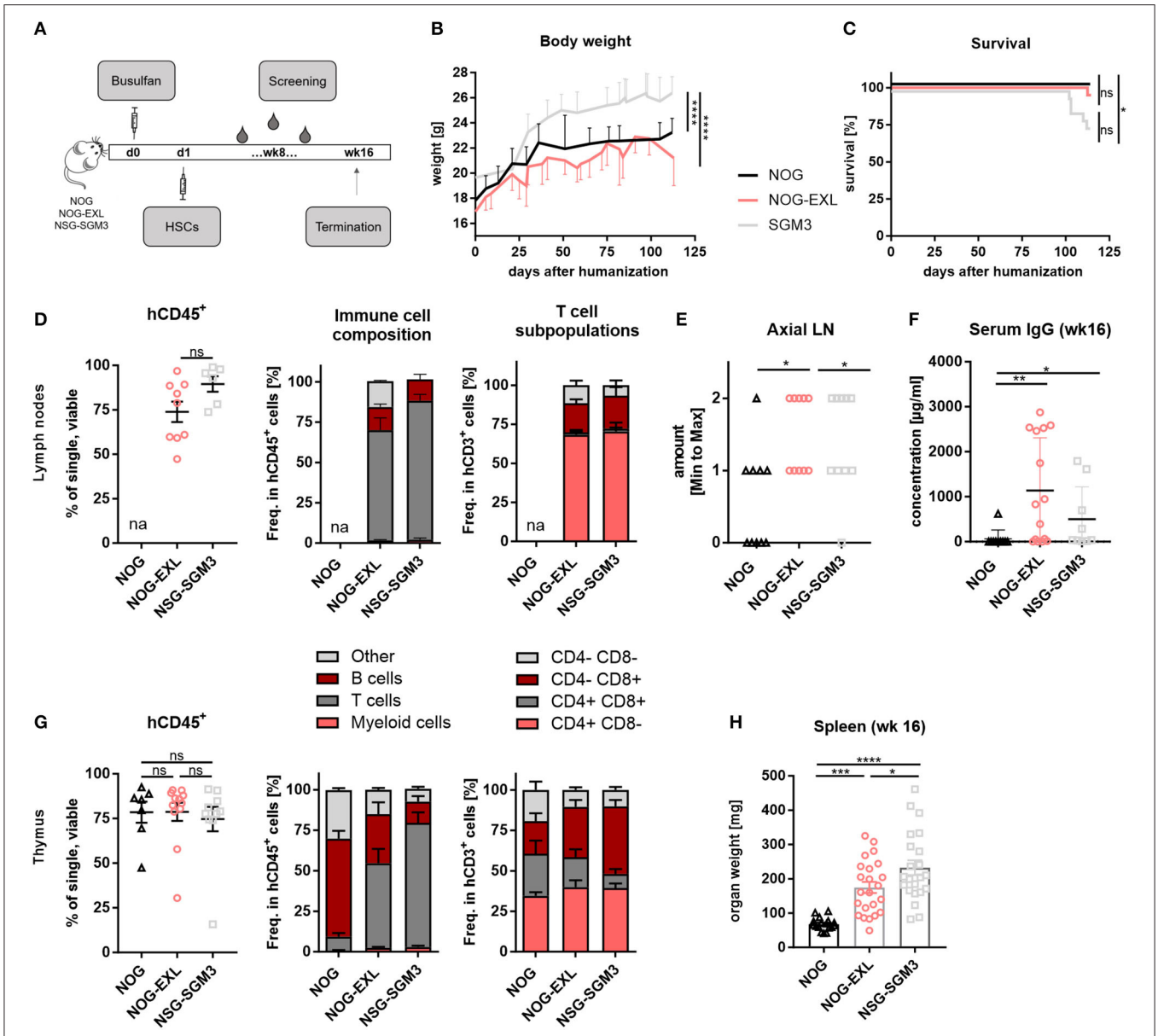

FIGURE 1 | Differences between identically humanized mouse strains in body weight, survival and immune cell composition. **(A)** Reconstitution protocol, graphic overview: NOG, NOG-EXL, and NSG-SGM3 (5–6 weeks) were pretreated with Busulfan and injected with human HSCs. Body weight (BW) and peripheral blood was screened biweekly. At termination (week 16), different peripheral organs were analyzed for human leukocytes. **(B)** BW kinetic: NOG, NOG-EXL, and NSG-SGM3 were monitored from day 0 until termination, $n = 18–341$, one-way ANOVA, Tukey's multiple comparison test. ****$p < 0.0001$. **(C)** Survival curve comparison, log-rank (Mantel-Cox) or Gehan-Breslow-Wilcoxon test provided same statistical results, error bars indicate mean ± SD, $n = 20$/strain, *$p < 0.05$. **(D)** Human leukocyte composition (CD45$^+$) in lymph nodes (LNs) as percentage, $n = 6–10$, one-way ANOVA, Tukey's multiple comparison test, ****$p < 0.0001$; Immune cell composition in CD45$^+$ and T cells in CD3$^+$. huNOG was excluded from analysis due to human CD45 levels < 25%. **(E)** Axial LN amount from all humanized mouse strains analyzed, $n = 10$/strain. One-way ANOVA, Tukey's multiple comparison test. *$p < 0.05$. **(F)** Total human IgG concentration in serum (week 16), $n = 10$/strain, Kruskal-Wallis ANOVA with Dunn's multiple comparison test, error bars indicate median ± IQR, *$p < 0.05$; **$p < 0.01$. **(G)** Human leukocyte composition in thymus as percentage, $n = 6–10$, one-way ANOVA, Tukey's multiple comparison test, ****$p < 0.0001$, Immune cell composition in CD45+ and T cell subsets. **(H)** Spleen weight in mg (week 16), one-way ANOVA, Tukey's multiple comparison test, $n = 17–23$. *$p < 0.05$; ***$p < 0.001$; ****$p < 0.0001$.

mice had higher frequencies of CD56$^+$ NK cells at early time points while only HIS-NOG-EXL mice maintained their NK population. Strikingly, increased frequencies of myeloid cells (CD33$^+$/CD14$^+$) were only observed in HIS-NOG-EXL mice throughout the screening period (**Figure 2E**). Despite transgene expression for enhanced myeloid reconstitution, HIS-NSG-SGM3 mice displayed decreasing NK-, B and myeloid cell frequencies over time.

Besides cellular immune composition, we were also interested in the human cytokine profile. Both myeloid-enhanced HIS

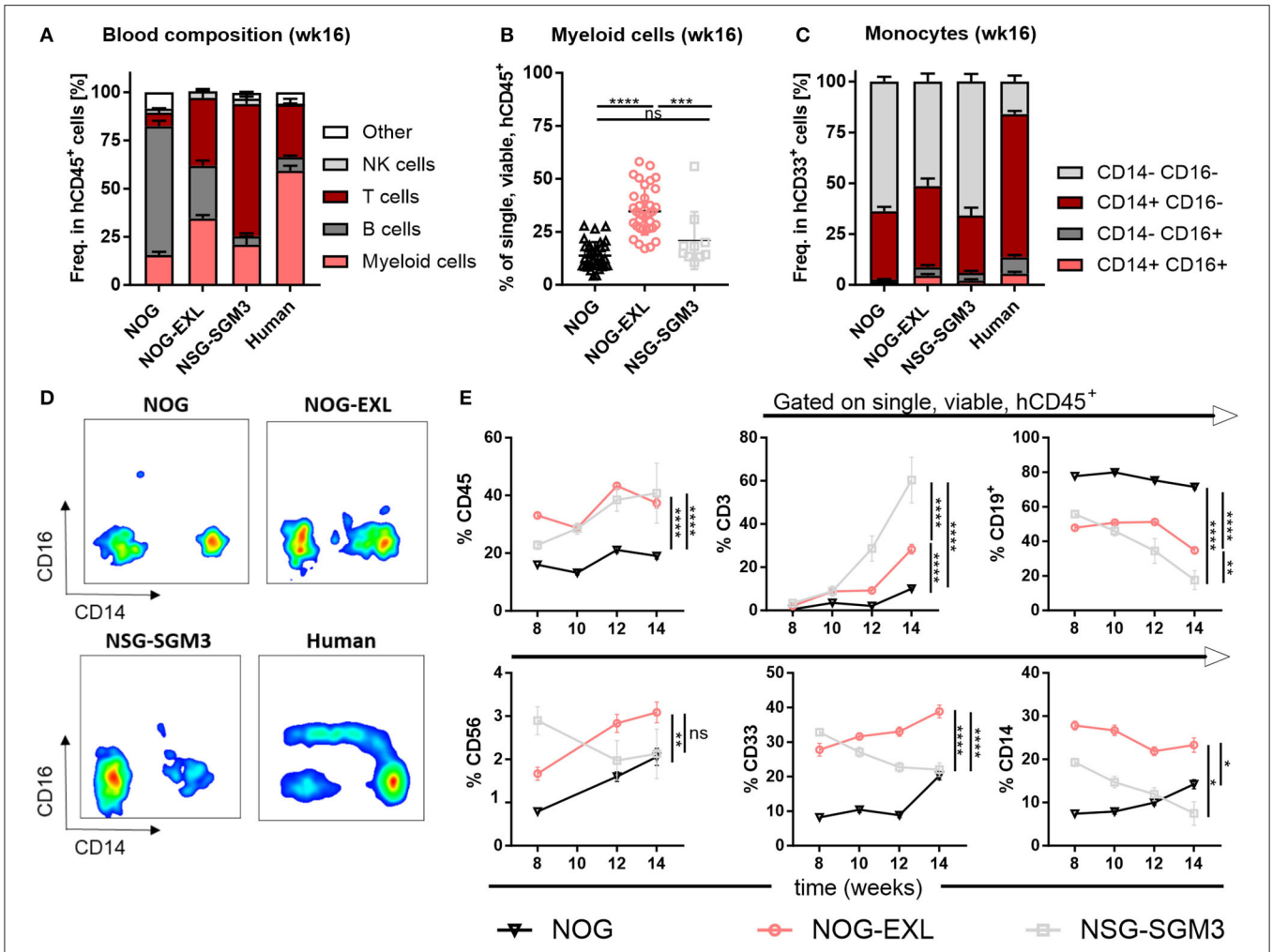

FIGURE 2 | Peripheral blood analysis demonstrates improved human immune cell reconstitution. **(A)** Human leukocytes composition (CD45$^+$) in peripheral blood (PB) 16 weeks after reconstitution as percentage, $n = 28–40$. **(B)** Comparison of human myeloid cells (CD33$^+$) in human leukocytes (CD45$^+$) as percentage from same mice as in A, one-way ANOVA, Tukey's multiple comparison test. $^*p < 0.05$; $^{***}p < 0.0005$; $^{****}p < 0.0001$, $n = 10–39$. **(C)** Human monocyte composition in total CD33$^+$ in PB 16 weeks after reconstitution or in human PBMCs as percentage, $n = 5–40$. **(D)** Representative FACS plots for human monocyte populations (CD16$^{+/-}$/CD14$^{+/-}$ in CD45$^+$) in PB of humanized mice in week 16 or in human PBMCs. **(E)** Different immune cell populations (CD45$^+$ in single viable; CD19$^+$, CD3$^+$, CD33$^+$, CD56$^+$, and CD14$^+$ in CD45$^+$) in HIS-NOG, HIS-NOG-EXL and HIS-NSG-SGM3 over time (week 8–14), ordinary 2-way ANOVA, $^*p < 0.05$; $^{**}p < 0.001$; $^{***}p < 0.0005$; $^{****}p < 0.0001$, $n = 28–121$.

mice showed significantly increased cytokine levels (**Figure 3**, **Supplementary Figure 3**). In line with published data (36, 37) we found cytokines/chemokines elevated especially in HIS-NSG-SGM3, such as the pro-inflammatory IL-1β, IL-6, IL-8, TNF-α, IFN-γ, MCP-1, and MIP-1β as well as anti-inflammatory IL-10 (**Figure 3**). Besides, cytokines and chemokines involved in T cell differentiation, e.g., IL-4, CX3CL1, and CCL17, but also Treg recruitment such as CCL22 were significantly elevated (**Figure 3**). Moreover, additional proinflammatory molecules showed a trend for upregulation (**Supplementary Figure 3**). As expected, human GM-CSF serum levels were strongly increased in sera of transgenic mice, in particular of HIS-NSG-SGM3 mice with ∼2 ng/ml. Non-humanized mice control sera were used to confirm the specificity of the multiplex assay for human cytokines (data not shown).

Collectively, we confirmed an enhanced human myeloid reconstitution in both mouse strains. However, HIS-NOG-EXL outperform HIS-NSG-SGM3 mice in maintaining long-term human myeloid cell reconstitution together with a more physiologic, low inflammatory cytokine profile.

HIS-NOG-EXL Mice Develop DC Subsets in Spleen and Have Functional Human pDCs

Major subsets of myeloid cells undergo terminal differentiation in tissues (38). Following the analysis of immune cell composition in LN and thymus (**Figures 1D–H**), we subjected spleen and BM samples of the same mice to flow cytometry analysis of human myeloid cells (DCs, macrophages and granulocytes) (**Supplementary Figures 4A–C**). Contrary to both HIS-NOG strains, HIS-NSG-SGM3 mice showed lower BM humanization,

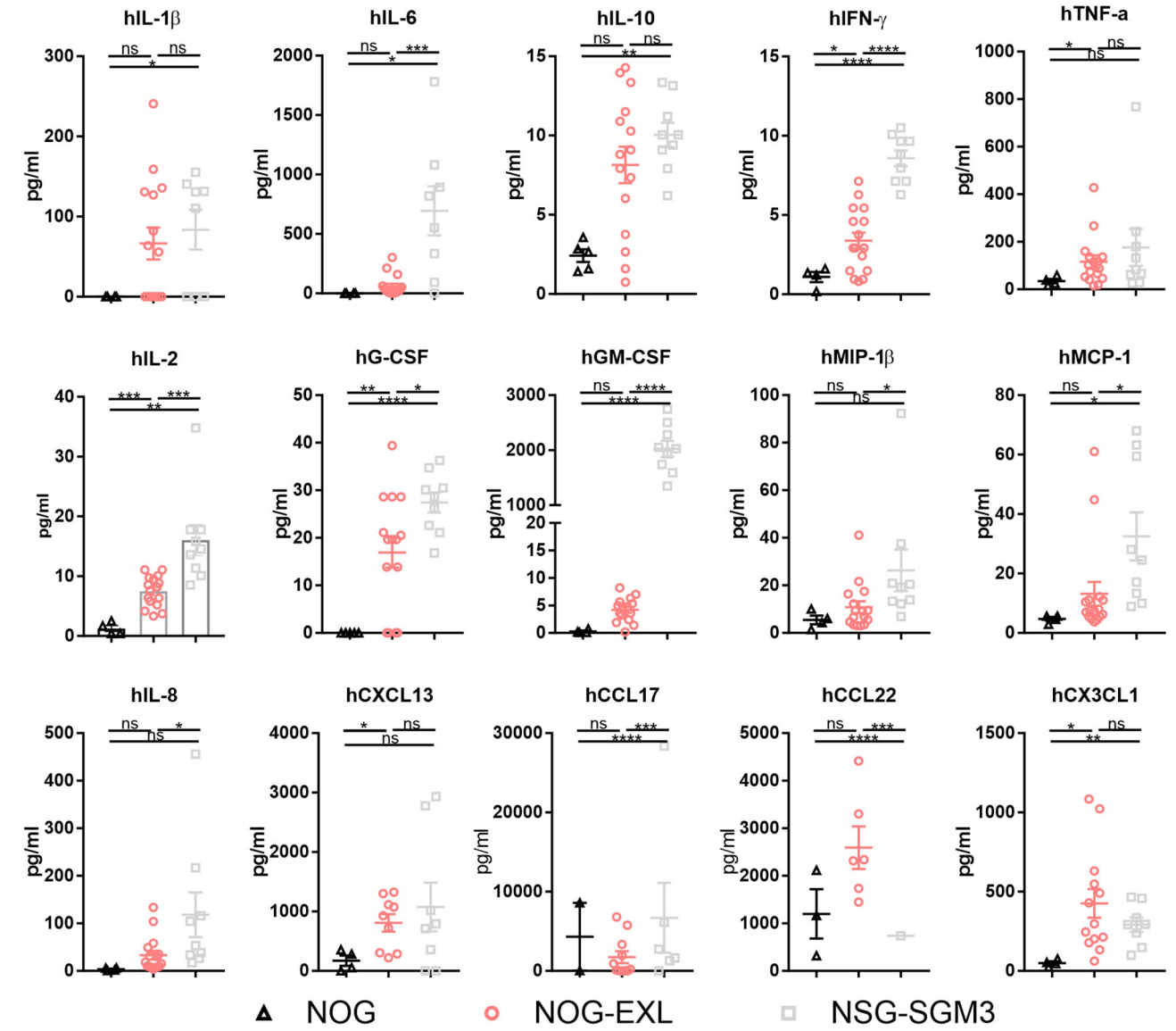

FIGURE 3 | Myeloid-enhanced mice show increased inflammatory profile. Human cytokines and chemokines analysis by Bio-Plex in sera of humanized NOG, NOG-EXL and NSG-SGM3 mice, two-tailed unpaired *t*-test, error bars indicate mean ± SEM, $^{*}p < 0.05$; $^{**}p < 0.005$; $^{***}p < 0.0005$; $^{****}p < 0.0001$; ns, not significant, $n = 4$–16.

while HIS-NOG-EXL had a high humanization level in spleen (**Figures 4A,B**). Concomitantly to the increased myeloid cell frequency in transgenic mice, we found increased T and NK cell numbers, while B cells were reduced in both lymphoid organs (**Figures 4C,D**). Similar to peripheral blood, HIS-NSG-SGM3 exhibited the highest $CD3^{+}$ T cell frequency in BM and spleen. Notably, increased numbers were not only observed for $CD4^{+}$ and $CD8^{+}$, but also Tregs (**Supplementary Figures 4D,E**), confirming previously published data (29).

Surprisingly, obvious differences were detected within the myeloid compartment of both transgenic GM-CSF and IL-3 HIS-models. While $CD66b^{-}CD68^{+}$ myeloid cells were the most abundant subset in BM and spleens of HIS-NOG and HIS-NOG-EXL, $CD66b^{+}CD68^{-}$ granulocytes were enriched in HIS-NSG-SGM3 (**Figures 4E,F**), which might be attributed to their elevated G-CSF levels (35). Of note, $CD66b^{+}CD68^{+}$ cells represent a substantial fraction of myeloid cells in BM that is reduced in transgenic HIS mice. We interpret these unusual $CD68^{+}/CD66b^{+}$ cells as common myeloid progenitors that retain expression of both markers.

Next, we detected all major subsets of human DCs ($CLEC9A^{+}$ cDC1s, $CD1c^{+}$ cDC2s, and $CD303^{+}$ pDCs) in BM and spleens of all HIS-mice independent of the transgene (**Figures 4G–J**, **Supplementary Figure 4F**). In general, higher DC frequencies

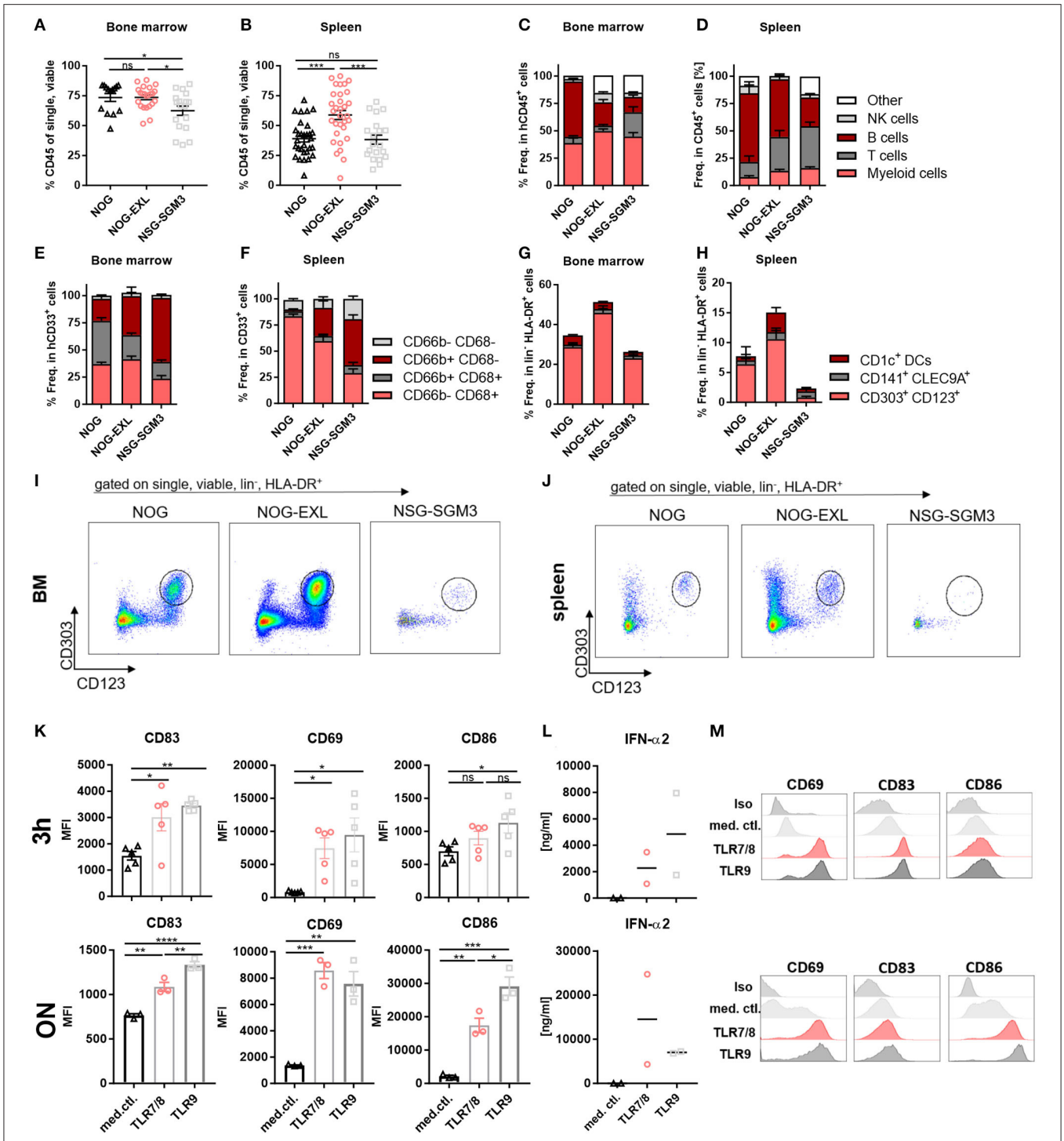

FIGURE 4 | HIS-NOG-EXL mice develop functional human pDCs. **(A)** Human CD45$^+$ in BM, ordinary one-way ANOVA, Tukey's multiple comparison test, $^*p < 0.05$, $n = 14$–23. **(B)** Human CD45$^+$ comparison in spleens, one-way ANOVA, Tukey's multiple comparison test, $^*p < 0.05$, $n = 20$–32. **(C)** Immune cell composition in CD45$^+$ from BM; **(D)** or splenocytes. **(E)** Myeloid cells in CD33$^+$ from BM; **(F)** from splenocytes. **(G)** DC subpopulations in HLA-DR$^+$ from BM, **(H)** from splenocytes. **(I)** Representative FACS plots of human pDCs (CD303$^+$/CD123$^+$) gated on single, viable, lineage negative, HLA-DR$^+$ in HIS-NOG or HIS-NOG-EXL BM and **(J)** spleen. **(K)** Activation marker MFIs (CD83, CD69, CD86), gated on pDCs (CD123$^+$/CD303$^+$) enriched from ten pooled HIS-NOG-EXL BM with TLR7/8 or TLR9, duplicates were performed, one-way ANOVA, Tukey's multiple comparison test. $^*p < 0.05$; $^{**}p < 0.001$; $^{***}p < 0.0005$; $^{****}p < 0.0001$, $n = 3$/condition. **(L)** IFN-α2 levels in supernatant of TLR-agonist treated or non-treated pDCs enriched from pooled HIS-NOG-EXL BM, measured after 3 h or overnight (ON) stimulation in duplicates. **(M)** Representative activation marker histograms with (TLR7/8 or TLR9) or without stimulation (media control = med. ctl.) ON, gated on lin$^-$, HLA-DR$^+$, pDC$^+$.

were found in BM compared to spleens with pDCs being the most abundant subset in both organs. Among the three strains, HIS-NOG-EXL exhibited the highest overall DC level. Notably, only in HIS-NSG-SGM3 DC frequencies correlated between BM and periphery.

Further, we tested the functionality of DC subsets in HIS-NOG and HIS-NOG-EXL mice, as they phenotypically resembled human blood-derived cells. Here we focused on the functional characterization of pDCs in HIS-NOG-EXL mice, due to lower immune cell counts in BM of HIS-NOG and the very low frequency of conventional DCs in general. Induced cytokine release upon TLR activation has been conducted before as reliable readout for pDC function (13, 15). Hence, we cultivated isolated pDCs from pooled BM for 3 h or overnight in presence or absence of TLR agonists. TLR7/8 and TLR9 stimulation of pDCs resulted in increased expression of early activation marker CD69, activation marker CD83 and co-stimulatory molecule CD86. Further, pDCs secreted IFN-α2 upon TLR activation (**Figures 4K–M**). IFN-α2 levels were maintained and resulted in increased concentrations upon overnight incubation (**Figure 4L**). Thus, human pDCs isolated from a humanized mouse model are not only reconstituted in sufficient numbers, but are also functional.

The Tumor Model Dictates Intratumoral Human Immune Cell Composition

Encouraged by the reasonable numbers of tissue resident pDCs in both NOG strains, we asked whether pDCs could be found in tumors implanted into humanized mice. Hence, two ovarian cancer cell lines and one patient derived breast cancer model were analyzed in parallel in HIS-NOG and HIS-NOG-EXL mice. All tumor models engrafted efficiently into both HIS-NOG strains. SK-OV-3 tumor growth did not differ between the two strains, whereas OVCAR-5 showed a considerably reduced tumor growth in HIS-NOG-EXL (**Figure 5A**, **Supplementary Figure 5A**). BC_038 breast tumor growth onset was delayed and at later stages tumor growth accelerated in HIS-NOG-EXL as compared to HIS-NOG (**Figure 5A**).

To elucidate whether tumors can influence the engrafted human immune system, we analyzed blood samples during tumor growth. Human $CD45^+$ immune cell and $CD33^+$ myeloid cell frequencies were maintained in peripheral blood independent of tumor growth, with higher myeloid counts in HIS-NOG-EXL as previously described for non-tumor-bearing mice (**Figure 5B**, **Supplementary Figure 5B**). Flow cytometric analysis of the tumor immune infiltrate revealed that SK-OV-3 showed the highest frequency of $CD45^+$ cells in both mouse strains followed by BC_038 and OVCAR-5. Of note, OVCAR-5 tumors retained their sparse human immune cell infiltrate despite the better humanization of HIS-NOG-EXL mice. In contrast, SK-OV-3 and BC_038 tumors had higher immune infiltration in HIS-NOG-EXL mice (**Figure 5C**). However, the immune cell composition was clearly influenced by the tumor rather than the HIS mouse strain (**Figure 5D**). While SK-OV-3 tumors had remarkably high NK cell frequencies, BC_038 and OVCAR-5 showed strong T cell infiltration (**Figure 5D**).

Analogous, also the myeloid subset distribution was rather shaped by the tumor than the HIS-strain. The three tumor models showed infiltration of human $CD68^+CD66b^-$ TAMs and $CD68^-CD66b^+$ granulocytes, but to different degrees. Whereas, in SK-OV-3 human TAMs were enriched, an equal distribution of granulocytes and TAMs was detected in OVCAR-5 and BC_038 with a higher number of $CD66b^-$ $CD68^-$ immune cells that might account for immature MDSCs. However, OVCAR-5 and BC_038 tumor-bearing HIS-NOG-EXL mice showed higher TAM infiltration compared to HIS-NOG (**Figure 5E**). A closer analysis of HLA-DR^+ myeloid cells revealed presence of human DC subsets in all tumor models albeit at different frequencies (**Figure 5E**). Human pDCs were primarily detected in OVCAR-5 and BC_038 tumors (**Figure 5E**, **Supplementary Figure 5C**).

pDC Infiltration of Tumors Is Associated With the Presence of pDC-Recruiting Chemokines

We were able to detect pDCs in OVCAR-5 and BC_038, but not in SK-OV-3 tumors. Therefore, we investigated the expression of factors that are associated with pDC function and recruitment. hFLT3-L, hGM-CSF and hIL-3 are well known to correlate with pDC survival and differentiation (39–41). In addition, various migratory cues have been identified to direct pDCs from BM into the blood or diseased tissues including tumor-derived CXCL12 (SDF-1), CXCR3 ligands CXCL9/10 and CCR7 ligands CCL19 and CCL21 (6, 9, 42–47).

Hence, we investigated expression levels of these cytokines and chemokines in tumor lysates of humanized mice bearing SK-OV-3, OVCAR-5 and BC_038 tumors. hGM-CSF and hIL-3 transgene expression in NOG-EXL mice had no effect on the inoculated tumors as their levels were comparable between the two mouse strains (**Figure 6**). However, we detected striking differences among individual tumor models: SK-OV-3 tumors for example expressed significantly higher levels of hGM-CSF (**Figure 6**). In contrast, the breast cancer PDX BC_038 showed uniquely high human FLT3-L expression. hIL-3 only showed residual levels barely above the detection limit in all tumors and are therefore not shown. OVCAR-5 and BC_038 had in general a more pronounced and diverse pDC recruiting chemokine profile compared to SK-OV-3 tumors comprising the CXCR3 ligands CXCL9 and CXCL10 as well as CCL19 and CXCL12 (**Figure 6**). Highest CCL21 expression levels were found in BC_038 (**Figure 6**). These findings suggest that each tumor generates its specific pDC-recruiting and sustaining network of chemokines and cytokines.

Intratumoral Stimulation With TLR7/8 Agonist Results in pDCs Activation and IFN-α2 Release

To further characterize the pDC population in OVCAR-5 and BC_038 we carried out functional analysis of pDCs in these two tumor models transplanted into both NOG strains by

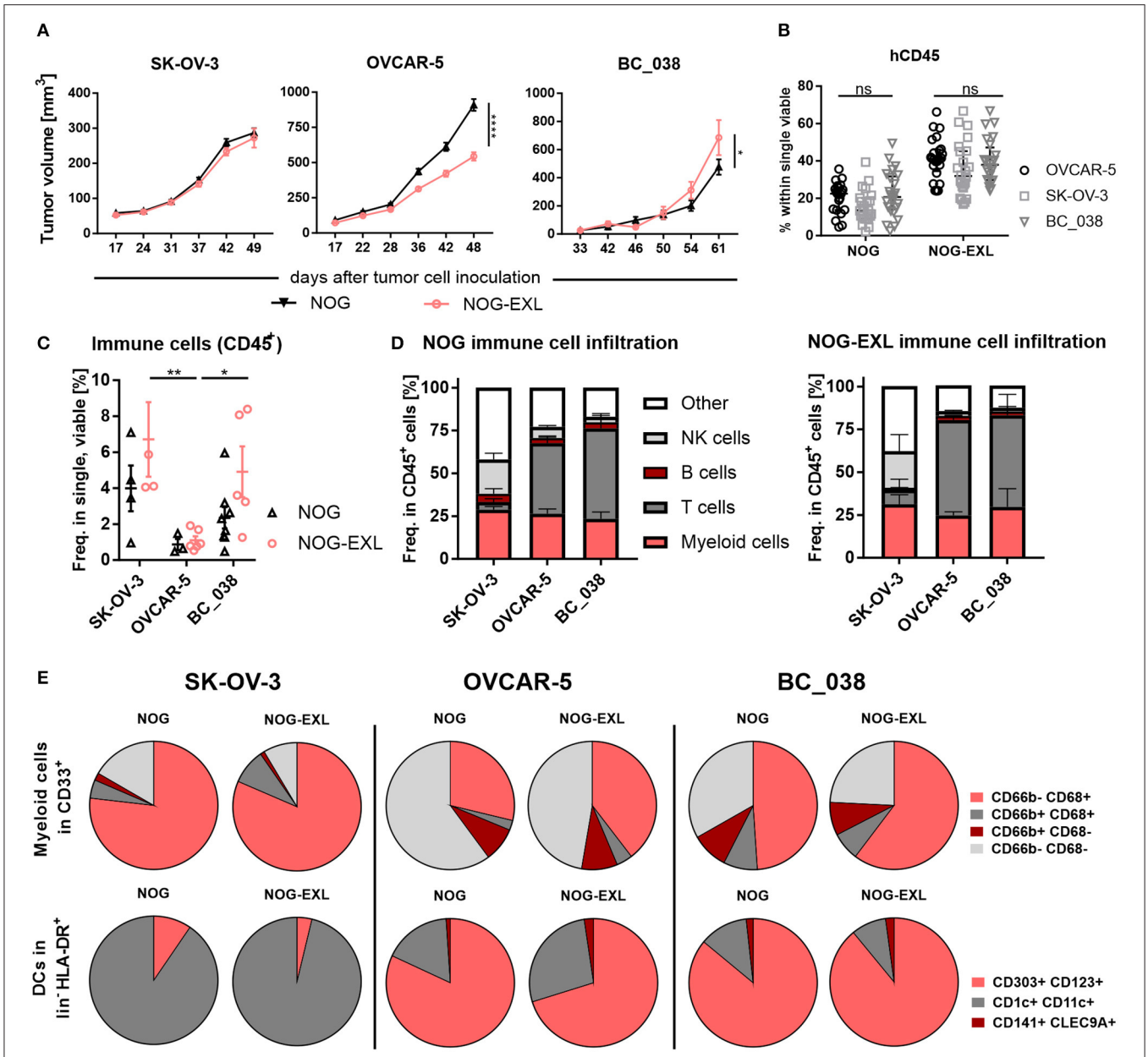

FIGURE 5 | The tumor model dictates intratumoral human immune cell composition. **(A)** Tumor volume [mm^3±SEM] in humanized mice injected with different tumor models. 2-way ANOVA, $^*p < 0.05$; $^{**}p < 0.001$; $^{****}p < 0.0001$, error bars indicate median ± 95% CI, $n = 27$–67. **(B)** Comparison of human $CD45^+$ in PB of mice inoculated with either SK-OV-3, OVCAR-5 or patient-derived xenograft BC_038, week 20. 2-way ANOVA, error bars indicate median ± IQR. $n = 22$–26, ns, not significant. **(C)** Total immune cell infiltrate in different tumor models from HIS-NOG-EXL and HIS-NOG, 2-way ANOVA, HIS-NOG + SK-OV-3 $n = 4$, HIS-NOG-EXL + SK-OV-3 $n = 4$, HIS-NOG + OVCAR-5 $n = 3$, HIS-NOG-EXL + OVCAR-5 $n = 6$, HIS-NOG + BC_038 $n = 8$, HIS-NOG-EXL + BC_038 $n = 5$. **(D)** Human leukocytes composition ($CD45^+$) in different tumor models in HIS-NOG and HIS-NOG-EXL mice, HIS-NOG + SK-OV-3 $n = 4$, HIS-NOG + OVCAR-5 $n = 7$, HIS-NOG + BC_038 $n = 4$, HIS-NOG-EXL + SK-OV-3 $n = 4$, HIS-NOG-EXL + OVCAR-5 $n = 12$, HIS-NOG-EXL + BC_038 $n = 5$. **(E)** Pie charts of immune subsets in SK-OV-3, OVCAR-5 or BC_038 tumors, Myeloid cells (CD68/CD66b) in CD33+: HIS-NOG + SK-OV-3 $n = 4$, HIS-NOG-EXL + SK-OV-3 $n = 4$, HIS-NOG + OVCAR-5 $n = 6$, HIS-NOG-EXL + OVCAR-5 $n = 12$, HIS-NOG + BC_038 $n = 3$, HIS-NOG-EXL + BC_038 $n = 4$ and DCs (CD303+/CD123+, CD1c+/CD11c+, CD141+/CLEC9A+) in HLA-DR+: HIS-NOG + SK-OV-3 $n = 4$, HIS-NOG-EXL + SK-OV-3 $n = 4$, HIS-NOG + OVCAR-5 $n = 7$, HIS-NOG-EXL + OVCAR-5 $n = 4$, HIS-NOG + BC_038 $n = 4$, HIS-NOG-EXL + BC_038 $n = 5$.

injecting the TLR7/8 agonist R848. Notably, tumor-derived pDCs responded to TLR stimulation with upregulation of CD69, CD86, and CD83 after 4 h. Consistently, we also detected increased IFN-α2 secretion in whole tumor lysates (**Figure 7**). Previous reports demonstrated that TLR7/8 agonist treatment results in secretion of proinflammatory cytokines (13–15, 48–50).

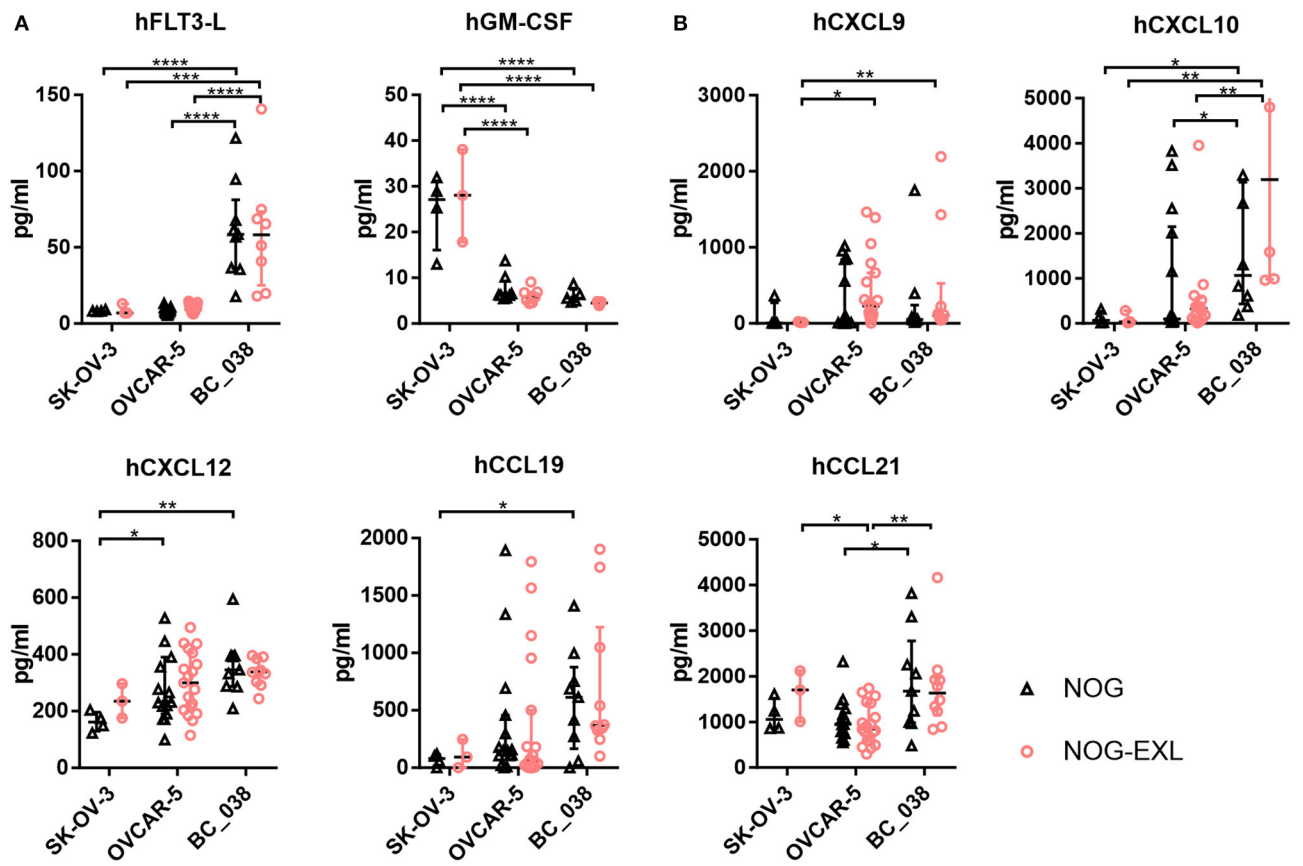

FIGURE 6 | Intratumoral analysis of pDC trafficking and survival associated chemokines and cytokines of different tumors in NOG and NOG-EXL mice. **(A)** Cytokines hFLT-3L, hGM-CSF, and hIL-3 analyzed by Bio-Plex from tumor lysates of humanized mice inoculated with SK-OV-3, OVCAR-5 or BC_038, Kruskal-Wallis ANOVA, error bars indicate median ± IQR, ***$p < 0.0005$, ****$p < 0.0001$, error bars indicate median ± IQR, $n = 3$–19. **(B)** Chemokines associated with pDC migration hCXCL9, hCXCL10. hCXCL12, hCCL19, and hCCL21 analyzed by Bio-Plex from tumor lysates of humanized mice inoculated with SK-OV-3, OVCAR-5 or BC_038, Kruskal-Wallis ANOVA, error bars indicate median ± IQR, *$p < 0.05$; **$p < 0.01$, ***$p < 0.0005$, ****$p < 0.0001$, $n = 3$–19.

Therefore, we profiled other human cytokines in the TME and found elevated levels of IL-6, IL-8, MIP-1β, and TNF-α upon short-term TLR7/8 stimulation (**Figure 7**). To confirm that cytokine secretion was immune cell dependent, we stimulated OVCAR-5 tumor cells *in vitro* with TLR7/8 and were not able to detect tumor cell line-derived IFN-α2 (data not shown). We were not able to perform a similar experiment using BC_038, which is a primary patient-derived xenograft without an existing cell line.

TLR agonist administration can stimulate dramatic cytokine release in the periphery. Excessive cytokine levels however are also associated with common side effects of immunotherapies. We found that i.t. TLR activation resulted in systemic serum cytokine increase as early as 4 h (**Supplementary Figure 6A**). For comparison, we injected non-tumor-bearing, humanized mice i.p. with R848 and found relatively higher IFN-α2 levels in serum of both NOG strains compared to i.t injected tumor-bearing mice. This indicates that TLR agonists and the subsequently induced cytokine response are primarily retained within the tumor tissue (**Supplementary Figure 6B**).

DISCUSSION

Therapeutic targeting of innate immunity holds great promise for the treatment of immune checkpoint blockade resistant cancer patients, because these patients are likely to have malfunctions in the early, innate immunity-regulated steps of mounting an anti-tumoral immune response or harbor an immune suppressive TME. Targeting of pDCs in the TME could potentially reprogram intratumoral immune cells by triggering the release of a broad type I interferon spectrum shown to reduce tumor growth and activate other immune cells such as NK cells (5, 11, 51). TLR7 and TLR9 agonists are able to activate pDCs and are currently at various stages in clinical development as drug or adjuvants (52, 53). Identification of synergistic combination partners, novel biomarkers or alternative pDC-targeting strategies requires preclinical models that provide sufficient and functional human pDCs in a human TME. In our study, we aimed to find a suitable preclinical, tumor-bearing HIS model taking into account the local tumor milieu and the general quality of human hematopoiesis. Furthermore, we assessed whether improved systemic reconstitution of the

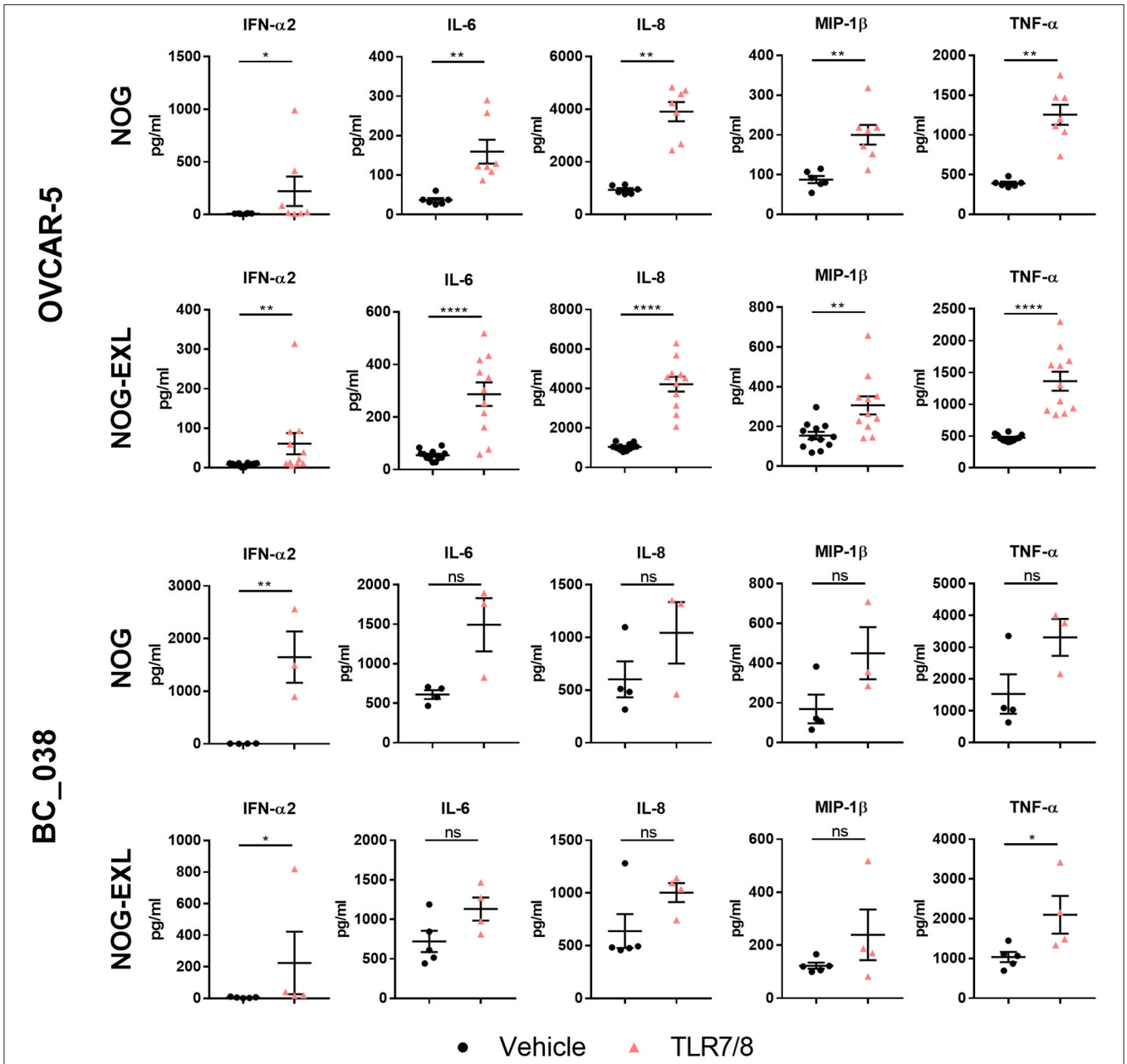

FIGURE 7 | TLR7/8 treatment increases intratumoral cytokine release. Human cytokines analyzed by Multiplex from tumor lysates of humanized mice treated i.t. with TLR7/8 or Vehicle for 4 h in OVCAR-5 and BC_038 tumors; Mann Whitney test; error bars indicate median ± IQR, $^{*}p < 0.05$; $^{**}p < 0.001$; $^{****}p < 0.0001$; $n = 4$–12.

human immune system would facilitate a more pronounced tumor-associated pDCs infiltrate to allow *in vivo* functional characterization of this notoriously difficult to study, rare pDCs population.

Despite their limitations, humanized mice are a highly useful and important model system for cancer immunotherapy studies as they provide an *in vivo* testing opportunity for human therapeutic targets that lack a functional mouse homolog. HIS mice come in many different flavors and diverse immune cell reconstitution levels (21). Classical humanized mice, such as BRG, NOG and NSG mainly develop B and T cells and provide a robust model to study tumor interaction with those lymphoid populations e.g., for checkpoint inhibitor or T cell recruitment studies (21, 26, 28, 54–56). However, they lack proper antigen-specific immune responses and suffer from compromised innate immune cell development due to limited cross-reactivity between human and murine cytokines (21, 26, 34). To overcome the latter obstacle, human cytokines e.g., M-CSF, GM-CSF, IL-3, and SCF were introduced using different methods such as hydrodynamic plasmid injection, daily

injections of recombinant FLT3-L, genetic transgene or knock-in replacement (28–30, 51, 57, 58). However, also tumor cells can serve as a rich source of human cytokines. That prompted us to ask whether tumor implantation could further boost human myeloid cell reconstitution in tumors transplanted into next generation humanized mouse strains. Therefore, we first performed a comprehensive characterization of two novel, non-tumor-bearing, myeloid enhanced HIS models (HIS-NOG-EXL and HIS-NSG-SGM3), followed by comparison with tumor-bearing HIS-NOG and HIS-NOG-EXL mice to delineate the contributions of tumor and transgene-derived cytokines to human immune cell reconstitution.

We confirmed higher overall engraftment and increased frequency of myeloid cells in peripheral blood of both transgenic mouse strains as compared to non-transgenic HIS-NOG mice (29, 30). Additionally, HIS-NOG-EXL mice showed increased NK cell reconstitution, while NSG-SGM-3 mice are characterized by rather high Treg frequencies and development of granulocytes. Although NOG-EXL and NSG-SGM3 strains harbor the hGM-CSF transgene, we detected 400-fold higher GM-CSF serum levels in NSG-SGM-3 mice that potentially, together with additionally increased G-CSF, favor granulocyte formation over macrophages and DCs. These unusually high GM-CSF levels in HIS-NSG-SGM3 mice may inhibit pDC survival or egress from bone marrow and explain the absence of peripheral pDCs in this strain despite the reported presence of pDC in bone marrow (29, 39, 59). Notably, the pDC inhibitory effect of GM-CSF seems to be dose-dependent in pDCs cultured *in vitro* (60, 61). On the other hand, it was shown that GM-CSF and IL-3 are essential for human pDC viability and differentiation (60). As those two cytokines are systemically expressed in both transgenic mouse strains, albeit to different levels, we hypothesize that GM-CSF levels in HIS-NSG-SGM3 exceed a certain threshold and become inhibitory for pDCs, whereas lower GM-CSF levels in HIS-NOG-EXL promote pDC viability and differentiation. NSG-SGM3 mice also had higher peripheral T cell frequencies and IFN-γ level compared to NOG-EXL. Furthermore, additional inflammatory signals such as IL-6, IL-8, IL-16, MCP-1, TNF-α, CX3CL1, were increased in HIS-NSG-SGM3 mice confirming previous reports (36, 37). Furthermore, the Treg recruiting chemokine CCL22 was significantly elevated. Thus, it is tempting to speculate that the high numbers of immunosuppressive Tregs associated with higher IL-10 levels suppress the activated T cell phenotype. Collectively, the observed hepatosplenomegaly and reduced overall survival suggest that human myeloid cells induce a continuous, smoldering inflammation in HIS-NSG-SGM3 (35–37). This assumption is supported by the notion that depletion of myeloid cells using an anti-CD33 antibody ameliorated these symptoms (36). Another major difference lies in the additional transgene encoding stem cell factor (SCF) in SGM-3 mice that may explain some of the observed differences between NOG-EXL and SGM-3 mice.

Furthermore, the different mouse background may also tune differential immune composition of HIS-NSG-SGM3 compared to HIS-NOG-EXL mice. Consistently, DCs were previously reported in higher numbers in BM of HIS-NOG mice compared to NSG mice (62, 63). HIS-NOG-EXL myeloid cell frequencies are substantially below human levels, although these mice show enhanced myelopoiesis and reconstitute even major subsets of DCs at high frequencies in spleens indicating terminal differentiation and successful egress of these cells from BM (64). Accordingly, also $CD14^+$ monocyte count in HIS-NOG-EXL is lower compared to the human situation, while the $CD14^+CD16^+$ non-classical monocyte population is almost absent. Notably, we were able to detect TAMs in SK-OV-3 tumors that express M-CSF, the cytokine responsible for macrophage differentiation and survival (28, 65). In contrast, HIS-NOG-EXL mice had low levels of macrophages in spleens and in general a more immature monocyte phenotype in peripheral blood that may be attributed to the lack of M-CSF (28). Importantly, pDC frequencies in blood and lymphoid organs of HIS-NOG-EXL mice are substantially higher compared to humans (66). This fact enables functional studies of the rare pDC population without further manipulation such as *ex vivo* expansion. The transgene-derived hIL-3 levels that are about 10-fold higher than the transgene-derived hGM-CSF levels (**Supplementary Figure 7A**), might result in augmented pDC viability in response to activated IL-3R (CD123) signaling.

Based on the important role of pDCs in ovarian and breast cancer, we selected two ovarian cancer cell lines with high and low cytokine producing profile and one breast cancer PDX for detailed human immune analysis in the myeloid enhanced HIS-NOG-EXL as compared to HIS-NOG mice. We compared tumor growth kinetics and found that SK-OV-3 tumor growth is similar in HIS-NOG and HIS-NOG-EXL, whereas OVCAR-5 and BC_038 tumors grew faster or slower in HIS-NOG mice, respectively. GM-CSF and IL-3 are both known to stimulate tumor cell proliferation (67, 68), so their direct effects on tumor growth cannot be excluded. Despite the remarkably altered WBC composition between the different strains, the tumor immune infiltrates were largely comparable between the three different tumor models, albeit striking differences were observed in frequency of individual immune subsets. In contrast to BC_038 and OVCAR-5 tumors, the SK-OV-3 tumor failed to recruit and sustain pDCs.

The molecular mechanism underlying the trafficking of pDCs to the tumor remain largely elusive. Unlike other immune subsets, pDCs can express non-functional chemokine receptors. Under homeostatic conditions pDCs are confined to lymphoid tissues in response to CXCL12 (SDF1)-mediated recruitment via CXCR4 expressed on pDCs (43). However, circulating pDCs express additional chemokine receptors that fail to migrate toward inflammatory stimuli. In pathological tissues pDCs are detectable. Several factors have been described, which may contribute to pDC recruitment into tumors: (i) tumor cells are capable to hijack the CXCL12/CXCR4 axis by producing SDF-1 (9, 46, 69); (ii) pDC maturation in the tumor increases CCR7 or CXCR3 levels and allows these receptors to engage with the migration machinery upon binding to CCL19/CCL21 and CXCL9/CXCL10, respectively (42–44); (iii) Maturation is induced e.g., by extracellular self-DNA bound to HMGB1 protein that prevents its degradation and is recognized by pDCs

as TLR ligand (47). High expression levels of CXCL12 were first described in ovarian tumors, later also in various solid tumor entities including breast cancer. CXCL12 was reported to attract pDCs into the tumor environment and to protect them against tumor-induced apoptosis (46, 47, 69, 70). Indeed, BC_038 and OVCAR-5 tumors had higher expression levels of the migratory chemokines CXCL10, CXCL12, and CCL19 (**Figure 6**) compared to SK-OV-3 and also shared a rather similar cytokine/chemokine profile (**Supplementary Figure 7B**) and immune cell composition, despite their different origin as PDX and established cancer cell line from a different tumor entity. Moreover, SK-OV-3 tumors expressed strikingly higher GM-CSF levels that may be above the threshold of acquiring pDC-inhibitory function. On the other hand elevated GM-CSF level could benefit SK-OV-3 tumors in shaping their rich TAM-infiltrate along with M-CSF.

Further characterization of tumor-associated pDCs showed upregulation of activation markers and increased IFN-α2 levels upon TLR-agonist treatment. Considering the intratumoral TLR agonist application and the early readout 4 h after agonist injection associated with increased activation marker expression by the pDCs, it is very likely that the observed IFN-α2 increase in tumor lysates originates from pDCs. This is further supported by another study using TLR7/8 agonist stimulated human PBMCs where pDCs were the only producers of IFN-α2 after 4 h of stimulation. Neither T nor B cells responded to TLR treatment while monocytes were strongly activated through the TLR8 agonist and produced TNF-a, IL-6 and IL-1β but not IFN-α2. Furthermore, activated pDCs produced TNF-α and IL-1β (71), confirming findings described in earlier studies (48, 49), which independently showed that pDCs produce not only IFN-α but also TNF-α, IL-6, IL-8, and MIP-1β upon TLR stimulation. The tumor lysate analysis is limited by the lack of analyzing the isolated, pure pDC subset. Purification of sufficient pDC cell numbers from tumors was technically not feasible due to the substantial loss of pDCs during the tumor digestion and immune cell enrichment processes. Therefore, we performed an *in vitro* assay with TLR7/8 agonist treated tumor cell lines as additional control demonstrating no IFN-α2 release. Regarding the other TLR7/8 agonist-induced cytokines we cannot exclude potential contributions from other immune cells such as monocytes. To unequivocally demonstrate that pDC are the predominant IFN-α source, pDC depleting/blocking studies e.g., with the anti-BDCA-2 monoclonal antibody 15B (72–74) or with the BDCA-2-DTR transgenic mice (75) would be necessary.

Thus, our data clearly indicate that local cytokine production by tumor xenografts have a more significant impact on tumor immune infiltrate than the selected humanized mouse strain. Consequently, different tumor-associated immune subsets can potentially be generated in conventional HIS models by selecting the appropriate tumor model. Instead of investing in expensive mice or developing time-consuming new mouse models, screening of the right tumor cell line or PDX model may present a faster and more efficient way to identify tumor models enriched with human pDCs. *In silico* criteria for tumor selection may include the presence of GM-CSF, IL-3 and FLT3-L, ligand expression of chemokine receptors CXCR4, CCR7, and CXCR3 and the absence of very high GM-CSF level. For melanoma models presence of $BRAF^{V600E}$ and absence of NRAS mutations may serve as additional predictors for higher tumor-resident pDC probability (76).

In the current report, we describe an acute setting, where we measured the effects of TLR7/8 agonists 4 h after injection. The next step to be addressed in future studies is to evaluate long-term effects of pDC infiltration as well as IFN-α production on tumor growth and other tumor-resident immune cells. Particularly, we expect that the investigation of the cross talk between activated pDCs and T cells is experimentally challenging in HIS mice considering the uncertainties around mouse MHC restriction and how reconstitution of additional human APC would interfere with T cell priming (77).

As an additional and unexpected finding, to our knowledge we here show for the first time that myeloid enhanced mice have significantly elevated serum IgG levels indicating improved B cell maturation and function. This was surprising because B cells of classical humanized mice have impaired class switch resulting in minimal antigen-specific IgG production (27, 34). Our findings are accompanied by improved LN development especially in HIS-NOG-EXL. Unlike mouse models that were specifically designed for improved LN development, the LNs in our animals had mostly T cells instead of B cells. However, further experiments, e.g., immunization assays, are needed for a more elaborate functional B cell characterization. In summary, HIS-NOG-EXL mice outperform HIS-NOG and HIS-NSG-SGM3 mice in terms of humanization quality.

Our study provides a comprehensive head-to-head comparison of two myeloid enhanced HIS strains using identical humanization protocols including stem cell donors. Those next-generation HIS strains proved to be superior in terms of a more diverse human immune system reconstitution. In particular, the HIS-NOG-EXL mice represent a robust mouse model to study human innate immune cells in homeostasis and in tumor context. In our view, HIS-NOG-EXL provide the clinically most relevant HIS model to study e.g., immunomodulatory drugs due to the enhanced myeloid and NK cell reconstitution, elevated IgG levels and the ability to reconstitute major immune subsets in different tumor models. Additionally, the relatively high proportion of human pDCs in this mouse model allows studying this rare cell population in more detail without any further manipulation in the context of high quality humanization. Although advanced transgenic HIS models clearly showed improved innate immune subset reconstitution in the periphery, this advantage was lost in TME. Our experimental setup delivers a fertile ground to expand the knowledge on how tumors regulate molecular circuits *in vivo* to shape and exploit human immune cells; a knowledge that potentially unravels novel targets for cancer immunotherapy.

DATA AVAILABILITY STATEMENT

All datasets generated for this study are included in the article/**Supplementary Material**.

ETHICS STATEMENT

The animal study was reviewed and approved by Regierung von Oberbayern, Az. ROB-55.2-2532.Vet_02-17-19.

AUTHOR CONTRIBUTIONS

I-PM, GH, SH, JE, and CR designed experiments. I-PM and CB performed experiments. I-PM, GH, SH, FN, JE, and CR analyzed and interpreted data. CR, SH, and JE wrote the paper together with I-PM and input from all authors. All authors contributed to the article and approved the submitted version.

FUNDING

This work was funded by Roche Diagnostics GmbH. The funder was not involved in the study design, collection, analysis, and interpretation of data, the writing of this article or the decision to submit it for publication.

ACKNOWLEDGMENTS

We are deeply thankful for the excellent technical support of: Petra Ulrich, Petra Falkner, and Stefanie Lechner for *in vivo* assistance; Stefan Gottwald, Monika Friedrich, Theresia Manger-Harasim, and Melanie Winter for *ex vivo* analyses; Frank Herting for animal model support and veterinary affairs, Stefanie Lechner and Jakob Rosenhauer for protein analysis, Jakob Rosenhauer for proliferation and phagocytosis assays, Afsaneh Abdolzade-Bavil for IgG measurement, Said Aktas for his support with Spotfire, Dr. Julia Schueler (Julia.Schueler@crl.com, Charles River) for the supply of the breast cancer PDX model, Dr. Lena Vockentanz for the establishment and expansion of the PDX model and Dr. William Vermi for fruitful discussions.

SUPPLEMENTARY MATERIAL

The Supplementary Material for this article can be found online at: https://www.frontiersin.org/articles/10.3389/fimmu.2020.02082/full#supplementary-material

REFERENCES

1. Awad RM, De Vlaeminck Y, Maebe J, Goyvaerts C, Breckpot K. Turn back the TIMe: targeting tumor infiltrating myeloid cells to revert cancer progression. *Front Immunol*. (2018) 9:1977. doi: 10.3389/fimmu.2018.01977
2. Dhodapkar MV, Dhodapkar KM, Palucka AK. Interactions of tumor cells with dendritic cells: balancing immunity and tolerance. *Cell Death Differ*. (2008) 15:39–50. doi: 10.1038/sj.cdd.4402247
3. Collin M, Mcgovern N, Haniffa M. Human dendritic cell subsets. *Immunology*. (2013) 140:22–30. doi: 10.1111/imm.12117
4. Minoda Y, Virshup I, Leal Rojas I, Haigh O, Wong Y, Miles JJ, et al. Human CD141(+) dendritic cell and CD1c(+) dendritic cell undergo concordant early genetic programming after activation in humanized mice *in vivo*. *Front Immunol*. (2017) 8:1419. doi: 10.3389/fimmu.2017.01419
5. Koucky V, Boucek J, Fialova A. Immunology of plasmacytoid dendritic cells in solid tumors: a brief review. *Cancers*. (2019) 11:470. doi: 10.3390/cancers11040470
6. Swiecki M, Colonna M. The multifaceted biology of plasmacytoid dendritic cells. *Nat Rev Immunol*. (2015) 15:471–85. doi: 10.1038/nri3865
7. Hirsch I, Caux C, Hasan U, Bendriss-Vermare N, Olive D. Impaired Toll-like receptor 7 and 9 signaling; from chronic viral infections to cancer. *Trends Immunol*. (2010) 31:391–7. doi: 10.1016/j.it.2010.07.004
8. Barrat FJ, Su L. A pathogenic role of plasmacytoid dendritic cells in autoimmunity and chronic viral infection. *J Exp Med*. (2019) 216:1974–85. doi: 10.1084/jem.20181359
9. Vermi W, Bonecchi R, Facchetti F, Bianchi D, Sozzani S, Festa S, et al. Recruitment of immature plasmacytoid dendritic cells (plasmacytoid monocytes) and myeloid dendritic cells in primary cutaneous melanomas. *J Pathol*. (2003) 200:255–68. doi: 10.1002/path.1344
10. Labidi-Galy SI, Sisirak V, Meeus P, Gobert M, Treilleux I, Bajard A, et al. Quantitative and functional alterations of plasmacytoid dendritic cells contribute to immune tolerance in ovarian cancer. *Cancer Res*. (2011) 71:5423–34. doi: 10.1158/0008-5472.CAN-11-0367
11. Vermi W, Soncini M, Melocchi L, Sozzani S, Facchetti F. Plasmacytoid dendritic cells and cancer. *J Leukoc Biol*. (2011) 90:681–90. doi: 10.1189/jlb.0411190
12. Sisirak V, Faget J, Gobert M, Goutagny N, Vey N, Treilleux I, et al. Impaired IFN-alpha production by plasmacytoid dendritic cells favors regulatory T-cell expansion that may contribute to breast cancer progression. *Cancer Res*. (2012) 72:5188–97. doi: 10.1158/0008-5472.CAN-11-3468
13. Aspord C, Leccia MT, Charles J, Plumas J. Plasmacytoid dendritic cells support melanoma progression by promoting Th2 and regulatory immunity through OX40L and ICOSL. *Cancer Immunol Res*. (2013) 1:402–15. doi: 10.1158/2326-6066.CIR-13-0114-T
14. Wu J, Li S, Yang Y, Zhu S, Zhang M, Qiao Y. TLR-activated plasmacytoid dendritic cells inhibit breast cancer cell growth *in vitro* and *in vivo*. *Oncotarget*. (2017) 8:11708–18. doi: 10.18632/oncotarget.14315
15. Aspord C, Tramcourt L, Leloup C, Molens JP, Leccia MT, Charles J, et al. Imiquimod inhibits melanoma development by promoting pDC cytotoxic functions and impeding tumor vascularization. *J Investig Dermatol*. (2014) 134:2551–61. doi: 10.1038/jid.2014.194
16. Traggiai E, Chicha L, Mazzucchelli L, Bronz L, Piffaretti JC, Lanzavecchia A, et al. Development of a human adaptive immune system in cord blood cell-transplanted mice. *Science*. (2004) 304:104–7. doi: 10.1126/science.1093933
17. Zhang L, Jiang Q, Li G, Jeffrey J, Kovalev GI, Su L. Efficient infection, activation, and impairment of pDCs in the BM and peripheral lymphoid organs during early HIV-1 infection in humanized rag2(-)/(-)gamma C(-)/(-) mice *in vivo*. *Blood*. (2011) 117:6184–92. doi: 10.1182/blood-2011-01-331173
18. Tanaka S, Saito Y, Kunisawa J, Kurashima Y, Wake T, Suzuki N, et al. Development of mature and functional human myeloid subsets in hematopoietic stem cell-engrafted NOD/SCID/IL2rgammaKO mice. *J Immunol*. (2012) 188:6145–55. doi: 10.4049/jimmunol.1103660
19. Shultz LD, Brehm MA, Garcia-Martinez JV, Greiner DL. Humanized mice for immune system investigation: progress, promise and challenges. *Nat Rev Immunol*. (2012) 12:786–98. doi: 10.1038/nri3311
20. Drake AC, Chen Q, Chen J. Engineering humanized mice for improved hematopoietic reconstitution. *Cell Mol Immunol*. (2012) 9:215–24. doi: 10.1038/cmi.2012.6
21. Theocharides AP, Rongvaux A, Fritsch K, Flavell RA, Manz MG. Humanized hemato-lymphoid system mice. *Haematologica*. (2016) 101:5–19. doi: 10.3324/haematol.2014.115212
22. Hofer U, Schlaepfer E, Baenziger S, Nischang M, Regenass S, Schwendener R, et al. Inadequate clearance of translocated bacterial products in HIV-infected humanized mice. *PLoS Pathog*. (2010) 6:e1000867. doi: 10.1371/journal.ppat.1000867
23. Seiler M. The role of immunodeficient animal models in advancing immuno-oncology research. *Drug Discov World Spring*. (2016) 1–6.

24. De La Rochere P, Guil-Luna S, Decaudin D, Azar G, Sidhu SS, Piaggio E. Humanized mice for the study of immuno-oncology. *Trends Immunol*. (2018) 39:748–63. doi: 10.1016/j.it.2018.07.001
25. Adigbli G, Menoret S, Cross AR, Hester J, Issa F, Anegon I. Humanization of immunodeficient animals for the modeling of transplantation graft versus host disease and regenerative medicine. *Transplantation*. (2020). doi: 10.1097/TP.0000000000003177. [Epub ahead of print].
26. Yong KSM, Her Z, Chen Q. Humanized mice as unique tools for human-specific studies. *Arch Immunol Ther Exp*. (2018) 66:245–66. doi: 10.1007/s00005-018-0506-x
27. Yu H, Borsotti C, Schickel JN, Zhu S, Strowig T, Eynon EE, et al. A novel humanized mouse model with significant improvement of class-switched, antigen-specific antibody production. *Blood*. (2017) 129:959–69. doi: 10.1182/blood-2016-04-709584
28. Chen Q, Khoury M, Chen J. Expression of human cytokines dramatically improves reconstitution of specific human-blood lineage cells in humanized mice. *PNAS*. (2009) 106:21783–8. doi: 10.1073/pnas.0912274106
29. Billerbeck E, Barry WT, Mu K, Dorner M, Rice CM, Ploss A. Development of human CD4+FoxP3+ regulatory T cells in human stem cell factor-, granulocyte-macrophage colony-stimulating factor-, and interleukin-3-expressing NOD-SCID IL2Rgamma(null) humanized mice. *Blood*. (2011) 117:3076–86. doi: 10.1182/blood-2010-08-301507
30. Ito R, Takahashi T, Katano I, Kawai K, Kamisako T, Ogura T, et al. Establishment of a human allergy model using human IL-3/GM-CSF-transgenic NOG mice. *J Immunol*. (2013) 191:2890–9. doi: 10.4049/jimmunol.1203543
31. Stubenrauch K, Wessels U, Lenz H. Evaluation of an immunoassay for human-specific quantitation of therapeutic antibodies in serum samples from non-human primates. *J Pharm Biomed Anal*. (2009) 49:1003–8. doi: 10.1016/j.jpba.2009.01.030
32. Legrand N, Huntington ND, Nagasawa M, Bakker AQ, Schotte R, Strick-Marchand H, et al. Functional CD47/signal regulatory protein alpha (SIRP(alpha)) interaction is required for optimal human T- and natural killer-(NK) cell homeostasis *in vivo*. *Proc Natl Acad Sci USA*. (2011) 108:13224–9. doi: 10.1073/pnas.1101398108
33. Jangalwe S, Shultz LD, Mathew A, Brehm MA. Improved B cell development in humanized NOD-scid IL2Rgamma(null) mice transgenically expressing human stem cell factor, granulocyte-macrophage colony-stimulating factor and interleukin-3. *Immun Inflamm Dis*. (2016) 4:427–40. doi: 10.1002/iid3.124
34. Li Y, Masse-Ranson G, Garcia Z, Bruel T, Kok A, Strick-Marchand H, et al. A human immune system mouse model with robust lymph node development. *Nat Methods*. (2018) 15:623–30. doi: 10.1038/s41592-018-0071-6
35. Coughlan AM, Harmon C, Whelan S, O'brien EC, O'reilly VP, Crotty P, et al. Myeloid engraftment in humanized mice: impact of granulocyte-colony stimulating factor treatment and transgenic mouse strain. *Stem Cells Dev*. (2016) 25:530–41. doi: 10.1089/scd.2015.0289
36. Wunderlich M, Stockman C, Devarajan M, Ravishankar N, Sexton C, Kumar AR, et al. A xenograft model of macrophage activation syndrome amenable to anti-CD33 and anti-IL-6R treatment. *JCI Insight*. (2016) 1:e88181. doi: 10.1172/jci.insight.88181
37. Yoshihara S, Li Y, Xia J, Danzl N, Sykes M, Yang YG. Posttransplant hemophagocytic lymphohistiocytosis driven by myeloid cytokines and vicious cycles of T-cell and macrophage activation in humanized mice. *Front Immunol*. (2019) 10:186. doi: 10.3389/fimmu.2019.00186
38. Mortha A, Burrows K. Cytokine networks between innate lymphoid cells and myeloid cells. *Front Immunol*. (2018) 9:191. doi: 10.3389/fimmu.2018.00191
39. Gilliet M, Boonstra A, Paturel C, Antonenko S, Xu XL, Trinchieri G, et al. The development of murine plasmacytoid dendritic cell precursors is differentially regulated by FLT3-ligand and granulocyte/macrophage colony-stimulating factor. *J Exp Med*. (2002) 195:953–8. doi: 10.1084/jem.20020045
40. Demoulin S, Roncarati P, Delvenne P, Hubert P. Production of large numbers of plasmacytoid dendritic cells with functional activities from CD34(+) hematopoietic progenitor cells: use of interleukin-3. *Exp Hematol*. (2012) 40:268–78. doi: 10.1016/j.exphem.2012.01.002
41. Zhang H, Gregorio JD, Iwahori T, Zhang X, Choi O, Tolentino LL, et al. A distinct subset of plasmacytoid dendritic cells induces activation and differentiation of B and T lymphocytes. *Proc Natl Acad Sci USA*. (2017) 114:1988–93. doi: 10.1073/pnas.1610630114
42. Krug A, Uppaluri R, Facchetti F, Dorner BG, Sheehan KC, Schreiber RD, et al. IFN-producing cells respond to CXCR3 ligands in the presence of CXCL12 and secrete inflammatory chemokines upon activation. *J Immunol*. (2002) 169:6079–83. doi: 10.4049/jimmunol.169.11.6079
43. Penna G, Vulcano M, Sozzani S, Adorini L. Differential migration behavior and chemokine production by myeloid and plasmacytoid dendritic cells. *Hum Immunol*. (2002) 63:1164–71. doi: 10.1016/S0198-8859(02)00755-3
44. Bendriss-Vermare N, Chaperot L, Peoc'h M, Vanbervliet B, Jacob MC, Briere F, et al. *In situ* leukemic plasmacytoid dendritic cells pattern of chemokine receptors expression and *in vitro* migratory response. *Leukemia*. (2004) 18:1491–8. doi: 10.1038/sj.leu.2403452
45. Shurin MR, Shurin GV, Lokshin A, Yurkovetsky ZR, Gutkin DW, Chatta G, et al. Intratumoral cytokines/chemokines/growth factors and tumor infiltrating dendritic cells: friends or enemies? *Cancer Metastasis Rev*. (2006) 25:333–56. doi: 10.1007/s10555-006-9010-6
46. Kryczek I, Wei S, Keller E, Liu R, Zou W. Stroma-derived factor (SDF-1/CXCL12) and human tumor pathogenesis. *Am J Physiol Cell Physiol*. (2007) 292:C987–95. doi: 10.1152/ajpcell.00406.2006
47. Sozzani S, Vermi W, Del Prete A, Facchetti F. Trafficking properties of plasmacytoid dendritic cells in health and disease. *Trends Immunol*. (2010) 31:270–7. doi: 10.1016/j.it.2010.05.004
48. Decalf J, Fernandes S, Longman R, Ahloulay M, Audat F, Lefrerre F, et al. Plasmacytoid dendritic cells initiate a complex chemokine and cytokine network and are a viable drug target in chronic HCV patients. *J Exp Med*. (2007) 204:2423–37. doi: 10.1084/jem.20070814
49. Ogata M, Ito T, Shimamoto K, Nakanishi T, Satsutani N, Miyamoto R, et al. Plasmacytoid dendritic cells have a cytokine-producing capacity to enhance ICOS ligand-mediated IL-10 production during T-cell priming. *Int Immunol*. (2013) 25:171–82. doi: 10.1093/intimm/dxs103
50. Hjorton K, Hagberg N, Israelsson E, Jinton L, Berggren O, Sandling JK, et al. Cytokine production by activated plasmacytoid dendritic cells and natural killer cells is suppressed by an IRAK4 inhibitor. *Arthritis Res Ther*. (2018) 20:238. doi: 10.1186/s13075-018-1702-0
51. Lee S, Margolin K. Cytokines in cancer immunotherapy. *Cancers*. (2011) 3:3856–93. doi: 10.3390/cancers3043856
52. Kim YH, Gratzinger D, Harrison C, Brody JD, Czerwinski DK, Ai WZ, et al. *In situ* vaccination against mycosis fungoides by intratumoral injection of a TLR9 agonist combined with radiation: a phase 1/2 study. *Blood*. (2012) 119:355–63. doi: 10.1182/blood-2011-05-355222
53. Gungor B, Yagci FC, Tincer G, Bayyurt B, Alpdundar E, Yildiz S, et al. CpG ODN nanorings induce IFNa from plasmacytoid dendritic cells and demonstrate potent vaccine adjuvant activity. *Sci Transl Med*. (2014) 6:1–11. doi: 10.1126/scitranslmed.3007909
54. Bacac M, Colombetti S, Herter S, Sam J, Perro M, Chen S, et al. CD20-TCB with obinutuzumab pretreatment as next-generation treatment of hematologic malignancies. *Clin Cancer Res*. (2018) 24:4785–97. doi: 10.1158/1078-0432.CCR-18-0455
55. Wang M, Yao LC, Cheng M, Cai D, Martinek J, Pan CX, et al. Humanized mice in studying efficacy and mechanisms of PD-1-targeted cancer immunotherapy. *FASEB J*. (2018) 32:1537–49. doi: 10.1096/fj.201700740R
56. Claus C, Ferrara C, Xu W, Sam J, Lang S, Uhlenbrock F, et al. Tumor-targeted 4-1BB agonists for combination with T cell bispecific antibodies as off-the-shelf therapy. *Sci Transl Med*. (2019) 11:eaav5989. doi: 10.1126/scitranslmed.aav5989
57. Rongvaux A, Willinger T, Martinek J, Strowig T, Gearty SV, Teichmann LL, et al. Development and function of human innate immune cells in a humanized mouse model. *Nat Biotechnol*. (2014) 32:364–72. doi: 10.1038/nbt.2858
58. Cheng L, Zhang Z, Li G, Li F, Wang L, Zhang L, et al. Human innate responses and adjuvant activity of TLR ligands *in vivo* in mice reconstituted with a human immune system. *Vaccine*. (2017) 35:6143–53. doi: 10.1016/j.vaccine.2017.09.052
59. Esashi E, Wang YH, Perng O, Qin XF, Liu YJ, Watowich SS. The signal transducer STAT5 inhibits plasmacytoid dendritic cell development by suppressing transcription factor IRF8. *Immunity*. (2008) 28:509–20. doi: 10.1016/j.immuni.2008.02.013

60. Ghirelli C, Zollinger R, Soumelis V. Systematic cytokine receptor profiling reveals GM-CSF as a novel TLR-independent activator of human plasmacytoid predendritic cells. *Blood*. (2010) 115:5037–40. doi: 10.1182/blood-2010-01-266932
61. Zhan Y, Vega-Ramos J, Carrington EM, Villadangos JA, Lew AM, Xu Y. The inflammatory cytokine, GM-CSF, alters the developmental outcome of murine dendritic cells. *Eur J Immunol*. (2012) 42:2889–900. doi: 10.1002/eji.201242477
62. Ishikawa F, Niiro H, Iino T, Yoshida S, Saito N, Onohara S, et al. The developmental program of human dendritic cells is operated independently of conventional myeloid and lymphoid pathways. *Blood*. (2007) 110:3591–600. doi: 10.1182/blood-2007-02-071613
63. Audige A, Rochat MA, Li D, Ivic S, Fahrny A, Muller CKS, et al. Long-term leukocyte reconstitution in NSG mice transplanted with human cord blood hematopoietic stem and progenitor cells. *BMC Immunol*. (2017) 18:28. doi: 10.1186/s12865-017-0209-9
64. Perdomo-Celis F, Medina-Moreno S, Davis H, Bryant J, Zapata JC. HIV Replication in humanized IL-3/GM-CSF-transgenic NOG mice. *Pathogens*. (2019) 8:33. doi: 10.3390/pathogens8010033
65. Mantovani A, Schioppa T, Porta C, Allavena P, Sica A. Role of tumor-associated macrophages in tumor progression and invasion. *Cancer Metastasis Rev*. (2006) 25:315–22. doi: 10.1007/s10555-006-9001-7
66. Heidkamp GF, Sander J, Lehmann CHK, Heger L, Eissing N, Baranska A, et al. Human lymphoid organ dendritic cell identity is predominantly dictated by ontogeny, not tissue microenvironment. *Sci Immunol*. (2016) 1:eaai7677. doi: 10.1126/sciimmunol.aai7677
67. Dentelli P, Rosso A, Olgasi C, Camussi G, Brizzi MF. IL-3 is a novel target to interfere with tumor vasculature. *Oncogene*. (2011) 30:4930–40. doi: 10.1038/onc.2011.204
68. Hong IS. Stimulatory versus suppressive effects of GM-CSF on tumor progression in multiple cancer types. *Exp Mol Med*. (2016) 48:e242. doi: 10.1038/emm.2016.64
69. Zou W, Machelon V, Coulomb-L'hermin A, Borvak J, Nome F, Isaeva T, et al. Stromal-derived factor-1 in human tumors recruits and alters the function of plasmacytoid precursor dendritic cells. *Nat Med*. (2001) 7:1339–46. doi: 10.1038/nm1201-1339
70. Charles J, Di Domizio J, Salameire D, Bendriss-Vermare N, Aspord C, Muhammad R, et al. Characterization of circulating dendritic cells in melanoma: role of CCR6 in plasmacytoid dendritic cell recruitment to the tumor. *J Invest Dermatol*. (2010) 130:1646–56. doi: 10.1038/jid.2010.24
71. Bender AT, Tzvetkov E, Pereira A, Wu Y, Kasar S, Przetak MM, et al. TLR7 and TLR8 differentially activate the IRF and NF-kappaB pathways in specific cell types to promote inflammation. *Immunohorizons*. (2020) 4:93–107. doi: 10.4049/immunohorizons.2000002
72. Li G, Cheng M, Nunoya J, Cheng L, Guo H, Yu H, et al. Plasmacytoid dendritic cells suppress HIV-1 replication but contribute to HIV-1 induced immunopathogenesis in humanized mice. *PLoS Pathog*. (2014) 10:e1004291. doi: 10.1371/journal.ppat.1004291
73. Li G, Zhao J, Cheng L, Jiang Q, Kan S, Qin E, et al. HIV-1 infection depletes human CD34+CD38- hematopoietic progenitor cells via pDC-dependent mechanisms. *PLoS Pathog*. (2017) 13:e1006505. doi: 10.1371/journal.ppat.1006505
74. Pham TNQ, Meziane O, Miah MA, Volodina O, Colas C, Beland K, et al. Flt3L-mediated expansion of plasmacytoid dendritic cells suppresses HIV infection in humanized mice. *Cell Rep*. (2019) 29:2770–82 e2775. doi: 10.1016/j.celrep.2019.10.094
75. Swiecki M, Gilfillan S, Vermi W, Wang Y, Colonna M. Plasmacytoid dendritic cell ablation impacts early interferon responses and antiviral NK and CD8(+) T cell accrual. *Immunity*. (2010) 33:955–66. doi: 10.1016/j.immuni.2010.11.020
76. Monti M, Consoli F, Vescovi R, Bugatti M, Vermi W. Human plasmacytoid dendritic cells and cutaneous melanoma. *Cells*. (2020) 9:417. doi: 10.3390/cells9020417
77. Halkias J, Yen B, Taylor KT, Reinhartz O, Winoto A, Robey EA, et al. Conserved and divergent aspects of human T-cell development and migration in humanized mice. *Immunol Cell Biol*. (2015) 93:716–26. doi: 10.1038/icb.2015.38

Conflict of Interest: I-PM, GH, SH, JE, and CR are current or former Roche employees. CR was employed by Dr. Carola Ries Consulting.

The remaining authors declare that the research was conducted in the absence of any commercial or financial relationships that could be construed as a potential conflict of interest.

Copyright © 2020 Maser, Hoves, Bayer, Heidkamp, Nimmerjahn, Eckmann and Ries. This is an open-access article distributed under the terms of the Creative Commons Attribution License (CC BY). The use, distribution or reproduction in other forums is permitted, provided the original author(s) and the copyright owner(s) are credited and that the original publication in this journal is cited, in accordance with accepted academic practice. No use, distribution or reproduction is permitted which does not comply with these terms.

frontiers in Immunology

MINI REVIEW
published: 09 September 2020
doi: 10.3389/fimmu.2020.581419

Probing Reconstituted Human Immune Systems in Mice With Oncogenic γ-Herpesvirus Infections

*Christian Münz**

Viral Immunobiology, Institute of Experimental Immunology, Zurich, Switzerland

Mice with reconstituted human immune systems can mount cell-mediated immune responses against the human tumor viruses Epstein Barr virus (EBV) and Kaposi sarcoma associated herpesvirus (KSHV). Primarily cytotoxic lymphocytes protect the vast majority of persistently infected carriers of these tumor viruses from the respective malignancies for life. Thus, EBV and KSHV infection can teach us how this potent immune control is induced, what phenotype and functions characterize the protective lymphocyte compartments and if similar immune responses could be induced by vaccination. This review will summarize similarities and differences between EBV and KSHV associated pathologies and their immune control in patients and mice with reconstituted human immune systems. Furthermore, it will high-light which aspects of the near perfect immune control can be modeled in the latter preclinical animal models and discuss their relevance for cancer immunology in general.

Keywords: Epstein Barr virus, Kaposi sarcoma associated herpesvirus, primary effusions lymphoma, diffuse large B cell lymphoma, T cells, NK cells, NKT cells

OPEN ACCESS

Edited by:
Yasuyuki Saito,
Kobe University, Japan

Reviewed by:
Shigeyoshi Fujiwara,
National Center for Child Health and Development (NCCHD), Japan
Baochun Zhang,
Dana–Farber Cancer Institute, United States

***Correspondence:**
Christian Münz
christian.muenz@uzh.ch

Specialty section:
This article was submitted to Cancer Immunity and Immunotherapy, a section of the journal Frontiers in Immunology

Received: *08 July 2020*
Accepted: *17 August 2020*
Published: *09 September 2020*

Citation:
Münz C (2020) Probing Reconstituted Human Immune Systems in Mice With Oncogenic γ-Herpesvirus Infections. Front. Immunol. 11:581419. doi: 10.3389/fimmu.2020.581419

INTRODUCTION ON EBV AND KSHV SPECIFIC IMMUNE CONTROL

The two human γ-herpesviruses Epstein Barr virus (EBV) and Kaposi sarcoma associated herpesvirus (KSHV) are WHO class I carcinogens (1–3). They are associated with lymphomas, Hodgkin's and Burkitt's in the case of EBV, and primary effusion lymphoma (PEL), and multicentric Castleman's disease (MCD) for KSHV (4). Furthermore, EBV causes epithelial cell tumors, like nasopharyngeal and 10% of gastric carcinoma (5), while KSHV is the etiological cause of the endothelial cell derived cancer Kaposi sarcoma (3). Fortunately, these malignancies are rare with incidence rates of less than 1 in 10^4 individuals, even so more than 95% of the human adult population is persistently infected with EBV, and more than 50% of the Sub-Saharan African population with KSHV (3, 6). However, EBV and KSHV associated lymphomas as well as Kaposi sarcoma develop at increased frequencies after immune suppression, due to for example human immunodeficiency virus (HIV) infection or iatrogenic treatment after transplantation (7, 8). Moreover, primary immunodeficiencies, often caused by individual gene mutations, can predispose for EBV and KSHV associated diseases (9). Interestingly, the affected genes point toward well defined immune compartments that control EBV and KSHV infection and prevent associated malignancies in most virus carriers. Even so EBV and KSHV are closely related γ-herpesviruses, the requirements for their immune control seem to be quite dissimilar. Primary immunodeficiencies that predispose for EBV associated diseases affect the cytotoxic machinery of lymphocytes,

including natural killer (NK) and CD8$^+$ T cells (10, 11). In addition, co-stimulatory molecules on these cytotoxic lymphocytes, like CD27, 4-1BB, 2B4, and NKG2D, seem to be required to control EBV. A third group of molecules that are required for EBV specific immune control, are involved in T cell receptor signaling, such as interleukin-2 inducible T cell kinase (ITK), ZAP70, and PI3K. Finally, gene products that support and sustain cytotoxic lymphocyte development and expansions, like MCM4, CTPS1, and XIAP, are required for EBV specific immune control. Surprisingly, type I and II interferons (IFNs) as well as antibody responses are dispensable for the immune control of EBV (11). In contrast, type II IFN signaling with IFN-γ receptor 1 and STAT4 protects from Kaposi sarcoma (9, 12). In addition, OX40 instead of the above mentioned co-stimulatory molecules is required to protect from Kaposi sarcoma (13). Thus, primary immunodeficiencies suggest that cytotoxic lymphocytes keep persistent EBV infection in check, while their cytokine production protects in addition from KSHV. Accordingly, these two pathogens are suitable to challenge human immune systems with their tumorigenic potential and test their robustness in raising cell-mediated immune responses.

VIRUS ASSOCIATED MALIGNANCIES

Such challenges are for example applied to immune compromised mice with reconstituted human immune system components, such as NOD-*scid* $\gamma_c^{-/-}$ that are neonatally injected with human CD34$^+$ hematopoietic progenitor cells (HPCs) and then develop human leucocytes during three to 6 months (humanized mice) (14, 15) (**Figure 1**). In order, however, to explore the protective capacity of the reconstituted human immune system compartments, at least some of the EBV and KSHV associated pathologies must be recapitulated in these humanized mouse systems. Accordingly, the viral gene expression patterns have been analyzed after EBV infection of humanized mice (16–21). In most of these studies a high dose of infectious viral particles from the B95-8 EBV strain, originally isolated during symptomatic primary infection called infectious mononucleosis (IM), was used. As in secondary lymphoid tissues, including tonsils, of IM patients (22) primarily EBV infected B cells expressing the latency III infection program with six nuclear antigen (EBNA1, 2, 3A-C, and LP), two latent membrane proteins (LMP1,2) as well as non-translated EBER and viral miRNAs, were observed (21). In addition, however, low levels of latency I and II with EBNA1 as the sole or in addition LMP1 and 2 protein expression could be detected (18, 23). Low levels of these lower latencies were also verified by detection of characteristic viral transcripts (21, 24, 25). While latency III is found in naïve B cells of healthy EBV carriers, latency II predominates in germinal center B cells and latency I in homeostatically replicating memory B cells (26, 27). It is unclear if the respective latencies are also in similar B cell differentiation stages in humanized mice. In humans, EBV persists without viral protein expression in circulating memory B cells of so-called latency 0 (28). This latency 0 can also be reached in humanized mice (20). From latency 0 and I EBV switches into lytic replication upon plasma cell differentiation in healthy virus carriers (29). Such reactivation only rarely occurs with the B95-8 EBV virus in humanized mice (30), but other viruses such as the M81 EBV strain are more prone to lytic replication (31, 32). In contrast to these IM-like infections, lower viral doses might mimic asymptomatic primary infection, as it occurs in the vast majority of humans (6), but these have so far not extensively been explored in humanized mice (33). Nevertheless, all EBV infection programs can be found upon usually intraperitoneal inoculation of humanized mice.

According to the predominance of EBV latency III infection the virus-associated lymphomas that develop in up to one third of infected mice also carry this strongly growth transforming gene expression program akin to some diffuse large B cell lymphomas (DLBCL) and *in vitro* EBV transformed, B cell derived lymphoblastoid cell lines (LCLs) (2). Burkitt's and Hodgkin's lymphomas that carry latency I and II have so far not been reported. DLBCL-like lymphomagenesis can further be increased by infection with an EBV strain that is deficient in the viral tumor suppressor EBNA3B (34). Accordingly, EBNA3B loss has also be found in a subset of DLBCLs in human patients (34, 35). Furthermore, both EBV and KSHV are present in most PELs (36). Of all KSHV associated malignancies PEL cells are also the only one that maintains KSHV in culture (37). Interestingly, KSHV infection only persists in humanized mice upon co-infection with EBV (23, 38). Similarly, both viruses or their monkey orthologues seem to be co-transmitted in both macaques and humans (39, 40). Furthermore, EBV supports KSHV infection of B cells *in vitro* (41). KSHV and EBV co-infection of humanized mice also allows for the development of PEL-like lymphomas (**Figure 1**) with characteristics of plasma cell differentiation that have previously been defined for PELs (23, 42). Consistent with lytic EBV replication being associated with plasma cell differentiation (29) both PEL-like tumors in humanized mice and human PELs displayed elevated lytic viral gene products and this lytic EBV replication contributed to enhanced tumor formation in double-infected humanized mice (23). Thus, EBV associated DLBCLs and KSHV as well as EBV positive PELs can be elicited in humanized mice.

IMMUNE CONTROL BY INNATE LEUKOCYTES

The symptomatic primary EBV infection IM is an immunopathology caused by massive expansion of CD8$^+$ T cells that are predominantly directed against lytic EBV antigens (43). This disease is rare in children but can make up 30 to 50% of primary infections in adolescents (6). Therefore, EBV infection at young age seems to trigger a different immune response than later in life. One reason for this altered immune response could be more robust innate immune control of lytic EBV infection in children. Along these lines it has been shown that NK cells protect from lytic EBV infection in humanized mice (19, 44) (**Figure 1**). In both humanized mice and pediatric IM patients primarily early differentiated CD56^{dim}NKG2A$^+$killer immunolglobulin-like receptor (KIR)$^-$ NK cells expand (19, 45–48). While these

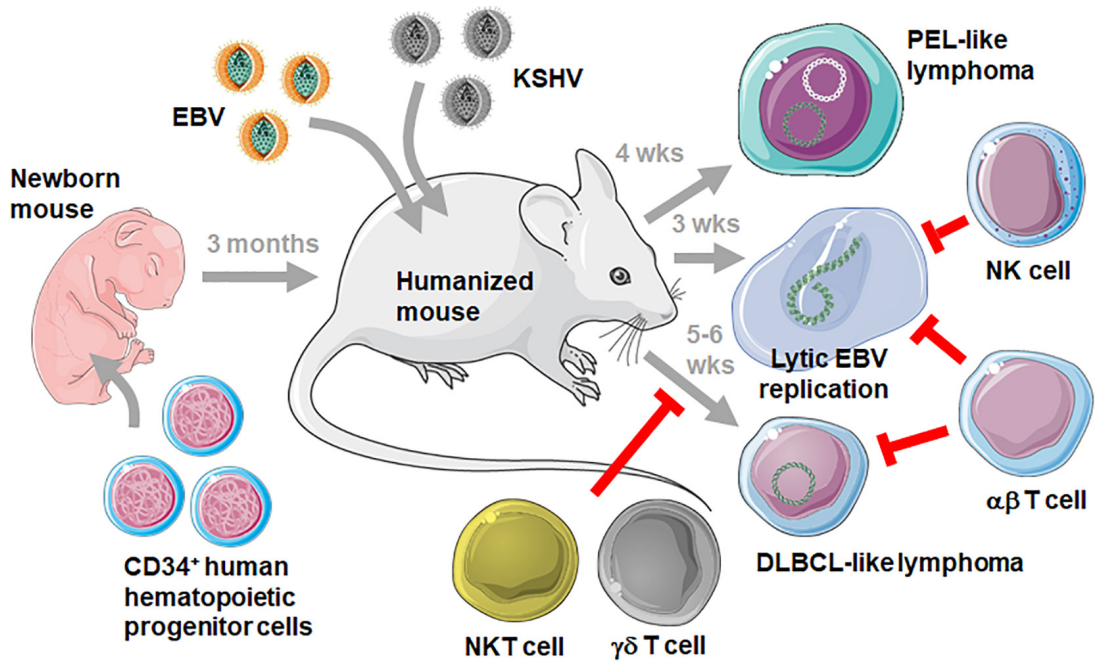

FIGURE 1 | Challenging humanized mice with EBV and KSHV infection. Mice with reconstituted human immune system compartments (humanized mice) are generated by injecting human CD34$^+$ HPCs into immune compromised mice, such as the NOD-*scid* $\gamma_c^{-/-}$ mouse strain. After 3 months humanized mice can be infected with EBV with and without KSHV. Persistent infection with these two viruses develops into PEL-like lymphomas after double infection after 4 weeks (wks), EBV lytic replication can be observed after 3 weeks and DLBCL-like lymphomas develop after 5–6 weeks. While the immune control of KSHV in humanized mice still needs to be defined, NK and αβ T cells control lytic EBV replication, and NKT, γδ T and αβ T cells prevent DLBCL-like tumorigenesis by targeting latent EBV infection. This figure was created in part with modified Servier Medical Art templates, which are licensed under a Creative Commons Attribution 3.0 unported license: https://smart.servier.com.

are the most abundant NK cell subpopulation after birth in humans, they differentiate to CD56^{dim}NKG2A$^-$KIR$^+$ NK cells during the first decade of life (45), possibly rendering adolescents more susceptible to IM. It has been suggested that ligands for the activating NK cell receptors NKG2D and DNAM1 get up-regulated on B cells that undergo lytic EBV reactivation, and that NKG2D and DNAM1 mediate NK cell cytotoxicity against the respective targets (49). Thus, NK cell differentiation could diminish protective NK cell populations during the first decade of life, compromising innate immune control of lytic EBV infection which in turn would trigger the massive expansion of lytic EBV antigen specific CD8$^+$ T cells, causing IM.

However, in addition to NK cells other innate lymphocyte populations might play a role during EBV infection. Along these lines it has been shown that Vγ9Vδ2 T cells that recognize mevalonate metabolism intermediates presented by butyrophilin 2A1 (BTN2A1) prevent EBV associated lymphoproliferative disease in humanized mice (50). Similarly, the transfer of Vγ9Vδ2 T cells inhibited tumor growth in EBV transformed B cell carrying mice (51). Vγ9Vδ2 T cells recognized EBV infected B cells by their T cell receptor and NKG2D as a co-receptor (50). Especially EBV latency I Burkitt's lymphoma cell lines expanded human Vγ9Vδ2 T cells (52). These lymphoma cell lines displayed the highest levels of mevalonate metabolite presentations on BTN2A1. Interestingly, only around 50% of human individuals could raise these protective Vγ9Vδ2 T cell responses against EBV infected targets (52). These so-called group 1 individuals harbor a high frequency of Vγ9Vδ2 T cells with T cell receptors that utilize JγP segments (53). These Vγ9JγP T cells expanded upon stimulation with Burkitt's lymphoma cell lines. Thus, Vγ9Vδ2 T cells might protect preferentially against EBV latency I infected B cells.

Finally, there might also be a role for NKT cells that recognize glycolipid presentation on CD1d non-classical MHC class I molecules (54, 55). Adoptive transfer of NKT cells into mice that carried EBV transformed B cells reduced their tumor formation (54). They seemed to recognize freshly EBV infected B cells and EBV latency II infected tumor cells, while CD1d is down-regulated on EBV latency III infected B cells (55). Along these lines, X-linked lymphoproliferative (XLP-1) disease which affects primarily boys due to mutations in the 2B4 adaptor SAP and which confers life-threatening susceptibility to EBV associated pathogenesis, lack NKT cells (56). Thus, NKT cells might also contribute to innate immune control of latently EBV infected B cells, possibly preferentially expressing the latency II program. Humanized mice have contributed to demonstrate immune control by NK, Vγ9Vδ2 T cells, and NKT cells against lytic and latent EBV infected B cells, respectively. Only fully transformed EBV latency III B cells, resembling DLBCLs, do not seem to be efficiently recognized by innate lymphocytes, but these seem to target EBV infected precursors that are required for DLBCL-like tumor development in humanized mice (**Figure 1**).

CYTOTOXIC T CELL RESPONSES

In contrast to innate lymphocytes, EBV latency III infected B cells that can be also generated *in vitro* by EBV infection of human B cells, are highly immunogenic for T cells. Indeed, adoptive transfer of LCL stimulated T cell lines into patients with EBV induced post-transplant lymphoproliferative disease (PTLD) was one of the first cellular therapies and was able to cause PTLD regression (57). The EBV antigens EBNA1, LMP1, and LMP2 have proven to be sufficient as T cell targets for such adoptive T cell transfer therapies against EBV associated malignancies (58, 59). Similarly in humanized mice antibody mediated T cell depletion increased EBV viral loads and DLBCL-like lymphomagenesis (16, 60) (**Figure 1**). While primarily $CD8^+$ T cells seemed to protect from EBV induced lymphomagenesis in humanized mice, antibody depletion, pharmacological inhibition by FK506 or destruction of $CD4^+$ T cells by HIV co-infection also compromised EBV specific immune control in humanized mice (16, 21, 25). Along these lines, late lytic EBV antigen specific $CD4^+$ T cells have been reported to restrict EBV transformed B cell growth in mice (61). Thus, both cytotoxic $CD8^+$ T cells and helper T cell functions seem to be required for adaptive immune control of EBV in humanized mice.

Antibody blocking and recombinant EBV mutant infection experiments have revealed crucial aspects of this T cell mediated immune control of EBV in humanized mice and helped to explain the mechanistic underpinnings of EBV susceptibility in patients with the above mentioned primary immunodeficiencies. Among the co-stimulatory molecules, blocking of 2B4, one of the receptors that depends on SAP for activating signaling and is affected in XLP-1, led to increased EBV loads and lymphomagenesis (62). This 2B4 requirement was mainly on $CD8^+$ T cells because their antibody mediated depletion did not further increase viral titers and tumor formation. In addition, $CD8^+$ T cells with the inhibitory co-receptor PD-1 expanded during IM and in EBV infected humanized mice (33, 63). They included both latent (LMP2) and lytic (BMLF1) EBV antigen specific $CD8^+$ T cells. These PD-1 positive $CD8^+$ T cells carried the highest cytotoxic ability during EBV infection of humanized mice. Furthermore, they expressed CXCR5, Tim-3, KLRG1, and TCF-1 (33) and resembled germinal center homing $CD8^+$ T cells which have previously been described to contain EBV specific $CD8^+$ T cells in human tonsils (64). Interestingly, antibody blocking of PD-1 led to increased EBV viral loads and lymphomagenesis. This was associated with IL-10 production and might therefore represent activation of a regulatory $CD4^+$ T cell population during PD-1 inhibition that compromises EBV specific immune control. Along these lines, at least a subset of patients that undergo PD-1 blockade for tumor treatment and develop neurological side effects, have recently been shown to harbor elevated EBV loads and accumulate EBV infected B cells and EBV reactive $CD4^+$ and $CD8^+$ T cells in their central nervous system (65). In contrast to PD-1 blockade on regulatory $CD4^+$ T cells, humanized mouse models that sustained only T and EBV transformed B cell reconstitution developed exhausted, presumably $CD8^+$ T cell populations and antibody blocking of their PD-1 and CTLA-4 inhibitory receptors restored EBV specific immune control (66). Antibody blocking studies have, therefore, suggested essential roles for PD-1, CTLA-4, and 2B4 during EBV specific immune control in humanized mice.

Additional characteristics of protective EBV specific T cell responses have been revealed by recombinant EBV mutant viruses. In addition to secondary lymphoid tissue homing, CXCR3 dependent T cell homing to inflamed tissues has been found to be critical for immune control of EBV in humanized mice by studying EBNA3B deficiency (34). EBNA3B deficiency which was observed in some patients with DLBCL (34, 35), elicited elevated lymphomagenesis in humanized mice (34). The respective tumors were devoid of T cell infiltrates and EBNA3B deficient LCLs were found to produce less of the CXCR3 stimulating CXCL9 and 10 chemokines. Transgenic CXCL10 expression by EBNA3B deficient LCLs restored their T cell mediated immune control *in vivo*. In addition, compromised MHC class I antigen presentation by EBV miRNAs limits EBV specific immune control (67). miRNA deficient EBV did not induce any DBLCL-like lymphomas in humanized mice, but tumor formation was restored upon antibody mediated $CD8^+$ T cell depletion. Both latent and at least early lytic $CD8^+$ T cell responses might contribute to $CD8^+$ T cell mediated immune protection against EBV associated lymphomagenesis in humanized mice (18, 30). EBV deficient in the immediate early lytic EBV transactivator BZLF1 was compromised in its ability to cause DLBCL-like lymphomas in humanized mice, KSHV co-infection increased lytic EBV replication and lymphomagenesis, and BMLF1 specific $CD8^+$ T cells were able to transiently control lytic EBV infection after their adoptive transfer (18, 23, 30). These studies define CXCR3 dependent homing, targeting of early lytic EBV antigens and efficient MHC class I antigen presentation as additional characteristics of EBV specific immune control by T cells.

In contrast to $CD8^+$ T cells, $CD4^+$ T cells can, however, also mediate pro-tumorigenic effects. LMP1 deficient EBV required $CD4^+$ T cells for DLBCL-like lymphoma formation in humanized mice (68). Furthermore, $CD4^+$ T cells allowed EBV to access the Burkitt's and Hodgkin's lymphoma associated EBV latencies I and II in humanized mice, even so no tumors with these viral gene expression patterns have so far been observed in any humanized mouse model (24). Therefore, both anti- and pro-tumorigenic functions of T cells can be studied during EBV infection of humanized mice, and so far, $CXCR3^+CXCR5^+2B4^+CD8^+$ T cells have emerged as the main protective entity.

VACCINATION

Epstein Barr virus specific immune control is uniquely dependent on cell mediated immunity and cytotoxic lymphocytes, while individuals with deficient antibody responses do not suffer from EBV associated pathologies (9–11). This cytotoxic immune

control of EBV can be recapitulated in humanized mice (14). Therefore, humanized mice should be well suited to test EBV specific vaccine candidates and develop vaccines that efficiently prime cytotoxic lymphocytes and are also required to stimulate other anti-tumor immune protection (69). Unfortunately, it has been quite frustrating to identify vaccine candidates that manage to induce such protective T cell responses. Antigen targeting to dendritic cells (DCs), recombinant viral vectors, and virus like particles (VLP) have been explored.

Even so EBNA1 specific T cells have been therapeutically used against PTLD (58) and this antigen is incorporated in many vaccine formulations (70–74), targeting of EBNA1 to DCs and uptake via their DEC-205 receptor has elicited only weak $CD4^+$ T cell responses (75, 76). However, even in regular mice this vaccine formulation was even with a boost by a recombinant adenovirus encoding EBNA1 less efficient in inducing T cell responses than heterologous prime-boost vaccination with EBNA1 encoding adenovirus and modified vaccinia virus Ankara (MVA) (74). In contrast, an EBV derived VLP into which EBNA1 was incorporated as a tegument component elicited protective $CD4^+$ T cell responses against EBV challenge in humanized mice (77). This VLP targets B cells as EBV does, and the abundance of these antigen presenting cells (APCs) in humanized mice could facilitate the priming of sufficient numbers of protective T cells. Similarly, yellow fever virus (YFV) specific vaccination that is based on the attenuated viral strain YFV17D required human DC expansion prior to YFV17D injection to prime significant T cell responses (78). Such expanded APC populations, as exemplified by the high constitutive B cell reconstitution in humanized mice and Flt3L mediated DC expansion might overcome the paucity in secondary lymphoid tissue development that most humanized mouse models suffer from (79). Interestingly, adoptive transfer of DC populations did not only increase these APC populations and allowed for more efficient induction of human cytomegalovirus (HCMV) specific immune responses in humanized mice, but also induced the formation of secondary lymphoid tissues like lymph nodes (80). These structures then did not only facilitate the priming of T cell, but also antibody responses (80). Thus, humanized mice allow for the evaluation of vaccines, but might require expansion of APC populations and secondary lymphoid tissues for them to meet naïve T cells for adaptive cell-mediated and possibly even humoral immune response induction.

CONCLUSION AND OUTLOOK

Humanized mice hold the promise that human immune responses and their modulation by immunotherapies as well as vaccinations can be studied. However, at least humoral immune responses are severely attenuated in these mice and mucosal immune reconstitution is only rudimentary. As a result, only few pathogens have been shown to elicit protective immune responses in humanized mouse systems. As these models get further improved by introduction of human MHC and cytokine genes, as well as additional human organoids (15) immunocompetence will probably increase. However, already with the available models strongly T cell immunogenic pathogens like EBV and KSHV can be characterized for their infection, tumorigenesis, and cell-mediated immune control. Indeed, EBV is the pathogen that most often leads to even pathogenic $CD8^+$ T cell expansions in humans, as in IM, and primary immunodeficiencies as well as therapeutic adoptive T cell transfer suggest that such cytotoxic lymphocyte responses are necessary and sufficient for its immune control (9, 43, 81). This suggests that EBV is well suited to interrogate the immunocompetence of cytotoxic lymphocyte compartments in humanized mice and should be able to reveal improvements of these preclinical *in vivo* models.

At the same time any manipulation of T cell mediated immune control, like immune checkpoint inhibition, can be assessed for its ability to improve or compromise EBV specific immune control, even if the respective treatments are developed for other tumors than EBV associated malignancies. The influence of these treatments on EBV infection should still be of interest because the vast majority of adult humans (>95%) are persistently infected with EBV (2) and, therefore, any immune modulation of anti-tumor T cell responses will also affect EBV specific immune control in the respective patients, as becomes apparent during immunosuppressive treatment after transplantation, increasing the risk for PTLD (7, 21). Thus, EBV infected humanized mice constitute an interesting preclinical *in vivo* system to test human immune modulators.

Finally, it remains difficult to construct humanized mice with tumors and long-term engraftment of diverse autologous human immune system components (15). However, the growth transforming ability of EBV allows for the generation of autologous tumor cells that can be genetically manipulated and afterward implanted into humanized mice that have been reconstituted with $CD34^+$ HPCs from the same donor. Therefore, it is one of the few systems that currently allow studying tumor interaction with human immune system components in an autologously xenografted humanized mouse model. All these advantages should allow us to interrogate human immune responses and design vaccines as well as other immunotherapies to elicit them more comprehensively.

AUTHOR CONTRIBUTIONS

CM wrote the manuscript.

FUNDING

Research in CM's laboratory is supported by Cancer Research Switzerland (KFS-4091-02-2017 and KFS-4962-02-2020), KFSP-Precision^{MS} and HMZ ImmunoTargET of the University of Zurich, Cancer Research Center Zurich, the Sobek Foundation, the Vontobel Foundation, the Baugarten Foundation, the Swiss Vaccine Research Institute, Roche, Novartis, and the Swiss National Science Foundation (310030B_182827 and CRSII5_180323).

REFERENCES

1. Bouvard V, Baan R, Straif K, Grosse Y, Secretan B, El Ghissassi F, et al. A review of human carcinogens–Part B: biological agents. *Lancet Oncol*. (2009) 10:321–2. doi: 10.1016/s1470-2045(09)70096-8
2. Münz C. Latency and lytic replication in the oncogenesis of the Epstein Barr virus. *Nat Rev Micobiol*. (2019) 17:691–700. doi: 10.1038/s41579-019-0249-7
3. Cesarman E, Damania B, Krown SE, Martin J, Bower M, Whitby D. Kaposi sarcoma. *Nat Rev Dis Primers*. (2019) 5:9.
4. Cesarman E. Gammaherpesviruses and lymphoproliferative disorders. *Annu Rev Pathol*. (2014) 9:349–72. doi: 10.1146/annurev-pathol-012513-104656
5. Shannon-Lowe C, Rickinson A. The global landscape of EBV-associated tumors. *Front Oncol*. (2019) 9:713. doi: 10.3389/fonc.2019.00713
6. Dunmire SK, Verghese PS, Balfour HH Jr. Primary Epstein-Barr virus infection. *J Clin Virol*. (2018) 102:84–92.
7. Gottschalk S, Rooney CM, Heslop HE. Post-transplant lymphoproliferative disorders. *Annu Rev Med*. (2005) 56:29–44.
8. Totonchy J, Cesarman E. Does persistent HIV replication explain continued lymphoma incidence in the era of effective antiretroviral therapy? *Curr Opin Virol*. (2016) 20:71–7. doi: 10.1016/j.coviro.2016.09.001
9. Damania B, Münz C. Immunodeficiencies that predispose to pathologies by human oncogenic gamma-herpesviruses. *FEMS Microbiol Rev*. (2019) 43:181–92. doi: 10.1093/femsre/fuy044
10. Tangye SG, Latour S. Primary immunodeficiencies reveal the molecular requirements for effective host defense against EBV infection. *Blood*. (2020) 135:644–55. doi: 10.1182/blood.2019000928
11. Latour S, Fischer A. Signaling pathways involved in the T-cell-mediated immunity against Epstein-Barr virus: lessons from genetic diseases. *Immunol Rev*. (2019) 291:174–89. doi: 10.1111/imr.12791
12. Jackson CC, Dickson MA, Sadjadi M, Gessain A, Abel L, Jouanguy E, et al. Kaposi sarcoma of childhood: inborn or acquired immunodeficiency to oncogenic HHV-8. *Pediatr Blood Cancer*. (2016) 63:392–7. doi: 10.1002/pbc.25779
13. Byun M, Ma CS, Akcay A, Pedergnana V, Palendira U, Myoung J, et al. Inherited human OX40 deficiency underlying classic Kaposi sarcoma of childhood. *J Exp Med*. (2013) 210:1743–59. doi: 10.1084/jem.20130592
14. McHugh D, Caduff N, Murer A, Engelmann C, Deng Y, Zdimerova H, et al. Infection and immune control of human oncogenic gamma-herpesviruses in humanized mice. *Philos Trans R Soc Lond B Biol Sci*. (2019) 374:20180296. doi: 10.1098/rstb.2018.0296
15. Stripecke R, Münz C, Schuringa JJ, Bissig KD, Soper B, Meeham T, et al. Innovations, challenges, and minimal information for standardization of humanized mice. *EMBO Mol Med*. (2020) 12:e8662.
16. Strowig T, Gurer C, Ploss A, Liu YF, Arrey F, Sashihara J, et al. Priming of protective T cell responses against virus-induced tumors in mice with human immune system components. *J Exp Med*. (2009) 206:1423–34. doi: 10.1084/jem.20081720
17. Yajima M, Imadome K, Nakagawa A, Watanabe S, Terashima K, Nakamura H, et al. A new humanized mouse model of Epstein-Barr virus infection that reproduces persistent infection, lymphoproliferative disorder, and cell-mediated and humoral immune responses. *J Infect Dis*. (2008) 198:673–82. doi: 10.1086/590502
18. Ma SD, Hegde S, Young KH, Sullivan R, Rajesh D, Zhou Y, et al. A new model of Epstein-Barr virus infection reveals an important role for early lytic viral protein expression in the development of lymphomas. *J Virol*. (2011) 85:165–77. doi: 10.1128/jvi.01512-10
19. Chijioke O, Muller A, Feederle R, Barros MH, Krieg C, Emmel V, et al. Human natural killer cells prevent infectious mononucleosis features by targeting lytic Epstein-Barr virus infection. *Cell Rep*. (2013) 5:1489–98. doi: 10.1016/j.celrep.2013.11.041
20. Murer A, McHugh D, Caduff N, Kalchschmidt JS, Barros MH, Zbinden A, et al. EBV persistence without its EBNA3A and 3C oncogenes in vivo. *PLoS Pathog*. (2018) 14:e1007039. doi: 10.1371/journal.ppat.1007039
21. Caduff N, McHugh D, Murer A, Ramer P, Raykova A, Landtwing V, et al. Immunosuppressive FK506 treatment leads to more frequent EBV-associated lymphoproliferative disease in humanized mice. *PLoS Pathog*. (2020) 16:e1008477. doi: 10.1371/journal.ppat.1008477
22. Kurth J, Spieker T, Wustrow J, Strickler GJ, Hansmann LM, Rajewsky K, et al. EBV-infected B cells in infectious mononucleosis: viral strategies for spreading in the B cell compartment and establishing latency. *Immunity*. (2000) 13:485–95. doi: 10.1016/s1074-7613(00)00048-0
23. McHugh D, Caduff N, Barros MHM, Rämer P, Raykova A, Murer A, et al. Persistent KSHV infection increases EBV-associated tumor formation in vivo via enhanced EBV lytic gene expression. *Cell Host Microbe*. (2017) 22:61–73. doi: 10.1016/j.chom.2017.06.009
24. Heuts F, Rottenberg ME, Salamon D, Rasul E, Adori M, Klein G, et al. T cells modulate Epstein-Barr virus latency phenotypes during infection of humanized mice. *J Virol*. (2014) 88:3235–45. doi: 10.1128/jvi.02885-13
25. McHugh D, Myburgh R, Caduff N, Spohn M, Kok YL, Keller CW, et al. EBV renders B cells susceptible to HIV-1 in humanized mice. *Life Sci Alliance*. (2020) 3:e202000640.
26. Babcock JG, Hochberg D, Thorley-Lawson AD. The expression pattern of Epstein-Barr virus latent genes in vivo is dependent upon the differentiation stage of the infected B cell. *Immunity*. (2000) 13:497–506. doi: 10.1016/s1074-7613(00)00049-2
27. Hochberg D, Middeldorp JM, Catalina M, Sullivan JL, Luzuriaga K, Thorley-Lawson DA. Demonstration of the Burkitt's lymphoma Epstein-Barr virus phenotype in dividing latently infected memory cells in vivo. *Proc Natl Acad Sci USA*. (2004) 101:239–44. doi: 10.1073/pnas.2237267100
28. Babcock GJ, Decker LL, Volk M, Thorley-Lawson DA. EBV persistence in memory B cells in vivo. *Immunity*. (1998) 9:395–404. doi: 10.1016/s1074-7613(00)80622-6
29. Laichalk LL, Thorley-Lawson DA. Terminal differentiation into plasma cells initiates the replicative cycle of Epstein-Barr virus in vivo. *J Virol*. (2005) 79:1296–307. doi: 10.1128/jvi.79.2.1296-1307.2005
30. Antsiferova O, Müller A, Rämer P, Chijioke O, Chatterjee B, Raykova A, et al. Adoptive transfer of EBV specific $CD8^+$ T cell clones can transiently control EBV infection in humanized mice. *PLoS Pathog*. (2014) 10:e1004333. doi: 10.1371/journal.ppat.1004333
31. Tsai MH, Raykova A, Klinke O, Bernhardt K, Gartner K, Leung CS, et al. Spontaneous lytic replication and epitheliotropism define an Epstein-Barr virus strain found in carcinomas. *Cell Rep*. (2013) 5:458–70. doi: 10.1016/j.celrep.2013.09.012
32. Tsai MH, Lin X, Shumilov A, Bernhardt K, Feederle R, Poirey R, et al. The biological properties of different Epstein-Barr virus strains explain their association with various types of cancers. *Oncotarget*. (2017) 8:10238–54. doi: 10.18632/oncotarget.14380
33. Chatterjee B, Deng Y, Holler A, Nunez N, Azzi T, Vanoaica LD, et al. $CD8^+$ T cells retain protective functions despite sustained inhibitory receptor expression during Epstein-Barr virus infection in vivo. *PLoS Pathog*. (2019) 15:e1007748. doi: 10.1371/journal.ppat.1007748
34. White RE, Ramer PC, Naresh KN, Meixlsperger S, Pinaud L, Rooney C, et al. EBNA3B-deficient EBV promotes B cell lymphomagenesis in humanized mice and is found in human tumors. *J Clin Invest*. (2012) 122:1487–502.
35. Gottschalk S, Ng CY, Perez M, Smith CA, Sample C, Brenner MK, et al. An Epstein-Barr virus deletion mutant associated with fatal lymphoproliferative disease unresponsive to therapy with virus-specific CTLs. *Blood*. (2001) 97:835–43. doi: 10.1182/blood.v97.4.835
36. Cesarman E, Chang Y, Moore PS, Said JW, Knowles DM. Kaposi's sarcoma-associated herpesvirus-like DNA sequences in AIDS-related body-cavity-based lymphomas. *N Engl J Med*. (1995) 332:1186–91. doi: 10.1056/nejm199505043321802
37. Carbone A, Cilia AM, Gloghini A, Capello D, Todesco M, Quattrone S, et al. Establishment and characterization of EBV-positive and EBV-negative primary effusion lymphoma cell lines harbouring human herpesvirus type-8. *Br J Haematol*. (1998) 102:1081–9. doi: 10.1046/j.1365-2141.1998.00877.x
38. Wang LX, Kang G, Kumar P, Lu W, Li Y, Zhou Y, et al. Humanized-BLT mouse model of Kaposi's sarcoma-associated herpesvirus infection. *Proc Natl Acad Sci USA*. (2014) 111:3146–51. doi: 10.1073/pnas.1318175111
39. Bruce AG, Barcy S, Staheli J, Bielefeldt-Ohmann H, Ikoma M, Howard K, et al. Experimental co-transmission of simian immunodeficiency virus (SIV) and the macaque homologs of the Kaposi Sarcoma-associated herpesvirus (KSHV) and Epstein-Barr Virus (EBV). *PLoS One*. (2018) 13:e0205632. doi: 10.1371/journal.pone.0205632

40. Labo N, Marshall V, Miley W, Davis E, McCann B, Stolka KB, et al. Mutual detection of Kaposi's sarcoma-associated herpesvirus and Epstein-Barr virus in blood and saliva of cameroonians with and without Kaposi's sarcoma. *Int J Cancer*. (2019) 145:2468–77. doi: 10.1002/ijc.32546
41. Faure A, Hayes M, Sugden B. How Kaposi's sarcoma-associated herpesvirus stably transforms peripheral B cells towards lymphomagenesis. *Proc Natl Acad Sci USA*. (2019) 116:16519–28. doi: 10.1073/pnas.1905025116
42. Klein U, Gloghini A, Gaidano G, Chadburn A, Cesarman E, Dalla-Favera R, et al. Gene expression profile analysis of AIDS-related primary effusion lymphoma (PEL) suggests a plasmablastic derivation and identifies PEL-specific transcripts. *Blood*. (2003) 101:4115–21. doi: 10.1182/blood-2002-10-3090
43. Luzuriaga K, Sullivan JL. Infectious mononucleosis. *N Engl J Med*. (2010) 362:1993–2000.
44. Landtwing V, Raykova A, Pezzino G, Beziat V, Marcenaro E, Graf C, et al. Cognate HLA absence in trans diminishes human NK cell education. *J Clin Invest*. (2016) 126:3772–82. doi: 10.1172/jci86923
45. Azzi T, Lunemann A, Murer A, Ueda S, Beziat V, Malmberg KJ, et al. Role for early-differentiated natural killer cells in infectious mononucleosis. *Blood*. (2014) 124:2533–43. doi: 10.1182/blood-2014-01-553024
46. Hendricks DW, Balfour HH Jr., Dunmire SK, Schmeling DO, Hogquist KA, Lanier LL. Cutting edge: NKG2C^{hi}CD57^{+} NK cells respond specifically to acute infection with cytomegalovirus and not Epstein-Barr virus. *J Immunol*. (2014) 192:4492–6. doi: 10.4049/jimmunol.1303211
47. Williams H, McAulay K, Macsween KF, Gallacher NJ, Higgins CD, Harrison N, et al. The immune response to primary EBV infection: a role for natural killer cells. *Br J Haematol*. (2005) 129:266–74. doi: 10.1111/j.1365-2141.2005.05452.x
48. Balfour HH Jr., Odumade OA, Schmeling DO, Mullan BD, Ed JA, Knight JA, et al. Behavioral, virologic, and immunologic factors associated with acquisition and severity of primary Epstein-Barr virus infection in university students. *J Infect Dis*. (2013) 207:80–8. doi: 10.1093/infdis/jis646
49. Pappworth IY, Wang EC, Rowe M. The switch from latent to productive infection in Epstein-Barr virus-infected B cells is associated with sensitization to NK cell killing. *J Virol*. (2007) 81:474–82. doi: 10.1128/jvi.01777-06
50. Xiang Z, Liu Y, Zheng J, Liu M, Lv A, Gao Y, et al. Targeted activation of human Vgamma9Vdelta2-T cells controls Epstein-Barr virus-induced B cell lymphoproliferative disease. *Cancer Cell*. (2014) 26:565–76. doi: 10.1016/j.ccr.2014.07.026
51. Zumwalde NA, Sharma A, Xu X, Ma S, Schneider CL, Romero-Masters JC, et al. Adoptively transferred Vgamma9Vdelta2 T cells show potent antitumor effects in a preclinical B cell lymphomagenesis model. *JCI Insight*. (2017) 2:e93179.
52. Djaoud Z, Guethlein LA, Horowitz A, Azzi T, Nemat-Gorgani N, Olive D, et al. Two alternate strategies for innate immunity to Epstein-Barr virus: one using NK cells and the other NK cells and gammadelta T cells. *J Exp Med*. (2017) 214:1827–41. doi: 10.1084/jem.20161017
53. Djaoud Z, Parham P. Dimorphism in the TCRgamma-chain repertoire defines 2 types of human immunity to Epstein-Barr virus. *Blood Adv*. (2020) 4:1198–205. doi: 10.1182/bloodadvances.2019001179
54. Yuling H, Ruijing X, Li L, Xiang J, Rui Z, Yujuan W, et al. EBV-induced human CD8^{+} NKT cells suppress tumorigenesis by EBV-associated malignancies. *Cancer Res*. (2009) 69:7935–44. doi: 10.1158/0008-5472.can-09-0828
55. Chung BK, Tsai K, Allan LL, Zheng DJ, Nie JC, Biggs CM, et al. Innate immune control of EBV-infected B cells by invariant natural killer T cells. *Blood*. (2013) 122:2600–8. doi: 10.1182/blood-2013-01-480665
56. Pasquier B, Yin L, Fondaneche MC, Relouzat F, Bloch-Queyrat C, Lambert N, et al. Defective NKT cell development in mice and humans lacking the adapter SAP, the X-linked lymphoproliferative syndrome gene product. *J Exp Med*. (2005) 201:695–701. doi: 10.1084/jem.20042432
57. Heslop HE, Brenner MK, Rooney CM. Donor T cells to treat EBV-associated lymphoma. *N Engl J Med*. (1994) 331:679–80. doi: 10.1056/nejm199409083311017
58. Icheva V, Kayser S, Wolff D, Tuve S, Kyzirakos C, Bethge W, et al. Adoptive transfer of epstein-barr virus (EBV) nuclear antigen 1-specific T cells as treatment for EBV reactivation and lymphoproliferative disorders after allogeneic stem-cell transplantation. *J Clin Oncol*. (2013) 31:39–48. doi: 10.1200/jco.2011.39.8495
59. Bollard CM, Gottschalk S, Torrano V, Diouf O, Ku S, Hazrat Y, et al. Sustained complete responses in patients with lymphoma receiving autologous cytotoxic T lymphocytes targeting Epstein-Barr virus latent membrane proteins. *J Clin Oncol*. (2014) 32:798–808. doi: 10.1200/jco.2013.51.5304
60. Yajima M, Imadome K, Nakagawa A, Watanabe S, Terashima K, Nakamura H, et al. T cell-mediated control of Epstein-Barr virus infection in humanized mice. *J Infect Dis*. (2009) 200:1611–5. doi: 10.1086/644644
61. Linnerbauer S, Behrends U, Adhikary D, Witter K, Bornkamm GW, Mautner J. Virus and autoantigen-specific CD4^{+} T cells are key effectors in a SCID mouse model of EBV-associated post-transplant lymphoproliferative disorders. *PLoS Pathog*. (2014) 10:e1004068. doi: 10.1371/journal.ppat.1004068
62. Chijioke O, Marcenaro E, Moretta A, Capaul R, Münz C. The SAP-dependent 2B4 receptor mediates CD8^{+} T cell dependent immune control of Epstein Barr virus infection in mice with reconstituted human immune system components. *J Infect Dis*. (2015) 212:803–7. doi: 10.1093/infdis/jiv114
63. Danisch S, Slabik C, Cornelius A, Albanese M, Tagawa T, Chen YA, et al. Spatiotemporally skewed activation of programmed cell death receptor 1-positive T cells after Epstein-Barr virus infection and tumor development in long-term fully humanized mice. *Am J Pathol*. (2019) 189:521–39. doi: 10.1016/j.ajpath.2018.11.014
64. Leong YA, Chen Y, Ong HS, Wu D, Man K, Deleage C, et al. CXCR5^{+} follicular cytotoxic T cells control viral infection in B cell follicles. *Nat Immunol*. (2016) 17:1187–96.
65. Johnson DB, McDonnell WJ, Gonzalez-Ericsson PI, Al-Rohil RN, Mobley BC, Salem JE, et al. A case report of clonal EBV-like memory CD4^{+} T cell activation in fatal checkpoint inhibitor-induced encephalitis. *Nat Med*. (2019) 25:1243–50. doi: 10.1038/s41591-019-0523-2
66. Ma SD, Xu X, Jones R, Delecluse HJ, Zumwalde NA, Sharma A, et al. PD-1/CTLA-4 blockade inhibits Epstein-Barr virus-induced lymphoma growth in a cord blood humanized-mouse model. *PLoS Pathog*. (2016) 12:e1005642. doi: 10.1371/journal.ppat.1005642
67. Murer A, Ruhl J, Zbinden A, Capaul R, Hammerschmidt W, Chijioke O, et al. MicroRNAs of Epstein-Barr virus attenuate T-cell-mediated immune control in vivo. *MBio*. (2019) 10:e01941-18.
68. Ma SD, Xu X, Plowshay J, Ranheim EA, Burlingham WJ, Jensen JL, et al. LMP1-deficient Epstein-Barr virus mutant requires T cells for lymphomagenesis. *J Clin Invest*. (2015) 125:304–15. doi: 10.1172/jci76357
69. Rühl J, Leung CS, Münz C. Vaccination against the Epstein-Barr virus. *Cell Mol Life Sci*. (2020) 1–10. doi: 10.1007/s00018-020-03538-3
70. Taylor GS, Haigh TA, Gudgeon NH, Phelps RJ, Lee SP, Steven NM, et al. Dual stimulation of Epstein-Barr Virus (EBV)-specific CD4^{+}- and CD8^{+}-T-cell responses by a chimeric antigen construct: potential therapeutic vaccine for EBV-positive nasopharyngeal carcinoma. *J Virol*. (2004) 78:768–78. doi: 10.1128/jvi.78.2.768-778.2004
71. Taylor GS, Jia H, Harrington K, Lee LW, Turner J, Ladell K, et al. A recombinant modified vaccinia Ankara vaccine encoding Epstein-Barr virus (EBV) target antigens: a phase I trial in UK patients with EBV-positive cancer. *Clin Cancer Res*. (2014) 20:5009–22. doi: 10.1158/1078-0432.ccr-14-1122-t
72. Hui EP, Taylor GS, Jia H, Ma BB, Chan SL, Ho R, et al. Phase I trial of recombinant modified vaccinia Ankara encoding Epstein-Barr viral tumor antigens in nasopharyngeal carcinoma patients. *Cancer Res*. (2013) 73:1676–88. doi: 10.1158/0008-5472.can-12-2448
73. Smith C, Tsang J, Beagley L, Chua D, Lee V, Li V, et al. Effective treatment of metastatic forms of Epstein-Barr virus-associated nasopharyngeal carcinoma with a novel adenovirus-based adoptive immunotherapy. *Cancer Res*. (2012) 72:1116–25. doi: 10.1158/0008-5472.can-11-3399
74. Rühl J, Citterio C, Engelmann C, Haigh TA, Dzionek A, Dreyer JH, et al. Heterologous prime-boost vaccination protects from EBV antigen expressing lymphomas. *J Clin Invest*. (2019) 129:2071–87. doi: 10.1172/jci125364
75. Gurer C, Strowig T, Brilot F, Pack M, Trumpfheller C, Arrey F, et al. Targeting the nuclear antigen 1 of Epstein Barr virus to the human endocytic receptor DEC-205 stimulates protective T-cell responses. *Blood*. (2008) 112:1231–9. doi: 10.1182/blood-2008-03-148072
76. Meixlsperger S, Leung CS, Ramer PC, Pack M, Vanoaica LD, Breton G, et al. CD141^{+} dendritic cells produce prominent amounts of IFN-alpha after dsRNA recognition and can be targeted via DEC-205 in humanized mice. *Blood*. (2013) 121:5034–44. doi: 10.1182/blood-2012-12-473413

77. van Zyl DG, Tsai MH, Shumilov A, Schneidt V, Poirey R, Schlehe B, et al. Immunogenic particles with a broad antigenic spectrum stimulate cytolytic T cells and offer increased protection against EBV infection ex vivo and in mice. *PLoS Pathog*. (2018) 14:e1007464. doi: 10.1371/journal.ppat.1007464
78. Douam F, Ziegler CGK, Hrebikova G, Fant B, Leach R, Parsons L, et al. Selective expansion of myeloid and NK cells in humanized mice yields human-like vaccine responses. *Nat Commun*. (2018) 9:5031.
79. Li Y, Masse-Ranson G, Garcia Z, Bruel T, Kok A, Strick-Marchand H, et al. A human immune system mouse model with robust lymph node development. *Nat Methods*. (2018) 15:623–30. doi: 10.1038/s41592-018-0071-6
80. Salguero G, Daenthanasanmak A, Münz C, Raykova A, Guzman CA, Riese P, et al. Dendritic cell-mediated immune humanization of mice: implications for allogeneic and xenogeneic stem cell transplantation. *J Immunol*. (2014) 192:4636–47. doi: 10.4049/jimmunol.1302887
81. Grant ML, Bollard CM. Cell therapies for hematological malignancies: don't forget non-gene-modified t cells! *Blood Rev*. (2018) 32:203–24. doi: 10.1016/j.blre.2017.11.004

Conflict of Interest: The author declares that the research was conducted in the absence of any commercial or financial relationships that could be construed as a potential conflict of interest.

Copyright © 2020 Münz. This is an open-access article distributed under the terms of the Creative Commons Attribution License (CC BY). The use, distribution or reproduction in other forums is permitted, provided the original author(s) and the copyright owner(s) are credited and that the original publication in this journal is cited, in accordance with accepted academic practice. No use, distribution or reproduction is permitted which does not comply with these terms.

frontiers in Immunology

ORIGINAL RESEARCH
published: 07 October 2020
doi: 10.3389/fimmu.2020.532684

Improved Detection of *in vivo* Human NK Cell-Mediated Antibody-Dependent Cellular Cytotoxicity Using a Novel NOG-FcγR-Deficient Human IL-15 Transgenic Mouse

Ikumi Katano[1], *Ryoji Ito*[1], *Kenji Kawai*[2] *and Takeshi Takahashi*[1]*

[1] Laboratory Animal Research Department, Central Institute for Experimental Animals (CIEA), Kawasaki, Japan, [2] Pathological Analysis Center, Central Institute for Experimental Animals (CIEA), Kawasaki, Japan

OPEN ACCESS

Edited by:
Tim Willinger,
Karolinska Institutet, Sweden

Reviewed by:
Anthony Rongvaux,
Fred Hutchinson Cancer Research Center, United States
Nicholas D. Huntington,
Walter and Eliza Hall Institute of Medical Research, Australia

***Correspondence:**
Takeshi Takahashi
takeshi-takahashi@ciea.or.jp

Specialty section:
This article was submitted to Cancer Immunity and Immunotherapy, a section of the journal Frontiers in Immunology

Received: 05 February 2020
Accepted: 07 September 2020
Published: 07 October 2020

Citation:
Katano I, Ito R, Kawai K and Takahashi T (2020) Improved Detection of in vivo Human NK Cell-Mediated Antibody-Dependent Cellular Cytotoxicity Using a Novel NOG-FcγR-Deficient Human IL-15 Transgenic Mouse. Front. Immunol. 11:532684. doi: 10.3389/fimmu.2020.532684

We generated an NOD/Shi-*scid*-IL2Rγ^{null} (NOG) mouse deficient for the *Fcer1g* and *Fcgr2b* genes (NOG-FcγR$^{-/-}$ mice), in which monocytes/macrophages do not express activating (FcγRI, III, and IV) or inhibitory (FcγRIIB) Fcγ receptors. Antibody-dependent cellular cytotoxicity (ADCC) by innate immune cells was strongly reduced in this strain. Thus, while the growth of xenogeneic human tumors engrafted in conventional NOG mice was suppressed by innate cells upon specific antibody treatment, such growth inhibition was abrogated in NOG-FcγR$^{-/-}$ mice. Using this novel strain, we further produced NOG-FcγR$^{-/-}$-mice expressing human IL-15 (NOG-FcγR$^{-/-}$-hIL-15 Tg). The mice inherited unique features from each strain, i.e., the long-term sustenance of human natural killer (NK) cells, and the elimination of mouse innate cell-mediated ADCC. As a result, segregation of human NK cell-mediated ADCC from mouse cell-mediated ADCC was possible in the NOG-FcγR$^{-/-}$-hIL-15 Tg mice. Our results suggest that NOG-FcγR$^{-/-}$-hIL-15 Tg mice are useful for validating the *in vivo* function of antibody drug candidates.

Keywords: humanized mice, NK cell, FcγR, ADCC, mouse innate immunity

INTRODUCTION

Antibody-dependent cellular cytotoxicity (ADCC) by natural killer (NK) cells has been considered a critical mechanism in antibody therapy for various malignant diseases, including hematopoietic malignancies and some solid tumors (1). Advances in technology have dramatically accelerated the development of various types of novel antibody (2–4), whereas there are few *in vivo* animal models to use to validate candidates in terms of pharmacokinetics (5) and pharmacodynamics, as they are directed against human antigens and are often developed in the form of humanized or even human IgG molecules. The absence of target antigens in conventional mouse models has limited the progress of drug discovery. Xenograft models in immune-deficient mice or genetically manipulated mice, which express human antigens (6) as surrogate targets, have been employed as *in vivo* models. However, they do not always assure faithful extrapolation to human situations, because

such models lack human effectors cells, including NK cells or T cells. Thus, innovative experimental animal models are sought to enable the accurate predictions of drug efficacy and effects on human cells and tissues.

Humanized mice, which stably and autonomously maintain human tissues, have attracted significant attention (7–9). Extremely immunodeficient mice, such as NOD/Shi-*scid*-IL2Rγ^{null} (NOG) (10), NOD/LtSz-scid IL-2Rγ^{null} (NSG) (11), or BALB-RAG2$^{-/-}$-IL-2Rγ$^{-/-}$ double knockout (BRG) mice (12) or the derivative strain, BRG-human signal-regulatory protein α (SIRPA) (BRGS) (13), are among the best platforms for the reconstitution of human hematopoietic and immune systems, by transplantation of human hematopoietic stem cells (HSCs) or human peripheral blood mononuclear cells (PBMCs). Application of these mice in the evaluation of ADCC has also been attempted (14–16). Our group previously reported that two NOG variant strains, that express either human IL-2 (hIL-2) or human IL-15 (hIL-15); NOG-hIL-2 transgenic (Tg) or NOG-hIL-15 Tg, respectively, are suitable for human NK cell development (17) and/or long-term persistence of human NK cells (18). These human NK cells suppress human tumor growth *in vivo* by cognate or therapeutic antibody-dependent mechanisms (17, 18). In the course of studies using various therapeutic and research antibodies, however, we have realized that tumor growth is significantly suppressed by antibody treatment alone in some cases, even in the absence of human NK cells. Thus, the capability of antibodies to induce human NK-cell mediated ADCC is often masked by this background effect.

In this study, we established an NOG-FcγR deficient (NOG-FcγR$^{-/-}$) strain. While administered therapeutic antibody in NOG mice was mainly captured by innate cells, primarily neutrophils and monocytes/macrophages, this did not occur in NOG-FcγR$^{-/-}$ mice. Accordingly, innate cell-mediated ADCC was strongly suppressed in NOG-FcγR$^{-/-}$ mice. Furthermore, we generated an NOG-FcγR$^{-/-}$-hIL-15 Tg mouse, and demonstrated that specific detection of human NK cell-mediated ADCC was possible, suppressing interference from mouse innate cells.

MATERIALS AND METHODS

Mice

NOG, NOG-hIL-15 Tg [formally NOD.Cg-*Prkdc*^{scid}*il2rg*^{tm1Sug} *Tg (CMV-IL15)1 Jic*/Jic] (18), and NOG-FcγR$^{-/-}$ mice were used in this study. These strains were maintained in the Central Institute for Experimental Animals (CIEA) under specific pathogen-free conditions. To generate NOG-FcγR$^{-/-}$ mice, frozen embryos of NOD.Cg-Fcer1g$^{<tm1Rav>}$ Fcgr2b$^{<tm1Ttk>}$ were obtained from RIKEN BRC (RBRC02330, Tsukuba, Japan) (19). The mice were backcrossed with NOG mice to introduce the *scid* mutation and the IL-2Rγc targeted allele (20). NOG-hIL-15 Tg and NOG-FcγR$^{-/-}$ mice were crossed to produce NOG-FcγR$^{-/-}$-hIL-15 Tg mice. All experiments were performed in accordance with institutional guidelines (14038, 17025, 20044), which were approved by the Animal Experimentation Committee of CIEA.

Reagents

Antibodies for flow cytometric analyses were as follows.

For staining mouse cells, anti-FcεRIα-fluorescent isothiocyanate (FITC; clone, Mar-1), anti-CD64 (FcγRI)-Phycoerythrin (PE; X54-5/7.1), anti-F4/80-PE (BM8), anti-CD16/32 (FcγRIII/II)-PE/Cyanine 7 (Cy7; 93), anti-Gr-1-Allophycocyanin (APC; RB6-8C5), and anti-CD45- APC/Cy7 (30-F11) were from Biolegend (San Diego, CA). For human NK cell staining, anti-CD45-Brilliant Violet (BV) 510 (HI30), anti-CD3-BV421 (UCHT1), anti-CD56-AlexaFluor700 (HCD56), anti-CD56-PE/Cy7 (HCD56), anti-CD16-BV605 (3G8), and anti-CD335 (NKp46)-PE (9E2) were from Biolegend. Anti-CD19-BUV395 (SJ25C1), anti-CD14-APC/Cy7 (HCD14), and anti-CD314 (NKG2D)-APC (1D11) were from BD Biosciences (San Jose, CA). For detecting human IgG captured by mouse cells, anti-human IgG-FITC (G18-145, BD Biosciences) was used.

Anti-HER2 antibody (Trastuzumab, Herceptin®) and anti-CD20 antibody (Rituximab, Rituxan®) were purchased from Chugai (Tokyo, Japan). Anti-CCR4 antibody (Mogamulizumab, Poteligeo®) was from Kyowa-Kirin (Tokyo, Japan).

Flow Cytometry

Spleen cells were prepared by smashing the tissues between two glass slides and filtration over nylon mesh. Red blood cells (RBCs) were lysed with RBC lysing solution (Pharm Lyse; BD Biosciences). After washing, the cell pellet was resuspended in PBS containing 0.1% bovine serum albumin (BSA). Bone marrow (BM) cells were recovered by flushing femurs with PBS + 0.5% BSA. After debris removal over nylon mesh and centrifugation, the pellets were resuspended in 1 mL PBS + 0.1% BSA. Thus, prepared single mononuclear cell suspensions were stained with the indicated antibodies in fluorescence-activated cell sorting (FACS) buffer (PBS containng 0.1% BSA and 0.05% NaN_3) for 30 min at 4°C in the dark. After washing in FACS buffer, cells were resuspended in FACS buffer containing propidium iodide (PI) and subsequently subjected to multicolor flow cytometric analyses on a FACSCanto or Fortessa instrument (BD Biosciences). The data were analyzed using FACSDiva software (ver. 6.0.4 or 8.0.3; BD Biosciences) or FlowJo™ (ver10; BD Biosciences).

Quantification of Immunoglobulin by Enzyme-Linked Immunosorbent Assay (ELISA)

The levels of human IgG or mouse IgG in the plasma of mice injected with therapeutic or control antibodies, respectively, were determined using ELISA kits from Bethyl Laboratories (Human IgG or Mouse IgG ELISA Quantitation Sets, Montgomery, TX) according to the manufacturer's protocol. Peripheral blood (PB) was collected at the indicated time points from the retro-orbital venous plexus after anesthetization of mice with isoflurane. The plasma was recovered by centrifugation (400 g × 10 min) and subjected to ELISA.

To determine the levels of human IL-15 or mouse IL-15 in mouse plasma, we used a LEGEND MAX™ Human IL-15 ELISA

kit (Biolegend) or mouse IL-15 DuoSet® ELISA (R&D systems, Inc., Minneapolis, MN), respectively.

Cell Culture

Daudi ($CD20^+$ Burkitt lymphoma) and 4–1ST ($HER\text{-}2^+$ gastric cancer) (21, 22) cell lines were used in this study. Daudi cells were cultured in complete RPMI-1640 medium (Gibco, Grand Island, NY, USA) with 10% FCS and antibiotics (penicillin-streptomycin, Gibco). The 4–1ST cells were maintained by serial transplantation in NOG mice, i.e., a 2–3 mm^3 piece of tumor was excised from an established tumor by razor blade and inoculated into the flank of a new recipient mouse under anesthesia.

Human NK cells were expanded using BINKIT® (Biotherapy Institute of Japan inc., Tokyo, Japan), according to the manufacturer's instructions. Briefly, 25 mL peripheral blood was collected from donors after obtaining informed consent. Total PBMCs were separated over a density gradient, using Lymphoprep™ (Alere Technologies AS, Oslo, Norway) and subsequent washing. We used BINKIT to culture 8.5 $\times 10^7$ PBMC (containing about 2.5 $\times 10^7$ NK cells). After 15 days expansion, cultured NK cells were purified by negative sorting, using a human $CD56^+$ NK cell isolation kit and magnetic cell separation (MACS, Miltenyi Biotec, Bergisch Gladbach, Germany). The degree of amplification of NK cells was about 18-fold. The expanded cells were frozen in Cell Banker1® (Takara, Shiga, Japan) and cryopreserved in a LN2 tank. For *in vivo* transplantation, thawed NK cells were further purified by eliminating human $CD3^+$ T cells (EasySep™ Human CD3 positive selection kit II, STEMCELL™ technologies, Vancouver, Canada). Typical purity after sorting was more than 99%, and the cells included $CD56^+$ $CD16^+$ $NKp46^+$ $NKG2D^+$, with few $CD3^+$ human T cells (**Supplementary Figure 1**).

In vivo Tumor Transplantation Model

NOG-$FcγR^{+/-}$ and NOG-$FcγR^{-/-}$ mice were inoculated subcutaneously in the flank with 4–1ST cells as mentioned above. Antibody treatment was begun at 7 days post inoculation. Anti-HER2 antibody (Trastuzumab, 50 μg) was injected i.p. twice per week for 2 weeks. Tumor size was measured every week using a caliper and calculated using the following formula: tumor volume (mm^3) = 1/2 × length (mm) × [width (mm)]^2.

For experiments using Daudi cells and anti-CD20 antibody (Rituximab), mice were transplanted with 1.5 × 10^6 Daudi cells via tail vein (day 0) and injected i.p. with 50 μg Rituximab once per week over 3 weeks. In some experiments, *in vitro* expanded NK cells (5 × 10^6) were transplanted twice, on days 3 and 10. The engraftment of Daudi cells was monitored every week by flowcytometry of peripheral blood samples.

Immunohistochemistry and Pathological Examination

Kidneys from Daudi-bearing mice were fixed in 10% neutralized formalin (Mildform, FUJIFILM Wako Pure Chemical, Osaka, Japan). Formalin-fixed tissues were embedded in paraffin and analyzed by either hematoxylin-eosin staining (H&E) or immunohistochemistry. Staining of sections with mouse monoclonal anti-human CD20 (clone L26, Leica Microsystems, Tokyo, Japan) was performed on a fully automated BOND-MAX system (Leica Biosystems, Mount Waverley, VIC, Australia). The images of two or four independent cross-sections from one kidney were captured by a Nanozoomer S60 (Hamamatsu Photonics, Hamamatsu, Japan) and the degree of Daudi dissemination in the kidney was quantified using Image J.

Statistics

The statistical significance was determined by Prism software (ver.7, GraphPad Prism, San Diego, CA).

RESULTS AND DISCUSSION

Establishment of NOG-$FcγR^{-/-}$ Mice

NOG mice and NOD-$FcγR^{-/-}$ mice were crossed to introduce the defective mutations in both alleles of the *scid, IL-2rg, Fcer1g, and Fcgr2b* loci. FcεRIγ (FcR common γ) is the common subunit for FcγRI, III, and IV, and its deficiency leads to the absence of expression of FcγRI, III, and IV (23, 24). Due to the additional absence of FcγRIIB, NOG-$FcγR^{-/-}$ mice had no expression of any mouse FcγR. Indeed, flow cytometric analyses of spleen cells and PB confirmed the absence of mouse FcγRI (CD64), FcγRIII/II (CD16/32), and FcεRIα in the mononuclear cells of NOG-$FcγR^{-/-}$ mice, while those present in NOG or NOG-$FcγR^{+/-}$ mice (**Figures 1A,B**).

To establish that there was functional FcγR deficiency, we administered 100 μg Trastuzumab (anti-HER-2 antibody, human IgG1) into NOG-$FcγR^{+/-}$ and NOG-$FcγR^{-/-}$ mice by intraperitoneal injection. Analyses of PB 3 days after injection showed that a significant amount of human IgG was present on the surface of about 15% of mouse $CD45^+$ cells in NOG-$FcγR^{+/-}$ mice, and that these consisted of about 75% mouse neutrophils and 25% mouse macrophages/monocytes. In contrast, such human IgG was not detected in NOG-$FcγR^{-/-}$ mice (**Figure 1C**), although the composition of mouse neutrophils and macrophages/monocytes was not different between the two strains (**Figure 1D**). This suggests that Trastuzumab was captured by FcγR on mouse phagocytic cells, including neutrophils and monocytes/macrophages.

We also measured the half-life of human IgG in NOG-$FcγR^{-/-}$ mice, as a recent report demonstrated that Fc-FcγR interaction is a determinant for the rapid clearance of antibody in NOG or NSG (25). Doses (100 μg) of Rituximab (anti-CD20, human IgG1), Trastuzumab, or Mogamulizumab (anti-CCR4, human IgG1) were injected i.p. and levels of human IgG were monitored over 4 weeks. A plateau level of human IgG was maintained for 1 week, but rapidly decreased over the following week and became undetectable after about 2 weeks after injection. The rapid clearance of human IgG was not different between NOG-$FcγR^{+/-}$ and NOG-$FcγR^{-/-}$ mice. This result markedly contrasts with the long-term circulation of mouse IgG1 (MOPC-21) in PB, which persisted beyond 12 weeks (**Supplementary Figure 2**). Hence, our results demonstrate that mouse FcγR molecules are not involved in the pharmacokinetics of human IgG antibody. Another Fc receptor, neonatal FcR

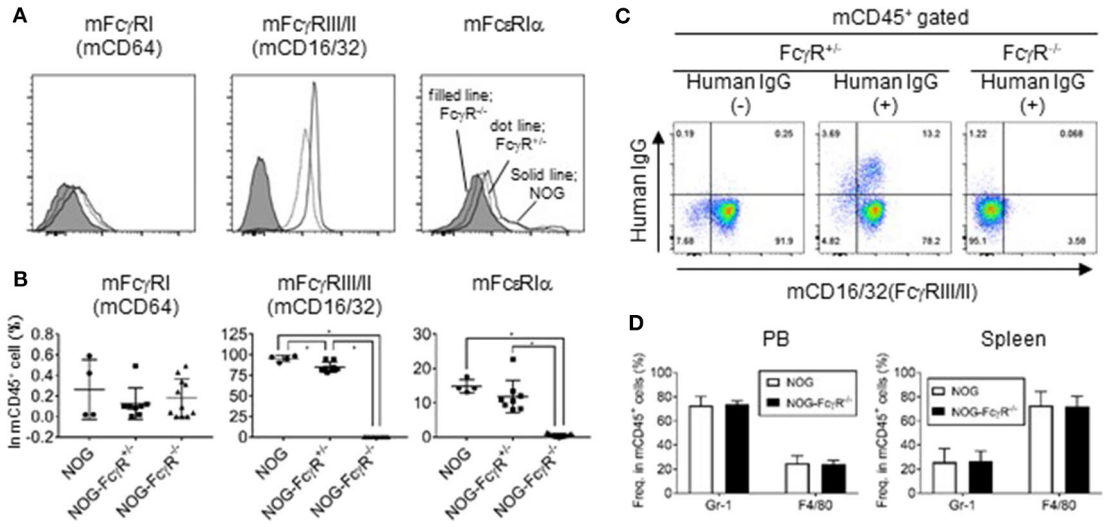

FIGURE 1 | Absence of FcγR in leukocytes of NOG-FcγR$^{-/-}$ mice. **(A)** Spleen cells from NOG, NOG-FcγR$^{+/-}$, and NOG-FcγR$^{-/-}$ mice were stained with the indicated antibodies and analyzed by flow cytometry. Representative FACS histograms for mouse FcγRI (CD64), FcγRIII/II (CD16/32), and FcεRIα. Solid line for NOG, dotted line for NOG-FcγR$^{+/-}$ and filled histogram for NOG-FcγR$^{-/-}$ mice. **(B)** The frequencies of FcR-positive cells among total mononuclear cells are plotted for NOG ($n = 4$), NOG-FcγR$^{+/-}$ ($n = 8$), and NOG-FcγR$^{-/-}$ mice ($n = 11$). **(C)** Failure of mouse monocytes from NOG-FcγR$^{-/-}$ mice to capture human IgG. Trastuzumab (100 μg anti-HER-2 human IgG) was injected i.p. into NOG-FcγR$^{+/-}$ and NOG-FcγR$^{-/-}$ mice. Mononuclear cells prepared from peripheral blood (PB) 3 days after administration were stained with anti-human IgG, together with anti-mouse CD45 and CD16/32 antibodies for gating. Representative FACS plots are from three independent experiments. **(D)** Frequencies of mouse Gr-1^{+} neutrophils and F4/80^{+} macrophage/monocytes in peripheral blood (PB) and spleen. Means ± SDs are shown for NOG mice ($n = 7$ for PB and $n = 4$ for spleen) and NOG-FcγR$^{-/-}$ mice ($n = 7$ for PB and $n = 4$ for spleen). Asterisks indicate the statistical significance by one-way ANOVA (*$p < 0.001$).

(FcRn), may be more relevant to the maintenance of human IgG proteins in mice (5, 26, 27).

Antibody-Dependent Cytotoxic Effects of Innate Cells in NOG Mice

Attempts to detect human NK-cell specific ADCC activity have often been confounded by regression of tumors after antibody treatment. For example, in our study, when a gastric cancer-derived HER-2^{+} cell line, 4–1ST, was inoculated into NOG mice and subsequently treated with Trastuzumab, tumor growth was strongly suppressed (**Figure 2A**). Interestingly, the inhibition of 4–1ST tumor growth was totally abrogated in NOG-FcγR$^{-/-}$ mice (**Figure 2A**, **Supplementary Table 1**, **Supplementary Figure 3**). In another model, when we intravenously transplanted the CD20^{+} Daudi Burkitt lymphoma cell line in NOG- FcγR$^{+/-}$ mice, Rituximab treatment alone strongly suppressed swelling in kidneys, where Daudi preferentially accumulates and forms colonies (**Figures 2B,C**). In contrast, the degree of the suppression of Daudi growth by Rituximab treatment in NOG-FcγR$^{-/-}$ mice was reduced to about 30–40% of the level in NOG- FcγR$^{+/-}$ mice (**Figure 2C**, **Supplementary Table 2**). This was also confirmed by immunohistochemistry using anti-CD20 antibody (data not shown). These results suggest that innate cells in mice, which include macrophages and neutrophils, actively killed human tumor cells by antibody-dependent mechanisms through the mouse FcγR molecules, and that NOG-FcγR$^{-/-}$ mice were useful for eliminating these endogenous effects.

Specific Detection of Human NK-Cell Mediated ADCC in NOG-FcγR$^{-/-}$-hIL-15 Tg Mice

Previously, our group established NOG-hIL-2 Tg and NOG-hIL-15 Tg strains, which supported the development of human NK cells and the long-term persistence of human NK cells, respectively. These models are useful for examining the capacity of antibody drugs to activate human NK cells to induce ADCC. However, our results suggest that this ADCC involves two types of effector cells, human NK cells and mouse innate phagocytic cells. To segregate these two components, we generated NOG-FcγR$^{-/-}$-hIL-15 Tg mice. The level of human IL-15 in NOG-FcγR$^{-/-}$-hIL-15 Tg mice was comparable to that in NOG-hIL-15 Tg mice, and the period of persistence of human NK cells was not different between these strains (**Supplementary Figure 4**).

Next, we examined whether human NK-cell mediated ADCC was specifically detected in the new strain. Mice were inoculated with Daudi cells and subsequently subjected to three different therapeutic protocols: human NK cells, Rituximab, or a combination of the two (**Figure 3A**). When we used NOG or NOG-FcγR$^{-/-}$ mice, transferred human NK cells were rapidly lost, and we could not detect protective effects in any of the mice (data not shown). When we compared NOG-hIL-15 Tg and NOG-FcγR$^{-/-}$-hIL-15 Tg mice, transfer of human NK cells alone did not induce tumor suppression in either strain, as shown by increases of kidney weight (**Figure 3B**). As in NOG mice, Rituximab treatment strongly inhibited kidney swelling in NOG-hIL-15 Tg mice, and this inhibition

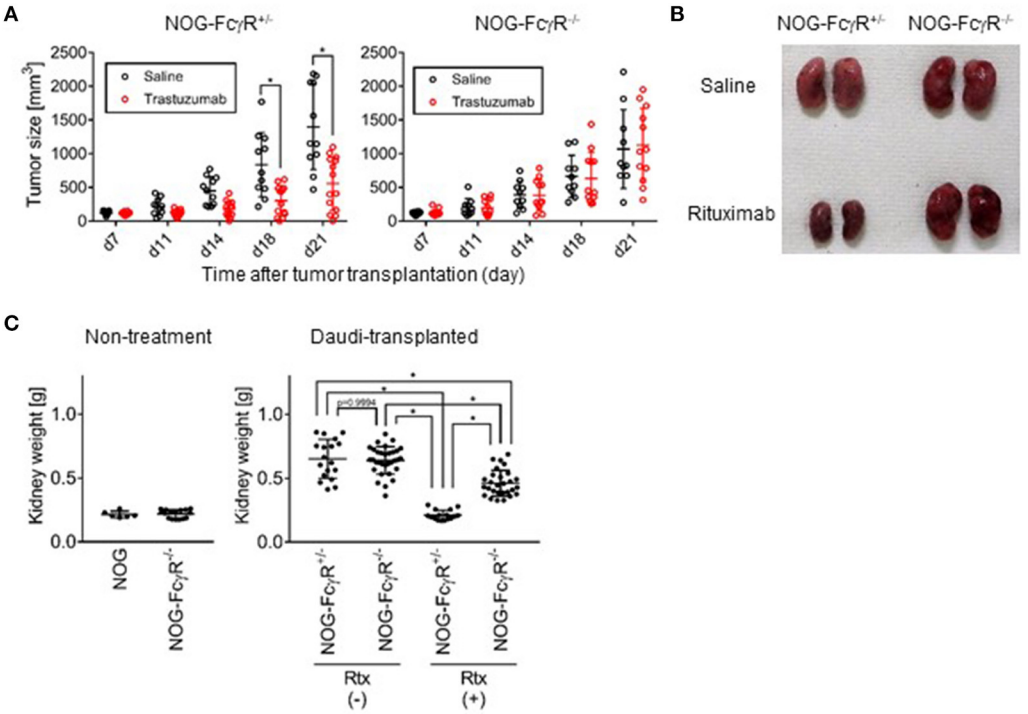

FIGURE 2 | Abrogation of mouse innate cell mediated antibody dependent cytotoxicity in NOG-FcγR$^{-/-}$ mice. **(A)** NOG-FcγR$^{+/-}$ or NOG-FcγR$^{-/-}$ mice were subcutaneously transplanted with a 2–3mm^3 piece of 4–1ST tumor on day 0, and administered 50 μg Trastuzumab or saline by i.p. injection twice per week over 2 weeks starting from day 7. The tumor volume from individual mice is plotted with the average. NOG-FcγR$^{+/-}$ ($n = 11$ or 14 for saline- or Trastuzumab-treated mice, respectively) or NOG-FcγR$^{-/-}$ mice ($n = 10$ or 12 for saline- or Trastuzumab-treated, respectively); bars represent SD. Cumulative data from three independent experiments are shown. Asterisks indicate statistical significance by a repeated measure ANOVA with Sidak's multiple comparison test (*$p < 0.0001$, All the raw data, statistics, and plots of tumor sizes in each experiment are available in **Supplementary Table 1**). **(B)** NOG-FcγR$^{+/-}$ or NOG-FcγR$^{-/-}$ mice received 1.5×10^6 Daudi cells intravenously, and 50 μg Rituximab or saline was injected i.p. on days 7, 14, and 21. The image shows representative kidneys resected from the indicated mice at day 23. **(C)** Plots of kidney weight from individual mice with mean ± SD for the indicated groups: normal NOG ($n = 3$), NOG-FcγR$^{-/-}$ mice ($n = 8$), Daudi-engrafted NOG-FcγR$^{+/-}$ ($n = 9$ or 8 for saline- or Rituximab-treated mice, respectively from two independent experiments), and Daudi-engrafted NOG-FcγR$^{-/-}$ mice ($n = 16$ or 14 for saline- or Rituximab-treated mice from four or three independent experiments, respectively). Asterisks indicate statistical significance by two-way ANOVA with Sidak's multiple comparison test (*$p < 0.0001$, All the raw data and statistics are available in **Supplementary Table 2**).

was evident irrespective of the presence of human NK cells (**Figure 3B**, left). In contrast, in NOG-FcγR$^{-/-}$-hIL-15 Tg mice, the combined therapy of human NK cells and Rituximab induced significant reductions in kidney weight compared to saline -treated or NK-cell transferred group. Rituximab-treated mice showed intermediate reduction in kidney weight and there was no statistical significance between this group and the combined therapy group (**Figure 3B**, right, **Supplementary Table 3**, **Supplementary Figure 5**). Immunohistochemical analyses also gave the consistent results (**Figures 3C,D**, **Supplementary Table 4**, **Supplementary Figure 6**). It was interesting, however, the image analysis of the multiple sections from immunohistochemistry demonstrated that the mice with combined therapy showed further enhanced suppression of Daudi when compared to the rituximab-treatment group, suggesting that human NK cells killed Daudi cells through ADCC (**Figures 3C,D**).

Bone marrow (BM) analyses also demonstrated that combined therapy was effective for preventing otherwise devastating BM destruction by Daudi cells. In NOG mice, Daudi cells cause a severe reduction of mouse CD45$^+$ cells in BM by unknown mechanisms (data not shown). In NOG-hIL-15 Tg mice, Rituximab treatment rescued mouse CD45$^+$ cells, irrespective of NK-cell transplantation, and mice without treatment or mice who received human NK cell transfer alone showed severe reductions in mouse CD45$^+$ cells (**Figure 3E**). On the other hand, in NOG-FcγR$^{-/-}$-hIL-15 Tg mice, only the group that received combined therapy avoided the destruction of BM (**Figure 3E**). These results suggest that specific detection of human NK cell-mediated ADCC is possible in this novel mouse strain.

Along with advances in antibody technology, the development of animal models providing "a proof of concept" for drug candidates has been urgently needed. In this study, we used Rituximab and Trastuzumab, which are specific for human CD20 and HER-2, respectively. We found that NOG-FcγR$^{-/-}$ mice protected tumor cells from mouse innate cell-mediated cytotoxicity after antibody treatment. It is important to note that such cytotoxicity by innate cells in mice would affect various combinations of antibody and target cells, and that

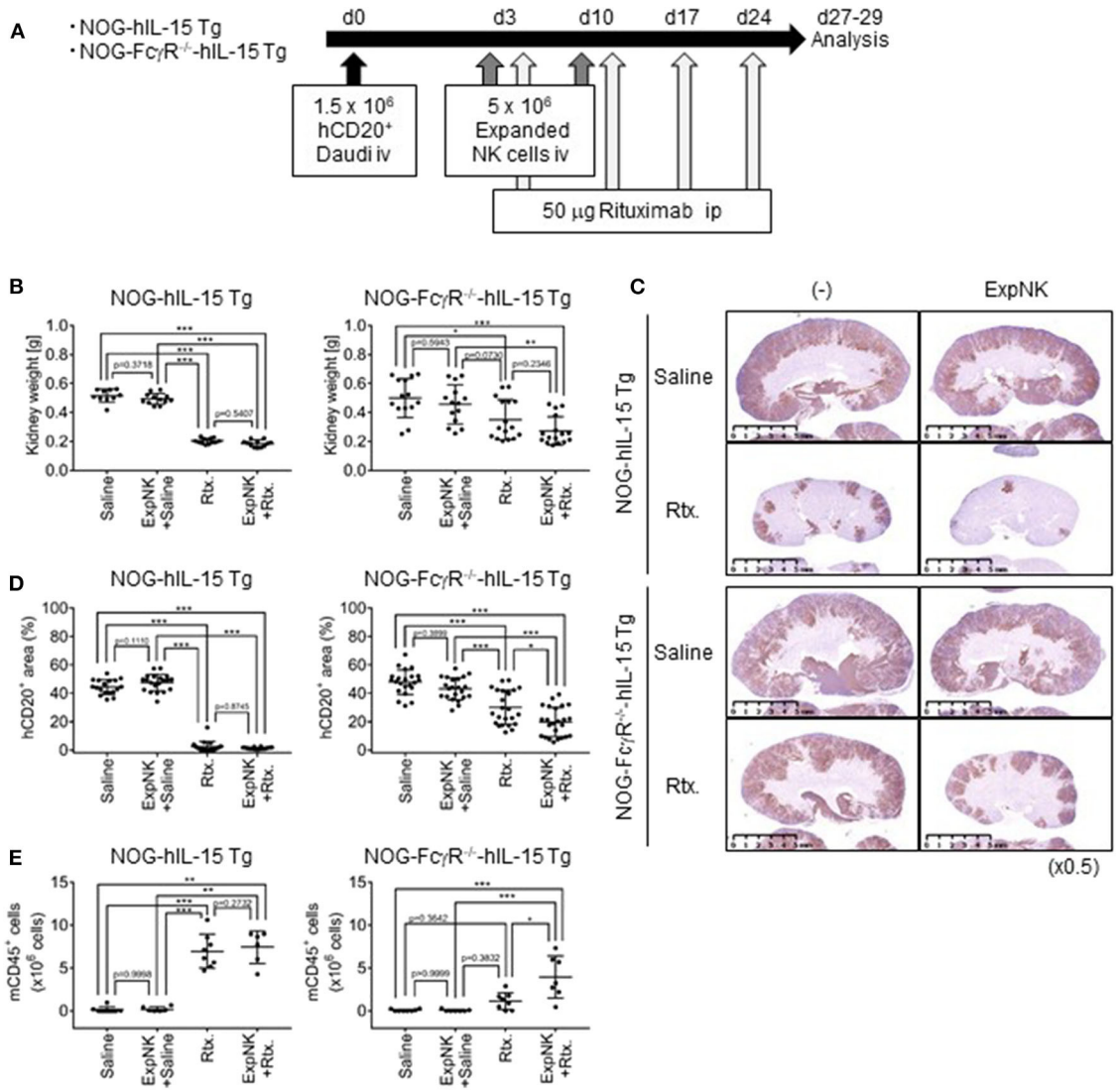

FIGURE 3 | Specific detection of human NK cell-mediated ADCC in NOG-FcγR$^{-/-}$-hIL-15 Tg mice. **(A)** Schema of experiments. NOG-hIL-15 Tg and NOG-FcγR$^{-/-}$-hIL-15 Tg male mice received 1.5 × 10^6 Daudi cells i.v., followed by 5 × 10^6 *in vitro* expanded human NK cells at days 3 and 10. Rituximab (50 μg) was administered once per week over 3 weeks, starting at day 3; mice were analyzed at days 27 and 29. **(B)** Prevention of kidney swelling in NOG-FcγR$^{-/-}$-hIL-15 Tg mice treated with combined therapy. Kidney weights from individual NOG-hIL-15 Tg (left) or NOG-FcγR$^{-/-}$-hIL-15 Tg (right) mice are plotted with the mean ± SD in each mouse group. The NOG-hIL-15 Tg group consisted of five saline-treated, six NK-treated, six Rituximab-treated, six combined therapy-treated mice. For NOG-FcγR$^{-/-}$-hIL-15 Tg, seven saline-treated, seven NK-treated, eight Rituximab-treated, eight combined therapy-treated mice. **(C)** Immunohistochemistry of kidneys from Daudi bearing mice in **(B)**. Tumors in kidney were detected using anti-CD20 antibody. Representative images are shown. **(D)** Quantification of Daudi dissemination by image analyses. **(E)** Prevention of BM destruction in NOG-FcγR$^{-/-}$-hIL-15 Tg mice with combined therapy. The absolute numbers of mouse CD45$^+$ cells in BM from individual mice are plotted with means and SDs. Cumulative results from two independent experiments are shown. Asterisks indicate the statistical significance by two-way ANOVA with Tukey's multiple comparisons test (*$p < 0.005$, **$p < 0.001$, ***$p < 0.0001$, All the raw data and statistics are available in **Supplementary Tables 3, 4**).

the degree of cytotoxicity is often difficult to predict for *in vivo* settings. For example, when we previously used an L428 cell line and anti-CCR4 antibody (Mogamulizumab), we found modest influences on cell growth (17). In addition, our previous report showed that HER-2-positive NCI-N87 was resistant to Trastuzumab treatment (18) in contrast to 4–1ST in this study. Furthermore, it was demonstrated that the growth of CD20$^+$ Raji cells was not affected by Rituximab in human SIRPA and IL-15 knock-in (SRG-15) mice (16), while another group demonstrated that Raji cells were partially suppressed by Rituximab in NSG mice (28). Those differences in the biological consequences of treatments indicate that sensitivity to antibody drugs is partly determined by the features of immunological interactions between cancer cells and mouse innate cells. In the presence of antibody drugs, resistant cells like NCI-N87 and Raji may avoid mouse innate immunity by some mechanisms such as

providing inhibitory signals, absence of stimulatory molecules, or expressing protective molecules, whereas susceptible tumor cell lines like 4–1ST or Daudi may strongly activate mouse innate cells through various molecules including FcγR. Interestingly, the degree of dependency on FcγR was different between 4–1ST and Daudi. The killing of 4–1ST was almost totally dependent on FcγR. In contrast, the partial suppression of Daudi by Rituximab in NOG-FcγR$^{-/-}$-hIL-15 Tg mice suggests that some FcγR-independent killing mechanisms function in this combination. Although the amount of hIL-15 in NOG-hIL-15Tg mice was much higher than that of the level of endogenous mIL-15 (**Supplementary Figure 7**), it is not likely that the abundant hIL-15 activates such FcγR-independent mechanisms in mouse innate cells because of the absence of IL-2Rγ in NOG mice to transduce the cytokine signal. One possibility is complement-dependent cytotoxicity (CDC) (29, 30). Although activation of the complement system is incomplete in NOG mice due to a nonsense mutation in the C5 gene (31), other factors like the C3 fragments may mediate the partial elimination of Daudi cells. It was also suggested that the resistance of Raji cells to Rituximab was due to the modest level of CD20 and high levels of CD55 or CD59, both complement regulatory proteins (32). CD59, especially, might prevent the formation of C5-mediated membrane attack complex in SRG-15 mice. Disruption of the C3 or C1q genes in NOG-FcγR$^{-/-}$-hIL-15 Tg mice will clarify the involvement of the complement pathway in the FcγR-independent mechanisms in the future and the development of NOG- FcγR$^{-/-}$/C3$^{-/-}$-, and NOG- FcγR$^{-/-}$/C1q$^{-/-}$-double deficient NOG mice is underway. Those models will be useful for evaluating ADCC in a wide variety of cancer cell lines and patient-derived cell lines (PDX).

Activation of mouse innate cells through FcγR may also be a problem in the development of novel forms of antibody with dual specificity, called bispecific antibodies (BsAbs). BsAbs include molecules with many types of architecture, with or without Fc portions (33), and are expected to have a broad range of functions, such as engaging two different cells or crosslinking different molecules on the surface of a single cell. When BsAbs have an Fc portion with binding capacity for mouse FcRs, the targeted cells could be affected by FcγR-expressing innate cells in mice, and validation of function could be compromised. It is rational to expect that NOG-FcγR$^{-/-}$ mice could improve such situations.

A mouse strain that expresses human FcγRs and lacks all mouse FcγRs has been reported to be useful for antibody development (34, 35). In this strain, human IgG is captured by human FcγRs on mouse cells and activates pharmacodynamic pathways in a way similar to that in humans, although the effector cells are mice. Our NOG-FcγR$^{-/-}$ mice should be able to provide another complementary model, when combined with NOG-hGM-CSF/IL-3 (36) or NOG-hIL-6 Tg mice (37). Because those models can induce development of human myeloid cells from human hematopoietic stem (HSC) cells, human HSC-transplanted NOG-FcγR$^{-/-}$-hGM-CSF/IL-3 Tg or NOG-FcγR$^{-/-}$-hIL-6 Tg mice would reconstitute a wide variety of human FcγR-expressing myeloid cells, together with human lymphocytes, in the absence of mouse FcγRs. The biological function of human IgG drugs could be better examined in these models than in mouse FcγR-competent models.

Finally, antibodies for human target molecules are still often produced in mice for research purposes. Such mouse IgG is easily captured by mouse FcγR molecules and activates mouse phagocytes. In this context, our NOG-FcγR$^{-/-}$ mice would also be useful for small-scale pilot studies to obtain proofs of concept for academic research.

DATA AVAILABILITY STATEMENT

All datasets generated for this study are included in the article/**Supplementary Material**.

ETHICS STATEMENT

The studies involving human participants were reviewed and approved by Research Ethics committee of CIEA. The patients/participants provided their written informed consent to participate in this study. The animal study was reviewed and approved by The Animal Experimentation Committee of CIEA.

AUTHOR CONTRIBUTIONS

IK and TT designed the project and completed the manuscript. IK and RI conducted experiments. KK performed the pathological examinations. All authors contributed to the article and approved the submitted version.

FUNDING

This work was supported in part by a Grant in Aid (B) (18H02368 to TT) and Grant in Aid for young researcher (B) (16K18405 to IK). This project was commissioned by a Grant-in-Aid for Research on Hepatitis from the Japan Agency for Medical Research and Development.

ACKNOWLEDGMENTS

We thank Iyo Ootsuka for her technical assistance and for genotyping the mice. We thank Mika Yagoto and Misa Mochidsuki for contributing their histology expertise, Motohito Goto and Takahiro Kagawa for mouse embryo manipulation, and Kayo Tomiyama and Yasuhiko Ando for their work in animal production and care. We also acknowledge our colleagues at CIEA for their suggestions and helpful discussion.

SUPPLEMENTARY MATERIAL

The Supplementary Material for this article can be found online at: https://www.frontiersin.org/articles/10.3389/fimmu.2020.532684/full#supplementary-material

REFERENCES

1. Wang W, Erbe AK, Hank JA, Morris ZS, Sondel PM. NK cell-mediated antibody-dependent cellular cytotoxicity in cancer immunotherapy. *Front Immunol.* (2015) 6:368. doi: 10.3389/fimmu.2015.00368
2. Weiner GJ. Building better monoclonal antibody-based therapeutics. *Nat Rev Cancer.* (2015) 15:361–70. doi: 10.1038/nrc3930
3. Carter PJ, Lazar GA. Next generation antibody drugs: pursuit of the 'high-hanging fruit'. *Nat Rev Drug Discov.* (2018) 17:197–223. doi: 10.1038/nrd.2017.227
4. Mayes PA, Hance KW, Hoos A. The promise and challenges of immune agonist antibody development in cancer. *Nat Rev Drug Discov.* (2018) 17:509–27. doi: 10.1038/nrd.2018.75
5. Proetzel G, Roopenian DC. Humanized FcRn mouse models for evaluating pharmacokinetics of human IgG antibodies. *Methods.* (2014) 65:148–53. doi: 10.1016/j.ymeth.2013.07.005
6. Zhu F, Nair RR, Fisher EMC, Cunningham TJ. Humanising the mouse genome piece by piece. *Nat Commun.* (2019) 10:1845. doi: 10.1038/s41467-019-09716-7
7. Ito R, Takahashi T, Katano I, Ito M. Current advances in humanized mouse models. *Cell Mol Immunol.* (2012) 9:208–14. doi: 10.1038/cmi.2012.2
8. Shultz LD, Brehm MA, Garcia-Martinez JV, Greiner DL. Humanized mice for immune system investigation: progress, promise and challenges. *Nat Rev Immunol.* (2012) 12:786–98. doi: 10.1038/nri3311
9. Allen TM, Brehm MA, Bridges S, Ferguson S, Kumar P, Mirochnitchenko O, et al. Humanized immune system mouse models: progress, challenges and opportunities. *Nat Immunol.* (2019) 20:770–4. doi: 10.1038/s41590-019-0416-z
10. Ito M, Hiramatsu H, Kobayashi K, Suzue K, Kawahata M, Hioki K, et al. NOD/SCID/gamma(c)(null) mouse: an excellent recipient mouse model for engraftment of human cells. *Blood.* (2002) 100:3175–82. doi: 10.1182/blood-2001-12-0207
11. Ishikawa F, Yasukawa M, Lyons B, Yoshida S, Miyamoto T, Yoshimoto G, et al. Development of functional human blood and immune systems in NOD/SCID/IL2 receptor {gamma} chain(null) mice. *Blood.* (2005) 106:1565–73. doi: 10.1182/blood-2005-02-0516
12. Traggiai E, Chicha L, Mazzucchelli L, Bronz L, Piffaretti JC, Lanzavecchia A, et al. Development of a human adaptive immune system in cord blood cell-transplanted mice. *Science.* (2004) 304:104–7. doi: 10.1126/science.1093933
13. Strowig T, Rongvaux A, Rathinam C, Takizawa H, Borsotti C, Philbrick W, et al. Transgenic expression of human signal regulatory protein alpha in Rag2-/-gamma(c)-/- mice improves engraftment of human hematopoietic cells in humanized mice. *Proc Natl Acad Sci USA.* (2011) 108:13218–23. doi: 10.1073/pnas.1109769108
14. Ito A, Ishida T, Yano H, Inagaki A, Suzuki S, Sato F, et al. Defucosylated anti-CCR4 monoclonal antibody exercises potent ADCC-mediated antitumor effect in the novel tumor-bearing humanized NOD/Shi-scid, IL-2Rgamma(null) mouse model. *Cancer Immunol Immunother.* (2009) 58:1195–206. doi: 10.1007/s00262-008-0632-0
15. Shiokawa M, Takahashi T, Murakami A, Kita S, Ito M, Sugamura K, et al. *In vivo* assay of human NK-dependent ADCC using NOD/SCID/gammac(null) (NOG) mice. *Biochem Biophys Res Commun.* (2010) 399:733–7. doi: 10.1016/j.bbrc.2010.07.145
16. Herndler-Brandstetter D, Shan L, Yao Y, Stecher C, Plajer V, Lietzenmayer M, et al. Humanized mouse model supports development, function, and tissue residency of human natural killer cells. *Proc Natl Acad Sci USA.* (2017) 114:E9626–34. doi: 10.1073/pnas.1705301114
17. Katano I, Takahashi T, Ito R, Kamisako T, Mizusawa T, Ka Y, et al. Predominant development of mature and functional human NK cells in a novel human IL-2-producing transgenic NOG mouse. *J Immunol.* (2015) 194:3513–25. doi: 10.4049/jimmunol.1401323
18. Katano I, Nishime C, Ito R, Kamisako T, Mizusawa T, Ka Y, et al. Long-term maintenance of peripheral blood derived human NK cells in a novel human IL-15- transgenic NOG mouse. *Sci Rep.* (2017) 7:17230. doi: 10.1038/s41598-017-17442-7
19. Inoue Y, Kaifu T, Sugahara-Tobinai A, Nakamura A, Miyazaki J, Takai T. Activating Fc gamma receptors participate in the development of autoimmune diabetes in NOD mice. *J Immunol.* (2007) 179:764–74. doi: 10.4049/jimmunol.179.2.764
20. Ohbo K, Suda T, Hashiyama M, Mantani A, Ikebe M, Miyakawa K, et al. Modulation of hematopoiesis in mice with a truncated mutant of the interleukin-2 receptor gamma chain. *Blood.* (1996) 87:956–67. doi: 10.1182/blood.V87.3.956.bloodjournal873956
21. Ohnishi Y, Nakamura H, Yoshimura M, Tokuda Y, Iwasawa M, Ueyama Y, et al. Prolonged survival of mice with human gastric cancer treated with an anti-c-ErbB-2 monoclonal antibody. *Br J Cancer.* (1995) 71:969–73. doi: 10.1038/bjc.1995.187
22. Yamashita-Kashima Y, Iijima S, Yorozu K, Furugaki K, Kurasawa M, Ohta M, et al. Pertuzumab in combination with trastuzumab shows significantly enhanced antitumor activity in HER2-positive human gastric cancer xenograft models. *Clin Cancer Res.* (2011) 17:5060–70. doi: 10.1158/1078-0432.CCR-10-2927
23. Takai T, Li M, Sylvestre D, Clynes R, Ravetch JV. FcR gamma chain deletion results in pleiotrophic effector cell defects. *Cell.* (1994) 76:519–29. doi: 10.1016/0092-8674(94)90115-5
24. Nimmerjahn F, Bruhns P, Horiuchi K, Ravetch JV. FcgammaRIV: a novel FcR with distinct IgG subclass specificity. *Immunity.* (2005) 23:41–51. doi: 10.1016/j.immuni.2005.05.010
25. Li F, Ulrich ML, Shih VF, Cochran JH, Hunter JH, Westendorf L, et al. Mouse strains influence clearance and efficacy of antibody and antibody-drug conjugate via Fc-FcgammaR interaction. *Mol Cancer Ther.* (2019) 18:780–7. doi: 10.1158/1535-7163.MCT-18-0977
26. Roopenian DC, Christianson GJ, Sproule TJ, Brown AC, Akilesh S, Jung N, et al. The MHC class I-like IgG receptor controls perinatal IgG transport, IgG homeostasis, and fate of IgG-Fc-coupled drugs. *J Immunol.* (2003) 170:3528–33. doi: 10.4049/jimmunol.170.7.3528
27. Roopenian DC, Christianson GJ, Sproule TJ. Human FcRn transgenic mice for pharmacokinetic evaluation of therapeutic antibodies. *Methods Mol Biol.* (2010) 602:93–104. doi: 10.1007/978-1-60761-058-8_6
28. Chao MP, Alizadeh AA, Tang C, Myklebust JH, Varghese B, Gill S, et al. Anti-CD47 antibody synergizes with rituximab to promote phagocytosis and eradicate non-Hodgkin lymphoma. *Cell.* (2010) 142:699–713. doi: 10.1016/j.cell.2010.07.044
29. Reff ME, Carner K, Chambers KS, Chinn PC, Leonard JE, Raab R, et al. Depletion of B cells *in vivo* by a chimeric mouse human monoclonal antibody to CD20. *Blood.* (1994) 83:435–45. doi: 10.1182/blood.V83.2.435.435
30. Kennedy AD, Solga MD, Schuman TA, Chi AW, Lindorfer MA, Sutherland WM, et al. An anti-C3b(i) mAb enhances complement activation, C3b(i) deposition, and killing of CD20+ cells by rituximab. *Blood.* (2003) 101:1071–9. doi: 10.1182/blood-2002-03-0876
31. Wetsel RA, Fleischer DT, Haviland DL. Deficiency of the murine fifth complement component (C5). A 2-base pair gene deletion in a 5'-exon. *J Biol Chem.* (1990) 265:2435–40.
32. Teeling JL, French RR, Cragg MS, van den Brakel J, Pluyter M, Huang H, et al. Characterization of new human CD20 monoclonal antibodies with potent cytolytic activity against non-Hodgkin lymphomas. *Blood.* (2004) 104:1793–800. doi: 10.1182/blood-2004-01-0039
33. Labrijn AF, Janmaat ML, Reichert JM, Parren P. Bispecific antibodies: a mechanistic review of the pipeline. *Nat Rev Drug Discov.* (2019) 18:585–608. doi: 10.1038/s41573-019-0028-1

34. Smith P, DiLillo DJ, Bournazos S, Li F, Ravetch JV. Mouse model recapitulating human Fcgamma receptor structural and functional diversity. *Proc Natl Acad Sci USA*. (2012) 109:6181–6. doi: 10.1073/pnas.1203954109
35. Dahan R, Barnhart BC, Li F, Yamniuk AP, Korman AJ, Ravetch JV. Therapeutic activity of agonistic, human anti-CD40 monoclonal antibodies requires selective FcgammaR engagement. *Cancer Cell*. (2016) 29:820–31. doi: 10.1016/j.ccell.2016.05.001
36. Ito R, Takahashi T, Katano I, Kawai K, Kamisako T, Ogura T, et al. Establishment of a human allergy model using human IL-3/GM-CSF-transgenic NOG mice. *J Immunol*. (2013) 191:2890–9. doi: 10.4049/jimmunol.1203543
37. Hanazawa A, Ito R, Katano I, Kawai K, Goto M, Suemizu H, et al. Generation of human immunosuppressive myeloid cell populations in human interleukin-6 transgenic NOG mice. *Front Immunol*. (2018) 9:152. doi: 10.3389/fimmu.2018.00152

Conflict of Interest: The authors declare that the research was conducted in the absence of any commercial or financial relationships that could be construed as a potential conflict of interest.

Copyright © 2020 Katano, Ito, Kawai and Takahashi. This is an open-access article distributed under the terms of the Creative Commons Attribution License (CC BY). The use, distribution or reproduction in other forums is permitted, provided the original author(s) and the copyright owner(s) are credited and that the original publication in this journal is cited, in accordance with accepted academic practice. No use, distribution or reproduction is permitted which does not comply with these terms.

frontiers in Immunology

MINI REVIEW
published: 08 October 2020
doi: 10.3389/fimmu.2020.591669

Human Immune System Mice With Autologous Tumor for Modeling Cancer Immunotherapies

Liguang Sun[1,2], Chun-Hui Jin[1,3], Shulian Tan[1,2], Wentao Liu[1,2] and Yong-Guang Yang[1,2,4]**

[1] Key Laboratory of Organ Regeneration & Transplantation of the Ministry of Education, The First Hospital of Jilin University, Changchun, China, [2] National-local Joint Engineering Laboratory of Animal Models for Human Diseases, Jilin University, Changchun, China, [3] Department of Pathology, The First Hospital of Jilin University, Changchun, China, [4] International Center of Future Science, Jilin University, Changchun, China

Mouse models are the most commonly used *in vivo* system for biomedical research, in which immune-related diseases and therapies can be investigated in syngeneic and immunologically intact hosts. However, because there are significant differences between rodent and human, most findings from conventional mouse models cannot be applied to humans. The humanized mouse with a functional human immune system, also referred to as human immune system (HIS) mouse, is the only model available to date for *in vivo* studies in real-time of human immune function under physiological and pathological conditions. HIS mice with human tumor xenografts are considered an emerging and promising *in vivo* model for modeling human cancer immunotherapy. In this review, we briefly discuss the protocols to construct HIS mice and elaborate their pros and cons. Particular attention is given to HIS mouse models with human tumor that is autologous or genetically identical to the human immune system, which are discussed with examples of their usefulness in modeling human cancer immunotherapies.

Keywords: humanized mouse, cancer, immunotherapy, CAR T cell, human immune system mouse, allogeneic hematopoietic cell transplantation

OPEN ACCESS

Edited by:
Yasuyuki Saito,
Kobe University, Japan

Reviewed by:
Susumu Goyama,
The University of Tokyo, Japan
Todd Pitts,
University of Colorado, United States

***Correspondence:**
Yong-Guang Yang
yongg@jlu.edu.cn
Wentao Liu
liuwtt70@163.com

Specialty section:
This article was submitted to Cancer Immunity and Immunotherapy, a section of the journal Frontiers in Immunology

Received: *05 August 2020*
Accepted: *22 September 2020*
Published: *08 October 2020*

Citation:
Sun L, Jin C-H, Tan S, Liu W and Yang Y-G (2020) Human Immune System Mice With Autologous Tumor for Modeling Cancer Immunotherapies. Front. Immunol. 11:591669. doi: 10.3389/fimmu.2020.591669

INTRODUCTION

Human immune system (HIS) mice have been highly instrumental for *in vivo* studies of human immune function and immune disorders. The HIS mouse was the first model that made it possible to study human immune responses in real time *in vivo* under physiologic or pathogenic conditions, such as HIV pathogenesis (1), human xeno-immune responses (2), complex interplay between hypercholesterolemia and human adaptive immunity (3), and intrathymic selections of human T cells (4). HIS mice, conjunct with tissue chimeras (i.e., with organ repopulation by human parenchymal cells), were found highly valuable in elucidating immunopathology of human-tropic viral infections, such as hepatitis B and hepatitis C viruses (5, 6) and respiratory viruses (7). HIS mice were also increasingly used in the studies of human cancer immunology and immunotherapy. However, most of the models used in these studies were either

immunocompromised or involving allogeneic and/or xenogeneic immune responses, making the host immune environment different from that of patients. Thus, there is an urgent and unmet need for a preclinical mouse model mimicking the patients, in which both the immunity and the tumor are of human origin and genetically identical. In this review, we first briefly overview the development and evolution of HIS mouse protocols, then discuss progress to date in creating HIS mice with autologous or genetically identical human tumors.

BRIEF REVIEW OF HIS MOUSE CONSTRUCTION

There has been a long-standing effort to create and optimize HIS mouse models. While different HIS mouse construction protocols have been reported, all involve transplantation of human hematopoietic and/or lymphoid cells (e.g., peripheral blood lymphocytes (PBLs), bone marrow cells, cord blood cells, or fetal liver hematopoietic cells) into immunodeficient mice. Current HIS mouse models are in general derived from three HIS mouse models reported in the late 1980s. Mosier and colleagues reported in 1988 that injection of human PBLs into C.B-17 severe combined immunodeficiency (SCID) mice resulted in durable reconstitution with human T cells, B cells and monocytes/macrophages, providing a useful model for the study of human immune function (known as hu-PBL-SCID mouse) (8). During the same period, McCune and colleagues reported another HIS mouse model (referred to as SCID-hu mouse by the authors), in which human immune reconstitution was achieved in C.B-17 SCID mice by transplantation of fetal thymus, liver and lymph node (9). Subsequently, using bg/nu/xid mice Kamel-Reid and Dick found that transplantation of human hematopoietic stem/progenitor cells (HSCs/HPCs) into immunodeficient mice could achieve human HSC/HPC engraftment and differentiation, offering an additional HIS mouse model (referred to as chimeric human/immune-deficient (HID) mice by the authors) (10). However, this HID model or similarly created HIS mouse models (i.e., constructed by human HSCs/HPCs of different sources) were not very useful for the study of human immunity due to poor T cell function until better immunodeficient mouse strains became available (see discussion below), and was further improved by using newborn immunodeficient mice as the recipients (11, 12). Despite these improvements, human T cells developing in the xenogeneic mouse thymus were increasingly reported to be functionally abnormal, likely caused by poor HLA-restricted antigen recognition (13–15).

The hu-PBL-SCID model is simple, but it needs to be cautious when using this model because of the potential of infused human T cells to induce xenogeneic graft-versus-host disease (GVHD) that may confound assessment of human immunity and result in human effector T cell anergy (16). Although there are apparent differences between xenogeneic and allogeneic GVHD, the hu-PBL-SCID model was found useful in the study of human GVHD pathogenesis (17). Xenogeneic GVHD was effectively prevented in the human fetal thymus/liver (Thy/Liv)-grafted SCID-hu model, in which the majority of human T cells developed *de novo* in the murine host and therefore, those reactive to mouse antigens were purged during the negative selection process (9). However, we found that, due to the lack of sufficient repopulation with human dendritic cells (DCs) and B cells, the SCID-hu mice were inefficient in mounting antigen-specific immune responses *in vivo* (18). To solve this problem, we developed a new protocol in which HIS mice were made by combined transplantation of human fetal thymus (under renal capsule) and $CD34^+$ HSCs/HPCs (i.v.) (18, 19). The resultant HIS mice showed reconstitution with human T cells, B cells and DCs, and acquired the ability to mediate robust antigen-specific immune responses *in vivo* and reject pig xenografts (19–22). These human Thy/HSC-grafted HIS mice were also found able to mediate anti-viral responses and were termed BLT mice in some other studies (23, 24). A disadvantage of the Thy/HSC-based HIS mouse model is the need to use fetal tissues. Therefore, increasing efforts are currently undertaken to optimize the potential of animal thymi to support human thymopoiesis. However, until such animal becomes available, the Thy/HSC HIS mouse model will likely still be instrumental.

Regardless of which protocol is used to construct HIS mice, magnificent improvements in engraftment and function of human hematopoietic and lymphoid cells were made by using more sophisticated immunodeficient mouse strains, such as nonobese diabetic/LtSz-*scid*/*scid* (NOD/SCID) (25) and NOD-*scid IL2R*γ^{null} (NSG) (26) mice. C.B-17 SCID mice, which were most commonly used in HIS mouse construction before the availability of NOD/SCID mice, have high complement activity that mediates antibody-independent rejection of xenogeneic cells (27). CD47 is ligand of SIRPα, an inhibitory receptor on macrophages and DCs, and its engagement with SIRPα inhibits phagocytosis and endocytosis (28, 29). In a xenogeneic transplant setting, the inability of donor CD47 to interact with the recipient SIRPα is an important mechanism triggering donor cell rejection by macrophages (30, 31). NOD/SCID mice lack hemolytic complement, and express signal regulatory protein (SIRP)α capable of cross-reacting with human CD47 (32). In addition, substantial effort was made to improve the engraftment, differentiation, survival, and function of human hematopoietic and lymphoid cells in immunodeficient mice by introducing human cytokines. The MISTRG mouse is a good example, in which human M-CSF, GM-CSF/IL-3, and TPO genes are knocked into their respective mouse loci (33). HIS mice made with MISTRG mice showed markedly improved development and function of human innate immune cells than those made with NSG mice (33). However, it is worth mention that HIS mice carrying transgenes of human immunostimulatory cytokines under a constitutive promoter, e.g., the SGM3-NSG mice expressing human SCF, GM-CSF, and IL-3, are prone to develop fatal disease characterized by activation and widespread tissue infiltration of human T cells and macrophages, and show significant elevation in human proinflammatory cytokines including IL-6, IL-18, IFN-γ, and TNF-α (34, 35). The vigorous proinflammatory responses would likely confound the evaluation of interested immune functions in these HIS mice, such as cytokine storm or cytokine release syndrome induced by immunotherapies (36).

CONSTRUCTION OF HIS MICE WITH AUTOLOGOUS TUMOR

There has been an emerging effort in developing human tumor-bearing HIS mouse models. Both human tumor cell derived xenograft (CDX; immunodeficient mice grafted with human cancer cell line cells) and patient-derived xenograft (PDX; immunodeficient mice grafted with patient cancer cells) models were widely and successfully used in understanding oncogenesis and testing anti-cancer drugs (37), these models, however, were not useful in the study of cancer immunology or immunotherapy due to the lack of human immune system. A conceivable approach to solve this problem is to construct human tumor-bearing HIS mouse models, in which both the tumor cells and the immune system are of human origin, which permit assessment of tumor-associated immune responses and immunotherapies. However, a notable limitation of such human tumor-bearing HIS mouse models is that the tumor cells are allogeneic to human immune system, so anti-tumor immune responses are expected to be largely driven by allogenicity rather than tumorigenicity. Although co-transplantation of tumor cells with immune cells (e.g., PBMCs) from the same patient may resolve this issue, this model will also suffer the same problem as the hu-PBL-SCID model discussed above (i.e., xenogeneic GVHD and human effector T cell anergy).

HIS Mice With Autologous Human Leukemia

An ideal approach to resolving allogenicity would be to construct HIS mice with autologous tumor. Recently, we developed a HIS mouse model with spontaneous autologous leukemia and validated its usefulness in exploring anti-human leukemia immunotherapies. In this model, we transplanted sublethally-irradiated NSG mice with human fetal thymus and fetal liver $CD34^+$ cells that were virally transduced with a mixed-lineage leukemia (MLL) fusion gene MLL-AF9 (**Figure 1A**) (38). It has been shown that MLL-AF9 expression drives the development of acute leukemia that resembles several clinical hallmarks of MLL leukemias (39). The NSG mice grafted with Thy/MLL-AF9-HSC appeared normal and showed a gradual increase in the levels of human PBMCs, including T cells, B cells and myeloid cells for about 3 to 4 months, then became progressively ill with a sharp increase in MLL-AF9-expressing HSC-derived $CD19^+$ cells in blood. Autopsy revealed splenomegaly, enlarged lymph nodes, and hepatomegaly in all moribund mice. Histology demonstrated massive leukemic cell infiltration in bone marrow, spleen, lung, liver, and kidney. The MLL-AF9-expressing HSC-derived leukemic cells exhibited a high nucleus/cytoplasm ratio with a B-ALL phenotype, i.e., $CD19^+CD10^+CD20^-sIgM^{low/-}sIgD^{low/-}CD44^{hi}MHC\text{-}I^+MHC\text{-}II^{hi}$ and negative for other lineage markers, i.e., $CD33^-CD15^{low/-}CD14^-CD11b^-CD3^-CD4^-CD8^-CD56^-$. The study demonstrated that the Thy/MLL-AF9-HSC HIS mice not only develop human lymphohematopoietic cells, but also autologous B-ALL, offering a model to study human leukemia immunopathology and anti-leukemia immunotherapy in an autologous setting.

B-ALL cells developed in MLL-AF9-HSC-grafted HIS mice are transplantable in immunodeficient mice and in HIS mice with an established autologous human immune system (i.e., HIS mice made with human Thy/HSC from the same fetus from which $CD34^+$ cells were used to develop the B-ALL) (38). However, rejection was seen when the B-ALL cells were transplanted in HIS mice with an allogeneic immune system. Adoptive transfer of cryopreserved B-ALL cells in pre-established HIS mice with an autologous immune system would present a much simpler model than spontaneous leukemia model described above (**Figure 1B**).

HIS Mice With Autologous Human Solid Tumor

This model may also possibly be applied to set up HIS mice bearing autologous solid tumor. Although there has been no report of successful construction of autologous human solid tumor-bearing

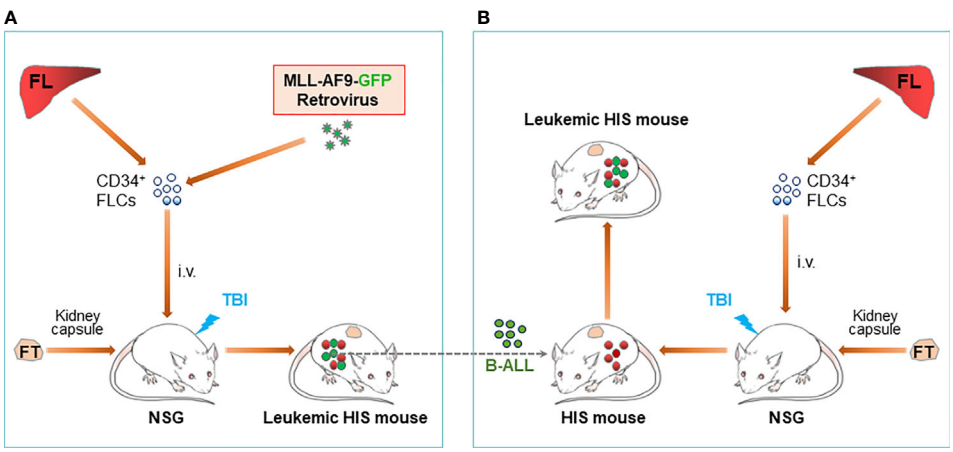

FIGURE 1 | Construction of leukemic HIS mice with human immune system and leukemia derived from genetically identical HSCs/HPCs. **(A)** Schematic showing preparation of HIS mice with spontaneous development of B-ALL autologous to the human immune system. **(B)**. Schematic of leukemic HIS mouse construction by injection of autologous B-ALL [made as described in **(A)**] into preestablished HIS mice. FL, fetal liver; FLC, fetal liver cell; FT, fetal thymus; TBI, total body irradiation.

HIS mice, the feasibility of developing such HIS mouse models is supported by progress in understanding oncogenic changes causing tumorigenic transformation of normal cells. Previous studies were successful in inducing melanocytic transformation by engineering normal melanocytes to express a combination of specific mutations found in human melanoma, and the engineered human melanocytes could develop into melanocytic tumor in immunodeficient mice (40). Other studies identified combinations of oncogenic mutants that may drive tumorigenic transformation of human lung epithelial cells (41, 42). These studies suggested the possibility of establishing tumorigenic cells from normal fetal tissue cells. Successful generation of tumorigenic cells from fetal tissue cells would make it possible to construct HIS mice bearing autologous solid tumors by injecting the tumor cells into autologous HIS mice (i.e., HIS mice made with human Thy/HSC from the fetus from which parenchymal tissue cells are engineered for tumorigenesis). The feasibility of this approach is supported by a previous study, in which HIS mice were successfully used to assess the immunogenicity of autologous human induced pluripotent stem (iPS) cells (i.e., iPS cells reprogramed from fetal liver fibroblasts of the same fetus used for constructing HIS mice) (43).

Personalized HIS Mice With Patient-Specific Immunity and Tumor

HIS mouse models were also used to study human immune function in a personalized manner, in which immunodeficient mice were grafted with patient-derived CD34$^+$ bone marrow cells along with partially HLA allele-matched fetal thymic tissue (44). In this model, although human T cells were more "naïve" than those of the adult CD34$^+$ cell donors, the immune recognition mimicked that of the adult donor, offering a model for individualized analysis of human immune function (44, 45). Furthermore, while the fetal thymus used was partially HLA-matched to the patient, human T cells developing in personalized HIS mice showed specific "self" tolerance (i.e., tolerance to the CD34$^+$ cell donor patient). Combining this personalized HIS mouse with PDX model would provide a means of constructing patient-specific tumor-bearing HIS mice, in which both the tumor (leukemia or solid tumor) and immune system are derived from the same patient (**Figure 2**). Such a patient-specific tumor-bearing HIS mouse model should be highly valuable in personalized therapies.

MODELING ANTI-LEUKEMIA IMMUNOTHERAPY IN HIS MICE WITH AUTOLOGOUS B-ALL

Anti-Leukemic Responses Induced by Recipient Leukocyte Infusion

Following allogeneic hematopoietic cell transplantation (allo-HCT), donor T cells mediate beneficial graft-vs.-tumor (GVT) effects. However, allogeneic donor T cells also attack recipient normal tissues, resulting in GVHD. It has been reported that, in patients receiving nonmyeloablative allo-HCT, some of the patients who rejected donor grafts unexpectedly showed sustained remissions, suggesting an anti-donor alloresponse-associated antitumor activity (46). In support of this possibility, studies in mice found that administration of recipient leukocyte infusion (RLI) to mixed allogeneic chimeras results in rejection of donor hematopoietic chimerism and significant anti-host leukemia responses (47). RLI is apparently less effective than alloreactive donor T cells in killing recipient leukemia (48), but it does not induce GVHD, offering a potentially safe treatment for use in combination with other immunostimulatory therapies.

We have tested the potential of lymphopenia to enhance antitumor effects of RLI in leukemic HIS mice (**Figure 1**) (38). Lymphopenia is common in patients with leukemia who receive allo-HCT (49, 50), which is a factor that triggers GVHD (51, 52)

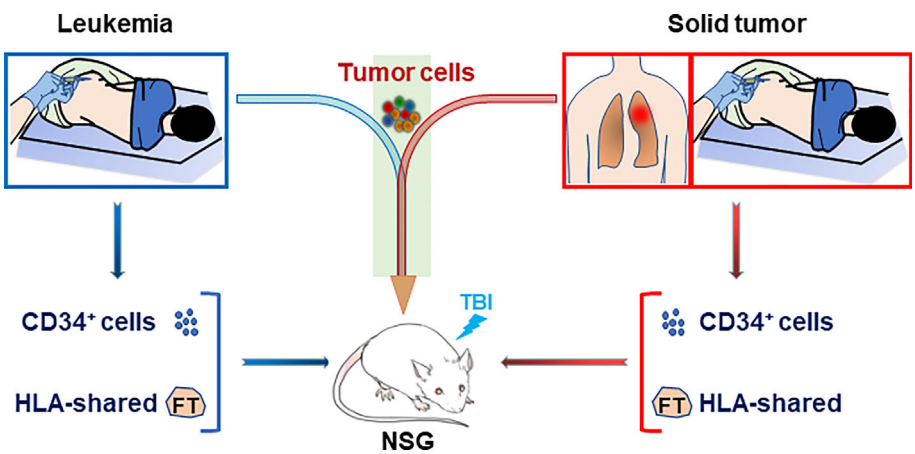

FIGURE 2 | Construction of personalized HIS mice with patient-specific immunity and cancer. Personalized HIS mice are constructed by transplantation of CD34$^+$ bone marrow cells (i.v.) from a patient bearing leukemia (Left) or solid tumor (Right) along with HLA allele-matched fetal thymic tissue (under renal capsule). The HIS mice will be followed for human immune reconstitution by flow cytometric analysis of blood cells and inoculated with the leukemic or solid tumor cells from the same patient when human immune reconstitution is confirmed. FT, fetal thymus; TBI, total body irradiation.

but also promotes antitumor responses (53, 54). In this study, mixed chimeric (MC) HIS mice were established by transplantation of human Thy along with a mixture of 'recipient' (genetically identical to the Thy graft) and allogeneic 'donor' $CD34^+$ HSCs, and lymphopenia was made by treatment with anti-huCD3-immunotoxin. Spleen cells from HIS mice made by transplantation of 'recipient' Thy/$CD34^+$ cells were used as the RLI cells, which were autologous to the 'recipient' and allogeneic to the 'donor' origin of the MC HIS mice. Using this model, it was found that, in a human immune system, RLI was significantly more effective in inducing antitumor responses in lymphopenic than non-lymphopenic recipients, and that the antitumor response was associated with rejection of donor hematopoietic chimerism (38). The findings suggested that RLI offers a potentially safer clinical treatment option for leukemic patients who have profound lymphopenia.

CD19-Targeted CAR T Cell Therapy

Recently, we made use of these leukemic HIS mice to model adoptive immunotherapy using human T cells that were genetically engineered to express anti-CD19 chimeric antigen receptors (CARs). CD19-targeted CAR T cell therapy has achieved promising results in patients with B-cell malignancies (55–57). However, despite the impressive response rates, many patients showed relapse or severe adverse reaction after anti-CD19 CAR T cell therapy (58, 59). Although memory CAR T cells were detected in patients (60), our understanding of these memory T cells, including their differentiation, function, self-renewal, and survival factors/signaling, remains limited. In addition, it remains largely unknown about the mechanisms responsible for the toxicities associated with anti-CD19 CAR T cell therapy, such as cytokine-release syndrome (CRS), which can be severe or even fatal (61). Thus, there is an urgent need to develop a preclinical model, which can be used to understand relapse and toxicity associated with human CAR T cell therapy, and to test the efficacy of new CAR T cells. Immunodeficient mice grafted with human B-ALL (PDX models) were found useful in testing CD19-targeted human CAR T cell therapy (62), but these models are either lacking host immunity or involving allo- and/or xeno-immune responses. Because the leukemic HIS mouse model described above has a functional human immune system and genetically-matched (autologous) primary B-ALL, this model was used to model CD19-targeted CAR T cell therapy (63). Another unique feature of this model is that the anti-CD19 CAR-expressing human T cells are also genetically-identical (autologous) to the human components (both normal and malignant human cells) and tolerant to mouse antigens of the HIS mice, and therefore do not mediate alloresponses against human or xenoresponses against mouse antigens. In leukemic HIS mice receiving CAR T cell therapy, the kinetics and levels of anti-CD19 CAR T cells in the peripheral blood were similar to those in patients (60). In agreement with clinical studies (55, 56), the frequency of CAR T cells in blood showed an inverse correlation with B-ALL burden but a positive correlation with survival times in CAR T cell-treated leukemic HIS mice. Moreover, this model was also found useful in characterizing cytokine profiles and regulatory T (Treg) cell generation and function following CAR T cell therapy. These observations provide a proof-of-principle that this leukemic HIS mouse model has the potential to be used to evaluate human CAR T cell therapy and help design new CARs with enhanced antitumor activity.

CONCLUDING REMARKS

Apparently, the HIS mouse is not identical to a human host. However, there is strong experimental evidence for the value and feasibility of using HIS mice to study human immunity, including antigen-specific T cell and antibody responses (18–23, 64, 65). Thus, HIS mice with autologous tumors, either leukemia or solid tumor, would provide a highly valuable preclinical model for *in vivo* studies of human cancer immunology and immunotherapy.

AUTHOR CONTRIBUTIONS

All authors contributed to the article and approved the submitted version.

REFERENCES

1. McCune J, Kaneshima H, Krowka J, Namikawa R, Outzen H, Peault B, et al. The SCID-hu mouse: a small animal model for HIV infection and pathogenesis. *Annu Rev Immunol* (1991) 9:399–429. doi: 10.1146/annurev.iy.09.040191.002151
2. Hu Z, Yang YG. Human lymphohematopoietic reconstitution and immune function in immunodeficient mice receiving cotransplantation of human thymic tissue and CD34(+) cells. *Cell Mol Immunol* (2012) 9:232–6. doi: 10.1038/cmi.2011.63
3. Proto JD, Doran AC, Subramanian M, Wang H, Zhang M, Sozen E, et al. Hypercholesterolemia induces T cell expansion in humanized immune mice. *J Clin Invest* (2018) 128:2370–5. doi: 10.1172/JCI97785
4. Li Y, Teteloshvili N, Tan S, Rao S, Han A, Yang YG, et al. Humanized Mice Reveal New Insights Into the Thymic Selection of Human Autoreactive CD8(+) T Cells. *Front Immunol* (2019) 10:63. doi: 10.3389/fimmu.2019.00063
5. Barth H, Robinet E, Liang TJ, Baumert TF. Mouse models for the study of HCV infection and virus-host interactions. *J Hepatol* (2008) 49:134–42. doi: 10.1016/j.jhep.2008.03.012
6. Cheng L, Li F, Bility MT, Murphy CM, Su L. Modeling hepatitis B virus infection, immunopathology and therapy in mice. *Antiviral Res* (2015) 121:1–8. doi: 10.1016/j.antiviral.2015.06.012
7. Wahl A, De C, Abad Fernandez M, Lenarcic EM, Xu Y, Cockrell AS, et al. Precision mouse models with expanded tropism for human pathogens. *Nat Biotechnol* (2019) 37:1163–73. doi: 10.1038/s41587-019-0225-9
8. Mosier DE, Gulizia RJ, Baird SM, Wilson DB. Transfer of a functional human immune system to mice with severe combined immunodeficiency. *Nature* (1988) 335:256–9. doi: 10.1038/335256a0
9. McCune J, Namikawa R, Kaneshima H, Shultz L, Lieberman M, Weissman I. The SCID-hu mouse: murine model for the analysis of human hematolymphoid differentiation and function. *Science* (1988) 241:1632–9. doi: 10.1126/science.2971269

10. Kamel-Reid S, Dick J. Engraftment of immune-deficient mice with human hematopoietic stem cells. *Science* (1988) 242:1706–9. doi: 10.1126/science.2904703
11. Traggiai E, Chicha L, Mazzucchelli L, Bronz L, Piffaretti JC, Lanzavecchia A, et al. Development of a human adaptive immune system in cord blood cell-transplanted mice. *Science* (2004) 304:104–7. doi: 10.1126/science.1093933
12. Ishikawa F, Yasukawa M, Lyons B, Yoshida S, Miyamoto T, Yoshimoto G, et al. Development of functional human blood and immune systems in NOD/SCID/IL2 receptor {gamma} chain(null) mice. *Blood* (2005) 106:1565–73. doi: 10.1182/blood-2005-02-0516
13. Shultz LD, Saito Y, Najima Y, Tanaka S, Ochi T, Tomizawa M, et al. Generation of functional human T-cell subsets with HLA-restricted immune responses in HLA class I expressing NOD/SCID/IL2r gamma(null) humanized mice. *Proc Natl Acad Sci U S A* (2010) 107:13022–7. doi: 10.1073/pnas.1000475107
14. Strowig T, Gurer C, Ploss A, Liu YF, Arrey F, Sashihara J, et al. Priming of protective T cell responses against virus-induced tumors in mice with human immune system components. *J Exp Med* (2009) 206:1423–34. doi: 10.1084/jem.20081720
15. Watanabe Y, Takahashi T, Okajima A, Shiokawa M, Ishii N, Katano I, et al. The analysis of the functions of human B and T cells in humanized NOD/shi-scid/gammac(null) (NOG) mice (hu-HSC NOG mice). *Int Immunol* (2009) 21:843–58. doi: 10.1093/intimm/dxp050
16. Tary-Lehmann M, Lehmann PV, Schols D, Roncarolo MG, Saxon A. Anti-SCID mouse reactivity shapes the human CD4+ T cell repertoire in hu-PBL-SCID chimeras. *J Exp Med* (1994) 180:1817–27. doi: 10.1084/jem.180.5.1817
17. Purtilo DT, Falk K, Pirruccello SJ, Nakamine H, Kleveland K, Davis JR, et al. SCID mouse model of Epstein-Barr virus-induced lymphomagenesis of immunodeficient humans. *Int J Cancer* (1991) 47:510–7. doi: 10.1002/ijc.2910470407
18. Lan P, Wang L, Diouf B, Eguchi H, Su H, Bronson R, et al. Induction of human T-cell tolerance to porcine xenoantigens through mixed hematopoietic chimerism. *Blood* (2004) 103:3964–9. doi: 10.1182/blood-2003-10-3697
19. Lan P, Tonomura N, Shimizu A, Wang S, Yang YG. Reconstitution of a functional human immune system in immunodeficient mice through combined human fetal thymus/liver and CD34+ cell transplantation. *Blood* (2006) 108:487–92. doi: 10.1182/blood-2005-11-4388
20. Tonomura N, Habiro K, Shimizu A, Sykes M, Yang YG. Antigen-specific human T-cell responses and T cell-dependent production of human antibodies in a humanized mouse model. *Blood* (2008) 111:4293–6. doi: 10.1182/blood-2007-11-121319
21. Tonomura N, Shimizu A, Wang S, Yamada K, Tchipashvili V, Weir GC, et al. Pig islet xenograft rejection in a mouse model with an established human immune system. *Xenotransplantation* (2008) 15:129–35. doi: 10.1111/j.1399-3089.2008.00450.x
22. Habiro K, Sykes M, Yang YG. Induction of human T-cell tolerance to pig xenoantigens via thymus transplantation in mice with an established human immune system. *Am J Transplant* (2009) 9:1324–9. doi: 10.1111/j.1600-6143.2009.02646.x
23. Melkus MW, Estes JD, Padgett-Thomas A, Gatlin J, Denton PW, Othieno FA, et al. Humanized mice mount specific adaptive and innate immune responses to EBV and TSST-1. *Nat Med* (2006) 12:1316–22. doi: 10.1038/nm1431
24. Brainard DM, Seung E, Frahm N, Cariappa A, Bailey CC, Hart WK, et al. Induction of robust cellular and humoral virus-specific adaptive immune responses in human immunodeficiency virus-infected humanized BLT mice. *J Virol* (2009) 83:7305–21. doi: 10.1128/JVI.02207-08
25. Shultz LD, Schweitzer PA, Christianson SW, Gott B, Schweitzer IB, Tennent B, et al. Multiple defects in innate and adaptive immunologic function in NOD/LtSz-scid mice. *J Immunol* (1995) 154:180–91.
26. Shultz LD, Lyons BL, Burzenski LM, Gott B, Chen X, Chaleff S, et al. Human lymphoid and myeloid cell development in NOD/LtSz-scid IL2R gamma null mice engrafted with mobilized human hemopoietic stem cells. *J Immunol* (2005) 174:6477–89. doi: 10.4049/jimmunol.174.10.6477
27. Yang YG, Chen AM, Sergio JJ, Zhou Y, Sykes M. Role of antibody-independent complement activation in rejection of porcine bone marrow cells in mice. *Transplantation* (2000) 69:163–5. doi: 10.1097/00007890-200001150-00027
28. Oldenborg PA, Zheleznyak A, Fang YF, Lagenaur CF, Gresham HD, Lindberg FP. Role of CD47 as a marker of self on red blood cells. *Science* (2000) 288:2051–4. doi: 10.1038/ni1527
29. Wang H, Madariaga ML, Wang S, Van Rooijen N, Oldenborg PA, Yang YG. Lack of CD47 on nonhematopoietic cells induces split macrophage tolerance to CD47null cells. *Proc Natl Acad Sci U S A* (2007) 104:13744–9. doi: 10.1126/science.288.5473.2051
30. Wang H, VerHalen J, Madariaga ML, Xiang S, Wang S, Lan P, et al. Attenuation of phagocytosis of xenogeneic cells by manipulating CD47. *Blood* (2007) 109:836–42. doi: 10.1073/pnas.0702881104
31. Ide K, Wang H, Tahara H, Liu J, Wang X, Asahara T, et al. Role for CD47-SIRPα signaling in xenograft rejection by macrophages. *Proc Natl Acad Sci* (2007) 104:5062–6. doi: 10.1182/blood-2006-04-019794
32. Takenaka K, Prasolava TK, Wang JC, Mortin-Toth SM, Khalouei S, Gan OI, et al. Polymorphism in Sirpa modulates engraftment of human hematopoietic stem cells. *Nat Immunol* (2007) 8:1313–23. doi: 10.1073/pnas.0609661104
33. Rongvaux A, Willinger T, Martinek J, Strowig T, Gearty SV, Teichmann LL, et al. Development and function of human innate immune cells in a humanized mouse model. *Nat Biotechnol* (2014) 32:364–72. doi: 10.1038/nbt.2858
34. Yoshihara S, Li Y, Xia J, Danzl N, Sykes M, Yang YG. Posttransplant Hemophagocytic Lymphohistiocytosis Driven by Myeloid Cytokines and Vicious Cycles of T-Cell and Macrophage Activation in Humanized Mice. *Front Immunol* (2019) 10:186. doi: 10.3389/fimmu.2019.00186
35. Wunderlich M, Stockman C, Devarajan M, Ravishankar N, Sexton C, Kumar AR, et al. A xenograft model of macrophage activation syndrome amenable to anti-CD33 and anti-IL-6R treatment. *JCI Insight* (2016) 1:e88181. doi: 10.1172/jci.insight.88181
36. Norelli M, Camisa B, Barbiera G, Falcone L, Purevdorj A, Genua M, et al. Monocyte-derived IL-1 and IL-6 are differentially required for cytokine-release syndrome and neurotoxicity due to CAR T cells. *Nat Med* (2018) 24:739–48. doi: 10.1038/s41591-018-0036-4
37. Hidalgo M, Amant F, Biankin AV, Budinska E, Byrne AT, Caldas C, et al. Patient-derived xenograft models: an emerging platform for translational cancer research. *Cancer Discov* (2014) 4:998–1013. doi: 10.1158/2159-8290.CD-14-0001
38. Xia J, Hu Z, Yoshihara S, Li Y, Jin CH, Tan S, et al. Modeling Human Leukemia Immunotherapy in Humanized Mice. *EBioMedicine* (2016) 10:101–8. doi: 10.1016/j.ebiom.2016.06.028
39. Barabe F, Kennedy JA, Hope KJ, Dick JE. Modeling the initiation and progression of human acute leukemia in mice. *Science* (2007) 316:600–4. doi: 10.1126/science.1139851
40. Chudnovsky Y, Adams AE, Robbins PB, Lin Q, Khavari PA. Use of human tissue to assess the oncogenic activity of melanoma-associated mutations. *Nat Genet* (2005) 37:745–9. doi: 10.1038/ng1586
41. Sato M, Larsen JE, Lee W, Sun H, Shames DS, Dalvi MP, et al. Human lung epithelial cells progressed to malignancy through specific oncogenic manipulations. *Mol Cancer Res* (2013) 11:638–50. doi: 10.1158/1541-7786.MCR-12-0634-T
42. Sato M, Shay JW, Minna JD. Immortalized normal human lung epithelial cell models for studying lung cancer biology. *Respir Invest* (2020) 58:344–54. doi: 10.1016/j.resinv.2020.04.005
43. Zhao T, Zhang ZN, Westenskow PD, Todorova D, Hu Z, Lin T, et al. Humanized Mice Reveal Differential Immunogenicity of Cells Derived from Autologous Induced Pluripotent Stem Cells. *Cell Stem Cell* (2015) 17:353–9. doi: 10.1016/j.stem.2015.07.021
44. Kalscheuer H, Danzl N, Onoe T, Faust T, Winchester R, Goland R, et al. A model for personalized in vivo analysis of human immune responsiveness. *Sci Transl Med* (2012) 4:125ra30. doi: 10.1126/scitranslmed.3003481
45. Borsotti C, Danzl NM, Nauman G, Holzl MA, French C, Chavez E, et al. HSC extrinsic sex-related and intrinsic autoimmune disease-related human B-cell variation is recapitulated in humanized mice. *Blood Adv* (2017) 1:2007–18. doi: 10.1182/bloodadvances.2017006932
46. Dey BR, McAfee S, Colby C, Cieply K, Caron M, Saidman S, et al. Anti-tumour response despite loss of donor chimaerism in patients treated with non-myeloablative conditioning and allogeneic stem cell transplantation. *Br J Haematol* (2005) 128:351–9. doi: 10.1111/j.1365-2141.2004.05328.x

47. Rubio MT, Kim YM, Sachs T, Mapara M, Zhao G, Sykes M. Antitumor effect of donor marrow graft rejection induced by recipient leukocyte infusions in mixed chimeras prepared with nonmyeloablative conditioning: critical role for recipient-derived IFN-gamma. *Blood* (2003) 102:2300–7. doi: 10.1182/blood-2002-12-3949
48. Saito TI, Rubio MT, Sykes M. Clinical relevance of recipient leukocyte infusion as antitumor therapy following nonmyeloablative allogeneic hematopoietic cell transplantation. *Exp Hematol* (2006) 34:1270–6. doi: 10.1016/j.exphem.2006.04.022
49. Heining C, Spyridonidis A, Bernhardt E, Schulte-Monting J, Behringer D, Grullich C, et al. Lymphocyte reconstitution following allogeneic hematopoietic stem cell transplantation: a retrospective study including 148 patients. *Bone Marrow Transplant* (2007) 39:613–22. doi: 10.1038/sj.bmt.1705648
50. Small TN, Papadopoulos EB, Boulad F, Black P, Castro-Malaspina H, Childs BH, et al. Comparison of immune reconstitution after unrelated and related T-cell-depleted bone marrow transplantation: effect of patient age and donor leukocyte infusions. *Blood* (1999) 93:467–80. doi: 10.1182/blood.V93.2.467.402k22_467_480
51. Li HW, Sachs J, Pichardo C, Bronson R, Zhao G, Sykes M. Nonalloreactive T cells prevent donor lymphocyte infusion-induced graft-versus-host disease by controlling microbial stimuli. *J Immunol* (2012) 189:5572–81. doi: 10.4049/jimmunol.120004
52. Miller JS, Weisdorf DJ, Burns LJ, Slungaard A, Wagner JE, Verneris MR, et al. Lymphodepletion followed by donor lymphocyte infusion (DLI) causes significantly more acute graft-versus-host disease than DLI alone. *Blood* (2007) 110:2761–3. doi: 10.1182/blood-2007-05-090340
53. Dudley ME, Wunderlich JR, Robbins PF, Yang JC, Hwu P, Schwartzentruber DJ, et al. Cancer regression and autoimmunity in patients after clonal repopulation with antitumor lymphocytes. *Science* (2002) 298:850–4. doi: 10.1126/science.1076514
54. Quezada SA, Simpson TR, Peggs KS, Merghoub T, Vider J, Fan X, et al. Tumor-reactive CD4+ T cells develop cytotoxic activity and eradicate large established melanoma after transfer into lymphopenic hosts. *J Exp Med* (2010) 207:637–50. doi: 10.1084/jem.20091918
55. Brentjens RJ, Davila ML, Riviere I, Park J, Wang X, Cowell LG, et al. CD19-targeted T cells rapidly induce molecular remissions in adults with chemotherapy-refractory acute lymphoblastic leukemia. *Sci Transl Med* (2013) 5:177ra38. doi: 10.1126/scitranslmed.3005930
56. Grupp SA, Kalos M, Barrett D, Aplenc R, Porter DL, Rheingold SR, et al. Chimeric antigen receptor-modified T cells for acute lymphoid leukemia. *N Engl J Med* (2013) 368:1509–18. doi: 10.1056/NEJMoa1215134
57. Park JH, Riviere I, Gonen M, Wang X, Senechal B, Curran KJ, et al. Long-Term Follow-up of CD19 CAR Therapy in Acute Lymphoblastic Leukemia. *N Engl J Med* (2018) 378:449–59. doi: 10.1056/NEJMoa1709919
58. Sotillo E, Barrett DM, Black KL, Bagashev A, Oldridge D, Wu G, et al. Convergence of Acquired Mutations and Alternative Splicing of CD19 Enables Resistance to CART-19 Immunotherapy. *Cancer Discov* (2015) 5:1282–95. doi: 10.1158/2159-8290.CD-15-1020
59. Jackson HJ, Brentjens RJ. Overcoming Antigen Escape with CAR T-cell Therapy. *Cancer Discov* (2015) 5:1238–40. doi: 10.1158/2159-8290.CD-15-1275
60. Kalos M, Levine BL, Porter DL, Katz S, Grupp SA, Bagg A, et al. T cells with chimeric antigen receptors have potent antitumor effects and can establish memory in patients with advanced leukemia. *Sci Transl Med* (2011) 3:95ra73. doi: 10.1126/scitranslmed.3002842
61. Neelapu SS, Tummala S, Kebriaei P, Wierda W, Gutierrez C, Locke FL, et al. Chimeric antigen receptor T-cell therapy - assessment and management of toxicities. *Nat Rev Clin Oncol* (2018) 15:47–62. doi: 10.1038/nrclinonc.2017.148
62. Qin H, Cho M, Haso W, Zhang L, Tasian SK, Oo HZ, et al. Eradication of B-ALL using chimeric antigen receptor-expressing T cells targeting the TSLPR oncoprotein. *Blood* (2015) 126:629–39. doi: 10.1182/blood-2014-11-612903
63. Jin CH, Xia J, Rafiq S, Huang X, Hu Z, Zhou X, et al. Modeling anti-CD19 CAR T cell therapy in humanized mice with human immunity and autologous leukemia. *EBioMedicine* (2019) 39:173–81. doi: 10.1016/j.ebiom.2018.12.013
64. Tan S, Li Y, Xia J, Jin CH, Hu Z, Duinkerken G, et al. Type 1 diabetes induction in humanized mice. *Proc Natl Acad Sci U S A* (2017) 114:10954–9. doi: 10.1073/pnas.1710415114
65. Rong Z, Wang M, Hu Z, Stradner M, Zhu S, Kong H, et al. An effective approach to prevent immune rejection of human ESC-derived allografts. *Cell Stem Cell* (2014) 14:121–30. doi: 10.1016/j.stem.2013.11.014

Conflict of Interest: The authors declare that the research was conducted in the absence of any commercial or financial relationships that could be construed as a potential conflict of interest.

Copyright © 2020 Sun, Jin, Tan, Liu and Yang. This is an open-access article distributed under the terms of the Creative Commons Attribution License (CC BY). The use, distribution or reproduction in other forums is permitted, provided the original author(s) and the copyright owner(s) are credited and that the original publication in this journal is cited, in accordance with accepted academic practice. No use, distribution or reproduction is permitted which does not comply with these terms.

frontiers in Immunology

ORIGINAL RESEARCH
published: 15 October 2020
doi: 10.3389/fimmu.2020.553362

Humanized Mouse as a Tool to Predict Immunotoxicity of Human Biologics

*Kylie Su Mei Yong[1], Zhisheng Her[1], Sue Yee Tan[1], Wilson Wei Sheng Tan[1], Min Liu[1], Fritz Lai[1], Shi Min Heng[1], Yong Fan[2], Kenneth Tou En Chang[3,4], Cheng-I Wang[5], Jerry Kok Yen Chan[6,7], Jianzhu Chen[8,9] and Qingfeng Chen[1,3,10]**

[1] Institute of Molecular and Cell Biology, Agency for Science, Technology and Research (A*STAR), Singapore, Singapore, [2] Key Laboratory for Major Obstetric Diseases of Guangdong Province, The Third Affiliated Hospital of Guangzhou Medical University, Guangzhou, China, [3] Department of Pathology and Laboratory Medicine, KK Women's and Children's Hospital, Singapore, Singapore, [4] Department of Pathology, Duke-NUS Graduate Medical School, Singapore, Singapore, [5] Singapore Immunology Network, Agency for Science, Technology and Research (A*STAR), Singapore, Singapore, [6] Department of Reproductive Medicine, KK Women's and Children's Hospital, Singapore, Singapore, [7] Experimental Fetal Medicine Group, Yong Loo Lin School of Medicine, National University of Singapore, Singapore, Singapore, [8] Interdisciplinary Research Group in Infectious Diseases, Singapore-Massachusetts Institute of Technology Alliance for Research and Technology, Singapore, Singapore, [9] The Koch Institute for Integrative Cancer Research and Department of Biology, Massachusetts Institute of Technology, Cambridge, MA, United States, [10] Department of Microbiology and Immunology, Yong Loo Lin School of Medicine, National University of Singapore, Singapore, Singapore

OPEN ACCESS

Edited by:
Alexandre P. A. Theocharides,
University Hospital Zürich, Switzerland

Reviewed by:
Onur Boyman,
University of Zurich, Switzerland
Yasuyuki Saito,
Kobe University, Japan

***Correspondence:**
Qingfeng Chen
qchen@imcb.a-star.edu.sg

Specialty section:
This article was submitted to Cancer Immunity and Immunotherapy, a section of the journal Frontiers in Immunology

Received: 18 April 2020
Accepted: 28 September 2020
Published: 15 October 2020

Citation:
Yong KSM, Her Z, Tan SY, Tan WWS, Liu M, Lai F, Heng SM, Fan Y, Chang KTE, Wang C-I, Chan JKY, Chen J and Chen Q (2020) Humanized Mouse as a Tool to Predict Immunotoxicity of Human Biologics. Front. Immunol. 11:553362. doi: 10.3389/fimmu.2020.553362

Advancements in science enable researchers to constantly innovate and create novel biologics. However, the use of non-human animal models during the development of biologics impedes identification of precise *in vivo* interactions between the human immune system and treatments. Due to lack of this understanding, adverse effects are frequently observed in healthy volunteers and patients exposed to potential biologics during clinical trials. In this study, we evaluated and compared the effects of known immunotoxic biologics, Proleukin®/IL-2 and OKT3 in humanized mice (reconstituted with human fetal cells) to published clinical outcomes. We demonstrated that humanized mice were able to recapitulate *in vivo* pathological changes and human-specific immune responses, such as elevated cytokine levels and modulated lymphocytes and myeloid subsets. Given the high similarities of immunological side effects observed between humanized mice and clinical studies, this model could be used to assess immunotoxicity of biologics at a pre-clinical stage, without placing research participants and/or patients at risk.

Keywords: cytokine storm, biologic testing, humanized mice, immunotoxicity, inflammation

INTRODUCTION

The pharmaceutical industry is constantly developing new biologics; however, accurate pre-clinical evaluation of human immune responses to biologics is an existing challenge (1, 2). The immune system is a complex biological system which can be affected by biologics that have an ability to alter immune-mediated activities and are major immunotoxic risk factors to humans (3, 4). Even though many aspects of the human immune system are found to be species-specific (5) and most antibody-based biologics are designed for human targets (6), non-human animal models are often used to

evaluate if biologics may cause immunological toxicity at a pre-clinical stage (7, 8). Due to evolutionary divergence in the immune systems between humans and animals, it is common that pre-clinical studies fail to identify exact immunological side effects of biologics, making it difficult to extrapolate conclusions from experimental data, therefore slowing or halting the translation of treatments (9, 10). For example, cell expression marker CD28 is only expressed on 80% of $CD4^+$ and 50% of $CD8^+$ T cells in humans but on 100% of $CD4^+$ and $CD8^+$ T cells in mice (11). In addition to this, human-specific CD3, upregulation of HLA-DR on activated T cells, production of IL-8 and Toll-like receptor 10 (TLR10) are not found in non-humanized mice (12). Due to these differences, it is common that animal models are refractory to an array of biologics that are human-specific. Therefore, to expand the existing range of treatments available and minimize the test of biologics with severe immunological side effects on humans, it is paramount to utilize animal models with high human-specificity (13, 14). The aim of this study is to investigate if mice reconstituted with a human immune system can be used as a platform for screening immunotoxicity and recapitulating mechanisms of the human immune responses to biologics such as, Proleukin®/IL-2 and OKT3.

An example of a biologic that causes severe immunological side effects in clinical patients is Proleukin®/IL-2. Proleukin®/IL-2 is a form of recombinant IL-2 used for the treatment of cancers such as, malignant melanoma and metastatic renal cell carcinoma (15, 16). IL-2 mediated toxicity is triggered by the direct binding of IL-2 to endothelial cells expressing IL-2 (17) and *via* the stimulation of IL-2 receptor-positive effector immune cells which releases vasoactive factors (18–20). IL-2 has a great propensity to induce adverse effects which includes "cytokine storm", capillary leak syndrome and breathing difficulties (21, 22) which limits the widespread use of Proleukin®/IL-2 therapy in clinics. These toxic effects require some patients to turn to alternative therapies including the use of IL-2 variants (17, 23, 24) that circumvent CD25 binding or completely withdraw from therapy after a limited number of treatment cycles even though Proleukin®/IL-2 is capable of inducing long-term clinical remission at a low cost (25, 26).

Another biologic known to trigger severe immunological side effects in clinics is OKT3. Utilizing hybridoma technology, OKT3 was engineered to target CD3 receptor, a membrane protein on the surface of circulating T cells (27, 28). During the initial stage, OKT3 activates T cells but subsequently promotes activated T cells to undergo apoptosis (29, 30). Due to the activation of T cells, a common side effect observed post-administration of OKT3 is the induction of a cytokine storm, which results in systemic release of inflammatory cytokines, predominantly interferon-γ (IFN-γ) and tumor necrosis factor alpha (TNF-α), which may cause a variety of adverse clinical conditions including, organ failure and pulmonary edema (31–33). Even though pre-clinical tests were conducted *in vitro* on human lymphocytes and *in vivo* on animal models, these studies failed to precisely identify the full spectrum of immunological side effects caused by a range of biologics (34–39).

Abbreviations: BFA, Brefeldin A; CM, Central memory; EM, Effector memory; IFN-γ, Interferon-γ; N, Naïve; NK, Natural Killer; PBMCs, Peripheral blood mononuclear cells; PD-1, Programmed cell death protein 1; SEM, Standard error of mean; TCR, T cell receptor; TEMRA, Effector memory RA; TNF-α, Tumor necrosis factor alpha.

METHODS

Fetal Liver Processing and Cell Isolation

Human fetal liver (FL) samples, male and female, 16–23 weeks of age were obtained from Kandang Kerbau Women's and Children's Hospital (KKH) with informed and written consent from patients. SingHealth and National Health Care Group Research Ethics Committees Singapore specifically approved this study (CIRB Ref: 2012/064/B), and all experimental procedures were conducted in accordance to the protocol. FLs were processed and digested with collagenase VI (2 mg/ml in Dulbecco's modified Eagle's medium (DMEM)) (Thermo Fisher Scientific, USA) for 15 min at 37°C with constant rotation. Digested tissue was passed through a 100 μm mesh to obtain single-cell suspension and isolated for human $CD34^+$ cells with a CD34-positive selection kit (STEMCELL Technologies, USA), according to the manufacturer's instructions. The purity of the $CD34^+$ cells was 90–99% as determined by flow cytometry.

Mice

NOD-*SCID IL2R*$\gamma^{-/-}$ (NSG) mice (Stock #005557) were obtained from the Jackson Laboratory and bred in the animal facility at A*STAR, Biological Resource Centre (BRC). Neonate mice were sub-lethally irradiated (100 rads) within 72 h of birth and infused with human $CD34^+$ fetal liver hematopoietic stem/progenitor cells (HSPCs) *via* intra-hepatic injection [96]. At 12-weeks post-transplantation, flow cytometry was used to determine human immune cell reconstitution levels in the peripheral blood of mice. A random mix of 13–15-week-old male and female mice were used in this study. Different donors were used for Proleukin®/IL-2 (n = 3) and OKT3 (n = 3) experiments. The International Animal Care and Use Committee (IACUC), A*STAR specifically approved this study with the protocol number (BRC #151034). All animal experimental procedures were conducted in accordance to the protocol.

Proleukin®/IL-2 and OKT3 Treatment

Proleukin®/IL-2 (Aldesleukin, Prometheus Laboratories Inc., USA) and OKT3 (Biolegend, USA) were procured. Dosage as per clinical scenarios, humanized mice were administered intravenously (IV) with either saline (n = 5), Proleukin®/IL-2 (600,000 IU) once daily for 5 days (n = 10) or a single dose of OKT3 (1 mg) injected only once (n = 9).

Sample Preparation for Flow Cytometry

To detect intracellular cytokines and chemokines by flow cytometry, mice administered with Proleukin®/IL-2 and saline-treated control groups of the same experiment were injected with 0.25 mg of BFA (Sigma-Aldrich, USA) at the endpoint of the

experiment (144 h) and sacrificed 6 h later. Submandibular blood collection was carried out in EDTA tubes (Greiner Bio-One, Austria), and red blood cells (RBCs) were lysed using RBC lysis buffer (Life Technologies, USA) prior to flow cytometry staining. Spleen and lymph nodes were digested in a mixture of collagenase IV (GIBCO, UK), DNase I (Sigma Aldrich, USA) and meshed through a 70 μm filter (Thermo Fisher Scientific, USA) in DMEM medium (Thermo Fisher Scientific, USA). When necessary, cell suspensions were subjected to red blood cell lysis (GIBCO, UK). The single-cell suspension was washed and re-suspended in media supplemented with 10% fetal bovine serum (FBS) (Thermo Fisher Scientific, USA).

Flow Cytometry

Single cell suspensions from spleen or blood (PBMCs) were stained with LIVE/DEAD fixable blue dead cell stain kit (Life Technologies, USA) for 30 min at 4°C and washed in PBS containing 0.2% BSA and 0.05% sodium azide. For staining of surface markers, the cells were incubated first with primary antibodies, CD45.1 (A20; Biolegend, USA), CD3 (UCHT1; BD Biosciences, USA), CD4 (RPA-T4; BD Biosciences, USA), CD8 (SK1; Biolegend, USA), CD11c (3.9; Biolegend, USA), CD16 (3G8; BD Biosciences, USA), CD19 (HIB19; Biolegend, USA), CD25 (2A3; BD Biosciences, USA), CD39 (TU66; BD Biosciences, USA), CD45 (HI30; BD Biosciences, USA), CD45RA (HI100; BD Biosciences, USA), CD56 (NCAM 16.2; BD Biosciences, USA), CD123 (7G3; BD Biosciences, USA), CD127/IL-7α (A019D5; Biolegend, USA), CD197/CCR7 (3D12; BD Biosciences, USA), CD278/ICOS (DX29; BD Biosciences, USA), CD279/PD-1 (MIH4; BD Biosciences, USA) and HLA-DR (G46-6; BD Biosciences, USA), CD3 (17A2; Biolegend, USA), CD4 (V4; BD Biosciences, USA), CD8a (53-6.7; Biolegend, USA), CD11b (M1/70; Biolegend, USA), CD11c (HL3; BD Biosciences, USA), CD25 (PC61; Biolegend, USA), CD19 (SJ25C1; Biolegend, USA), CD24 (M1/69; Biolegend, USA), CD44 (IM7; BD Biosciences, USA), CD49b (HMα2; Biolegend, USA), CD62L (MEL-14; BD Biosciences, USA), CD69 (H1.2F3; Biolegend, USA), CD127 (A7R34; Biolegend, USA), CD206 (068C2; Biolegend, USA), CD278 (DX29; BD Biosciences, USA), CD335 (29A1.4; Biolegend, USA), FOXP3 (MF23; BD Biosciences, USA), Ly6C (HK1.4; Biolegend, USA), Ly6G (1A8; BD Biosciences, USA), NK 1.1 (PK136; BD Biosciences, USA), and NKG2D (CX5; Biolegend, USA) in 100 μl of FACS buffer for 30 min at 4°C. For staining of intracellular proteins (including transcription factors, cytokines and chemokines), FACS buffer supplemented with 10 μg/ml of BFA was used. The cells were stained with LIVE/DEAD fixable blue dead cell stain kit (Life Technologies, USA), primary antibodies and then fixed and permeabilized using the Fixation/Permeabilization staining kit (BD Cytofix/Cytoperm™; BD Biosciences, USA) as per manufacturer's protocol. Staining was performed for 30 min at room temperature in the dark with the following antibodies, FOXP3 (206D; Biolegend, USA), IFN-γ(4S.B3; Biolegend, USA) and IL-10 (JES3-9D7; Biolegend, USA). Absolute count of cells in peripheral blood was determined using CountBright™ Absolute Counting Beads (ThermoFisher Scientific, USA). Data was acquired using a LSR II flow cytometer (BD Biosciences, USA) with FACSDiva software and analyzed using the Flowjo software version 10 (Treestar, USA).

Cytokine and Chemokine Protein Quantification

A premixed LEGENDplex™ Human Inflammation Panel (13-plex) (Biolegend, USA) was used to measure plasma cytokine and chemokine levels. The 13 cytokines and chemokines assayed simultaneously include IL-1β, IFN-α, IFN-γ, TNF-α, MCP-1 (CCL2), IL-6, IL-8 (CXCL8), IL-10, IL-12p70, IL-17A, IL-18, IL-23, and IL-33. Samples, reagents, and immunoassay procedures were prepared and performed according to the manufacturer's instructions. Data was acquired using a LSR II flow cytometer (BD Biosciences, USA) with FACSDiva software, and analysis was performed using LEGENDplex™ Data Analysis software (Biolegend, USA) based on standard curves plotted through a five-parameter logistic curve setting. Mice treated with Proleukin®/IL-2 had levels of IL-1β, IFN-α, TNF-α and IL-6 below detection limit and were excluded from subsequent analysis. For mice treated with OKT3, levels of IL-1β and IFN-α were below detection limit and excluded from analysis.

T Cell Activation and ELISA

Mice were administered with a single dose of OKT3 and sacrificed 5 days later. EasySep™ PE Positive Selection Kit (Stem Cell Technologies, Vancouver, BC), CD4 PE (OKT4, Biolegend, USA) and CD8 PE (OKT4, Biolegend, USA) antibodies were used to isolate $CD4^+$ and $CD8^+$ T cells from blood (PBMCs) as per manufacturer's instructions. Activation of $CD4^+$ and $CD8^+$ T cells was carried out with human T Cell Activation/Expansion Kit (Miltenyi, Germany) as per manufacturer's instructions. After T cell stimulation, supernatant in the culture was harvested and analyzed with IFN-γ (Biolegend, USA) and TNF-α (Biolegend, USA) ELISA kits.

Quantitative RT-PCR

RNA isolation was performed with RNeasy Mini and Micro kits (Qiagen, USA). Reverse transcription was performed using the iScript cDNA Synthesis Kit (Bio-Rad, USA) according to manufacturer's specifications. All values were normalized with β-actin as an endogenous control. Data were analyzed with the comparative CT method in which gene expression is calculated as $2^{-\Delta\Delta CT}$, where Delta Ct = (Ct gene of interest − Ct β-actin internal control). The primer sequences used are listed in **Supplementary Table 1**.

Histology

Mouse organs were collected, fixed with 10% formalin and embedded in paraffin for processing into sections. Formalin-fixed paraffin sections (5 μm) were dewaxed by melting for 30 min at 65°C, cleared in xylene twice for 5 min, and rehydrated in water–ethanol solutions containing decreasing percentages of ethanol. To determine tissue morphology, sections were stained with hematoxylin–eosin (Gill 2 Hematoxylin and Eosin Y alcoholic; Thermo Sandon, UK) following standard procedures.

For Immunohistochemistry, mouse organs were subjected to heat-mediated antigen retrieval with sodium citrate (pH6), incubated with anti-human CD45 (Abcam, UK) and stained with SuperPicture 3rd Gen IHC Detection Kit (Life Technologies, USA) according to the manufacturer's instructions. Sections were imaged and analyzed under an Olympus BX-61 microscope (Olympus, Japan).

Statistical Analysis

Statistical analysis was performed using GraphPad Prism 5.0 software (GraphPad Software Inc., USA). The correlation strength between the variables was assessed using the Spearman's rank correlation coefficient. Pairwise comparison was performed using two-tailed Mann–Whitney *U* test/two-way Analysis of variance (ANOVA), *p* value less than 0.05 is considered statistically significant.

RESULTS

Proleukin®/IL-2 Triggers an Inflammatory Response in Humanized Mice

To assess *in vivo* immunotoxic effects of Proleukin®/IL-2, humanized mice were administered with Proleukin®/IL-2 (600,000 IU/mouse) once daily for 5 days (40, 41). Peripheral blood mononuclear cells (PBMCs) were collected from the mice at 0 hours (h), 1 h after first administration and 72 h. At 144 h (endpoint), the mice were sacrifice and their PBMCs and organs were harvested for analysis (**Figure 1A**). Histological analysis showed that the lungs, liver, and kidneys of Proleukin®/IL-2-treated humanized mice developed massive immune cell infiltrations (**Figure 1B**).

A life-threatening side effect of prescribing Proleukin®/IL-2 to patients is the development of pulmonary edema (23, 42–44). This condition is commonly attributed to pulmonary capillary permeability, which causes fluid build-up and an increase in hydrostatic pressure within a patient's lung, in turn affecting air exchange leading to eventual death. To assess if humanized mice treated with Proleukin®/IL-2 experienced similar conditions to humans, we weighed the lungs at endpoint and observed that the lung weight of treated humanized mice were significantly heavier than that of saline-treated control mice (**Figure 1C**).

Administration of Proleukin®/IL-2 to patients usually results in "cytokine storm", which is the release of cytokines at high levels, leading to many clinical symptoms (22, 45). To identify if humanized mice would respond by producing cytokine storms as akin to human subjects, we evaluated human cytokine and chemokine levels within the plasma of these mice at 0 h, 1 h after the first administration, 72 h, and at 144 h after the last

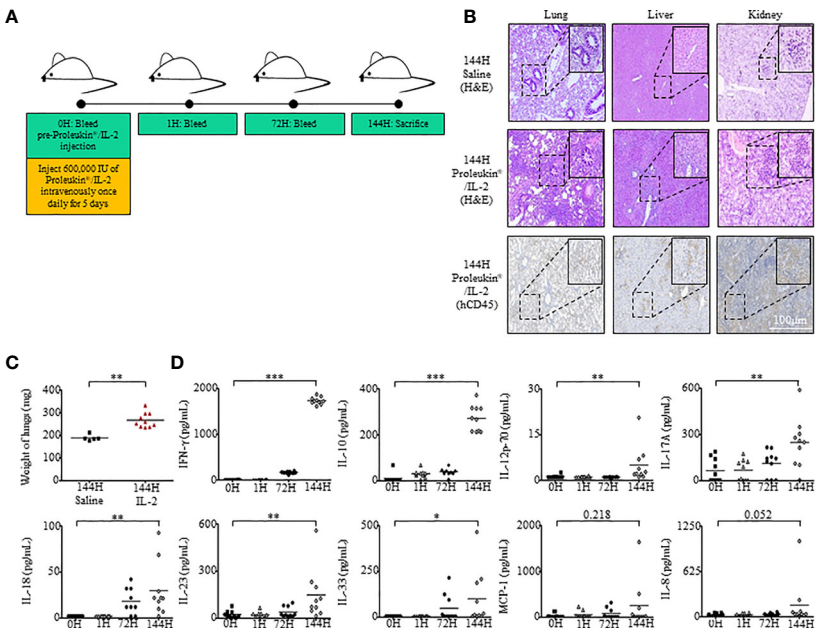

FIGURE 1 | Humanized mice exhibit inflammatory responses when administered with Proleukin®/IL-2. **(A)** Adult humanized mice were bled at 0 h to obtain peripheral blood mononuclear cells (PBMCs) and plasma for baseline analysis (n = 15). Each mouse was injected with 600,000 IU of Proleukin®/IL-2 daily for 5 days (n = 10). Mice were bled at 1 h after Proleukin®/IL-2 administration, at 72 h before day 3 administration of Proleukin®/IL-2 and sacrificed at 144 h to collect organs, PBMCs and plasma for analysis. **(B)** Histological analysis of organs from both saline treated (n = 5) and Proleukin®/IL-2 treated (n = 10) humanized mice. Paraffin slides from indicated organs were processed and stained with H&E or anti-human CD45 antibody. Representative images are shown. Scale bar applies to all panels. **(C)** Weight of lungs from saline (n = 5) and Proleukin®/IL-2- (n = 10) treated humanized mice. Each symbol represents one mouse and the horizontal line indicates the mean value. **(D)** Human-specific cytokine and chemokine release of IFN-γ, IL-10, IL-12p70, IL-17A, IL-18, IL-23, IL-33, MCP-1, and IL-8 were measured in the plasma of humanized mice administered with saline (n = 5) or Proleukin®/IL-2 (n = 10). Each symbol represents one mouse and the horizontal line indicates the mean value. Two-tailed Mann–Whitney *U* test; (*$p < 0.05$, **$p < 0.01$, ***$p < 0.001$). Data are from a single experiment; one independent experiment was performed.

administration of Proleukin®/IL-2. Similar to the clinical scenario (16), Proleukin®/IL-2 treatment in humanized mice induced an elevation of major chemokines and pro-inflammatory cytokines such as, IFN-γ, IL-12p70, IL-17A, IL-18, IL-23, IL-33, as well as an immunosuppressive cytokine, IL-10 at 144 h post-Proleukin®/IL-2 treatment but not at earlier time points (**Figure 1D**).

Multiple Immune Cell Subsets Expand Drastically During Proleukin®/IL-2 Treatment

We performed a comprehensive multiparameter flow cytometry evaluation on PBMCs, spleen, and lymph nodes (**Supplementary Figure 1**) of humanized mice, at 0 and at 144 h (endpoint) after Proleukin®/IL-2, utilizing markers that covered both lymphoid (**Supplementary Figure 2**) and myeloid (**Supplementary Figures 3A–C**) cell subsets.

In clinical settings, ICOS$^+$ regulatory T cells (CD4$^+$CD25$^+$ FOXP3$^+$ICOS$^+$ Tregs) have been identified as a potential predicative biomarker to determine if a patient would be responsive to Proleukin®/IL-2 treatment (16). It has been reported that patients who produce high levels of ICOS$^+$ Tregs during Proleukin®/IL-2 administration have an increased chance of responding to treatment (16). As shown in humanized mice, immunosuppressive cytokine IL-10 was produced in addition to chemokines and pro-inflammatory cytokines. Therefore, the frequency and phenotypes of human ICOS$^+$ Tregs in Proleukin®/IL-2-treated humanized mice were analyzed.

Consistent to cytokine and chemokine levels in the plasma, there were minimal changes in the levels of immune cell subsets in PBMCs from 0 to 72 h, with most significant changes observed at 144 h. Spearman's rank correlation coefficient revealed significantly positive correlation between the levels of CD45$^+$ cells to the release of cytokines such as IFN-γ (r = 0.940, p < 0.001) and IL-10 (r = 0.903, p > 0.001) (**Supplementary Figure 3D**). Among the human immune cell subsets analyzed, CD4$^+$ T cells, CD8$^+$ T cells and ICOS$^+$ Tregs expanded robustly, in terms of percentage relative to total live human leukocytes and absolute cell counts within PBMCs (**Figures 2A, B**) and spleen (**Figures 2D, E**) of humanized mice treated with Proleukin®/IL-2. There was also a significant increase in CD56$^+$ natural killer (NK) cells within both PBMCs (**Figure 2C**) and spleen (**Figure 2F**) of Proleukin®/IL-2-treated humanized mice. Similar to clinical settings CD14$^+$ monocytes and CD19$^+$ B cells decreased in both PBMCs (**Figure 2C**) and splenocytes (**Figure 2F**) post-Proleukin®/IL-2 therapy (16).

To compare our findings in humanized mice to wild type mice, we administered C57BL/6 mice with the same dose of

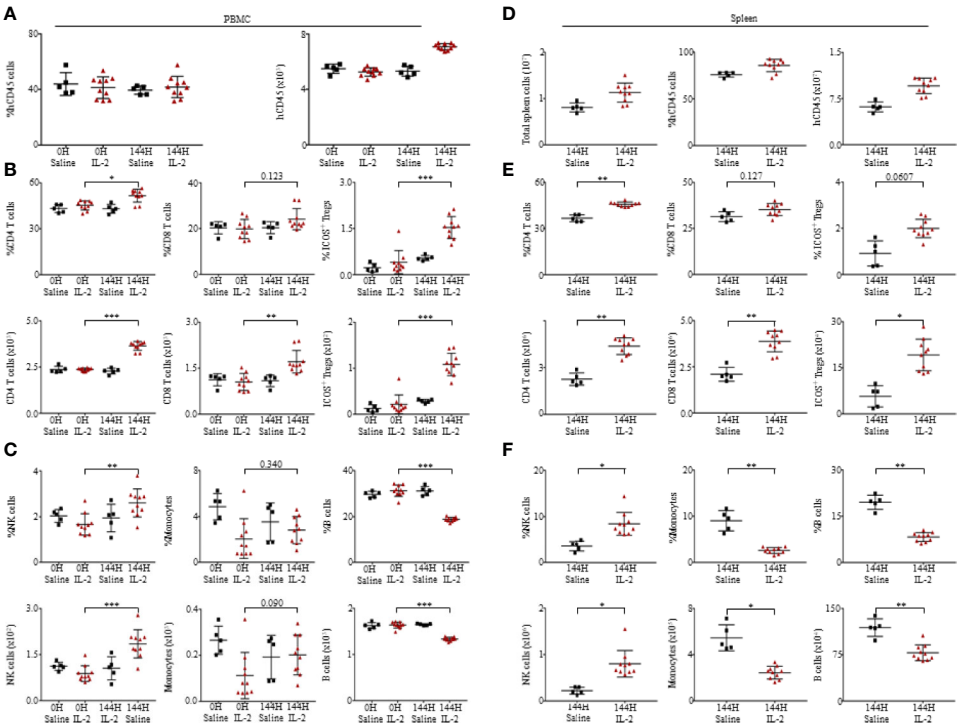

FIGURE 2 | Proleukin®/IL-2 triggers expansion of human immune cell subsets. **(A)** Mean frequency of PBMCs and absolute count over human CD45$^+$ cells ± SEM. Immunophenotypic analysis of **(B)** CD4$^+$ T cells, CD8$^+$ T cells, ICOS$^+$ Treg, **(C)** NK cells, monocytes and B cell subsets within peripheral blood mononuclear cells (PBMCs) of saline (n = 5) and Proleukin®/IL-2 recipient mice (n = 10). **(D)** Mean frequency and absolute cell count of splenocytes are based on total human CD45$^+$ cells ± SEM. Immune profile analysis of **(E)** CD4$^+$ T cells, CD8$^+$ T cells, ICOS$^+$ Treg, **(F)** NK cells, monocytes and B cell subsets in splenocytes of saline (n = 5) and Proleukin®/IL-2 recipient mice (n = 10). Two-tailed Mann–Whitney U test; (*p < 0.05, **p < 0.01, ***p < 0.001). Data are from a single experiment; one independent experiment was performed.

Proleukin®/IL-2 and observed that there was an increase in percentage of CD4$^+$ T cells, CD8$^+$ T cells, ICOS$^+$ Tregs, activation of CD4$^+$ and CD8$^+$ T cells (by CD69$^+$ upregulation) in PBMCs (**Supplementary Figure 4A**) and spleen (**Supplementary Figure 4B**) of these mice. While absolute cell counts of CD4$^+$ T cells, CD8$^+$ T cells, ICOS$^+$ Tregs, monocytes, NK cells, B cells, and activation of CD4$^+$ and CD8$^+$ T cells (by CD69$^+$ upregulation) increased in PBMCs (**Supplementary Figure 4A**), there was an increase in absolute cell counts of CD4$^+$ T cells, CD8$^+$ T cells, ICOS$^+$ Tregs, monocytes, NK cells, B cells in the spleen (**Supplementary Figure 4B**). Even though C57BL/6 could also respond to Proleukin®/IL-2 with immune cell expansion and activation (by upregulation of CD69), it lacked human-specific responses for example, the expression of MHC-II on activated T cells. This study strongly supports that humanized mice can more accurately recapitulate clinical responses and should be used to reduce the total number of animals utilized for research and clinical trials.

Proleukin®/IL-2 Activates T Cells Toward Terminally Differentiated Phenotype

As T cells expanded in response to Proleukin®/IL-2, we further investigated the immunophenotype of both CD4$^+$ and CD8$^+$ T cells. After Proleukin®/IL-2 administration, both CD4$^+$ (**Figure 3A**) and CD8$^+$ T cells (**Figure 3B**) lost characteristics of Naïve (N; CD45RA$^+$CCR7$^+$) and effector memory (EM; CD45RA$^-$CCR7$^-$) phenotypes. Instead, T cells with effector memory RA (TEMRA; CD45RA$^+$CCR7$^-$) increased. We examined the activation status of CD4$^+$ and CD8$^+$ T cells by analyzing the expression of HLA-DR, a molecule upregulated upon human T cell activation not usually observed in mice. Proleukin®/IL-2 treatment activated CD4$^+$ and CD8$^+$ T cells to upregulate HLA-DR expression in both PBMCs and spleen (**Figure 3C**). To detect intracellular cytokines, mice were injected with Brefeldin A (BFA). Upon activation, both CD4$^+$ and CD8$^+$ T cells had a greater number of IFN-γ producing cells as compared to monocytes and NK cells (**Figure 3D**). Together with absolute cell numbers, the cytokine production data confirmed that T cells were the main effector cells for the immunotoxicity induced by Proleukin®/IL-2.

ICOS$^+$ Tregs Have Phenotypic Characteristics of Tregs

In published clinical studies, FOXP3 expression has been associated in T cells with a regulatory or suppressive phenotype (46, 47). In some situations, a transient expression of FOXP3 at low levels can occur when effector, non-Treg CD4$^+$ cells are activated (48, 49). Prior to Proleukin®/IL-2 treatment, Tregs were ICOS$^-$;, however, after Proleukin®/IL-2 therapy, ICOS$^+$ Tregs increased drastically. Therefore, we investigated if these cells had immunosuppressive and regulatory phenotypic characteristics of Tregs seen in patients and were not merely non-Treg CD4$^+$FOXP3$^+$ T cells with an ICOS activation marker (16).

First, in accordance with previous studies (50–54), we observed the staining of CD25 and FOXP3 on ICOS$^+$ and

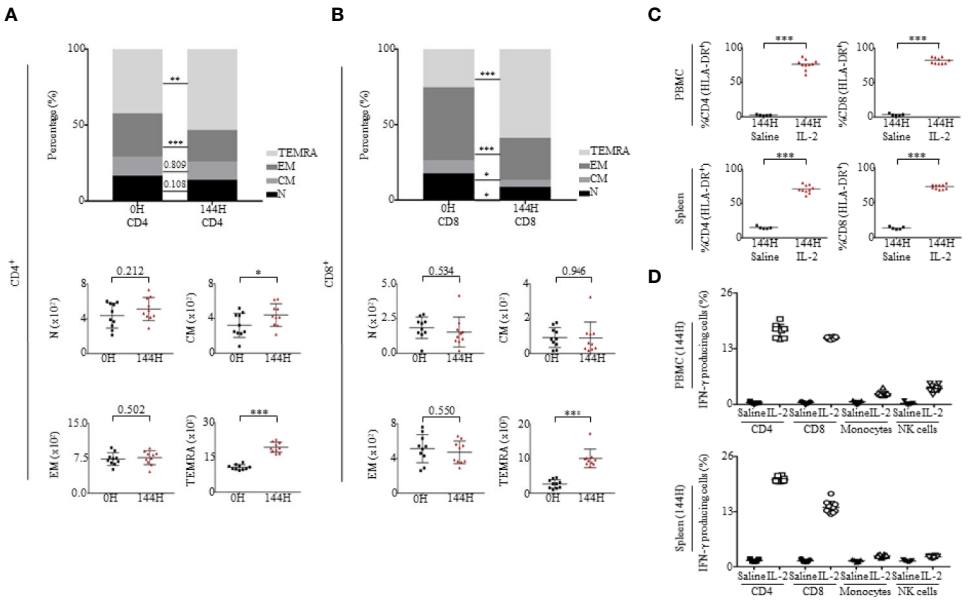

FIGURE 3 | Proleukin®/IL-2 activates T cells toward memory phenotypes. **(A, B)** Immunophenotypic analysis of both CD4 and CD8 subsets of Naïve (N; CD45RA$^+$CCR7$^+$), central memory (CM; CD45RA$^-$CCR7$^+$), effector memory (EM; CD45RA$^-$CCR7$^-$) and effector memory RA (TEMRA; CD45RA$^+$CCR7$^-$) in PBMCs at 0 and 144 h of mice administered with Proleukin®/IL-2 (n = 10). Mean frequency of (**A**, top panel) CD4$^+$ T cells and (**A**, bottom panel) absolute count over total human CD45$^+$ cells ± SEM. Mean frequency of (**B**, top panel) CD8$^+$ T cells and (**B**, bottom panel) absolute count of human CD45$^+$ cells ± SEM. **(C)** Percentage of CD4$^+$HLA-DR$^+$ and CD8$^+$HLA-DR$^+$ cells in the (**C**, top panel) PBMCs and (**C**, bottom panel) spleen of saline (n = 5) and Proleukin®/IL-2-treated mice (n = 10) at 144 h. **(D)** Percentage of IFN-γ was measured within T cells in (**D**, top panel) PBMCs and (**D**, bottom panel) spleen at 144 h of saline (n = 5) and Proleukin®/IL-2-treated mice (n = 10), injected with BFA. Two-way ANOVA/Two-tailed Mann–Whitney *U* test; (*$p < 0.05$, **$p < 0.01$, ***$p < 0.001$). Data are from a single experiment; one independent experiment was performed.

ICOS⁻ cells. Cells which were ICOS⁺ had a higher intensity staining of CD25 and FOXP3 than ICOS⁻ cells (**Supplementary Figure 2**). Second, ICOS⁺ Tregs expressed low levels of CD127/IL-7α in both PBMCs and spleen of humanized mice (**Figure 4A**). Third, we observed the expression of programmed cell death protein 1 (PD-1) and found that ICOS⁺ Tregs had a higher level of PD-1 than ICOS⁻ Tregs in both PBMCs and spleen of humanized mice (**Figure 4B**). Fourth, studies have linked highly suppressive Tregs to CD39 ectonucleotidase expression (55–57). In our experiment, we observed that ICOS⁺ Tregs were CD39⁺ while non-Tregs were CD39⁻, which was similar in both PBMCs and spleen of humanized mice (**Figure 4C**). Fifth, at 144 h post Proleukin®/IL-2 treatment, mice had heightened expression of FOXP3 and demethylation of Treg-specific-demethylated region (TSDR), suggesting activation of Tregs (**Figure 4D**). Lastly, it has been demonstrated that suppressive ICOS⁺ Tregs are able to secrete high levels of IL-10 and low levels of IFN-γ in response to stimulation. In agreement with published findings (16, 58), the intracellular cytokine staining revealed that ICOS⁺ cells produced high levels of IL-10 (**Figure 4E**) but did not produce IFN-γ at 144 h post-Proleukin®/IL-2 stimulation in both PBMCs (**Supplementary Figure 2B**) and spleen (**Supplementary Figure 2C**) of humanized mice. These results indicate that expanded ICOS⁺ Tregs in humanized mice treated with Proleukin®/IL-2 treatment display phenotypic attributes of Tregs similar to clinical scenarios (16).

OKT3 Induces Immunotoxic Effects in Humanized Mice

Besides cytokine treatments such as Proleukin®/IL-2, antibody therapy can also induce Immunotoxicity (31, 59). To determine whether humanized mice were able to recapitulate antibody-mediated immunotoxicity in humans, we evaluated a T cell receptor (TCR) triggering antibody, OKT3 (anti-CD3) in humanized mice. Humanized mice were analyzed at 0 h to obtain baseline levels of cytokines, chemokines, and immune cell subsets. As per clinical practice, in contrast to Proleukin®/IL-2 treatment which usually requires a longer duration of treatment to observe side effects, OKT3-mediated immunotoxicity occurs within a shorter time frame (60, 61). Mice were analyzed at 1 h post-administration of OKT3, 24 h, and sacrificed 96 h later (**Figure 5A**). Human chemokine and cytokine analysis in plasma showed that human chemokines and pro-inflammatory cytokines, such as IFN-γ, TNF-α, IL-6, IL-8, MCP-1, IL-17A, IL-18, IL-23, IL-33 and an immunosuppressive cytokine IL-10, started to elevate at 1 h post-OKT3 treatment (**Figure 5B**) with some cytokines and chemokines, IFN-γ, IL-8, IL-6, MCP-1 and IL-10 reaching its peak at 24 h. Most of the cytokines and chemokines returned to baseline levels by 96 h post-OKT3 treatment. Spearman's rank correlation coefficient revealed that there was a significant positive correlation between CD45⁺ cell levels and cytokines including IFN-γ (r = 0.950, p < 0.001) and IL-10 (r = 0.933, p < 0.001) production

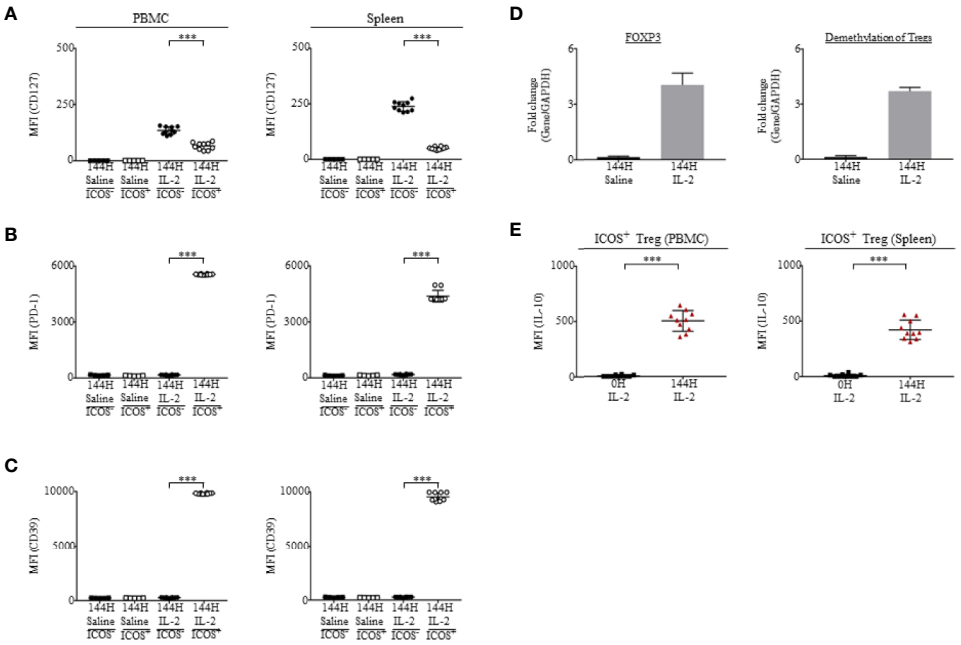

FIGURE 4 | Tregs from mice administered with Proleukin®/IL-2 display highly immunosuppressive phenotypes. **(A–C)** In saline treated (n = 5) mice, Tregs were ICOS⁻. ICOS was upregulated on Tregs upon Proleukin®/IL-2 treatment (n = 10) (**Supplementary Figure 2B**). Mean fluorescence intensity (MFI) in PBMCs and splenocytes, illustrating the expression of **(A)** CD127, **(B)** PD-1 and **(C)** CD39 on ICOS⁺ and ICOS⁻ Tregs in saline treated mice and ICOS⁺ and ICOS⁻ Tregs in Proleukin®/IL-2-treated mice at 144 h was shown. **(D)** Transcript expression of FOXP3 and demethylation of Tregs 144 h post saline (n = 5) and IL-2 treatment (n = 10). **(E)** Mean fluorescence intensity (MFI) in PBMCs and splenocytes, illustrating the production of IL-10 by ICOS⁺ Treg after IL-2 administration. Two-tailed Mann–Whitney U test; (*p < 0.05, **p < 0.01, ***p < 0.001). Data are from a single experiment; one independent experiment was performed.

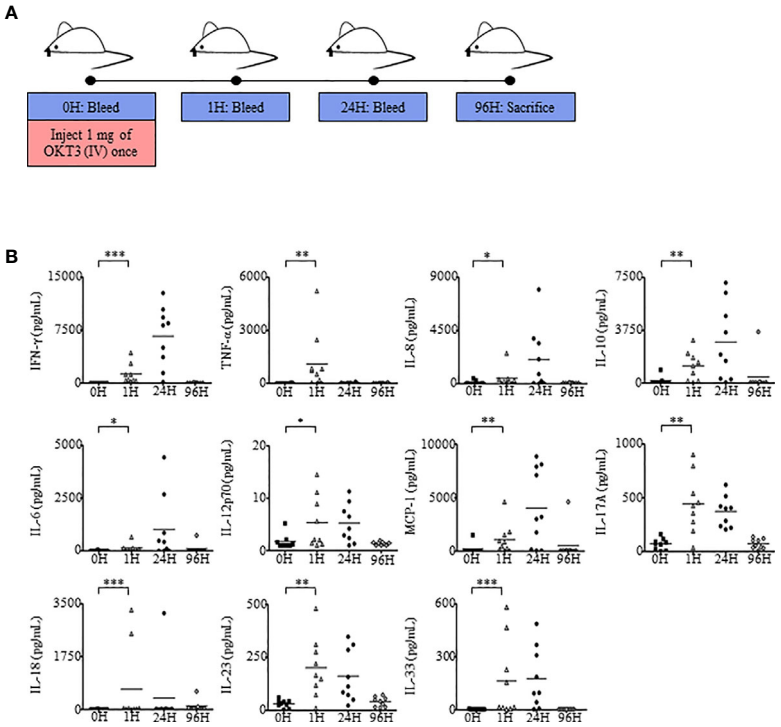

FIGURE 5 | Humanized mice administered with OKT3 exhibit heightened cytokine and chemokine production. **(A)** Adult humanized mice were bled at 0 h to obtain PBMCs and plasma for baseline analysis (n = 9). Each mouse was injected with 1 mg of OKT3 only once, bled at 1 h after OKT3 administration, 24 h and sacrificed at 96 h (endpoint). Organs, PBMCs, and plasma were collected, processed, and analyzed. **(B)** Human-specific cytokine and chemokine release of IFN-γ, TNF-α, IL-6, IL-8, IL-10, IL-12p70, MCP-1, IL-17A, IL-18, IL-23, and IL-33 were measured in the plasma of humanized mice administered with OKT3 (n = 9). Each symbol represents one mouse and the horizontal line indicates the mean value. Two-tailed Mann–Whitney *U* test; (*$p < 0.05$, **$p < 0.01$, ***$p < 0.001$). Data are from a single experiment; one independent experiment was performed.

(**Supplementary Figure 5C**). These results demonstrated that similar to clinical data, cytokine storm induced by immunotoxic antibody can be reproduced in humanized mice.

We further examined the effects of OKT3 stimulation on the regulation of immune cell subsets such as, $CD4^+$ T cells, $CD8^+$ T cells, NK cells, monocytes, and B cells (**Supplementary Figure 5**) within PBMCs (**Figures 6A, B**) and splenocytes (**Supplementary Figure 6**) of humanized mice. In addition, as it has been reported that upregulation of ICOS is greatly dependent on TCR activation (62), the involvement of $CD4^+ICOS^+$ T cells was also analyzed. At 24 h post-OKT3 treatment, humanized mice had drastically reduced frequencies and absolute numbers of $CD4^+$ and $CD8^+$ T cells due to the depletion effects of OKT3 antibody to CD3 T cells. However, the frequencies and number of $CD4^+$ and $CD8^+$ T cells recovered to baseline levels by 96H post-treatment, and there was an increase in $CD4^+ICOS^+$ T cells at 24 to 96 h post-OKT3 administration (**Figure 6A**). Treatment of humanized mice with OKT3 did not result in changes to the actual cell counts of NK cells and monocytes (**Figure 6B**).

To evaluate the functionality of T cells in pre-treated (0 h) and post-treated OKT3 (96 h) mice, we isolated $CD4^+$ and $CD8^+$ T cells and stimulated them with a T cell activation/expansion kit. Post-activation, the supernatant of $CD4^+$ and $CD8^+$ stimulated T cells was harvested and tested for the presence of IFN-γ and TNF-α *via* ELISA. Even though levels of IFN-γ and TNF-α were slightly lower in 96 h $CD4^+$ and $CD8^+$ T cells as compared to 0 h, the production of cytokines suggest that T cells that returned to the blood after OKT3 treatment were functional (**Figure 7A**). Although T cell numbers recovered 96 h post-OKT3 treatment, the composition of T cell subsets had changed significantly. Both $CD4^+$ T cells (**Figure 7B**) and $CD8^+$ T cells (**Figure 7C**) developed distinctive terminally differentiated phenotypes where percentages and absolute numbers of N, CM, and EM cells decreased while TEMRA cells were significantly elevated. These results from humanized mice correlate to published studies on patient responses (16, 27, 28, 63).

DISCUSSION

A pivotal reason for inferior success rates of biologics evaluated during clinical development may be due to conventional application of *in vitro* tests and non-human animal models

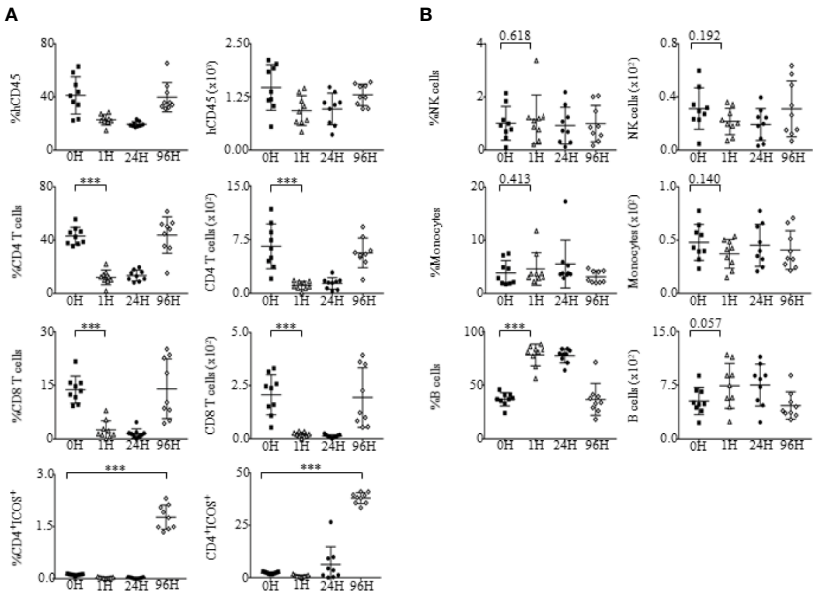

FIGURE 6 | Changes in immune cell subsets upon administration of OKT3. **(A)** Immunophenotypic analysis of CD4$^+$ T cells, CD8$^+$ T cells and CD4$^+$ICOS$^+$ T cell subsets within the PBMCs of OKT3 recipient mice (n = 9). (**A**, left panel) Mean frequency and (**A**, right panel) absolute count of CD4$^+$ T cells, CD8$^+$ T cells and CD4$^+$ICOS$^+$ T cells of total human CD45$^+$ cells ± SEM. **(B)** Immune profile analysis of NK cells, monocytes and B cell subsets within the PBMCs of mice administered with OKT3. (**B**, left panel) Mean frequency and (**B**, right panel) absolute count of NK cells, monocytes, and B cells over total human CD45$^+$ cells ± SEM. Two-tailed Mann–Whitney *U* test; (*$p < 0.05$, **$p < 0.01$, ***$p < 0.001$). Data are from a single experiment; one independent experiment was performed.

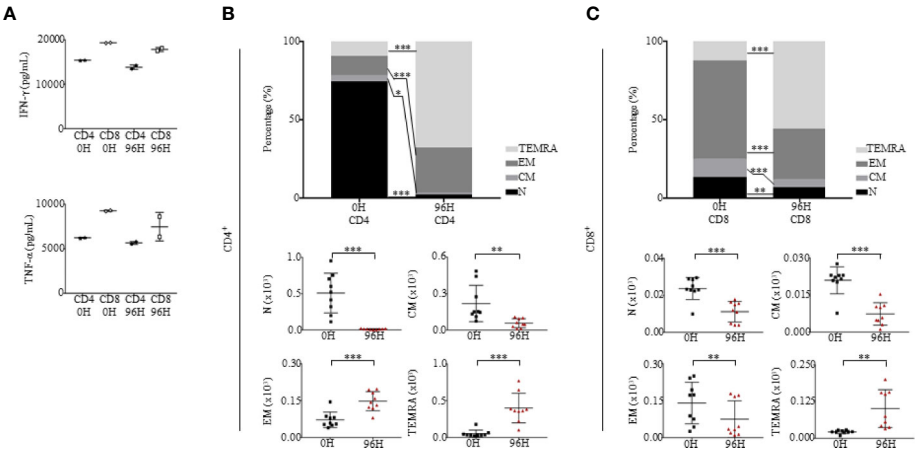

FIGURE 7 | Humanized mice treated with OKT3 have functional T cells and express altered CD4 and CD8 differentiation profiles. **(A)** T cells were stimulated with human T Cell Activation/Expansion Kit and levels of human IFN-γ and TNF-α were measured by ELISA (n = 2). **(B, C)** Immunophenotypic analysis of both CD4 and CD8 subsets of Naïve (N; CD45RA$^+$CCR7$^+$), central memory (CM; CD45RA$^-$CCR7$^+$), effector memory (EM; CD45RA$^-$CCR7$^-$) and effector memory RA (TEMRA; CD45RA$^+$CCR7$^-$) in PBMCs at 0H and 96H of mice administered with OKT3 (n = 9). (**B**, top panel) Mean frequency of CD4$^+$ T cells and (**B**, bottom panel) absolute count based on total human CD45$^+$ cells ± SEM. (**C**, top panel) Mean frequency of CD8$^+$ T cells and (**C**, bottom panel) absolute count over total human CD45$^+$ cells ± SEM. Two-way ANOVA/Two-tailed Mann–Whitney *U* test; (*$p < 0.05$, **$p < 0.01$, ***$p < 0.001$). Data are from a single experiment; one independent experiment was performed.

used to evaluate biologics specific for human targets during pre-clinical development (9, 10). Currently, the most suitable species for preclinical safety assessment of biologics are non-human primates (NHPs); however, the use of these animals raise critical ethical and economic issues including heighten level of sentience, scarcity, and high costs (35). In addition, analysis of NHPs demonstrated differences in biological systems particularly that of the immune system, resulting in inconsistent correlation of possible immunotoxic side effects when tested with biologics designed with human-specific targets (5, 7, 64). For example, the

use of cynomolgus and rhesus monkeys to screen for side effects of TGN1412 showed extremely different safety and efficacy profiles as compared to humans due to their dissimilarities in CD28 sequence and molecule (38, 64–66). Shortcomings in these assessments, suggest that the selection of a cost-effective, validated, predictive animal model, containing human-specific cells will add substantial value in identifying *in vivo* human-specific clinical toxicity, particularly for biologics with novel mechanisms of action, therefore allowing accurate safety assessment, determination of exact dose and timing of administration to patients (5, 8, 67).

In published studies, research teams constructed different humanized mice by using a myriad of immunodeficient mouse strains, reconstituted with human PBMCs, cord blood or fetal liver. Some of these humanized mice have been applied as a platform to test plasmids, antibodies and biologics (68–75). For example, Li et al. tested IL-2 plasmid and CD3 antibody in human immune system (HIS) mice [generated in BALB/cR-ag2$^{-/-}$ Il2r-$\gamma^{-/-}$ SIRPA^{NOD} (BRGS) hosts] reconstituted with fetal liver CD34^{+} cells (75). Different from published work, we utilized one of the most well-studied and accessible immunodeficient mouse strain, NSG. To prevent unwanted side effects that have been reported with the use of PBMCs, we reconstituted mice with human fetal liver stem cells and recapitulated clinical scenarios closely by using the exact clinical drug, dose and administration method to evaluate the effects of Proleukin®/IL-2 in humanized mice (40).

In this study, we have shown that mice reconstituted with a human immune system, more accurately recapitulated human immune responses to immunotoxic biologics. Humanized mice treated with Proleukin®/IL-2 for 5 consecutive days at a dose of 600,000 IU demonstrated an increase in total lung weight, immune cell infiltration into organs, elevated levels of chemokines and pro-inflammatory cytokines, IFN-γ, IL-12p70, IL-17A, IL-18, IL-23 and IL-33 and an immunosuppressive cytokine, IL-10 (15, 76). Additionally, percentages and absolute numbers of CD4^{+} T cells, CD8^{+} T cells, ICOS^{+} Tregs and NK cells were upregulated, while levels of monocytes and B cells decreased (15, 21, 26, 76). To further validate this model, we administered an anti-CD3 antibody—OKT3—to humanized mice and observed that massive amounts of chemokines and pro-inflammatory cytokines, IFN-γ, TNF-α, IL-6, IL-8, MCP-1, IL-17A, IL-18, IL-23, and IL-33 were secreted predominantly at 1 h post-treatment (77, 78). At 96 h, levels of T cells gradually recovered; this phenomenon could be due to a homeostatic mechanism to maintain constant T cell numbers in the circulation known as lymphopenia-induced proliferation (LIP) (79). Interestingly, in addition to inflammatory responses, which were considered to be the main cause of immunotoxicity, immunosuppressive responses, such as the expansion of ICOS^{+} Treg cells and production of immunosuppressive cytokine, IL-10, occurred concurrently. These results suggest that immunotoxicity may be a competitive dynamic process between inflammation and immunosuppression (80). Besides the effort on reducing inflammation (44), development of strategies to enhance immunosuppression may provide new options to the treatments of an array of conditions and diseases (81, 82). Most importantly, our results are in concordance with that of published clinical studies (16), therefore enabling the use of humanized mice as a pre-clinical platform to determine human-specific biologic mechanisms of action.

Despite the advantages and significant findings from using humanized mice, limitations in this work include firstly, the measurement of lung total weight which could have been further optimized by analyzing lung wet weight so as to differentiate between intrapulmonary cellular infiltrates and lung edema (17). Secondly, TNF-α was not upregulated in Proleukin®/IL-2-treated humanized mice (18–20). Possible reasons for this observation could be that our current model relies on the transplantation of HSPCs which do not give rise to endothelial cells of human-origin. Endothelial cells together with IL-2 receptor-positive immune cells are essential for the release of vasoactive factors such as TNF-α (18–20). In addition, our model requires further optimization to improve levels of human cell engraftment and functionality of immune subsets such as myeloid cells, which are crucial for TNF-α production but are relatively low in the current model (83). In recent years, humanized mouse strains such as NSG-SGM3, HuNOG-EXL, and MISTRG mice have been created with improved human immune cell reconstitution (84). However, despite the increase of reconstitution in these mice, drawbacks include the need for matched donors to create thymus, liver, and hematopoietic stem cell engrafted mice (NSG-SGM3, HuNOG-EXL), human immune cell reconstitution that lasts not more than 5 months (NSG-SGM3), anemia and short lifespan after human cell engraftment (HuNOG-EXL, MISTRG), undetermined long-term effects of irradiation tolerance and incidences of lymphoma (NSG-SGM3, HuNOG-EXL, MISTRG) and impaired innate immune cells including macrophages and dendritic cells (NSG-SGM3, HuNOG-EXL, MISTRG) (85–88). To improve current versions of humanized mice, murine cells should be completely depleted to allow an increase in human cell reconstitution which can be supplemented by hydrodynamically boosting mice with high affinity cytokines (*e.g.* IL-1β, IL-2, IL-7, and GM-CSF) to induce immune cell differentiation, maturation and function (83, 89, 90). Overcoming obstacles and improving humanized mice would undoubtedly provide exciting opportunities for the scientific community to evaluate novel therapeutics including biologics that would greatly benefit society.

Outcomes for specific therapeutic developments are largely dependent on selected animal models which allow the validation of therapeutic mechanisms and prediction of clinical efficacy (5, 91). When properly designed and carried out, animal models can contribute essential information to our knowledge of biology and medicine, including the discovery and development of new therapies (1, 2). However, due to the evolutionary gap between species, existing animal models are unable to fully recapitulate human biological responses, particularly that of the immune system (5). Advantages of utilizing humanized mice are its ability to more accurately mimic and reproduce human-specific responses (92, 93) for example, allowing the test of biologics

specific to human CD3, production of human cytokine, IL-8 and the expression of HLA-DR on activated T cells, as demonstrated in this study. Therefore, in addition to current *in vitro* and *in vivo* pre-clinical tests, we advocate the use of humanized mice as a key for successful and safe clinical translation, so as to develop, optimize, validate, and create treatments.

In summary, humanized mice are small, easy to manipulate, cost-effective and robust platform that recapitulates the immune responses of human subjects. Because of the similarities in cellular and molecular mechanisms between humanized mice and humans (13, 84, 94), it unquestionably provides valuable data on the clinical performance of treatments, allowing researchers to learn human immunological mechanisms or be alerted of potential adverse effects of therapeutics before testing them on human subjects, therefore enabling the translation of a plethora of treatments which will benefit patients.

DATA AVAILABILITY STATEMENT

All datasets presented in this study are included in the article/ **Supplementary Material**.

ETHICS STATEMENT

The studies involving human participants were reviewed and approved by SingHealth and National Health Care Group Research Ethics Committees Singapore. The patients/participants provided their written informed consent to participate in this study. The animal study was reviewed and approved by International Animal Care and Use Committee (IACUC), A*STAR.

AUTHOR CONTRIBUTIONS

KY designed and performed experiments, analyzed and interpreted data, and prepared the manuscript. ZH, ST, WT, ML, FL, and SH performed experiments. YF, KC, C-IW, MK, JKYC, and JC provided the research tools, were involved in discussions, and prepared the manuscript. QC conceived the study, supervised the project and prepared the manuscript. All authors contributed to the article and approved the submitted version.

FUNDING

This work was supported by the following grants: National Medical Research Council Singapore, VICTORY programme (NMRC/OFLCG/003/2018) and CS-IRG (CIRG19may-0051), A*STAR IAF-PP IMPACT programme (H18/01/a0/022) and National Research Foundation Fellowship Singapore NRF-NRFF2017-03, Competitive Research Programme NRF2016-CRP001-103 and NRF2019-NRF-ISF003-3127 to QC.

SUPPLEMENTARY MATERIAL

The Supplementary Material for this article can be found online at: https://www.frontiersin.org/articles/10.3389/fimmu.2020.553362/full#supplementary-material

SUPPLEMENTARY TABLE 1 | Primers for qPCR. Primer sequences for FOXP3-TSDR demethylation-specific, FOXP3-TSDR methylation-specific, FOXP3, and β-actin.

REFERENCES

1. Otto MW, Nierenberg AA. Assay sensitivity, failed clinical trials, and the conduct of science. *Psychother Psychosom* (2002) 71(5):241–3. doi: 10.1159/000064813
2. Kola I. The state of innovation in drug development. *Clin Pharmacol Ther* (2008) 83(2):227–30. doi: 10.1038/sj.clpt.6100479
3. Dansette PM, Bonierbale E, Minoletti C, Beaune PH, Pessayre D, Mansuy D. Drug-induced immunotoxicity. *Eur J Drug Metab Pharmacokinet* (1998) 23 (4):443–51. doi: 10.1007/BF03189993
4. Descotes J. Immunotoxicology. *Drug Saf* (2005) 28(2):127–36. doi: 10.2165/00002018-200528020-00004
5. Mestas J, Hughes CCW. Of mice and not men: differences between mouse and human immunology. *J Immunol* (2004) 172(5):2731–8. doi: 10.4049/jimmunol.172.5.2731
6. Ito S, Bollard CM, Carlsten M, Melenhorst JJ, Biancotto A, Wang E. Ultra-low dose interleukin-2 promotes immune-modulating function of regulatory T cells and natural killer cells in healthy volunteers. *Mol Ther* (2014) 22(7):1388–95. doi: 10.1038/mt.2014.50
7. van Wijk F, Nierkens S. Assessment of drug-induced immunotoxicity in animal models. *Drug Discov Today Technol* (2006) 3(1):103–9. doi: 10.1016/j.ddtec.2006.03.003
8. Begley CG, Ellis LM. Drug development: raise standards for preclinical cancer research. *Nature* (2012) 483(7391):531–3. doi: 10.1038/483531a
9. Arrowsmith J. Phase II failures: 2008–2010. *Nat Rev Drug Discov* (2011) 10:328–9. doi: 10.1038/nrd3439
10. Harrison RK. Phase II and phase III failures: 2013–2015. *Nat Rev Drug Discov* (2016) 15:817–8. doi: 10.1038/nrd.2016.184
11. Beyersdorf N, Kerkau T, Hünig T. CD28 co-stimulation in T-cell homeostasis: a recent perspective. *ImmunoTargets Ther* (2015) 4:111–22. doi: 10.2147/ITT.S61647
12. Oosting M, Cheng SC, Bolscher JM, Vestering-Stenger R, Plantinga TS, Verschueren IC, et al. Human TLR10 is an anti-inflammatory pattern-recognition receptor. *Proc Natl Acad Sci U S A* (2014) 111(42):E4478–84. doi: 10.1073/pnas.1410293111
13. Pearson T, Greiner DL, Shultz LD. Creation of "humanized" mice to study human immunity. *Curr Protoc Immunol* (2008) Chapter 15, Unit-15.21. doi: 10.1002/0471142735.im1521s81
14. Shultz LD, Brehm MA, Garcia JV, Greiner DL. Humanized mice for immune system investigation: progress, promise and challenges. *Nat Rev Immunol* (2012) 12(11):786–98. doi: 10.1038/nri3311
15. Antony GK, Dudek AZ. Interleukin 2 in cancer therapy. *Curr Med Chem* (2010) 17(29):3297–302. doi: 10.2174/092986710793176410
16. Sim GC, Martin-Orozco N, Jin L, Yang Y, Wu S, Washington E, et al. IL-2 therapy promotes suppressive ICOS(+) Treg expansion in melanoma patients. *J Clin Invest* (2014) 124(1):99–110. doi: 10.1172/JCI46266
17. Krieg C, Létourneau S, Pantaleo G, Boyman O. Improved IL-2 immunotherapy by selective stimulation of IL-2 receptors on lymphocytes and endothelial cells. *Proc Natl Acad Sci U S A* (2010) 107(26):11906–11. doi: 10.1073/pnas.1002569107
18. Boyman O, Sprent J. The role of interleukin-2 during homeostasis and activation of the immune system. *Nat Rev Immunol* (2012) 12(3):180–90. doi: 10.1038/nri3156

19. Arenas-Ramirez N, Woytschak J, Boyman O. Interleukin-2: Biology, Design and Application. *Trends Immunol* (2015) 36(12):763–77. doi: 10.1016/j.it.2015.10.003
20. Boyman O, Arenas-Ramirez N. Development of a novel class of interleukin-2 immunotherapies for metastatic cancer. *Swiss Med Wkly* (2019) 149:w14697. doi: 10.4414/smw.2019.14697
21. Atkins MB, Lotze MT, Dutcher JP, Fisher RI, Weiss G, Margolin K, et al. High-dose recombinant interleukin 2 therapy for patients with metastatic melanoma: analysis of 270 patients treated between 1985 and 1993. *J Clin Oncol* (1999) 17(7):2105–5. doi: 10.1200/JCO.1999.17.7.2105
22. Tisoncik JR, Korth MJ, Simmons CP, Farrar J, Martin TR, Katze MG. Into the eye of the cytokine storm. *Microbiol Mol Biol Rev* (2012) 76(1):16–32. doi: 10.1128/MMBR.05015-11
23. Levin AM, Bates DL, Ring AM, Krieg C, Lin JT, Su L, et al. Exploiting a natural conformational switch to engineer an interleukin-2 'superkine'. *Nature* (2012) 484(7395):529–33. doi: 10.1038/nature10975
24. Arenas-Ramirez N, Zou C, Popp S, Zingg D, Brannetti B, Wirth E, et al. Improved cancer immunotherapy by a CD25-mimobody conferring selectivity to human interleukin-2. *Sci Transl Med* (2016) 8(367):367ra166. doi: 10.1126/scitranslmed.aag3187
25. Fyfe GA, Fisher RI, Rosenberg SA, Sznol M, Parkinson DR, Louie AC. Long-term response data for 255 patients with metastatic renal cell carcinoma treated with high-dose recombinant interleukin-2 therapy. *J Clin Oncol* (1996) 14(8):2410–1. doi: 10.1200/JCO.1996.14.8.2410
26. Jolliffe LK. Humanized antibodies: enhancing therapeutic utility through antibody engineering. *Int Rev Immunol* (1993) 10(2-3):241–50. doi: 10.3109/08830189309061699
27. Adair JR, Athwal DS, Bodmer MW, Bright SM, Collins AM, Pulito VL, et al. Humanization of the murine anti-human CD3 monoclonal antibody OKT3. *Hum Antibodies Hybridomas* (1994) 5(1–2):41–7. doi: 10.3233/HAB-1994-51-206
28. Debure A, Chkoff N, Chatenoud L, Lacombe M, Campos H, Noël LH, et al. One-month prophylactic use of OKT3 in cadaver kidney transplant recipients. *J Urol* (1989) 45(3):546–53. doi: 10.1097/00007890-198803000-00009
29. Carpenter PA, Pavlovic S, Tso JY, Press OW, Gooley T, Yu XZ, et al. Non-Fc receptor-binding humanized anti-CD3 antibodies induce apoptosis of activated human T cells. *J Immunol* (2000) 165(11):6205–13. doi: 10.4049/jimmunol.165.11.6205
30. Chatenoud L, Baudrihaye MF, Kreis H, Goldstein G, Schindler J, Bach JF. Human *in vivo* antigenic modulation induced by the anti-T cell OKT3 monoclonal antibody. *Eur J Immunol* (1982) 12(11):979–82. doi: 10.1002/eji.1830121116
31. Martin A, Tisch RM, Getts DR. Manipulating T cell-mediated pathology: targets and functions of monoclonal antibody immunotherapy. *Clin Immunol* (2013) 148(1):136–47. doi: 10.1016/j.clim.2013.04.011
32. Shiheido H, Chen C, Hikida M, Watanabe T, Shimizu J. Modulation of the human T cell response by a novel non-mitogenic anti-CD3 antibody. *PLoS One* (2014) 9(4):e94324. doi: 10.1371/journal.pone.0094324
33. Loisel S, Ohresser M, Pallardy M, Daydé D, Berthou C, Cartron G, et al. Relevance, advantages and limitations of animal models used in the development of monoclonal antibodies for cancer treatment. *Crit Rev Oncol Hematol* (2007) 62(1):34–42. doi: 10.1016/j.critrevonc.2006.11.010
34. Chapman K, Pullen N, Coney L, Dempster M, Andrews L, Bajramovic J, et al. Preclinical development of monoclonal antibodies: considerations for the use of non-human primates. *mAbs* (2009) 1(5):505–16. doi: 10.4161/mabs.1.5.9676
35. Eastwood D, Findlay L, Poole S, Bird C, Wadhwa M, Moore M, et al. Monoclonal antibody TGN1412 trial failure explained by species differences in CD28 expression on CD4(+) effector memory T-cells. *Br J Pharmacol* (2010) 161(3):512–26. doi: 10.1111/j.1476-5381.2010.00922.x
36. Hünig T. The storm has cleared: lessons from the CD28 superagonist TGN1412 trial. *Nat Rev Immunol* (2012) 12(5):317–8. doi: 10.1038/nri3192
37. Hünig T. The rise and fall of the CD28 superagonist TGN1412 and its return as TAB08: a personal account. *FEBS J* (2016) 283(18):3325–34. doi: 10.1111/febs.13754
38. Kuhn C, Weiner HL. Therapeutic anti-CD3 monoclonal antibodies: from bench to bedside. *Immunotherapy* (2016) 8(8):889–906. doi: 10.2217/imt-2016-0049
39. Amaria RN, Reuben A, Cooper ZA, Wargo JA. Update on use of aldesleukin for treatment of high-risk metastatic melanoma. *Immunotargets Ther* (2015) 4:79–89. doi: 10.2147/itt.s61590
40. Nair AB, Jacob S. A simple practice guide for dose conversion between animals and human. *J Basic Clin Pharm* (2016) 7(2):27–31. doi: 10.4103/0976-0105.177703
41. Ferro TJ, Johnson A, Everitt J, Malik AB. IL-2 induces pulmonary edema and vasoconstriction independent of circulating lymphocytes. *J Immunol* (1989) 142(6):1916.
42. Saxon RR, Klein JS, Bar MH, Blanc P, Gamsu G, Webb WR, et al. Pathogenesis of pulmonary edema during interleukin-2 therapy: correlation of chest radiographic and clinical findings in 54 patients. *AJR Am J Roentgenol* (1991) 156(2):281–5. doi: 10.2214/ajr.156.2.1898799
43. Berthiaume Y, Boiteau P, Fick G, Kloiber R, Sinclair GD, Fong C, et al. Pulmonary edema during IL-2 therapy: combined effect of increased permeability and hydrostatic pressure. *Am J Respir Crit Care Med* (1995) 152(1):329–35. doi: 10.1164/ajrccm.152.1.7599842
44. Clark IA. The advent of the cytokine storm. *Immunol Cell Biol* (2007) 85 (4):271–3. doi: 10.1038/sj.icb.7100062
45. Campbell DJ, Koch MA. Phenotypic and functional specialization of FOXP3 (+) regulatory T cells. *Nat Rev Immunol* (2011) 11(2):119–30. doi: 10.1038/nri2916
46. Li Z, Li D, Tsun A, Li B. FOXP3$^+$ regulatory T cells and their functional regulation. *Cell Mol Immunol* (2015) 12(5):558–65. doi: 10.1038/cmi.2015.10
47. Wang J, Ioan-Facsinay A, van der voort EIH, Huizinga TWJ, Toes REM. Transient expression of FOXP3 in human activated nonregulatory CD4$^+$ T cells. *Eur J Immunol* (2007) 37(1):129–38. doi: 10.1002/eji.200636435
48. Ziegler SF. FOXP3: Not just for regulatory T cells anymore. *Eur J Immunol* (2007) 37(1):21–3. doi: 10.1002/eji.200636929
49. Sakaguchi S. Naturally arising Foxp3-expressing CD25$^+$CD4$^+$ regulatory T cells in immunological tolerance to self and non-self. *Nat Immunol* (2005) 6(4):345–52. doi: 10.1038/ni1178
50. Sakaguchi S, Wing K, Miyara M. Regulatory T cells – a brief history and perspective. *Eur J Immunol* (2007) 37(S1):S116–23. doi: 10.1007/978-1-61737-979-6_1
51. Wei S, Kryczek I, Edwards RP, Zou L, Szeliga W, Banerjee M, et al. Interleukin-2 administration alters the CD4$^+$FOXP3$^+$ T-cell pool and tumor trafficking in patients with ovarian carcinoma. *Cancer Res* (2007) 67(15):7487. doi: 10.1158/0008-5472.CAN-07-0565
52. Venken K, Hellings N, Broekmans T, Hensen K, Rummens JL, Stinissen P. Natural naive CD4$^+$CD25$^+$CD127^{low} regulatory T cell (Treg) development function are disturbed in multiple sclerosis patients: recovery of memory Treg homeostasis during disease progression. *J Immunol* (2008) 180(9):6411. doi: 10.4049/jimmunol.180.9.6411
53. Miyara M, Yoshioka Y, Kitoh A, Shima T, Wing K, Niwa A, et al. Functional delineation and differentiation dynamics of human CD4$^+$ T cells expressing the FoxP3 transcription factor. *Immunity* (2009) 30(6):899–911. doi: 10.1016/j.immuni.2009.03.019
54. Borsellino G, Kleinewietfeld M, Di Mitri D, Sternjak A, Diamantini A, Giometto R, et al. Expression of ectonucleotidase CD39 by Foxp3$^+$ Treg cells: hydrolysis of extracellular ATP and immune suppression. *Blood* (2007) 110(4):1225. doi: 10.1182/blood-2006-12-064527
55. Fletcher JM, Lonergan R, Costelloe L, Kinsella K, Moran B, O'Farrelly C, et al. CD39$^+$Foxp3$^+$ regulatory T cells suppress pathogenic Th17 cells and are impaired in Multiple Sclerosis. *J Immunol* (2009) 183(11):7602. doi: 10.4049/jimmunol.0901881
56. Mandapathil M, Lang S, Gorelik E, Whiteside TL. Isolation of functional human regulatory T cells (Treg) from the peripheral blood based on the CD39 expression. *J Immunol Methods* (2009) 346(1-2):55–63. doi: 10.1016/j.jim.2009.05.004
57. Kryczek I, Liu R, Wang G, Wu K, Shu X, Szeliga W, et al. FOXP3 defines regulatory T cells in human tumor and autoimmune disease. *Cancer Res* (2009) 69(9):3995. doi: 10.1158/0008-5472.CAN-08-3804
58. Ohira M, Nishida S, Matsuura T, Muraoka I, Tryphonopoulos P, Fan J, et al. Comparative analysis of T-cell depletion method for clinical immunotherapy —anti–Hepatitis C effects of Natural Killer cells via interferon-γ production. *Transplant Proc* (2013) 45(5):2045–50. doi: 10.1016/j.transproceed.2013.01.046
59. Gaston RS, Deierhoi MH, Patterson T, Prasthofer E, Julian BA, Barber WH, et al. OKT3 first-dose reaction: association with T cell subsets and cytokine release. *Kidney Int* (1991) 39(1):141–8. doi: 10.1038/ki.1991.18

60. Meloni G, Trisolini SM, Capria S, Torelli GF, Baldacci E, Torromeo C, et al. How long can we give interleukin-2? Clinical and immunological evaluation of AML patients after 10 or more years of IL2 administration. *Leukemia* (2002) 16:2016–8. doi: 10.1038/sj.leu.2402566
61. Martin-Orozco N, Li Y, Wang Y, Liu S, Hwu P, Liu YJ, et al. Melanoma cells express ICOS ligand to promote the activation and expansion of T-regulatory cells. *Cancer Res* (2010) 70(23):9581–90. doi: 10.1158/0008-5472.CAN-10-1379
62. Isaacs JD. Therapeutic T-cell manipulation in rheumatoid arthritis: past, present and future. *Rheumatology* (2008) 47(10):1461–8. doi: 10.1093/rheumatology/ken163
63. Attarwala H. TGN1412: from discovery to disaster. *J Young Pharm* (2010) 2 (3):332–6. doi: 10.4103/0975-1483.66810
64. Suntharalingam G, Perry MR, Ward S, Brett SJ, Castello-Cortes A, Brunner MD, et al. Cytokine storm in a phase 1 trial of the anti-CD28 monoclonal antibody TGN1412. *N Engl J Med* (2006) 355(10):1018–28. doi: 10.1056/NEJMoa063842
65. Tranter E, Peters G, Boyce M, Warrington S. Giving monoclonal antibodies to healthy volunteers in phase 1 trials: is it safe? *Br J Clin Pharmacol* (2013) 76 (2):164–72. doi: 10.1111/bcp.12096
66. Brady JL, Harrison LC, Goodman DJ, Cowan PJ, Hawthorne WJ, O'Connell P, et al. Preclinical screening for acute toxicity of therapeutic monoclonal antibodies in a hu-SCID model. *Clin Transl Immunol* (2014) 3(12):e29. doi: 10.1038/cti.2014.28
67. Malcolm SL, Smith EL, Bourne T, Shaw S. A humanised mouse model of cytokine release: Comparison of CD3-specific antibody fragments. *J Immunol Methods* (2012) 384(1):33–42. doi: 10.1016/j.jim.2012.07.001
68. Waldron-Lynch F, Henegariu O, Deng S, Preston-Hurlburt P, Tooley J, Flavell R, et al. Teplizumab induces human gut-tropic regulatory cells in humanized mice and patients. *Sci Transl Med* (2012) 4(118):118ra112–118ra112. doi: 10.1126/scitranslmed.3003401
69. Alcantar-Orozco EM, Gornall H, Baldan V, Hawkins RE, Gilham DE. Potential limitations of the NSG humanized mouse as a model system to optimize engineered human T cell therapy for cancer. *Hum Gene Ther Methods* (2013) 24(5):310–20. doi: 10.1089/hgtb.2013.022
70. Durost P, Shultz L, Brehm M. Evaluation of IL-2 therapy on human immune system homeostasis in humanized mice (LYM8P.731). *J Immunol* (2014) 192 (1 Supplement):194.192.
71. Katano I, Takahashi T, Ito R, Kamisako T, Mizusawa T, Ka Y, et al. Predominant development of mature and functional human NK cells in a novel human IL-2–producing transgenic NOG mouse. *J Immunol* (2015) 194 (7):3513–25. doi: 10.4049/jimmunol.1401323
72. Weißmüller S, Kronhart S, Kreuz D, Schnierle B, Kalinke U, Kirberg J, et al. TGN1412 induces lymphopenia and human cytokine release in a humanized mouse model. *PLoS One* (2016) 11(3):e0149093. doi: 10.1371/journal.pone.0149093
73. Abraham S, Guo H, Choi J, Ye C, Thomas MB, Ortega N, et al. Combination of IL-10 and IL-2 induces oligoclonal human CD4 T cell expansion during xenogeneic and allogeneic GVHD in humanized mice. *Heliyon* (2017) 3(4): e00276–6. doi: 10.1016/j.heliyon.2017.e00276
74. Li Y, Strick-Marchand H, Lim AI, Ren J, Masse-Ranson G, Li D, et al. Regulatory T cells control toxicity in a humanized model of IL-2 therapy. *Nat Commun* (2017) 8(1):1762. doi: 10.1038/s41467-017-01570-9
75. Shablak A, Sikand K, Shanks JH, Thistlethwaite F, Spencer-Shaw A, Hawkins RE. High-dose interleukin-2 can produce a high rate of response and durable remissions in appropriately selected patients with metastatic renal cancer. *J Immunother* (2011) 34(1):107–12. doi: 10.1097/CJI.0b013e3181fb659f
76. Roayaie S, Sheiner PA, Emre S, Guy S, Schwartz ME, Boros P, et al. Cytokine profiles in early rejection following OKT3 treatment in liver transplant patients. *Mediators Inflamm* (2000) 9(3-4):141–6. doi: 10.1080/09629350020002877
77. Ilan Y, Zigmond E, Lalazar G, Dembinsky A, Ya'acov AB, Hemed N, et al. Oral administration of OKT3 monoclonal antibody to human subjects induces a dose-dependent immunologic effect in T cells and dendritic cells. *J Clin Immunol* (2010) 30(1):167–77. doi: 10.1007/s10875-009-9323-7
78. Sheu TT, Chiang BL, Yen JH, Lin WC. Premature $CD4^+$ T Cell Aging and Its Contribution to Lymphopenia-Induced Proliferation of Memory Cells in Autoimmune-Prone Non-Obese Diabetic Mice. *PLoS One* (2014) 9(2): e89379. doi: 10.1371/journal.pone.0089379
79. Henson PM. Dampening inflammation. *Nat Immunol* (2005) 6(12):1179–81. doi: 10.1038/ni1205-1179
80. Halloran PF. Immunosuppressive drugs for kidney transplantation. *N Engl J Med* (2004) 351(26):2715–29. doi: 10.1056/NEJMra033540
81. Stegall MD, Morris RE, Alloway RR, Mannon RB. Developing new immunosuppression for the next generation of transplant recipients: the path forward. *Am J Transplant* (2016) 16(4):1094–101. doi: 10.1111/ajt.13582
82. Chen Q, Khoury M, Chen J. Expression of human cytokines dramatically improves reconstitution of specific human-blood lineage cells in humanized mice. *Proc Natl Acad Sci U S A* (2009) 106(51):21783–8. doi: 10.1073/pnas.0912274106. pnas.0912274106
83. Yong KSM, Her Z, Chen Q. Humanized mice as unique tools for human-specific studies. *Arch Immunol Ther Exp* (2018 66(4):245–66. doi: 10.1007/s00005-018-0506-x
84. Fukuchi Y, Miyakawa Y, Kobayashi K, Kuramochi T, Shimamura K, Tamaoki N, et al. Cytokine dependent growth of human TF-1 leukemic cell line in human GM-CSF and IL-3 producing transgenic SCID mice. *Leuk Res* (1998) 22(9):837–43. doi: 10.1016/s0145-2126(98)00084-8
85. Billerbeck E, Barry WT, Mu K, Dorner M, Rice CM, Ploss A. Development of human CD4+FoxP3+ regulatory T cells in human stem cell factor-, granulocyte-macrophage colony-stimulating factor-, and interleukin-3-expressing NOD-SCID IL2Rγ(null) humanized mice. *Blood* (2011) 117 (11):3076–86. doi: 10.1182/blood-2010-08-301507
86. Ito R, Takahashi T, Katano I, Kawai K, Kamisako T, Ogura T, et al. Establishment of a human allergy model using human IL-3/GM-CSF-transgenic NOG mice. *J Immunol* (2013) 191(6):2890–9. doi: 10.4049/jimmunol.1203543
87. Rongvaux A, Willinger T, Martinek J, Strowig T, Gearty SV, Teichmann LL, et al. Development and function of human innate immune cells in a humanized mouse model. *Nat Biotechnol* (2014) 32(4):364–72. doi: 10.1038/nbt.2858
88. Yong SMK, Keng CT, Tan SQ, Loh E, Chang KT, Tan TC, et al. Human CD34 (lo)CD133(lo) fetal liver cells support the expansion of human CD34(hi) CD133(hi) hematopoietic stem cells. *Cell Mol Immunol* (2016) 13(5):605–14. doi: 10.1038/cmi.2015.40
89. Lim AI, Li Y, Lopez-Lastra S, Stadhouders R, Paul F, Casrouge A, et al. Systemic Human ILC Precursors Provide a Substrate for Tissue ILC Differentiation. *Cell* (2017) 168(6):1086–1100.e10. doi: 10.1016/j.cell.2017.02.021
90. Denayer T, Stöhr T, Van Roy M. Animal models in translational medicine: validation and prediction. *New Horiz Transl Med* (2014) 2(1):5–11. doi: 10.1016/j.nhtm.2014.08.001
91. Taneja V, David CS. HLA transgenic mice as humanized mouse models of disease and immunity. *J Clin Invest* (1998) 101(5):921–6. doi: 10.1172/JCI2860
92. Cacev T, Radosević S, Krizanac S, Kapitanović S. Influence of interleukin-8 and interleukin-10 on sporadic colon cancer development and progression. *Carcinogenesis* (2008) 29(8):1572–80. doi: 10.1093/carcin/bgn164
93. Brehm MA, Shultz LD, Greiner DL. Humanized mouse models to study human diseases. *Curr Opin Endocrinol Diabetes Obes* (2010) 17(2):120–5. doi: 10.1097/MED.0b013e328337282f
94. Chen Q, Chen J. Serial transfer of human hematopoietic and hepatic stem/progenitor cells. *Bio Protoc* (2013) 3(23):e992. doi: 10.21769/BioProtoc.992

Conflict of Interest: The authors declare that the research was conducted in the absence of any commercial or financial relationships that could be construed as a potential conflict of interest.

Copyright © 2020 Yong, Her, Tan, Tan, Liu, Lai, Heng, Fan, Chang, Wang, Chan, Chen and Chen. This is an open-access article distributed under the terms of the Creative Commons Attribution License (CC BY). The use, distribution or reproduction in other forums is permitted, provided the original author(s) and the copyright owner(s) are credited and that the original publication in this journal is cited, in accordance with accepted academic practice. No use, distribution or reproduction is permitted which does not comply with these terms.

frontiers in Immunology

ORIGINAL RESEARCH
published: 19 October 2020
doi: 10.3389/fimmu.2020.573406

Different Human Immune Lineage Compositions Are Generated in Non-Conditioned NBSGW Mice Depending on HSPC Source

Nicholas J. Hess[1†], Payton N. Lindner[2], Jessica Vazquez[2], Samuel Grindel[3], Amy W. Hudson[4], Aleksandar K. Stanic[2], Akihiro Ikeda[3], Peiman Hematti[5] and Jenny E. Gumperz[1†]*

[1] Department of Medical Microbiology and Immunology, University of Wisconsin-Madison School of Medicine and Public Health, Madison, WI, United States, [2] Department of Obstetrics and Gynecology, University of Wisconsin-Madison School of Medicine and Public Health, Madison, WI, United States, [3] Department of Medical Genetics, University of Wisconsin-Madison School of Medicine and Public Health, Madison, WI, United States, [4] Department of Microbiology and Immunology, Medical College of Wisconsin, Milwaukee, WI, United States, [5] Division of Hematology/Oncology, Department of Medicine, University of Wisconsin-Madison School of Medicine and Public Health, Madison, WI, United States

OPEN ACCESS

Edited by:
Alexandre P. A. Theocharides,
University Hospital Zürich, Switzerland

Reviewed by:
Claudia Waskow,
Fritz Lipmann Institute (FLI), Germany
Andreas Reinisch,
Medizinische Universität Graz, Austria

***Correspondence:**
Jenny E. Gumperz
jegumperz@wisc.edu

†ORCID:
Nicholas J. Hess
orcid.org/0000-0001-5720-9305
Jenny E. Gumperz
orcid.org/0000-0003-1852-2192

Specialty section:
This article was submitted
Cancer Immunity and
Immunotherapy,
a section of the journal
Frontiers in Immunology

Received: 16 June 2020
Accepted: 28 September 2020
Published: 19 October 2020

Citation:
Hess NJ, Lindner PN, Vazquez J, Grindel S, Hudson AW, Stanic AK, Ikeda A, Hematti P and Gumperz JE (2020) Different Human Immune Lineage Compositions Are Generated in Non-Conditioned NBSGW Mice Depending on HSPC Source. Front. Immunol. 11:573406. doi: 10.3389/fimmu.2020.573406

NBSGW mice are highly immunodeficient and carry a hypomorphic mutation in the *c-kit* gene, providing a host environment that supports robust human hematopoietic expansion without pre-conditioning. These mice thus provide a model to investigate human hematopoietic engraftment in the absence of conditioning-associated damage. We compared transplantation of human $CD34^+$ HSPCs purified from three different sources: umbilical cord blood, adult bone marrow, and adult G-CSF mobilized peripheral blood. HSPCs from mobilized peripheral blood were significantly more efficient (as a function of starting HSPC dose) than either cord blood or bone marrow HSPCs at generating high levels of human chimerism in the murine blood and bone marrow by 12 weeks post-transplantation. While T cells do not develop in this model due to thymic atrophy, all three HSPC sources generated a human compartment that included B lymphocytic, myeloid, and granulocytic lineages. However, the proportions of these lineages varied significantly according to HSPC source. Mobilized blood HSPCs produced a strikingly higher proportion of granulocyte lineage cells (~35% as compared to ~5%), whereas bone marrow HSPC output was dominated by B lymphocytic cells, and cord blood HSPC output was enriched for myeloid lineages. Following transplantation, all three HSPC sources showed a shift in the $CD34^+$ subset towards $CD45RA^+$ progenitors along with a complete loss of the $CD45RA^-CD49f^+$ long-term HSC subpopulation, suggesting this model promotes mainly short-term HSC activity. Mice transplanted with cord blood HSPCs maintained a diversified human immune compartment for at least 36 weeks after the primary transplant, although mice given adult bone marrow HSPCs had lost diversity and contained only myeloid cells by this time point. Finally, to assess the impact of non-HSPCs on transplantation outcome, we also tested mice transplanted with total or T cell-depleted adult bone marrow mononuclear cells. Total bone marrow mononuclear cell

transplants produced significantly lower human chimerism compared to purified HSPCs, and T-depletion rescued B cell levels but not other lineages. Together these results reveal marked differences in engraftment efficiency and lineage commitment according to HSPC source and suggest that T cells and other non-HSPC populations affect lineage output even in the absence of conditioning-associated inflammation.

Keywords: human immune system mice, HSC, HPSC, c-KIT mutation, bone marrow, umbilical cord blood, human neutrophil engraftment, G-CSF mobilized peripheral blood

INTRODUCTION

Hematopoietic stem cell transplantation (HSCT) using autologous or allogeneic graft tissue sources is a potentially curative treatment for patients with malignant and non-malignant blood diseases. However, the clinical value of HSCT remains limited by its high potential for complications, including graft-*vs*-host-disease (GVHD), delayed immune reconstitution, and graft failure (1, 2). Recovery of neutrophil and platelet populations is a key indicator of engraftment success that usually occurs between 14 and 25 days post-transplant, with delays beyond this window increasing the chances of mortality due to infection (3, 4). Furthermore, the late reconstitution of other immune lineages, which can also demonstrate substantial variability, may carry long-term consequences for patient health, including influencing the likelihood of disease relapse (1–4). Factors that impact the capacity of human hematopoietic stem and progenitor cells (HSPCs) to engraft and differentiate, and the resulting dynamics of human hematopoietic reconstitution remain poorly understood, underscoring the need for new research strategies.

Xenogeneic models involving transplantation of human cells into animal hosts have the potential to shed new light on hematopoietic cell-intrinsic and -extrinsic factors that influence engraftment results and may thus provide an important path towards improving clinical outcomes (5–7). A key advance in this area was the development of immunodeficient mouse strains (*e.g.* NSG) that are highly permissive for engraftment of human hematopoietic cells because they lack adaptive lymphocytes due to a mutation that abrogates antigen receptor recombination (Prkdc^{scid}) and are also deficient in innate lymphocytes due to the deletion of a key cytokine receptor gene (γc or CD132) (6, 7). Further genetic modification of these strains has led to a variety of new options for modeling human hematopoietic engraftment. For example, mouse strains containing human knock-in gene replacements for key hematopoietic factors have recently been developed. These include NSG-SGM3 mice that have a triple knock-in of human stem cell factor (SCF), granulocyte–macrophage colony-stimulating-factor (GM-CSF) and interleukin-3 (IL-3), and MISTRG mice that contain human macrophage colony-stimulating-factor (M-CSF), GM-CSF, IL-3, thrombopoietin, and signal regulatory protein alpha (SIRPα) (8–10). Both strains have been shown to support high levels of multi-lineage human hematopoietic engraftment with superior representation of myeloid lineages and the MISTRG mouse also appears to sustain long-term hematopoietic progenitors (10). However, for efficient engraftment of human HSPCs in these strains it is necessary to administer pre-transplant conditioning (*e.g.* γ-irradiation).

Pre-transplant conditioning induces a variety of different inflammatory pathways and produces damage that may alter bone marrow microenvironment in ways that are still not fully understood (11). While pre-transplant conditioning is routinely used in clinical settings, there is substantial variation in the specifics of the regimens used, and the nature of the conditioning regimen is known to influence both the recovery of the immune compartment and the risk of GVHD (1–4). Myeloablative conditioning is associated with the fastest engraftment, though this is balanced by an increased probability of GVHD (1, 2, 12). Non-myeloablative and reduced intensity conditioning are less damaging and are associated with lower rates of GVHD, but show higher rates of delayed or failed engraftment (12). Thus, model systems that allow for analysis of transplantation outcomes in the absence of host conditioning may help to shed light on damage-independent factors that influence engraftment success. To this end, mouse strains containing mutations in the c-kit (SCF receptor or CD117) protein are particularly valuable, as they have been shown to support either murine or human HSPC engraftment in the absence of pre-conditioning (13–20).

An additional important factor influencing both hematopoietic recovery and GVHD is the source of tissue used for transplantation. The most common graft tissues used for clinical transplantation protocols are G-CSF mobilized peripheral blood (MB), bone marrow (BM), and umbilical cord blood (CB), in that order (21, 22). While the incidence of GVHD and times to immune recovery vary according to the source of graft tissue (3, 4), it remains unclear how these outcomes are impacted by intrinsic differences in the HSPCs found in different types of human graft tissue or by non-HSPC populations that are co-transplanted as part of these grafts. In this study, we sought to compare engraftment outcomes resulting from transplantation of human HSPCs isolated from BM, MB, or CB and to assess the impact of lineage-committed cells on hematopoietic reconstitution. Since the inflammatory status of the host environment may significantly affect the functions of both HSPCs and differentiated cells, to avoid conditioning-associated damage we used NBSGW mice, in which a hypomorphic mutation in the *c-kit* gene (Kit^{W41J}) has been crossed into the highly immunodeficient NSG (NOD.Cg-Prkdc^{scid}Il2rg^{tm1Wjl}) strain (13–20). Remarkably, while prior

studies have demonstrated improved human myeloid engraftment in these or related *c-kit* mutated mice (13–20), the comparison performed here demonstrates that the NBSGW strain supports marked differences in human granulocytic, B lymphocytic, and myeloid lineage output depending on the HSPC source and points to an unexpected impact on B cell engraftment levels when T lymphocytes are present within graft tissue.

METHODS

Isolation of Primary Human HSPCs

All work involving human cells was performed under UW Minimal Risk IRB protocols 2018-0304 (JG), 2016-0298 (PH), and 2017-0870 (JG). Human BM and MB tssues were collected from the remnants of left-over bags and filters used for clinical HSCT procedures at the University of Wisconsin-Madison. CB samples were acquired either from the University of Colorado's ClinImmune Labs cord blood bank or the Medical College of Wisconsin's tissue bank. Mononuclear cells were isolated by ficoll density-gradient centrifugation (1,100×g for 15 min with 0 brake) to remove red blood cells (RBCs), neutrophils, and other non-leukocytes. Where indicated, T cells were depleted using StemCell Technologies RosetteSep T cell-depletion kit (catalog #15661), and HSPCs were isolated using StemCell Technologies EasySep Human CD34 positive selection kit II (catalog #17856), which first depletes lineage positive cells, then positively selects $CD34^+$ cells. The resulting cell population was typically >90% $CD34^+$, with the remaining cells all lineage negative. Prior to transplantation, cells were counted, washed, and resuspended in phosphate buffered saline (PBS).

Transplantation Into NBSGW Mice

All animal work was completed in accordance with UW-Madison IACUC protocol M005199. NBSGW immunodeficient mice (NOD.CG-$Kit^{W-41J}Tyr^+Prkdc^{scid}IL2rg^{tm1Wjl}$/ThomJ) were initially purchased from Jackson Laboratories, then bred and maintained in a specific pathogen free facility using aseptic housing. Experiments were performed using both male and female mice (equal numbers of each sex); results are not stratified according to sex, since no significant differences in results were observed between the sexes. All mice were between the ages of 6–10 weeks at the time of transplantation. Human cells suspended in a volume of 150 μl of PBS were injected retro-orbitally while the mice were under isoflurane anesthesia. Blood draws were performed at indicated time points by retro-orbital bleeding, using heparin coated capillary tubes with the mouse under isoflurane anesthesia. At the experiment endpoint, mice were euthanized by CO_2, and tissues collected for analysis. Bone marrow was prepared by flushing tissue from the inside of the femur and tibia of the left leg. Mice were monitored for signs of GVHD (weight loss ≥5% of maximum body weight) by weekly weighing as described previously (23). Mice characterized as experiencing GVHD were removed from the analysis.

For analysis of engraftment following secondary transplantation, primary transplants were first performed on four mice using a dose of $2.5E^6$ purified HSPCs. After 12 weeks, bone marrow (both femurs) from these four mice was pooled and purified by density gradient centrifugation (Ficoll) to remove non-leukocytes. Four naïve mice were then transplanted with $3E^7$ pooled bone marrow cells. Flow cytometric analysis of the pooled MNC used for the secondary transplant showed that ~$2.5E^6$ HSPC of the injected cells were human cells expressing CD34.

Flow Cytometry

Singe cell suspensions were blocked in PBS with 10% human serum and stained for flow cytometry using fluorophore-conjugated antibodies purchased from BioLegend: CD3 (OKT3), CD10 (HI10A), CD19 (HIB19), CD33 (HIM3-4), CD34 (8G12), CD38 (HIT2), mCD45.1 (A20), CD45RA (HI100), CD56 (HCD56), CD66b (610F5), CD123 (6H6), and PanHLA (w6/32). All samples were analyzed on a BD LSRII flow cytometer equipped with three lasers (nine filter channels), quantified using Precision Count Beads (BioLegend) and analyzed using FlowJo V10.5.

Immunofluorescence of Murine Bone Tissue

Following CO_2 euthanasia, mice were immediately perfused with PBS, followed by 4% paraformaldehyde (PFA). Femurs were removed and immersion fixed in 4% paraformaldehyde (PFA) for 24 h at 4°C. Femurs were then decalcified in 20% EDTA for 4 days at room temperature. Femurs were rinsed, dehydrated, and embedded in paraffin. Paraffin blocks were sectioned 5 μm thick and mounted on glass slides. Sections were de-paraffinized, rehydrated to PBS, and heated in citric acid buffer (10 mM sodium citrate, 0.05% tween-20, pH 6.0) for antigen retrieval. Sections were blocked in PBS with 0.5% Triton X-100 and 2% normal donkey serum for 1 h at room temperature. Sections were then incubated at 4°C overnight with Leukocyte Common Antigen (LCA) Cocktail (Biocare Medical, Pacheco, CA) diluted at 1:100 in the diluent solution supplied by the manufacturer. Sections were rinsed in PBS and incubated in 1:400 diluted secondary antibody (Cy3-conjugated anti mouse IgG, Jackson ImmunoResearch Laboratories, West Grove, PA) in block solution for 1 h at room temperature. Following PBS rinse, sections were stained with 4′,6-diamidino-2-phenylindole (DAPI). Slides were imaged using a Nikon A1R+ confocal microscope (Nikon, Tokyo, Japan).

Statistics

Replicate mice were transplanted in each experiment using the indicated graft sources and doses, and results from like conditions of independent experiments were aggregated for statistical analyses. Data were analyzed for significance using a two-tailed, unpaired, non-parametric t-test (Mann–Whitney analysis). Symbols on plots represent results from individual mice (or individual graft samples in **Figure 1**), and bars or lines show the means. Data sets from analyses of cell number are plotted using a logarithmic scale with geometric means shown, while analyses of cell frequencies (percentages) are plotted using a linear scale with bars or lines showing the arithmetic means.

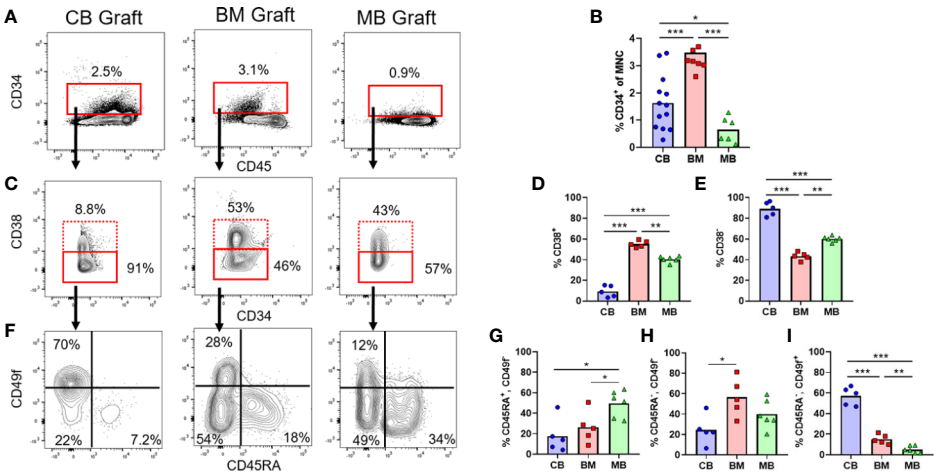

FIGURE 1 | Composition of human HSPC populations varies among graft sources. Flow cytometric analysis of HSPC populations in primary graft tissues. **(A)** Representative plots of panHLA-class-I$^+$ human cells from umbilical cord blood (CB), bone marrow (BM), and G-CSF mobilized peripheral blood (MB), showing the percentage of CD34$^+$ cells (red box) in each graft. **(B)** Aggregated results showing percentage of CD34$^+$ cells detected in individual graft samples. Symbols show results from individual samples of CB (blue), BM (red), or MB (green) tissue, with bars representing the arithmetic means. **(C)** Representative plots showing flow cytometric staining of CD34$^+$ cells for CD38. **(D, E)** Aggregated results showing the percentage of cells in the CD38$^+$ **(D)** or CD38$^-$ **(E)** gates. **(F)** Representative plots showing flow cytometric staining of CD34$^+$CD38$^-$ cells for CD45RA and CD49f. **(G–I)** Aggregated results showing the percentage of CD34$^+$CD38$^-$ cells corresponding to uncommitted progenitors (CD45RA$^+$CD49f$^-$, **G**), multipotent progenitors (CD45RA$^-$CD49f$^-$, **H**), and long-term HSCs (CD45RA$^-$CD49f$^+$, **I**). *$p < 0.05$; **$p < 0.01$; ***$p < 0.001$.

RESULTS

Characterization of Human HSPCs From Different Graft Sources

The three commonly used HSCT graft tissues (CB, BM, and MB) all contain CD34$^+$ HSPCs capable of re-populating hosts but are collected from different physiological niches (umbilical cord/placental blood, bone marrow interstitial space, and peripheral blood, respectively). Additionally, donors of MB grafts undergo pre-treatment with G-CSF, which may be associated with changes to HSPC function in addition to inducing migration of HSPCs from the bone marrow into the blood, while CB grafts are from less developmentally mature donors and are exposed to factors associated with pregnancy (24–26). Therefore, HSPCs in these three graft tissues are expected to differ in multiple ways. We performed flow cytometric analysis to gain an initial assessment of HSPCs from these three tissue types. Similar to previous findings, our analysis revealed that on average the percent of CD34$^+$ cells was lowest in MB graft tissue, while BM had the highest average, and cord blood samples were highly variable yielding an intermediate average (**Figures 1A, B**) (23). We performed flow cytometric analysis using a previously published gating strategy to further identify the CD38$^+$ committed progenitors and CD38$^-$ uncommitted progenitor populations within the CD34$^+$ pool (**Figures 1C–E**) (27, 28). We observed that CB grafts had the highest percentage of uncommitted progenitors followed by MB and BM, respectively (**Figures 1D, E**). We further divided the CD38$^-$ population into long-term HSC (CD45RA$^-$, CD49f$^+$), MPP (CD45RA$^-$, CD49f$^-$) and an uncommitted progenitor (CD45RA$^+$, CD49f$^-$) population. From this analysis, CB grafts had the highest percentage of long-term HSCs, while the MPP population was dominant in BM, and MB showed enrichment for the uncommitted progenitor population (**Figures 1F–I**). These results are consistent with clinical data showing that a lower absolute number of CB-CD34$^+$ cells is required for engraftment, but hematopoietic recovery takes longer than for grafts of other tissue sources, presumably because CB grafts contain fewer differentiated progenitors (3, 4, 29, 30).

Human Cell Chimerism Is Established in Murine Bone Marrow and Peripheral Tissues

To confirm successful engraftment of human immune cells in this model, we performed flow cytometric analyses to test them in bone marrow and peripheral tissues. Human cells were detectable at 12 weeks post-engraftment in the bone marrow and also in all other murine tissues tested, including spleen, blood, small intestine, and uterus (**Figures 2A–F**). The abundance of human cells at these sites appeared dependent on the dose of HSPCs used for engraftment (**Figure 2F**). The bone marrow typically showed the highest levels of human chimerism as a percentage of the total cells within the murine tissue (**Figure 2F**). To further characterize the bone marrow engraftment, we performed immunofluorescence staining on sections of whole femur (**Figure 2G**). Femur of an engrafted mouse showed abundant cells staining positively for human CD45 that were distributed throughout the bone and appeared most concentrated near endosteal areas (**Figure 2G**, right side), and analysis of similarly prepared femur from an unengrafted mouse indicated that non-specifically stained cells were rare (**Figure 2G**, left side). Together, these results strongly support

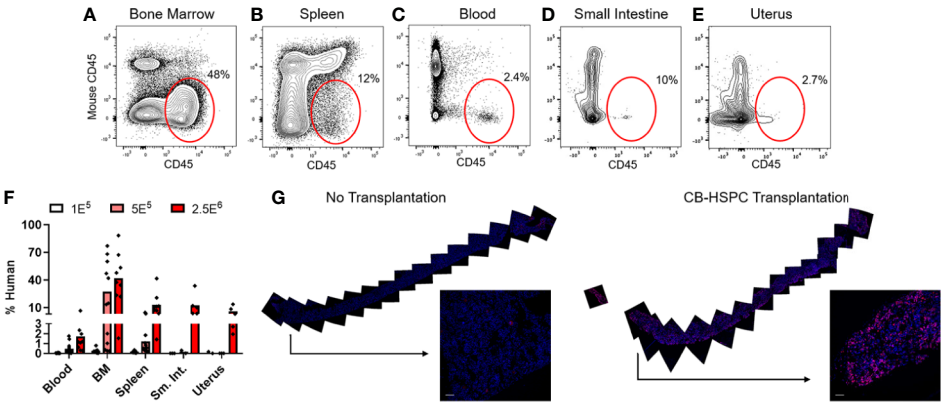

FIGURE 2 | Transplantation of HSPCs is associated with colonization of bone marrow and peripheral tissues by human cells. Bone marrow and peripheral tissues (spleen, blood, small intestine, and uterus) were collected at 12 weeks post-transplantation from mice given varying doses of BM-HSPCs ($1E^5$, $5E^5$, $2.5E^6$). **(A–E)** Representative plots showing flow cytometric staining of human cells (red oval gates) in a mouse transplanted with $2.5E^6$ BM-HSPCs. **(F)** Aggregated data showing percentages of human cells within the total (human $CD45^+$ + murine $CD45^+$) hematopoietic compartment from the indicated tissues of mice engrafted with the indicated BM-HSPC doses. Symbols show results from individual mice, bars represent the arithmetic means. **(G)** Cells expressing human CD45 were detected by immunofluorescence of whole bone tissue collected at 12 weeks post-transplant from a mouse given $2.5E^6$ CB-HSPCs (right side), compared to a negative control unengrafted mouse (left side). Staining of human CD45 is shown in red; blue color shows staining of cell nuclei by DAPI.

that non-conditioned NBSGW mice are productively engrafted following transplantation of purified human HSPCs.

Efficiency of Engraftment According to HSPC Source

To investigate hematopoietic output of HSPCs from the three different graft sources, we transplanted titrated doses of lineage-negative $CD34^+$ cells from each type of graft tissue into NBSGW mice, and after 12 weeks we assessed the total number of human cells in one femur (**Figure 3A**) or in the spleen (**Figure 3B**). Dose response curves appeared similar for murine bone marrow and spleen transplanted with CB- and BM-HSPCs (**Figures 3A, B**). Remarkably, MB-HSPCs generated one to three orders of magnitude more total human cells in these murine tissues as a function of starting HSPC dose (**Figures 3A, B**). We also assessed the number of human cells present in 100 µl murine blood, at 3 week intervals following transplantation (**Figure 3C**). This analysis demonstrated that mice transplanted with MB-HSPCs reached significantly higher levels of human chimerism within 9 weeks. Thus, compared to CB- or BM-HSPCs, MB-HSPCs engrafted more efficiently at low doses and also produced more rapid peripheral reconstitution in this model.

HSPC Source Influences Lineage Output

We next characterized the composition of the human compartments generated within mice transplanted with the three sources of HSPCs. Flow cytometric analysis of the murine bone marrow at 12 weeks after transplantation showed a heterogeneous population of human cells that we further identified as B lymphocytic [$CD19^+$, $CD38^{high}$, $CD10^+$ (not

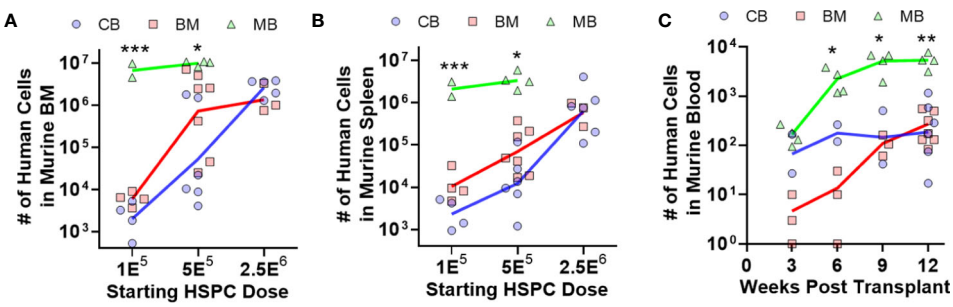

FIGURE 3 | Human hematopoietic output is dependent on HSPC dose. The relative abundance and kinetics of human HSPC expansion in NBSGW mice was determined for each graft source. **(A)** Total number of human cells in the bone marrow collected from one leg (femur + tibia) at 12 weeks post-transplantation according to the starting HSPC dose. Symbols show individual mice that received HSPCs isolated from CB (blue), BM (red), or MB (green), with lines indicating geometric means. **(B)** Total number of human cells in the murine spleens at 12 weeks post-transplantation. **(C)** Total number of human cells in 100 µl of murine peripheral blood, collected at the indicated times post-transplantation. Results are from transplantation of $5E^5$ HSPCs. *$p < 0.05$; **$p < 0.01$; ***$p < 0.001$.

shown)], neutrophilic (CD11b$^+$, CD66b$^+$), myeloid cells consisting of monocytic (CD33$^+$, CD14$^+$) and dendritic (CD33$^+$, CD1c$^+$) cells, and a progenitor population that was low/intermediate for CD33 and positive for CD123 (**Figures 4A–C**). T cells (*i.e.* CD3$^+$) were not detected following transplantation of any of the types of HSPCs, which is mostly likely a consequence of thymic atrophy in these mice.

Strikingly, the composition of the human compartment in the murine bone marrow at 12 weeks showed marked differences according to the source of HSPC transplanted. The human immune compartment of mice transplanted with BM-HSPCs was dominated by B lineage cells (~60%), whereas B lymphocytic cells comprised only about 30–40% of the human immune compartment of mice transplanted with CB- and MB-HSPCs (**Figure 4D**). Mice transplanted with MB-HSPCs showed a dramatic enrichment for neutrophilic lineage cells (~35%), whereas neutrophilic cells comprised only about 5% of the human compartment in mice that received BM- or CB-HSPCs (**Figure 4E**). Finally, mice that received CB-HSPCs showed an approximate twofold and threefold enrichment for CD33$^+$ and CD123$^+$ lineages respectively compared to mice transplanted with BM- or MB-HSPCs (**Figures 4F, G**). The percentage of monocytic cells ranged from about 5% in mice that received BM- or MB-HSPCs to about 10% in mice transplanted with CB-HSPCs (**Figure 4H**), while the percentage of CD1c$^+$ DCs (~3%) did not show significant differences according to HSPC source (**Figure 4I**).

HSPC Population Shifts Towards Progenitor Phenotypes Following Transplantation

We next evaluated the characteristics of the CD34$^+$ HSPC population in the bone marrow of transplanted mice (**Figure 5A**). Regardless of the source of HSPCs, the percentage of human cells expressing CD34 was significantly expanded at 12 weeks post-transplantation compared to the starting graft tissue (**Figure 5B**). We performed the same sequential gating strategy used to characterize the CD34$^+$ subset of the starting grafts (**Figure 1**). Compared to the respective starting grafts, the percentage of committed progenitors (CD38$^+$) was markedly increased for CB-, but somewhat decreased after transplantation of BM- and MB-HSPCs (**Figures 5C–E**). Strikingly, for all HSPC sources, the CD38$^-$ population showed a dramatic shift towards uncommitted progenitors (CD45$^+$CD49f$^-$) and away from MPPs (CD45$^-$CD49f$^-$) and long-term HSCs (CD45$^-$CD49f$^+$) (**Figures 5F–I**). Indeed, we did not detect any human cells bearing a long-term HSC phenotype in the bone marrow from any of the mice analyzed, and even cells bearing an MPP phenotype appeared extremely rare (**Figures 5F–I**).

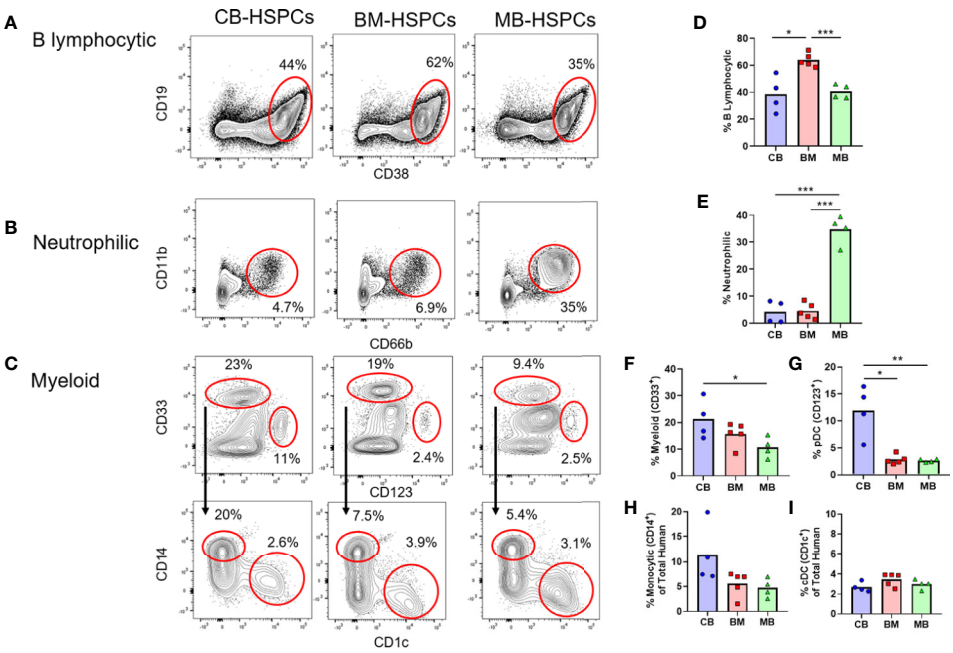

FIGURE 4 | Source of human HSPCs influences hematopoietic output. The lineage output resulting from transplantation of CB-, BM-, or MB-HSPCs was examined by flow cytometry of murine bone marrow after 12 weeks. **(A–C)** Representative plots showing flow cytometric analysis of human cells (panHLA-I$^+$, murine CD45$^-$) in the bone marrow of NBSGW mice given 5E^5 HSPCs. **(A)** Identification of B lymphocytic cells (CD19$^+$, CD38^{high}). **(B)** Identification of neutrophilic cells (CD11b$^+$, CD66b$^+$). **(C)** Identification of myeloid lineage cells (CD33$^+$ gate in top row), that are comprised of monocytic cells (CD14$^+$ gate in bottom row) and DCs (CD1c$^+$ gate in bottom row). Additionally, a progenitor population that is thought to give rise to plasmacytoid DCs and other cells is present (CD33$^-$CD123$^+$ gate in top row). **(D–I)** Plots showing the percent of each population within the human compartment of mice given the indicated sources of HSPCs. Symbols show results from individual mice, bars represent the arithmetic means. *$p < 0.05$; **$p < 0.01$; ***$p < 0.001$.

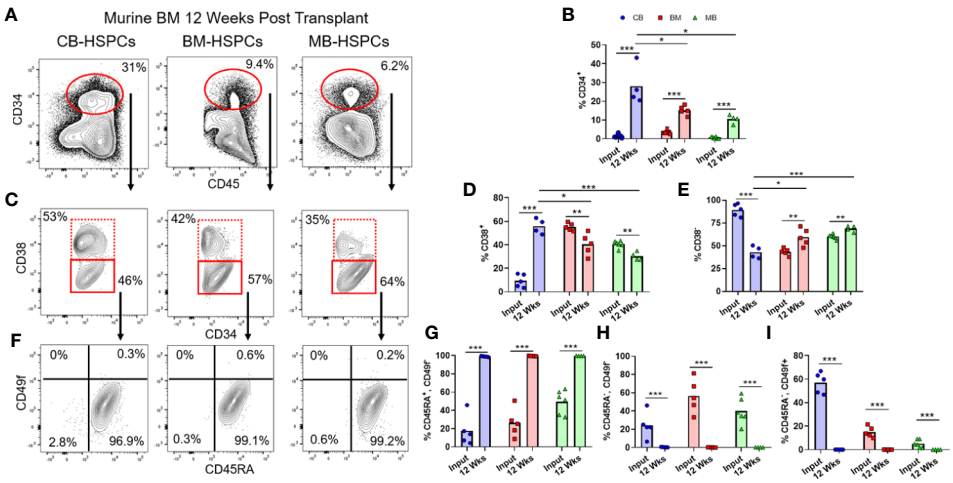

FIGURE 5 | Shift towards short-term HSPC phenotype after transplantation. Flow cytometric analysis was performed to assess the composition of the CD34$^+$ HSPC population within the human compartment in the murine bone marrow at 12 weeks post-transplantation. **(A)** Representative flow cytometry plots showing identification of human CD34$^+$ population. **(B)** Plot showing percentage of CD34$^+$ cells detected in bone marrow of mice transplanted with the indicated sources of HSPCs compared to the frequency of total CD34$^+$ cells in the starting graft tissue (Input). **(C)** Representative plots showing flow cytometric staining of human CD34$^+$ cells in murine bone marrow for CD38. **(D, E)** Percentage of cells in the CD38$^+$ **(D)** or CD38$^-$ **(E)** gates after transplantation compared to the starting graft (Input). **(F)** Representative plots showing flow cytometric staining of human CD34$^+$CD38$^-$ cells in the murine bone marrow for CD45RA and CD49f. **(G–I)** Percentage of CD34$^+$CD38$^-$ cells corresponding to uncommitted progenitor (CD45RA$^+$CD49f$^-$, **G**), multipotent progenitor (CD45RA$^-$CD49f$^-$, **H**), and long-term HSC (CD45RA$^-$CD49f$^+$, **I**) gates after transplantation compared to the starting graft (Input). Symbols show results from individual mice; bars represent the arithmetic means. *$p < 0.05$; **$p < 0.01$; ***$p < 0.001$.

Since prior studies have established that the transition from HSC to MPP to uncommitted progenitors occurs as a step-wise process, with each population capable of repopulating itself as well as giving rise to more committed populations (27, 28), the absence of HSC and MPP populations in the murine bone marrow after 12 weeks suggested that the NBSGW host promotes short-term hematopoietic activity with little stem cell self-renewal. To investigate further, we evaluated the duration of engraftment in mice transplanted with CB- or BM-HSPCs. In both cases, human chimerism was maintained in peripheral blood for at least 36 weeks post-transplantation (**Figures 6A, D**), but the total number of human cells in the bone marrow declined by about 10-fold (**Figures 6B, E**). In mice transplanted with CB-HSPCs, the human compartment in the murine bone marrow shifted over time towards increased representation of B lymphocytes and myeloid lineages and reduced frequency of progenitors (**Figure 6B**). In contrast, mice transplanted with BM-HSPCs underwent a dramatic loss of lineage diversity and by 36 weeks post-transplantation the human compartment in the murine bone marrow was comprised almost exclusively of CD33$^+$ myeloid cells (**Figure 6E**). To directly evaluate the capacity for self renewal, we performed a serial transfer of murine bone marrow from mice transplanted with CB- or BM-HSPCs into naïve NBSGW mice. Bone marrow was collected at 12 weeks post-transplantation from four mice given CB- or BM-HSPCs, pooled and subjected to density gradient centrifugation to isolate mononuclear cells, then split into equal doses and transplanted into four naive mice. Murine bone marrow was harvested for analysis at 12 weeks after the secondary transplant. For mice given either CB- or BM-HSPCs, the number of human cells in the murine bone marrow was about 2 logs lower than the primary transplant, and the human compartment was almost exclusively comprised of CD33$^+$ myeloid cells (**Figures 6C, F**). Together, these results suggest the NBSGW strain promotes short-term hematopoietic activity of transplanted human HSPCs.

Impact of Non-HSPCs in Graft Tissue

Most clinical HSCT protocols are performed using graft tissues that contain a wide variety of immune cells, including a substantial proportion of mature T lymphocytes (29, 30). To determine how the presence of such donor-derived immune cells in graft tissue affects hematopoietic outcomes, we transplanted NBSGW mice with either isolated human BM-HSPCs, total BM mononuclear cells (MNC), or T cell-depleted MNC. Compared to transplantation of isolated BM-HSPCs, transplantation of total MNCs containing the same number of HSPCs led to approximately 2 logs lower levels of human chimerism in the murine bone marrow after 12 weeks (**Figure 7A**). However, transplantation of T cell-depleted MNCs resulted in human chimerism levels approaching those of mice that received isolated BM-HSPCs (**Figure 7A**). Since mice that showed evidence of GVHD were excluded from these analyses, this suggested that the presence of donor-derived T cells adversely affects hematopoietic output independently of GVHD pathology. Remarkably, further analysis revealed that mice receiving T-depleted MNCs showed recovery of B lymphocytic cell numbers, but that other lineages and HSPC numbers remained reduced, similar to mice that received total MNCs (**Figures 7B–F**). Thus, the presence of donor-derived T cells appeared to selectively

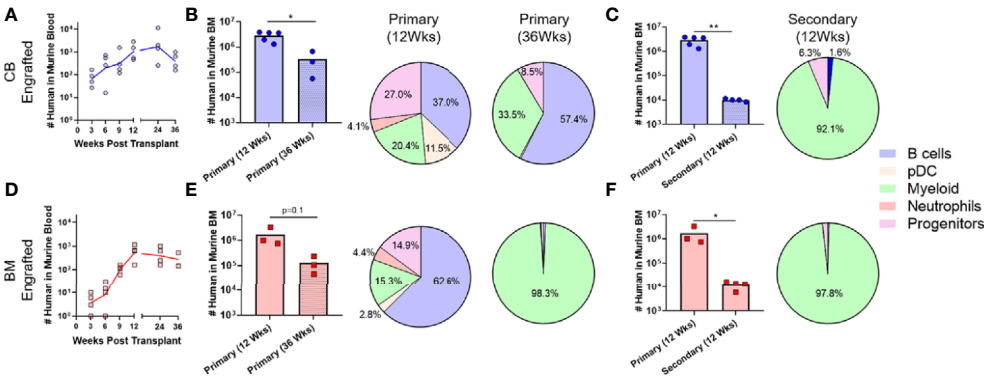

FIGURE 6 | Transplantation of CB-HSPCs produces a longer duration of multi-lineage engraftment than BM-HSPCs. Analyses were performed to evaluate the duration of the multi-lineage expansion produced by the initial HSPC transplantation as well as the ability of engrafted HSPC to re-populate a naïve host. **(A)** Blood draws were performed every 3 weeks on NBSGW given $2.5E^6$ CB-HSPCs until week 12 after which they were performed every 12 weeks until 36 weeks. **(B)** Bar graph showing the total number of human cells in the bone marrow collected from one leg (femur + tibia) as determined by flow cytometry in mice 12 or 36 weeks post-transplant. The lineage composition of the human cells is shown as a pie graph. **(C)** Bone marrow collected from four mice initially transplanted with $2.5E^6$ CB-HSPCs was combined and subjected to density gradient centrifugation, then $3E^7$ mononuclear cells was transplanted into each of four naïve NBSGW mice. The number of transplanted HSPCs was approximately $2.5E^6$/mouse. The plot shows total number of human cells in the bone marrow collected from one leg (femur + tibia) at 12 weeks after primary *vs.* secondary transplant. Pie chart shows lineage composition at 12 weeks after secondary transplant. **(D–F)** Results from similar analysis using BM-HSPCs. Symbols show results from individual mice, and lines or bars show the geometric means. *$p < 0.05$; **$p < 0.01$.

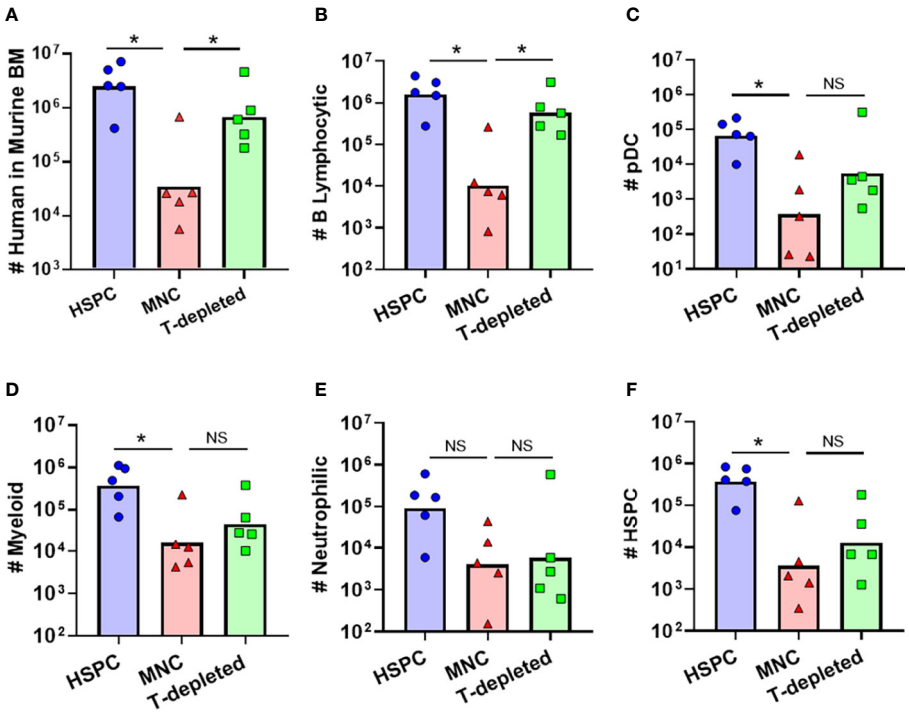

FIGURE 7 | Impact of other donor-derived cells on hematopoietic output. To determine how graft composition alters hematopoietic potential and lineage commitment, transplantation of isolated BM-HSPC (blue) was compared to total bone marrow mononuclear cells (MNC, red), or T cell-depleted MNC (green). For all conditions, the grafts contained $5E^5$ HSPCs. **(A)** Plot showing total number of human cells in the bone marrow collected from one leg (femur + tibia) at 12 weeks post-transplantation. **(B–F)** Plots showing the total number of human cells of the indicated lineages for each graft condition. Symbols show results from individual mice, and bars show the geometric means. *$p < 0.05$.

reduce the hematopoietic output of B lineage cells, while other donor-derived cells adversely affected the production of myeloid, neutrophilic, and progenitor populations.

DISCUSSION

In this study, we used the NBSGW mouse strain as a model system to investigate hematopoietic output by human HSPCs. Consistent with results from prior studies that transplanted human HSPCs into immunodeficient mice bearing hypomorphic c-kit mutations (13–20), we found that a complex multi-lineage human immune compartment was generated that included B lymphocytic, neutrophilic, and multiple myeloid lineage populations. However, whereas prior studies have highlighted that Kit-mutant mice support enhanced engraftment of human myeloid cells (13–15, 17–20), our analysis revealed marked differences in the composition and duration of the human immune compartment depending on the source of the HSPCs. Of particular interest, we found that transplantation of HSPCs purified from G-CSF mobilized blood led to the generation of abundant human neutrophilic lineage cells, whereas HSPCs from the bone marrow favored B lymphocytic reconstitution, and HSPCs from the umbilical cord blood led to more durable B lymphocytic engraftment. Thus, our findings suggest that while the host environment of NBSGW mice is favorable for human myelopoiesis, it also does not overridingly skew hematopoietic output toward myeloid lineages and thus allows for distinct programs of human HSPC differentiation.

Prior human HSPC engraftment studies using irradiated immunodeficient mice with wild-type *c-kit* led to the production of a human immune compartment dominated by B cells, with comparatively low representation of myeloid lineages and little or no evidence of granulocytic lineage development (31–33). This B lymphocytic lineage bias was thought to be due to the abundance of murine IL-7, which promotes lymphopoiesis and is cross-reactive between mouse and humans (34), while murine IL-3 and GM-CSF do not appear to efficiently promote human myelopoiesis. To address this limitation, the NSG-SGM3 and MISTRG next-generation immunodeficient mouse strains were designed to support myeloid development by providing human GM-CSF and IL-3 through gene knock-in technology (8–10). While these mouse strains do support human myeloid development exceptionally well, it is not clear whether they may skew HSPCs towards myelopoiesis and thus may mask the impact on hematopoiesis of other biological features of HSPCs or of accessory cell populations. Thus, immunodeficient Kit-mutant mouse strains provide an important alternative, since the presence of hypofunctional c-kit in the endogenous murine cells and the cross-reactivity of murine SCF apparently provide a sufficient advantage to transplanted human HSPCs so that they can successfully engraft, while also supporting varied differentiation outputs.

Another important factor is that pre-transplant conditioning is not required for human hematopoietic engraftment in Kit-mutant strains, such as NBSGW. Eliminating pre-conditioning removes the influx of DAMPs, alarmins, and other inflammatory signals that could alter survival of the donor HSPCs or affect lineage differentiation and that are now known to promote the development of GVHD (3, 4, 23). Additionally, eliminating pre-conditioning leaves mesenchymal and endothelial cells undamaged, which is likely to promote hematopoietic reconstitution as it has recently been shown that HSPCs reside in specific pockets within bone marrow tissue, where they are surrounded by mesenchymal and endothelial cells that secrete cytokines important for HSPC survival and differentiation (11). Indeed, recognition of the adverse impact of pre-transplant conditioning has led to increasing interest in the use of reduced intensity conditioning or alternative protocols for clinical HSCT. For example, it has recently been shown that depleting endogenous murine HSPCs by administering an antibody-bead conjugate against CD117, allows for the survival and differentiation of human HSPCs in non-conditioned NSG mice (35, 36). With this approach now entering phase-I clinical trials, murine models that provide an HSPC-deficient host environment will likely become increasingly useful tools for further research.

A highly novel observation from this study is the efficient engraftment and abundant neutrophilic population generated by transplantation of MB-HSPCs (**Figures 4B, E**). Clinical reports have shown that patients given MB grafts tend to achieve neutrophil and platelet reconstitution faster than those receiving either BM or CB grafts (3, 4). The robust granulocytic differentiation we observed is most likely due to the prior systemic G-CSF treatment of mobilized blood donors, since G-CSF is known to induce granulopoiesis as well as mobilizing HSPCs to leave the bone marrow (25, 26). One possibility is that G-CSF treatment preferentially mobilizes HSPCs that are already committed towards granulocytic lineage differentiation. However, our analysis of the HSPC population in MB graft tissue revealed a higher frequency of $CD38^{-}$ uncommitted progenitors than BM (**Figures 1E–H**), suggesting that the granulocytic differentiation bias of MB-HSPCs may be due to changes prior to lineage commitment. It will thus be of great interest to determine in future studies whether exposure to G-CSF alters the composition or programming of uncommitted HSPCs or instead results in selective mobilization of specific HSPC populations from the bone marrow (37). Additionally, we observed that the percentage of long-term HSCs ($CD45RA^{-}/CD49f^{+}$) was significantly lower in MB than BM (**Figure 1I**). Thus, an additional important question not addressed by our study is whether the enhanced early hematopoietic output and granulopoiesis of MB-HSPCs is accompanied by a shorter duration of engraftment in NBSGW compared to clinical transplantation protocols are typically performed using grafts that contain an abundance of lineage-committed cell types in addition to HSPCs, we also investigated the impact of such cells on hematopoietic output in our model. Prior studies have established adverse effects from the presence of T cells within graft tissues that occur even in the absence of GVHD (23, 38, 39). This may be due to low levels of IFN-γ production, since this cytokine has been shown to have bi-specific activity on HSPCs. Acute IFN-γ exposure has been shown to induce both myelopoiesis and granulopoiesis in response to an infection, but

chronic IFN-γ exposure has been shown to cause HSPC arrest through the binding and occlusion of the HSPC pro-survival factor thrombopoietin (TPO) to its cognate receptor c-MPL (40, 41). Surprisingly, we found that removing donor-derived T cells from total MNC grafts resulted in a selective enhancement of B cell numbers, but did not significantly improve the output for other populations (**Figure 7**). This suggests that T cells may inhibit B cell engraftment, but other cells found within the MNCs may suppress the differentiation of other populations. Alternatively, T cells may override the B cell promoting effects of another population found in the MNCs. Consistent with this possibility, it has recently been shown that B lymphocytes may engage in a feed-back loop that promotes B cell development *via* a GABAergic pathway (42). Thus, a key area of future investigation will be to determine the mechanisms involved in the impact of non-HSPCs on hematopoietic output.

Lastly, it is important to acknowledge that a limitation of our study is that we did not address the functionality of the human immune lineages produced in these models. In particular, it will be important to determine whether the neutrophilic cells observed in the bone marrow develop into fully mature and functional human neutrophils, and whether these exit to the periphery. Nevertheless, this study demonstrates the potential for using NBSGW mice engrafted with human MB-HSPCs to study aspects of human granulopoiesis *in vivo*. Similarly, we show the utility of the NBSGW strain as a tool to investigate differences within HSPC populations from different human graft tissues, which remains an understudied aspect of the many variables that influence immune reconstitution following allogeneic HSCT.

DATA AVAILABILITY STATEMENT

The raw data supporting the conclusions of this article will be made available by the authors, without undue reservation.

ETHICS STATEMENT

The studies involving human participants were reviewed and approved by University of Wisconsin Minimal Risk Institutional Review Board. Written informed consent for participation was not required for this study in accordance with the national legislation and the institutional requirements. The animal study was reviewed and approved by University of Wisconsin Care and Use Committee.

AUTHOR CONTRIBUTIONS

NJH and JEG designed the study. AWH and PH procured samples. NJH, PNL, JV and SG performed the research and analyzed the data. NJH and JEG wrote the manuscript. NJH, AWH, AKS, AI, PH and JEG edited the manuscript. All authors approved the submitted version.

FUNDING

NJH was supported by NIH T32 AI125231 and T32 HL07899. Additional support from NIH R21 AI116007 and R01 AI135600 (JEG) and R21 AI105841 (AWH).

ACKNOWLEDGMENTS

The authors would like to acknowledge the UW-Madison BRMS Mouse Breeding Core for their assistance with this study, and to thank Satoshi Kinoshita and the University of Wisconsin Translational Research Initiatives in Pathology laboratory (TRIP) for the use of facilities and services.

REFERENCES

1. McCurdy SR, Luznik L. How we perform haploidentical stem cell transplantation with posttransplant cyclophosphamide. *Hematol Am Soc Hematol Educ Program* (2019) 2019:513–21. doi: 10.1182/hematology.2019001323
2. Juric MK, Ghimire S, Ogonek J, Weissinger EM, Holler E, van Rood JJ, et al. Milestones of Hematopoietic Stem Cell Transplantation - From First Human Studies to Current Developments. *Front Immunol* (2016) 7:470. doi: 10.3389/fimmu.2016.00470
3. Seggewiss R, Einsele H. Immune reconstitution after allogeneic transplantation and expanding options for immunomodulation: an update. *Blood* (2010) 115:3861–8. doi: 10.1182/blood-2009-12-234096
4. Ogonek J, Kralj Juric M, Ghimire S, Varanasi PR, Holler E, Greinix H, et al. Immune Reconstitution after Allogeneic Hematopoietic Stem Cell Transplantation. *Front Immunol* (2016) 7:507. doi: 10.3389/fimmu.2016.00507
5. Mestas J, Hughes CCW. Of mice and not men: differences between mouse and human immunology. *J Immunol* (2004) 172:2731–8. doi: 10.4049/jimmunol.172.5.2731
6. Allen TM, Brehm MA, Bridges S, Ferguson S, Kumar P, Mirochnitchenko O, et al. Humanized immune system mouse models: progress, challenges and opportunities. *Nat Immunol* (2019) 20:770–4. doi: 10.1038/s41590-019-0416-z
7. Zumwalde NA, Gumperz JE. Modeling Human Antitumor Responses In Vivo Using Umbilical Cord Blood-Engrafted Mice. *Front Immunol* (2018) 9:54. doi: 10.3389/fimmu.2018.00054
8. Rongvaux A, Willinger T, Martinek J, Strowig T, Gearty SV, Teichmann LL, et al. Development and function of human innate immune cells in a humanized mouse model. *Nat Biotechnol* (2014) 32:364–72. doi: 10.1038/nbt.2858
9. Jangalwe S, Shultz LD, Mathew A, Brehm MA. Improved B cell development in humanized NOD-scid IL2Rγnull mice transgenically expressing human stem cell factor, granulocyte-macrophage colony-stimulating factor and interleukin-3. *Immun Inflamm Dis* (2016) 4:427–40. doi: 10.1002/iid3.124
10. Sippel TR, Radtke S, Olsen TM, Kiem H-P, Rongvaux A. Human hematopoietic stem cell maintenance and myeloid cell development in next-generation humanized mouse models. *Blood Adv* (2019) 3:268–74. doi: 10.1182/bloodadvances.2018023887
11. Tamplin OJ, Durand EM, Carr LA, Childs SJ, Hagedorn EJ, Li P, et al. Hematopoietic stem cell arrival triggers dynamic remodeling of the perivascular niche. *Cell* (2015) 160:241–52. doi: 10.1016/j.cell.2014.12.032
12. Solomon SR, St Martin A, Shah NN, Fatobene G, Al Malki MM, Ballen KK, et al. Myeloablative vs reduced intensity T-cell-replete haploidentical transplantation for hematologic malignancy. *Blood Adv* (2019) 3:2836–44. doi: 10.1182/bloodadvances.2019000627

13. Geissler EN, Russell ES. Analysis of the hematopoietic effects of new dominant spotting (W) mutations of the mouse. I. Influence upon hematopoietic stem cells. *Exp Hematol* (1983) 11:452–60.
14. Thorén LA, Liuba K, Bryder D, Nygren JM, Jensen CT, Qian H, et al. Kit regulates maintenance of quiescent hematopoietic stem cells. *J Immunol* (2008) 180:2045–53. doi: 10.4049/jimmunol.180.4.2045
15. Waskow C, Madan V, Bartels S, Costa C, Blasig R, Rodewald H-R. Hematopoietic stem cell transplantation without irradiation. *Nat Methods* (2009) 6:267–9. doi: 10.1038/nmeth.1309
16. Cosgun KN, Rahmig S, Mende N, Reinke S, Hauber I, Schäfer C, et al. Kit regulates HSC engraftment across the human-mouse species barrier. *Cell Stem Cell* (2014) 15:227–38. doi: 10.1016/j.stem.2014.06.001
17. Yurino A, Takenaka K, Yamauchi T, Nunomura T, Uehara Y, Jinnouchi F, et al. Enhanced Reconstitution of Human Erythropoiesis and Thrombopoiesis in an Immunodeficient Mouse Model with Kit(Wv) Mutations. *Stem Cell Rep* (2016) 7:425–38. doi: 10.1016/j.stemcr.2016.07.002
18. McIntosh BE, Brown ME, Duffin BM, Maufort JP, Vereide DT, Slukvin II, et al. B6.SCID Il2rγ-/- Kit(W41/W41) (NBSGW) mice support multilineage engraftment of human hematopoietic cells. *Stem Cell Rep* (2015) 4:171–80. doi: 10.1016/j.stemcr.2014.12.005
19. Rahmig S, Bornstein SR, Chavakis T, Jaeckel E, Waskow C. Humanized mouse models for type 1 diabetes including pancreatic islet transplantation. *Horm Metab Res* (2015) 47:43–7. doi: 10.1055/s-0034-1390446
20. Rahmig S, Kronstein-Wiedemann R, Fohgrub J, Kronstein N, Nevmerzhitskaya A, Bornhäuser M, et al. Improved Human Erythropoiesis and Platelet Formation in Humanized NSGW41 Mice. *Stem Cell Rep* (2016) 7:591–601. doi: 10.1016/j.stemcr.2016.08.005
21. Keating AK, Langenhorst J, Wagner JE, Page KM, Veys P, Wynn RF, et al. The influence of stem cell source on transplant outcomes for pediatric patients with acute myeloid leukemia. *Blood Adv* (2019) 3:1118–28. doi: 10.1182/bloodadvances.2018025908
22. Anasetti C, Logan BR, Lee SJ, Waller EK, Weisdorf DJ, Wingard JR, et al. Peripheral-blood stem cells versus bone marrow from unrelated donors. *N Engl J Med* (2012) 367:1487–96. doi: 10.1056/NEJMoa1203517
23. Hess NJ, Hudson AW, Hematti P, Gumperz JE. Early T Cell Activation Metrics Predict Graft-versus-Host Disease in a Humanized Mouse Model of Hematopoietic Stem Cell Transplantation. *J Immunol* (2020) 205:272–81. doi: 10.4049/jimmunol.2000054
24. Hiwarkar P, Hubank M, Qasim W, Chiesa R, Gilmour KC, Saudemont A, et al. Cord blood transplantation recapitulates fetal ontogeny with a distinct molecular signature that supports CD4+ T-cell reconstitution. *Blood Adv* (2017) 1:2206–16. doi: 10.1182/bloodadvances.2017010827
25. Tay J, Levesque J-P, Winkler IG. Cellular players of hematopoietic stem cell mobilization in the bone marrow niche. *Int J Hematol* (2017) 105:129–40. doi: 10.1007/s12185-016-2162-4
26. Greenbaum AM, Link DC. Mechanisms of G-CSF-mediated hematopoietic stem and progenitor mobilization. *Leukemia* (2011) 25:211–7. doi: 10.1038/leu.2010.248
27. Notta F, Zandi S, Takayama N, Dobson S, Gan OI, Wilson G, et al. Distinct routes of lineage development reshape the human blood hierarchy across ontogeny. *Science* (2016) 351:aab2116. doi: 10.1126/science.aab2116
28. Majeti R, Park CY, Weissman IL. Identification of a hierarchy of multipotent hematopoietic progenitors in human cord blood. *Cell Stem Cell* (2007) 1:635–45. doi: 10.1016/j.stem.2007.10.001
29. Kasow KA, Sims-Poston L, Eldridge P, Hale GA. CD34(+) hematopoietic progenitor cell selection of bone marrow grafts for autologous transplantation in pediatric patients. *Biol Blood Marrow Transplant* (2007) 13:608–14. doi: 10.1016/j.bbmt.2007.01.074
30. Salzmann-Manrique E, Bremm M, Huenecke S, Stech M, Orth A, Eyrich M, et al. Joint Modeling of Immune Reconstitution Post Haploidentical Stem Cell Transplantation in Pediatric Patients With Acute Leukemia Comparing CD34+-Selected to CD3/CD19-Depleted Grafts in a Retrospective Multicenter Study. *Front Immunol* (2018) 9:1841. doi: 10.3389/fimmu.2018.01841
31. Matsumura T, Kametani Y, Ando K, Hirano Y, Katano I, Ito R, et al. Functional CD5+ B cells develop predominantly in the spleen of NOD/SCID/gammac(null) (NOG) mice transplanted either with human umbilical cord blood, bone marrow, or mobilized peripheral blood CD34+ cells. *Exp Hematol* (2003) 31:789–97. doi: 10.1016/S0301-472X(03)00193-0
32. Shultz LD, Lyons BL, Burzenski LM, Gott B, Chen X, Chaleff S, et al. Human lymphoid and myeloid cell development in NOD/LtSz-scid IL2R gamma null mice engrafted with mobilized human hemopoietic stem cells. *J Immunol* (2005) 174:6477–89. doi: 10.4049/jimmunol.174.10.6477
33. McDermott SP, Eppert K, Lechman ER, Doedens M, Dick JE. Comparison of human cord blood engraftment between immunocompromised mouse strains. *Blood* (2010) 116:193–200. doi: 10.1182/blood-2010-02-271841
34. Barata JT, Silva A, Abecasis M, Carlesso N, Cumano A, Cardoso AA. Molecular and functional evidence for activity of murine IL-7 on human lymphocytes. *Exp Hematol* (2006) 34:1133–42. doi: 10.1016/j.exphem.2006.05.001
35. Pang WW, Czechowicz A, Logan AC, Bhardwaj R, Poyser J, Park CY, et al. Anti-CD117 antibody depletes normal and myelodysplastic syndrome human hematopoietic stem cells in xenografted mice. *Blood* (2019) 133:2069–78. doi: 10.1182/blood-2018-06-858159
36. Czechowicz A, Palchaudhuri R, Scheck A, Hu Y, Hoggatt J, Saez B, et al. Selective hematopoietic stem cell ablation using CD117-antibody-drug-conjugates enables safe and effective transplantation with immunity preservation. *Nat Commun* (2019) 10:617. doi: 10.1038/s41467-018-08201
37. Six E, Guilloux A, Denis A, Lecoules A, Magnani A, Vilette R, et al. Clonal tracking in gene therapy patients reveals a diversity of human hematopoietic differentiation programs. *Blood* (2020) 135:1219–31. doi: 10.1182/blood.2019002350
38. Capitini CM, Herby S, Milliron M, Anver MR, Mackall CL, Fry TJ. Bone marrow deficient in IFN-{gamma} signaling selectively reverses GVHD-associated immunosuppression and enhances a tumor-specific GVT effect. *Blood* (2009) 113:5002–9. doi: 10.1182/blood-2008-11-187385
39. Yoshihara S, Li Y, Xia J, Danzl N, Sykes M, Yang Y-G. Posttransplant Hemophagocytic Lymphohistiocytosis Driven by Myeloid Cytokines and Vicious Cycles of T-Cell and Macrophage Activation in Humanized Mice. *Front Immunol* (2019) 10:186. doi: 10.3389/fimmu.2019.00186
40. Alvarado LJ, Huntsman HD, Cheng H, Townsley DM, Winkler T, Feng X, et al. Eltrombopag maintains human hematopoietic stem and progenitor cells under inflammatory conditions mediated by IFN-γ. *Blood* (2019) 133:2043–55. doi: 10.1182/blood-2018-11-884486
41. Merli P, Caruana I, De Vito R, Strocchio L, Weber G, Del Bufalo F, et al. Role of IFNγ in immune-mediated graft failure occurring after allogeneic hematopoietic stem cell transplantation. *Haematologica* (2019) 104:2314–2323. doi: 10.3324/haematol.2019.216101
42. Shao L, Elujoba-Bridenstine A, Zink KE, Sanchez LM, Cox BJ, Pollok KE, et al. The neurotransmitter receptor Gabbr1 regulates proliferation and function of hematopoietic stem and progenitor cells. *Blood* (2020) [published online ahead of print, 2020 Sep 3]. doi: 10.1182/blood.2019004415.

Conflict of Interest: The authors declare that the research was conducted in the absence of any commercial or financial relationships that could be construed as a potential conflict of interest.

Copyright © 2020 Hess, Lindner, Vazquez, Grindel, Hudson, Stanic, Ikeda, Hematti and Gumperz. This is an open-access article distributed under the terms of the Creative Commons Attribution License (CC BY). The use, distribution or reproduction in other forums is permitted, provided the original author(s) and the copyright owner(s) are credited and that the original publication in this journal is cited, in accordance with accepted academic practice. No use, distribution or reproduction is permitted which does not comply with these terms.

frontiers in Oncology

ORIGINAL RESEARCH
published: 12 January 2021
doi: 10.3389/fonc.2020.614876

PD-1 Blockade Aggravates Epstein–Barr Virus$^+$ Post-Transplant Lymphoproliferative Disorder in Humanized Mice Resulting in Central Nervous System Involvement and CD4$^+$ T Cell Dysregulations

Valery Volk[1,2,3†], Sebastian J. Theobald[1,2†], Simon Danisch[1,2†], Sahamoddin Khailaie[4], Maja Kalbarczyk[1,2], Andreas Schneider[1], Julia Bialek-Waldmann[1], Nicole Krönke[3], Yun Deng[5], Britta Eiz-Vesper[6], Anna Christina Dragon[6], Constantin von Kaisenberg[7], Stefan Lienenklaus[8], Andre Bleich[8], James Keck[9], Michael Meyer-Hermann[4], Frank Klawonn[10,11], Wolfgang Hammerschmidt[12], Henri-Jacques Delecluse[13], Christian Münz[5], Friedrich Feuerhake[3,14‡] and Renata Stripecke[1,2‡]*

[1] Laboratory of Regenerative Immune Therapies Applied, REBIRTH - Research Center for Translational Regenerative Medicine, Department of Hematology, Hemostasis, Oncology and Stem Cell Transplantation, Hannover Medical School, Hannover, Germany, [2] German Centre for Infection Research (DZIF), Partner site Hannover, Hannover, Germany, [3] Institute for Pathology, Hannover Medical School, Hannover, Germany, [4] Department of Systems Immunology, Braunschweig Integrated Centre of Systems Biology, Helmholtz Centre for Infection Research, Braunschweig, Germany, [5] Viral Immunobiology, Institute of Experimental Immunology, University of Zürich, Zürich, Switzerland, [6] Institute for Transfusion Medicine and Transplant Engineering, Hannover Medical School, Hannover, Germany, [7] Department of Obstetrics, Gynecology and Reproductive Medicine, Hannover Medical School, Hannover, Germany, [8] Institute for Laboratory Animal Science, Hannover Medical School, Hannover, Germany, [9] The Jackson Laboratory, Sacramento, CA, United States, [10] Biostatistics Group, Helmholtz Centre for Infection Research, Braunschweig, Germany, [11] Institute for Information Engineering, Ostfalia University, Wolfenbuettel, Germany, [12] Research Unit Gene Vectors, Helmholtz Zentrum München, German Research Center for Environmental Health and German Centre for Infection Research (DZIF), Partner site Munich, Munich, Germany, [13] German Cancer Research Center (DKFZ), Institut National de la Santé et de la Recherche Médicale (INSERM) Unit U1074, Heidelberg, Germany, [14] Institute for Neuropathology, University Clinic Freiburg, Freiburg, Germany

Post-transplant lymphoproliferative disorder (PTLD) is one of the most common malignancies after solid organ or allogeneic stem cell transplantation. Most PTLD cases are B cell neoplasias carrying Epstein-Barr virus (EBV). A therapeutic approach is reduction of immunosuppression to allow T cells to develop and combat EBV. If this is not effective, approaches include immunotherapies such as monoclonal antibodies targeting CD20 and adoptive T cells. Immune checkpoint inhibition (ICI) to treat EBV$^+$ PTLD was not established clinically due to the risks of organ rejection and graft-*versus*-host disease. Previously, blockade of the programmed death receptor (PD)-1 by a monoclonal antibody (mAb) during *ex vivo* infection of mononuclear cells with the EBV/M81$^+$ strain showed lower xenografted lymphoma development in mice. Subsequently, fully humanized mice infected with the EBV/B95-8 strain and treated *in vivo* with a PD-1 blocking mAb showed aggravation of PTLD and lymphoma development. Here, we evaluated *vis-a-vis* in fully humanized mice after EBV/B95-8 or EBV/M81 infections the

OPEN ACCESS

Edited by:
Yasuyuki Saito,
Kobe University, Japan

Reviewed by:
Maher Gandhi,
University of Queensland, Australia
Gilles Marodon,
INSERM U1135 Centre d'Immunologie et de Maladies Infectieuses, France
Ali Roghanian,
University of Southampton, United Kingdom

***Correspondence:**
Renata Stripecke
stripecke.renata@mh-hannover.de

†These authors have contributed equally to this work

‡These authors share senior authorship

Specialty section:
This article was submitted to Cancer Immunity and Immunotherapy, a section of the journal Frontiers in Oncology

Received: 07 October 2020
Accepted: 16 November 2020
Published: 12 January 2021

Citation:
Volk V, Theobald SJ, Danisch S, Khailaie S, Kalbarczyk M, Schneider A, Bialek-Waldmann J, Krönke N, Deng Y, Eiz-Vesper B, Dragon AC, von Kaisenberg C, Lienenklaus S, Bleich A, Keck J, Meyer-Hermann M, Klawonn F, Hammerschmidt W, Delecluse H-J, Münz C, Feuerhake F and Stripecke R (2021) PD-1 Blockade Aggravates Epstein–Barr Virus$^+$ Post-Transplant Lymphoproliferative Disorder in Humanized Mice Resulting in Central Nervous System Involvement and CD4$^+$ T Cell Dysregulations. Front. Oncol. 10:614876. doi: 10.3389/fonc.2020.614876

effects of a clinically used PD-1 blocker. Fifteen to 17 weeks after human CD34$^+$ stem cell transplantation, Nod.Rag.Gamma mice were infected with two types of EBV laboratory strains expressing firefly luciferase. Dynamic optical imaging analyses showed systemic EBV infections and this triggered vigorous human CD8$^+$ T cell expansion. Pembrolizumab administered from 2 to 5 weeks post-infections significantly aggravated EBV systemic spread and, for the M81 model, significantly increased the mortality of mice. ICI promoted Ki67$^+$CD30$^+$CD20$^+$EBER$^+$PD-L1$^+$ PTLD with central nervous system (CNS) involvement, mirroring EBV$^+$ CNS PTLD in humans. PD-1 blockade was associated with lower frequencies of circulating T cells in blood and with a profound collapse of CD4$^+$ T cells in lymphatic tissues. Mice treated with pembrolizumab showed an escalation of exhausted T cells expressing TIM-3, and LAG-3 in tissues, higher levels of several human cytokines in plasma and high densities of FoxP3$^+$ regulatory CD4$^+$ and CD8$^+$ T cells in the tumor microenvironment. We conclude that PD-1 blockade during acute EBV infections driving strong CD8$^+$ T cell priming decompensates T cell development towards immunosuppression. Given the variety of preclinical models available, our models conferred a cautionary note indicating that PD-1 blockade aggravated the progression of EBV$^+$ PTLD.

Keywords: humanized mice, immuno-oncology, Epstein-Barr Virus (EBV), immune checkpoint inhibition (ICI), post-transplant lymphoproliferative disease (PTLD), lymphoma, PD-1, pembrolizumab

INTRODUCTION

EBV is an oncogenic γ-herpesvirus associated with around 2% of all human cancers such as hematologic and epithelial malignancies (1). After the primary infection, EBV lytic reactivations are immunologically controlled, but the virus is not cleared. The life-long EBV maintenance in the host does not always lead to cellular transformations, but dysfunctional immunity can predispose opportunistic flares of EBV reactivations and eventually lead to EBV$^+$ infectious mononucleosis (IM), lymphoproliferative diseases (LPD), or malignancies (2). Thus, novel immunotherapeutic options are being developed and tested for treatment of EBV infections and/or EBV-associated malignancies. For example, immune checkpoint inhibition (ICI) with monoclonal antibodies (mAbs) became a major breakthrough immunotherapy for cancer treatment over the past decade and showed to be effective against several types of tumors. Currently, several mAbs blocking the programmed death receptor protein (PD)-1 or its ligand PD-L1 have been approved or are in clinical development against several types of cancer (3, 4). ICI has demonstrated impressive high response rates as salvage therapy in relapsed/refractory (R/R) classical Hodgkin lymphoma (cHL) (5), the most common cancer among young people. Incidentally, EBV contributes to the chronic inflammatory microenvironment of a subset of cHL with high expression of PD-L1. Indeed, the interaction of PD-L1 with PD-1 on inflammatory T cells constitutes one of the major immune escape mechanisms in cHL, associated with development of dysfunctional and tolerogenic T cell responses (5). The preclinical observation of PD-L1 overexpression in cHL led to the evaluation of ICI administration in several clinical trials and the subsequent clinical approval of nivolumab, a mAb blocking PD-1, for cHL therapy (6). In 2017, The U.S. Food and Drug Administration also granted approval to pembrolizumab (KEYTRUDA®), another PD-1 blocking mAb, for the treatment of adult and pediatric patients with refractory cHL.

Another important clinical scenario is the EBV-associated post-transplant lymphoproliferative disorder (PTLD), a severe complication occurring in immunocompromised hosts after allogeneic hematopoietic stem cell transplantation (allo-HCT) or solid organ transplantation (SOT). The diagnostic of PTLD categories proposed by World Health Organization (WHO) are early lesions, polymorphic PTLD, monomorphic PTLD, and also cHL (7). Diffuse large B-cell lymphoma (DLBCL) accounts for the majority of the cases of PTLD. Development of aggressive EBV$^+$ DLBCL has been associated with both latent and lytic viral cycles (8). The EBV$^+$ DLBCL subtype is amonomorphic B cell lymphoma positive for EBV-encoded small RNAs (EBER) and characteristically expressing pan-B-cell markers (CD19, CD20, and occasionally CD30) with an EBV latency pattern type III in which all latency genes are expressed [for an expert review see (9)]. A small number of lytic infected cells can be found in tumors and show expression of lytic transcripts (such as BZLF1 and gp350) (8). A biomarker for these malignancies is the frequently detectable high expression of PD-L1 (CD274 and also known as B7-H1) in EBV$^+$ PTLD, cHL, and DLBCL (10–12). PD-L1 induction in EBV$^+$ malignancies occurs *via* AP-1 and JAK/STAT pathways (10) and also through the cooperation of EBV-LMP-1 and IFN-γ signaling (13). For EBV$^+$ DLBCL, the PD-L1 positive tumors express high levels of indoleamine 2,3-dioxygenase (IDO), indicating a tolerogenic tumor microenvironment (TME) (11). Furthermore, EBV$^+$ DLBCL

presents with a distinct tolerogenic TME than EBV⁻ DLBCL, characterized by elevated expression of immune checkpoints [PD-L1, PD-L2, lymphocyte activation gene 3 (LAG-3) and T cell immunoglobulin and mucin domain-containing protein 3 (TIM-3)] and high levels of immunosuppressive M2-type macrophages (12). Thirty to 40% of DLBCL patients show primary resistance or early relapse after standard therapy and there is no standard treatment approach specifically for aggressive EBV$^+$ DLBCL (9).

The standard of care for PTLD/DLBCL is first a reduction in immunosuppression, that needs to be adjusted to the clinical situation, e.g. potential risks for transplant rejection or graft-*versus*-host disease (GvHD) (2). Additionally, treatment with rituximab, a mAb that targets the CD20$^+$ malignant cells, produces response rates of about 65% (14). Clinical trials in specialized centers demonstrated that adoptive administration of third party or donor-derived or T cells specific for EBV could effectively restore virus-specific immunity and confer protection in 60 to 90% of transplant recipients with a PTLD (15). In addition to these measures, use of ICI could be a promising approach to treat EBV$^+$ PTLD (10). Nonetheless, since the immunity of patients after transplantations is not in the normal homeostatic steady state, the clinical use of ICI against PTLD demands careful preclinical testing, particularly due to the associated risks of graft rejection and graft-versus host disease (GvHD).

EBV strictly infects human cells and therefore special *in vivo* models are required for preclinical testing of therapies targeting an EBV$^+$ malignancy or immunopathology. During the last decade, mice reconstituted with the human immune system ("HIS mice") became the state-of-the art *in vivo* models to test human-specific therapies against several human infections, malignancies, immunological and metabolic diseases (16–18). Infection of HIS mice with different EBV strains recapitulated several hallmarks of PTLD and lymphoma development and, concurrently, allowed studies of the human T cell inflammatory immune responses (19–22). The EBV/B95-8 strain was originally isolated from a patient with infectious mononucleosis and was later modified into the engineered B95-8/GFP strain, produced in the laboratory with the bac-mid technology. B95-8/GFP promotes a high B cell transformation rate and B-cell lymphoma growth (23). We have previously shown that, a few weeks after infection of HIS mice with B95-8/GFP, a dramatic expansion of CD8$^+$ T cells expressing the inhibitory receptors PD-1, LAG-3, and TIM-3 followed (24, 25). Another strain, EBV/M81, was originally isolated from a patient with nasopharyngeal carcinoma (26). The M81/GFP engineered laboratory derivative induces potent lytic replication in B cells both *in vitro* and in humanized mice also leading to development of tumors (23).

Previously, therapeutic effects of PD-1 blockade in a xenograft mouse model of M81/GFP$^+$ lymphoma were reported (27) (**Table 1**). Mononuclear cells obtained from cord blood (CB) were infected *in vitro w*ith the M81/GFP strain and then injected *i.p.* into Nod.Scid.Gamma (NSG) mice. Tumors resembling diffuse large B cells lymphoma (DLBCL) developed 3–5 weeks after in spleen. Pre-treatment of the cells with mAbs *in vitro*, i.e., prior to administration into the mice, significantly lowered the development of EBV$^+$ tumors, particularly when anti-PD-1 and anti-CTLA-4 mAbs were combined (27). More recently, the Münz laboratory showed that fully humanized mice infected with B95-8/GFP and afterwards treated with a PD-1 blocking mAb showed significant increase in EBV viral load and tumor development (25) (**Table 1**). The interpretation of these results was that the disruption of the PD-1/PD-L1 axis during the T cell priming phase abrogated functionality of CD8$^+$ CTLs, required to keep EBV infection and tumor development under control (25).

In view of these opposite results, we sought to clarify these discrepancies in fully humanized mice comparing head-to-head the two EBV strains used for infection models (**Table 1**). NOD.Rag.Gamma (NRG) HIS mice were infected either with EBV/B95-8/fLuc or EBV/M81/fLuc and dynamic non-invasive monitoring of viral spread and post-mortem immunological and histological analyses were performed as previously reported (24, 28). We show a dose-dependent effect of pembrolizumab augmenting the EBV systemic dissemination, lymphomagenesis, and increasing mortality. Remarkably, pembrolizumab treatment promoted EBV spread into the central nervous system (CNS) recapitulating CNS-PTLD. These severe effects of PD-1 blockade were associated with a decompensation of the systemic and intra-tumoral pattern of CD4$^+$ T cells and accumulation of cytokines and FoxP3$^+$ T cells. Thus, although PD-1 blockade may be a favorable therapeutic option against some EBV$^+$ tumors, these models show that it can aggravate the EBV infections in the context of PTLD, promoting hyper-progressive disease (HPD), morbidity, and mortality.

MATERIAL AND METHODS

Generation of Humanized NRG Mice

Collection of CB was performed at the Department of Gynecology and Obstetrics (Hannover Medical School) and obtained according to study protocols approved by the Ethics Committee of the Hannover Medical School and after informed consent obtained from the mothers. Human CD34$^+$ hematopoietic cells were isolated from CB after two rounds of positive selection using immune magnetic beads (Direct CD34 Progenitor Cell Isolation Kit, human, MACS Miltenyi Biotec, Bergisch Gladbach, Germany) as described (24, 28–30). All experiments involving mice were approved by the Lower Saxony Office for Consumer Protection and Food Safety–LAVES (permit number: 16/2222) and performed in accordance with the German animal welfare act and the EU-directive 2010/63. Breeding pairs of NOD.Cg – $Rag1^{tm1Mom}IL-2R\gamma_c^{tm1Wjl}$ (NRG) mice were obtained from the Jackson Laboratory (JAX; Bar Harbor, USA) and bred under pathogen-free conditions. Prior to HCT, 5–6 weeks-old mice were sublethally irradiated (450 cGy) using a [^{137}Cs] column

TABLE 1 | Summary of experimental approaches and conclusions from three different animal studies evaluating *in vivo* the effects of PD-1 blockade on EBV infection and tumor development.

	Ma et al. (27)	Chatterjee et al. (25)	This Study
Human Donor Human Cells or Tissues	Newborn cord blood Commercial CD34-depleted mononuclear cells. Dose: 12–25× 10e6 cells/mouse	Fetal liver tissue Commercial HLA-A2$^+$ CD34$^+$ isolated HSCs Dose: 1–3 × 10e5 HSCs/mouse	Newborn cord blood On site collection CD34$^+$ isolated HSC Dose: 2 × 10e5 cells/mouse
Mouse Recipient	NSG/Jackson Laboratory/3–5 weeks old at cell transfer	NSG w.t. or expressing HLA-A2/Jackson Laboratory/HCT in newborns up to 5 days of age	NRG/Breeding pairs Jackson Laboratory/HCT in 5–6 weeks old mice/Females
Mouse Handling	Human xenograft model/Intraperitoneal cell transfer after *in vitro* infection/Euthanasia at endpoint 4 weeks after cell transfer, or earlier if clinically ill	Fully humanized model/Sublethally irradiated (1 Gy)/intrahepatic HCT/EBV infection 12 weeks after HCT/Bleedings 2, 3, 4, 5 wpi/Euthanasia at endpoint 5 wpi, or earlier if ill	Fully humanized model/Sublethally irradiated (4.5 Gy)/IV HCT/EBV infection 15–17 weeks after HCT/Bleedings 0, 2, 3–4, 5–6, 8 wpi/Optical Imaging 2, 3–4, 5–6 wpi/Euthanasia at endpoint 8 wpi, or earlier if ill
Human Immunity	Spleen and tumors at endpoints. FACS: HLA-A/B/C, CD45, CD3, CD19, CD20, PD-L1, PD-L2, PD-1, CTLA-4	Blood FACS: CD45, CD19, CD3, CD4, CD8 Endpoint FACS CD3, CD8, CD19, CD27, CD28, CD45, CD45RA, CD62L, CTLA4, HLA-DR, Ki67 LAG-3, PD-1, PD-L1, Tim-3 and other analyses of human cytokines in plasma	Blood analyses FACS: CD45, CD19, CD3, CD4, CD8 Endpoint FACS CD3, CD8, CD19, CD45, PD-1, LAG-3, TIM-3 FoxP3 Analyses of human cytokines in plasma
Human Infections	EBV M81/GFP produced in HEK293/tittered on Raji cells/CB cells infected *in vitro* with 2,000 to 5,000 infectious units for 1.5 h	B95-8/GFP produced in HEK293/Tittered on Raji cells/EBV infection IP with 10e5 infectious units/Viral load: DNA isolated from spleen and whole blood and RT-qPCR	B95-8/fLuc/GFP and EBV M81/fLuc/GFP produced in HEK293/tittered on Raji cells/B95-8 10e5 and M81 10e6 infectious units IV/Followed for up 8 wpi/Viral load: DNA isolated from spleen and bone marrow and RT-qPCR
Human Oncology	Lymphoma development 4 weeks after cell transfer/spleen and organs H&E staining/IHC staining CD20, CD8, CD4/EBV antigens: EBER, EBNA2, LMP1, BZLF1, BMRF	PTLD and lymphoma terminal analyses 5 wpi/Spleen IHC EBNA1, EBNA2, EBER	PTLD and lymphoma terminal analyses 8 wpi/Spleen, liver, brain, IHC CD20, CD30, Ki67, CD3, CD4, CD8, PD-1, PD-L1, LMP1, EBNA2, EBER
Pre-clinical Study and Outcomes	No ICI *in vivo*/Anti-CTLA-4 mAb (Ipilimumab)/anti-PD-1 mAb (anti-hCD279, clone J116 BioXcell)/3× weekly (100 μg i.p.), starting 5–10 days after cell transfer until 4 weeks after cell transfer/Control hIgG ICI applied *in vitro* reduced lymphomas as single therapies (*P=0.06*) or combination (*P=0.03*)/combination, lowered # latently, and lyrically infected B cells, increased EBV-specific T cell responses **ICI considered useful for treating EBV-induced diseases**	ICI starting 3 wpi applied a total of 7× until 5 wpi/Anti-PD-1 mAb (clone EH12.2H7 Biolegend) 100–150 μg per administration/7× administrations/Control: PBS or 150 μg of isotype control antibody ICI applied during *in vivo* T cell priming resulted in elevated viral load (blood $P < 0.05$, spleen $P < 0.001$), elevated tumor burden ($P < 0.05$./CD3 T cell numbers in blood not changed/Lower frequencies of PD-1$^+$ CD8 T cells ($P < 0.0001$)/Elevated levels of cytokines (IFN-γ, TNF-α, IL-10, IL-8 $P < 0.05$ to $P < 0.001$) **Function of PD-1 axis necessary for control of EBV infection and tumorigenesis**	ICI low dose: 1st administration 3.33 mg/kg at 2 wpi; 1.7 mg/kg every other week applied 6×)/ICI high dose (1st 10 mg/kg at 2 wpi; 5 mg/kg every other week applied 6×) ICI applied during *in vivo* T cell priming resulted in elevated viral spread (BLI) load (spleen and bone marrow), elevated tumor burden (also in CNS) and higher mortality/CD4 and CD8 T cell numbers in blood reduced, lower frequencies of PD-1$^+$ CD8 and CD4 T cells/Increased frequencies of TIM-3$^+$, LAG-3$^+$ and Tregs/elevated levels of cytokines (IFN-α, IL-10, IL-33, IL-12) **PD-1 blockade worsens PTLD and lymphomagenesis with the emergence of immune dysfunctional T cells**

irradiator (Gammacell 3000 Elan; Best Theratronics, Ottawa, Canada). Four hours after irradiation, 2.0×10^5 CD34$^+$ cells were injected through the tail vein. Body weight and occurrence of GvHD were monitored weekly after HCT. For the sake of reproducibility, we used preferentially female NRG mice because they show more consistent and stable human immune reconstitution and immune responses >15 weeks after HCT (29). Further, CD34$^+$ HSC units were pretested in a couple of transplanted NRG mice and only those resulting in 20% or higher frequencies of human CD45$^+$ cells in mouse blood at 10–15 weeks post-HCT were used for experiments with EBV infections. These parameters were extensively optimized for preclinical testing of vaccines and chimeric antigen receptor (CAR) T cell therapies (28, 30–33).

EBV Infections and Treatment of Humanized Mice With Pembrolizumab

Stable human hematopoietic engraftment was confirmed in peripheral blood at 15–17 weeks after HCT, and at this point mice were infected with the B95-8/fLuc (24) or with the M81/fLuc strain (28, 34). The engineered B95-8/fLuc strain expresses the reporter gene firefly luciferase downstream of the viral Epstein-Barr nuclear antigen 2 (EBNA2) (24), while the EBV/M81/fLuc strain expresses fLuc under the control of an inserted CMV immediately early (IE)1 promoter sequence (34). EBV titers were defined as green Raji units (GRU) after infection of Raji cells with serial dilutions of the virus stocks. The percentage of GFP$^+$ cells was analyzed by flow cytometry 3 days later and the viral titers were calculated by the following formula: "total

number of Raji cells infected" × "percentage of GFP+ cells"/ "volume of the virus stock used." After pilot experiments to evaluate the relationship between the viral dose and reproducible bioluminescent signals detectable at 2 weeks post infection (wpi), the viral doses diluted in 100 µl PBS were established: 10^5 GRU for EBV/B95-8/fLuc and 10^6 GRU for EBV/M81/fLuc (**Table 1**). Using these viral doses, we have reported that most of the infected HIS mice survive for more than 8 wpi with some mice showing progressive disease while others are able to control the tumor development with stable disease (24, 28). Euthanasia was performed at the endpoint 8 wpi for collection of biopsies or earlier if symptoms of distress due to tumor development or weight loss were detected. At 2 wpi, mice were randomized based on their bioluminescence signal between PBS control, pembrolizumab high dose (HD) and pembrolizumab low dose (LD). Pembrolizumab (MSD; Kenilworth; USA) was diluted in PBS for administration as a low dose (LD: First administration 3.33 mg/kg at 2 wpi; 1.7 mg/kg every other week applied six times) or as a high dose (HD: First administration 10 mg/kg at 2 wpi; 5 mg/kg every other week applied six times). As treatment controls PBS or human pooled immunoglobulin (KIOVIG, a clinically used pooled polyclonal IgG product obtained from human donors) were injected intraperitoneally every week after 2 wpi.

Flow Cytometry Analysis of Blood and Lymphatic Tissues

Peripheral blood (BL) obtained at different time-points and tissues obtained from humanized mice at the endpoint [lymph node (LN), spleen (SPL), bone marrow (BM), thymus (Thy)] were processed as previously described (24, 29, 30). For BL and SPL, a hypotonic solution (0.83% ammonium chloride/20 mM HEPES, pH 7.2, for 5 min at room temperature) was used to remove erythrocytes. Flow cytometry acquisitions were performed with fresh or cryopreserved/thawed cells after immune staining (see antibodies used in **Table S10**). After washing of unbound antibodies, cells were acquired with an LSR II cytometer (BD bioscience) or Cytoflex cytometer (Beckman Coulter). Data was analyzed with FlowJo (LLC, USA).

Dynamic Bioluminescence Imaging (BLI) Analysis

Viral infection and spread in the mice were monitored by expression of luciferase in tissues infected with EBV/B95-8/fLuc or with EBV/M81/fLuc. Dynamic BLI analyses were performed with the IVIS SpectrumCT apparatus (PerkinElmer, Waltham, MA, USA). Before imaging, mice were anesthetized using isoflurane. Mice were imaged 5 min after luciferin administration [2.5 mg D-luciferin potassium salt intraperitoneally (SYNCHEM, ELK Grove Village, IL, USA) reconstituted in 100 µl PBS]. Data was analyzed using the Living Image Software (PerkinElmer, Waltham, MA, USA).

Quantification of Epstein–Barr Virus by Real-Time Quantitative PCR

DNA was isolated from tissues using the DNeasy Blood&Tissue Kit (QIAGEN, Venlo, Netherlands) following the manufacturer´s protocol. In order to detect EBV DNA, a quantitative PCR (qPCR) was performed by amplifying a fragment of the BALF5 gene using following primers: 5´-CTTTGGCGCGGATCCTC-3´ (forward) and 5´-AGTCCTTCTTGGCTAGTCTGTTGAC-3´ (reverse). Detection of the amplification was performed with the following Taqman probe: 5´-Fam-CATCAAGAAGCTGCTGGCGGCC-Tamra-3´. EBV copy number was normalized per µg of isolated DNA. The Taqman PCR assays were run in duplicates on the StepOnePlusTM Real-time system (Applied Biosystems, Life Technologies, Darmstadt, Germany). Data was analyzed using the StepOnePlusTM software (Applied Biosystems, Life Technologies, Version 2.3).

Cytokine Analysis in Mouse Plasma

Cytokine concentrations in plasma samples were determined using the LEDGENDplex™ Human Inflammation Panel 1 Multi-Analyte Flow Assay (BioLegend, San Diego, USA), which allowed for the simultaneous detection of IFN-α, IFN-γ, IL-1β, IL-6, IL-8, IL-10, IL-12p70, IL-17A, IL-18, IL-23, IL-33, MCP-1, and TNF-α. The assay was performed according to the manufacturer's instructions. Briefly, undiluted samples and standards were incubated with antibody-coated premixed beads overnight at 4°C followed by incubation with detection antibody for 1 h at room temperature and streptavidin-PE for 30 min at room temperature. Samples were read on a BD FACSCanto™ Flow Cytometer (BD Biosciences, Heidelberg, Germany) and analyzed with the LEGENDplex v8.0 Software (BioLegend, San Diego, USA).

Histopathology, Immunohistochemistry, and Image Analysis

Three-µm-thick tissue sections were cut from formalin-fixed, paraffin-embedded (FFPE) tissue blocks containing mouse SPL and LI. Staining was performed according to standard protocols for Giemsa. Immunohistochemistry analyses were performed using the Benchmark Ultra automated instrument (Ventana/Roche Tissue Diagnostics, Mannheim, Germany). Following antibodies were used for tissue staining: Ki67 (clone RM9106-S1; ThermoScientific), CD20 (clone M0755; Dako), CD30 (Ber-H2; Dako), CD3 (clone M7254; Dako), programmed cell death ligand 1 (PD-L1; clone 22C3; Dako), CD8 (clone C8/144B; Dako, Copenhagen, Denmark), CD4 (clone SP35; Zytomed Systems, Berlin, Germany), PD-1 (MRQ-22; Medac Diagnostika, Wedel, Germany), FoxP3 (cat. number 560046; BD) (vendor information available in **Table S10**). For antibody binding detection, the 3,3-diaminobenzidine based UltraView reagent was used according to the manufacturer's recommendations. EBER-1 detection was performed by an *in situ* hybridization method (EBER 1 DNP Probe, Ventana/Roche Tissue Diagnostics) and the automated Benchmark Ultra instrument. Whole Slide Scans were produced using an Aperio AT2 scanner (Leica Biosystems), images were taken using the ImageScope software, and trained pathologists evaluated staining results.

Quantitative Multispectral Immunohistochemistry

Three-µm-thick FFPE tissue slides were deparaffinized and antigen retrieval was performed according to "Opal Multiplex IHC Assay Development Guide" instructions. Blocking was done

using Protein Block Serum-free (Dako) solution before each staining cycle. Staining panel was designed to include primary antibodies against human CD4, CD8, FoxP3 (or CD30 for brain tissue staining), CD20, and Ki67. Secondary HRP Labelled Polymer mouse/rabbit (Dako EnVision+ System- HRP Labelled Polymer) antibodies were applied after washing step and maintained for 10 min at room temperature, followed by 10 min incubation with tyramide fluorophores (Opal 520, Opal 570, Opal 620, Opal 650 or Opal 690, Akoya) used for signal amplification. DAPI (Akoya) was used for nuclear staining and Fluoromount-G mounting medium (ThermoScientific) was applied to cover slides before imaging. Whole slide tissue scanning was done at 40× magnification using the "Vectra Polaris" (Akoya) platform. Spectral libraries were generated using single stained scans of tonsil tissue for each marker and images deconvolution was done with the inForm Advanced Image Analysis software (inForm v2.4.8; Akoya). Several representative spleen and liver images were used to train pre-designed machine learning algorithms within inForm software to define tissue classes (tumor, parenchyma, and blank area), adjust cell segmentation settings, and phenotype cells. All the settings from the training images were applied for batch analysis of scanned images.

Statistical Analyses

Log-rank (Mantel-Cox) test was used to compare survival curves. Fisher's exact test was applied to compare the number of macroscopically visible tumors between treatment groups. Unpaired Welch's t test was used to calculate statistical significance for kinetics of immune reconstitution, EBV and T cell levels in tissues. Mann-Whitney t test was used for analyses of cytokines concentrations. $P < 0.05$ was considered statistically significant. Log-transformation of absolute numbers was done for BLI, RT-qPCR, PD1/CD4, and PD1/CD8 MFI, and cell count results, to compare the distribution of measurements within different groups; we also tested the equality of one-dimensional probability distributions using a two-sample Kolmogorov-Smirnov (KS) test. The KS statistic (D), defined as the maximal vertical distance between the empirical cumulative distributions between the groups, and significance level (p-value) were calculated and used as two criteria for finding biomarkers with significant difference between experimental groups. The biomarkers with high KS statistics and low p-value are reported. Statistical analyses were performed using GraphPad Prism v7 software (GraphPad Software Inc., La Jolla, CA, USA). KS test was performed using the statistical computing software R (version 3.4.3).

Data Analyses

Quantitative imaging analyses of data tables exported from inForm 2.4.8. (Akoya) were performed using "R" packages "Phenoptr" and "PhenoptrReports" (Kent S Johnson (2019). phenoptr: inForm Helper Functions. R package version 0.2.3.). Analyses were performed using Rstudio (Rstudio v1.1.456). See also: https://www.r-project.org/foundation/. The readout protocols combined results for "Cell absolute counts," "Cell percentages," "Cell densities," and "Counts within" following manufacturer's instructions (Phenoptics™, Akoya).

RESULTS

PD-1 Blockade in Fully Humanized Mice Promoted Epstein–Barr Virus Spread, Tumor Development, and Mortality

Pembrolizumab administration ("Pembro") or the control treatment ("CTR", PBS or KIOVIG) were initiated at 2 wpi, after a baseline BLI measurement was performed in order to allocate mice in comparable treatment arms (**Figure 1A**). The pembrolizumab low and high dose were previously determined in studies of humanized mice challenged with breast cancer and treated with the drug (35). EBV-infected mice were monitored for clinical signs of disease and euthanized based on humane endpoint criteria. BLI analyses were performed serially until 8 wpi. All B95-8/fLuc-infected mice treated with ICI survived until the end of the experiments (**Figure 1B**). In contrast, several mice infected with M81/fLuc and ICI-treated died prematurely and could not be analyzed or were euthanized (3/6 mice in the LD and in 6/6 in the HD cohort (survival of CTR *vs* HD, $P < 0.01$) (**Figure 1C**, **Table S1**). Mice infected with B95-8/fLuc treated with pembrolizumab or PBS showed comparable body weights (**Figure 1D**), while mice infected with M81/fLuc treated with HD pembrolizumab showed weight loss compared with the other arms (**Figure 1E**). For control infected mice, tumors typically developed in the spleen, while most ICI-treated mice showed multiple tumors located in different organs, such as liver, lung, and kidney (**Figures 1F, G**). At the baseline analyses before ICI treatment (2 wpi), EBV infection levels assessed by BLI analyses were comparable, and over time showed dynamic changes in intensities and bio-distribution. Remarkably, the BLI signals in the ICI-treated animals increased dramatically after 6–8 wpi indicating higher EBV dissemination (8 wpi: B95-8: CTR vs Pembro, $P < 0.0001$; M81: CTR vs Pembro, $P = 0.1387$) (**Figures 1H, I, J, L**, **Table 2**, **Table S2**). The EBV copy numbers in SPL and BM were higher in ICI-treated mice infected with B95-8/fLuc (**Figure 1K**, **Table 2**, **Table S3**, $P = 0.199$ and $P = 0.111$, respectively) or with M81/fLuc than in controls (**Figure 1M**, **Table 2**, **Table S3**, $P < 0.05$). In summary, pembrolizumab administration caused higher viral spread, viral load, tumor development for both EBV infection models. The M81/fLuc lytic model showed the highest severity leading to early mortality occurrences.

PD-1 Blockade Promotes Development of Larger Epstein–Barr Virus+ PD-L1+ Tumor Masses With Lower Densities of Tumor-Infiltrating Lymphocytes

Next, we dissected the effects of pembrolizumab at the tissue level and analyzed the histological signatures of the tumor formation. Post-mortem BLI analyses of explanted SPL and LI showed high levels of bioluminescence signals in ICI-treated mice (**Figures 2A, B**). Histopathological analyses confirmed numerous EBV+ lymphoid neoplastic lesions with a blast-like phenotype and a CD20+ and partially CD30+ immunophenotype of different size and cellular composition. The lesions ranged from relatively small, diffusely infiltrating or sheet-like tumor formations, often observed in perivascular localization (**Figures 2C–F**, left panels, arrows), to confluent lesions and massive compact tumor masses

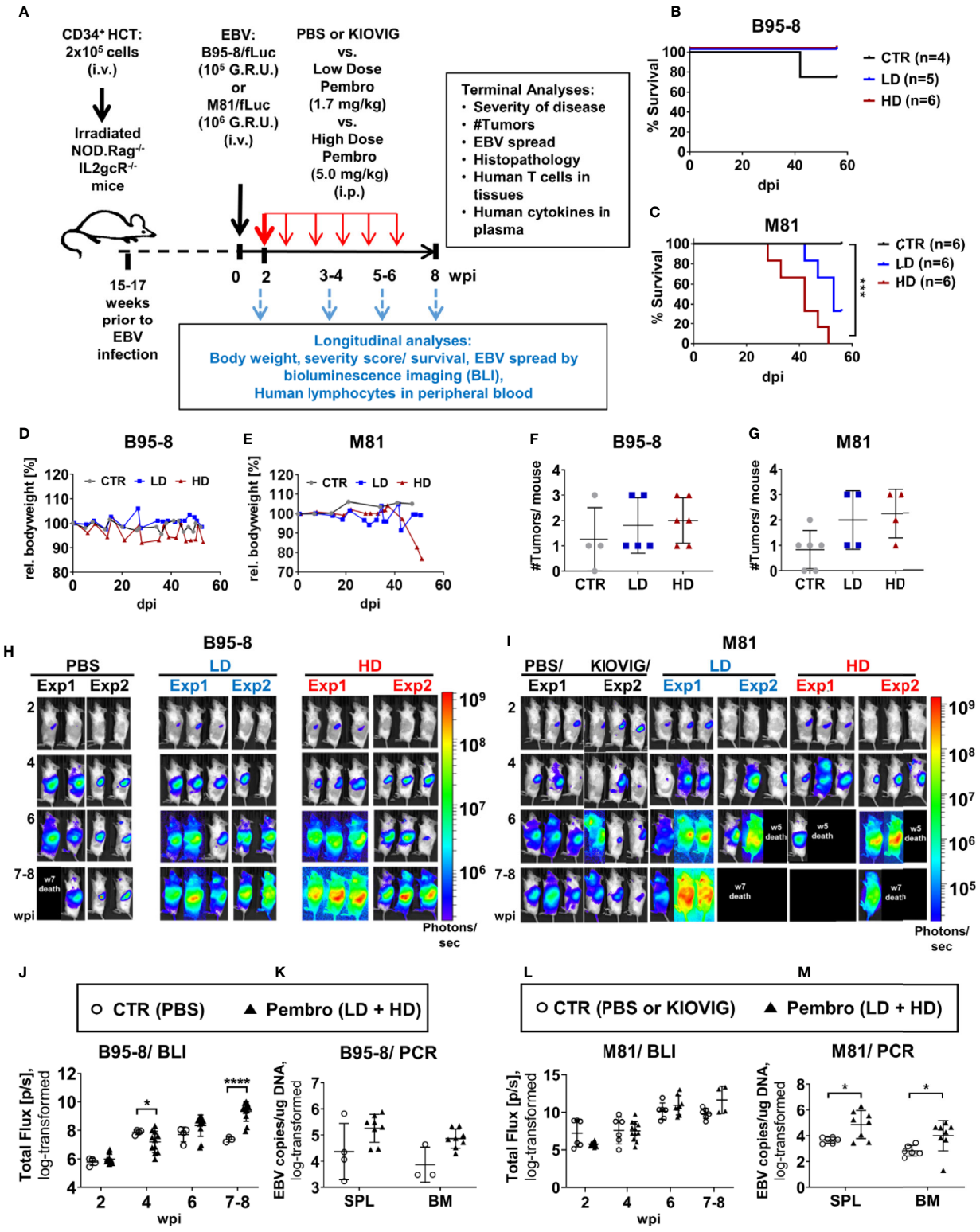

FIGURE 1 | Continued

FIGURE 1 | Humanized mice infected with EBV/fLuc and treated with pembrolizumab show high mortality associated with increased EBV spread and tumor development. **(A)** Scheme of the experiments. 2×10^5 human $CD34^+$ cord blood (CB) purified hematopoietic stem cells (HSCs) were used for hematopoietic stem cell transplantation (HCT) of sub-lethally irradiated NRG mice. Fifteen to 17 weeks after HCT, the long-term human immune reconstitution in blood ($huCD45^+$) was confirmed. At this point, mice were infected i.v., with the preferentially latent EBV B95-8/fLuc strain (10^5 GRU) or with the lytic EBV M81/fLuc strain (10^6 GRU). Two independent experiments using HSCs from two different CB donors were performed for each EBV model. At 2 weeks post-infections (wpi), bioluminescence imaging (BLI) analyses were performed to determine the baseline of EBV infection level and to randomize the mice among three cohorts: (i) injected i.p. with phosphate-buffered saline (PBS, corresponding to the control group, CTR), (ii) injected i.p. a low dose (LD: First administration 3.33 mg/kg at 2 wpi; 1.7 mg/kg every other week applied six times), or with (iii) a high dose (HD: First administration 10 mg/kg at 2 wpi; 5 mg/kg every other week applied six times). Mice were monitored for disease severity every 2–3 days and body weights were measured weekly. Scores of disease severity or loss of 20% of body weight were used as termination criteria. Optical imaging analyses and analyses of human immune reconstitution in peripheral blood collections were performed longitudinally (2, 4, 6, 8 wpi). The experimental endpoint was eight weeks post-infections. The following data was acquired for terminal analyses: % survival, occurrence of weight loss, occurrence of tumors, EBV load, histopathology, characterization of T cells in blood and tissues, human cytokine profile in plasma. **(B, C)** Survival curves for humanized mice infected with the B95-8/fLuc strain **(B)** or with the M81/fLuc strain **(C)**. A log-rank test (Mantel-Cox) was applied to evaluate the differences in survival. Cohorts: CTR (gray line), LD (blue line); HD (red line). **(D, E)** Measurements of body weight relative to the baseline weights on the day of EBV infection. Mice infected with B95-8/fLuc strain **(D)** or M81/fLuc strain **(E)**. Cohorts: CTR (grea line), LD (blue line); HD (red line). **(F, G)** Numbers of macroscopically detectable tumors in mice infected with B95-8/fLuc **(F)** or with M81/fLuc **(G)**. Cohorts: CTR (gray dots), LD (blue dots); HD (red dots). **(H, I)** BLI pictures generated sequentially from week 2 to 8 after EBV infection performed in duplicate experiments for each EBV model and treatment. Pictures were taken of left body side of mice infected with B95-8/fLuc **(H)** or with M81/fLuc **(I)**. Bioluminescence signal intensities (photons/sec) are depicted by the color bars on the right side. Black boxes depict dead mice. **(J–L)** Quantification of EBV spread by BLI for the B95-8/fLuc **(J)** or M81/fLuc **(L)** strain. *Total Flux* corresponds to the radiance (photons/sec) in each pixel summed over the regions of interest (ROI) area containing the whole left side of the body. The dots represent quantifications at 2, 4, 6, 8 wpi for each mouse in CTR (open circles) or in pembrolizumab treatment cohorts (filled triangles, LD and HD were combined). **(K–M)** Quantification of EBV spread by RT-qPCR. EBV copies per µg DNA were quantified in spleen (SPL) and bone marrow (BM) of mice infected with B95-8/fLuc **(K)** or with M81/fLuc **(M)**. The dots represent quantifications for each mouse in CTR (open circles, PBS and KIOVIG controls combined) or in pembrolizumab treatment cohort (filled triangles, LD and HD were combined). Results of measurements were log-transformed and statistical analyses were performed using unpaired t test with Welch's correction. Standard deviation is indicated. Statistical significances are indicated with $^{*}P < 0.05$, $^{****}P < 0.0001$.

TABLE 2 | Summary of EBV spread (by BLI and PCR) and immunologic effects (by FACS, cytokine measurement of plasma and histopathology analyses by multiplex immunohistochemistry) observed after PD-1 blockade.

A) B95-8	**Endpoint wpi**	**Control**			**Pembrolizumab**			
Analyses		**N =**	**Mean**	**ST Dev**	**N =**	**Mean**	**ST Dev**	**P values**
BLI p/s*	8	3	7.35	0.17	11	9.32	0.68	***<0.0001***
PCR BM copy/µg DNA*	8	3	3.87	0.67	8	4.87	0.36	0.1110
CD4-PD1 MFI PBL*	8	3	4.38	0.14	11	3.36	0.24	***0.0001***
CD4-PD1 MFI SPL*	8	3	4.94	0.24	11	3.50	0.29	***0.0013***
% Treg inCD4. SPL	8	3	2.80	1.80	11	6.50	5.70	*0.0876*
IL-17A pg/ml	8	3	1.63	0.93	10	8.87	9.81	***0.0490***
IL-10 pg/ml	8	3	416.73	681.52	10	825.43	718.53	0.2867
IL-33 pg/ml	8	3	3.90	0.48	10	10.57	17.06	0.1608
IFN-α pg/ml	8	3	3.07	3.15	10	11.39	12.09	*0.0769*
IL-12 pg/ml	8	3	10.29	16.37	10	3.56	2.79	0.5734
IL-1β pg/ml	8	3	1.89	0.52	10	2.89	2.59	0.8357
Treg near CD4 LI	8	3	0.02	0.023	11	0.35	0.40	***0.0193***
Treg near CD8 LI	8	3	0.001	0.02	11	0.25	0.30	***0.0251***
B) M81	**Endpoint wpi**	**Control**			**Pembrolizumab**			
Analyses		**N =**	**Mean**	**ST Dev**	**N =**	**Mean**	**ST Dev**	**P values**
BLI p/s*	8	6	9.84	0.68	4	11.65	1.82	0.1387
PCR BM copy/µg DNA*	5, 7, 8	6	2.83	0.41	8	4.00	1.18	***0.0283***
CD4-PD1 MFI PBL*	7, 8	6	4.84	0.08	5	3.96	0.41	***0.0074***
CD4-PD1 MFI SPL*	7, 8	6	5.15	0.06	5	3.99	0.59	***0.0112***
% Treg in CD4, SPL	7, 8	6	2.80	0.60	5	5.70	7.60	***0.0407***
IL-17A pg/ml	7, 8	6	3.71	1.73	5	4.07	4.04	0.6623
IL-10 pg/ml	7, 8	6	18.23	10.03	5	9189.12	11248.73	***0.0173***
IL-33 pg/ml	7, 8	6	3.35	1.03	5	51.80	70.27	***0.0087***
IFN-α pg/ml	7, 8	6	0.97	0.20	5	25.13	22.94	***0.0043***
IL-12 pg/ml	7, 8	6	1.51	0.51	5	59.21	105.47	***0.0043***
IL-1β pg/ml	7, 8	6	1.72	0.46	5	3.84	2.12	***0.0498***

(A) B95-8 infection. (B) M81 infection. The statistical methods used for analyses are shown in the ***Supplementary Tables****. Significant differences between control and pembrolizumab-treated mice are shown in bold and italics. The original values for PD-1 MFI (*) were log-transformed before statistical tests. The reduced detections of PD-1 on $CD4^+$ T cells were highly significant for both models (p values are underlined). The frequencies of $CD4^+$ Tregs in spleens were increased for both models. The proximity of Tregs to T cells of liver for the B95-8 model was analyzed by multiplex immunohistochemistry analyses. The cytokine responses were variable for the two models.*

(**Figures 2C–F**, right panels, see areas marked with asterisks). In LI, large coherent tumor formations were almost exclusively observed in pembrolizumab treatment groups, while in control animals tumors tended to be smaller and only rarely confluent. In ICI-treated mice, large, partially necrotic tumor masses in SPL (**Figures 2C–E**, left panel) and LI (**Figures 2C–E**, right panels) were consistently present. The neoplastic partially CD30$^+$ and CD20$^+$ cells were associated with a dense CD3$^+$ T-lymphocytic infiltrate (**Figures 2E, F**). Immune subtyping revealed that this T cell infiltrate was mainly composed of CD8$^+$ cytotoxic T lymphocytes (CTLs) and CD4$^+$ T helper cells (Th) (**Figures 2G, H**). Brisk T cell infiltrates were predominantly observed in small, presumably early-stage perivascular lesions (**Figures 2C–H**, arrows), where fewer neoplastic cells expressing EBER were present in relation to the overall amount of cells, and at the margins of coherent tumor masses. In contrast, the center of larger tumor formations (**Figures**

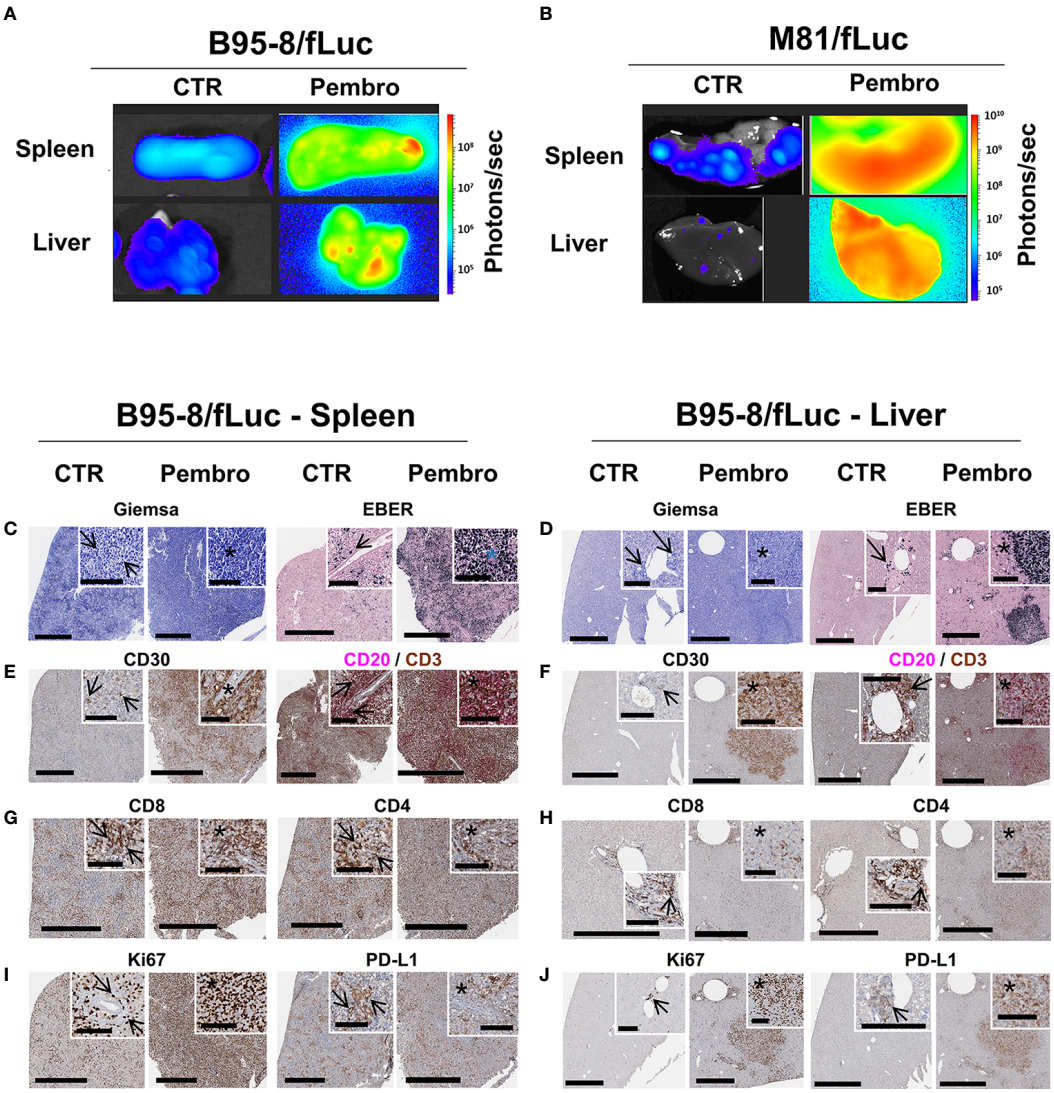

FIGURE 2 | Analyses of explanted spleen and liver showed increased EBV/fLuc spread, inflammation, and neoplasia after pembrolizumab treatment. **(A, B)** Bioluminescence imaging analyses performed with explanted spleen and liver from representative B95-8/fLuc **(A)** or from representative M81/fLuc-infected mice **(B)**. Tissues from representative non-treated control (CTR) mice are shown. Bioluminescence signal intensities (photons/sec) are depicted by the color bars on the right side. **(C–J)** Histopathological analyses of spleen **(C–I)** and liver **(D–J)** of representative mice infected with EBV/B95-8/fLuc and non-treated (CTR, left side) or treated with pembrolizumab (Pembro, right side). **(C, D)** Giemsa, EBER: In both organs, the perivascular spread of EBV/B95-8/fLuc infected neoplastic cells is observed. More disseminated infection and larger tumors were observed in pembrolizumab-treated than in control mice. Stars indicate perivascular angiocentric neoplastic growth. **(E, F)** CD30, CD20/CD3 duplex: The CD30- and CD20-expressing tumors and perivascular infiltrates resemble human B-cell neoplasia, corresponding to diffuse large B-cell lymphoma, and are surrounded or invaded by variable amounts of tumor-infiltrating CD3$^+$ lymphocytes (TILs). **(G, H)** CD8, CD4: Early perivascular lesions display a largely balanced CD4/CD8 ratio. In the center of tumor bulk mass, the balance is shifted towards CD8$^+$ cytotoxic T lymphocytes (CTLs). **(I, J)** Ki67, PD-L1: proliferating cells observed at a higher density in tumor areas, which also correlates with PD-L1 expression. Digital whole slides scanned at 40×; black bars correspond to 600 µm (full image) and 100 µm (inserts).

2C–H, see areas marked with asterisks) showed relatively fewer T cells, particularly fewer CD4+ Th cells, if compared to tumor margins and smaller perivascular tumor cell groups (**Figures 2G, H**). The tumor areas corresponded to proliferative activity: Ki67+ cells with morphological features indicative of neoplastic lymphoproliferation were more prominent in tissues of ICI-treated mice and tumor formations were associated with higher expression of PD-L1 (**Figures 2I, J**). Altogether, these descriptive analyses indicated that infiltrating T lymphocytes were more pronounced, and potentially more active, in early stages of tumor invasion and at the invasive edges, but less prominent in the center of the large tumor masses observed in ICI-treated mice, a pattern resembling "immune excluded" tumors (36).

PD-1 Blockade Promotes Epstein–Barr Virus Spread into the Central Nervous System

Brains explanted of ICI-treated mice showed detectable BLI signals, but this was not the case for brains of control mice (**Figures 3A, B**). Histopathology confirmed presence of EBER+ cells in brains of infected mice. In two cases of the ICI-treated group, both from the B95-8 model, three distinctive patterns of

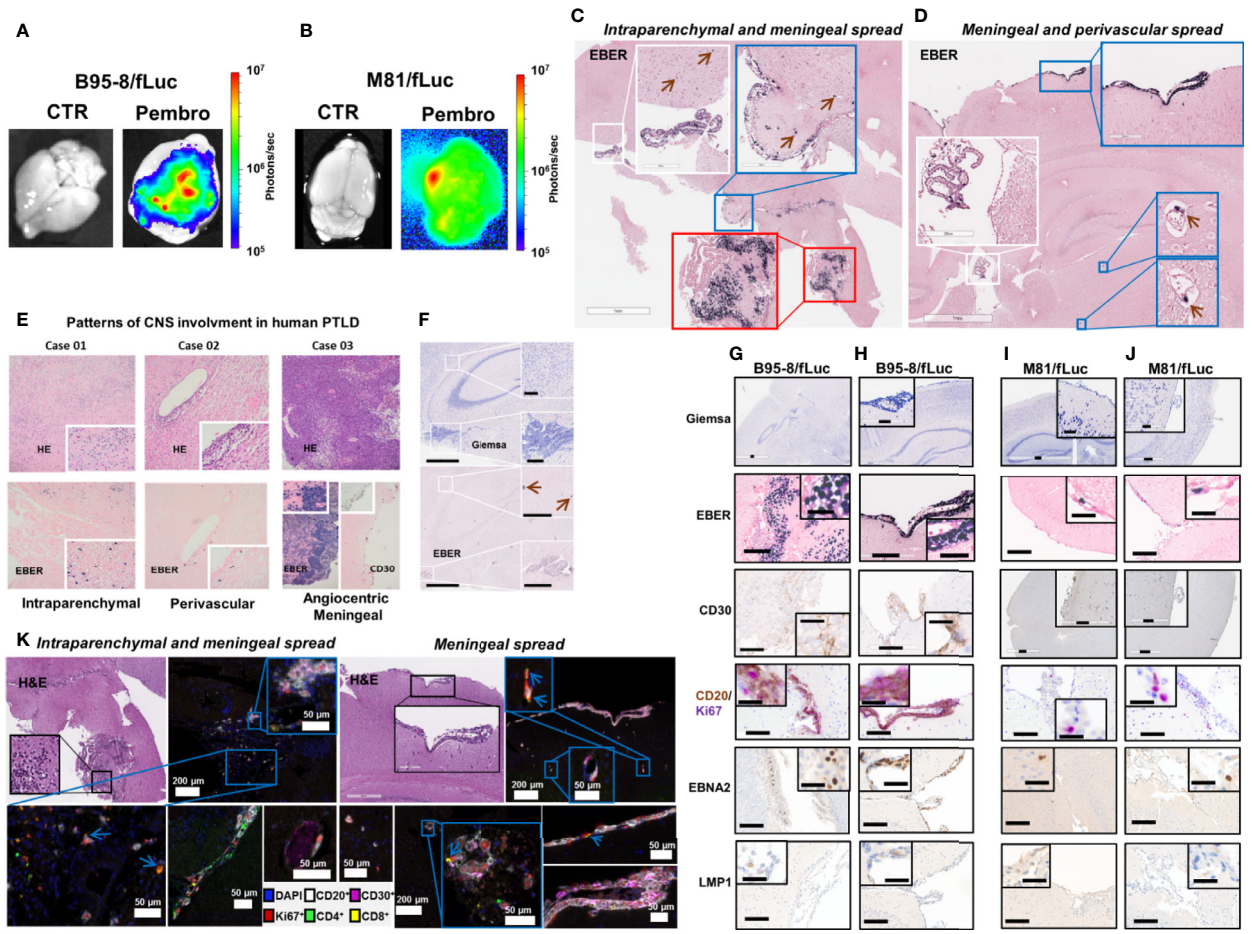

FIGURE 3 | Pembrolizumab treatment is associated with spread of EBV/fLuc to the central nervous system. **(A, B)** Bioluminescence images showing representative EBV signal patterns in brains from mice infected with B95-8/fLuc **(A)** or with M81/fLuc **(B)** and treated with pembrolizumab (Pembro; most severely affected animals shown in each group), compared with non-treated controls (CTR). The bioluminescence signal intensities (photons/sec) are depicted by the color bar on the right side. **(C, D)** *In-situ* hybridization for detection of Epstein-Barr encoded RNA (EBER)-1 in brains of mice infected with B95-8/fLuc and treated with pembrolizumab. Observed patterns include invasion of tumor cells into the plexus choroideus (white inserts), as well as into periventricular brain parenchyma (red insert) and meningeal tumor spread (blue inserts). The green arrows indicate single tumor cells associated with blood vessels. **(E)** Comparison with three representative examples of human EBV-positive monomorphic transplantation-associated B-PTLD, with clinical manifestation as primary CNS lymphoma (PCNSL) revealed similar patterns of intraparenchymal (Case 01), perivascular (Case 02), and massive angiocentric/diffuse growth with meningeal spread (Case 03). **(F)** Control animals did not show any involvement of the plexus choroideus or periventricular brain areas. Only single EBER-positive cells in intravascular localization were detected (green arrows). **(G–J)** The immunophenotype of the neoplastic cells invading the brain of ICI-treated mice corresponded to the phenotype of the peripheral neoplastic population with variable CD30+, and constant CD20+ expression. The majority of neoplastic cells expressed EBNA2 but not LMP1 and were actively proliferating (CD20+/Ki67+). **(G–H)** and **(I–J)** Analyses of duplicate mice infected with B95-8/fLuc and M81/fLuc and treated with pembrolizumab, respectively. **(K)** Multiplexed image of two mouse brains from B95-8/fLuc infection model after pembrolizumab treatment confirmed co-localization of neoplastic cells (CD20+, white; CD30+, magenta) and T lymphocytes (CD8+ yellow; CD4+, green). Lymphocytes were actively proliferating (Ki67+, red), particularly CD8 (blue arrows). DAPI (blue) is used to mark cell nucleus. Bars correspond to 200 µm (full image) and 50 µm (inserts).

local CNS manifestations of EBER$^+$ LPD were observed with blast-like morphological appearance (**Figures 3C, D**): (i) Intra- or perivascular spread: single tumor cells were found within the lumen of small, mostly capillary blood vessels (**Figure 3C**, blue and white inserts, brown arrows) and close to the vessel walls in small veins (**Figure 3D**, blue inserts, brown arrows), resembling patterns observed in brain manifestations of human PTLD (**Figure 3E**, Case 01 and 02); (ii) Meningeal spread: coherent sheets of tumor cells forming a meningeal infiltration at the brain surface (**Figures 3C, D**) and resembling neoplastic meningitis in corresponding human diseases, e.g., EBV$^+$ PTLD (**Figure 3E**, Case 03); (iii) Diffuse brain infiltration: diffusely infiltrating tumor cells formed a partially perivascular tumor mass, mixed with pre-existing brain tissue (**Figure 3C**, red insert), corresponding to the characteristic patterns of human (primary) CNS lymphoma and/or monomorphic PTLD (**Figure 3E**, Case 01 and 03). In addition to these patterns, there was also diffuse involvement of the choroid plexus in treated mice. In contrast, the control animals showed only occasionally single EBER$^+$ cells associated with blood vessels but no meningeal or intraparenchymal involvement and no positive cells in the choroid plexus (**Figure 3F**). The morphological phenotype of the EBER$^+$ tumor cells corresponded to the extracerebral manifestations (**Figures 3G–J**, top panels), as well as the immune phenotype with inconsistent CD30 expression, CD20 positivity, and high Ki67$^+$ proliferative activity (**Figures 3G–J**, middle panels). EBNA2 and LMP1 staining indicated latently-infected EBV$^+$ cell population (**Figures 3G–J** lower panels). In-depth analysis of the tumor spread to the CNS by multiplex-immunohistochemistry confirmed the B cell lineage of the blast-like tumor cells, the high proliferative activity, the partial expression of CD30, and a scarce bystanding infiltration with some CD4$^+$ and CD8$^+$ lymphocytes, the latter frequently co-expressing the proliferation marker Ki67 (**Figure 3K**).

PD-1 Blockade Results in Lower Frequencies of Circulating Cytotoxic T Lymphocytes and Th Cells and Reduced Detection of PD-1 on T Cells

Longitudinal analyses of blood samples were performed to monitor the frequencies of circulating human T cells (see **Figure S1A** for the flow cytometry gating strategy). The frequencies of huCD45$^+$ hematopoietic cells at the time of EBV infections were comparable for both models (B95-8/fLuc: mean 26.4%; M81/fLuc: mean 33.7%). Relative to controls, the frequency of blood huCD45$^+$ cells was significantly reduced for mice infected with M81/fLuc and treated with ICI (M81 model 7–8 wpi: CTR *vs* Pembro, $P = 0.0017$; **Figures S2A, B**; see **Tables S4**, **5** for descriptive data). Consistent with our previous observations after EBV/B95-8 infection (24), significant increase in CD3$^+$ frequencies in blood (**Figures 4A, B**, **Tables S4**, **5**) and significant decrease in frequencies of CD19$^+$ B cells were observed from 4 to 8 wpi (**Figures S2C, D**, **Tables S4**, **5**). ICI treated mice at 6–8 wpi, however, showed lower frequencies of CD3$^+$, CD8$^+$, and CD4$^+$ T cells compared with controls (**Figures 4A–D, G, H**; **Tables S4**, **5**). We have observed that T cells pre-treated with pembrolizumab for 30 min *in vitro*, washed and then stained with the fluorochrome-labeled monoclonal anti-PD-1 antibody (clone EH12.2H7) showed a drastic reduction on the detectable PD-1 (**Figure S2E**). The most likely explanation is that the epitope is bound by pembrolizumab and this blocks the antibody used for immune staining of T cells, resulting in epitope "masking." This "masking" effect was confirmed by measurement of the mean fluorescence intensity (MFI) of PD-1 analyses of T cells from 3 to 4 wpi, *i.e.* 2 weeks after initiation of therapy (**Figures 4E, F, I, J**; **Figure S1A**; **Table 2**, **Tables S4**, **5**). For both models, this PD-1 masking effect was consistently more pronounced for CD4$^+$ (CTR *vs* Pembro, $P < 0.01$ to $P < 0.0001$) compared to CD8$^+$ T cells.

PD-1 Blockade Results in Increased Levels of Several Human Cytokines in Plasma of Epstein–Barr Virus Infected Mice

Plasma was collected at the endpoint for analyses of human cytokines in the circulation. The levels of both pro-inflammatory (IL-6, IL-8, IFN-α, IFN-γ, MCP-1, and TNF-α) and immune-suppressive (IL-10) cytokines were elevated in ICI-treated mice (**Figures 4K, L**, **Figures S2F, G**, **Table 2**, **Table S6**). Treatment of EBV-M81/fLuc-infected mice with KIOVIG did not affect the immune reconstitution profile nor cytokine levels and, therefore, these immune-modulations were only seen in mice after EBV infection and PD-1 blockade (**Figures S2H–J**). Administration of pembrolizumab alone, in absence of EBV did not have a comparable effect with either treated or untreated groups (**Figures S2H–J**).

Biomarkers Identified in Blood and Plasma After Immune Checkpoint Inhibition Treatment

The datasets of both EBV-models were merged for the identification of concordant biomarkers defining a response to pembrolizumab treatment (**Figure 4M**). Overall, in comparison with control mice, ICI-treated mice showed significant: (i) lower frequencies of CD3$^+$/CD45$^+$ and CD4$^+$/CD45$^+$ T cells, (ii) lower MFI of PD-1 detectable on CD4$^+$ cells; (iii) elevated levels of IL-10 and IFN-α. In summary, PD-1 blockade applied during an active EBV infection resulted in lower detection of PD-1^{high} circulating lymphocytes (particularly for CD4$^+$ T cells) and in a profound modulation of the cytokine levels in plasma.

PD-1 Blockade Promotes a Quantitative Loss of CD4$^+$ T Cells in Lymphatic Tissues

The immune composition of total human T cell counts in lymphatic tissues (SPL, LN, BM, and Thy) was performed to characterize the immunologic effects of ICI on CD8$^+$ and CD4$^+$ T cells in further detail (**Figure 5**, see **Tables S7**, **8** for descriptive data). For the B95-8/fLuc model, ICI treatment promoted a modest expansion of the CD8$^+$ T cell compartment in lymphatic tissues (**Figure 5A**), whereas for the M81/fLuc model a significant reduction was seen (**Figure 5B**,

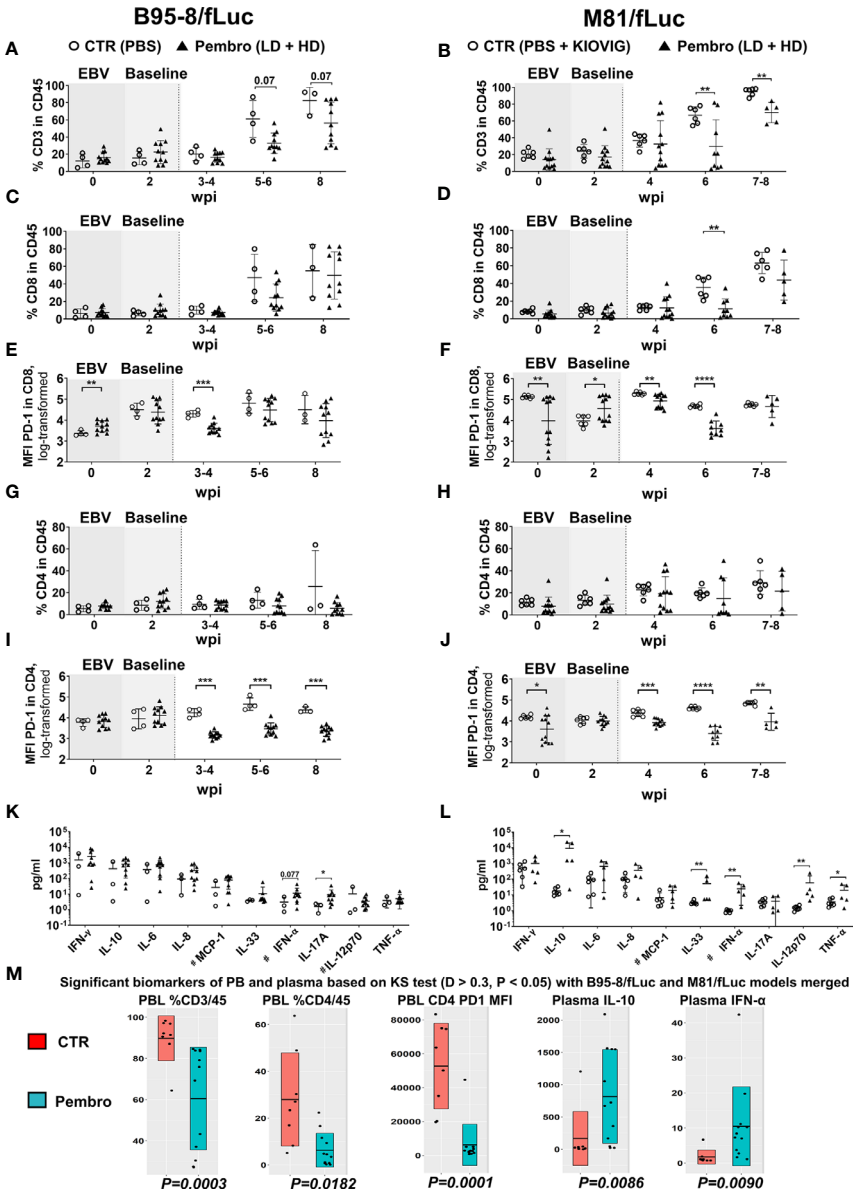

FIGURE 4 | Reduced frequencies of human T lymphocytes in peripheral blood and increased concentrations of human cytokines in plasma after PD-1 blockade during active EBV infections. Peripheral blood was collected on the day prior to EBV infection (time-point 0) and 2 weeks post-infections (wpi), as baseline values for randomization (shaded graphs). Non-treated control mice (CTR, open circles) and pembrolizumab treated cohorts are shown (filled triangles; low-dose and high-dose treatments were merged for the analyses, each dot represents a mouse analyzed at the corresponding time point). After initiation of pembrolizumab treatment, peripheral blood was collected at 3–4, 5–6, and 8 wpi. The different EBV infection models (B95-8/fLuc; left panels and M81/fLuc; right panels) were analyzed separately regarding lymphocytes and cytokines and then the data was merged for power analyses and identification of markers associated with response. **(A–J)** Flow cytometry analyses of peripheral blood lymphocytes. **(A, B)** Frequencies (%) of human $CD45^+/CD3^+$ lymphocytes were reduced after pembrolizumab treatment. **(C, D)** Frequencies (%) of human $CD45^+/CD8^+$ lymphocytes were reduced after pembrolizumab treatment. **(E, F)** Mean fluorescence intensities (MFI) of PD-1 detected on the surface of $CD8^+$ T cells were reduced after pembrolizumab treatment. **(G, H)** Frequencies (%) of human $CD45^+/CD4^+$ lymphocytes were reduced after pembrolizumab treatment. **(I, J)** MFI of PD-1 detected on the surface of $CD4^+$ T cells were significantly reduced after pembrolizumab treatment. Statistical analyses for flow cytometry data was performed using unpaired t test with Welch's correction. Standard deviation is indicated. *$P < 0.05$, **$P < 0.01$, ***$P < 0.001$, ****$P < 0.0001$. **(K, L)** Concentration human cytokines (pg/ml) at 8 wpi showing elevation for several cytokines in plasma of mice infected B95-8/fLuc **(K)** or M81/fLuc **(L)** treated with pembrolizumab. Mann-Whitney t test was used to compare the control and treatment groups. Standard deviation is indicated. *$P < 0.05$, **$P < 0.01$. # indicates parameters with some values being beyond the lower limit of detection (LOD), LOD was used for these samples to analyze the differences. **(M)** Global analysis for power analyses and identification of T cell and cytokine patterns at 8 wpi. The datasets from the B95-8/fLuc and M81/fLuc infection models were merged. Kolmogorov-Smirnov-Test (KS test; $D > 0.3$, $P < 0.05$) is depicted for flow cytometry and cytokine datasets showing markers with significant difference between control (CTR, red) and pembrolizumab treatment (Pembro, blue). P-values determined for each biomarker are indicated below the box plots. The top biomarkers associated with pembrolizumab treatment were: Reduced %CD3/CD45 ($P = 0.0003$), reduced %CD4/CD45 ($P = 0.0182$), reduced MFI of PD-1 expression on $CD4^+$ cells ($P = 0.0001$), increased IL-10 ($P = 0.0086$) and IFN-α ($P = 0.0090$) levels in plasma.

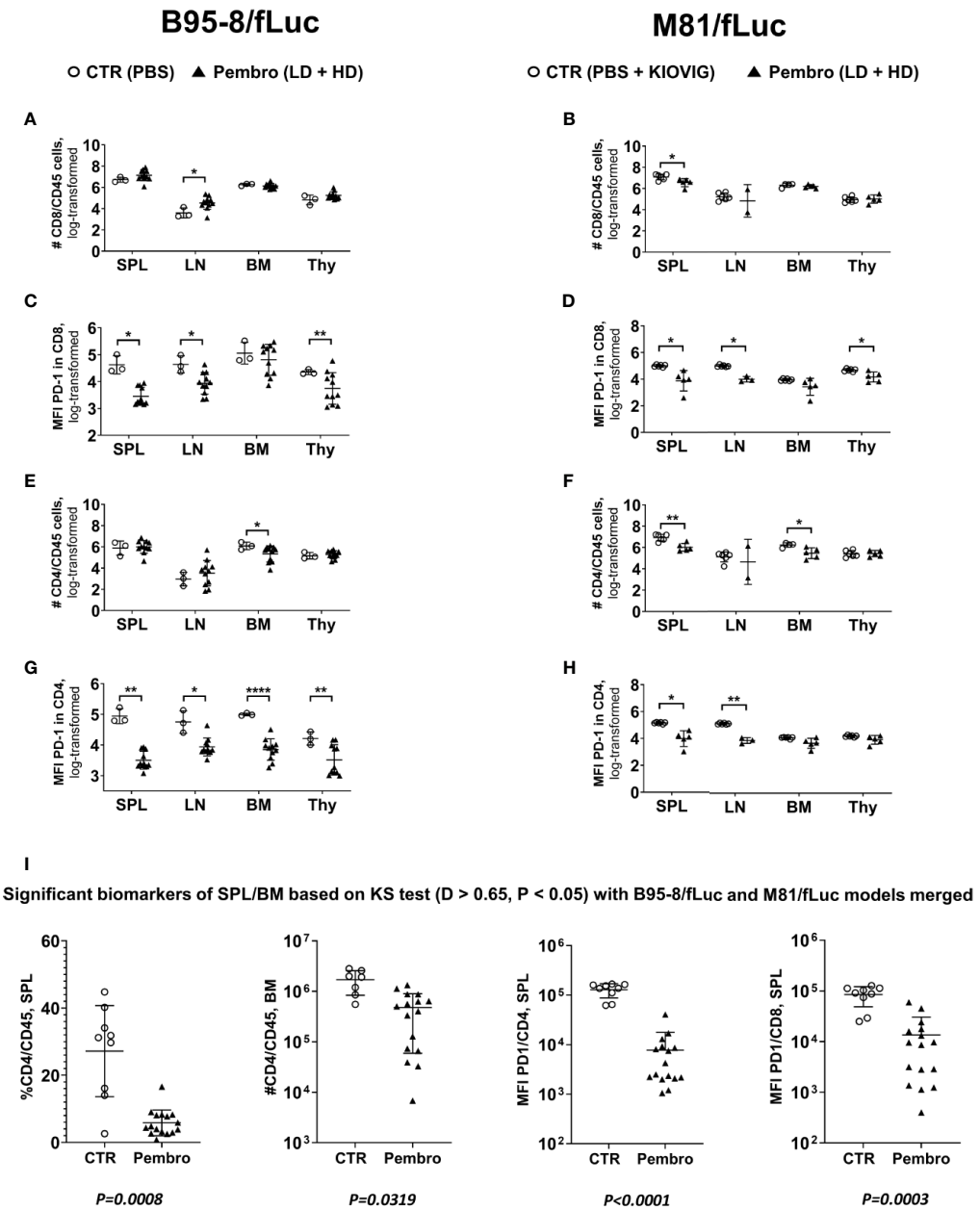

FIGURE 5 | The absolute numbers of human T lymphocytes in lymphatic tissues increased for the B95-8/fLuc model and decreased for the M81/fLuc model after PD-1 blockade. The absolute numbers of viable lymphocytes recovered from spleen (SPL), lymph nodes (LN), bone marrow (BM), and thymus (Thy) were counted and, after flow cytometry analyses, the absolute numbers of each lineage was calculated. Non-treated control mice (CTR, open circles) and pembrolizumab-treated cohorts are shown (filled triangles; low-dose and high-dose treatments were merged for the analyses; each dot represents a mouse analyzed at the terminal time point). Only mice surviving until the terminal analyses at 8 wpi were included in the terminal flow cytometry analyses. **(A, B, E, F)**. Quantified total lymphocyte numbers (# cells) calculated for $CD8^+$ T cells **(A, B)** and $CD4^+$ T cells **(E, F)** for each organ. Note the increased numbers of lymphocytes for the B95-8/fLuc models and the decreased numbers for the M81/fLuc models for the pembrolizumab-treated mice. **(C, D, G, H)** Mean fluorescence intensity (MFI) for PD-1 detection for $CD8^+$ T cells **(C, D)** and $CD4^+$ T cells **(G, H)** showing overall significantly reduced PD-1 detection after pembrolizumab treatment for both models. Unpaired t test with Welch's correction was used to compare treatment groups. *$P < 0.05$, **$P < 0.01$, ****$P < 0.0001$. Standard deviation is indicated. **(I)** Global power analyses and biomarker identification. The flow cytometry datasets of spleen of B95-8/fLuc and M81/fLuc models were merged. Kolmogorov-Smirnov Test (KS test; D > 0.65, $P < 0.05$) is depicted. The biomarkers identified with significant differences between control (CTR, open circles) and pembrolizumab treatment (Pembro, filled triangles) were: Lower SPL % CD4/CD45 ($P = 0.0008$); lower BM #CD4/CD45 ($P = 0.0319$); lower MFI for PD-1 in $CD4^+$ cells ($P < 0.0001$); lower MFI for PD-1 in $CD8^+$ cells ($P = 0.0003$). P-values determined for each marker are indicated below the graphs.

P < 0.05). The CD8$^+$ T cells from ICI-treated mice were PD-1^{Low}, recapitulating the epitope masking effect (**Figures 5C, D**). Numbers of CD4$^+$ T cells were reduced compared to control in BM of ICI-treated mice for both EBV models (*P < 0.05*), as well as in the SPL of M81 model (*P < 0.01*) (**Figures 5E, F**). For the mice surviving until the endpoint analyses, PD-1 masking of CD4$^+$ T cells was more pronounced in lymphatic tissues of mice infected with B95-8 than infected with M81 (*P < 0.05 to P < 0.0001*, **Figures 5G, H**; **Tables S7**, **8**). Overall, the MFIs measured for PD-1 in CD4$^+$ T cells were significantly reduced in ICI-treated mice compared to controls, although this varied for different tissues (*P < 0.05 to P < 0.0001*, **Figures 5G, H**; **Tables S7**, **8**).

Biomarkers Identified in Lymphatic Tissues After Immune Checkpoint Inhibition Treatment

The datasets of tissue analyses of both EBV-models were merged for identification of biomarkers of response to pembrolizumab, showing: (i) lower frequencies and lower absolute numbers of CD4$^+$/CD45$^+$ in SPL (*P = 0.0008*) and BM (*P = 0.0319*) and (ii) lower MFI of PD-1 detection on CD4$^+$ cells (*P < 0.0001*) and CD8$^+$ T cells (*P = 0.0003*) (**Figure 5I**). In summary, pembrolizumab treatment after EBV infection consistently lowered the numbers of PD-1$^+$CD4$^+$ T cells in lymphatic tissues.

PD-1 Blockade Promotes T Cell Exhaustion and High Frequencies of Regulatory T Cells in Spleen

Splenocytes were analyzed to identify markers of immune exhaustion. TIM-3 analyses were included because TIM-3 cooperates with PD-1 in T cell dysfunction in chronic viral infections and PD-1$^+$/TIM-3$^+$ CD8$^+$ T cells express high levels of IL-10 (37). For both CD8$^+$ and CD4$^+$ T cell sub-populations, treated mice showed higher frequencies of TIM-3$^+$ cells (**Figures 6A–D**; **Tables S7**, **8**; see the gating strategy in **Figure S1B**). Higher frequencies of cells expressing TIM-3 were observed for PD-1^{high} cells, indicating that T cells evading or not masked with pembrolizumab were more exhausted. In another panel, LAG-3 was analyzed in conjunction with the activation marker CD69 (**Figures 6E–H**; **Tables S7**, **8**, see gating strategy in **Figure S1C**). LAG-3 is another checkpoint receptor that defines a potent regulatory T cell subset that occurs more frequently in cancer patients and is expanded at tumor sites (38). The frequencies of CD8$^+$ and CD4$^+$ T cells positive for both CD69 and LAG-3 were moderately increased for treated mice infected with B95-8/fLuc, while significantly increased for M81/fLuc infected and ICI-treated mice (**Figures 6E–H**). Altogether, these results indicated that the PD-1 blockade after EBV infection magnified T cell exhaustion. As complementary analyses, the presence of CD25$^+$/FoxP3$^+$/CD4$^+$ regulatory T cells (Tregs) in spleen was determined. A modest increase of Tregs proportion in CD4 cells was observed for the B95-8/fLuc-infected treated mice relative to controls (**Figures 6I, J**, **Tables S7**), while the Tregs were significantly amplified in mice infected with M81/fLuc after ICI treatment (**Figures 6K, L**, **Table S8**, for gating strategy see **Figure S1D**). Therefore, both exhaustion of CD4$^+$ and CD8$^+$ T cells and higher frequencies of Tregs were promoted by PD-1 blockade after EBV-infection, and this signature was even more noticeable for the M81/fLuc lytic model.

PD-1 Blockade Is Associated With Increased Densities of CD4$^+$/FoxP3$^+$ T Cells Within Tumors

The tumor immune microenvironment was assessed using a multiplexed immunohistochemistry approach. The cell densities and distance metrics within the tumor or parenchyma areas using tissues obtained from B95-8/fLuc-infected mice were analyzed (**Figures 7A–C**, representative example of immune cell phenotyping in a liver tumor and adjacent parenchyma by co-staining for DAPI, CD20, CD8, CD4, the proliferation marker Ki67, and the Treg marker FoxP3; for corresponding analyses in spleen tissue see **Figure S3A**). The density of proliferating CD4$^+$ T cells showed an overall modest reduction for ICI-treated mice compared with controls, however, this did not occur for CD8$^+$ T cells (**Figures 7D, E**, liver; **Figures S3C, D**, spleen; **Table S9**). Further, higher densities of CD4$^+$/FoxP3$^+$ T cells, were observed within the tumor area (**Figure 7F**, liver; **Figure S3E**, spleen). CD8$^+$/FoxP3$^+$ T cells, another subset of immunosuppressive cells, were also present in liver parenchyma of ICI-treated, but not in the control group (**Figure 7G**, liver; **Figure S3F**, spleen). The analysis of distance metrics between different T cell subtypes in liver tissues (**Figure 7C**, liver; for spleen see **Figure S3B**) showed that the average presence of CD4$^+$/FoxP3$^+$ Tregs in up to 200 μm radius around any single FoxP3$^-$ T cell (both CD4$^+$/FoxP3$^-$ or CD8$^+$/FoxP3$^-$) was higher in the pembrolizumab-treated group than in controls (*P < 0.05*, **Figures 7H, I**, liver; **Table 2**, **Table S9**), suggesting that immune regulatory T cells with CD4$^+$/FoxP3$^+$ and CD8$^+$/FoxP3$^+$ phenotypes were enriched. This was observed in the immediate microenvironment of T-effector and helper cells of ICI-treated mice with more advanced tumors indicating a higher chance of direct cell-to-cell interactions, potentially associated with immune suppression and aggravation of EBV spread upon PD-1 blockade.

DISCUSSION

Several human malignancies are initiated by viral oncogenesis, such as EBV, human papillomavirus (HPV), hepatitis B virus (HBV), and hepatitis C virus (HCV). Currently, there are several ongoing clinical trials of ICIs to combat virus-associated cancers (39). For example, pembrolizumab is currently being tested for the treatment of EBV$^+$ nasopharyngeal carcinoma (NPC), EBV$^+$ Non-Hodgkin's disease, EBV$^+$ NK/T cell lymphoma, EBV$^+$ gastric cancer, HPV$^+$ cervical cancer, and HPV$^+$ head and neck squamous cell carcinoma (39). One potential risk to be evaluated is that viral immune evasion mechanisms may develop to counteract the human immune responses affecting the mode of action of ICI. On the other hand, a substantial amount of cancer patients treated with ICI occasionally show HPD, but the etiological reasons (such as for example action of underlying infections) are not yet fully understood (40–42). To avoid HPD or to mitigate its risks, the causes and early predictors associated

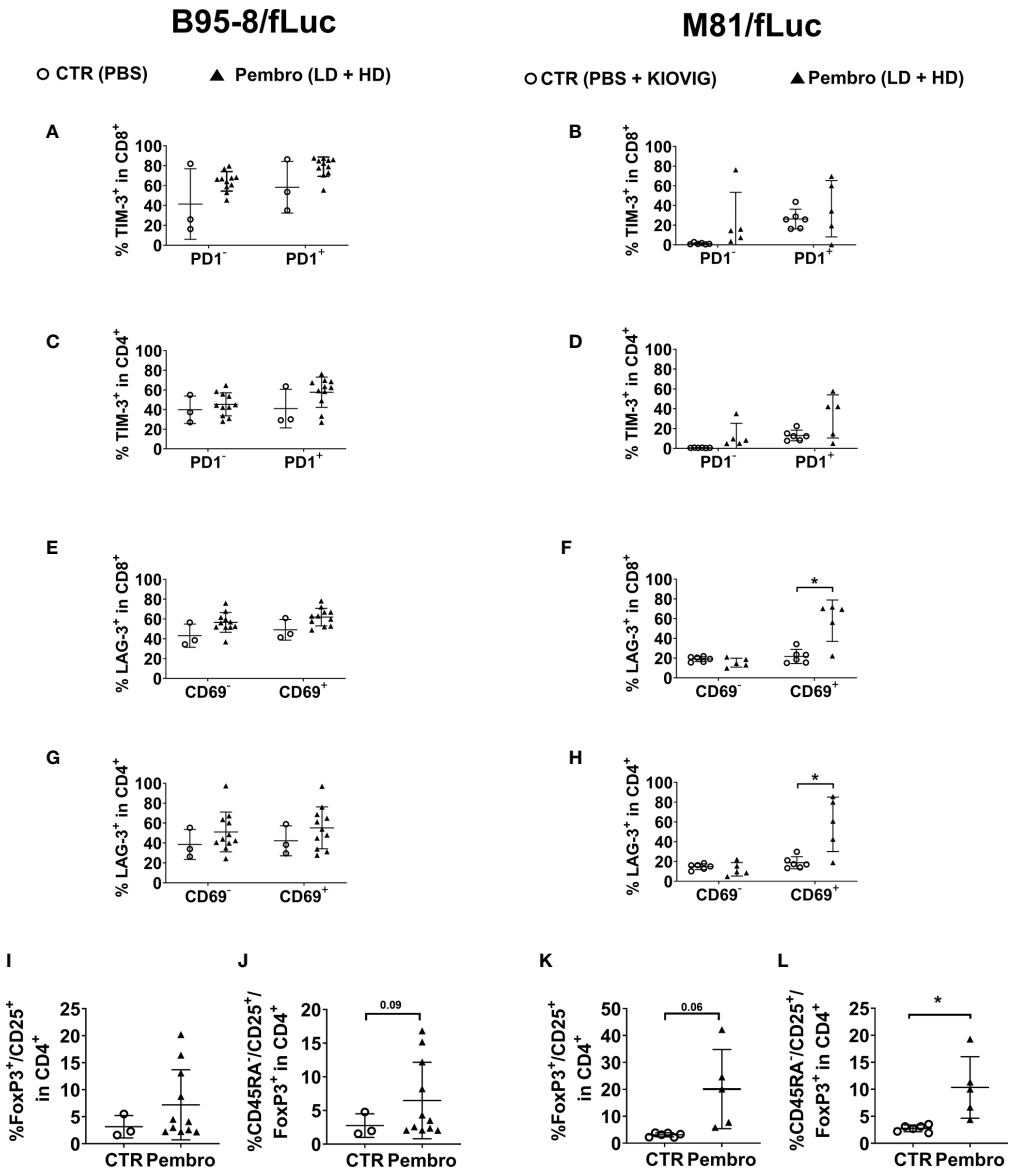

FIGURE 6 | The frequencies of T cells expressing TIM-3 or LAG-3 exhaustion markers or a regulatory T cell immunophenotype increased after pembrolizumab treatment. Frequencies of marker-positive lymphocytes recovered from spleen (SPL) comparing non-treated control mice (CTR, open circles) and pembrolizumab-treated cohorts are shown (filled triangles; low-dose and high-dose treatments were merged for the analyses). Only mice surviving until the terminal analyses at 8 wpi were included in the terminal flow cytometry analyses. **(A–D)** Frequencies (%) of TIM-3$^+$ in CD45$^+$/CD8$^+$ **(A, B)** and of TIM-3$^+$ in CD45$^+$/CD4$^+$ **(C, D)** T cells are shown. PD-1$^+$ (left side) or PD-1$^-$ (right side) CD8 or CD4 subpopulations were analyzed separately. Higher proportion of TIM-3$^+$ cells was observed more clearly for PD1$^+$ T cells for both models. **(E–H)** Frequencies (%) of LAG-3$^+$ in CD45$^+$/CD8$^+$ **(E, F)** and LAG-3$^+$ in CD45$^+$/CD4$^+$ **(G, H)** T cells are shown. CD69$^+$ (left side) or CD69$^-$ (right side) CD8 or CD4 subpopulations were analyzed separately. Significantly higher proportion of LAG-3$^+$ T cells were observed for activated CD69$^+$ T cells for mice infected with M81/EBV/fLuc and treated with pembrolizumab. **(I–L)** Frequencies (%) of CD25$^+$/FoxP3$^+$/CD45$^+$ regulatory **(I, K)** and CD45RA$^-$/CD25$^+$/FoxP3$^+$/CD45$^+$ activated regulatory T cells **(J, L)** detected within the human CD4$^+$ cells for B95-8 **(I, J)** and M81 model **(K, L)**. Pembrolizumab treatment was associated with higher proportion of regulatory T cells for both models. Unpaired Welch's t test was used to compare treatment groups. *$P < 0.05$. Standard deviation is indicated.

with this phenomenon require investigation. The tumor burden, level of immune infiltration in the tumor, quality of immune responses, immune biomarkers, and existence immunomodulatory PD-1 positive lymphocytes have all been associated with HPD (43–47). Wong et al. reported a case series of four patients with advanced hepatocellular carcinoma with chronic HBV infections treated with ICIs and demonstrating rapid radiological progression and HPD (48). A recent review summarizing the results on the safety and efficacy of ICI in HBV/HCV-infected advanced cancer patients concluded that it was safe and effective, but warned about the reactivation of hepatitis virus in some cases (49). Currently, there is no clear relationship embracing ICI, cancer, chronic infections, irAEs, and HPD. Recently, it was shown in a mouse model and in patients with tuberculosis that PD-1 blockade

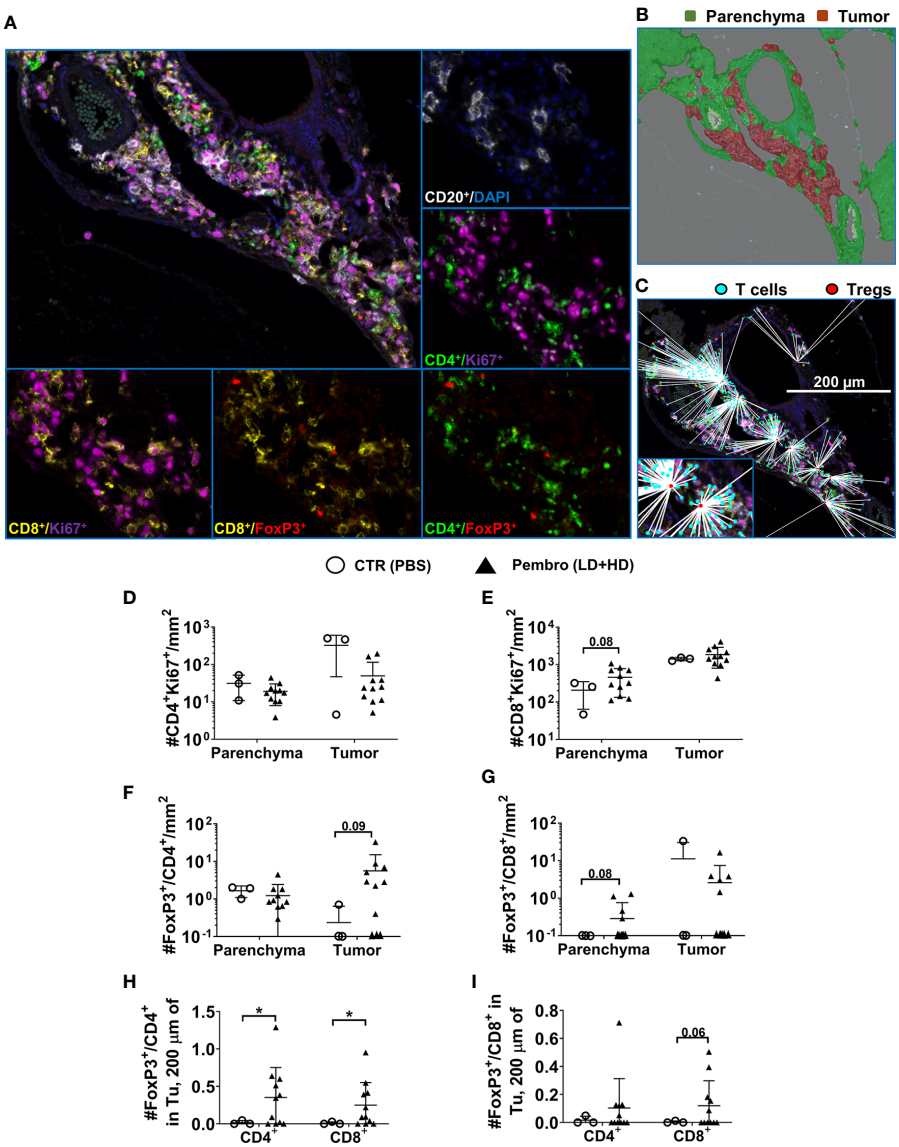

FIGURE 7 | Lower overall infiltration of CD4+ T cells but higher density and chance of intercellular interactions of regulatory T cells in tumors of mice infected with EBV/B95-8/fLuc and treated with pembrolizumab. **(A)** Representative example of a multiplexed immunohistochemical (mIHC) staining of liver tissue of a B95-8/fLuc-infected and pembrolizumab-treated humanized mouse followed by multispectral image (MSI) analysis/color deconvolution into six channels representing CD20+ (white), Ki67+ (magenta), CD4+ (green), CD8+ (yellow), FoxP3+ (red), and DAPI (blue) markers. **(B)** Tissue segmentation between the perivascular tumor mass (red) and the non-neoplastic parenchyma (green). Expectedly, the tumor area corresponds with high density of proliferating CD20+ blast-like cells **(A, B)**. **(C)** Comprehensive distance mapping between FoxP3+ (red dots) and FoxP3- T-cells (cyan dots). **(D)** The tumor areas of treated animals (black triangles, n = 11) showed fewer CD4+ T cells than controls (open circles, n = 3). **(E)** The parenchyma area is characterized by a prominent population of proliferating CD8+ cells, with a trend towards higher densities in treated animals (not significant). **(F)** Densities of proliferating Ki67+CD4+ Treg cells in the parenchyma or in the tumor tissue, with an increase of tumor-infiltrating FoxP3+/CD4+ Treg cells in the pembrolizumab-treated group (not significant), **(G)** that was also observed for parenchyma FoxP3+/CD8+ Treg cells (not significant). **(H)** Distance metrics between FoxP3+/CD4+ Tregs or **(I)** FoxP3+/CD8+ Tregs revealing significantly increased average number of FoxP3+/CD4+ within a radius of 200 µm around any single CD4+ or CD8+ T cells residing in the tumor area for pembrolizumab-treated (black triangles) mice compared with control (open circles) mice. Unpaired t test with Welch's correction was applied to calculate statistical significance. Standard deviation is indicated. *$P < 0.05$.

mounted rampant CD4+ T helper type 1 (Th1) responses driving lethal disseminated tuberculosis (50). In another alarming report, metastatic melanoma patient suffered fatal encephalitis after PD-1 blockade therapy with pembrolizumab. The affected brain tissue contained lymphocytes infected with EBV with a concurrent infiltration of memory cytotoxic CD4+ and CD8+ T cells reactive against EBV (51). Therefore, as these clinical case reports are summing up, there is a significant need to examine pre-clinically the potency and potential side effects of ICIs affecting virus-related malignancies.

There were previously two discordant reports in the literature concerning the effects of PD-1 blockade tested pre-clinically in mouse models for the treatment of EBV-related PTLD and DLBCL (**Table 1**). Corroborating our results, Münz and colleagues showed that fully humanized mice infected with the B95-8 strain and treated with a PD-1 blocking mAb developed rampant EBV spread and inflammatory reactions (25) (**Table 1**). Here, we showed that these results could be reproduced with pembrolizumab and for both the B95-8 (preferentially latent) and M81 (preferentially lytic) EBV infection models. Therefore, we suggest that PD-1 blocking in the setting of a primary infection and T cell priming can lead to uncontrolled and widespread EBV infections and development of neoplasias (PTLD and DLBCL-like tumors). Incidentally, pembrolizumab treatment affected even more drastically mice infected with M81, resulting in significantly accelerated and increased death rates. One aspect that has to be acknowledged in respect to the fully humanized mouse models of EBV infection presented by Chatterjee et al. (25) and by this current work is that their immune reconstitution at the time of infection was biased towards a high abundance of B cells (>50%) relative to T cells (<30%). These high levels of B cells, which are not seen in humans after transplantation, may have predisposed a more aggressive PTLD development in the mice. Taking this bias in consideration, we may be overestimating the substantial detrimental immunomodulatory effects caused by pembrolizumab.

Of note, there is a clear discrepancy between our results and those of Kenney and collaborators who observed lower tumor burden after PD-1 blockade when using the M81 viral strain in a not fully humanized model (27) (**Table 1**). The most straightforward explanation for the different results is that they pre-treated the mature B and T cell mixture *in vitro* with the PD-1 and CTLA-4 blocking mAbs and then administered the cells into the mice. Therefore, this *ex vivo* pre-treatment *per se* may have stimulated the adoptively transferred human T cells to become more xeno-reactive in the mice and to expand more strongly than the co-administered infected B cells. The activated and expanded T cells could eventually kill or inhibit the outgrowth of EBV-infected malignant B cells *in vivo*. This xenograft model was carried on only for 4 weeks, as the adoptively transferred human T cells can strongly react against mouse tissues and eventually result into lethal xeno-GvHD. This adoptive transfer mouse model strongly deviates from PTLD in humans, since after HCT the adoptively transferred T cells from the donor are at least partially matched through the major histocompatibility complexes (MHCs) to the recipient and there is also donor-derived thymopoiesis.

On the other hand, in fully humanized mouse models reported by Chatterjee and by this current work, the human T cells undergo an endogenous development (18, 25). The hematopoietic progenitors home in the bone marrow, travel through the thymus for positive and negative selection of functional non self-reactive T cell receptors (TCRs). TCR restriction is mediated by the MHC of the mouse and of the HSC donor. The developed human $TCR^+/CD4^+$ T cells and in lower frequencies $TCR^+/CD8^+$ T cells, eventually home in the lymphatic tissues and organs. Upon vaccination of fully humanized mice, the naïve human T cells show typical signs of priming, and change their immunophenotype from naïve to memory subtypes (29). Functional human B cells binding to viral antigens also develop in humanized mice with full maturation after class switch (30). Thus, these HIS models reflect homeostatic modulations and are multidimensional, as T cells with diverse functions and at several stages of differentiation co-exist in different tissues. From the preclinical perspective, it is indeed more challenging to perform studies in fully humanized mice, but these complexities reflect intrinsic mechanisms that may be missed in *in vitro* or in simpler xenograft models.

Primarily, the main mechanistic prospect of ICI is the release of inhibited $CD8^+$ memory TILs through the blockade of the PD-1/PD-L1 axis in order to revert their functionality (3, 43). Nonetheless, less is reported about the blockade of the PD-1/PD-L1 axis during the priming and expansion phase of naïve $CD8^+$ T cells, which occurs in humans and mice with acute infections, such as lytic EBV infections (24, 25). Indeed, it has previously been shown that downregulation of PD-1 expression prevented T cell proliferation by accelerating a T cell early differentiation (52).

The significant amplification of several human cytokines that we observed in the plasma of M81-infected mice after PD-1 blockade (IL-10, IL-33, IFN-α, IL-12p70, and IL-1β) revealed the ignition of a profound inflammatory response. The spread of viral infection systemically and the remarkable infiltration of EBV^+ PTLD into the CNS indicated a defaulted TIL response. This worrisome finding suggested that the aggravated infection and/or inflammation could potentially weaken the blood-brain-barrier. Of note, we observed that LAG-3 was strongly upregulated on $CD8^+$ and $CD4^+$ T cells after PD-1 blockade. Therefore, it is possible that the viral immune escape maneuvered the T cell exhaustion through upregulation of other suppressive receptors, like LAG-3.

In addition, our data also underscored bystander effects involving the participation of $CD4^+PD\text{-}1^+$ T cells. Their collapse and/or conversion into dysfunctional exhausted cells or Tregs likely contributed to viral escape and to irAEs. The role of Tregs seemed to be particularly critical within the tumor microenvironment on the initial stages of tumor development. Although we have not yet identified an EBV-specific molecular and immunologic mechanism by which PD-1 blockade may have affected the $CD4^+$ Tregs function, some correlations exist with neoplasias caused by EBV. For example, *in vitro* studies showed that EBV latency III–transformed B cells promoted expansion of autologous $FoxP3^+$ $CD39^{high}$ $PD\text{-}1^+$ $CTLA\text{-}4^+$ $Helios^+$ $GITR^+$ $LAG\text{-}3^+$ CD4 Tregs (53). Another study showed that homing of Tregs in EBV^+ HL tumor microenvironment is significantly increased around EBV-infected cell nests (54). Tregs also effectively populate EBV^+ gastric carcinoma tumors and express PD-1 (55). In EBV^+ NPC, EBNA-1-and LMP2-specific $CD8^+$ CTL responses can be suppressed *in vitro* by Tregs and their depletion with a recombinant fusion protein (Ontak) reverted this immune suppression (56). Therefore, Treg depletion combined with PD-1 blockade could be eventually tested, with the caveat that persistent CD25 immune depletion can lead to immune deficiency. Future studies are needed to clarify the participation of Tregs in EBV^+ HPD.

Remarkably, we also noticed a conspicuous presence of $CD8^+$/$FoxP3^+$ cells in tumors, endorsing that TILs can be subverted to immunosuppressive Tregs. Incidentally, $CD25^+CD8^+FoxP3^+$ Tregs were previously described as cells showing rapid expansion in blood and tissues of rhesus macaques during the acute phase of simian immune deficiency (SIV) infection (57). $CD8^+$ Tregs were also observed in humans infected with the human immune deficiency virus and expressed low levels of granzyme B and perforin, suggesting that they did not possess killing potential but were related to immune suppressor functions (57). Thus, development of virus-induced $CD8^+$ Tregs during acute infection may be a mechanism to curb the primary immune response so that the pathogen can take hold. Nonetheless, variability of PD-1^+ T cell populations emerging in different infections has been shown, pointing to diverse mechanisms inducing suppressive T cell types. For example, for acute influenza A virus infection, mainly central memory $CD8^+$ T cells with a PD-$1^+2B4^+CXCR5^+$ phenotype thrive after viral clearance (58). In contrast, $CD8^+$ T cells with these characteristics were completely absent in viremic HIV infected individuals (58).

Concluding, our study endorsed preclinical (25) and clinical observations (51) regarding the interaction of EBV infection with PD-1 blockade in sparking EBV spread. One novel mechanistic insight provided is the possible role of immunosuppressive $PD1^+CD4^+$ Tregs cells. One limitation of our current studies was that a single agent, pembrolizumab, was tested for ICI and in a single treatment schedule. It is possible that other ICIs or treatments at different doses or time points may give different results. For instance, blocking PD-L1 on the tumor side may produce less immunosuppressive effects on T cell effects primed against EBV^+ PTLD or DLBCL. Additional studies in humanized mice using ICI drugs in the preclinical testing pipeline can provide predictive information for very critical decisions that clinicians will eventually have to make, i.e., to opt for single or combinations of targets for treatment of EBV^+ tumors. From the translational perspective, as clinical trials against different malignancies exploring the use of ICI in combination with chemotherapy, rituximab, or small drugs against EBV^+ malignancies are emerging, it would be recommendable to first evaluate if the patients have active EBV infections and second to monitor the patients for possible EBV reactivations. Therefore, these findings warrant careful preclinical assessment of the EBV status in patients in order to minimize the side effects and improve the outcomes for patients treated with PD-1 blockade to avoid irAEs and HPD. Noteworthy, this report illustrates discordant interpretations of preclinical results (**Table 1**), advocating for a transparent reporting of the methodological approaches used towards the "Minimal Information for Standardization of Humanized Mice" (MISHUM) so that the field can further evolve (18).

DATA AVAILABILITY STATEMENT

The original contributions with the descriptive data and corresponding statistical analyses presented in the study are included in the article/**Supplementary Material**; further inquiries can be directed to the corresponding author.

ETHICS STATEMENT

Collection of CB was performed at the Department of Gynecology and Obstetrics (Hannover Medical School) and obtained according to study protocols approved by the Ethics Committee of the Hannover Medical School and after informed consent obtained from the mothers (Study protocol Nr.4837). The patients/participants provided their written informed consent to participate in this study. All experiments involving mice were approved by the Lower Saxony Office for Consumer Protection and Food Safety—LAVES (permit number: 16/2222) and performed in accordance with the German animal welfare act and the EU-directive 2010/63.

AUTHOR CONTRIBUTIONS

VV, ST, and SD conducted the experiments, analyzed the data, and wrote the first manuscript draft and revised the manuscript. SK and MM-H performed the computational analysis. MK, AS, and JB-W conducted the experiments and helped with humanized mouse work. NK performed the histological analysis. YD and CM performed the EBV histological analysis. BE-V and AD conducted the cytokine analysis. CK provided the CB units. SL and AB assisted with the mouse breeding and *in vivo* optical imaging analyses. JK provided the concept for the dosage of pembrolizumab for use in humanized mice. FK conducted the statistical analysis. WH provided the EBV/B95-8/fLuc EBV strain and technical assistance. H-JD provided the EBV/M81/fLuc stain and technical assistance. RS and FF planned the project, designed the experiments, obtained funding and regulatory approvals, enrolled the collaborators, interpreted the data, and wrote, edited, and revised the manuscript. All authors contributed to the article and approved the submitted version.

FUNDING

This work was financed by grants of the German Center for Infections Research (DZIF-TTU07.803 and DZIF-TTU07.805 to RS), by a research grant of the "The Jackson Laboratory" and a research grant from Else Kröner-Fresenius/Fortra (T04 to RS). MK received DZIF MD stipends. ST received a RegSci Ph.D. fellowship. FF was funded by the German Ministry of Education and Research (BMBF), DLR project management (e:Med) grants #01ZX1710A and #01ZX1608A.

ACKNOWLEDGMENTS

We acknowledge Dr. Dirk Wedekind (Animal Facility, Hannover Medical School), who kindly assisted with the preparation of the animal study protocols. The authors thank other members of the Regenerative Immune Therapies Applied Laboratory, in particular, Benjamin Ostermann, for his valuable technical contributions.

SUPPLEMENTARY MATERIAL

The Supplementary Material for this article can be found online at: https://www.frontiersin.org/articles/10.3389/fonc.2020.614876/full#supplementary-material

SUPPLEMENTARY TABLE 1 | Data presented in **Figures 1B, C** regarding survival of humanized mice.

SUPPLEMENTARY TABLE 2 | Data presented in **Figures 1J, L**. Descriptive statistics regarding the bioluminescence signal quantified as photons per second (p/sec).

SUPPLEMENTARY TABLE 3 | Data presented in **Figures 1K, M**. Descriptive statistics regarding the RT-qPCR analyses.

SUPPLEMENTARY TABLE 4 | Data presented in **Figures 4A, C, E, G, I**. Descriptive statistics regarding the B95-8 model for blood kinetic analyses of human immunophenotypic markers measured by flow cytometry.

SUPPLEMENTARY TABLE 5 | Data presented in **Figures 4B, D, F, H, J**. Descriptive statistics regarding the M81 model for blood kinetic analyses of human immunophenotypic markers measured by flow cytometry.

SUPPLEMENTARY TABLE 6 | Data presented in **Figures 4K, L**. Descriptive statistics regarding the analyses of human cytokines measured in plasma of mice.

SUPPLEMENTARY TABLE 7 | Data presented in **Figures 5A, C, E, G** and **6A, C, E, G, I, J**. Descriptive statistics regarding the B95-8 model for tissue analyses of human immunophenotypic markers measured by flow cytometry.

SUPPLEMENTARY TABLE 8 | Data presented in **Figures 5B, D, F, H** and **6B, D, F, H, K, L**. Descriptive statistics regarding the M81 model for tissue analyses of human immunophenotypic markers measured by flow cytometry.

SUPPLEMENTARY TABLE 9 | Data presented in **Figures 7D–I**. Descriptive statistics regarding tissue multiplex IHC analyses of spleen and liver tissues explanted from B95-8-infected mice.

SUPPLEMENTARY TABLE 10 | Antibodies used for flow cytometry and histopathology analyses.

REFERENCES

1. Shannon-Lowe C, Rickinson A. The Global Landscape of EBV-Associated Tumors. *Front Oncol* (2019) 9:713. doi: 10.3389/fonc.2019.00713
2. Crombie JL, LaCasce AS. Epstein Barr Virus Associated B-Cell Lymphomas and Iatrogenic Lymphoproliferative Disorders. *Front Oncol* (2019) 9:109. doi: 10.3389/fonc.2019.00109
3. Topalian SL, Drake CG, Pardoll DM. Immune checkpoint blockade: a common denominator approach to cancer therapy. *Cancer Cell* (2015) 27 (4):450–61. doi: 10.1016/j.ccell.2015.03.001
4. Balar AV, Weber JS. PD-1 and PD-L1 antibodies in cancer: current status and future directions. *Cancer Immunol Immunother* (2017) 66(5):551–64. doi: 10.1007/s00262-017-1954-6
5. De Goycoechea D, Stalder G, Martins F, Duchosal MA. Immune Checkpoint Inhibition in Classical Hodgkin Lymphoma: From Early Achievements towards New Perspectives. *J Oncol* (2019) 2019:9513701. doi: 10.1155/2019/9513701
6. Ansell SM, Lesokhin AM, Borrello I, Halwani A, Scott EC, Gutierrez M, et al. PD-1 blockade with nivolumab in relapsed or refractory Hodgkin's lymphoma. *N Engl J Med* (2015) 372(4):311–9. doi: 10.1056/NEJMoa1411087
7. Dierickx D, Tousseyn T, Gheysens O. How I treat posttransplant lymphoproliferative disorders. *Blood* (2015) 126(20):2274–83. doi: 10.1182/blood-2015-05-615872
8. Cohen M, Vistarop AG, Huaman F, Narbaitz M, Metrebian F, De Matteo E, et al. Epstein-Barr virus lytic cycle involvement in diffuse large B cell lymphoma. *Hematol Oncol* (2018) 36(1):98–103. doi: 10.1002/hon.2465
9. Castillo JJ, Beltran BE, Miranda RN, Young KH, Chavez JC, Sotomayor EM. EBV-positive diffuse large B-cell lymphoma, not otherwise specified: 2018 update on diagnosis, risk-stratification and management. *Am J Hematol* (2018) 93(7):953–62. doi: 10.1002/ajh.25112
10. Green MR, Rodig S, Juszczynski P, Ouyang J, Sinha P, O'Donnell E, et al. Constitutive AP-1 activity and EBV infection induce PD-L1 in Hodgkin lymphomas and posttransplant lymphoproliferative disorders: implications for targeted therapy. *Clin Cancer Res* (2012) 18(6):1611–8. doi: 10.1158/1078-0432.CCR-11-1942
11. Nicolae A, Pittaluga S, Abdullah S, Steinberg SM, Pham TA, Davies-Hill T, et al. EBV-positive large B-cell lymphomas in young patients: a nodal lymphoma with evidence for a tolerogenic immune environment. *Blood* (2015) 126(7):863–72. doi: 10.1182/blood-2015-02-630632
12. Keane C, Tobin J, Gunawardana J, Francis S, Gifford G, Gabrielli S, et al. The tumour microenvironment is immuno-tolerogenic and a principal determinant of patient outcome in EBV-positive diffuse large B-cell lymphoma. *Eur J Haematol* (2019) 103(3):200–7. doi: 10.1111/ejh.13274
13. Fang W, Zhang J, Hong S, Zhan J, Chen N, Qin T, et al. EBV-driven LMP1 and IFN-gamma up-regulate PD-L1 in nasopharyngeal carcinoma: Implications for oncotargeted therapy. *Oncotarget* (2014) 5(23):12189–202. doi: 10.18632/oncotarget.2608
14. Al Hamed R, Bazarbachi AH, Mohty M. Epstein-Barr virus-related post-transplant lymphoproliferative disease (EBV-PTLD) in the setting of allogeneic stem cell transplantation: a comprehensive review from pathogenesis to forthcoming treatment modalities. *Bone Marrow Transplant* (2020) 55(1):25–39. doi: 10.1038/s41409-019-0548-7
15. Bollard CM, Heslop HE. T cells for viral infections after allogeneic hematopoietic stem cell transplant. *Blood* (2016) 127(26):3331–40. doi: 10.1182/blood-2016-01-628982
16. Shultz LD, Brehm MA, Garcia-Martinez JV, Greiner DL. Humanized mice for immune system investigation: progress, promise and challenges. *Nat Rev Immunol* (2012) 12(11):786–98. doi: 10.1038/nri3311
17. Allen TM, Brehm MA, Bridges S, Ferguson S, Kumar P, Mirochnitchenko O, et al. Humanized immune system mouse models: progress, challenges and opportunities. *Nat Immunol* (2019) 20(7):770–4. doi: 10.1038/s41590-019-0416-z
18. Stripecke R, Munz C, Schuringa JJ, Bissig KD, Soper B, Meeham T, et al. Innovations, challenges, and minimal information for standardization of humanized mice. *EMBO Mol Med* (2020) 12(7):e8662. doi: 10.15252/emmm.201708662
19. Cocco M, Bellan C, Tussiwand R, Corti D, Traggiai E, Lazzi S, et al. CD34+ cord blood cell-transplanted Rag2-/- gamma(c)-/- mice as a model for Epstein-Barr virus infection. *Am J Pathol* (2008) 173(5):1369–78. doi: 10.2353/ajpath.2008.071186
20. Lee EK, Joo EH, Song KA, Choi B, Kim M, Kim SH, et al. Effects of lymphocyte profile on development of EBV-induced lymphoma subtypes in humanized mice. *Proc Natl Acad Sci USA* (2015) 112(42):13081–6. doi: 10.1073/pnas.1407075112
21. Munz C. Humanized mouse models for Epstein Barr virus infection. *Curr Opin Virol* (2017) 25:113–8. doi: 10.1016/j.coviro.2017.07.026
22. Fujiwara S, Imadome K, Takei M. Modeling EBV infection and pathogenesis in new-generation humanized mice. *Exp Mol Med* (2015) 47:e135. doi: 10.1038/emm.2014.88
23. Tsai MH, Lin X, Shumilov A, Bernhardt K, Feederle R, Poirey R, et al. The biological properties of different Epstein-Barr virus strains explain their association with various types of cancers. *Oncotarget* (2017) 8(6):10238–54. doi: 10.18632/oncotarget.14380
24. Danisch S, Slabik C, Cornelius A, Albanese M, Tagawa T, Chen YA, et al. Spatiotemporally Skewed Activation of Programmed Cell Death Receptor 1-Positive T Cells after Epstein-Barr Virus Infection and Tumor Development in Long-Term Fully Humanized Mice. *Am J Pathol* (2019) 189(3):521–39. doi: 10.1016/j.ajpath.2018.11.014
25. Chatterjee B, Deng Y, Holler A, Nunez N, Azzi T, Vanoaica LD, et al. CD8+ T cells retain protective functions despite sustained inhibitory receptor expression during Epstein-Barr virus infection in vivo. *PLoS Pathog* (2019) 15(5):e1007748. doi: 10.1371/journal.ppat.1007748
26. Tsai MH, Raykova A, Klinke O, Bernhardt K, Gartner K, Leung CS, et al. Spontaneous lytic replication and epitheliotropism define an Epstein-Barr

virus strain found in carcinomas. *Cell Rep* (2013) 5(2):458–70. doi: 10.1016/j.celrep.2013.09.012
27. Ma SD, Xu X, Jones R, Delecluse HJ, Zumwalde NA, Sharma A, et al. PD-1/CTLA-4 Blockade Inhibits Epstein-Barr Virus-Induced Lymphoma Growth in a Cord Blood Humanized-Mouse Model. *PLoS Pathog* (2016) 12(5):e1005642. doi: 10.1371/journal.ppat.1005642
28. Slabik C, Kalbarczyk M, Danisch S, Zeidler R, Klawonn F, Volk V, et al. CAR-T Cells Targeting Epstein-Barr Virus gp350 Validated in a Humanized Mouse Model of EBV Infection and Lymphoproliferative Disease. *Mol Ther Oncolytics* (2020) 18:504–24. doi: 10.1016/j.omto.2020.08.005
29. Volk V, Reppas AII, Robert PA, Spineli LM, Sundarasetty BS, Theobald SJ, et al. Multidimensional Analysis Integrating Human T-Cell Signatures in Lymphatic Tissues with Sex of Humanized Mice for Prediction of Responses after Dendritic Cell Immunization. *Front Immunol* (2017) 8:1709. doi: 10.3389/fimmu.2017.01709
30. Theobald SJ, Khailaie S, Meyer-Hermann M, Volk V, Olbrich H, Danisch S, et al. Signatures of T and B Cell Development, Functional Responses and PD-1 Upregulation After HCMV Latent Infections and Reactivations in Nod.Rag.Gamma Mice Humanized With Cord Blood CD34(+) Cells. *Front Immunol* (2018) 9:2734. doi: 10.3389/fimmu.2018.02734
31. Sundarasetty B, Volk V, Theobald SJ, Rittinghausen S, Schaudien D, Neuhaus V, et al. Human Effector Memory T Helper Cells Engage with Mouse Macrophages and Cause Graft-versus-Host-Like Pathology in Skin of Humanized Mice Used in a Nonclinical Immunization Study. *Am J Pathol* (2017) 187(6):1380–98. doi: 10.1016/j.ajpath.2017.02.015
32. Olbrich H, Theobald SJ, Slabik C, Gerasch L, Schneider A, Mach M, et al. Adult and cord blood-derived high affinity gB-CAR-T cells effectively react against human cytomegalovirus infections. *Hum Gene Ther* (2020) 31(7-8):423–39. doi: 10.1089/hum.2019.149
33. Theobald SJ, Kreer C, Khailaie S, Bonifacius A, Eiz-Vesper B, Figueiredo C, et al. Repertoire characterization and validation of gB-specific human IgGs directly cloned from humanized mice vaccinated with dendritic cells and protected against HCMV. *PLoS Pathog* (2020) 16(7):e1008560. doi: 10.1371/journal.ppat.1008560
34. Bilger A, Plowshay J, Ma S, Nawandar D, Barlow EA, Romero-Masters JC, et al. Leflunomide/teriflunomide inhibit Epstein-Barr virus (EBV)- induced lymphoproliferative disease and lytic viral replication. *Oncotarget* (2017) 8 (27):44266–80. doi: 10.18632/oncotarget.17863
35. Wang M, Yao LC, Cheng M, Cai D, Martinek J, Pan CX, et al. Humanized mice in studying efficacy and mechanisms of PD-1-targeted cancer immunotherapy. *FASEB J* (2018) 32(3):1537–49. doi: 10.1096/fj.201700740R
36. Chen DS, Mellman I. Elements of cancer immunity and the cancer-immune set point. *Nature* (2017) 541(7637):321–30. doi: 10.1038/nature21349
37. Jin HT, Anderson AC, Tan WG, West EE, Ha SJ, Araki K, et al. Cooperation of Tim-3 and PD-1 in CD8 T-cell exhaustion during chronic viral infection. *Proc Natl Acad Sci USA* (2010) 107(33):14733–8. doi: 10.1073/pnas.1009731107
38. Camisaschi C, Casati C, Rini F, Perego M, De Filippo A, Triebel F, et al. LAG-3 expression defines a subset of CD4(+)CD25(high)Foxp3(+) regulatory T cells that are expanded at tumor sites. *J Immunol* (2010) 184(11):6545–51. doi: 10.4049/jimmunol.0903879
39. Gao P, Lazare C, Cao C, Meng Y, Wu P, Zhi W, et al. Immune checkpoint inhibitors in the treatment of virus-associated cancers. *J Hematol Oncol* (2019) 12(1):58. doi: 10.1186/s13045-019-0743-4
40. Champiat S, Ferrara R, Massard C, Besse B, Marabelle A, Soria JC, et al. Hyperprogressive disease: recognizing a novel pattern to improve patient management. *Nat Rev Clin Oncol* (2018) 15(12):748–62. doi: 10.1038/s41571-018-0111-2
41. Popat V, Gerber DE. Hyperprogressive disease: a distinct effect of immunotherapy? *J Thorac Dis* (2019) 11(Suppl 3):S262–5. doi: 10.21037/jtd.2019.01.97
42. Kim JY, Lee KH, Kang J, Borcoman E, Saada-Bouzid E, Kronbichler A, et al. Hyperprogressive Disease during Anti-PD-1 (PDCD1) / PD-L1 (CD274) Therapy: A Systematic Review and Meta-Analysis. *Cancers (Basel)* (2019) 11(11):1699. doi: 10.3390/cancers11111699
43. Huang AC, Postow MA, Orlowski RJ, Mick R, Bengsch B, Manne S, et al. T-cell invigoration to tumour burden ratio associated with anti-PD-1 response. *Nature* (2017) 545(7652):60–5. doi: 10.1038/nature22079
44. Kim CG, Kim KH, Pyo KH, Xin CF, Hong MH, Ahn BC, et al. Hyperprogressive disease during PD-1/PD-L1 blockade in patients with non-small-cell lung cancer. *Ann Oncol* (2019) 30(7):1104–13. doi: 10.1093/annonc/mdz123
45. Kamada T, Togashi Y, Tay C, Ha D, Sasaki A, Nakamura Y, et al. PD-1(+) regulatory T cells amplified by PD-1 blockade promote hyperprogression of cancer. *Proc Natl Acad Sci USA* (2019) 116(20):9999–10008. doi: 10.1073/pnas.1822001116
46. Sasaki A, Nakamura Y, Mishima S, Kawazoe A, Kuboki Y, Bando H, et al. Predictive factors for hyperprogressive disease during nivolumab as anti-PD1 treatment in patients with advanced gastric cancer. *Gastric Cancer* (2019) 22 (4):793–802. doi: 10.1007/s10120-018-00922-8
47. Suda K. The ABCs of preventing hyperprogressive disease after immunotherapy: awareness, biomarkers, and combination. *J Thorac Dis* (2019) 11(Suppl 3):S347–51. doi: 10.21037/jtd.2018.12.112
48. Wong DJ, Lee J, Choo SP, Thng CH, Hennedige T. Hyperprogressive disease in hepatocellular carcinoma with immune checkpoint inhibitor use: a case series. *Immunotherapy* (2019) 11(3):167–75. doi: 10.2217/imt-2018-0126
49. Pu D, Yin L, Zhou Y, Li W, Huang L, Cai L, et al. Safety and efficacy of immune checkpoint inhibitors in patients with HBV/HCV infection and advanced-stage cancer: A systematic review. *Medicine (Baltimore)* (2020) 99 (5):e19013. doi: 10.1097/MD.0000000000019013
50. Barber DL, Sakai S, Kudchadkar RR, Fling SP, Day TA, Vergara JA, et al. Tuberculosis following PD-1 blockade for cancer immunotherapy. *Sci Transl Med* (2019) 11(475):eaat2702. doi: 10.1126/scitranslmed.aat2702
51. Johnson DB, McDonnell WJ, Gonzalez-Ericsson PII, Al-Rohil RN, Mobley BC, Salem JE, et al. A case report of clonal EBV-like memory CD4(+) T cell activation in fatal checkpoint inhibitor-induced encephalitis. *Nat Med* (2019) 25(8):1243–50. doi: 10.1038/s41591-019-0523-2
52. Wei J, Luo C, Wang Y, Guo Y, Dai H, Tong C, et al. PD-1 silencing impairs the anti-tumor function of chimeric antigen receptor modified T cells by inhibiting proliferation activity. *J Immunother Cancer* (2019) 7(1):209. doi: 10.1186/s40425-019-0685-y
53. Auclair H, Ouk-Martin C, Roland L, Santa P, Al Mohamad H, Faumont N, et al. EBV Latency III-Transformed B Cells Are Inducers of Conventional and Unconventional Regulatory T Cells in a PD-L1-Dependent Manner. *J Immunol* (2019) 203(6):1665–74. doi: 10.4049/jimmunol.1801420
54. Assis MC, Campos AH, Oliveira JS, Soares FA, Silva JM, Silva PB, et al. Increased expression of CD4+CD25 +FOXP3+ regulatory T cells correlates with Epstein-Barr virus and has no impact on survival in patients with classical Hodgkin lymphoma in Brazil. *Med Oncol* (2012) 29(5):3614–9. doi: 10.1007/s12032-012-0299-4
55. Zhao L, Zhou X, Zhou X, Wang H, Gu L, Ke Y, et al. Low expressions of PD-L1 and CTLA-4 by induced CD4(+)CD25(+) Foxp3(+) Tregs in patients with SLE and their correlation with the disease activity. *Cytokine* (2020) 133:155119. doi: 10.1016/j.cyto.2020.155119
56. Fogg M, Murphy JR, Lorch J, Posner M, Wang F. Therapeutic targeting of regulatory T cells enhances tumor-specific CD8+ T cell responses in Epstein-Barr virus associated nasopharyngeal carcinoma. *Virology* (2013) 441(2):107–13. doi: 10.1016/j.virol.2013.03.016
57. Nigam P, Velu V, Kannanganat S, Chennareddi L, Kwa S, Siddiqui M, et al. Expansion of FOXP3+ CD8 T cells with suppressive potential in colorectal mucosa following a pathogenic simian immunodeficiency virus infection correlates with diminished antiviral T cell response and viral control. *J Immunol* (2010) 184(4):1690–701. doi: 10.4049/jimmunol.0902955
58. Bengsch B, Ohtani T, Khan O, Setty M, Manne S, O'Brien S, et al. Epigenomic-Guided Mass Cytometry Profiling Reveals Disease-Specific Features of Exhausted CD8 T Cells. *Immunity* (2018) 48(5):1029–45.e5. doi: 10.1016/j.immuni.2018.04.026

Conflict of Interest: The authors declare that the research was conducted in the absence of any commercial or financial relationships that could be construed as a potential conflict of interest.

Copyright © 2021 Volk, Theobald, Danisch, Khailaie, Kalbarczyk, Schneider, Bialek-Waldmann, Krönke, Deng, Eiz-Vesper, Dragon, von Kaisenberg, Lienenklaus, Bleich, Keck, Meyer-Hermann, Klawonn, Hammerschmidt, Delecluse, Münz, Feuerhake and Stripecke. This is an open-access article distributed under the terms of the Creative Commons Attribution License (CC BY). The use, distribution or reproduction in other forums is permitted, provided the original author(s) and the copyright owner(s) are credited and that the original publication in this journal is cited, in accordance with accepted academic practice. No use, distribution or reproduction is permitted which does not comply with these terms.

frontiers in Immunology

REVIEW
published: 02 February 2021
doi: 10.3389/fimmu.2020.619236

Advances in Human Immune System Mouse Models for Studying Human Hematopoiesis and Cancer Immunotherapy

Syed A. Mian[1,2†], *Fernando Anjos-Afonso*[3†] *and Dominique Bonnet*[1*†]

[1] Haematopoietic Stem Cell Lab, The Francis Crick Institute, London, United Kingdom, [2] Department of Haematology, School of Cancer and Pharmaceutical Sciences, King's College London, London, United Kingdom, [3] Haematopoietic Signalling Group, European Cancer Stem Cell Institute, School of Biosciences, Cardiff University, Cardiff, United Kingdom

Immunotherapy has established itself as a promising tool for cancer treatment. There are many challenges that remain including lack of targets and some patients across various cancers who have not shown robust clinical response. One of the major problems that have hindered the progress in the field is the dearth of appropriate mouse models that can reliably recapitulate the complexity of human immune-microenvironment as well as the malignancy itself. Immunodeficient mice reconstituted with human immune cells offer a unique opportunity to comprehensively evaluate immunotherapeutic strategies. These immunosuppressed and genetically modified mice, with some overexpressing human growth factors, have improved human hematopoietic engraftment as well as created more functional immune cell development in primary and secondary lymphoid tissues in these mice. In addition, several new approaches to modify or to add human niche elements to further humanize these immunodeficient mice have allowed a more precise characterization of human hematopoiesis. These important refinements have opened the possibility to evaluate not only human immune responses to different tumor cells but also to investigate how malignant cells interact with their niche and most importantly to test immunotherapies in a more preclinically relevant setting, which can ultimately lead to better success of these drugs in clinical trials.

Keywords: immunodeficient mice models, immunotherapy, human hematopoiesis, xenotransplantation models, immune reconstitution

OPEN ACCESS

Edited by:
Tim Willinger,
Karolinska Institutet, Sweden

Reviewed by:
Anthony Rongvaux,
Fred Hutchinson Cancer Research Center, United States
Stephanie Halene,
School of Medicine Yale University, United States

****Correspondence:***
Dominique Bonnet
dominique.bonnet@crick.ac.uk

†These authors have contributed equally to this work

Specialty section:
This article was submitted to Cancer Immunity and Immunotherapy, a section of the journal Frontiers in Immunology

Received: *19 October 2020*
Accepted: *18 December 2020*
Published: *02 February 2021*

Citation:
Mian SA, Anjos-Afonso F and Bonnet D (2021) Advances in Human Immune System Mouse Models for Studying Human Hematopoiesis and Cancer Immunotherapy. Front. Immunol. 11:619236. doi: 10.3389/fimmu.2020.619236

BRIEF HISTORY OF HUMAN HEMATOPOIESIS

HSCs are rare (one in 10^6 bone marrow cells) undifferentiated multipotent stem cells with the ability to perpetuate themselves for indefinite time through self-renewal. These HSCs differentiate to all the downstream mature blood cell lineages that control the homeostasis balance, immune function, and response to infections. Since the pioneering work of Till and McCulloch in the early 1960s, the understanding of HSCs has progressed enormously from observational to functional studies. The regenerative potential of HSCs was further established with the development of various clonal repopulation assays pioneered by Becker et al. (1), McCulloch et al. (2, 3), Moore and Metcalf (4, 5),

Griffin and Löwenberg (6) and Dicke et al. (7). Even though our understanding of hematopoiesis largely comes from the mouse system, our ability to characterize human HSCs has improved. Since the discovery of a ligand for L-selectin (namely CD34) by Civin et al. (8), that for decades became the cornerstone, cell surface marker for enriching human HSCs, is still being used alongside newly well-established antigens (such as CD38, CD45RA, CD90, and CD49f) (9–15). However, the concept of SCID-repopulating cell (SRC) assay by Dick and colleagues was the game changing idea that enabled to accurately measure the primitive HSC populations using NOD/SCID mice (16, 17). Altogether, thanks to the use of robust *in vivo* and *in vitro* clonal assays, xenotransplantation as well as refined sorting strategies using cell surface antigens, significant insights toward understanding the human hematopoietic hierarchy have been made. Today it is well established that human HSCs are present within the $CD34^{+}CD38^{-}CD90^{+}CD45RA^{-}CD49f^{+}$ fraction of the hematopoietic compartment, with an SRC frequency of one in 10 cells (15). There is also emerging evidence suggesting the existence of some HSCs within the $CD34^{-}$ faction of the human bone marrow cells, however the frequency of these HSCs is low (18–21).

A BRIEF NOTE ON THE DEVELOPMENT AND REFINEMENT OF IMMUNODEFICIENT MOUSE MODELS TO STUDY HUMAN HEMATOPOIESIS

Gaining knowledge of human physiology and pathophysiology has been often hampered by restricted access to human tissues or limited to performing *in vitro* assays. Over the last few decades, advances made from inbred wild-type to more state-of-the-art genetically engineered humanized strains have enabled researchers to gain novel insights into the complex biological underpinnings of human hematopoiesis. The development of humanized mouse models started with the identification of the severe combined immunodeficient (Scid; mutation in $Prkdc^{scid}$) mice that lacked B and T cells (22). These mice were shown to allow human T and B cell reconstitution (23). However, the SCID mouse model has limited usage due to the spontaneous generation of mouse T and B cells during aging (also known as leakiness) and high levels of host NK cell activity, that limits the engraftment of human cells. Further attempts to modify the SCID mouse model were made to increase the human hematopoietic cell engraftment which eventually led to the development of the non-obese diabetic-SCID (NOD-SCID) mice. This hybrid model was developed by backcrossing the SCID mice onto the non-obese diabetic (NOD) mouse background, which resulted in immunological multi-dysfunction, including defective NK cell activity and complement-dependent hemolytic activity (24). The NOD background is supportive of human cells due to a specific mutation in *Sirpa* that confers high affinity to human CD47, resulting in host macrophage tolerance to human cells (25). These NOD-*Scid* mice supported high levels of human cell engraftment compared to other non-NOD derived immunodeficient mice. However, the use of this hybrid NOD-SCID mice remained limited due to relatively short life span (median survival = 257 days) as well as the residual activity of NK cell and some of the other innate components (26, 27) of the immune system, thereby impeding the engraftment of the human cells. These mice also have a propensity to developing thymic lymphomas with age, similar to SCID mice.

The next revolution in the development of advanced immunodeficient mice occurred with the backcrossing of NOD-*Scid* mice with either truncated (NOG) or deleted (NSG) interleukin-2 receptor (IL-2R) common γ chain. Both of these models have deficiency in the IL-2R γ-chain that leads to the multiple defects in the innate as well as the adaptive immune system and prevents NK cell development (28–30). In addition, the lack of the IL-2Rγc activity limits the spontaneous development of thymoma, therefore allowing for long-term human cell engraftment experiments (median survival >89 weeks) (31). Although NOD-*Scid*, NOG, and NSG mice are the three most commonly used models for xenotransplantation, there are also other strains that have been developed over the years. For example, Rag-deficient mice that lack the expression of functional Rag1 or Rag2 proteins cannot perform somatic recombination of the T cell receptor (TCR) and immunoglobulin (Ig) genes, and the absence of either of these genes results in T and B cell deficiency. Mice that carry either the *Rag1* or *Rag2* mutations have very similar phenotypes and are also commonly used nowadays (BALB/c-$Rag2^{-/-}Il2r\gamma^{-/-}$ or BRG and the NOD-$Rag1^{-/-}Il2r\gamma^{-/-}$ or NRG mice). Despite these improvements, all of the hybrid $Il2r\gamma^{-/-}$ mice strains still require conditioning with either sublethal radiation or with a myeloablative agent such as bulsulfan prior to cell injection of low number of human cells for optimal engraftment. Further detailed reviews on the historical development of the different mouse models have been extensively covered elsewhere (32–34). Instead, we will critically discuss the recent advancements and pitfalls concerning the development of the different human blood cells in these mice, particularly focusing on their use to investigate cancer immunotherapies (**Figure 1**). Nevertheless, a brief description of such models described here is summarized in **Table 1**.

IMPROVED ERYTHROPOIESIS AND MEGAKARYOPOIESIS IN CURRENT IMMUNODEFICIENT MOUSE MODELS

Despite the successes seen over the last few decades in improving immunodeficient mouse models, significant challenges still remain. For example, NSG mice only allow low human myeloid cell development with high proportion of immature B cells (56, 57) with minimal production of antigen-specific IgG class antibodies (58) and very reduced production of erythrocytes (59). In fact, human cells that have proven most difficult to generate in these immunodeficient mice have been the erythrocytic and megakaryocytic lineages in which their *de novo* production from human hematopoietic stem and progenitor cells (HSPCs) normally peaks at 5–7 weeks following the xenotransplantation. This skewing

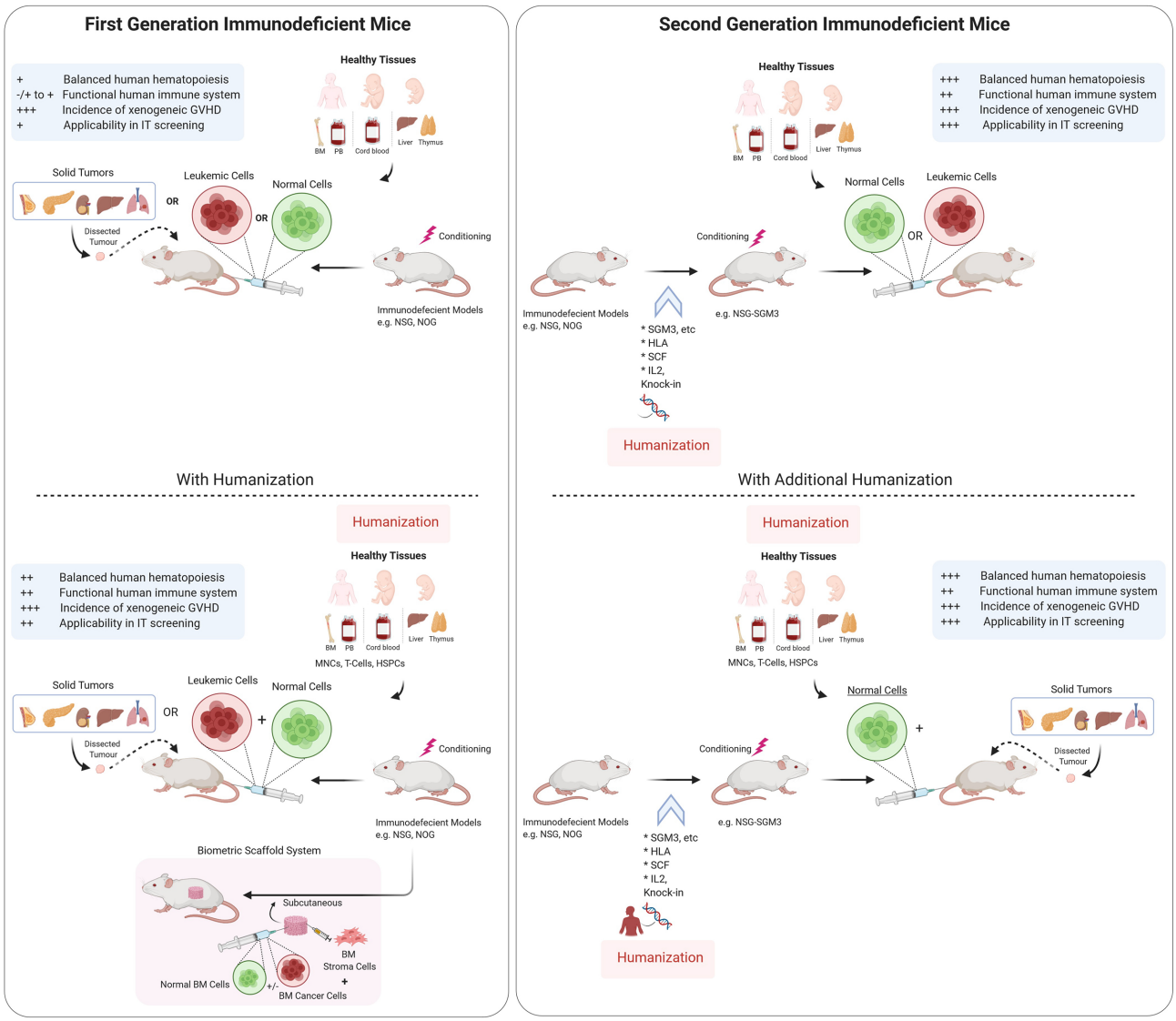

FIGURE 1 | Schematic representation of Immunodeficient mouse models and humanization strategies used to establish preclinical models. Tumor tissues from cancer patients are either injected (for hematological cancers) or implanted subcutaneously or orthotopically into immunodeficient mice with or without humanization. Scaffold implantation approach has also be used for hematological cancers in mice. Immunodeficient mouse models are either used for understanding the normal hematopoiesis or pathophysiology of the cancer tissues and for testing theurapeutic strategies. There are varying degrees of benefits for using different immunodeficient mouse models as depecited in the panel (+/–). IT, Immunotherapy, GVHD, Graft *vs* host disease, I.V., Intravenous route, BM, bone marrow, HSPC, hematopoietic stem and progenitor cells. Illustration was created with Biorender.com.

in the lineage development of human cells could be multifactorial. The insufficient cross-reactivity of mouse cytokines to human cells may explain, at least in part, the poor development of these cell lineages. Certainly, humanized mice do not allow an efficient production of human megakaryocyte erythroid progenitors (MEPs). However, this deficiency is not corrected in *Rag2*$^{-/-}$*Il2ry*$^{-/-}$ mice expressing human thrombopoietin (TPO). Interestingly, this mouse strain generated increased levels of human cell engraftment, as well as higher multilineage differentiation of HSCs, with an increased ratio of myelomonocytic *versus* lymphoid cells (38). In addition, injection of plasmid DNA-encoding human erythropoietin (EPO) and IL-3 was found to modestly improve human red blood cell (RBC) reconstitution in NSG mice that were engrafted with CD34^{+} HSPCs (60). It is worth to note that phagocytosis of human RBCs and platelets by murine macrophages has been shown to play a larger role in the elimination of such human cells. This could explain the absence of these cell types in the peripheral blood of the humanized mice. Interestingly, human late-stage immature erythroid cells (CD235a^{+}CD45^{-} nucleated normoblasts) are normally detected in the mouse BM; however, as these cells reach their maturity to form RBC, they are efficiently eliminated by murine macrophages

TABLE 1 | Summary of the immunodeficient mouse strains developed over the last few decades described in this review.

Name of the strain (genetic description) (reference when first described)	Features of the mice
BRG or **BALB/c-*Rag2*$^{-/-}$*Il2r*γ$^{-/-}$** (C.Cg-*Rag2*^{tm1Fwa} *Il2rg*^{tm1Sug}/JicTac (Taconic) or **C;129S4-*Rag2*$^{tm1.1Flv}$ *Il2rg*$^{tm1.1Flv}$/J** (Jackson)) (35)	-BALB/c background with *Rag2 and Il2rg* knockout; Taconic strain is completely congenic on BALB/c background whereas Jackson is on a 129 background -both models have higher radiation tolerance due to *Rag2* mutation compared to Scid models -both models lack T, B, and NK cells and dysfunctional DCs
BRG-*IL3/CSF2* (C;129S4-*Rag2*$^{tm1.1Flv}$ *Csf2/Il3*$^{tm1.1(CSF2,IL3)Flv}$ *Il2rg*$^{tm1.1Flv}$/J) (36)	-similar to BRG -targeted replacement of mouse *Il3* and *Csf2* with coding regions with those of human -improve human myeloid cell reconstitution in the lung in particular alveolar macrophages
BRGS (C;129S4-Rag2$^{tm1.1Flv}$ IL2rg$^{tm1.1F1v}$Tg(SIRPA)1Flv (37)	-similar to BRG -heterozygous human *SIRPA* BAC transgene expression -allow better engraftment and maintenance of human hematopoietic cells compared to BRG mice to levels comparable to NSG mice
BRG-*TPO* or *Rag2*$^{-/-}$*Il2ry*$^{-/-}$-*TPO* (C;129S4-*Rag2*$^{tm1.1Flv}$ *Thpotm1.1(TPO)Flv Il2rgtm1.1Flv*)/J (38)	-similar to BRG -human *TPO* knock-in replacing mouse *Tpo* -support higher human myeloid-lymphoid and HSC engraftment compared to BRG -have reduced mouse platelets compared to BRG
Rag2*$^{-/-Il2ry-/--}$SIRPA$^{h/m}$*IL6*$^{h/h}$** *or* **RGSKI-*IL6 (39)	-similar to BRG -heterozygous human *SIRPA BAC* transgene expression and homozygous *IL6* knock-in replacing mouse *Il6* -CD47 expressed on human cells binds efficiently to the mouse BAC transgene-encoded human SIRPα enabling mouse phagocytes to tolerate and not engulf engrafted human cells -allow improved thymopoiesis and peripheral T cell reconstitution -allow higher frequencies of human memory and IgG producing B cells development with increased in total IgG and antigen-specific IgG levels
Rag2*$^{-/-Il2ry-/--}$SIRPA$^{h/m}$*IL15*$^{h/m}$** *or* ***SRG-15 (40)	-similar to BRG -heterozygous human *SIRPA* knock-in -homozygous knock-in *IL15* replacing mouse *Il15* -expression of human SIRP*α* enables mouse phagocytes to tolerate and not engulf engrafted human cells -support efficient development of human circulating and tissue-resident NK cells, intraepithelial lymphocytes and innate lymphoid cell subsets
MITRG (C;129S4-*Rag2*$^{tm1.1Flv}$ *Csf1*$^{tm1(CSF1)Flv}$ *Csf2/Il3*$^{tm1.1(CSF2,IL3)Flv}$ *Thpo*$^{tm1.1(TPO)Flv}$ *Il2rg*$^{tm1.1Flv}$/J) (41)	-similar to BRG -*human CSF1, CSF2/IL3* and TPO knock-in replacing the respective mouse genes -enable the full recapitulation of human myeloid development and function due to the expression of human cytokines
MISTRG (C;A29S4-*Rag2*$^{tm1.1Flv}$ *Csf1*^{tm1}*(CSF1)FlvCsf2*$^{/Il3tm1.1(CSF2,IL3)Flv}$ *Thpo*$^{tm1.1}$*(TPO)Flv Il2rg*$^{tm1.1Flv}$ Tg (SIRPA)1Flv/J) (41)	-similar to MITRG -human *SIRPA* BAC transgene expression -CD47 expressed on human cells binds efficiently to the mouse BAC transgene-encoded human SIRPα enabling mouse phagocytes to tolerate and not engulf engrafted human cells
MISTRG6 (42)	-similar to MISTRG -homozygous *IL6* knock-in replacing mouse Il6 -allow the development of entire spectrum of human plasma cell neoplasia
Scid *(Prkdcscid)* (22)	-lack functional lymphocytes because of impaired VDJ rearrangement -have severe combined immunodeficiency affecting both B and T lymphocytes
NOD-*Scid* (NOD.Cg-*Prkdc*^{scid}/J) (24)	-as *Scid* mice -NOD/ShiJic strain background contributes to defective mouse DCs and macrophages -have reduced complement and NK cells -harbour *Sirpa* polymorphism that allows interactions between mouse macrophages and human CD47
NOD-*Scid*-SGM3 (NOD.Cg-*Prkdc*^{scid} Tg(CMV-IL3,CSF2,KITLG)1Eav (43)	-as NOD-*Scid* -transgenic expression of human IL-3, GM-CSF, and SCF under the CMV promoter -support higher level of human myeloid cell engraftment -induce exhaustion of human HSCs
NOG (NOD.Cg-*Prkdc*^{scid}*Il2rgtm*^{1Sug}/JicTac) (29)	-features similar to NOD-*Scid* -truncated intracytoplasmic domain of IL-2Rg leading to no signalling -have defective mouse NK cell development
NOG-EXL or **NOG-*IL3/CSF2*** (NOD.Cg-*Prkdc*^{scid}*Il2rg*^{tm1Sug}(SV40/HTLV-IL3,CSF2) 10-7Jic/JicTac) (44)	-similar to NOG -transgenic expression of human GM-CSF and IL-3 driven by the SRα promoter -support higher levels of human myeloid cell differentiation -support higher human DC and mast cells differentiation -allow more efficient human HSC engraftment
NOG-*IL6* (NOD.Cg-*Prkdc*^{scid}*Il2rg*^{tm1SugTg}(CMV-IL6)1-1Jic/JicTac) (45)	-similar to NOG -transgenic expression of human IL-6 driven by the CMV promoter -allow enhanced human monocytes development

(Continued)

TABLE 1 | Continued

Name of the strain (genetic description) (reference when first described)	Features of the mice
NOG-*IL15* (NOD.Cg-*Prkdc*^{scid}*Il2rg*^{tm1SugTg}(CMV-IL2/IL15)1-1Jic/JicTac) (46)	-similar to NOG -transgenic expression of human IL-15 with a IL-2 signal peptide driven by the CMV promoter -allow extensive human NK cell proliferation and differentiation and human NK cells produce both granzyme A and perforin upon stimulation -allow engraftment and expansion of human NK cells following engraftment with CD56+ NK cells derived from human PBMCs
NRG or **NOD-*Rag1*$^{-/-}$*Il2ry* $^{-/-}$** (NOD.Cg-*Rag1t*^{m1MomIl}*2rg*^{tm1Wjl}*/SzJ)* (47)	-harbor *Rag1*^{null} and *IL2rγ*^{null} mutations -lack T, B, and NK cells and dysfunctional DCs and macrophages -have *Sirpa* polymorphism that allows interactions between mouse macrophages and human CD47
NRG-HLA-A2-DR4 or **DRAG** (NOD.Cg-*Rag1*^{tm1Mom} *Il2rg*^{tm1Wjl} Tg(HLA-DRA,HLA-DRB1*0401)39-2Kito/ScasJ) (48)	-similar to NRG -express chimeric human-mouse class II transgenes HLA-DRA/HLA-DRB1*0401 fused to the *I-E*^{d} MHC class II molecule -allow enhanced HLA-DR-matched HSC engraftment and subsequent human T cell and B cell development to study the development of autoimmune diseases -allow vaccine testing and generation of human IgM, IgG, IgA or IgE monoclonal antibodies
NSG (NOD.Cg-*Prkdc*^{scidIl}*2rg*^{tm1Wjl}/SzJ) (28)	-features similar *to* NOD-*Scid* -target mutation of Il2rg leading to no expression of IL-2 -have defective NK cell development
NSG-*B2M*^{null} *(*NOD.Cg-*B2m*^{tm1Unc} *Prkdc*^{scid} *Il2rg*^{tm1Wjl}/SzJ) (49)	-similar to NSG -are relatively resistant to GVHD
NSG-*CSF1* (NOD.Cg-*Prkdc*^{scid} *Il2rg*^{tm1Wjl} Tg(CSF1)3Sz/SzJ) (50)	-similar to NSG -transgenic expression of human M-CSF -support higher human macrophage development
NSG-*HLA-A2/HHD* (NOD.Cg-*Prkdc*^{scid} *Il2rg*^{tm1Wjl} Tg(HLA-A/H2-D/B2M) 1Dvs/SzJ) (51)	-similar to NSG -express human HLA class 1 heavy and light chains with B2M covalently linked to the MHC class 1, alpha1 and alpha2 binding domains of the human *HLA-A2.1* gene, and the alpha3, cytoplasmic and transmembrane domains of the murine *H2-D*^{b} -support T cell maturation and responses to human antigens presented by HLA-A2.1 molecule
NSG-*HLA-A24/HHD* (NOD.Cg-*Prkdc*^{scid} Il2rg^{tm1Wjl} Tg(HLA-A24/H2-D/B2M)3Dvs/Sz) (52)	-similar to NSG -express human *HLA-A24.2* with *B2M* and murine *H2-D*^{b} -support human T cell maturation and responses to human antigens presented by HLA-A24.2 molecule
NSG-*HLA-A2/DR1* (NOD.Cg-*Prkdc*^{scid} *IL2rg*^{tmlWjl}*/Sz* Tg[HLA-DRA*0101, HLA-DRB1*0101]1Dmz/GckRolyJ *Mcph1*$^{Tg(HLA-A2.1)1Enge}$/SzJ (48)	-similar to NSG -express human/mouse chimeric MHC Class II transgene (Tg(HLA-DRB1*01)1Dmz): parts of mouse MHC Class II *H2-Ea* and *H2-Eb1* were replaced by the corresponding amino acids of the human MHC Class II protein -Tg(HLA-A2.1)1Enge integrated into chromosome 8 causing a duplication in *Mcph1* resulting into functional knock-out of *Mcph1* in homozygous mice -support human T cell maturation and responses to human antigens presented by the respective HLA molecules. -allow the engraftment of functional human Th1, Th2 and Th17 T cells
NSG-(*K*^{b}*D*^{b})*null*(*IA*^{null}) (NOD.Cg-*Prkdc*^{scid} *H2-K1*^{tm1Bpe} *H2-Ab1*^{em1Mvw} *H2-D1*^{tm1Bpe} *Il2rg*^{tm1Wjl}/SzJ) (49)	-similar to NSG -have MHC class I molecule (H2-K and D) and MHC class II deficiencies (IA) -are resistant to GVHD
NSG-*IL6* NOD.Cg-*Prkdc*^{scid}*Il2rg*^{tm1Wjl} *Tg(IL6)/Sz)* (53)	-similar to NSG -transgenic expression of human IL-6 -allow higher levels of human CD3^{+} and Th17 T cell development -allow higher plasma levels of human IgM and IgG
NSG-SGM3 (NOD.Cg-*Prkdc*^{scid}*Il2rg*^{tm1Wjl} Tg(CMV-IL3,CSF2, KITLG)1Eav/MloySzJ) (54)	-similar to NSG -transgenic expression of human IL-3, GM-CSF and SCF under the CMV promoter -induce exhaustion of human HSCs -allow higher level of human myeloid cell and AML engraftment -allow rapid reconstitution of human T cells, with improved B cell differentiation and increased levels of NK cells
NSG-SGM3-*CSF1* or **QUAD** (NOD.Cg-*Prkdc*^{scid} *Il2rg*^{tm1Wjl} Tg(CMV-IL3,CSF2, KITLG)1Eav Tg(CSF1)3Sz/J) (33)	- similar to NSG-SGM3 combined with features of NSG-*CSF1*
NSG Kit$^{W41/W41}$ or **NSGW41** (NOD.Cg-*Kit*$^{W-41J}$ *Prkdc*^{scid} *Il2rg*^{tm1Wjl}/WaskJ) (55)	-similar to NSG -loss of endogenous *Kit* function, conferred by the *Kit*$^{W-41J}$ allele -have impaired endogenous mouse HSCs, allowing engraftment of human HSCs without irradiation -support better human erythropoiesis and platelet formation

(59, 61). As previously mentioned, NOD SIRPα is capable of cross-reacting with human CD47, suggesting that the rejection of human RBCs in humanized mice is unlikely to be induced by the inability of human CD47 to interact with the recipient SIRPα. Indeed, it was demonstrated that the rejection rates of human RBCs were significantly higher than CD47 knockout mouse RBCs, indicating that the rejection of human RBCs in immunodeficient mice is mainly induced by CD47-SIRPα independent mechanisms, such as

xenoantigens present on human RBCs that can activate host macrophages (62, 63). Interestingly, intravenous injection of liposome-encapsulated clodronate into mice was shown to deplete recipient macrophages, resulting in robust, albeit transient, generation of both human RBCs and platelets (59, 61).

The recent generation of NSGW41 (with partial deficiency in Kit function) mice (**Table 1**) has definitely helped to improve human erythropoiesis and platelet formation in murine microenvironment (55, 64). Furthermore, human thrombopoiesis was observed in these mice following xenotransplantation, with increased proportions of human mature thrombocytes and erythroblasts in the murine BM. In addition, the morphology and composition of *de novo* generated human erythroblasts were found to be similar to that observed in the human BM. The most likely mechanism resulting in enhanced BM erythropoiesis in kit mutant mice is the cell intrinsic impairment of erythropoiesis in these mice (65). Interestingly, human erythro- and megakaryopoiesis were also found to be enhanced in an another recently developed immunodeficient mouse model (namely MISTRG mice), following the xenotransplantation of human HSPCs (66). The authors of this work postulated that the expression of human cytokines from the endogenous murine loci (replacing murine encoding cytokines), by providing a more physiologic expression of human cytokines, synergistically promotes a more competitive human hematopoiesis including the efficient development of human RBCs and platelets (66).

IMMUNE INNATE CELL DIFFERENTIATION OUTPUTS ARE MUCH NEEDED

In a healthy human adult individual, myeloid cells comprise ~55–70% of all leukocytes both in the peripheral blood and BM. As discussed earlier, the current common immunodeficient mouse models poorly recapitulate the normal myelopoiesis that is observed in human hematopoietic tissues, particularly the human macrophages that are poorly generated in mice. Cytokines play a key role not only in the maintenance of human HSCs but also in their differentiation to mature myeloid progeny. One of the main reasons responsible for poor human myelopoiesis in mice could be the evolutionary divergence between human and mouse cytokines, that are species-specific (*i.e.*, the mouse cytokines do not function in human cells). Early attempts were made to resolve these limitations which included the direct delivery of human cytokines (recombinant cytokines or plasmids encoding for cytokines) into the immunodeficient mice (60, 67, 68). However, these methods are expensive and not suitable for long-term experiments. Further quest for a "better" humanized mouse model led to the development of transgenic mice that are generated by overexpression of human cytokine-encoding genes under the control of a strong constitutive promoter. The NOD-SCID-SGM3 and NSG-SGM3 mouse strains (see **Table 1**) that overexpress SCF, GM-CSF, and IL-3 under the cytomegalovirus (CMV) promoter have been shown to increase the level of human myeloid cells upon engraftment with human HSPCs (43, 69). The latter mouse strain was also found to facilitate a more rapid reconstitution of T cells, with improved B cell differentiation and increased levels of NK cells as compared to the parental NSG strain. However, the supra-physiological levels of these cytokines in these mice were shown to almost abolish the human platelets that are normally detected in NSG mice at a low level, and more importantly cause exhaustion of the engrafted human HSCs (69). A closely related strain such as NOG-*IL3*/*CSF2* (NOG-EXL) mice that overexpresses human IL-3 and GM-CSF, was also shown to have increased levels of human myeloid cells, in particular basophils, mast cells, and myeloid derived dendritic cells (DCs). However, this mouse strain appears to preserve the human HSPCs (44). It is unclear why this mouse strain does not seem to exhaust the human HSPCs. One of the reasons for such a behavior could be the level of the transgene expression that is driven by different promoters in these models (*i.e.* SRα instead of the CMV promoter) (44). However, BRG mice with human *IL3* and *CSF2* knock-in genes (BRG-*IL3*/*CSF2*) were found to have no significant increase in human T, B, and NK cells as well as human HSPCs, $CD34^+CD33^+$ myeloid progenitors, total $CD33^+$ myeloid cells, $CD14^+$ monocytes/macrophages and $CD66^+$ granulocytes in the bone marrow, blood, and spleen of these mice (36). However, BRG-*IL3*/*CSF2* mice were shown to support the development and replacement of human alveolar marcophages (36). This may suggest that additional factors other than only the lack of cross-reactivity of the cytokines between the species, are also important for generating robust human myelopoiesis in hematopoietic tissues in mice. In another model, a transgenic NOG mouse was generated using human *IL6* cDNA under the control of the CMV promoter (NOG-*IL6*). These mice generated significant levels of $CD14^+HLA\text{-}DR^{lo/neg}$ human monocytic myeloid derived suppressor cells, following HSPC xenotransplantation. In addition, infiltration of human $CD163^+$ tumor-associated macrophages was evidently detected in a head and neck squamous cell carcinoma engrafted model (45).To specifically increase macrophage development, human macrophage colony stimulating factor (M-CSF; NSG-*CSF1*) gene was overexpressed in NSG mice (50), which when crossed with NSG-SGM3 mice, led to the generation of NSG-SGM3-*CSF1* (QUAD) mice. Interestingly, these mice showed increased human myeloid and mature macrophage development when engrafted with human HSPCs (33). In order to further refine the expression of these critical cytokines, Rongvaux and colleagues used 129×BALB/c-*Rag2*$^{-/-}$*Il2r*$\gamma^{-/-}$ mice to knock-in human *IL3*, *CSF2*, *TPO* (MITRG) and in addition *SIRPA* (MISTRG mice; see **Table 1**) in these mice. These mice allowed a robust development of human myelopoiesis and showed a strong human innate immune response to viral and bacterial infections. The authors also observed a functional human NK cell development that could be attributed to the production of IL-15 by the human monocytes developed in these mice (41). However, these mice eventually developed severe anemia as a result of the high human cell engraftment, which resulted in shorter lifespan of these mice. This was due to the destruction of mouse RBCs as a result of the enhanced human myeloid cell function (41).

Another innate immune cell population that displays suboptimal development in immunodeficient mice are the NK cells. Early effort to boost NK cell formation was demonstrated when BRG mice engrafted with human HSPCs were injected

with recombinant IL-15/IL-15-receptor complexes that induced extensive NK cell proliferation and differentiation. This resulted in accumulation of $CD16^+KIR^+$ NK cells in these mice (70). This study led to the generation of NOG-*IL15* mice (see **Table 1**). The high levels of circulating IL-15 cytokines in these mice were shown to support the survival of human peripheral blood-derived NK cells (46). Interestingly, human *SIRPA* and *IL15* knock-in RAG (SRG-*IL15*) mice have more physiological levels of IL-15 but upon poly I:C stimulation these mice can express high levels of IL-15, resulting in an efficient functional human NK cells that can mediate antibody-dependent cellular cytotoxicity (40). Furthermore, compared to the all above innate immune cells, human $CD123^+$ plasmacytoid and myeloid $CD11c^+$ DCs are efficiently developed in most immunodeficient mouse models (71) even in NOD-*Scid* mice (72) without the requirement of exogenous human cytokines or the use of additional human transgene expression. Nevertheless, administration of recombinant FLT3-L was demonstrated to induce HSPC differentiation towards fully functional human $CD141^+$ and $CD1c^+$ DCs (73). As $CD141^+$ DCs are endowed with the capacity to cross-present viral antigens after their uptake of necrotic virus-infected cells, produce high levels of IL-12, and induce Th1 responses, $CD1c^+$ DCs, on the other hand, play a key role in driving adaptive immune responses to extracellular pathogens, owing to their capacity to promote Th2 and Th17 responses. Both DC fractions can serve important bridges for the elaboration of more complex human immune response studies in these immunodeficient mice.

CAN HUMAN B CELLS FULLY DEVELOP IN MICE?

Recent efforts to further enhance human immune system development and function in humanized mouse models have focused on improving specific innate immune cell lineages. An early study using mice with partial immunodeficiency has shown incomplete human B cell development, with large proportion of engrafted B cells having an immature (CD10+) and B1-type phenotype (CD5+) (74). Subsequent reports that used NSG mice demonstrated improved B cell function including class switching in which the VH-DH-JH composition was seen to be similar to the mice engrafted with cord blood cells. In these mice, the production of IgM, IgA, and IgG antibodies were also observed (75, 76). The general view in the field appears to be that B cell maturation in human HSPC engrafted mice increases with time, reaching up to 60% of the B cells having a mature phenotype ($CD20^+CD10^-$) after 24 weeks (57). Human *de novo* B cells isolated from NSG mice have also been shown to undergo somatic hypermutation (77). In fact, several studies have observed the production of antigen-specific human IgM and IgG antibodies in humanized mice in response to infection or immunization with varied degrees of responses (74, 78–80). Some of these humanized mice generated functional neutralizing antibodies in a model of Dengue virus infection (79). Furthermore, these mice have also been used to test the selection process of human autoreactive B cells. Indeed, Lang and colleagues used BRG mice that express a synthetic self-antigen specific constant region of human Igκ and demonstrated that developing human autoreactive (κ+) B cells undergo central tolerance by both receptor editing as well as clonal deletion (81). Other studies have supported this notion of autoreactive human B cell development, therefore confirming the intact central B cell tolerance in immunodeficient mice (82, 83). Therefore, humanized mouse models could also be used to elucidate some aspects of the molecular mechanisms of autoimmunity.

To further enhance class switching and somatic hypermutation, Flavell and colleagues generated immunodeficient $Rag2^{-/-}Il2r\gamma^{-/-}$ mice in which *IL6* was integrated into its orthologous mouse locus (39). These RGSKI-*IL6* mice expressing human IL-6 not only allowed the improvement of thymopoiesis and peripheral T cell reconstitution but also showed significant increase in total IgG and antigen-specific IgG levels. The authors of this work also observed higher frequencies of memory and IgG producing B cells. Interestingly, once these mice were challenged with ovalbumin (OVA), the OVA-specific antibodies displayed high frequency of somatic mutations (39). This mouse model then led to the development of the MISTRG6 mice, that enabled further improvement of B cell development. Consequently, MISTRG6 mouse model was used to investigate the entire spectrum of human plasma cell neoplasia (42). Recently, IL-6 transgenic strain was created on the NSG background using human *IL6* BAC (NSG-IL6) (33). These NSG-*IL6* mice engrafted with human HSPCs displayed increased levels of $CD3^+$ and Th17 T cells compared to NSG mice. In addition, higher plasma levels of IgM and IgG were observed in these mice (33). In summary, human IL6-expressing immunodeficient mice could be a useful tool to evaluate the elicitation of antigen-specific antibody responses.

HUMAN THYMOPOIESIS: A PROPER T SELECTION WITH HUMAN LEUKOCYTE ANTIGEN-RESTRICTED IMMUNE RESPONSES IN MICE?

Human conventional T cells' response relies on the ability of their TCRs to recognize a specific peptide (and subsequently bind) in the context of an MHC molecule that is solely expressed in the thymus during their initial developmental phase. To examine human immune responses in immunodeficient mice, leukocytes can be engrafted by intravenous or intraperitoneal injection of human peripheral blood mononuclear cells (PBMCs) into mice. This model is less laborious and time consuming compared to the *de novo* generation of leukocytes through BM xenotransplantation using HSPCs. Although human leukocytes, in particular T cells, can be found circulating in the murine peripheral blood within days following the injection; however, this process can lead to a rapid xenogeneic graft *versus* host disease (GvHD) (84, 85). One of the major drawbacks of this system includes the limited T cell repertoire and prevalence of uncontrolled B cell activation with the production of human

xenoreactive antibodies (86, 87). However, some of these concerns can be circumvented by using new mouse strains that are for the major histocompatibility complex (MHC) class I/II [such as, NSG-$B2M^{null}$ and NSG-$(K^bD^b)^{null}(IA^{null})$ mice]. Injection of human PBMCs into these strains enables long-term engraftment of human $CD4^+$ and $CD8^+$ T cells without causing acute GvHD (49, 51). Alternatively, xenogeneic GvHD in immunodeficient mice can be eliminated by a more classical approach that enables the reconstitution of human immune system including T cells through the transplantation of HSPCs. This method enables the generation of human T cells that can be detected in murine thymus at around 12 weeks, depending upon the level of human cell engraftment in the mouse BM. However, this process can be accelerated when human HSPC transplantation is performed in new-born mouse (88–90), that perhaps occurs as a result of a faster seeding of primitive precursors in the mouse thymus. On the other hand, adult NSG-SGM3 mice also have improved T cell development (69). The exact mechanism and the particular changes responsible for this improved lymphopoiesis remain unknown. It is worth to note that this process still requires an extended developmental time, but interestingly different human T cell populations and diverse T cell receptor variable beta chain (TCR Vβ) repertoire can be generated in these mice (89, 91, 92). However, one of the caveats in human T cell development in humanized NSG murine microenvironment is that Th1, Th2, and Th17 cells were found at very low levels (51, 93), although the quantification of these cells was performed following an *in vitro* stimulation.

Development of human T cells in NOD-*Scid* and Rag-deficient derived mice undergoes maturation as well as selection *via* recognition of mouse MHC molecules expressed by thymus mouse epithelial cells and DCs. As these human T cells are educated and restricted solely to murine MHC, therefore they are not suitable for studies investigating T cell responses with human antigen presenting cells (APCs), which express human MHC receptors. To acquire the immune sensitivities with high diversity for human cells, education of T cells must be performed by the human MHC molecules in a murine environment. This major issue was addressed by transplanting human HSPCs isolated from human fetal liver into NOD-*Scid* mice that were implanted with human liver and thymus (under the mouse kidney capsule) from the same fetus (BLT model). This BLT model demonstrated that human T cells developed in the human thymus (implanted in mouse) were human Human Leukocyte antigen and generated immune response, with development of a mucosal system similar to humans (94–96). Despite these advantages, this model is still time consuming and technically difficult, and mice can still develop xenogeneic GvHD (97). In a recent development, NSG-*HLA-A2/HHD* mice expressing human HLA class I showed the development of virus-specific HLA-A2-restricted human T cell responses to Dengue virus infection (79). In a subsequent study, this mouse model generated functionally HLA-restricted cytotoxic T cells against Epstein–Barr virus (EBV) virus, therefore suggesting that the recognition and education of human HLA can take place in NSG mouse with a functional thymus. Furthermore, interferon gamma (IFNγ)-producing human T cells against multiple EBV HLA-A2 epitopes were observed showing similar patterns of reactivity to that detected in human infections, including the development of $CD8^+CD45RO^+$ memory T cells (51). These two reports described that HLA expressed in murine thymus allows human T cells to be positively selected and in fact these cells can induce HLA-restricted immune responses in murine environment. There are other HLA-transgenic immunodeficient mice that have recently been established, such as NSG mice expressing HLA-A*0201 and A*2402. This study showed that human cytotoxic T cells upon stimulation with Wilms' tumor 1 (WT1) peptide in *in vitro* conditions, produced IFNγ and cytotoxic activity against leukemic cells in an antigen-specific and HLA-restricted manner (52). In another report, NSG-*HLA-A2/DR1* mice were used to study human antiviral adaptive responses during hepatotropic virus infection (98). It was reported that these mice allowed the engraftment of functional human Th1, Th2, and Th17 T cells, and some of these T cells were polyfunctional effector cells ($CD62L^-$ $CCR7^-$HLA-DR^+). Interestingly, these cells secreted a variety of cytokines such as IFNγ, tumor necrosis factor alpha (TNFα), IL-4 and IL-17 (98). The HLA-*DR4* single knock-in mice (DRAG mice; NRG-*HLA-A2-DR4*; see **Table 1**) offer further improved polyfunctionality and antigen specificity of effector $CD8^+$ cells over the HLA-A2 NSG mice (99). Interestingly, these mice were also shown to allow the generation of high levels of $CD4^+CXCR5^+PD1^+$ T follicular helper cells that were efficiently disseminated into the gut-associated lymphoid tissues (100). Therefore, HLA class I and II transgenic NSG mouse models may serve as a preclinical tool to develop effective immunotherapy against human malignancies.

IS MORE HUMANIZATION OF IMMUNODEFICIENT MODELS NEEDED?

Even though the above mentioned immunodeficient mouse models have been useful, they still present various challenges. One of the biggest caveats is cross-species differences that exist between the engrafted human cells and mouse microenvironment (including immune-microenvironment) they reside in, and how this may influence various environmental clues that mediate cell–cell interactions, hematopoietic cell homing, survival, and expansion, among others. Recently, integration of biomaterials with immunodeficient mouse models has enabled researchers to generate a more physiological human microenvironment namely 'humanized ectopic scaffold niche', that provides architectural support for cell attachment and subsequent human BM-like tissue development. These humanized scaffold-based approaches can potentially enable the researchers to closely mimic the multicellular aspects of the human bone in a mouse model (101–104). This approach can provide an important tool to potentially generate patient-specific human microenvironment including endothelium in immunodeficient mice that can be used to unravel not only the role of human

tumor microenvironments, disease pathology but can potentially be used to gather physiological response to various immunotherapies.

PROFILING OF CANCER IMMUNOTHERAPIES IN MOUSE MODELS WITH HUMAN IMMUNO-MICROENVIRONMENT

Immunotherapies are considered to be the cornerstone of current therapeutic strategies against cancer, along with surgery, radiation, cytotoxic chemotherapy, and targeted drug therapy (105). Current strategies of immunotherapies are summarized in **Figure 2**. Intrinsic therapeutic modulation of the adaptive and innate components of the human immune system to enhance recognition that subsequently leads to improved response against tumors is widely adopted strategy in the clinical fight targeting different types of cancers. There are more than 3,000 types of cancer immunotherapies either in development or currently assessed in clinical trials, that include antibody-based immunotherapy, oncolytic virus therapy, cytokine therapy, cellular therapy (CAR-T, CAR-NK, TCR-T and DC-based), cancer vaccines and the combination of immunotherapy that targets multiple immune components (106). Although, these therapies focused on unleashing the immune system are considered a breakthrough; however, durable clinical responses only occur in a subset of patients. Furthermore, the development of novel therapeutics is tightly restricted by the use of human samples before moving to clinical trials, which is generally slow and costly. Therefore, considerable scientific resources are still needed in preclinical research to identify novel and improved approaches to cancer cell-specific immune response as well as testing of therapeutic strategies. Over the last half century, syngeneic mouse tumor models were the major *in vivo* systems used for understanding cancer immunology and associated immunotherapies. However, the paradigm shifted with the dramatic advances in our understanding of the interactions between tumor development and the immune microenvironment. Furthermore, immunotherapies such as immunomodulatory agents do not always react with mouse molecules due to cross species barriers. Together all these factors led to the increased humanization of immunodeficient mouse models in which both the human immune cells and human tumors are cohabiting with each other. However, these models are quite complex, and the fact that obtaining human immune cells as well as the malignant cells from the same patient still remains difficult, researchers are currently using HLA mismatched cord blood derived HSPCs or healthy donor derived PBMCs for humanization along with patient derived tumor cells or cancer cell lines (**Figure 1**). Even with these caveats, the use of these humanized models has emerged as an invaluable tool in providing a system not only to study normal human immune system interactions with the malignant cellular components but have also accelerated the development of the cancer immunotherapies. These preclinical model systems have enabled to better predict the clinical outcomes of immunotherapy regimens before moving to clinical trials.

FIRST GENERATION HUMANIZED MOUSE MODELS

To date, one of the most popular immunodeficient mouse models used in the field of cancer biology as well as immuno-oncology is the NSG mice. These models have enabled the generation of patient derived xenografts (PDXs) particularly in hematological malignancies where they have played an instrumental role in the identification and understanding of leukemia initiating cells (101, 107) (**Figure 1**). Furthermore, these humanized mouse models have enabled personalized tests on the sensitivity and specificity of the tumors to many therapeutic regimens. Among various cellular immunotherapies, anti-CD19 directed CAR-T cells that were shown to eliminate the $CD19^{+}$ B cell leukemia in NSG PDX model, resulted in prolonged survival of these mice, and this data set the basis for the first clinical trial and later on, approval of the first CAR T cell products by the FDA (108). In a recent development focusing on cellular therapies that could pave the way for off-the shelf cellular therapies, Li and colleagues used NSG mice to demonstrate the feasibility of using the next generation iPSC-derived CAR-NK cells as a treatment option for mesothelin-over expressing ovarian tumors (109). Monoclonal antibody (92R) tested in NSG mice to target T cell acute lymphoblastic leukemia cells strongly inhibited tumor growth *via* binding to the C-C chemokine receptor type 9 (CCR9) N-terminal domain. This leukemia killing response was observed in a model with compromised NK and complement activities, suggesting that other mechanisms (such as phagocytosis or apoptosis) might also be playing a role in tumor destruction (110).

One of the major drawbacks of these PDXs established in NSG model is the lack of immunosurveillance by the host. Considerable efforts that led to the generation of NSG-PBMC models have been used widely to study single and combination therapies. For example, IgG-based BCMA-T cell bispecific antibody (EM801) targeting B cell maturation antigen (BCMA) induced myeloma cell death by autologous T cells (111). Anti-tumor activity of ICBs (nivolumab, pembrolizumab, atezolizumab, cetuximab, and urelumab) was also observed in the PBMC-humanized mouse models (112–114). Interestingly, the differences in tumor growth were not significantly different between mono- and combination therapies; however, the humanized model was suitable to develop mechanistic studies that supported this combination in the subsequent clinical studies (113). This initial experience represented the first proof of concept report to demonstrate that immunotherapy combination strategies can be modeled in preclinical settings involving humanized mouse models. On the other hand, multiple DC-based vaccine tested in NSG-PBMC mouse model enabled assessment of melanoma antigen recognized by T cells-1 (MART-1)-specific immune responses and suppressive functions on melanoma cells (115). Although the ease of generating these

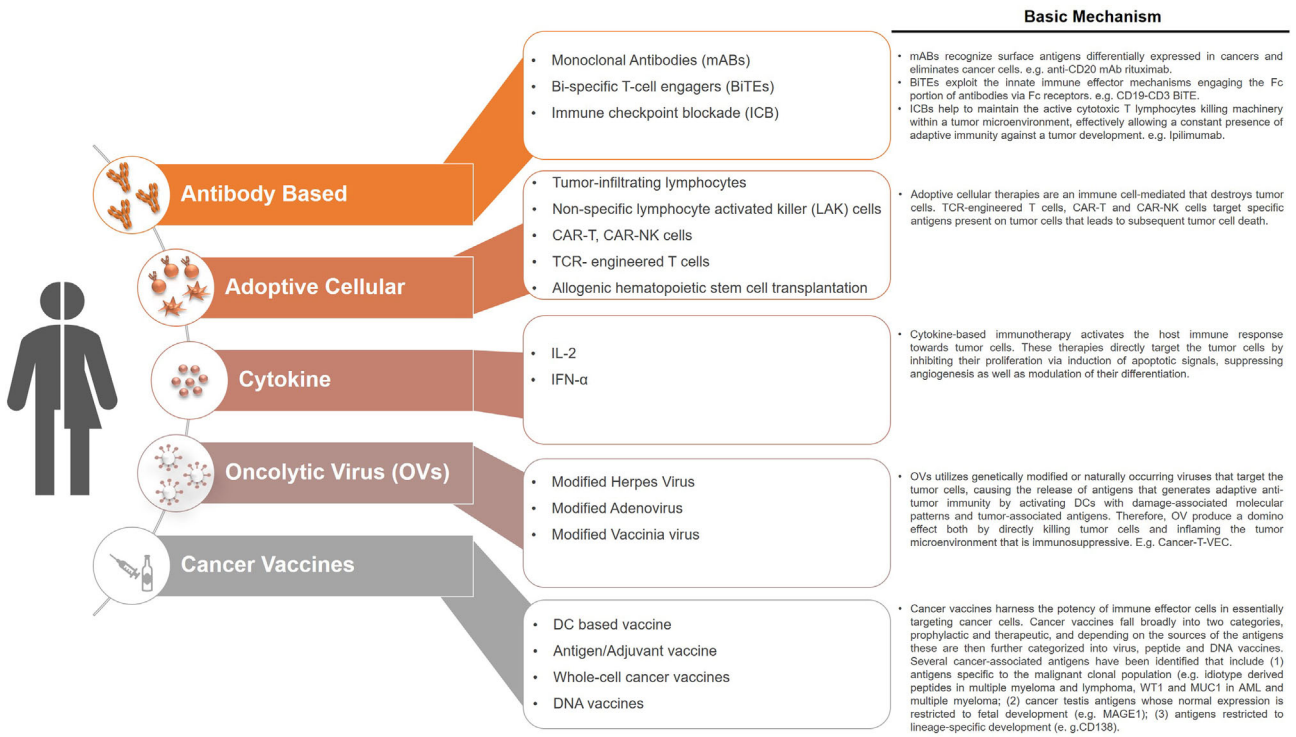

FIGURE 2 | Current immunotherapeutic strategies in cancers. Cancer immunotherapies target the patients own immune system by restoring and stimulating various immune components that ultimately had the potential to inhibit cancer growth and/or eradicate cancer. The various types of immunotherapies that are currently being used in the clinic or are under development include antibody-based immunotherapy, oncolytic virus therapy, cytokine therapy, cellular therapy, cancer vaccines. These therapies are also being used as combination therapies that target multiple immune components or with other established therapeutic options such as chemotherapy.

mice allows for their use in tumor-bearing PDXs, challenges arise with regard to the onset of xenogeneic robust GvHD, which occurs concomitant with T cell expansion (116, 117). The limited window of time (approximately 2–3 weeks) for taking observation could enable the investigations into T cell-mediated anti-tumor mechanisms; however, the use of NSG or NOG MHC knockout mice or alternatively xenotransplantation of purified $CD8^+$ T cells may enable long-term immune response studies (49, 118, 119). Using ICB-based (PD-1) immunotherapy in these mouse models, specific $CD8^+$ T cell population was identified that produced anti-tumor effect in an HLA restricted manner without needing to worry about xenogeneic GvHD (120).

HSPC-engrafted human immune system (HIS) models provide powerful tools for long-term studies and are increasingly being used for understanding T cell-mediated immunotherapy mechanisms. The caveat of this HSPC-HIS (NSG and NOG) model is the biased differentiation of HSPCs towards the lymphoid lineage, with the limited development of myeloid cells. However, despite this limitation, HSPC-HIS mice have successfully provided a model system to study T cell-dependent immunotherapy mechanisms (such as blocking PD-1, CTLA-4 alone or in combination with oncolytic viruses) and benefit from long experimental time scales (121–123). In cord blood derived HSPC-generated humanized mouse model, PD-1 blocking (using nivolumab) inhibited the growth of MDAMB-231 tumor cells and CRC172 tumor cells by enhancing anti-tumor T cell response, increasing GrB^+ or $IFN\gamma^+$ $CD8^+$ cells in tumors and reducing frequency of Treg and myeloid cells. However, combination of histone deacetylase (HDAC) inhibitors OKI-179 and nivolumab further inhibited cancer cell growth, therefore indicating that HDAC inhibitors could improve anti-tumor immune responses in cancers (124). In another study, a combination of anti-CD278 mAb and cyclophosphamide controlled the growth of breast cancer in NSG humanized mice. Administration of a neutralizing anti-CD278 mAb reduced human Treg proportions and numbers and improved $CD4^+$ T cell proliferation therefore highlighting the crucial implication of innate immunity in treatment efficacy, opening new perspectives for the treatment of breast cancer (125). In another study, transplantation of allogeneic but HLA partially matched donor HSPCs and tumor cells (non-small cell lung cancer, sarcoma, bladder cancer, and triple-negative breast cancer) in NSG mice demonstrated significant tumor growth delay following pembrolizumab (anti-PD-1) therapy (121). In a different approach, Haworth and colleagues reconstituted NSG

mice with human HSPCs that lead to the generation of matured human $CD3^+$ T cells, which can be isolated, genetically modified and then reinfused into the same mice (89). It is worth to note that no clinical symptoms of GvHD were observed in these mice, and therefore this model might represent a better system for long term evaluation of cellular immunotherapies such as CAR-T cells.

SECOND GENERATION HUMANIZED MOUSE MODELS

Until recently, the development of more balanced humanization by improving the differentiation and survival of various human immune cell populations has been a major goal; the function of these human immune cells in murine system was overlooked. These issues have led to the development of so called "second generation" immunodeficient models that express human transgenes. These models (*e.g.* NSG-SGM3, NOG-EXL, NSG HLA-A2 and MISTRG) not only allow more myeloid and NK cell development apart from lymphoid reconstitution, but also enable the function of engrafted human immune cells thus, improving the utility and translatability of these models in immunotherapy related studies (**Figure 1**). NOG-IL2 transgenic mice were able to overcome the previous problems and recapitulated the clinical responses of patient-derived TILs (126). In a preclinical model using HSPC transplanted humanized BRGS mice, Capasso and colleagues established breast cancer and colon cancer PDXs, and showed strong suppressive function of PD-1 blockade that resulted in tumor growth inhibition with increased CD8 IFNγ^+ tumor infiltrating T cells (124). Transgenic mice that express the human HLA-A2 allele, commonly detected in the Caucasian population, were developed to study immunologic interactions between human T cells and tumor cells (51, 127). Studies investigating the antigen-specific HLA-restricted response against Epstein–Barr virus (EBV)-associated tumors, found $CD8^+$ (and $CD4^+$) effector-to-target ratio-dependent cytotoxicity against EBV-infected lymphomas (128). The humanized transgenic NSG-SGM3 mice have shown enhanced human Treg cell differentiation, and these Treg cells were functional and were able to suppress the proliferation of T cells in PDX generated from HSPCs (93). Notably, similar data of T cell suppression by Tregs was reported in PDX models for autoimmune conditions such as aplastic anemia (129).

MISTRG mice that have recently been developed show robust differentiation of human innate as well as adaptive immune cells and have been used to study acute myeloid leukemia and diffuse large B-cell lymphoma (41, 130). Interestingly, human macrophages generated in MISTRG infiltrated a human tumor xenograft in a manner resembling that observed in tumors obtained from patients (41). Therefore, these MISTRG mice recapitulate the role of macrophages in tumor development and fulfil a critical need for models that enable study of the interaction between human tumors and human innate immune microenvironment. The major advantage of these humanized systems is the ability to observe the immune surveillance against human cancer tissues. However, one caveat of these models is that the reconstituted human immune system lacks physiological maturity due to the absence of human thymus tissue. To address these concerns, BLT mouse model developed, harbors an almost intact functional human immune system therefore providing a powerful tool to study cancer immunotherapy (131). In a recent study, implantation of human lung tissue into NSG mice pre-humanized with BM/liver/thymus resulted in robust antigen-specific humoral and T cell responses against cytomegalovirus infection (132). In a different study, Jin and colleagues developed an autologous NSG BLT-based model with a fully competent human immune system. Following the humanization, mice were transplanted with edited fetal HSPCs that recapitulated human B-ALL like disease. This model system was used to test autologous anti-CD19-CAR T cells. This preclinical model, though complex in its generation, was highly adapted to evaluate human CAR T cell efficacy, resistance and toxicity (133). These second-generation humanization strategies provide a promising tool for understanding the tumor immune microenvironment interactions and enable greater translational potential and expanded opportunities for therapeutic evaluation. However, BLT mice do require human fetal tissues which are difficult to source especially if needed in large quantities. However, surplus neonatal tissue can be a good viable alternative that can be used for mouse humanization (134).

FUTURE DEVELOPMENTS

Although immunodeficient mouse models along with increased humanization have been instrumental in gaining understanding of the cancer biology and develop various targeted immunotherapies, these models do have limitations that need to be addressed to create more appropriate model system that will fulfil the need of current and future research. There is an urgent need to develop new strategies that will enable us to further the humanization of these mice, particularly focusing on the development of comprehensive and functional human immune system. One of the ways to improve on the current sub-optimal development of human immune cells is to further characterize and identify the cytokines as well as growth factors that do not cross react between mouse and human. It is also important to identify and integrate novel approaches that would enable autologous experiments, where malignant tissues and immune cells from the same individual are used, that would provide more accurate understanding of disease progression, tumor-immune interactions and efficacy of personalized therapeutic options. Improving the humanization of these mice will also enable us to shed more light on the basic tumor immunology, particularly the roles of the immunosuppressive tumor immune-microenvironment and tumor neoantigens that often shape the development of cancer and influence therapeutic efficacy. Altogether, having an appropriate humanized preclinical model will enable speedier assessment of the efficacy and safety of

novel therapeutic approaches and will ultimately provide a faster bench to beside transition.

AUTHOR CONTRIBUTIONS

All authors listed have made a substantial, direct, and intellectual contribution to the work and approved it for publication.

FUNDING

This work was supported by the Francis Crick Institute (to DB), which receives its core funding from Cancer Research UK (FC0010045), the UK Medical Research Council (FC0010045), and the Wellcome Trust (FC001045) and by the UK Biotechnology and Biological Sciences Research Council (BB/S017097/1; to FA-A). We would like to thank Blood Cancer UK for their support to SAM.

REFERENCES

1. Becker AJ, Mc CE, Till JE. Cytological demonstration of the clonal nature of spleen colonies derived from transplanted mouse marrow cells. *Nature* (1963) 197:452–4. doi: 10.1038/197452a0
2. Buick RN, Till JE, McCulloch EA. Colony assay for proliferative blast cells circulating in myeloblastic leukaemia. *Lancet* (1977) 1(8016):862–3. doi: 10.1016/s0140-6736(77)92818-5
3. McCulloch EA. Stem cells in normal and leukemic hemopoiesis (Henry Stratton Lecture, 1982). *Blood* (1983) 62(1):1–13. doi: 10.1182/blood.V62.1.1.1
4. Moore MA, Williams N, Metcalf D. In vitro colony formation by normal and leukemic human hematopoietic cells: characterization of the colony-forming cells. *J Natl Cancer Inst* (1973) 50(3):603–23. doi: 10.1093/jnci/50.3.603
5. Metcalf D, Moore MA, Warner NL. Colony formation in vitro by myelomonocytic leukemic cells. *J Natl Cancer Inst* (1969) 43(4):983–1001. doi: 10.1093/jnci/43.4.983
6. Griffin JD, Lowenberg B. Clonogenic cells in acute myeloblastic leukemia. *Blood* (1986) 68(6):1185–95. doi: 10.1182/blood.V68.6.1185.1185
7. Dicke KA, Spitzer G, Ahearn MJ. Colony formation in vitro by leukaemic cells in acute myelogenous leukaemia with phytohaemagglutinin as stimulating factor. *Nature* (1976) 259(5539):129–30. doi: 10.1038/259129a0
8. Civin CI, Strauss LC, Brovall C, Fackler MJ, Schwartz JF, Shaper JH. Antigenic analysis of hematopoiesis. III. A hematopoietic progenitor cell surface antigen defined by a monoclonal antibody raised against KG-1a cells. *J Immunol* (1984) 133(1):157–65.
9. Bhatia M, Wang JC, Kapp U, Bonnet D, Dick JE. Purification of primitive human hematopoietic cells capable of repopulating immune-deficient mice. *Proc Natl Acad Sci U S A* (1997) 94(10):5320–5. doi: 10.1073/pnas.94.10.5320
10. Cashman JD, Lapidot T, Wang JC, Doedens M, Shultz LD, Lansdorp P, et al. Kinetic evidence of the regeneration of multilineage hematopoiesis from primitive cells in normal human bone marrow transplanted into immunodeficient mice. *Blood* (1997) 89(12):4307–16. doi: 10.1182/blood.V89.12.4307
11. Hogan CJ, Shpall EJ, Keller G. Differential long-term and multilineage engraftment potential from subfractions of human CD34+ cord blood cells transplanted into NOD/SCID mice. *Proc Natl Acad Sci U S A* (2002) 99(1):413–8. doi: 10.1073/pnas.012336799
12. Baum CM, Weissman IL, Tsukamoto AS, Buckle AM, Peault B. Isolation of a candidate human hematopoietic stem-cell population. *Proc Natl Acad Sci U S A* (1992) 89(7):2804–8. doi: 10.1073/pnas.89.7.2804
13. Murray L, Chen B, Galy A, Chen S, Tushinski R, Uchida N, et al. Enrichment of human hematopoietic stem cell activity in the CD34+Thy-1+Lin- subpopulation from mobilized peripheral blood. *Blood* (1995) 85(2):368–78. doi: 10.1182/blood.V85.2.368.368
14. Majeti R, Park CY, Weissman IL. Identification of a hierarchy of multipotent hematopoietic progenitors in human cord blood. *Cell Stem Cell* (2007) 1(6):635–45. doi: 10.1016/j.stem.2007.10.001
15. Notta F, Doulatov S, Laurenti E, Poeppl A, Jurisica I, Dick JE. Isolation of single human hematopoietic stem cells capable of long-term multilineage engraftment. *Science* (2011) 333(6039):218–21. doi: 10.1126/science.1201219
16. Guenechea G, Gan OI, Dorrell C, Dick JE. Distinct classes of human stem cells that differ in proliferative and self-renewal potential. *Nat Immunol* (2001) 2(1):75–82. doi: 10.1038/83199
17. Larochelle A, Vormoor J, Hanenberg H, Wang JC, Bhatia M, Lapidot T, et al. Identification of primitive human hematopoietic cells capable of repopulating NOD/SCID mouse bone marrow: implications for gene therapy. *Nat Med* (1996) 2(12):1329–37. doi: 10.1038/nm1296-1329
18. Bhatia M, Bonnet D, Murdoch B, Gan OI, Dick JE. A newly discovered class of human hematopoietic cells with SCID-repopulating activity. *Nat Med* (1998) 4(9):1038–45. doi: 10.1038/2023
19. Danet GH, Luongo JL, Butler G, Lu MM, Tenner AJ, Simon MC, et al. C1qRp defines a new human stem cell population with hematopoietic and hepatic potential. *Proc Natl Acad Sci U S A* (2002) 99(16):10441–5. doi: 10.1073/pnas.162104799
20. Wang J, Kimura T, Asada R, Harada S, Yokota S, Kawamoto Y, et al. SCID-repopulating cell activity of human cord blood-derived CD34- cells assured by intra-bone marrow injection. *Blood* (2003) 101(8):2924–31. doi: 10.1182/blood-2002-09-2782
21. Anjos-Afonso F, Currie E, Palmer HG, Foster KE, Taussig DC, Bonnet D. CD34(-) cells at the apex of the human hematopoietic stem cell hierarchy have distinctive cellular and molecular signatures. *Cell Stem Cell* (2013) 13(2):161–74. doi: 10.1016/j.stem.2013.05.025
22. Bosma GC, Custer RP, Bosma MJ. A severe combined immunodeficiency mutation in the mouse. *Nature* (1983) 301(5900):527–30. doi: 10.1038/301527a0
23. Mosier DE, Gulizia RJ, Baird SM, Wilson DB. Transfer of a functional human immune system to mice with severe combined immunodeficiency. *Nature* (1988) 335(6187):256–9. doi: 10.1038/335256a0
24. Shultz LD, Schweitzer PA, Christianson SW, Gott B, Schweitzer IB, Tennent B, et al. Multiple defects in innate and adaptive immunologic function in NOD/LtSz-scid mice. *J Immunol* (1995) 154(1):180–91.
25. Takenaka K, Prasolava TK, Wang JC, Mortin-Toth SM, Khalouei S, Gan OI, et al. Polymorphism in Sirpa modulates engraftment of human hematopoietic stem cells. *Nat Immunol* (2007) 8(12):1313–23. doi: 10.1038/ni1527
26. Pearson T, Markees TG, Serreze DV, Pierce MA, Marron MP, Wicker LS, et al. Genetic disassociation of autoimmunity and resistance to costimulation blockade-induced transplantation tolerance in nonobese diabetic mice. *J Immunol* (2003) 171(1):185–95. doi: 10.4049/jimmunol.171.1.185
27. Serreze DV, Gaedeke JW, Leiter EH. Hematopoietic stem-cell defects underlying abnormal macrophage development and maturation in NOD/Lt mice: defective regulation of cytokine receptors and protein kinase C. *Proc Natl Acad Sci U S A* (1993) 90(20):9625–9. doi: 10.1073/pnas.90.20.9625
28. Ishikawa F, Yasukawa M, Lyons B, Yoshida S, Miyamoto T, Yoshimoto G, et al. Development of functional human blood and immune systems in NOD/SCID/IL2 receptor {gamma} chain(null) mice. *Blood* (2005) 106(5):1565–73. doi: 10.1182/blood-2005-02-0516
29. Ito M, Hiramatsu H, Kobayashi K, Suzue K, Kawahata M, Hioki K, et al. NOD/SCID/gamma(c)(null) mouse: an excellent recipient mouse model for engraftment of human cells. *Blood* (2002) 100(9):3175–82. doi: 10.1182/blood-2001-12-0207
30. Shultz LD, Lyons BL, Burzenski LM, Gott B, Chen X, Chaleff S, et al. Human lymphoid and myeloid cell development in NOD/LtSz-scid IL2R gamma null mice engrafted with mobilized human hemopoietic stem cells. *J Immunol* (2005) 174(10):6477–89. doi: 10.4049/jimmunol.174.10.6477
31. Prochazka M, Gaskins HR, Shultz LD, Leiter EH. The nonobese diabetic scid mouse: model for spontaneous thymomagenesis associated with immunodeficiency. *Proc Natl Acad Sci U S A* (1992) 89(8):3290–4. doi: 10.1073/pnas.89.8.3290

32. Saito Y, Shultz LD, Ishikawa F. Understanding Normal and Malignant Human Hematopoiesis Using Next-Generation Humanized Mice. *Trends Immunol* (2020) 41(8):706–20. doi: 10.1016/j.it.2020.06.004
33. Shultz LD, Keck J, Burzenski L, Jangalwe S, Vaidya S, Greiner DL, et al. Humanized mouse models of immunological diseases and precision medicine. *Mamm Genome* (2019) 30(5-6):123–42. doi: 10.1007/s00335-019-09796-2
34. Theocharides AP, Rongvaux A, Fritsch K, Flavell RA, Manz MG. Humanized hemato-lymphoid system mice. *Haematologica* (2016) 101 (1):5–19. doi: 10.3324/haematol.2014.115212
35. Goldman JP, Blundell MP, Lopes L, Kinnon C, Di Santo JP, Thrasher AJ. Enhanced human cell engraftment in mice deficient in RAG2 and the common cytokine receptor gamma chain. *Br J Haematol* (1998) 103 (2):335–42. doi: 10.1046/j.1365-2141.1998.00980.x
36. Willinger T, Rongvaux A, Takizawa H, Yancopoulos GD, Valenzuela DM, Murphy AJ, et al. Human IL-3/GM-CSF knock-in mice support human alveolar macrophage development and human immune responses in the lung. *Proc Natl Acad Sci U S A* (2011) 108(6):2390–5. doi: 10.1073/pnas.1019682108
37. Strowig T, Rongvaux A, Rathinam C, Takizawa H, Borsotti C, Philbrick W, et al. Transgenic expression of human signal regulatory protein alpha in Rag2-/-gamma(c)-/- mice improves engraftment of human hematopoietic cells in humanized mice. *Proc Natl Acad Sci U S A* (2011) 108(32):13218–23. doi: 10.1073/pnas.1109769108
38. Rongvaux A, Willinger T, Takizawa H, Rathinam C, Auerbach W, Murphy AJ, et al. Human thrombopoietin knockin mice efficiently support human hematopoiesis in vivo. *Proc Natl Acad Sci U S A* (2011) 108(6):2378–83. doi: 10.1073/pnas.1019524108
39. Yu H, Borsotti C, Schickel JN, Zhu S, Strowig T, Eynon EE, et al. A novel humanized mouse model with significant improvement of class-switched, antigen-specific antibody production. *Blood* (2017) 129(8):959–69. doi: 10.1182/blood-2016-04-709584
40. Herndler-Brandstetter D, Shan L, Yao Y, Stecher C, Plajer V, Lietzenmayer M, et al. Humanized mouse model supports development, function, and tissue residency of human natural killer cells. *Proc Natl Acad Sci U S A* (2017) 114(45):E9626–E34. doi: 10.1073/pnas.1705301114
41. Rongvaux A, Willinger T, Martinek J, Strowig T, Gearty SV, Teichmann LL, et al. Development and function of human innate immune cells in a humanized mouse model. *Nat Biotechnol* (2014) 32(4):364–72. doi: 10.1038/nbt.2858
42. Das R, Strowig T, Verma R, Koduru S, Hafemann A, Hopf S, et al. Microenvironment-dependent growth of preneoplastic and malignant plasma cells in humanized mice. *Nat Med* (2016) 22(11):1351–7. doi: 10.1038/nm.4202
43. Nicolini FE, Cashman JD, Hogge DE, Humphries RK, Eaves CJ. NOD/SCID mice engineered to express human IL-3, GM-CSF and Steel factor constitutively mobilize engrafted human progenitors and compromise human stem cell regeneration. *Leukemia* (2004) 18(2):341–7. doi: 10.1038/sj.leu.2403222
44. Ito R, Takahashi T, Katano I, Kawai K, Kamisako T, Ogura T, et al. Establishment of a human allergy model using human IL-3/GM-CSF-transgenic NOG mice. *J Immunol* (2013) 191(6):2890–9. doi: 10.4049/jimmunol.1203543
45. Hanazawa A, Ito R, Katano I, Kawai K, Goto M, Suemizu H, et al. Generation of Human Immunosuppressive Myeloid Cell Populations in Human Interleukin-6 Transgenic NOG Mice. *Front Immunol* (2018) 9:152. doi: 10.3389/fimmu.2018.00152
46. Katano I, Nishime C, Ito R, Kamisako T, Mizusawa T, Ka Y, et al. Long-term maintenance of peripheral blood derived human NK cells in a novel human IL-15- transgenic NOG mouse. *Sci Rep* (2017) 7(1):17230. doi: 10.1038/s41598-017-17442-7
47. Pearson T, Shultz LD, Miller D, King M, Laning J, Fodor W, et al. Non-obese diabetic-recombination activating gene-1 (NOD-Rag1 null) interleukin (IL)-2 receptor common gamma chain (IL2r gamma null) null mice: a radioresistant model for human lymphohaematopoietic engraftment. *Clin Exp Immunol* (2008) 154(2):270–84. doi: 10.1111/j.1365-2249.2008.03753.x
48. Covassin L, Laning J, Abdi R, Langevin DL, Phillips NE, Shultz LD, et al. Human peripheral blood CD4 T cell-engrafted non-obese diabetic-scid IL2rgamma(null) H2-Ab1 (tm1Gru) Tg (human leucocyte antigen D-related 4) mice: a mouse model of human allogeneic graft-versus-host disease. *Clin Exp Immunol* (2011) 166(2):269–80. doi: 10.1111/j.1365-2249.2011.04462.x
49. Brehm MA, Kenney LL, Wiles MV, Low BE, Tisch RM, Burzenski L, et al. Lack of acute xenogeneic graft- versus-host disease, but retention of T-cell function following engraftment of human peripheral blood mononuclear cells in NSG mice deficient in MHC class I and II expression. *FASEB J* (2019) 33(3):3137–51. doi: 10.1096/fj.201800636R
50. Lee J, Brehm MA, Greiner D, Shultz LD, Kornfeld H. Engrafted human cells generate adaptive immune responses to Mycobacterium bovis BCG infection in humanized mice. *BMC Immunol* (2013) 14:53. doi: 10.1186/1471-2172-14-53
51. Shultz LD, Saito Y, Najima Y, Tanaka S, Ochi T, Tomizawa M, et al. Generation of functional human T-cell subsets with HLA-restricted immune responses in HLA class I expressing NOD/SCID/IL2r gamma(null) humanized mice. *Proc Natl Acad Sci U S A* (2010) 107(29):13022–7. doi: 10.1073/pnas.1000475107
52. Najima Y, Tomizawa-Murasawa M, Saito Y, Watanabe T, Ono R, Ochi T, et al. Induction of WT1-specific human CD8+ T cells from human HSCs in HLA class I Tg NOD/SCID/IL2rgKO mice. *Blood* (2016) 127(6):722–34. doi: 10.1182/blood-2014-10-604777
53. Ono R, Watanabe T, Kawakami E, Iwasaki M, Tomizawa-Murasawa M, Matsuda M, et al. Co-activation of macrophages and T cells contribute to chronic GVHD in human IL-6 transgenic humanised mouse model. *EBioMedicine* (2019) 41:584–96. doi: 10.1016/j.ebiom.2019.02.001
54. Wunderlich M, Chou FS, Link KA, Mizukawa B, Perry RL, Carroll M, et al. AML xenograft efficiency is significantly improved in NOD/SCID-IL2RG mice constitutively expressing human SCF, GM-CSF and IL-3. *Leukemia* (2010) 24(10):1785–8. doi: 10.1038/leu.2010.158
55. Cosgun KN, Rahmig S, Mende N, Reinke S, Hauber I, Schafer C, et al. Kit regulates HSC engraftment across the human-mouse species barrier. *Cell Stem Cell* (2014) 15(2):227–38. doi: 10.1016/j.stem.2014.06.001
56. Chen Q, He F, Kwang J, Chan JK, Chen J. GM-CSF and IL-4 stimulate antibody responses in humanized mice by promoting T, B, and dendritic cell maturation. *J Immunol* (2012) 189(11):5223–9. doi: 10.4049/jimmunol.1201789
57. Lang J, Kelly M, Freed BM, McCarter MD, Kedl RM, Torres RM, et al. Studies of lymphocyte reconstitution in a humanized mouse model reveal a requirement of T cells for human B cell maturation. *J Immunol* (2013) 190 (5):2090–101. doi: 10.4049/jimmunol.1202810
58. Jangalwe S, Shultz LD, Mathew A, Brehm MA. Improved B cell development in humanized NOD-scid IL2Rgamma(null) mice transgenically expressing human stem cell factor, granulocyte-macrophage colony-stimulating factor and interleukin-3. *Immun Inflammation Dis* (2016) 4(4):427–40. doi: 10.1002/iid3.124
59. Hu Z, Van Rooijen N, Yang YG. Macrophages prevent human red blood cell reconstitution in immunodeficient mice. *Blood* (2011) 118(22):5938–46. doi: 10.1182/blood-2010-11-321414
60. Chen Q, Khoury M, Chen J. Expression of human cytokines dramatically improves reconstitution of specific human-blood lineage cells in humanized mice. *Proc Natl Acad Sci U S A* (2009) 106(51):21783–8. doi: 10.1073/pnas.0912274106
61. Hu Z, Yang YG. Full reconstitution of human platelets in humanized mice after macrophage depletion. *Blood* (2012) 120(8):1713–6. doi: 10.1182/blood-2012-01-407890
62. Burlak C, Twining LM, Rees MA. Terminal sialic acid residues on human glycophorin A are recognized by porcine kupffer cells. *Transplantation* (2005) 80(3):344–52. doi: 10.1097/01.tp.0000162974.94890.9f
63. Jin R, Greenwald A, Peterson MD, Waddell TK. Human monocytes recognize porcine endothelium via the interaction of galectin 3 and alpha-GAL. *J Immunol* (2006) 177(2):1289–95. doi: 10.4049/jimmunol.177.2.1289
64. Rahmig S, Kronstein-Wiedemann R, Fohgrub J, Kronstein N, Nevmerzhitskaya A, Bornhauser M, et al. Improved Human Erythropoiesis and Platelet Formation in Humanized NSGW41 Mice. *Stem Cell Rep* (2016) 7(4):591–601. doi: 10.1016/j.stemcr.2016.08.005
65. Sharma Y, Astle CM, Harrison DE. Heterozygous kit mutants with little or no apparent anemia exhibit large defects in overall hematopoietic stem cell function. *Exp Hematol* (2007) 35(2):214–20. doi: 10.1016/j.exphem.2006.10.001

66. Song Y, Rongvaux A, Taylor A, Jiang T, Tebaldi T, Balasubramanian K, et al. A highly efficient and faithful MDS patient-derived xenotransplantation model for pre-clinical studies. *Nat Commun* (2019) 10:366. doi: 10.1038/s41467-018-08166-x
67. Li Y, Chen Q, Zheng D, Yin L, Chionh YH, Wong LH, et al. Induction of functional human macrophages from bone marrow promonocytes by M-CSF in humanized mice. *J Immunol* (2013) 191(6):3192–9. doi: 10.4049/jimmunol.1300742
68. Wang JC, Lapidot T, Cashman JD, Doedens M, Addy L, Sutherland DR, et al. High level engraftment of NOD/SCID mice by primitive normal and leukemic hematopoietic cells from patients with chronic myeloid leukemia in chronic phase. *Blood* (1998) 91(7):2406–14. doi: 10.1182/blood.V91.7.2406
69. Wunderlich M, Chou FS, Sexton C, Presicce P, Chougnet CA, Aliberti J, et al. Improved multilineage human hematopoietic reconstitution and function in NSGS mice. *PLoS One* (2018) 13(12):e0209034. doi: 10.1371/journal.pone.0209034
70. Huntington ND, Legrand N, Alves NL, Jaron B, Weijer K, Plet A, et al. IL-15 trans-presentation promotes human NK cell development and differentiation in vivo. *J Exp Med* (2009) 206(1):25–34. doi: 10.1084/jem.20082013
71. Helft J, Anjos-Afonso F, van der Veen AG, Chakravarty P, Bonnet D, Reis e Sousa C. Dendritic Cell Lineage Potential in Human Early Hematopoietic Progenitors. *Cell Rep* (2017) 20(3):529–37. doi: 10.1016/j.celrep.2017.06.075
72. Palucka AK, Gatlin J, Blanck JP, Melkus MW, Clayton S, Ueno H, et al. Human dendritic cell subsets in NOD/SCID mice engrafted with CD34+ hematopoietic progenitors. *Blood* (2003) 102(9):3302–10. doi: 10.1182/blood-2003-02-0384
73. Ding Y, Wilkinson A, Idris A, Fancke B, O'Keeffe M, Khalil D, et al. FLT3-ligand treatment of humanized mice results in the generation of large numbers of CD141+ and CD1c+ dendritic cells in vivo. *J Immunol* (2014) 192(4):1982–9. doi: 10.4049/jimmunol.1302391
74. Novelli EM, Ramirez M, Leung W, Civin CI. Human hematopoietic stem/progenitor cells generate CD5+ B lymphoid cells in NOD/SCID mice. *Stem Cells* (1999) 17(5):242–52. doi: 10.1002/stem.170242
75. Brainard DM, Seung E, Frahm N, Cariappa A, Bailey CC, Hart WK, et al. Induction of robust cellular and humoral virus-specific adaptive immune responses in human immunodeficiency virus-infected humanized BLT mice. *J Virol* (2009) 83(14):7305–21. doi: 10.1128/JVI.02207-08
76. Quach TD, Hopkins TJ, Holodick NE, Vuyyuru R, Manser T, Bayer RL, et al. Human B-1 and B-2 B Cells Develop from Lin-CD34+CD38lo Stem Cells. *J Immunol* (2016) 197(10):3950–8. doi: 10.4049/jimmunol.1600630
77. Chang H, Biswas S, Tallarico AS, Sarkis PT, Geng S, Panditrao MM, et al. Human B-cell ontogeny in humanized NOD/SCID gammac(null) mice generates a diverse yet auto/poly- and HIV-1-reactive antibody repertoire. *Genes Immun* (2012) 13(5):399–410. doi: 10.1038/gene.2012.16
78. Biswas S, Chang H, Sarkis PT, Fikrig E, Zhu Q, Marasco WA. Humoral immune responses in humanized BLT mice immunized with West Nile virus and HIV-1 envelope proteins are largely mediated via human CD5+ B cells. *Immunology* (2011) 134(4):419–33. doi: 10.1111/j.1365-2567.2011.03501.x
79. Jaiswal S, Pearson T, Friberg H, Shultz LD, Greiner DL, Rothman AL, et al. Dengue virus infection and virus-specific HLA-A2 restricted immune responses in humanized NOD-scid IL2rgammanull mice. *PLoS One* (2009) 4(10):e7251. doi: 10.1371/journal.pone.0007251
80. Sango K, Joseph A, Patel M, Osiecki K, Dutta M, Goldstein H. Highly active antiretroviral therapy potently suppresses HIV infection in humanized Rag2-/-gammac-/- mice. *AIDS Res Hum Retroviruses* (2010) 26(7):735–46. doi: 10.1089/aid.2009.0136
81. Lang J, Ota T, Kelly M, Strauch P, Freed BM, Torres RM, et al. Receptor editing and genetic variability in human autoreactive B cells. *J Exp Med* (2016) 213(1):93–108. doi: 10.1084/jem.20151039
82. Cantaert T, Schickel JN, Bannock JM, Ng YS, Massad C, Oe T, et al. Activation-Induced Cytidine Deaminase Expression in Human B Cell Precursors Is Essential for Central B Cell Tolerance. *Immunity* (2015) 43(5):884–95. doi: 10.1016/j.immuni.2015.10.002
83. Ippolito GC, Hoi KH, Reddy ST, Carroll SM, Ge X, Rogosch T, et al. Antibody repertoires in humanized NOD-scid-IL2Rgamma(null) mice and human B cells reveals human-like diversification and tolerance checkpoints in the mouse. *PLoS One* (2012) 7(4):e35497. doi: 10.1371/journal.pone.0035497
84. King M, Pearson T, Shultz LD, Leif J, Bottino R, Trucco M, et al. A new Hu-PBL model for the study of human islet alloreactivity based on NOD-scid mice bearing a targeted mutation in the IL-2 receptor gamma chain gene. *Clin Immunol* (2008) 126(3):303–14. doi: 10.1016/j.clim.2007.11.001
85. Pearson T, Greiner DL, Shultz LD. Creation of "humanized" mice to study human immunity. *Curr Protoc Immunol* (2008). 81:15.21.1–15.21.21 doi: 10.1002/0471142735.im1521s81. Chapter 15:Unit 15 21.
86. Abedi MR, Christensson B, Islam KB, Hammarstrom L, Smith CI. Immunoglobulin production in severe combined immunodeficient (SCID) mice reconstituted with human peripheral blood mononuclear cells. *Eur J Immunol* (1992) 22(3):823–8. doi: 10.1002/eji.1830220329
87. Garcia S, Dadaglio G, Gougeon ML. Limits of the human-PBL-SCID mice model: severe restriction of the V beta T-cell repertoire of engrafted human T cells. *Blood* (1997) 89(1):329–36. doi: 10.1182/blood.V89.1.329.329_329_336
88. Brehm MA, Cuthbert A, Yang C, Miller DM, DiIorio P, Laning J, et al. Parameters for establishing humanized mouse models to study human immunity: analysis of human hematopoietic stem cell engraftment in three immunodeficient strains of mice bearing the IL2rgamma(null) mutation.. *Clin Immunol* (2010) 135(1):84–98. doi: 10.1016/j.clim.2009.12.008
89. Haworth KG, Ironside C, Norgaard ZK, Obenza WM, Adair JE, Kiem HP. In Vivo Murine-Matured Human CD3(+) Cells as a Preclinical Model for T Cell-Based Immunotherapies. *Mol Ther Methods Clin Dev* (2017) 6:17–30. doi: 10.1016/j.omtm.2017.05.004
90. Traggiai E, Chicha L, Mazzucchelli L, Bronz L, Piffaretti JC, Lanzavecchia A, et al. Development of a human adaptive immune system in cord blood cell-transplanted mice. *Science* (2010) 304(55667):104–7. doi: 10.1126/science.1093933
91. Brugman MH, Wiekmeijer AS, van Eggermond M, Wolvers-Tettero I, Langerak AW, de Haas EF, et al. Development of a diverse human T-cell repertoire despite stringent restriction of hematopoietic clonality in the thymus. *Proc Natl Acad Sci U S A* (2015) 112(44):E6020–7. doi: 10.1073/pnas.1519118112
92. Hiramatsu H, Nishikomori R, Heike T, Ito M, Kobayashi K, Katamura K, et al. Complete reconstitution of human lymphocytes from cord blood CD34 + cells using the NOD/SCID/gammacnull mice model. *Blood* (2003) 102(3):873–80. doi: 10.1182/blood-2002-09-2755
93. Billerbeck E, Barry WT, Mu K, Dorner M, Rice CM, Ploss A. Development of human CD4+FoxP3+ regulatory T cells in human stem cell factor-, granulocyte-macrophage colony-stimulating factor-, and interleukin-3-expressing NOD-SCID IL2Rgamma(null) humanized mice. *Blood* (2011) 117(11):3076–86. doi: 10.1182/blood-2010-08-301507
94. Denton PW, Nochi T, Lim A, Krisko JF, Martinez-Torres F, Choudhary SK, et al. IL-2 receptor gamma-chain molecule is critical for intestinal T-cell reconstitution in humanized mice. *Mucosal Immunol* (2012) 5(5):555–66. doi: 10.1038/mi.2012.31
95. Lan P, Tonomura N, Shimizu A, Wang S, Yang YG. Reconstitution of a functional human immune system in immunodeficient mice through combined human fetal thymus/liver and CD34+ cell transplantation. *Blood* (2006) 108(2):487–92. doi: 10.1182/blood-2005-11-4388
96. Melkus MW, Estes JD, Padgett-Thomas A, Gatlin J, Denton PW, Othieno FA, et al. Humanized mice mount specific adaptive and innate immune responses to EBV and TSST-1. *Nat Med* (2006) 12(11):1316–22. doi: 10.1038/nm1431
97. Greenblatt MB, Vrbanac V, Tivey T, Tsang K, Tager AM, Aliprantis AO. Graft versus host disease in the bone marrow, liver and thymus humanized mouse model. *PLoS One* (2012) 7(9):e44664. doi: 10.1371/journal.pone.0044664
98. Billerbeck E, Horwitz JA, Labitt RN, Donovan BM, Vega K, Budell WC, et al. Characterization of human antiviral adaptive immune responses during hepatotropic virus infection in HLA-transgenic human immune system mice. *J Immunol* (2013) 191(4):1753–64. doi: 10.4049/jimmunol.1201518
99. Majji S, Wijayalath W, Shashikumar S, Pow-Sang L, Villasante E, Brumeanu TD, et al. Differential effect of HLA class-I versus class-II transgenes on human T and B cell reconstitution and function in NRG mice. *Sci Rep* (2016) 6:28093. doi: 10.1038/srep28093
100. Allam A, Majji S, Peachman K, Jagodzinski L, Kim J, Ratto-Kim S, et al. TFH cells accumulate in mucosal tissues of humanized-DRAG mice and are highly permissive to HIV-1. *Sci Rep* (2015) 5:10443. doi: 10.1038/srep10443

101. Abarrategi A, Mian SA, Passaro D, Rouault-Pierre K, Grey W, Bonnet D. Modeling the human bone marrow niche in mice: From host bone marrow engraftment to bioengineering approaches. *J Exp Med* (2018) 215(3):729–43. doi: 10.1084/jem.20172139
102. Abarrategi A, Foster K, Hamilton A, Mian SA, Passaro D, Gribben J, et al. Versatile humanized niche model enables study of normal and malignant human hematopoiesis. *J Clin Invest* (2017) 127(2):543–8. doi: 10.1172/JCI89364
103. Lee J, Li M, Milwid J, Dunham J, Vinegoni C, Gorbatov R, et al. Implantable microenvironments to attract hematopoietic stem/cancer cells. *Proc Natl Acad Sci U S A* (2012) 109(48):19638–43. doi: 10.1073/pnas.1208384109
104. Reinisch A, Hernandez DC, Schallmoser K, Majeti R. Generation and use of a humanized bone-marrow-ossicle niche for hematopoietic xenotransplantation into mice. *Nat Protoc* (2017) 12(10):2169–88. doi: 10.1038/nprot.2017.088
105. Waldman AD, Fritz JM, Lenardo MJ. A guide to cancer immunotherapy: from T cell basic science to clinical practice. *Nat Rev Immunol* (2020) 20: 651–68 doi: 10.1038/s41577-020-0306-5
106. Yang Y. Cancer immunotherapy: harnessing the immune system to battle cancer. *J Clin Invest* (2015) 125(9):3335–7. doi: 10.1172/JCI83871
107. Meyer LH, Debatin KM. Diversity of human leukemia xenograft mouse models: implications for disease biology. *Cancer Res* (2011) 71(23):7141–4. doi: 10.1158/0008-5472.CAN-11-1732
108. Barrett DM, Zhao Y, Liu X, Jiang S, Carpenito C, Kalos M, et al. Treatment of advanced leukemia in mice with mRNA engineered T cells. *Hum Gene Ther* (2011) 22(12):1575–86. doi: 10.1089/hum.2011.070
109. Li Y, Hermanson DL, Moriarity BS, Kaufman DS. Human iPSC-Derived Natural Killer Cells Engineered with Chimeric Antigen Receptors Enhance Anti-tumor Activity. *Cell Stem Cell* (2018) 23(2):181–92>e5. doi: 10.1016/j.stem.2018.06.002
110. Somovilla-Crespo B, Martin Monzon MT, Vela M, Corraliza-Gorjon I, Santamaria S, Garcia-Sanz JA, et al. 92R Monoclonal Antibody Inhibits Human CCR9(+) Leukemia Cells Growth in NSG Mice Xenografts. *Front Immunol* (2018) 9:77. doi: 10.3389/fimmu.2018.00077
111. Seckinger A, Delgado JA, Moser S, Moreno L, Neuber B, Grab A, et al. Target Expression, Generation, Preclinical Activity, and Pharmacokinetics of the BCMA-T Cell Bispecific Antibody EM801 for Multiple Myeloma Treatment. *Cancer Cell* (2017) 31(3):396–410. doi: 10.1016/j.ccell.2017.02.002
112. Hartkopf AD, Taran FA, Wallwiener M, Walter CB, Kramer B, Grischke EM, et al. PD-1 and PD-L1 Immune Checkpoint Blockade to Treat Breast Cancer. *Breast Care (Basel)* (2016) 11(6):385–90. doi: 10.1159/000453569
113. Sanmamed MF, Rodriguez I, Schalper KA, Onate C, Azpilikueta A, Rodriguez-Ruiz ME, et al. Nivolumab and Urelumab Enhance Antitumor Activity of Human T Lymphocytes Engrafted in Rag2-/-IL2Rgammanull Immunodeficient Mice. *Cancer Res* (2015) 75(17):3466–78. doi: 10.1158/0008-5472.CAN-14-3510
114. Lutterbuese R, Raum T, Kischel R, Hoffmann P, Mangold S, Rattel B, et al. T cell-engaging BiTE antibodies specific for EGFR potently eliminate KRAS- and BRAF-mutated colorectal cancer cells. *Proc Natl Acad Sci U S A* (2010) 107(28):12605–10. doi: 10.1073/pnas.1000976107
115. Hu Z, Xia J, Fan W, Wargo J, Yang YG. Human melanoma immunotherapy using tumor antigen-specific T cells generated in humanized mice. *Oncotarget* (2016) 7(6):6448–59. doi: 10.18632/oncotarget.7044
116. Ali N, Flutter B, Sanchez Rodriguez R, Sharif-Paghaleh E, Barber LD, Lombardi G, et al. Xenogeneic graft-versus-host-disease in NOD-scid IL-2Rgammanull mice display a T-effector memory phenotype. *PLoS One* (2012) 7(8):e44219. doi: 10.1371/journal.pone.0044219
117. Alcantar-Orozco EM, Gornall H, Baldan V, Hawkins RE, Gilham DE. Potential limitations of the NSG humanized mouse as a model system to optimize engineered human T cell therapy for cancer. *Hum Gene Ther Methods* (2013) 24(5):310–20. doi: 10.1089/hgtb.2013.022
118. Inoue M, Senju S, Hirata S, Irie A, Baba H, Nishimura Y. An in vivo model of priming of antigen-specific human CTL by Mo-DC in NOD/Shi-scid IL2rgamma(null) (NOG) mice. *Immunol Lett* (2009) 126(1-2):67–72. doi: 10.1016/j.imlet.2009.08.001
119. Yaguchi T, Kobayashi A, Inozume T, Morii K, Nagumo H, Nishio H, et al. Human PBMC-transferred murine MHC class I/II-deficient NOG mice enable long-term evaluation of human immune responses. *Cell Mol Immunol* (2018) 15(11):953–62. doi: 10.1038/cmi.2017.106
120. Ashizawa T, Iizuka A, Nonomura C, Kondou R, Maeda C, Miyata H, et al. Antitumor Effect of Programmed Death-1 (PD-1) Blockade in Humanized the NOG-MHC Double Knockout Mouse. *Clin Cancer Res* (2017) 23(1):149–58. doi: 10.1158/1078-0432.CCR-16-0122
121. Wang M, Yao LC, Cheng M, Cai D, Martinek J, Pan CX, et al. Humanized mice in studying efficacy and mechanisms of PD-1-targeted cancer immunotherapy. *FASEB J* (2018) 32(3):1537–49. doi: 10.1096/fj.201700740R
122. Kuryk L, Moller AW, Jaderberg M. Combination of immunogenic oncolytic adenovirus ONCOS-102 with anti-PD-1 pembrolizumab exhibits synergistic antitumor effect in humanized A2058 melanoma huNOG mouse model. *Oncoimmunology* (2019) 8(2):e1532763. doi: 10.1080/2162402X.2018.1532763
123. Tsoneva D, Minev B, Frentzen A, Zhang Q, Wege AK, Szalay AA. Humanized Mice with Subcutaneous Human Solid Tumors for Immune Response Analysis of Vaccinia Virus-Mediated Oncolysis. *Mol Ther Oncolytics* (2017) 5:41–61. doi: 10.1016/j.omto.2017.03.001
124. Capasso A, Lang J, Pitts TM, Jordan KR, Lieu CH, Davis SL, et al. Characterization of immune responses to anti-PD-1 mono and combination immunotherapy in hematopoietic humanized mice implanted with tumor xenografts. *J Immunother Cancer* (2019) 7(1):37. doi: 10.1186/s40425-019-0518-z
125. Burlion A, Ramos RN, Kc P, Sendeyo K, Corneau A, Menetrier-Caux C, et al. A novel combination of chemotherapy and immunotherapy controls tumor growth in mice with a human immune system. *Oncoimmunology* (2019) 8 (7):1596005. doi: 10.1080/2162402X.2019.1596005
126. Jespersen H, Lindberg MF, Donia M, Soderberg EMV, Andersen R, Keller U, et al. Clinical responses to adoptive T-cell transfer can be modeled in an autologous immune-humanized mouse model. *Nat Commun* (2017) 8 (1):707. doi: 10.1038/s41467-017-00786-z
127. Strowig T, Gurer C, Ploss A, Liu YF, Arrey F, Sashihara J, et al. Priming of protective T cell responses against virus-induced tumors in mice with human immune system components. *J Exp Med* (2009) 206(6):1423–34. doi: 10.1084/jem.20081720
128. Ruhl J, Citterio C, Engelmann C, Haigh T, Dzionek A, Dreyer J, et al. Heterologous prime-boost vaccination protects against EBV antigen-expressing lymphomas. *J Clin Invest* (2019) 129(5):2071–87. doi: 10.1172/JCI125364
129. Lim SP, Costantini B, Mian SA, Perez Abellan P, Gandhi S, Martinez Llordella M, et al. Treg sensitivity to FasL and relative IL-2 deprivation drive idiopathic aplastic anemia immune dysfunction. *Blood* (2020) 136 (7):885–97. doi: 10.1182/blood.2019001347
130. Stelling A, Hashwah H, Bertram K, Manz MG, Tzankov A, Muller A. The tumor suppressive TGF-beta/SMAD1/S1PR2 signaling axis is recurrently inactivated in diffuse large B-cell lymphoma. *Blood* (2018) 131(20):2235–46. doi: 10.1182/blood-2017-10-810630
131. Smith DJ, Lin LJ, Moon H, Pham AT, Wang X, Liu S, et al. Propagating Humanized BLT Mice for the Study of Human Immunology and Immunotherapy. *Stem Cells Dev* (2016) 25(24):1863–73. doi: 10.1089/scd.2016.0193
132. Wahl A, De C, Abad Fernandez M, Lenarcic EM, Xu Y, Cockrell AS, et al. Precision mouse models with expanded tropism for human pathogens. *Nat Biotechnol* (2019) 37(10):1163–73. doi: 10.1038/s41587-019-0225-9
133. Jin CH, Xia J, Rafiq S, Huang X, Hu Z, Zhou X, et al. Modeling anti-CD19 CAR T cell therapy in humanized mice with human immunity and autologous leukemia. *EBioMedicine* (2019) 39:173–81. doi: 10.1016/j.ebiom.2018.12.013
134. Brown ME, Zhou Y, McIntosh BE, Norman IG, Lou HE, Biermann M, et al. Humanized Mouse Model Generated Using Surplus Neonatal Tissue. *Stem Cell Rep.* (2018) doi: 10.1016/j.stemcr.2018.02.011

Conflict of Interest: The authors declare that the research was conducted in the absence of any commercial or financial relationships that could be construed as a potential conflict of interest.

Copyright © 2021 Mian, Anjos-Afonso and Bonnet. This is an open-access article distributed under the terms of the Creative Commons Attribution License (CC BY). The use, distribution or reproduction in other forums is permitted, provided the original author(s) and the copyright owner(s) are credited and that the original publication in this journal is cited, in accordance with accepted academic practice. No use, distribution or reproduction is permitted which does not comply with these terms.

GLOSSARY

Prkdc	gene encoding for protein kinase DNA-activated catalytic subunit which is required for the non-homologous end joining pathway of DNA repair during V(D)J recombination. Mutation of *Prkdc* leads to V(D)J recombination defects.
Sirpa	gene encoding for signal regulatory protein alpha; SIRPα acts as inhibitory receptor and interacts with the transmembrane protein CD47 also called the "don't eat me" signal. This interaction negatively controls effector function of innate immune cells such as host cell phagocytosis.
Rag1 or *Rag2*	recombination activating gene 1 or 2; the protein encoded by these genes are involved in antibody and T-cell receptor V(D)J recombination.
SCF	stem cell factor, is a cytokine that binds to the c-KIT receptor, and it plays a role in the regulation of HSCs in the niche by increasing the survival and self-renewal of HSCs.
GM-CSF	granulocyte macrophage colony stimulating factor; it stimulates stem cells to produce granulocytes and monocytes.
SRα	Simian virus 40 early promoter and the R segment and part of the U5 sequence of the long terminal repeat of human T cell leukemia virus type 1
CSF2	gene encoding for GM-CSF
FLT3-L	fms-related tyrosine kinase 3 ligand; is a hematopoietic cytokine; it stimulates the survival, proliferation, and differentiation of various blood cell progenitors.
CAR-T, CAR-NK	chimeric antigen receptor T-cell, chimeric antigen receptor NK-cell; CARs are receptor proteins that have been engineered to give T or NK cells the new ability to target a specific protein. The receptors are chimeric because they combine both antigen-binding and T/NK-cell activating functions into a single receptor.

frontiers in Immunology

MINI REVIEW
published: 18 February 2021
doi: 10.3389/fimmu.2021.643544

Advances in Human Immune System Mouse Models for Personalized Treg-Based Immunotherapies

Isabelle Serr[1,2], *Maria Kral*[1,2], *Martin G. Scherm*[1,2] *and Carolin Daniel*[1,2,3]*

[1] Group Immune Tolerance in Type 1 Diabetes, Helmholtz Diabetes Center at Helmholtz Zentrum München, Institute of Diabetes Research, Munich, Germany, [2] Deutsches Zentrum für Diabetesforschung (DZD), Neuherberg, Germany, [3] Division of Clinical Pharmacology, Department of Medicine IV, Ludwig-Maximilians-Universität München, Munich, Germany

Immunodeficient mice engrafted with a functional human immune system [Human immune system (HIS) mice] have paved the way to major advances for personalized medicine and translation of immune-based therapies. One prerequisite for advancing personalized medicine is modeling the immune system of individuals or disease groups in a preclinical setting. HIS mice engrafted with peripheral blood mononuclear cells have provided fundamental insights in underlying mechanisms guiding immune activation vs. regulation in several diseases including cancer. However, the development of Graft-vs.-host disease restrains relevant long-term studies in HIS mice. Alternatively, engraftment with hematopoietic stem cells (HSCs) enables mimicking different disease stages, however, low frequencies of HSCs in peripheral blood of adults impede engraftment efficacy. One possibility to overcome those limitations is the use of patient-derived induced pluripotent stem cells (iPSCs) reprogrammed into HSCs, a challenging process which has recently seen major advances. Personalized HIS mice bridge research in mice and human diseases thereby facilitating the translation of immunomodulatory therapies. Regulatory T cells (Tregs) are important mediators of immune suppression and thereby contribute to tumor immune evasion, which has made them a central target for cancer immunotherapies. Importantly, studying Tregs in the human immune system *in vivo* in HIS mice will help to determine requirements for efficient Treg-targeting. In this review article, we discuss advances on personalized HIS models using reprogrammed iPSCs and review the use of HIS mice to study requirements for efficient targeting of human Tregs for personalized cancer immunotherapies.

Keywords: HIS mice, Treg, cancer immunotherapy, personalized medicine, iPSC-derived HSCs, microRNA

OPEN ACCESS

Edited by:
Tim Willinger,
Karolinska Institutet, Sweden

Reviewed by:
Takeshi Takahashi,
Central Institute for Experimental Animals, Japan
Yan Li,
Nanjing University, China
Tomoyuki Yamaguchi,
Nozaki Tokushukai Hospital, Japan

****Correspondence:***
Carolin Daniel
carolin.daniel@helmholtz-muenchen.de

Specialty section:
This article was submitted to Cancer Immunity and Immunotherapy, a section of the journal Frontiers in Immunology

Received: *18 December 2020*
Accepted: *26 January 2021*
Published: *18 February 2021*

Citation:
Serr I, Kral M, Scherm MG and Daniel C (2021) Advances in Human Immune System Mouse Models for Personalized Treg-Based Immunotherapies. Front. Immunol. 12:643544. doi: 10.3389/fimmu.2021.643544

INTRODUCTION

With the discovery of checkpoint inhibitors and more recently, the use of chimeric antigen-receptor T cells, immunotherapies have taken center stage in oncology. The common goal for cancer immunotherapies is to boost the immune system to attack and destroy cancerous cells. The gold-standard for pre-clinical testing of cancer therapies has long been the use of xenograft models, where human cancer cell lines are engrafted into immunodeficient hosts. However, both development and evaluation of immunotherapies requires the presence of a functional immune system closely mirroring the immune reaction in the human disease. Immunodeficient

mice engrafted with a functional human immune system [human immune system (HIS) mice] have opened up new ways of evaluating immunotherapies directly *in vivo* in a pre-clinical setting. One main obstacle remaining in cancer therapy is intra-tumor heterogeneity. The use of personalized medicine offers a promising approach to tackle this major hurdle and HIS mice engrafted with patient-derived hematopoietic cells are an important tool for the development of personalized medicine.

HUMAN IMMUNE SYSTEM MOUSE MODELS FOR IMMUNOTHERAPIES

Since the discovery that severe combined immunodeficiency (*Prkcd*^{scid} or SCID) mice, engrafted with human hematopoietic stem cells (HSCs) or human peripheral blood mononuclear cells (PBMCs), can develop a human immune system (1), researchers are constantly working on improving xenoengraftment in such HIS mice to study human diseases. Advancements have been made especially regarding background strain, immunodeficiency mutation as well as engraftment method and material, thereby considerably improving engraftment efficacy (2). For example, mice on the NOD background present with the highest engraftment efficacy due to a polymorphism in the gene *Sirpa*, encoding the signal regulatory protein alpha (*Sirpa*) that shows enhanced interaction with human CD47 on hematopoietic cells, thereby preventing their phagocytosis by macrophages (3).

Moreover, to overcome human T cell xeno-reactivity directed against murine MHC molecules, strains of immunodeficient mice lacking murine MHC class I and class II were developed (4, 5). We have used murine MHC class II deficient NOD-*scid* IL2Rgamma^{null} (NSG)-HLA-DQ8 transgenic mice engrafted with fresh human cord blood (CB) HSCs and demonstrated a high engraftment efficacy in peripheral blood of these animals (6). Importantly, we identified autoreactive disease-relevant insulin-specific CD4^{+}T cells, indicating positive selection on HLA-DQ8 molecules in the thymus of humanized mice (6). The development of T cells with a TCR repertoire recapitulating that of the human donor is essential to analyze T cell responses, also in the setting of cancer immunotherapy. In this regard, in a mouse model for prostate adenocarcinoma, tumor-infiltrating regulatory T cells (Tregs) showed a significant enrichment for distinct TCR specificities targeting an antigen present in healthy pancreatic tissue and not specific to the tumor (7). Therefore, the use of HIS mice with transgenic expression of human HLA molecules will be important to permit for accurate representation of TCR repertoires to study T cell responses to the tumor.

In order to study tumor related immune responses in the human immune system *in vivo,* HIS mice engrafted with cell line-derived (CDX), or patient-derived xenografted tumors (PDXs) have been established (8, 9). Importantly, MART1-TCR-transgenic T cells from humanized mice reconstituted with fetal thymic tissue and human HSCs were able to mount efficient HLA/antigen-dependent anti-melanoma immune responses also after transfer into tumor-bearing recipients (10). Among others, especially the potent checkpoint inhibition with anti-PD1 humanized antibodies has been tested in HIS mice bearing various types of tumors (8, 9, 11), highlighting the value of PDX engrafted HIS models for cancer immunotherapies.

HIS MICE AS PRECLINICAL MODEL FOR THE TREATMENT OF CANCER

Despite the therapeutic advances indicated above, some hurdles remain which hinder efficient and safe implementation of cancer immunotherapies to the patient. During disease progression, genomic instability leads to genetic variations within tumor cells resulting in various distinct populations of cancer cells (12). This intra-tumor heterogeneity is a major obstacle for the success of efficient immunotherapies since it fosters resistance to therapy and leads to highly variable treatment outcomes thereby calling for personalized strategies.

The potential of personalized HIS mouse models for the analysis of patient specific immune responses was demonstrated in a PDX-bearing HIS mouse model based on NSG mice engrafted with autologous tumor-infiltrating T cells and tumor cells from the same patient. Importantly, the autologous T cell transfer was successful in eradicating tumors only in mice generated with material from patients that show a positive autologous cell transfer response in the clinic (13).

To investigate complex immune responses more closely in a preclinical personalized setting, the engraftment of HIS mice with autologous hematopoietic cells and tumor cells from the same patient is required. This can be achieved by engraftment with patient-derived PBMCs. However, such mice are not useful for long-term studies as they can develop severe Graft-vs.-Host-Disease (GvHD) within few weeks upon engraftment. Alternatives for long-term studies are the engraftment with patient-derived HSCs or HSCs originating from fetal liver or CB. Here, engraftment with patient-derived HSCs allows for positive selection of T and B cells based on murine antigens in the thymus and bone marrow, therefore limiting GvHD reactions and further enabling MHC compatibility with the autologous tumor tissue. One drawback of HSC engraftment, however, are low frequencies of HSCs in the peripheral blood of adults without mobilization, which impede an effective reconstitution of the human immune system in HIS mice. Of note, in 2006, a group led by Shinya Yamanaka generated pluripotent stem cells from adult cells. The discovery of these induced pluripotent stem cells (iPSCs) has thenceforward substantially revolutionized the field of translational research and personalized medicine (14) and enabled an unlimited source for the derivation of HSCs (15, 16).

NEXT GENERATION HIS MOUSE MODELS USING IPSC-DERIVED HSC FOR PERSONALIZED MEDICINE

The discovery that iPSCs are able to self-renew and differentiate into any cell type by introducing the reprogramming factors Oct4, Sox2, cMyc, and Klf4 (14, 17) has enabled the development of novel therapeutic strategies in personalized and regenerative medicine. Noteworthy, iPSCs can be derived from different sources of somatic cells, thereby evading the limitations of using

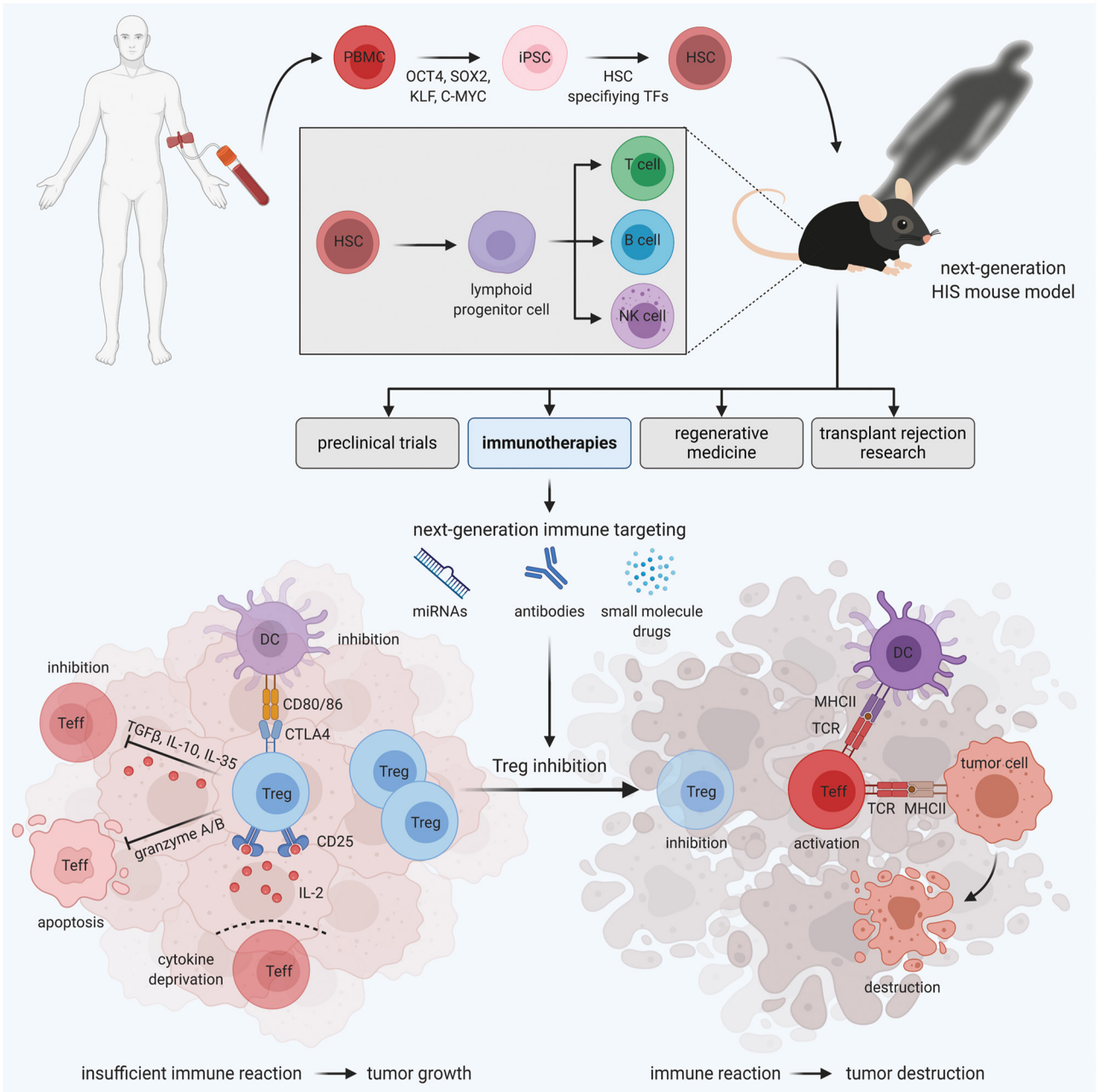

FIGURE 1 | HIS mouse models for personalized Treg-based cancer immunotherapies. Immunodeficient mice engrafted with human PBMC-derived HSCs develop a functional human immune system. These HIS mice are valuable tools for various areas of medical research, including preclinical trials, regenerative medicine, transplant rejection research, and immunotherapies. In the field of immunotherapies, next-generation HIS mouse models enable the development and testing of novel immune targeting strategies, aiming at Treg inhibition to boost the immune reaction against the tumor, in a human immune system *in vivo*.

primary, patient-derived disease affected cells for e.g., disease modeling (18) (**Figure 1**).

Yet, *de novo* generation of functional HSCs from iPSCs for efficient *in vivo* engraftment and multi-lineage potential remains challenging due to the complex nature of hematopoietic ontogeny (19). Recently, methods for the generation of self-renewing hematopoietic stem and progenitor cells with multi-lineage potential after engraftment into immunodeficient hosts have been developed. Although analysis was largely limited to the bone marrow, T and B cells, as well as myeloid cells were also detected in spleen, thymus and peripheral blood, showing a diverse TCR repertoire and functional antibody responses (16, 20). These initial studies highlight the potential use for the generation of HIS mice with iPSC-derived HSCs

(20). Furthermore, hPSCs generated from iPSCs from patients with Diamond-Blackfan anemia (DBA) were used to enable a new therapeutic pathway for the treatment of DBA (21) and immunodeficient mice reconstituted with patient-derived iPSCs were used to develop a drug-testing system for chronic myelomonocytic leukemia (22). Even though still low in number, such studies highlight the vast opportunities and potential therapeutic applications that are offered by iPSC technology, which have to be further explored and improved for future investigations.

Personalized HIS mice reconstituted with tumor cells and autologous patient-derived hematopoietic cells from the same donor are especially important, since they will help to mirror the immunological tumor microenvironment. Importantly, the tumor microenvironment contains immunosuppressive immune subsets [reviewed in (23)], including Tregs that promote tumor immune evasion and hence impede effective antitumor immune responses [reviewed in (24)].

TARGETING TREGS FOR CANCER IMMUNOTHERAPIES IN HIS MICE

Tregs are a specialized suppressive subtype of $CD4^+$T cells that controls the immune response in the periphery and prevents adverse immune reactions and autoimmunity (25). They are characterized by the high expression of the high-affinity interleukin-2 receptor alpha-chain (CD25) and the expression of the transcription factor Foxp3, which is the master regulator of their phenotype and function (26–28). Mutations in the *Foxp3* gene lead to defects in Treg development and function as illustrated by severe multiorgan autoimmunity in patients with the Immunodysregulation polyendocrinopathy enteropathy X-linked (IPEX) syndrome (29) and mice with Scurfy mutations (30). While defects in Treg function and reduced frequencies are associated with autoimmune disorders, increased Treg infiltration into solid tumors and the resulting suppression of effector immune cells are associated with poor prognosis in several types of cancer (31–35). Accordingly, the manipulation of Tregs has gained interest in the field of cancer immunotherapy. However, many aspects of Treg-mediated immune suppression in tumors remain to be determined. Importantly, HIS mice reconstituted with CB HSCs or PBMCs display comparable frequencies of Tregs in various tissues as non-humanized mice (6, 11, 36–40), making them a suitable tool to study human Tregs *in vivo* in a preclinical model (**Figure 1**). Notably, the development of immune cells in NSG mice is skewed to the lymphoid lineage, with cells of the myeloid lineage being under represented, due to limited cross-reactivity of murine cytokines with human hematopoietic cells [reviewed in (41)]. Therefore, novel humanized mouse strains such as NSG-SGM3 mice (42) and others (43) that transgenically express human cytokines and thereby support myeloid cell development have been developed. Importantly, it was demonstrated that NSG-SGM3 mice further support the development of $Foxp3^+$Tregs (44), thereby highlighting the importance of considering different HIS mouse models as basis for pre-clinical studies.

It is now established, that Tregs take residence in various tissues, where they express tissue specific signature genes and exert key non-canonical functions (45–49). Notably, a tissue specific signature has been likewise identified for tumor-infiltrating Tregs. Importantly, the investigation of gene expression of Tregs isolated from breast cancer, colorectal cancer, non-small cell lung cancer and hepatocellular carcinoma in comparison to Tregs from adjacent healthy tissue or peripheral blood identified a tumor-specific Treg gene expression signature (50–52). Some of these signature genes (e.g., *CTLA4*, *GITR*, *CCR4*) are likewise present on peripheral Tregs, whereas their expression is increased in tumor-infiltrating Tregs. Other tumor-specific Treg signature genes (e.g., *CCR8*, *FCRL3*, *IL1R2*) are exclusively expressed on tumor-infiltrating Tregs and absent in their peripheral counterparts. However, the functional consequence of this gene signature in tumor-infiltrating Tregs remains to be determined.

Checkpoint inhibitors have taken center stage in cancer immunotherapy research, since they block signaling through immune inhibitory molecules, especially programmed cell death protein 1 (PD-1) and cytotoxic T-lymphocyte associated protein 4 (CTLA4) (53, 54). Many tumors promote immune evasion by expression of PD-L1, a ligand for PD-1, which is in turn expressed on activated T cells. The engagement of PD-1 by PD-L1 is highly immunosuppressive and leads to T cell anergy and apoptosis. Accordingly, blocking PD-1/PD-L1 signaling has shown great efficacy in various cancers, however in a large proportion of patients PD-1/PD-L1 blockade shows limited success, highlighting the importance of understanding underlying mechanisms of checkpoint inhibitor blockade as well as defining biomarkers to predict treatment success (39). In addition to effector T cells, PD-1 is likewise expressed on Tregs and multiple studies indicate, that PD-1 blockade can increase Treg proliferation and suppression, which could account for the differences in treatment outcome (53). In this regard, the ratio of PD-$1^+$$CD8^+$T cells/PD-$1^+$Tregs in the tumor microenvironment can predict the efficacy of PD-1 blocking therapy (39). While PD-1 blockade has been studied extensively in HIS mice, only few studies investigated the specific effect on Tregs. In line with highly variable treatment outcomes in patients, two studies did not observe changes in tumor-infiltrating Treg frequencies (11, 38), while one study using a combination of anti-PD-1 antibody and CD137 antibody therapies reported an increase in CD8/Treg ratio in tumors of HIS mice xenotransplanted with gastric carcinoma and engrafted with autologous PBMCs from the same donor (55). These studies highlight the strength of personalized HIS mice using xenotransplanted tumors and autologous immune cells for the assessment of treatment outcome.

The identification of tumor-related Treg signature genes is an important step toward more specific targeting of tumor Tregs without affecting the peripheral Treg pool which could potentially lead to autoimmune reactions. CTLA4 mediated tolerization of antigen-presenting cells is an important mechanism of suppression by Tregs. Importantly, CTLA4 blockade has been studied extensively as checkpoint inhibitor in cancer immunotherapy, since CTLA4 is often upregulated by

tumor cells for immune evasion (54). However, the anti-tumor effects of anti-CTLA4 treatment largely rely on the antibody-dependent cellular cytotoxicity (ADCC) mediated depletion of tumor-infiltrating Tregs (56, 57). Here, HIS mice offer an important advantage over classical non-humanized mouse models in the pre-clinical assessment of depleting antibodies. ADCC relies on the interaction of the human IgG Fc region on depleting antibodies with human immune cells and can therefore be studied accurately only in the presence of these cells (58, 59). Anti-CTLA4 antibodies were used to successfully deplete Tregs in fetal liver engrafted HIS mice treated with low-dose IL2 to demonstrate that critical side effects and toxicity of high-dose IL2 treatment are largely dependent on the depletion of Tregs (40). This study highlights the usefulness of HIS mice to study not only treatment efficacy, but also critical side effects of cancer immunotherapy.

Like CTLA4 the chemokine receptor type 4 (CCR4), albeit being expressed on peripheral Tregs, is further upregulated on tumor-infiltrating Tregs, while additionally being expressed on different types of cancer cells. To test anti-CCR4 treatment in a pre-clinical setting, a humanized mouse model for lymphoma based on $CCR4^+$ lymphoma bearing NOG mice reconstituted with human PBMCs was used (60). The treatment with an anti-CCR4 antibody induced robust ADCC leading to reduced tumor mass, accompanied by decreased Treg frequencies in the tumor (60). The latter finding suggests that anti-CCR4 treatment might be more generally applicable also to CCR4-negative tumors, by targeting tumor-infiltrating Tregs. Accordingly, a Phase Ia clinical trial demonstrated efficient Treg depletion by an anti-CCR4 antibody in patients with CCR4-negative solid tumors resulting in stable disease in half of the patients 12 weeks after treatment start (61). However, CCR4 is likewise expressed on peripheral Tregs, albeit at lower levels, leading to the simultaneous depletion of peripheral Tregs by anti-CCR4 treatment. Tumor cells and cells in the tumor microenvironment secrete high amounts of CCL22, a ligand for CCR4, in various cancers (32, 62, 63). Therefore, small molecule CCR4 antagonists might be a safer alternative to block Treg migration to the tumor microenvironment without Treg depletion.

An alternative to Treg depletion is the manipulation of their functional properties. In this regard, glucocorticoid-induced tumor necrosis factor receptor-related protein (GITR) has been studied extensively as a target for cancer immunotherapies. GITR is a coreceptor, which is expressed at low levels on naïve CD4 and CD8 T cells and is upregulated upon activation with $Foxp3^+$Tregs harboring the highest levels of GITR (64, 65). Importantly, targeting GITR for cancer immunotherapy became of interest with the discovery that an agonist anti-GITR antibody could break self-tolerance in mice by making effector T cells resistant to Treg suppression (66). Accordingly, anti-GITR antibody treatment could induce strong anti-tumor immunity in mice (67–69). While these studies demonstrated that the anti-GITR antibody acts mainly by enhancing effector T cell frequencies through avoidance of Treg mediated suppression, the exact mechanism remains unclear. In addition to rendering effector T cells resistant to Treg mediated suppression, agonist anti-GITR treatment was suggested to likewise enhance the effector T cell: Treg ratio in the tumor (67, 70). This change was attributed to the agonist anti-GITR antibody rendering Tregs unstable, causing them to lose Foxp3 expression (67), or to Treg depletion (70) in different studies. In NSG mice reconstituted with human $hCD34^+$HSCs and grafted with melanoma tumors the treatment increased the effector T cell: Treg ratio in the spleen and the tumor, while remaining tumor-infiltrating Tregs showed reduced expression of activation markers such as ICOS (70). Overall, although the treatment was not able to clear the tumor completely, treated mice exhibited significantly reduced tumor growth (70). The exact mechanisms leading to the enhanced effector T cell: Treg ratio in this particular study remain to be defined. The loss of activation markers such as ICOS observed in the anti-GITR study in HIS mice could indicate that, in addition to Treg depletion, remaining Tregs are rendered phenotypically unstable by the treatment.

Destabilization of Tregs is a promising approach for Treg-based immunotherapy and mechanisms of Treg destabilization have been studied in the setting of autoimmune diseases. Treg stability is mainly mediated by epigenetic mechanisms, most importantly the demethylation of the conserved non-coding sequence 2 (CNS2) in the *Foxp3* locus (71). We were able to show that microRNA (miRNA) 142-3p contributes to Treg instability during progression of Type 1 Diabetes (T1D) by targeting TET2, a molecule that can actively demethylate DNA (37, 72, 73). MiRNAs are small non-coding RNAs that can sequence-specifically inhibit their target mRNAs, thereby regulating complex cellular states, such as T cell activation, which makes them important targets for immunotherapy (74). Importantly, miRNA modulation has been studied extensively in the setting of autoimmunity and infection. Accordingly, a miR122 inhibitor is currently being tested in clinical trials for hepatitis C virus (HCV) infections, highlighting the feasibility of targeting miRNAs for immune modulation in human diseases (75). Regarding miRNA modulation for Treg targeting, we used NSG mice reconstituted with PBMCs and were able to demonstrate that the blockade of miRNAs that impact Treg induction or stability *in vivo* enhances human Treg frequencies both in the periphery and in the pancreas (36, 37, 76). Lessons learned from the autoimmune setting could be used for cancer immunotherapy. Enhancing the function of these miRNAs using miRNA mimics could induce immune responses against cancer cells by reducing Treg-mediated suppression mechanisms. Importantly, miRNAs that induce autoimmunity when overexpressed in lymphocytes, can still have tumor-promoting properties because of their expression in other cell types (e.g., miR17∼92 cluster) (77, 78). Therefore, the implementation of miRNA modulation for immune targeting in cancer therapy relies on the development of targeted approaches that allow the modulation of these miRNAs specifically in immune cells or even specific subsets. Importantly, miRNA delivery systems are currently intensively studied [reviewed in (79)], as miRNA instability and degradation still hinder the development of a successful system. To improve the delivery of miRNAs in a preclinical setting that also enables the testing of drug safety and efficiency, HIS mouse models offer a suitable platform prior the translation to humans.

OUTLOOK AND CONCLUSIONS

The perpetual improvements of HIS mouse models have enabled the design of personalized immunotherapies for various diseases including cancer and the evaluation of their efficacy prior to the translation to the human setting. Using patient-specific HIS mice will enable us to better understand the heterogeneity of immune responses and advance the development of novel personalized immunotherapies for the treatment of cancer. Even though still in its infancy, the use of iPSC-derived HSCs for engraftment could be an important step toward personalized HIS models.

Additionally, the immunosuppressive tumor microenvironment influences antitumor responses and the efficiency of cancer immunotherapies. Targeting Tregs has therefore become an important tool in cancer immunotherapy and has been studied extensively in murine models. In order to target Tregs most efficiently in human diseases the development of novel models depicting the immune reaction of the human disease is pivotal. HIS mouse models offer the opportunity to study the interaction of human immune cells, including Tregs, with human tumors directly *in vivo*.

Overall, current advances in establishing a "truly" humanized mouse model for the development of immunotherapies and drug delivery systems will guide personalized medicine approaches further to the translation to the clinic.

AUTHOR CONTRIBUTIONS

IS and MK reviewed the literature and wrote the manuscript. MGS reviewed the manuscript and prepared the figure using BioRender. CD reviewed the literature and contributed to the conceptualization of the manuscript. All authors contributed to the article and approved the submitted version.

FUNDING

CD holds a professorship grant from the Excellence Program for Outstanding Female Scientists from the Helmholtz Association, was supported by a Research Group at Helmholtz Zentrum München, the German Center for Diabetes Research (DZD), through a membership in the CRC1054 of the Deutsche Forschungsgemeinschaft (B11), and is funded through an EFSD award supported by EFSD/JDRF/Lilly European Programme in Type 1 Diabetes Research. IS was supported by a Research Grant of the Deutsche Forschungsgemeinschaft (DFG, SE 3036/2-1).

ACKNOWLEDGMENTS

We would like to thank all former and current members of our group for valuable input and helpful discussion.

REFERENCES

1. Mosier DE, Gulizia RJ, Baird SM, Wilson DB. Transfer of a functional human immune system to mice with severe combined immunodeficiency. *Nature*. (1988) 335:256–9. doi: 10.1038/335256a0
2. Shultz LD, Keck J, Burzenski L, Jangalwe S, Vaidya S, Greiner DL, et al. Humanized mouse models of immunological diseases and precision medicine. *Mamm Genome*. (2019) 30:123–42. doi: 10.1007/s00335-019-09796-2
3. Kwong LS, Brown MH, Barclay AN, Hatherley D. Signal-regulatory protein alpha from the NOD mouse binds human CD47 with an exceptionally high affinity–implications for engraftment of human cells. *Immunology*. (2014) 143:61–7. doi: 10.1111/imm.12290
4. Brehm MA, Kenney LL, Wiles MV, Low BE, Tisch RM, Burzenski L, et al. Lack of acute xenogeneic graft- versus-host disease, but retention of T-cell function following engraftment of human peripheral blood mononuclear cells in NSG mice deficient in MHC class I and II expression. *FASEB J*. (2019) 33:3137–51. doi: 10.1096/fj.201800636R
5. Yaguchi T, Kobayashi A, Inozume T, Morii K, Nagumo H, Nishio H, et al. Human PBMC-transferred murine MHC class I/II-deficient NOG mice enable long-term evaluation of human immune responses. *Cell Mol Immunol*. (2018) 15:953–62. doi: 10.1038/cmi.2017.106
6. Serr I, Furst RW, Achenbach P, Scherm MG, Gokmen F, Haupt F, et al. Type 1 diabetes vaccine candidates promote human Foxp3(+)Treg induction in humanized mice. *Nat Commun*. (2016) 7:10991. doi: 10.1038/ncomms10991
7. Malchow S, Leventhal DS, Nishi S, Fischer BI, Shen L, Paner GP, et al. Aire-dependent thymic development of tumor-associated regulatory T cells. *Science*. (2013) 339:1219–24. doi: 10.1126/science.1233913
8. Choi B, Lee JS, Kim SJ, Hong D, Park JB, Lee KY. Anti-tumor effects of anti-PD-1 antibody, pembrolizumab, in humanized NSG PDX mice xenografted with dedifferentiated liposarcoma. *Cancer Lett*. (2020) 478:56–69. doi: 10.1016/j.canlet.2020.02.042
9. Wang M, Yao LC, Cheng M, Cai D, Martinek J, Pan CX, et al. Humanized mice in studying efficacy and mechanisms of PD-1-targeted cancer immunotherapy. *FASEB J*. (2018) 32:1537–49. doi: 10.1096/fj.201700740R
10. Hu Z, Xia J, Fan W, Wargo J, Yang YG. Human melanoma immunotherapy using tumor antigen-specific T cells generated in humanized mice. *Oncotarget*. (2016) 7:6448–59. doi: 10.18632/oncotarget.7044
11. Capasso A, Lang J, Pitts TM, Jordan KR, Lieu CH, Davis SL, et al. Characterization of immune responses to anti-PD-1 mono and combination immunotherapy in hematopoietic humanized mice implanted with tumor xenografts. *J Immunother Cancer*. (2019) 7:37. doi: 10.1186/s40425-019-0518-z
12. Dagogo-Jack I, Shaw AT, Tumour heterogeneity and resistance to cancer therapies. *Nat Rev Clin Oncol*. (2018) 15:81–94. doi: 10.1038/nrclinonc.2017.166
13. Jespersen H, Lindberg MF, Donia M, Soderberg EMV, Andersen R, Keller U, et al. Clinical responses to adoptive T-cell transfer can be modeled in an autologous immune-humanized mouse model. *Nat Commun*. (2017) 8:707. doi: 10.1038/s41467-017-00786-z
14. Takahashi K, Yamanaka S. Induction of pluripotent stem cells from mouse embryonic and adult fibroblast cultures by defined factors. *Cell*. (2006) 126:663–76. doi: 10.1016/j.cell.2006.07.024
15. Ferreira AF, Calin GA, Picanco-Castro V, Kashima S, Covas DT, de Castro FA. Hematopoietic stem cells from induced pluripotent stem cells-considering the role of microRNA as a cell differentiation regulator. *J Cell Sci*. (2018) 131:jcs203018. doi: 10.1242/jcs.203018
16. Tan YT, Ye L, Xie F, Beyer AI, Muench MO, Wang J, et al. Respecifying human iPSC-derived blood cells into highly engraftable hematopoietic stem and progenitor cells with a single factor. *Proc Natl Acad Sci USA*. (2018) 115:2180–5. doi: 10.1073/pnas.1718446115
17. Takahashi K, Okita K, Nakagawa M, Yamanaka S. Induction of pluripotent stem cells from fibroblast cultures. *Nat Protoc*. (2007) 2:3081–9. doi: 10.1038/nprot.2007.418
18. Elitt MS, Barbar L, Tesar PJ. Drug screening for human genetic diseases using iPSC models. *Hum Mol Genet*. (2018) 27:R89–98. doi: 10.1093/hmg/ddy186
19. Vo LT, Daley GQ. *De novo* generation of HSCs from somatic and pluripotent stem cell sources. *Blood*. (2015) 125:2641–8. doi: 10.1182/blood-2014-10-570234

20. Sugimura R, Jha DK, Han A, Soria-Valles C, da Rocha EL, Lu YF, et al. Haematopoietic stem and progenitor cells from human pluripotent stem cells. *Nature*. (2017) 545:432–8. doi: 10.1038/nature22370
21. Doulatov S, Vo LT, Chou SS, Kim PG, Arora N, Li H, et al. Induction of multipotential hematopoietic progenitors from human pluripotent stem cells via respecification of lineage-restricted precursors. *Cell Stem Cell*. (2013) 13:459–70. doi: 10.1016/j.stem.2013.09.002
22. Taoka K, Arai S, Kataoka K, Hosoi M, Miyauchi M, Yamazaki S, et al. Using patient-derived iPSCs to develop humanized mouse models for chronic myelomonocytic leukemia and therapeutic drug identification, including liposomal clodronate. *Sci Rep*. (2018) 8:15855. doi: 10.1038/s41598-018-34193-1
23. Whiteside TL. The tumor microenvironment and its role in promoting tumor growth. *Oncogene*. (2008) 27:5904–12. doi: 10.1038/onc.2008.271
24. Tormoen GW, Crittenden MR, Gough MJ. Role of the immunosuppressive microenvironment in immunotherapy. *Adv Radiat Oncol*. (2018) 3:520–6. doi: 10.1016/j.adro.2018.08.018
25. Sakaguchi S, Sakaguchi N, Asano M, Itoh M, Toda M. Immunologic self-tolerance maintained by activated T cells expressing IL-2 receptor alpha-chains (CD25). Breakdown of a single mechanism of self-tolerance causes various autoimmune diseases. *J Immunol*. (1995) 155:1151–64.
26. Fontenot JD, Gavin MA, Rudensky AY. Foxp3 programs the development and function of CD4+CD25+ regulatory T cells. *Nat Immunol*. (2003) 4:330–6. doi: 10.1038/ni904
27. Hori S, Nomura T, Sakaguchi S. Control of regulatory T cell development by the transcription factor Foxp3. *Science*. (2003) 299:1057–61. doi: 10.1126/science.1079490
28. Roncador G, Brown PJ, Maestre L, Hue S, Martinez-Torrecuadrada JL, Ling KL, et al. Analysis of FOXP3 protein expression in human CD4+CD25+ regulatory T cells at the single-cell level. *Eur J Immunol*. (2005) 35:1681–91. doi: 10.1002/eji.200526189
29. Bennett CL, Christie J, Ramsdell F, Brunkow ME, Ferguson PJ, Whitesell L, et al. The immune dysregulation, polyendocrinopathy, enteropathy, X-linked syndrome (IPEX) is caused by mutations of FOXP3. *Nat Genet*. (2001) 27:20–21. doi: 10.1038/83713
30. Brunkow ME, Jeffery EW, Hjerrild KA, Paeper B, Clark LB, Yasayko S-A, et al. Disruption of a new forkhead/winged-helix protein, scurfin, results in the fatal lymphoproliferative disorder of the scurfy mouse. *Nat Genet*. (2001) 27:68–73. doi: 10.1038/83784
31. Bates GJ, Fox SB, Han C, Leek RD, Garcia JF, Harris AL, et al. Quantification of regulatory T cells enables the identification of high-risk breast cancer patients and those at risk of late relapse. *J Clin Oncol*. (2006) 24:5373–80. doi: 10.1200/JCO.2006.05.9584
32. Curiel TJ, Coukos G, Zou L, Alvarez X, Cheng P, Mottram P, et al. Specific recruitment of regulatory T cells in ovarian carcinoma fosters immune privilege and predicts reduced survival. *Nat Med*. (2004) 10:942–9. doi: 10.1038/nm1093
33. Fu J, Xu D, Liu Z, Shi M, Zhao P, Fu B, et al. Increased regulatory T cells correlate with CD8 T-cell impairment and poor survival in hepatocellular carcinoma patients. *Gastroenterology*. (2007) 132:2328–39. doi: 10.1053/j.gastro.2007.03.102
34. Gobert M, Treilleux I, Bendriss-Vermare N, Bachelot T, Goddard-Leon S, Arfi V, et al. Regulatory T cells recruited through CCL22/CCR4 are selectively activated in lymphoid infiltrates surrounding primary breast tumors and lead to an adverse clinical outcome. *Cancer Res*. (2009) 69:2000–9. doi: 10.1158/0008-5472.CAN-08-2360
35. Shou J, Zhang Z, Lai Y, Chen Z, Huang J, Worse outcome in breast cancer with higher tumor-infiltrating FOXP3+ Tregs: a systematic review and meta-analysis. *BMC Cancer*. (2016) 16:687. doi: 10.1186/s12885-016-2732-0
36. Serr I, Scherm MG, Zahm AM, Schug J, Flynn VK, Hippich M, et al. A miRNA181a/NFAT5 axis links impaired T cell tolerance induction with autoimmune type 1 diabetes. *Sci Transl Med*. (2018) 10:eaag1782. doi: 10.1126/scitranslmed.aag1782
37. Scherm MG, Serr I, Zahm AM, Schug J, Bellusci S, Manfredini R, et al. miRNA142-3p targets Tet2 and impairs Treg differentiation and stability in models of type 1 diabetes. *Nat Commun*. (2019) 10:5697. doi: 10.1038/s41467-019-13587-3
38. Ma SD, Xu X, Jones R, Delecluse HJ, Zumwalde NA, Sharma A, et al. PD-1/CTLA-4 blockade inhibits epstein-barr virus-induced lymphoma growth in a cord blood humanized-mouse model. *PLoS Pathog*. (2016) 12:e1005642. doi: 10.1371/journal.ppat.1005642
39. Kumagai S, Togashi Y, Kamada T, Sugiyama E, Nishinakamura H, Takeuchi Y, et al. The PD-1 expression balance between effector and regulatory T cells predicts the clinical efficacy of PD-1 blockade therapies. *Nat Immunol*. (2020) 21:1346–58. doi: 10.1038/s41590-020-0769-3
40. Li Y, Strick-Marchand H, Lim AI, Ren J, Masse-Ranson G, Dan L, et al. Regulatory T cells control toxicity in a humanized model of IL-2 therapy. *Nat Commun*. (2017) 8:1762. doi: 10.1038/s41467-017-01570-9
41. Theocharides AP, Rongvaux A, Fritsch K, Flavell RA, Manz MG. Humanized hemato-lymphoid system mice. *Haematologica*. (2016) 101:5–19. doi: 10.3324/haematol.2014.115212
42. Wunderlich M, Chou FS, Link KA, Mizukawa B, Perry RL, Carroll M, et al. AML xenograft efficiency is significantly improved in NOD/SCID-IL2RG mice constitutively expressing human SCF, GM-CSF, and IL-3. *Leukemia*. (2010) 24:1785–8. doi: 10.1038/leu.2010.158
43. Rongvaux A, Willinger T, Martinek J, Strowig T, Gearty SV, Teichmann LL, et al. Development and function of human innate immune cells in a humanized mouse model. *Nat Biotechnol*. (2014) 32:364–72. doi: 10.1038/nbt.2858
44. Billerbeck E, Barry WT, Mu K, Dorner M, Rice CM, Ploss A. Development of human CD4+FoxP3+ regulatory T cells in human stem cell factor-, granulocyte-macrophage colony-stimulating factor-, and interleukin-3-expressing NOD-SCID IL2Rγ(null) humanized mice. *Blood*. (2011) 117:3076–86. doi: 10.1182/blood-2010-08-301507
45. Becker M, Serr I, Salb VK, Ott VB, Mengel L, Bluher M, et al. Short-term cold exposure supports human Treg induction *in vivo*. *Mol Metab*. (2019) 28:73–82. doi: 10.1016/j.molmet.2019.08.002
46. Burzyn D, Kuswanto W, Kolodin D, Shadrach JL, Cerletti M, Jang Y, et al. A special population of regulatory T cells potentiates muscle repair. *Cell*. (2013) 155:1282–95. doi: 10.1016/j.cell.2013.10.054
47. Cipolletta D, Feuerer M, Li A, Kamei N, Lee J, Shoelson SE, et al. PPAR-gamma is a major driver of the accumulation and phenotype of adipose tissue Treg cells. *Nature*. (2012) 486:549–53. doi: 10.1038/nature11132
48. Feuerer M, Herrero L, Cipolletta D, Naaz A, Wong J, Nayer A, et al. Lean, but not obese, fat is enriched for a unique population of regulatory T cells that affect metabolic parameters. *Nat Med*. (2009) 15:930–9. doi: 10.1038/nm.2002
49. Kalin S, Becker M, Ott VB, Serr I, Hosp F, Mollah MMH, et al. A Stat6/Pten axis links regulatory T cells with adipose tissue function. *Cell Metab*. (2017) 26:475–92.e7. doi: 10.1016/j.cmet.2017.08.008
50. Plitas G, Konopacki C, Wu K, Bos PD, Morrow M, Putintseva EV, et al. Regulatory T cells exhibit distinct features in human breast cancer. *Immunity*. (2016) 45:1122–34. doi: 10.1016/j.immuni.2016.10.032
51. De Simone M, Arrigoni A, Rossetti G, Gruarin P, Ranzani V, Politano C, et al. Transcriptional landscape of human tissue lymphocytes unveils uniqueness of tumor-infiltrating T regulatory cells. *Immunity*. (2016) 45:1135–47. doi: 10.1016/j.immuni.2016.10.021
52. Zheng C, Zheng L, Yoo JK, Guo H, Zhang Y, Guo X, et al. Landscape of infiltrating T cells in liver cancer revealed by single-cell sequencing. *Cell*. (2017) 169:1342–56.e16. doi: 10.1016/j.cell.2017.05.035
53. Togashi Y, Shitara K, Nishikawa H. Regulatory T cells in cancer immunosuppression—implications for anticancer therapy. *Nat Rev Clin Oncol*. (2019) 16:356–71. doi: 10.1038/s41571-019-0175-7
54. Tanaka A, Sakaguchi S. Targeting Treg cells in cancer immunotherapy. *Eur J Immunol*. (2019) 49:1140–6. doi: 10.1002/eji.201847659
55. Sanmamed MF, Rodriguez I, Schalper KA, Onate C, Azpilikueta A, Rodriguez-Ruiz ME, et al. Nivolumab and urelumab enhance antitumor activity of human T lymphocytes engrafted in Rag2-/-IL2Rgamma^{null} immunodeficient mice. *Cancer Res*. (2015) 75:3466–78. doi: 10.1158/0008-5472.CAN-14-3510
56. Selby MJ, Engelhardt JJ, Quigley M, Henning KA, Chen T, Srinivasan M, et al. Anti-CTLA-4 antibodies of IgG2a isotype enhance antitumor activity through reduction of intratumoral regulatory T cells. *Cancer Immunol Res*. (2013) 1:32–42. doi: 10.1158/2326-6066.CIR-13-0013
57. Arce Vargas F, Furness AJS, Litchfield K, Joshi K, Rosenthal R, Ghorani E, et al. Fc effector function contributes to the activity of human anti-CTLA-4 antibodies. *Cancer Cell*. (2018) 33:649–63.e4. doi: 10.1016/j.ccell.2018.02.010

58. Kang TH, Jung ST. Boosting therapeutic potency of antibodies by taming Fc domain functions. *Exp Mol Med*. (2019) 51:1–9. doi: 10.1038/s12276-019-0345-9
59. Clynes RA, Towers TL, Presta LG, Ravetch JV. Inhibitory Fc receptors modulate *in vivo* cytoxicity against tumor targets. *Nat Med*. (2000) 6:443–46. doi: 10.1038/74704
60. Ito A, Ishida T, Yano H, Inagaki A, Suzuki S, Sato F, et al. Defucosylated anti-CCR4 monoclonal antibody exercises potent ADCC-mediated antitumor effect in the novel tumor-bearing humanized NOD/Shi-scid, IL-2Rgamma(null) mouse model. *Cancer Immunol Immunother*. (2009) 58:1195–206. doi: 10.1007/s00262-008-0632-0
61. Kurose K, Ohue Y, Wada H, Iida S, Ishida T, Kojima T, et al. Phase ia study of FoxP3+ CD4 Treg depletion by infusion of a humanized anti-CCR4 antibody, KW-0761, in cancer patients. *Clin Cancer Res*, (2015) 21:4327–36. doi: 10.1158/1078-0432.CCR-15-0357
62. Mizukami Y, Kono K, Kawaguchi Y, Akaike H, Kamimura K, Sugai H. CCL17 and CCL22 chemokines within tumor microenvironment are related to accumulation of Foxp3+ regulatory T cells in gastric cancer. *Int J Cancer*. (2008) 122:2286–93. doi: 10.1002/ijc.23392
63. Ménétrier-Caux C, Faget J, Biota C, Gobert M, Blay J-Y, Caux C. Innate immune recognition of breast tumor cells mediates CCL22 secretion favoring Treg recruitment within tumor environment. *Oncoimmunology*. (2012) 1:759–61. doi: 10.4161/onci.19680
64. Ronchetti S, Nocentini G, Riccardi C, Pandolfi PP. Role of GITR in activation response of T lymphocytes. *Blood*. (2002) 100:350–2. doi: 10.1182/blood-2001-12-0276
65. Tone M, Tone Y, Adams E, Yates SF, Frewin MR, Cobbold SP, et al. Mouse glucocorticoid-induced tumor necrosis factor receptor ligand is costimulatory for T cells. *Proc Natl Acad Sci USA*. (2003) 100:15059–64. doi: 10.1073/pnas.2334901100
66. Shimizu J, Yamazaki S, Takahashi T, Ishida Y, Sakaguchi S. Stimulation of CD25(+)CD4(+) regulatory T cells through GITR breaks immunological self-tolerance. *Nat Immunol*. (2002) 3:135–42. doi: 10.1038/ni759
67. Cohen AD, Schaer DA, Liu C, Li Y, Hirschhorn-Cymmerman D, Kim SC, et al. Agonist anti-GITR monoclonal antibody induces melanoma tumor immunity in mice by altering regulatory T cell stability and intra-tumor accumulation. *PLoS ONE*. (2010) 5:e10436. doi: 10.1371/journal.pone.0010436
68. Ko K, Yamazaki S, Nakamura K, Nishioka T, Hirota K, Yamaguchi T, et al. Treatment of advanced tumors with agonistic anti-GITR mAb and its effects on tumor-infiltrating Foxp3+CD25+CD4+ regulatory T cells. *J Exp Med*. (2005) 202:885–91. doi: 10.1084/jem.20050940
69. Ramirez-Montagut T, Chow A, Hirschhorn-Cymerman D, Terwey TH, Kochman AA, Lu S, et al. Glucocorticoid-induced TNF receptor family related gene activation overcomes tolerance/ignorance to melanoma differentiation antigens and enhances antitumor immunity. *J Immunol*. (2006) 176:6434–42. doi: 10.4049/jimmunol.176.11.6434
70. Mahne AE, Mauze S, Joyce-Shaikh B, Xia J, Bowman EP, Beebe AM, et al. Dual roles for regulatory T-cell depletion and costimulatory signaling in agonistic GITR targeting for tumor immunotherapy. *Cancer Res*. (2017) 77:1108–18. doi: 10.1158/0008-5472.CAN-16-0797
71. Polansky JK, Kretschmer K, Freyer J, Floess S, Garbe A, Baron U, et al. DNA methylation controls Foxp3 gene expression. *Eur J Immunol*. (2008) 38:1654–63. doi: 10.1002/eji.200838105
72. Ito S, D'Alessio AC, Taranova OV, Hong K, Sowers LC, Zhang Y. Role of tet proteins in 5 mC to 5 hmC conversion, ES-cell self-renewal, and inner cell mass specification. *Nature*. (2010) 466:1129–33. doi: 10.1038/nature09303
73. Tahiliani M, Koh KP, Shen Y, Pastor WA, Bandukwala H, Brudno Y, et al. Conversion of 5-methylcytosine to 5-hydroxymethylcytosine in mammalian DNA by MLL partner TET1. *Science*. (2009) 324:930–5. doi: 10.1126/science.1170116
74. Cobb BS, Nesterova TB, Thompson E, Hertweck A, O'Connor E, Godwin J, et al. T cell lineage choice and differentiation in the absence of the RNase III enzyme Dicer. *J Exp Med*. (2005) 201:1367–73. doi: 10.1084/jem.20050572
75. van der Ree MH, de Vree JM, Stelma F, Willemse S, van der Valk M, Rietdijk S, et al. Safety, tolerability, and antiviral effect of RG-101 in patients with chronic hepatitis C: a phase 1B, double-blind, randomised controlled trial. *Lancet*. (2017) 389:709–17. doi: 10.1016/S0140-6736(16)31715-9
76. Serr I, Furst RW, Ott VB, Scherm MG, Nikolaev A, Gokmen F, et al. miRNA92a targets KLF2 and the phosphatase PTEN signaling to promote human T follicular helper precursors in T1D islet autoimmunity. *Proc Natl Acad Sci USA*. (2016) 113:E6659–68. doi: 10.1073/pnas.1606646113
77. He L, Thomson JM, Hemann MT, Hernando-Monge E, Mu D, Goodson S, et al. A microRNA polycistron as a potential human oncogene. *Nature*. (2005) 435:828–33. doi: 10.1038/nature03552
78. Xiao C, Srinivasan L, Calado DP, Patterson HC, Zhang B, Wang J, et al. Lymphoproliferative disease and autoimmunity in mice with increased miR-17-92 expression in lymphocytes. *Nat Immunol*. (2008) 9:405–14. doi: 10.1038/ni1575
79. Fu Y, Chen J, Huang Z. Recent progress in microRNA-based delivery systems for the treatment of human disease. *ExRNA*. (2019) 1:24. doi: 10.1186/s41544-019-0024-y

Conflict of Interest: The authors declare that the research was conducted in the absence of any commercial or financial relationships that could be construed as a potential conflict of interest.

Copyright © 2021 Serr, Kral, Scherm and Daniel. This is an open-access article distributed under the terms of the Creative Commons Attribution License (CC BY). The use, distribution or reproduction in other forums is permitted, provided the original author(s) and the copyright owner(s) are credited and that the original publication in this journal is cited, in accordance with accepted academic practice. No use, distribution or reproduction is permitted which does not comply with these terms.

frontiers in Immunology

REVIEW
published: 22 February 2021
doi: 10.3389/fimmu.2021.643852

Building the Next Generation of Humanized Hemato-Lymphoid System Mice

Tijana Martinov[1†], Kelly M. McKenna[1,2,3†], Wei Hong Tan[1†], Emily J. Collins[1], Allie R. Kehret[1], Jonathan D. Linton[1], Tayla M. Olsen[1], Nour Shobaki[1] and Anthony Rongvaux[1,4]*

[1] Clinical Research Division, Program in Immunology, Fred Hutchinson Cancer Research Center, Seattle, WA, United States, [2] Graduate Program in Molecular and Cellular Biology, University of Washington, Seattle, WA, United States, [3] Medical Scientist Training Program, University of Washington, Seattle, WA, United States, [4] Department of Immunology, University of Washington, Seattle, WA, United States

Since the late 1980s, mice have been repopulated with human hematopoietic cells to study the fundamental biology of human hematopoiesis and immunity, as well as a broad range of human diseases *in vivo*. Multiple mouse recipient strains have been developed and protocols optimized to efficiently generate these "humanized" mice. Here, we review three guiding principles that have been applied to the development of the currently available models: (1) establishing tolerance of the mouse host for the human graft; (2) opening hematopoietic niches so that they can be occupied by human cells; and (3) providing necessary support for human hematopoiesis. We then discuss four remaining challenges: (1) human hematopoietic lineages that poorly develop in mice; (2) limited antigen-specific adaptive immunity; (3) absent tolerance of the human immune system for its mouse host; and (4) sub-functional interactions between human immune effectors and target mouse tissues. While major advances are still needed, the current models can already be used to answer specific, clinically-relevant questions and hopefully inform the development of new, life-saving therapies.

Keywords: humanized mice, immunity, hematopoiesis, infectious diseases, cancer, immunotherapies

OPEN ACCESS

Edited by:
Tim Willinger, Karolinska Institutet, Sweden

Reviewed by:
Christian Muenz, University of Zurich, Switzerland
Hergen Spits, University of Amsterdam, Netherlands

****Correspondence:***
Anthony Rongvaux
rongvaux@fredhutch.org

† These authors share first authorship

Specialty section:
This article was submitted to Cancer Immunity and Immunotherapy, a section of the journal Frontiers in Immunology

Received: *18 December 2020*
Accepted: *27 January 2021*
Published: *22 February 2021*

Citation:
Martinov T, McKenna KM, Tan WH, Collins EJ, Kehret AR, Linton JD, Olsen TM, Shobaki N and Rongvaux A (2021) Building the Next Generation of Humanized Hemato-Lymphoid System Mice. Front. Immunol. 12:643852. doi: 10.3389/fimmu.2021.643852

INTRODUCTION

Biomedical research aims to provide a platform for the development and testing of new therapies that can reduce human suffering and deaths. *In vitro* studies using human cells or organoids are useful, but animal models can better elucidate the fundamental principles of complex biological processes in mammals. In particular, laboratory mice are often the model organism of choice, as their small size and short generation time enable extensive genetic engineering and invasive experimentation. Many fundamental characteristics of hematopoietic and immune systems are shared across mice and humans. However, with 91 million years of divergent evolution, differences exist and results from murine studies cannot always be directly translated into clinical applications, driving the development of experimental murine platforms that faithfully model human physiology and diseases. Specifically, mice can be transplanted with a human hemato-lymphoid system (1). Such "humanized mice" (**Box 1**) have been increasingly used since the late 1980s, and have

BOX 1 | What is a humanized mouse?

The Wikipedia definition of a humanized mouse is "a mouse carrying functioning human genes, cells, tissues, and/or organs." This review focuses on mice transplanted with human hematopoietic cells, colloquially referred to as "humanized mice" (6, 7). When used to study immune responses, such mice are better designated as "human(ized) immune system" (HIS) mice (5, 8, 9). However, not all hematopoietic cells contribute to the immune response, and "human(ized) hemato-lymphoid system" (HHLS) mice is a more encompassing term, particularly when human $CD34^+$ HSPCs are transplanted (1, 10, 11).

Many models combine multiple characteristics listed in the definition of humanized mice. In addition to human hematopoietic cell transplantation, diverse human tissues or tumors can be co-transplanted and the genome of the recipient mouse can be engineered to contain human genes.

contributed to major breakthroughs in several research fields, including human hematopoiesis (2), hematologic malignancies (3), and immunity to human-tropic pathogens (4, 5). Successful generation of humanized mice requires: (i) a source of human donor hematopoietic cells, (ii) an effective transplantation protocol, and (iii) an appropriate recipient mouse strain.

Human peripheral blood mononuclear cells (PBMCs) can be used as a source of hematopoietic cells for transplantation, but their engraftment favors T cell maintenance, resulting in an incomplete human immune system (7, 12). In contrast, hematopoietic stem and progenitor cells (HSPCs), enriched in the $CD34^+$ cell fraction, give rise to all human hematopoietic lineages upon transplantation in mice (7, 13). Human $CD34^+$ HSPCs can be obtained from different sources. Fetal $CD34^+$ cells, abundant in the liver, very efficiently engraft and undergo multilineage differentiation upon transplantation in mice, but ethical concerns limit access to fetal tissues (14). Other sources of $CD34^+$ cells, such as cord blood, bone marrow (BM) or peripheral blood following granulocyte colony-stimulating factor (G-CSF) mobilization, are more accessible with fewer ethical concerns. However, their stemness declines with the age of the donor (15, 16), resulting in lower engraftment potential (17, 18). Of note, donor cells can be obtained from patients affected by diverse hematopoietic diseases, thereby providing small animal models of human diseases including genetic immune disorders or hematological malignancies (3, 19).

Abbreviations: AM, Alveolar macrophages; BLT, bone marrow, liver, thymus; BM, Bone marrow; BRG, BALB/c *Rag2*$^{-/-}$ *Il2g*$^{-/-}$; BRGF, BALB/c *Rag2*$^{-/-}$ *Il2g*$^{-/-}$ *Flt3*$^{-/-}$; DCs, Dendritic cells; EBV, Epstein–Barr virus; EPO, Erythropoietin; G-CSF, Granulocyte colony-stimulating factor; GM-CSF, Granulocyte-macrophage colony-stimulating factor; GvHD, Graft-vs.-host disease; HCMV, Human Cytomegalovirus; HIV-1, human immunodeficiency virus 1; HLA, Human leukocyte antigen; HSPCs, Hematopoietic stem and progenitor cells; IL, Interleukin; MSCs, Mesenchymal stromal cells; MHC-I, Major histocompatibility complex class I; MHC-II, Major histocompatibility complex class II; MISTRG, M-CSF$^{h/h}$ IL-3/GM-CSF$^{h/h}$ SIRPα$^{h/m}$ THPO$^{h/h}$ RAG2$^{-/-}$ IL2Rγ$^{-/-}$; MISTRG6, M-CSF$^{h/h}$ IL-3/GM-CSF$^{h/h}$ SIRPα$^{h/m}$ THPO$^{h/h}$ RAG2$^{-/-}$ IL2Rγ$^{-/-}$ IL6$^{h/h}$; NK, Natural killer; NOD, Non-obese diabetic; NSG, NOD/SCID/*Il2rg*$^{-/-}$; NSGW41, NOD/SCID/*Il2rg*$^{-/-}$ *Kit*$^{W41/W41}$; PBMCs, peripheral blood mononuclear cells; PDX, Patient derived xenograft; RBCs, Red blood cells; SCF, Stem cell factor; SCID, severe-combined immunodeficient; TCR, T cell receptor; xGvHD, xenogeneic graft-vs.-host disease.

Human hematopoietic cells can be transplanted by systemic intravenous delivery or by orthotopic injection into a site of primary hematopoiesis. In adult mice, hematopoietic cells can be implanted in the BM niche by intrafemoral injection (20). Intrahepatic injection has also become a common route of $CD34^+$ cell implantation in newborn mice; the liver is a site of primary hematopoiesis during embryonic life and continues to be for several days after birth, until the hematopoietic niche is established in the BM and the mouse host naturally supports the expansion and multilineage differentiation of the hematopoietic system (21) (**Figure 1**).

The array of recipient mice for hematopoietic humanization has expanded over the past few decades, with advances in mouse genome engineering. This review focuses on these developments, highlighting the genetic engineering of the host, as well as the co-transplantation of human tissues to support human hematopoiesis. We first discuss three guiding principles that have been employed for the development of the currently available recipient mice (**Figure 2**): (i) preventing rejection of the human graft by the mouse immune system, (ii) opening the niche to make it accessible to human hematopoietic cells, and (iii) supporting human hematopoiesis in the mouse. We then consider how these principles are being applied to the development of newer mouse strains, aiming to resolve four remaining major challenges: (i) the development and function of missing human hematopoietic lineages, (ii) efficient and durable antigen-specific adaptive immunity, (iii) tolerance of the engrafted human immune system for the mouse host and (iv) functional cross-reactivity between the human graft and target tissues.

PRINCIPLE #1: PREVENTING REJECTION OF THE HUMAN GRAFT

The field of humanized mice was launched in the late 1980s, a few years after the discovery of mice with severe combined immunodeficiency (SCID). *Prkdc*^{scid} (protein kinase, DNA activated, catalytic polypeptide; severe combined immunodeficiency) is a spontaneous mutation identified in a colony of C.B-17 mice (22). The functional inactivation of the PRKDC enzyme in SCID mice leads to defective DNA repair and repair-dependent somatic V(D)J recombination of B and T cell receptor-encoding genes (23). As a result, lymphocyte development is arrested at an early stage and mature B and T lymphocytes are absent in SCID mice. Taking advantage of the severe immunodeficiency of these animals, several groups successfully transplanted human PBMCs (12), human BM cells (24), human fetal tissues (25) or human HSPCs (26) in SCID (12, 25, 26) or equivalent recipient mice (24). Coinciding with the early years of the HIV-1/AIDS epidemic, these pioneering models provided a much-needed tool for *in vivo* studies of HIV-1 infection (27–29). Recipient mouse strains have since undergone numerous iterative improvements, and this historical perspective has been comprehensively reviewed previously [e.g., (6)]. The most notable modifications include further preventing rejection of the human graft, through the elimination

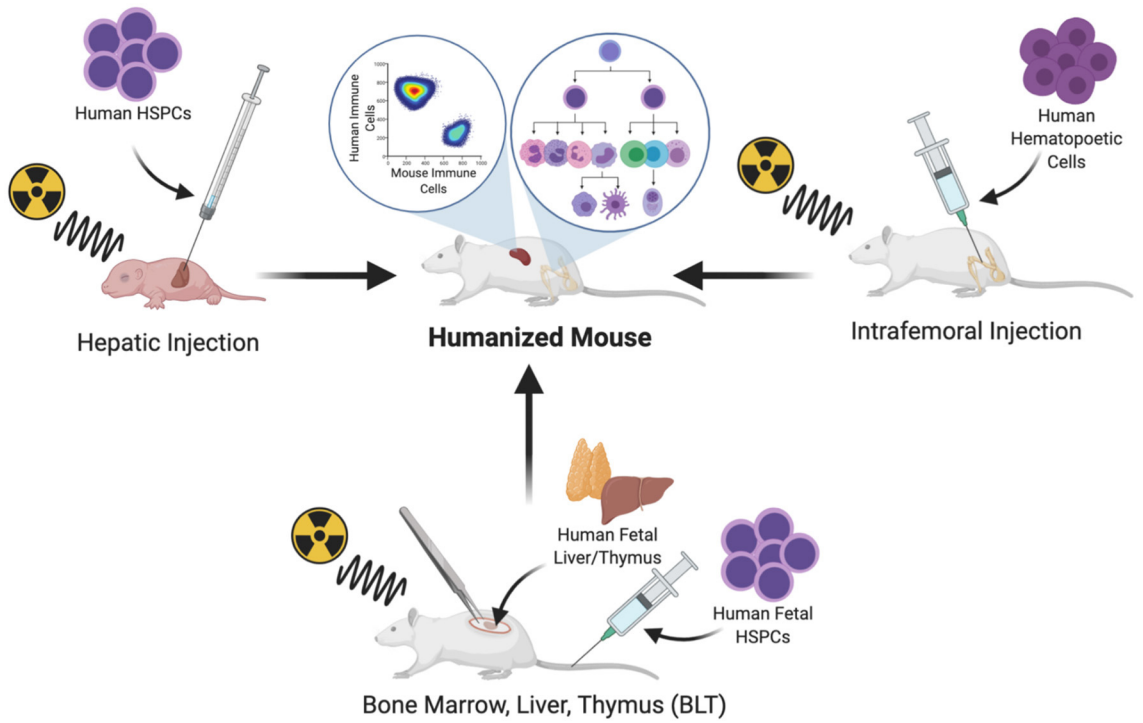

FIGURE 1 | Protocols commonly used for the generation of humanized mice.

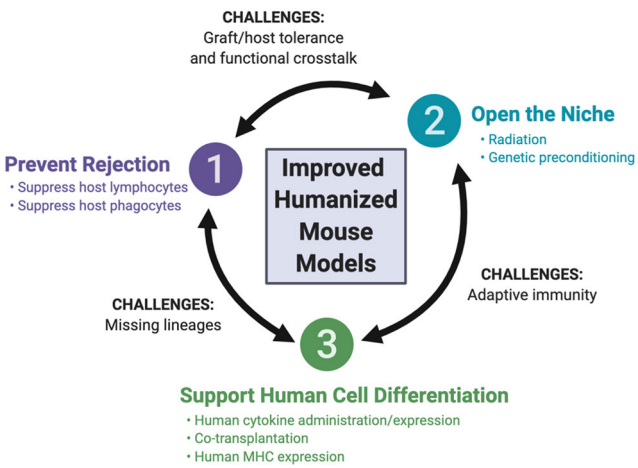

FIGURE 2 | Fundamental principles of mouse humanization and remaining challenges.

of endogenous natural killer (NK) cells and the induction of phagocytic tolerance, as discussed below.

NK cells are lymphoid cells that eliminate cells lacking major histocompatibility complex class I (MHC-I) molecules (30). Engrafted human cells express human MHC-I molecules that are not recognized by mouse NK cells. Therefore, depletion of mouse NK cells is essential, to prevent them from recognizing and eliminating the graft as "missing self." The interleukin-2 receptor γ chain (IL-2Rγ, encoded by *Il2rg*) is shared by multiple cytokines of the IL-2 family, including IL-15 that is essential for NK cell development (31). Consequently, *Il2rg* deficiency eliminates host NK cells and improves human hematopoietic cell engraftment in immunodeficient recipient mice (21, 32–35).

Transplanted human cells are also rejected through phagocytosis by mouse cells, such as monocytes and macrophages. Because phagocytes are essential for normal development and physiology, they cannot be easily depleted genetically without affecting mouse health and survival (36, 37). An alternative strategy is to alter their functional properties, by inducing phagocytic tolerance through the signal regulatory protein alpha (SIRPα) and CD47 axis (38). The polymorphic *Sirpa* gene in the non-obese diabetic (NOD) mouse strain encodes a variant of the SIRPα receptor that cross-reacts with the human CD47 ligand. As a result, human cells transplanted in NOD mice can engage the CD47/SIRPα "don't eat me" signal and are protected from phagocytosis by mouse macrophages (39). Consequently, backcrossing the *scid* mutation, and later the *Il2rg* deficiency, onto the NOD background significantly increased the efficiency of human cell transplantation (33–35, 40, 41). The resulting strains, NOD SCID *Il2rg*$^{-/-}$ (NOG and NSG), became very popular as they combine T, B and NK cell deficiencies with SIRPα-mediated phagocytic tolerance (33–35), but multiple other strains are functionally equivalent. These different strains abrogate V(D)J recombination [*Prkdc*^{scid} mutation (12, 25), or deletion of recombination activating gene (RAG)-1 or RAG-2

TABLE 1 | List of immunodeficient mice used as recipients for transplantation of human hemato-lymphoid system.

Acronym	Genetic background	T and B cell deficiency	NK cell deficiency	Phagocytic tolerance	References
SCID	C.B-17	*Prkdc*^{scid}	-	-	(12, 25, 26)
NOD-SCID	NOD	*Prkdc*^{scid}	-	*Sirpa*^{NOD}	(40, 41)
BRG	Balb/c	*Rag2*$^{-/-}$	*Il2rg*$^{-/-}$	-	(21, 32)
NOG	NOD	*Prkdc*^{scid}	*Il2rg*$^{-/-}$ (truncation)	*Sirpa*^{NOD}	(35)
NSG	NOD	*Prkdc*^{scid}	*Il2rg*$^{-/-}$	*Sirpa*^{NOD}	(33, 34)
NRG	NOD	*Rag1*$^{-/-}$	*Il2rg*$^{-/-}$	*Sirpa*^{NOD}	(42)
BRGS^{NOD}	Balb/c	*Rag2*$^{-/-}$	*Il2rg*$^{-/-}$	*Sirpa*^{NOD}	(43)
S^{tg}RG	Balb/c x 129	*Rag2*$^{-/-}$	*Il2rg*$^{-/-}$	Human *SIRPA* (BAC tg)	(45)
S^{KI}RG	Balb/c x 129	*Rag2*$^{-/-}$	*Il2rg*$^{-/-}$	Human *SIRPA* (KI extracellular domain)	(46)
B6RGS^{NOD}	C57BL/6	*Rag2*$^{-/-}$	*Il2rg*$^{-/-}$	*Sirpa*^{NOD}	(44)
B6RGS^{Human}	C57BL/6	*Rag2*$^{-/-}$	*Il2rg*$^{-/-}$	Human *SIRPA* (KI full-length)	(47)
B6RG-CD47	C57BL/6	*Rag2*$^{-/-}$	*Il2rg*$^{-/-}$	*Cd47*$^{-/-}$	(48)

SCID, NOD-SCID and BRG are historical models, that provided the basis for most currently used recipient mice. All other mice listed in this table have conceptually similar properties, with a few exceptions, as discussed in the text.

(21, 32, 42)] and IL-2Rγ [*Il2rg* gene deletion or truncation (21, 32–35)]. SIRPα/CD47-dependent cross-species tolerance can be achieved by expressing the mouse *Sirpa*^{NOD} variant (43, 44) or human *SIRPA* (45–47), or by employing a *Cd47* deficiency that produces tolerance by an unknown mechanism (48, 49). These strains are on diverse genetic backgrounds (NOD, BALB/c, C57BL/6), and are known by distinct acronyms, listed in **Table 1**. Upon transplantation of human CD34$^+$ HSPCs, all of these strains support the differentiation of high levels of human CD45$^+$ cells, reaching about 80% engraftment in the BM and 50% in the periphery. However, immune cell differentiation is disproportionately skewed toward the B and T lymphoid lineages (33, 35, 45). Human myelo-monocytic and NK cells are present only at low frequencies (50, 51), and human circulating red blood cells and platelets are barely detectable (52, 53). Investigators should carefully select the background strain they use, based on their research question, as the specific strain can impact the outcome of experiments. For example, SCID mice are highly susceptible to DNA damage; therefore RAG-deficient mice are the preferred recipient strain when testing chemo- and radiotherapies (42, 54). For studies involving complement-dependent cytotoxicity, the C57BL/6 or BALB/c backgrounds should be preferred, since NOD mice lack hemolytic complement C5 (41, 44).

PRINCIPLE #2: OPENING THE NICHE

Hematopoiesis is a complex and tightly regulated process during which hematopoietic progenitors undergo expansion and multilineage differentiation (2, 13). This process occurs primarily in the BM that uniquely provides supporting factors, such as cytokines at local physiological concentrations, and also provides a distinct microenvironment for developing cells (55). Accessibility of the transplanted human CD34$^+$ HSPCs to this niche is required for efficient engraftment in the mouse host. Reducing cellularity in the mouse BM creates the needed physical space, described as "opening the niche." Traditional protocols rely on irradiation as a preconditioning regimen (56–60), typically achieved using sub-lethal X-ray or ^{137}Cs irradiation to kill most hematopoietic cells while limiting toxicity. When no irradiator is available, alternative pre-conditioning protocols can be used, such as the myeloablative drug busulfan (61–63).

Recently, the requirement for radiation preconditioning has been alleviated with recipient mice engineered to have a less populated BM niche, thereby achieving a form of "genetic preconditioning." An example is provided by the *Kit*^{W41} mutation, in an NSG-derived mouse strain known as NSGW41 (64) (**Table 2**). The receptor tyrosine kinase Kit (also known as c-Kit or CD117, encoded by the *Kit* gene) is the receptor for the cytokine stem cell factor (or SCF, also known as steel factor or Kit ligand). SCF increases HSPC retention in the BM niche by increasing their adhesion to neighboring stromal cells and proteins in the extracellular matrix (75). The *Kit*^{W41} allelic variant encodes a protein with partially impaired kinase activity (76–78), producing functionally defective hematopoietic stem cells in *Kit*$^{W41/W41}$ mutant mice. In addition, because SCF is conserved between species [over 82% amino acid identity between mouse and human (1)], mouse SCF cross-reacts on the corresponding human Kit receptor. Consequently, when transplanted into NSGW41 mice, human HSPCs find a partially open BM niche and effectively compete for SCF against the mouse HSPCs that express the impaired Kit receptor. The impact of the *Kit*$^{W41/W41}$ mutation on mouse humanization is threefold: human CD34$^+$ HSPCs efficiently engraft without radiation preconditioning; even without radiation, engraftment levels in NSGW41 are higher than in irradiated NSG recipients; and better maintenance of functional human HSPCs favors their multilineage differentiation, including into the erythro-megakaryocytic lineage (64, 79).

Other genes can be inactivated to open the BM niche. *Thpo* encodes the cytokine, thrombopoietin, which is essential

TABLE 2 | List of genetically engineered mice, in the order discussed in this review.

Strain	Preventing graft rejection	Opening the niche	Providing support	Impact	References
NSGW41 *Kit*$^{W41/W41}$	NSG background	Mouse HSPC deficiency		- Genetic pre-conditioning (high engraftment without irradiation)	(64)
BRG-THPO *Thpo*$^{h/h}$	BRG background	Mouse HSPC deficiency	Human HSPC support by human THPO	- Increased BM engraftment - Thrombocytopenia	(65)
BRGF *Flt3*$^{-/-}$	BRG background	Mouse DC deficiency		- Only human DCs, increased by human Flt-3 ligand treatment	(66)
BRG-IL3/GM-CSF *Il3*$^{h/h}$ *Csf2*$^{h/h}$	BRG background	Mouse alveolar macrophage deficiency	Human alveolar macrophage support by human GM-CSF	- Alveolar macrophage replacement	(67)
NSG-SGM3 Human *SCF, CSF2, IL3* transgenes	NSG background		Transgenic overexpression of cytokines supporting myelopoiesis	- Increased myelopoiesis - Functional mast cells - Immature myeloid cells - Exhaustion of HSPCs	(18, 68–70)
SRG15 *Il15*$^{h/h}$	S^{KI}RG background		Human NK cells and T cells by human IL-15	- Functional human NK cells - Intraepithelial lymphocytes in mucosa	(46)
MISTRG *Csf1*$^{h/h}$, *Il3*$^{h/h}$, *Csf2*$^{h/h}$, *Thpo*$^{h/h}$	S^{tg}RG or S^{KI}RG background	Mouse HSPC and alveolar macrophage deficiency	Multiple human cytokines supporting HPSC maintenance and myelopoiesis	- Genetic pre-conditioning (high engraftment without irradiation) - Long-term hematopoiesis - Engraftment of patient-derived hematologic malignancies - Diverse and functional subsets of myelomonocytic cells - Functional NK cells - Thrombocytopenia - Hemophagocytosis	(17, 18, 71)
MISTRG6 *Il6*$^{h/h}$	MIS^{KI}TRG background		Support to IL-6 dependent cells	- Engraftment of patient-derived multiple myeloma	(72)
SRG6 *Il6*$^{h/h}$	S^{KI}RG background		Support to IL-6 dependent cells	- Increased thymic cellularity - Improved B cell response to immunization	(73)
BRGST Mouse *Tslp* transgene	BRGS^{NOD} background		Restore support for mouse LTi cells and LN architecture	- LN development - Improved antigen-specific adaptive immunity	(74)

Positive impacts are indicated in green, unintended detrimental effects in red. A more detailed version is provided as ***Supplementary Table 1****, including additional details of improvements and limitations of each model with regards to hematopoiesis, innate and adaptive immunity.*

for the maintenance of quiescent and self-renewing HSPCs (80–83). Mouse *Thpo* gene inactivation reduces frequencies of mouse HSPCs, thereby opening the niche for transplanted human HSPCs (65). The concept of genetic preconditioning also applies to non-HSPC cell types, and to niches other than the BM. Fms-like tyrosine kinase 3 (Flt-3) ligand is essential to the differentiation of dendritic cells (DCs) (84–87), while granulocyte-macrophage colony stimulating factor (GM-CSF) is required for the maturation of lung alveolar macrophages (AM) (88–90). Genetic inactivation of *Flt3* (encoding the receptor for Flt-3 ligand) or of *Csf2* (encoding GM-CSF) eliminates mouse DCs or AMs, respectively, thereby opening the niche for the development of the corresponding human cell lineages (66, 67). In these three cases (*Thpo*, *Ftl3,* or *Csf2* gene deficiencies), the elimination of mouse cell populations was supplemented with provision of the corresponding human cytokines (65–67), as discussed next.

PRINCIPLE #3: SUPPORTING THE DEVELOPMENT OF ENGRAFTED HUMAN CELLS

The spatial microenvironment of the BM niche includes diverse cell types, including endothelial cells and mesenchymal stromal/stem cells (MSCs) that are known to release cytokines, signaling mediators and growth factors, such as SCF, IL-3, IL-6, THPO, and GM-CSF (91–93). These molecules are important for the maintenance of human HSPCs and their differentiation into all hematopoietic and immune cell lineages (1, 2). Some of the cytokines supporting hematopoiesis are poorly conserved (e.g., 29% amino acid identity between human and mouse IL-3) and do not cross-react from mouse to human, while others are highly conserved and largely cross-reactive (e.g., SCF) (1). However, even when amino acid identity is high, cross-reactivity of cytokines is not always complete in local microenvironments at physiological concentrations. To account for this incomplete

cross-reactivity, various protocols were developed to promote the differentiation of a more complete human immune system upon human CD34$^+$ cell transplantation in mice.

Exogenous Cytokine Administration

The simplest method of supplying graft-supporting factors is the repeated injection of recombinant human cytokines. This approach was used in an early-generation SCID model and the injection of cytokines, including human SCF, IL-3, and GM-CSF, supported enhanced engraftment levels of human BM cells as well as their myeloid differentiation (26). Because human NK cell differentiation is limited in mice, humanized BRG mice were treated with recombinant human IL-15 coupled to IL-15Rα, which is an essential growth factor for NK cell development and homeostasis. This treatment resulted in a significant increase in the differentiation and homeostasis of human NK cells in mice transplanted with human CD34$^+$ cells (94).

A second cytokine delivery approach relies on hydrodynamic injection of a human cytokine-encoding DNA plasmid, resulting in the *in vivo* "transfection" of hepatocytes. In turn, hepatocytes produce high levels of the encoded cytokine and release it into the circulation for up to 5 days (95, 96). This method was used to demonstrate that human cytokines, such as GM-CSF and M-CSF, support myeloid differentiation of human CD34$^+$ cells in NSG mice, while IL-15 and Flt-3 ligand supported NK cell differentiation (96, 97).

The administration of human cytokines can be combined with genetic opening of the niche. In BRGF mice, which lack the *Flt3* gene, injection of human recombinant Flt-3 ligand boosts the development of human dendritic cells, in the absence of mouse dendritic cells (66).

Recombinant cytokine injection and hydrodynamic plasmid delivery are easy to implement, irrespective of the recipient mouse and protocol of human cell transplantation used. However, they both result in transient, systemic and generally supra-physiological cytokine expression.

Genetic Engineering of Human Cytokine Expression

To circumvent the requirement for repeated cytokine administrations, the genome of the recipient mouse can be engineered to express human cytokines (**Table 2**). The initial method relied on transgenic overexpression of a human cytokine-encoding cDNA, under the control of a strong promoter. Such transgenic mice are still in use, based on NSG or similar genetic backgrounds. However, results obtained with these mice need to be interpreted cautiously as the systemic overexpression of human cytokines frequently results in non-physiological hematopoiesis. For example, the transgenic pCMV promoter-driven overexpression of human SCF, GM-CSF, and IL-3 results in the mobilization of CD34$^+$ HSPCs in the NSG-SGM3 mouse and the loss of their functional properties (68). As a consequence, although high-level human hematopoietic engraftment is achieved in NSG-SGM3 mice, hematopoietic progenitors lose their stemness and long-term hematopoiesis is deficient, as demonstrated by their inability to serially engraft (18, 69). Nevertheless, transgenic overexpression of cytokines can support the development of specific cell lineages and provide useful models to study those cells. In NSG-SGM3, the overexpression of human SCF results in the development of abundant and functional human mast cells, which are effective in models of passive cutaneous and systemic anaphylaxis (98). Similarly, human IL-15 overexpression in NOG mice supports the maintenance and function of human NK cells isolated from human peripheral blood (99, 100). Such models can provide useful experimental systems to evaluate the effect of candidate drugs on specific human immune cell populations.

More physiological expression of human cytokines can be achieved by bacterial artificial chromosome (referred to as "BAC") transgenesis, inserting an entire human gene, including its regulatory elements, into the mouse genome. This method has been used to express human IL-6 and human IL-7 in NSG mice (101, 102). In another strategy, the mouse gene can be eliminated and corresponding human gene inserted in its place, including introns and exons from the start to the stop codon (**Figure 3A**) (103). This knock-in strategy has been used for a number of cytokine-encoding genes, including *Csf1*, *Csf2*, *Il3*, *Il6*, *Il15,* and *Thpo* (46, 65, 67, 72, 104). A slightly different approach was used for replacement of the *Il7*, *Il15,* and *Tnfsf13b* genes, through insertion of a human cDNA in frame with the start codon of the corresponding mouse gene, followed by a poly-adenylation signal (**Figure 3B**) (101, 105).

Because of its role in supporting NK cell development, human IL-15 is highly featured in the humanized mouse literature, and it has been delivered to recipient mice by each of the methods described above (46, 94, 96, 99, 101). Since these approaches have been reported by different groups, their direct comparison and the evaluation of respective merits and limitations are difficult. However, the SRG-15 recipient mouse stands out as a definitive solution to the limited development of human NK cells in humanized mice, owing to its simplicity of use (no cytokine administration is needed), the physiological expression of the cytokine by knock-in gene replacement, the comprehensive phenotypic comparison to human peripheral blood cells and rigorous functional *in vivo* characterization (46).

In addition to expressing a human cytokine, knock-in gene replacement abrogates expression of the corresponding mouse cytokine (**Figure 3**). If the human cytokine is not fully cross-reactive, this can result in the absence of the cytokine-dependent mouse cell population and niche opening (103). This is best illustrated in the case of GM-CSF (encoded by *Csf2/CSF2*), where only 56% of amino acids are shared between human and mouse (1, 67). In mice with homozygous humanization of the *Csf2* locus, the absence of mouse GM-CSF induces alveolar macrophage deficiency in the lung and a resulting pathology described as pulmonary alveolar proteinosis (67), recapitulating the phenotype of *Csf2* knockout mice (88–90). Upon human CD34$^+$ cell transplantation, human GM-CSF supports the development of human alveolar macrophages and partial rescue of the proteinosis pathology (67).

Importantly, because hematopoiesis is a stepwise process in which stem cells gradually differentiate toward more committed progenitors and multiple lineages of mature cells (1, 2),

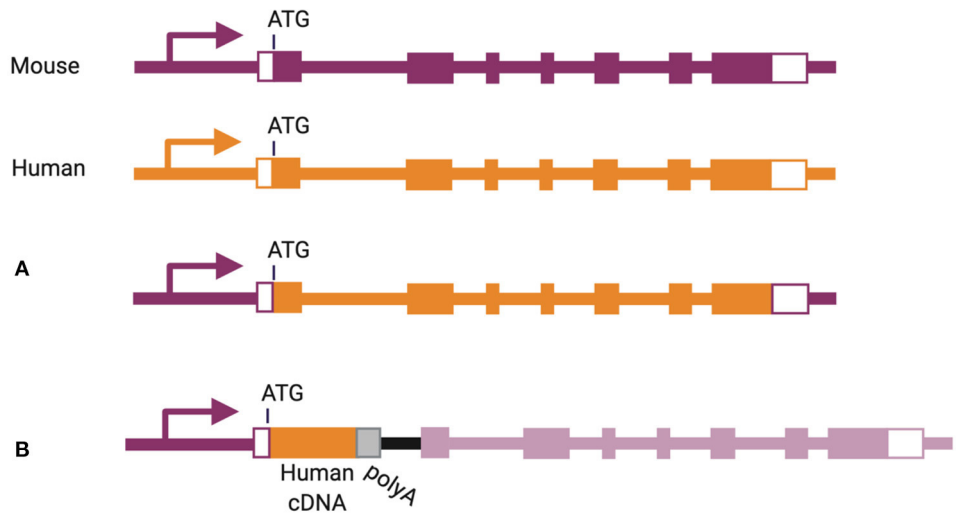

FIGURE 3 | Methods of knock-in gene humanization by **(A)** gene replacement or **(B)** cDNA insertion.

humanization of several cytokines is required to support the maintenance and multilineage differentiation of human HSPCs. This is exemplified in the MISTRG mouse in which M-CSF, IL-3, GM-CSF and THPO are humanized by knock-in replacement, on the SRG genetic background (17, 71). Niche opening and four human cytokines synergize to support the engraftment of human CD34$^+$ cells without radiation preconditioning (17, 18). The long-term maintenance of functional HSPCs is demonstrated by their serial transplantation for up to four generations of MISTRG recipients (18). These mice also support multilineage differentiation of human B, T and dendritic cells (similarly to NSG mice) as well as different subsets of functional myelo-monocytic cells in lymphoid and non-lymphoid tissues (17, 18). The myelo-monocytic cells themselves express human IL-15/IL-15Rα, which in turn supports the development and function of human NK cells (17). Overall, MISTRG mice emphasize the benefits of combining multiple strategies for the provision of human cytokines in the development of improved recipient mice by: niche opening by elimination of the corresponding mouse cytokines; physiological expression of each cytokine; synergy between multiple cytokines; and, indirectly, cross-support between different human immune cell lineages.

Co-transplantation of Supporting Human Cells or Tissues

Although providing specific cytokines can be effective, it would be a long and arduous journey to humanize the entire spectrum of hematopoiesis-supporting cytokines (and possibly other required factors). Therefore, co-transplantation of supporting human cells or tissues, naturally found in the BM niche or in other primary lymphoid organs, can be used to provide all required factors and more fully recapitulate human hematopoietic development and homeostasis.

A well-established protocol of such co-transplantation is the BM, liver, thymus (BLT) humanized mouse model (106, 107). BLT mice are generated by co-transplanting human fetal liver and thymus under the murine renal capsule in preconditioned adult immunodeficient mice, before injecting syngeneic CD34$^+$ HSPCs intravenously. The liver and thymus implants form a liver-thymus organoid that contains stromal microenvironments and provides cytokines at local physiological concentrations, requisite for the differentiation of functional B, T, and NK cells, dendritic cells and monocytes/macrophages, as well as long-term maintenance of human hematopoiesis and lymphopoiesis (106–108). Because human T cells develop in the context of thymic epithelial cells, the human thymus organoid contains significantly higher absolute numbers of thymocytes, compared to mouse thymus (109) and a repertoire of immunocompetent human leukocyte antigen (HLA) class I- and class II-restricted T lymphocytes is selected (106, 107, 110). The immune cell distribution in BLT humanized mice is well-described for both primary and secondary lymphoid organs, including BM, human and mouse thymus, intestines (lamina propria), mesenteric lymph nodes, vaginal tissues, liver and lungs (106, 107, 109, 111–113). Although the BLT protocol was first described using the NOD-SCID background (106, 107), this technique can be applied to any recipient mouse, and has been used successfully in NSG (109, 113), NSG-SGM3 (98), and B6RG-CD47 (48) mice. Thus, investigators can use the BLT protocol to enhance human T cell development in a mouse strain with immune characteristics that are appropriate for their study.

Intravenous or intrafemoral co-transplantation of human BM-derived MSCs along with CD34$^+$ cord blood cells is another strategy to improve engraftment of CD34$^+$ and CD45$^+$ cells in immunodeficient mice (114–117). Overall, co-transplantation of the BM-derived MSCs into humanized mice can improve human HSPC maintenance and expansion, and improve reconstitution

of the human hemato-lymphoid system in humanized mice. Furthermore, recent studies have used genetically engineered MSCs to deliver additional human factors to support human hematopoiesis, or to facilitate the expansion and maintenance of HSPCs to allow serial transplantation and generation of larger quantities of humanized mice (118, 119).

Recent studies have used human bone organoid (ossicles) as a method to add human BM microenvironment for engrafted HSPCs to occupy (120, 121). Ossicles are often generated by seeding 3D polymer scaffolds with human BM-derived MSCs. These are then implanted subcutaneously into NSG mice and become colonized with subsequently injected human HSPCs, enabling their expansion and differentiation (122–128). Humanized ossicles contain increased human immature and mature hematopoietic cells as compared to the bones of host mice implanted with only human $CD34^+$ cells, indicating homing of HSPCs (122, 128). Additionally, self-renewing HSPCs from humanized ossicles can reconstitute hematopoiesis in secondary recipient mice, demonstrating maintenance of their functional properties (129). Most importantly, high engraftment levels of $hCD45^+$ cells were measured in the blood, spleen and mouse bone (130, 131). High numbers of human erythroid lineage cells and robust differentiation of mature myeloid cells were also detected (132).

With the development of MISTRG and MISTRG6 mouse strains that express essential human cytokines, and protocols for co-transplantation of human fetal bone chips or ossicles, major progress has been made in transplanting patient-derived hematologic malignancies into humanized BM niches. Samples from patients with myelodysplastic syndromes, myeloproliferative neoplasms, low risk acute myeloid leukemia, diffuse large B cell lymphoma or multiple myeloma have been successfully engrafted, using diverse recipient mice and protocols (72, 123, 125, 133–136).

FUTURE CHALLENGE #1: THE MISSING LINEAGES

Provision of specific human cytokines significantly improved the development, homeostasis and function of human NK cells and myelo-monocytic cells in humanized mice. But several lineages remain defective. For example, human neutrophils are generally present in the BM of humanized mice, but their frequency is negligible in the periphery (50). Cytokine overexpression in NSG-SGM3 mice increases the frequency of granulocytic $CD33^+$ cells in the BM and the periphery (18, 69, 70), but these cells display the morphology and cell surface phenotype of immature cells (18). Human cytokine knock-in MISTRG mice also do not have improved mature neutrophil numbers in the periphery (17, 18). Therefore, the differentiation, egress, maturation and/or survival of human neutrophils likely requires additional factors.

Human red blood cells (RBCs) and platelets are probably the most challenging hematopoietic cells to develop in mice. They illustrate that additional strategies, beyond the provision of human cytokines, will likely be needed to support the complete spectrum of human hematopoietic lineages in mice. In the BM of humanized NSG mice, human erythroid ($CD235a^+$) and megakaryocytic ($CD41^+CD61^+$) progenitors are extremely rare. Their frequency is increased by at least an order of magnitude in NSGW41 and MISTRG recipient mice but surprisingly, overexpression of human erythropoietin (EPO) did not further improve human erythropoiesis (79, 133). The increase in genetically preconditioned mice is likely due to the better competition of human progenitors against mouse progenitors in the open hematopoietic niche, and/or support from knocked-in human factors. However, erythropoiesis is arrested at an immature ($CD71^+$ $CD235a^+$) stage. As a result, few mature $CD71^-CD235a^+$ human reticulocytes are detectable in the BM and human RBCs rarely exceed 1% in peripheral blood (79).

Several lines of evidence demonstrate that this deficiency is due to a developmental defect as well as impaired survival. Indeed, human RBCs are highly susceptible to destruction in mice. Expression of human SIRPα in BRG mice, or depletion of macrophages by clodronate treatment in NOD SCID mice, extends the lifespan of adoptively transferred human RBCs (45). However, in both cases, the half-life of human RBCs does not exceed ∼16 h, which is much shorter than the 10–20-days half-life of mouse RBCs in similar transfer experiments (137). Accordingly, clodronate treatment results in significant but transient and incomplete increase in human RBCs and platelets in mice humanized by $CD34^+$ cell transplantation (52, 53, 79). In those conditions, injection of the human cytokines, IL-3 and EPO, promotes an increase in peripheral RBC counts (52). But, because clodronate targets both mouse and human cells, the treatment results in a humanized mouse entirely lacking human phagocytic cells, which limits the applicability of the model for studies of human immunity.

Therefore, the entire panel of mechanisms limiting the half-life of human RBCs and platelets in mice will need to be identified and resolved. In addition, the adequate combination of human cytokines will have to be provided, to enable the mice to live with primarily human platelets and RBCs. Such a model would be highly useful for studying diseases caused by pathogens with exclusive tropism for human RBCs [e.g., malaria caused by *Plasmodium falciparum* (138)] or diseases in which platelets contribute to pathogenesis [e.g., dengue fever, autoimmune thrombocytopenia (139, 140)]. In the meantime, current models (such as MISTRG) have already demonstrated their utility for modeling the early BM stages of human erythropoiesis and thrombopoiesis, as well as for studying drug responses in pathologies, including myelodysplastic syndromes and myeloproliferative neoplasms (133, 134).

FUTURE CHALLENGE #2: ADAPTIVE IMMUNITY

As a result of advances discussed above, we now have humanized mice in which both cellular and humoral adaptive immune responses can be elicited. However, these responses are largely modest in magnitude, quality and duration, as outlined below.

Antigen-Specific Adaptive Immunity

Humanized mice generated by transplantation of CD34$^+$ cells, or following the BLT protocol, can mount antigen-specific adaptive immune responses (21, 107, 141, 142). Evidence of protective immunity, capable of controlling pathogen replication and resulting disease, was provided in the context of Epstein-Barr virus (EBV), dengue virus (DENV), and human immunodeficiency virus-1 (HIV-1) infection. Indeed, in CD34$^+$-humanized NSG mice, antibody-mediated depletion of T cells led to the development of EBV-associated tumors, suggesting that T cell-mediated immunity can control EBV infection in this setting (143). Robust CD4$^+$ and CD8$^+$ T cell responses were also detected after DENV and HIV-1 infection. Notably, in HIV-1-infected BLT mice, CD8$^+$ T cell responses were HLA-restricted and directed against epitopes previously described as immunogenic in humans. Furthermore, CD8$^+$ T cell-mediated viral recognition led to viral epitope evolution, closely resembling clinical observations (142).

Despite having detectable anti-viral T cells, CD34$^+$-humanized and BLT mice generally exhibit weak humoral responses after viral infection (144, 145). While neutralizing antibodies were detected in a subset of DENV-infected mice, in both CD34$^+$-only and BLT humanized mice, the anti-EBV or anti-HIV-1 antibody responses were either weak, equivocal or delayed (111, 141). This was also the case in humanized MISTRG mice, where enhanced innate immune cell engraftment led to improved T cell function after *Listeria monocytogenes* infection, but humoral immunity remained weak (17). Across these models, immunoglobulin class-switching and somatic hypermutation are rarely achieved, likely because most B cells fail to reach a fully mature phenotype in the periphery, T cell repertoire is selected on mouse and human MHC and is suboptimal, and recipient mice have disorganized lymph nodes and little capacity for germinal center formation (146).

While human B cells are detectable in high frequencies in humanized mice, most exhibit an immature phenotype, and remain blocked at the transitional stage of B cell development (1, 146). Since immature B cells have a reduced capacity to respond to antigen (147), several groups sought to improve B cell maturation and by extension, their function by knocking-in human cytokines that are known to support B cell development. Surprisingly, human B cell activation factor (BAFF, encoded by *TNFSF13B*) knock-in resulted in reduced numbers of mature naïve B cells, and reduced antibody production after immunization (105). Human IL-7 knock-in had no effect on B cell numbers and any effect on B cell function remains to be determined (101). In contrast, human IL-6 positively impacted B cell differentiation into plasmablasts and memory cells after immunization with model antigen, and promoted somatic hypermutation and class switching, albeit to a lower level than that observed in humans (73). IL-6 knock-in mice also had improved T cell development; therefore, it is possible that enhanced B cell responses were in part due to increased T cell help.

Thymic Lymphopoiesis and Repertoire Selection

Thymic lymphopoiesis is suboptimal in mice humanized by transplantation of CD34$^+$ HSPCs, in part due to a lack of thymopoiesis-supporting human cytokines. As a result, thymic cellularity is extremely low (only a few million cells) and CD4$^+$ CD8$^+$ double positive cells, which represent the vast majority of thymocytes in a healthy thymus, are frequently underrepresented. Human IL-6 knock-in produces increased thymic cellularity (73), but additional cytokines are likely required to restore the normal size of a mouse thymus, populated by human thymocytes. While a human IL-7 knock-in recipient mouse has been developed, a thorough characterization of thymic cellularity upon HSPC engraftment has not been reported to date (101).

Human T cell repertoire selection in the mouse thymus involves interactions with both mouse MHC and human HLA-expressing cells-expressing cells (1, 10, 21). Specifically, developing human T cells are positively selected by mouse epithelial cells and negatively selected by both mouse epithelial and mouse and human hematopoietic cells (148). The resulting T cell receptor (TCR) repertoire is weakly reactive to autologous human leukocyte antigen (HLA) class I and II, and tolerant to mouse MHC. Indeed, in *in vitro* re-stimulation assays, T cells from humanized mice were shown to proliferate better in response to allogeneic human DCs compared to autologous human DCs or mouse DCs (21). To improve the repertoire and function of human T cells, several recipient strains have been engineered to express HLA class I and class II (143, 144, 149–154). HLA-restricted T cell responses have been reported in these mice (143, 149). Additional characterization and comparison of these mice are required to rigorously evaluate how transgenic HLA expression in recipient HSPC-humanized mice impacts human T cell selection and function.

In BLT mice, T cells develop in the human thymus organoid and are positively and negatively selected on human autologous HLA molecules (106, 107, 155). Consequently, BLT mice are generally accepted as having a more diverse T cell repertoire, capable of mounting more robust adaptive immune responses, as discussed above. However, because the induction of tolerance for mouse MHC and mouse tissue-restricted antigens is incomplete, BLT mice are prone to the development of xenogeneic graft-vs.-host disease (xGvHD) (156, 157), as discussed below.

Few direct comparisons between BLT and HSPC-engrafted mice have been reported to date (144, 145). In both models, it is apparent that thymic lymphopoiesis and the selection of a diverse and tolerant T cell repertoire is a complex issue, and additional work is needed.

Secondary Lymphoid Organs

Secondary lymphoid organs including lymph nodes (LNs), spleen, Peyer's patches, and mucosa-associated lymphoid tissues normally provide niche microenvironments where T and B cells interact with hematopoietic antigen-presenting cells and stromal follicular dendritic cells (FDCs) to initiate the adaptive immune response (158, 159). LN formation requires IL-7- and

IL-2Rγ-dependent lymphoid tissue inducer (LTi) cells (160). However, because most immunodeficient recipient mice lack *Il2rg* to promote tolerance to the human graft through NK cell depletion, they also lack LTi cells and defined LN structures. This represents a major obstacle in recapitulating the human adaptive immune response in mice. While engraftment with human $CD34^+$ cells can partially rescue the LN anlagen, T and B cell zones remain poorly organized compared to those in normal human or normal mouse LNs. Furthermore, the germinal center formation is impaired, in part because it involves human B cells interacting with stromal FDCs of mouse origin (1, 159).

Given that the germinal center is the primary site of B cell-T cell collaboration, antibody affinity maturation and class switching, multiple groups sought to improve LN formation and germinal center development (158). Adoptive transfer of autologous human DCs lentivirally transduced to express GM-CSF, IFNα, and human cytomegalovirus (HCMV) viral antigen enhances LN development in humanized NRG mice, and by extension promotes T cell-B cell collaboration and the production of neutralizing anti-HCMV antibodies (161, 162). Human fetal organ co-transplantation also partially rescues secondary lymphoid organ development. BLT mice have improved lymphoid structure development in the spleen and lymph nodes compared to $CD34^+$-only engrafted mice, and as a result, they also have more robust antigen-specific adaptive immunity (106, 107). However, a comparison of IL-2Rγ-sufficient NOD-SCID BLT humanized mice and IL-2Rγ-deficient NSG BLT humanized mice showed that only NOD-SCID BLT mice contain mucosal tissue-associated T cells (109). This result emphasizes the critical nature of IL-2Rγ in the development of LN and other secondary lymphoid organs that are essential for adaptive immune responses and mucosal immunity. The importance of structured secondary lymphoid organs for adaptive immunity is further demonstrated by the addition of fetal spleen to BLT mice (163). Human fetal spleen implants grow into spleen organoids with prominent follicular lymphoid structure; implanted mice have improved B cell and T cell engraftment, compared to control mice without human spleen implants, and can mount antigen-specific responses to immunization (163).

Another strategy to overcome the near-absence of LNs in *Il2rg*$^{-/-}$ humanized mice involves transgenic overexpression of murine thymic stromal lymphopoietin (TSLP). TSLP is another cytokine of the IL-2 family, its receptor is independent of the IL-2Rγ chain and, when overexpressed under a keratin 14 promoter (specific for epithelial/mesenchymal cells), it rescues LN development in *Il7* deficient mice (164, 165). Crossing the transgene to BRGS resulted in the BRGST model, in which mouse LTi cells and LN structures are restored (74). Upon transplantation of $CD34^+$ HSPCs, BRGST mice support the development of a human immune system, including sizeable LNs with compartmentalized human T and B cell zones. BRGST mice also have more mature B cells and IL-21 producing follicular helper T cells, essential to promoting adaptive immunity. Consequently, BRGST mice mounted enhanced antigen-specific humoral immune responses upon immunization with an experimental antigen (74). Overall, this novel model successfully addresses a major limitation that had hampered immune function in most humanized mouse models to date.

FUTURE CHALLENGE #3: GRAFT-TO-HOST TOLERANCE

The transplantation of human cells into recipient mice is feasible because the recipient mice used are immunologically tolerant to the graft. As these mice support an increasingly functional human immune system, immunologic tolerance of the graft for its host can become an issue.

Xenogeneic Graft-vs.-Host Disease

Adoptive transfer of human T cells from donor PBMCs into immunodeficient recipient mice results in xGvHD, thereby limiting the potential duration of experiments with these mice. To prevent xGvHD, two strains of immunodeficient mice lacking mouse MHC-I and MHC-II have been developed, which prevented the onset of xGvHD, while retaining the functional properties of human T cells (166, 167). But, as discussed above, PBMC transfer results in an incomplete human hematopoietic system in the mice.

When mice are humanized by transplantation of $CD34^+$ HSPCs, developing human T cells undergo positive and negative selection in the mouse thymus. Consequently, they are tolerized for mouse MHC-I and MHC-II, and xGvHD is not a limitation in this model (1, 10, 21).

Finally, in BLT mice, T cells are educated in the human thymus organoid and once they reach the periphery, they are allogeneic to the mouse MHC molecules and can induce xGvHD (156, 157). Different levels of xGvHD are reported by different groups, suggesting that the disease could be affected by subtle differences in protocols, the microbiota of the mice, or the recipient strain used (48). The development of xGvHD in the BLT model is attributed to residual mature T cells present in the fetal human thymus grafts, and these passenger T cells can be removed by treating the thymic implants with 2′-deoxyguanosine, or by treating the mice with anti-human CD2 antibody post-surgery (168).

Xenogeneic Hemophagocytosis

The efficient development of human phagocytic cells of the myelo-monocytic lineage in MISTRG creates a new challenge; i.e., the absence of phagocytic tolerance from the human graft toward the mouse host. Mouse red blood cells are particularly susceptible to destruction by human phagocytic cells, and highly engrafted MISTRG mice develop lethal anemia (17). Consequently, the transplantation protocol in MISTRG needs to be optimized so that engraftment allows mouse erythropoiesis in the BM (or extramedullary erythropoiesis) to sufficiently compensate for the loss of mouse red blood cells by phagocytosis, as long as a specific experiment requires (17, 18, 58, 133). Long-term solutions will need to be implemented, either to establish human-to-mouse phagocytic tolerance or to enable human erythropoiesis to reach healthy human RBC counts and maintain mouse homeostasis, as discussed above.

Xenogeneic GvHD and hemophagocytosis remind us that activation and tolerance are two equally important features of the immune system and are inseparable. As human immune function improves in mouse recipients, it is likely that parallel strategies will need to be developed to maintain tolerance of the human immune graft for the mouse host.

FUTURE CHALLENGE #4: INTERACTIONS BETWEEN IMMUNE CELLS AND TARGET TISSUES OR TUMORS

Immune responses require functional interactions between immune cells and their target, either through direct cell-cell contact or via soluble factors. In humanized mice generated by transplantation of human HSPCs, this requirement is fulfilled when the target of the immune response is also a human hematopoietic cell. Accordingly, T and B cell-mediated immunity have been demonstrated in the context of infection by pathogens with tropism for human hematopoietic cells, such as EBV, HIV-1, or dengue virus (141, 143, 169). But, for pathogens that infect non-hematopoietic tissues, or for inflammatory mediators that induce systemic responses, the cross-reactivity between human immune effector mechanisms and mouse target tissues may be incomplete. Humanizing cytokine receptors or other factors, such as adhesion molecules, could improve the responsiveness of mouse tissues to human immune cells and soluble mediators.

Co-transplantation of the human target tissue along with the human hematopoietic system has been performed in the context of cancer and infectious diseases. Implantation of human tumors, either from an established cell line or from a "patient-derived xenograft" (PDX), in mice already repopulated with a human immune system, provides useful models for immuno-oncology and immunotherapy studies (170–173). However, developing such "immuno-PDX" models can be challenging as each patient-derived tumor or cell line has different growth characteristics in mice, and matching patient's HLA to the HLA of the HSPC donor is not always feasible. Additionally, many components of the tumor microenvironment (e.g., vasculature) remain of mouse origin. Consequently, antitumoral immunity, or the response to immunotherapies, can be highly variable from experiment to experiment (171). In the case of hematologic malignancies, new strains of recipient mice (i.e., MISTRG and MISTRG6) extend the range of transplantable diseases (72, 133–136) and provide new opportunities to evaluate candidate immunotherapies, such as adoptive T cell therapies (174, 175).

Transplantation of human liver tissue enables infection of the mouse host by human hepatotropic viruses. Because implantation of a liver fragment at an ectopic site does not fully recapitulate the architecture and function of the liver, protocols of orthotopic implantation have been developed. These methods follow the same principles as for the transplantation of human hematopoiesis (176): an immunodeficient strain to prevent immune rejection of the graft; engineering of the mouse to induce mouse liver injury and open the niche for human hepatocytes; and, in some instances, support from human growth factors (177). Several methods have been developed to eliminate mouse hepatocytes, relying on the expression of cytolytic proteins [e.g., overexpression of urokinase plasminogen activator under an albumin promoter in uPA mice (178, 179)] and/or inactivation of metabolic enzymes essential for hepatocyte homeostasis [e.g., inactivation of the fumarylacetoacetate hydrolase in *Fah*$^{-/-}$ mice (180, 181)]. Upon injection of human hepatocytes, these mice support high levels of liver chimerism and are permissive for infection by the human hepatotropic viruses, HBV and HCV. To study human immune responses to these pathogens, mice can be dually transplanted with human hepatocytes and CD34^{+} HSPCs; human immune cells are recruited to the human liver in these chimeric mice and immune responses are triggered upon viral infections (177, 182, 183).

Finally, subcutaneous implantation of a fragment of human fetal lung contains all cell types naturally present in this tissue, and extends the permissiveness of the host mouse to respiratory pathogens with human tropism, including respiratory syncytial

BOX 2 | Which humanized mouse model is best for your studies?

There is no one-size-fits-all model. Here are a few practical considerations:

(1) Which mice and human cells/tissue do you have access to?

(2) What question are you trying to answer?

(3) Which cell types are important to answer your question?

In addition to considering these practical questions, it is important to know what has been done before you. Take time to read the literature and critically analyze the experiments. If you are able to talk to the people who developed the model or to someone who has recently published on the model of interest, you may receive invaluable unpublished data and advice.

Finally, applying these criteria, we provide our own selection, subjective and probably slightly biased, of the models that we consider most suitable for specific applications.

Hematopoiesis

- HSPC biology: NSGW41, MISTRG, MISTRG6
- Erythropoiesis and thrombopoiesis: NSGW41, MISTRG, MISTRG6 (BM only, limited)
- Myelopoiesis: MISTRG, MISTRG6
- Hematologic malignancies: MISTRG, MISTRG6

Innate immunity

- Monocytes/macrophages: MISTRG, MISTRG6
- DCs: NSG (or any other strain, depending on additional requirements)
- Mast cells: NSG-SGM3
- Neutrophils: no suitable model available
- NK cells: SRG15, MISTRG
- Innate lymphoid cells: NSG (or any other strain, depending on additional requirements)

Adaptive immunity

BLT mice are generally considered as supporting more robust adaptive immunity than mice transplanted with HSPCs only. However, few direct comparisons have been reported and antigen-specific immune responses remain relatively weak or delayed, even in BLT mice. Importantly, the BLT protocol can be applied with any recipient mice.

Expression of HLA molecules by the mouse host qualitatively favors HLA-restricted immune responses. But the impact on the amplitude of responses remains to be rigorously quantified.

- B cells: BLT, SRG6, MISTRG6
- T cells: BLT, BRGST.

virus, Middle East respiratory syndrome coronavirus, and HCMV. This was recently accomplished by surgical implantation of a fragment of human lung tissue in BLT mice, resulting in the "BLT-L" model (184). Upon infection with HCMV, by direct injection in the lung implant, BLT-L mounted an antigen specific adaptive immune response, capable of controlling virus replication (184).

Thus, co-transplantation models greatly broaden the spectrum of human immune responses that can be studied in humanized mice. However, current approaches rely on highly specialized protocols and recipient mice, and should still be considered as prototypes under development.

CONCLUSION

Tremendous progress has been accomplished since pioneering humanized mouse models were developed in the late 1980s. In the past decade, a flurry of new opportunities have been enabled by the optimization of recipient mouse strains and humanization protocols. The most advanced models support long-term multilineage human hematopoiesis, and recapitulate essential aspects of innate immunity and antigen-specific adaptive immunity. Furthermore, numerous hematologic diseases can now be modeled by xenotransplantation of primary patient-derived samples.

Despite this progress, limitations remain. Rigorous evaluation and comparison of the new models is needed, while supporting additional innovations that might drive transformative advances. Until one or more humanized mouse model fully recapitulates human immunity, we can enthusiastically but critically use the currently available strains to answer specific, clinically-relevant questions and hopefully inform the development of new, life-saving therapies (**Box 2**).

AUTHOR CONTRIBUTIONS

All authors listed have made a substantial, direct and intellectual contribution to the work, and approved it for publication.

FUNDING

Research in our lab was supported by the NIH/NCI CA234720, NIH/NIAID AI138011, The Hartwell Foundation, The Emerson Collective, the Seattle Translational Tumor Research, the University of Washington Center for AIDS Research, and the Immunotherapy Integrated Research Center at Fred Hutch. TM was supported by a Parker Institute for Cancer Immunotherapy Scholar Award. EC was supported by a postdoctoral fellowship from Fred Hutch's Immunotherapy Integrated Research Center.

ACKNOWLEDGMENTS

We thank Deborah Banker for manuscript editing, and the Guest Editors for inviting us to submit this manuscript, which we wrote as an educational work from home activity. Figures created with BioRender.com.

SUPPLEMENTARY MATERIAL

The Supplementary Material for this article can be found online at: https://www.frontiersin.org/articles/10.3389/fimmu.2021.643852/full#supplementary-material

REFERENCES

1. Rongvaux A, Takizawa H, Strowig T, Willinger T, Eynon EE, Flavell RA, et al. Human hemato-lymphoid system mice: current use and future potential for medicine. *Annu Rev Immunol.* (2013) 31:635–74. doi: 10.1146/annurev-immunol-032712-095921
2. Doulatov S, Notta F, Laurenti E, Dick JE. Hematopoiesis: a human perspective. *Cell Stem Cell.* (2012) 10:120–36. doi: 10.1016/j.stem.2012.01.006
3. Gbyli R, Song Y, Halene S. Humanized mice as preclinical models for myeloid malignancies. *Biochem Pharmacol.* (2020) 174:113794. doi: 10.1016/j.bcp.2020.113794
4. Douam, F. and Ploss A, The use of humanized mice for studies of viral pathogenesis and immunity. *Curr Opin Virol.* (2018) 29:62–71. doi: 10.1016/j.coviro.2018.03.003
5. Li Y, Di Santo JP. Modeling infectious diseases in mice with a "humanized" immune system. *Microbiol Spectr.* (2019) 7:BAI-0019-2019. doi: 10.1128/microbiolspec.BAI-0019-2019
6. Shultz LD, Ishikawa F, Greiner DL. Humanized mice in translational biomedical research. *Nat Rev Immunol.* (2007) 7:118–30. doi: 10.1038/nri2017
7. Shultz LD, Brehm MA, Garcia-Martinez JV, Greiner DL. Humanized mice for immune system investigation: progress, promise and challenges. *Nat Rev Immunol.* (2012) 12:786–98. doi: 10.1038/nri3311
8. Huntington ND, Di Santo JP. Humanized immune system (HIS) mice as a tool to study human NK cell development. *Curr Top Microbiol Immunol.* (2008) 324:109–24. doi: 10.1007/978-3-540-75647-7_7
9. Li Y, Di Santo JP. Probing human NK cell biology using human immune system (HIS) Mice. *Curr Top Microbiol Immunol.* (2016) 395:191–208. doi: 10.1007/82_2015_488
10. Manz MG. Human-hemato-lymphoid-system mice: opportunities and challenges. *Immunity.* (2007). 26:537-41. doi: 10.1016/j.immuni.2007.05.001
11. Theocharides AP, Rongvaux A, Fritsch K, Flavell RA, Manz MG. Humanized hemato-lymphoid system mice. *Haematologica.* (2016) 101:5–19. doi: 10.3324/haematol.2014.115212
12. Mosier DE, Gulizia RJ, Baird SM, Wilson DB. Transfer of a functional human immune system to mice with severe combined immunodeficiency. *Nature.* (1988) 335:256–9. doi: 10.1038/335256a0
13. Kondo M, Wagers AJ, Manz MG, Prohaska SS, Scherer DC, Beilhack GF, et al. Biology of hematopoietic stem cells and progenitors: implications for clinical application. *Annu Rev Immunol.* (2003) 21:759–806. doi: 10.1146/annurev.immunol.21.120601.141007
14. Allen TM, Brehm MA, Bridges S, Ferguson S, Kumar P, Mirochnitchenko O, et al. Humanized immune system mouse models: progress, challenges and opportunities. *Nat Immunol.* (2019) 20:770–4. doi: 10.1038/s41590-019-0416-z
15. Holyoake TL, Nicolini FE, Eaves CJ. Functional differences between transplantable human hematopoietic stem cells from fetal liver, cord blood, adult marrow. *Exp Hematol.* (1999) 27:1418–27. doi: 10.1016/S0301-472X(99)00078-8
16. Nicolini FE, Holyoake TL, Cashman JD, Chu PP, Lambie K, Eaves CJ. Unique differentiation programs of human fetal liver stem cells shown both in vitro and in vivo in NOD/SCID mice. *Blood.* (1999) 94:2686–95. doi: 10.1182/blood.V94.8.2686.420k15_2686_2695

17. Rongvaux A, Willinger T, Martinek J, Strowig T, Gearty SV, Teichmann LL, et al. Development and function of human innate immune cells in a humanized mouse model. *Nat Biotechnol.* (2014). 32:364–72. doi: 10.1038/nbt.2858
18. Sippel TR, Radtke S, Olsen TM, Kiem HP, Rongvaux A. Human hematopoietic stem cell maintenance and myeloid cell development in next-generation humanized mouse models. *Blood Adv.* (2019) 3:268–274. doi: 10.1182/bloodadvances.2018023887
19. Tyagi RK, Li J, Jacobse J, Snapper SB, Shouval DS, Goettel JA. Humanized mouse models of genetic immune disorders and hematological malignancies. *Biochem Pharmacol.* (2020) 174:113671. doi: 10.1016/j.bcp.2019.113671
20. Mazurier F, Doedens M, Gan OI, Dick JE. Rapid myeloerythroid repopulation after intrafemoral transplantation of NOD-SCID mice reveals a new class of human stem cells. *Nat Med.* (2003) 9:959–63. doi: 10.1038/nm886
21. Traggiai E, Chicha L, Mazzucchelli L, Bronz L, Piffaretti JC, Lanzavecchia A, et al. Development of a human adaptive immune system in cord blood cell-transplanted mice. *Science.* (2004) 304:104–7. doi: 10.1126/science.1093933
22. Bosma GC, Custer RP, Bosma MJ. A severe combined immunodeficiency mutation in the mouse. *Nature.* (1983) 301:527–30. doi: 10.1038/301527a0
23. Blunt T, Finnie NJ, Taccioli GE, Smith GC, Demengeot J, Gottlieb TM, et al. Defective DNA-dependent protein kinase activity is linked to V(D)J recombination and DNA repair defects associated with the murine scid mutation. *Cell.* (1995) 80:813–23. doi: 10.1016/0092-8674(95)90360-7
24. Kamel-Reid S, Dick JE. Engraftment of immune-deficient mice with human hematopoietic stem cells. *Science.* (1988) 242:1706–9. doi: 10.1126/science.2904703
25. McCune JM, Namikawa R, Kaneshima H, Shultz LD, Lieberman M, Weissman IL. The SCID-hu mouse: murine model for the analysis of human hematolymphoid differentiation and function. *Science.* (1988) 241:1632–9. doi: 10.1126/science.2971269
26. Lapidot T, Pflumio F, Doedens M, Murdoch B, Williams DE, Dick JE. Cytokine stimulation of multilineage hematopoiesis from immature human cells engrafted in SCID mice. *Science.* (1992) 255:1137–41. doi: 10.1126/science.1372131
27. Namikawa R, Kaneshima H, Lieberman M, Weissman IL, McCune JM. Infection of the SCID-hu mouse by HIV-1. *Science.* (1988) 242:1684–6. doi: 10.1126/science.3201256
28. Mosier DE, Gulizia RJ, Baird SM, Wilson DB, Spector DH, Spector SA. Human immunodeficiency virus infection of human-PBL-SCID mice. *Science.* (1991) 251:791–4. doi: 10.1126/science.1990441
29. McCune J, Kaneshima H, Krowka J, Namikawa R, Outzen H, Peault B, et al. The SCID-hu mouse: a small animal model for HIV infection and pathogenesis. *Annu Rev Immunol.* (1991) 9:399–429. doi: 10.1146/annurev.iy.09.040191.002151
30. Miller JS, Lanier LL. Natural killer cells in cancer immunotherapy. *Annu Rev Cancer Biol.* (2019) 3:77–103. doi: 10.1146/annurev-cancerbio-030518-055653
31. Ma A, Koka R, Burkett P. Diverse functions of IL-2, IL-15, and IL-7 in lymphoid homeostasis. *Annu Rev Immunol.* (2006) 24:657–79. doi: 10.1146/annurev.immunol.24.021605.090727
32. Mazurier F, Fontanellas A, Salesse S, Taine L, Landriau S, Moreau-Gaudry F, et al. de Verneuil, A novel immunodeficient mouse model–RAG2 x common cytokine receptor gamma chain double mutants–requiring exogenous cytokine administration for human hematopoietic stem cell engraftment. *J Interferon Cytokine Res.* (1999) 19:533–41. doi: 10.1089/107999099313983
33. Ishikawa F, Yasukawa M, Lyons B, Yoshida S, Miyamoto T, Yoshimoto G, et al. Development of functional human blood and immune systems in NOD/SCID/IL2 receptor {gamma} chain(null) mice. *Blood.* (2005) 106:1565–73. doi: 10.1182/blood-2005-02-0516
34. Shultz LD, Lyons BL, Burzenski LM, Gott B, Chen X, Chaleff S, et al. Human lymphoid and myeloid cell development in NOD/LtSz-scid IL2R gamma null mice engrafted with mobilized human hemopoietic stem cells. *J Immunol.* (2005) 174:6477–89. doi: 10.4049/jimmunol.174.10.6477
35. Ito M, Hiramatsu H, Kobayashi K, Suzue K, Kawahata M, Hioki K, et al. NOD/SCID/gamma(c)(null) mouse: an excellent recipient mouse model for engraftment of human cells. *Blood.* (2002) 100:3175–82. doi: 10.1182/blood-2001-12-0207
36. Yoshida H, Hayashi S, Kunisada T, Ogawa M, Nishikawa S, Okamura H, et al. The murine mutation osteopetrosis is in the coding region of the macrophage colony stimulating factor gene. *Nature.* (1990) 345:442–4. doi: 10.1038/345442a0
37. Dai XM, Ryan GR, Hapel AJ, Dominguez MG, Russell RG, Kapp S, et al. Targeted disruption of the mouse colony-stimulating factor 1 receptor gene results in osteopetrosis, mononuclear phagocyte deficiency, increased primitive progenitor cell frequencies, reproductive defects. *Blood.* (2002) 99:111–20. doi: 10.1182/blood.V99.1.111
38. Barclay, A.N. and Brown MH, The SIRP family of receptors and immune regulation. *Nat Rev Immunol.* (2006) 6:457–64. doi: 10.1038/nri1859
39. Takenaka K, Prasolava TK, Wang JC, Mortin-Toth SM, Khalouei S, Gan OI, et al. Polymorphism in Sirpa modulates engraftment of human hematopoietic stem cells. *Nat Immunol.* (2007) 8:1313–23. doi: 10.1038/ni1527
40. Hesselton RM, Greiner DL, Mordes JP, Rajan TV, Sullivan JL, Shultz LD. High levels of human peripheral blood mononuclear cell engraftment and enhanced susceptibility to human immunodeficiency virus type 1 infection in NOD/LtSz-scid/scid mice. *J Infect Dis.* (1995) 172:974–82. doi: 10.1093/infdis/172.4.974
41. Shultz LD, Schweitzer PA, Christianson SW, Gott B, Schweitzer IB, Tennent B, et al. Multiple defects in innate and adaptive immunologic function in NOD/LtSz-scid mice. *J Immunol.* (1995) 154:180–91.
42. Pearson T, Shultz LD, Miller D, King M, Laning J, Fodor W, et al. Non-obese diabetic-recombination activating gene-1 (NOD-Rag1 null) interleukin (IL)-2 receptor common gamma chain (IL2r gamma null) null mice: a radioresistant model for human lymphohaematopoietic engraftment. *Clin Exp Immunol.* (2008) 154:270–84. doi: 10.1111/j.1365-2249.2008.03753.x
43. Legrand N, Huntington ND, Nagasawa M, Bakker AQ, Schotte R, Strick-Marchand H, et al. Functional CD47/signal regulatory protein alpha (SIRPα) interaction is required for optimal human T- and natural killer- (NK) cell homeostasis in vivo. *Proc Natl Acad Sci USA.* (2011) 108:13224–9. doi: 10.1073/pnas.1101398108
44. Yamauchi T, Takenaka K, Urata S, Shima T, Kikushige Y, Tokuyama T, et al. Polymorphic Sirpa is the genetic determinant for NOD-based mouse lines to achieve efficient human cell engraftment. *Blood.* (2013) 121:1316–25. doi: 10.1182/blood-2012-06-440354
45. Strowig T, Rongvaux A, Rathinam C, Takizawa H, Borsotti C, Philbrick W, et al. Transgenic expression of human signal regulatory protein alpha in Rag2-/-gamma(c)-/- mice improves engraftment of human hematopoietic cells in humanized mice. *Proc Natl Acad Sci USA.* (2011) 108:13218–23. doi: 10.1073/pnas.1109769108
46. Herndler-Brandstetter D, Shan L, Yao Y, Stecher C, Plajer V, Lietzenmayer M, et al. Humanized mouse model supports development, function, and tissue residency of human natural killer cells. *Proc Natl Acad Sci USA.* (2017) 114:E9626–34. doi: 10.1073/pnas.1705301114
47. Jinnouchi F, Yamauchi T, Yurino A, Nunomura T, Nakano M, Iwamoto C, et al. A human SIRPA knock-in xenograft mouse model to study human hematopoietic and cancer stem cells. *Blood.* (2020) 135:1661–72. doi: 10.1182/blood.2019002194
48. Lavender KJ, Pang WW, Messer RJ, Duley AK, Race B, Phillips K, et al. BLT-humanized C57BL/6 Rag2-/-γc-/-CD47-/- mice are resistant to GVHD and develop B- and T-cell immunity to HIV infection. *Blood.* (2013) 122:4013–20. doi: 10.1182/blood-2013-06-506949
49. Oldenborg PA, Zheleznyak A, Fang YF, Lagenaur CF, Gresham HD, Lindberg FP. Role of CD47 as a marker of self on red blood cells. *Science.* (2000) 288:2051–4. doi: 10.1126/science.288.5473.2051
50. Tanaka S, Saito Y, Kunisawa J, Kurashima Y, Wake T, Suzuki N, et al. Development of mature and functional human myeloid subsets in hematopoietic stem cell-engrafted NOD/SCID/IL2rgammaKO mice. *J Immunol.* (2012) 188:6145–55. doi: 10.4049/jimmunol.1103660
51. Strowig T, Chijioke O, Carrega P, Arrey F, Meixlsperger S, Ramer PC, et al. Human NK cells of mice with reconstituted human immune system components require preactivation to acquire functional competence. *Blood.* (2010) 116:4158–67. doi: 10.1182/blood-2010-02-270678

52. Hu Z, Van Rooijen N, Yang YG. Macrophages prevent human red blood cell reconstitution in immunodeficient mice. *Blood.* (2011) 118:5938–46. doi: 10.1182/blood-2010-11-321414
53. Hu Z, Yang YG. Full reconstitution of human platelets in humanized mice after macrophage depletion. *Blood*. (2012) 120:1713–6. doi: 10.1182/blood-2012-01-407890
54. Wunderlich M, Manning N, Sexton C, Sabulski A, Byerly L, O'Brien E, et al. Improved chemotherapy modeling with RAG-based immune deficient mice. *PLoS ONE.* (2019) 14:e0225532. doi: 10.1371/journal.pone.0225532
55. Crane GM, Jeffery E, Morrison SJ. Adult haematopoietic stem cell niches. *Nat Rev Immunol.* (2017) 17:573–590. doi: 10.1038/nri.2017.53
56. Saito Y, Ellegast JM, Manz MG. Generation of humanized mice for analysis of human dendritic cells. *Methods Mol Biol.* (2016) 1423:309–20. doi: 10.1007/978-1-4939-3606-9_22
57. Legrand N, Weijer K, Spits H. Experimental model for the study of the human immune system: production and monitoring of "human immune system" Rag2-/-gamma c-/- mice. *Methods Mol Biol.* (2008) 415:65–82. doi: 10.1007/978-1-59745-570-1_4
58. Song Y, Gbyli R, Fu X, Halene S. Functional analysis of human hematopoietic stem cells in vivo in humanized mice. *Methods Mol Biol.* (2020) 2097:273–89. doi: 10.1007/978-1-0716-0203-4_18
59. Hasgur S, Aryee KE, Shultz LD, Greiner DL, Brehm MA. Generation of immunodeficient mice bearing human immune systems by the engraftment of hematopoietic stem cells. *Methods Mol Biol.* (2016) 1438:67–78. doi: 10.1007/978-1-4939-3661-8_4
60. Vatakis DN, Bristol GC, Kim SG, Levin B, Liu W, Radu CG, et al. Using the BLT humanized mouse as a stem cell based gene therapy tumor model. *J Vis Exp.* (2012) 2012:e4181. doi: 10.3791/4181
61. Choi B, Chun E, Kim M, Kim ST, Yoon K, Lee KY, et al. Human B cell development and antibody production in humanized NOD/SCID/IL-2Rγ(null) (NSG) mice conditioned by busulfan. *J Clin Immunol.* (2011) 31:253–64. doi: 10.1007/s10875-010-9478-2
62. Hayakawa J, Hsieh MM, Uchida N, Phang O, Tisdale JF. Busulfan produces efficient human cell engraftment in NOD/LtSz-Scid IL2Rgamma(null) mice. *Stem Cells.* (2009) 27:175–82. doi: 10.1634/stemcells.2008-0583
63. Singh M, Singh P, Gaudray G, Musumeci L, Thielen C, Vaira D, et al. An improved protocol for efficient engraftment in NOD/LTSZ-SCIDIL-2Rγnull mice allows HIV replication and development of anti-HIV immune responses. *PLoS ONE.* (2012) 7:e38491. doi: 10.1371/journal.pone.0038491
64. Cosgun KN, Rahmig S, Mende N, Reinke S, Hauber I, Schafer C, et al. Kit regulates HSC engraftment across the human-mouse species barrier. *Cell Stem Cell.* (2014) 15:227–38. doi: 10.1016/j.stem.2014.06.001
65. Rongvaux A, Willinger T, Takizawa H, Rathinam C, Auerbach W, Murphy AJ, et al. Human thrombopoietin knockin mice efficiently support human hematopoiesis in vivo. *Proc Natl Acad Sci USA.* (2011) 108:2378–83. doi: 10.1073/pnas.1019524108
66. Li Y, Mention JJ, Court N, Masse-Ranson G, Toubert A, Spits H, et al. A novel Flt3-deficient HIS mouse model with selective enhancement of human DC development. *Eur J Immunol.* (2016) 46:1291–9. doi: 10.1002/eji.201546132
67. Willinger T, Rongvaux A, Takizawa H, Yancopoulos GD, Valenzuela DM, Murphy AJ, et al. Human IL-3/GM-CSF knock-in mice support human alveolar macrophage development and human immune responses in the lung. *Proc Natl Acad Sci USA.* (2011) 108:2390–5. doi: 10.1073/pnas.1019682108
68. Nicolini FE, Cashman JD, Hogge DE, Humphries RK, Eaves CJ. NOD/SCID mice engineered to express human IL-3, GM-CSF and Steel factor constitutively mobilize engrafted human progenitors and compromise human stem cell regeneration. *Leukemia.* (2004) 18:341–7. doi: 10.1038/sj.leu.2403222
69. Wunderlich M, Chou FS, Sexton C, Presicce P, Chougnet CA, Aliberti J, et al. Improved multilineage human hematopoietic reconstitution and function in NSGS mice. *PLoS ONE.* (2018) 13:e0209034. doi: 10.1371/journal.pone.0209034
70. Billerbeck E, Barry WT, Mu K, Dorner M, Rice CM, Ploss A. Development of human CD4+FoxP3+ regulatory T cells in human stem cell factor-, granulocyte-macrophage colony-stimulating factor-, and interleukin-3-expressing NOD-SCID IL2Rgamma(null) humanized mice. *Blood.* (2011) 117:3076–86. doi: 10.1182/blood-2010-08-301507
71. Deng K, Pertea M, Rongvaux A, Wang L, Durand CM, Ghiaur G, et al. Broad CTL response is required to clear latent HIV-1 due to dominance of escape mutations. *Nature.* (2015) 517:381–5. doi: 10.1038/nature14053
72. Das R, Strowig T, Verma R, Koduru S, Hafemann A, Hopf S, et al. Microenvironment-dependent growth of preneoplastic and malignant plasma cells in humanized mice. *Nat Med.* (2016) 22:1351–7. doi: 10.1038/nm.4202
73. Yu H, Borsotti C, Schickel JN, Zhu S, Strowig T, Eynon EE, et al. A novel humanized mouse model with significant improvement of class-switched, antigen-specific antibody production. *Blood.* (2017) 129:959–69. doi: 10.1182/blood-2016-04-709584
74. Li Y, Masse-Ranson G, Garcia Z, Bruel T, Kök A, Strick-Marchand H, et al. A human immune system mouse model with robust lymph node development. *Nat Methods.* (2018) 15:623–30. doi: 10.1038/s41592-018-0071-6
75. Broudy VC. Stem cell factor and hematopoiesis. *Blood.* (1997). 90:1345–64. doi: 10.1182/blood.V90.4.1345
76. Geissler EN, McFarland EC, Russell ES. Analysis of pleiotropism at the dominant white-spotting (W) locus of the house mouse: a description of ten new W alleles. *Genetics.* (1981) 97:337–61.
77. Geissler EN, Ryan MA, Housman DE. The dominant-white spotting (W) locus of the mouse encodes the c-kit proto-oncogene. *Cell.* (1988) 55:185–92. doi: 10.1016/0092-8674(88)90020-7
78. Nocka K, Tan JC, Chiu E, Chu TY, Ray P, Traktman P, et al. Molecular bases of dominant negative and loss of function mutations at the murine c-kit/white spotting locus: W37, Wv, W41 and W. *Embo j.* (1990) 9:1805–13. doi: 10.1002/j.1460-2075.1990.tb08305.x
79. Rahmig S, Kronstein-Wiedemann R, Fohgrub J, Kronstein N, Nevmerzhitskaya A, Bornhauser M, et al. Improved Human Erythropoiesis and Platelet Formation in Humanized NSGW41 Mice. *Stem Cell Reports.* (2016) 7:591–601. doi: 10.1016/j.stemcr.2016.08.005
80. Fox N, Priestley G, Papayannopoulou T, Kaushansky K. Thrombopoietin expands hematopoietic stem cells after transplantation. *J Clin Invest.* (2002) 110:389–94. doi: 10.1172/JCI0215430
81. Kirito K, Fox N, Kaushansky K. Thrombopoietin stimulates Hoxb4 expression: an explanation for the favorable effects of TPO on hematopoietic stem cells. *Blood.* (2003) 102:3172–8. doi: 10.1182/blood-2003-03-0944
82. Qian H, Buza-Vidas N, Hyland CD, Jensen CT, Antonchuk J, Mansson R, et al. Critical role of thrombopoietin in maintaining adult quiescent hematopoietic stem cells. *Cell Stem Cell.* (2007) 1:671–84. doi: 10.1016/j.stem.2007.10.008
83. Yoshihara H, Arai F, Hosokawa K, Hagiwara T, Takubo K, Nakamura Y, et al. Thrombopoietin/MPL signaling regulates hematopoietic stem cell quiescence and interaction with the osteoblastic niche. *Cell Stem Cell.* (2007) 1:685–97. doi: 10.1016/j.stem.2007.10.020
84. Lyman SD, James L, Vanden Bos T, de Vries P, Brasel K, Gliniak B, et al. Molecular cloning of a ligand for the flt3/flk-2 tyrosine kinase receptor: a proliferative factor for primitive hematopoietic cells. *Cell.* (1993) 75:1157–67. doi: 10.1016/0092-8674(93)90325-K
85. Maraskovsky E, Brasel K, Teepe M, Roux ER, Lyman SD, Shortman K, et al. Dramatic increase in the numbers of functionally mature dendritic cells in Flt3 ligand-treated mice: multiple dendritic cell subpopulations identified. *J Exp Med.* (1996) 184:1953–62. doi: 10.1084/jem.184.5.1953
86. McKenna HJ, Stocking KL, Miller RE, Brasel K, De Smedt T, Maraskovsky E, et al. Mice lacking flt3 ligand have deficient hematopoiesis affecting hematopoietic progenitor cells, dendritic cells, and natural killer cells. *Blood.* (2000) 95:3489–97. doi: 10.1182/blood.V95.11.3489
87. Waskow C, Liu K, Darrasse-Jèze G, Guermonprez P, Ginhoux F, Merad M, et al. The receptor tyrosine kinase Flt3 is required for dendritic cell development in peripheral lymphoid tissues. *Nat Immunol.* (2008) 9:676–83. doi: 10.1038/ni.1615

88. Dranoff G, Crawford AD, Sadelain M, Ream B, Rashid A, Bronson RT, et al. Involvement of granulocyte-macrophage colony-stimulating factor in pulmonary homeostasis. *Science.* (1994) 264:713–6. doi: 10.1126/science.8171324
89. Stanley E, Lieschke GJ, Grail D, Metcalf D, Hodgson G, Gall JA, et al. Granulocyte/macrophage colony-stimulating factor-deficient mice show no major perturbation of hematopoiesis but develop a characteristic pulmonary pathology. *Proc Natl Acad Sci USA.* (1994) 91:5592–6. doi: 10.1073/pnas.91.12.5592
90. Shibata Y, Berclaz PY, Chroneos ZC, Yoshida M, Whitsett JA, Trapnell BC. GM-CSF regulates alveolar macrophage differentiation and innate immunity in the lung through PU.1. *Immunity.* (2001) 15:557–67. doi: 10.1016/s1074-7613(01)00218-7
91. Ramasamy SK, Kusumbe AP, Itkin T, Gur-Cohen S, Lapidot T, Adams RH. Regulation of hematopoiesis and osteogenesis by blood vessel-derived signals. *Annu Rev Cell Dev Biol.* (2016) 32:649–75. doi: 10.1146/annurev-cellbio-111315-124936
92. Rafii S, Shapiro F, Pettengell R, Ferris B, Nachman R, Moore M, et al. Human bone marrow microvascular endothelial cells support long-term proliferation and differentiation of myeloid and megakaryocytic progenitors. *Blood.* (1995) 86:3353–63. doi: 10.1182/blood.V86.9.3353.bloodjournal8693353
93. Majumdar MK, Thiede MA, Haynesworth SE, Bruder SP, Gerson SL. Human marrow-derived mesenchymal stem cells (MSCs) express hematopoietic cytokines and support long-term hematopoiesis when differentiated toward stromal and osteogenic lineages. *J Hematother Stem Cell Res.* (2000) 9:841–8. doi: 10.1089/152581600750062264
94. Huntington ND, Legrand N, Alves NL, Jaron B, Weijer K, Plet A, et al. IL-15 trans-presentation promotes human NK cell development and differentiation *in vivo*. *J Exp Med.* (2009) 206:25–34. doi: 10.1084/jem.20082013
95. Liu F, Song Y, Liu D. Hydrodynamics-based transfection in animals by systemic administration of plasmid DNA. *Gene Ther.* (1999) 6:1258–66. doi: 10.1038/sj.gt.3300947
96. Chen Q, Khoury M, Chen J. Expression of human cytokines dramatically improves reconstitution of specific human-blood lineage cells in humanized mice. *Proc Natl Acad Sci USA.* (2009) 106:21783–8. doi: 10.1073/pnas.0912274106
97. Li Y, Chen Q, Zheng D, Yin L, Chionh YH, Wong LH, et al. Induction of functional human macrophages from bone marrow promonocytes by M-CSF in humanized mice. *J Immunol.* (2013) 191:3192–9. doi: 10.4049/jimmunol.1300742
98. Bryce PJ, Falahati R, Kenney LL, Leung J, Bebbington C, Tomasevic N, et al. Humanized mouse model of mast cell-mediated passive cutaneous anaphylaxis and passive systemic anaphylaxis. *J Allergy Clin Immunol.* (2016) 138:769–79. doi: 10.1016/j.jaci.2016.01.049
99. Katano I, Nishime C, Ito R, Kamisako T, Mizusawa T, Ka Y, et al. Long-term maintenance of peripheral blood derived human NK cells in a novel human IL-15- transgenic NOG mouse. *Sci Rep.* (2017) 7:17230. doi: 10.1038/s41598-017-17442-7
100. Katano I, Ito R, Kawai K, Takahashi T. Improved detection of in vivo human Nk cell-mediated antibody-dependent cellular cytotoxicity using a novel NOG-FcγR-Deficient Human IL-15 transgenic mouse. *Front Immunol.* (2020) 11:532684. doi: 10.3389/fimmu.2020.532684
101. Matsuda M, Ono R, Iyoda T, Endo T, Iwasaki M, Tomizawa-Murasawa M, et al. Human NK cell development in hIL-7 and hIL-15 knockin NOD/SCID/IL2rgKO mice. *Life Sci Alliance.* (2019) 2:e201800195. doi: 10.26508/lsa.201800195
102. Ono R, Watanabe T, Kawakami E, Iwasaki M, Tomizawa-Murasawa M, Matsuda M, et al. Co-activation of macrophages and T cells contribute to chronic GVHD in human IL-6 transgenic humanised mouse model. *EBioMedicine.* (2019) 41:584–596. doi: 10.1016/j.ebiom.2019.02.001
103. Willinger T, Rongvaux A, Strowig T, Manz MG, Flavell RA. Improving human hemato-lymphoid-system mice by cytokine knock-in gene replacement. *Trends Immunol.* (2011) 32:321–7. doi: 10.1016/j.it.2011.04.005
104. Rathinam C, Poueymirou WT, Rojas J, Murphy AJ, Valenzuela DM, Yancopoulos GD, et al. Efficient differentiation and function of human macrophages in humanized CSF-1 mice. *Blood.* (2011) 118:3119–28. doi: 10.1182/blood-2010-12-326926
105. Lang J, Zhang B, Kelly M, Peterson JN, Barbee J, Freed BM, et al. Replacing mouse BAFF with human BAFF does not improve B-cell maturation in hematopoietic humanized mice. *Blood Adv.* (2017) 1:2729–41. doi: 10.1182/bloodadvances.2017010090
106. Lan P, Tonomura N, Shimizu A, Wang S, Yang YG. Reconstitution of a functional human immune system in immunodeficient mice through combined human fetal thymus/liver and CD34+ cell transplantation. *Blood.* (2006) 108:487–92. doi: 10.1182/blood-2005-11-4388
107. Melkus MW, Estes JD, Padgett-Thomas A, Gatlin J, Denton PW, Othieno FA, et al. Humanized mice mount specific adaptive and innate immune responses to EBV and TSST-1. *Nat Med.* (2006) 12:1316–22. doi: 10.1038/nm1431
108. Smith DJ, Lin LJ, Moon H, Pham AT, Wang X, Liu S, et al. Propagating Humanized BLT Mice for the Study of Human Immunology and Immunotherapy. *Stem Cells Dev.* (2016) 25:1863–73. doi: 10.1089/scd.2016.0193
109. Denton PW, Nochi T, Lim A, Krisko JF, Martinez-Torres F, Choudhary SK, et al. IL-2 receptor gamma-chain molecule is critical for intestinal T-cell reconstitution in humanized mice. *Mucosal Immunol.* (2012) 5:555–66. doi: 10.1038/mi.2012.31
110. Rajesh D, Zhou Y, Jankowska-Gan E, Roenneburg DA, Dart ML, Torrealba J, et al. Th1 and Th17 immunocompetence in humanized NOD/SCID/IL2rgammanull mice. *Hum Immunol.* (2010) 71:551–9. doi: 10.1016/j.humimm.2010.02.019
111. Brainard DM, Seung E, Frahm N, Cariappa A, Bailey CC, Hart WK, et al. Induction of robust cellular and humoral virus-specific adaptive immune responses in human immunodeficiency virus-infected humanized BLT mice. *J Virol.* (2009) 83:7305–21. doi: 10.1128/JVI.02207-08
112. Denton PW, Estes JD, Sun Z, Othieno FA, Wei BL, Wege AK, et al. Antiretroviral pre-exposure prophylaxis prevents vaginal transmission of HIV-1 in humanized BLT mice. *PLoS Med.* (2008) 5:e16. doi: 10.1371/journal.pmed.0050016
113. Stoddart CA, Maidji E, Galkina SA, Kosikova G, Rivera JM, Moreno ME, et al. Superior human leukocyte reconstitution and susceptibility to vaginal HIV transmission in humanized NOD-scid IL-2Rgamma(-/-) (NSG) BLT mice. *Virology.* (2011) 417:154–60. doi: 10.1016/j.virol.2011.05.013
114. Lee ST, Maeng H, Chwae YJ, Oh DJ, Kim YM, Yang WI. Effect of mesenchymal stem cell transplantation on the engraftment of human hematopoietic stem cells and leukemic cells in mice model. *Int J Hematol.* (2008) 87:327–37. doi: 10.1007/s12185-008-0041-3
115. Fernandez-Garcia M, Yanez RM, Sanchez-Dominguez R, Hernando-Rodriguez M, Peces-Barba M, Herrera G, et al. Mesenchymal stromal cells enhance the engraftment of hematopoietic stem cells in an autologous mouse transplantation model. *Stem Cell Res Ther.* (2015) 6:165. doi: 10.1186/s13287-015-0155-5
116. Metheny L III, Eid S, Lingas K, Reese J, Meyerson H, Tong A, et al. Intra-osseous Co-transplantation of CD34-selected umbilical cord blood and mesenchymal stromal cells. *Hematol Med Oncol.* (2016) 1:25–9. doi: 10.15761/HMO.1000105
117. Morton JJ, Keysar SB, Perrenoud L, Chimed TS, Reisinger J, Jackson B, et al. Dual use of hematopoietic and mesenchymal stem cells enhances engraftment and immune cell trafficking in an allogeneic humanized mouse model of head and neck cancer. *Mol Carcinog.* (2018) 57:1651–63. doi: 10.1002/mc.22887
118. Khoury M, Drake A, Chen Q, Dong D, Leskov I, Fragoso MF, et al. Mesenchymal stem cells secreting angiopoietin-like-5 support efficient expansion of human hematopoietic stem cells without compromising their repopulating potential. *Stem Cells Dev.* (2011) 20:1371–81. doi: 10.1089/scd.2010.0456
119. Yin X, Hu L, Zhang Y, Zhu C, Cheng H, Xie X, et al. PDGFB-expressing mesenchymal stem cells improve human hematopoietic stem cell engraftment in immunodeficient mice. *Bone Marrow Transplant.* (2020) 55:1029–1040. doi: 10.1038/s41409-019-0766-z
120. Abarrategi A, Mian SA, Passaro D, Rouault-Pierre K, Grey W, Bonnet D. Modeling the human bone marrow niche in mice: from host bone marrow

engraftment to bioengineering approaches. *J Exp Med.* (2018) 215:729–43. doi: 10.1084/jem.20172139
121. Sommerkamp P, Mercier FE, Wilkinson AC, Bonnet D, Bourgine PE. Engineering human hematopoietic environments through ossicle and bioreactor technologies exploitation. *Exper Hematol.* (2020) 94:1–68. doi: 10.1016/j.exphem.2020.11.008
122. Antonelli A, Noort WA, Jaques J, de Boer B, de Jong-Korlaar R, Brouwers-Vos AZ, et al. Establishing human leukemia xenograft mouse models by implanting human bone marrow-like scaffold-based niches. *Blood.* (2016) 128:2949–59. doi: 10.1182/blood-2016-05-719021
123. Reinisch A, Thomas D, Corces MR, Zhang X, Gratzinger D, Hong WJ, et al. A humanized bone marrow ossicle xenotransplantation model enables improved engraftment of healthy and leukemic human hematopoietic cells. *Nat Med.* (2016) 22:812–21. doi: 10.1038/nm.4103
124. Reinisch A, Hernandez DC, Schallmoser K, Majeti R. Generation and use of a humanized bone-marrow-ossicle niche for hematopoietic xenotransplantation into mice. *Nat Protoc.* (2017). 12:2169–88. doi: 10.1038/nprot.2017.088
125. Abarrategi A, Foster K, Hamilton A, Mian SA, Passaro D, Gribben J, et al. Versatile humanized niche model enables study of normal and malignant human hematopoiesis. *J Clin Invest.* (2017) 127:543–8. doi: 10.1172/JCI89364
126. Vaiselbuh SR, Edelman M, Lipton JM, Liu JM. Ectopic human mesenchymal stem cell-coated scaffolds in NOD/SCID mice: an in vivo model of the leukemia niche. *Tissue Eng Part C Methods.* (2010) 16:1523–31. doi: 10.1089/ten.tec.2010.0179
127. Bourgine PE, Fritsch K, Pigeot S, Takizawa H, Kunz L, Kokkaliaris KD, et al. Fate distribution and regulatory role of human mesenchymal stromal cells in engineered hematopoietic bone organs. *iScience.* (2019) 19:504–513. doi: 10.1016/j.isci.2019.08.006
128. Fritsch K, Pigeot S, Feng X, Bourgine PE, Schroeder T, Martin I, et al. Engineered humanized bone organs maintain human hematopoiesis in vivo. *Exp Hematol.* (2018) 61:45–51 e5. doi: 10.1016/j.exphem.2018.01.004
129. Scotti C, Piccinini E, Takizawa H, Todorov A, Bourgine P, Papadimitropoulos A, et al. Engineering of a functional bone organ through endochondral ossification. *Proc Natl Acad Sci USA.* (2013) 110:3997–4002. doi: 10.1073/pnas.1220108110
130. Martine LC, Holzapfel BM, McGovern JA, Wagner F, Quent VM, Hesami P, et al. Engineering a humanized bone organ model in mice to study bone metastases. *Nat Protoc.* (2017) 12:639–63. doi: 10.1038/nprot.2017.002
131. Lee J, Li M, Milwid J, Dunham J, Vinegoni C, Gorbatov R, et al. Implantable microenvironments to attract hematopoietic stem/cancer cells. *Proc Natl Acad Sci USA.* (2012) 109:19638–43. doi: 10.1073/pnas.1208384109
132. Reinisch A, Etchart N, Thomas D, Hofmann NA, Fruehwirth M, Sinha S, et al. Epigenetic and in vivo comparison of diverse MSC sources reveals an endochondral signature for human hematopoietic niche formation. *Blood.* (2015) 125:249–60. doi: 10.1182/blood-2014-04-572255
133. Song Y, Rongvaux A, Taylor A, Jiang T, Tebaldi T, Balasubramanian K, et al. A highly efficient and faithful MDS patient-derived xenotransplantation model for pre-clinical studies. *Nat Commun.* (2019) 10:366. doi: 10.1038/s41467-018-08166-x
134. Lysenko V, Wildner-Verhey van Wijk N, Zimmermann K, Weller MC, Bühler M, Wildschut MHE, et al. Enhanced engraftment of human myelofibrosis stem and progenitor cells in MISTRG mice. *Blood Adv.* (2020) 4:2477–88. doi: 10.1182/bloodadvances.2019001364
135. Ellegast JM, Rauch PJ, Kovtonyuk LV, Muller R, Wagner U, Saito Y, et al. Minv(16) G, and NPM1mut AMLs engraft human cytokine knock-in mice. *Blood.* (2016) 128:2130–4. doi: 10.1182/blood-2015-12-6 89356
136. Hashwah H, Bertram K, Stirm K, Stelling A, Wu CT, Kasser S, et al. The IL-6 signaling complex is a critical driver, negative prognostic factor, and therapeutic target in diffuse large B-cell lymphoma. *EMBO Mol Med.* (2019) 11:e10576. doi: 10.15252/emmm.201910576
137. Lindsey ES, Donaldson GW, Woodruff MF. Erythrocyte survival in normal mice and in mice with autoimmune haemolytic anaemia. *Clin Exp Immunol.* (1966) 1:85–98.
138. Phillips MA, Burrows JN, Manyando C, van Huijsduijnen RH, Van Voorhis WC, Wells TNC. *Malaria Nat Rev Dis Primers.* (2017) 3:17050. doi: 10.1038/nrdp.2017.50
139. Guzman MG, Gubler DJ, Izquierdo A, Martinez E, Halstead SB. Dengue infection. *Nat Rev Dis Primers.* (2016) 2:16055. doi: 10.1038/nrdp.2016.55
140. Semple JW, Rebetz J, Maouia A, Kapur R. An update on the pathophysiology of immune thrombocytopenia. *Curr Opin Hematol.* (2020) 27:423–429. doi: 10.1097/MOH.0000000000000612
141. Baenziger S, Tussiwand R, Schlaepfer E, Mazzucchelli L, Heikenwalder M, Kurrer MO, et al. Disseminated and sustained HIV infection in CD34+ cord blood cell-transplanted Rag2-/-gamma c-/- mice. *Proc Natl Acad Sci USA.* (2006) 103:15951–6. doi: 10.1073/pnas.0604493103
142. Dudek TE, No DC, Seung E, Vrbanac VD, Fadda L, Bhoumik P, et al. Rapid evolution of HIV-1 to functional $CD8^+$ T cell responses in humanized BLT mice. *Sci Transl Med.* (2012) 4:143ra98. doi: 10.1126/scitranslmed.3003984
143. Strowig T, Gurer C, Ploss A, Liu YF, Arrey F, Sashihara J, et al. Priming of protective T cell responses against virus-induced tumors in mice with human immune system components. *J Exp Med.* (2009) 206:1423–34. doi: 10.1084/jem.20081720
144. Jaiswal S, Pazoles P, Woda M, Shultz LD, Greiner DL, Brehm MA, et al. Enhanced humoral and HLA-A2-restricted dengue virus-specific T-cell responses in humanized BLT NSG mice. *Immunology.* (2012) 136:334–43. doi: 10.1111/j.1365-2567.2012.03585.x
145. Seung, E. and Tager AM, Humoral immunity in humanized mice: a work in progress. *J Infect Dis.* (2013) 208 (Suppl. 2):S155–9. doi: 10.1093/infdis/jit448
146. Lang J, Kelly M, Freed BM, McCarter MD, Kedl RM, Torres RM, et al. Studies of lymphocyte reconstitution in a humanized mouse model reveal a requirement of T cells for human B cell maturation. *J Immunol.* (2013) 190:2090–101. doi: 10.4049/jimmunol.1202810
147. Cuss AK, Avery DT, Cannons JL, Yu LJ, Nichols KE, Shaw PJ, et al. Expansion of functionally immature transitional B cells is associated with human-immunodeficient states characterized by impaired humoral immunity. *J Immunol.* (2006) 176:1506–16. doi: 10.4049/jimmunol.176.3.1506
148. Klein L, Kyewski B, Allen PM, Hogquist KA. Positive and negative selection of the T cell repertoire: what thymocytes see (and don't see). *Nat Rev Immunol.* (2014) 14:377–91. doi: 10.1038/nri3667
149. Shultz LD, Saito Y, Najima Y, Tanaka S, Ochi T, Tomizawa M, et al. Generation of functional human T-cell subsets with HLA-restricted immune responses in HLA class I expressing NOD/SCID/IL2r gamma(null) humanized mice. *Proc Natl Acad Sci USA.* (2010) 107:13022–7. doi: 10.1073/pnas.1000475107
150. Danner R, Chaudhari SN, Rosenberger J, Surls J, Richie TL, Brumeanu TD, et al. Expression of HLA class II molecules in humanized NOD.Rag1KO.IL2RgcKO mice is critical for development and function of human T and B cells. *PLoS ONE.* (2011) 6:e19826. doi: 10.1371/journal.pone.0019826
151. Billerbeck E, Horwitz JA, Labitt RN, Donovan BM, Vega K, Budell WC, et al. Characterization of human antiviral adaptive immune responses during hepatotropic virus infection in HLA-transgenic human immune system mice. *J Immunol.* (2013) 191:1753–64. doi: 10.4049/jimmunol.1201518
152. Najima Y, Tomizawa-Murasawa M, Saito Y, Watanabe T, Ono R, Ochi T, et al. Induction of WT1-specific human CD8+ T cells from human HSCs in HLA class I Tg NOD/SCID/IL2rgKO mice. *Blood.* (2016) 127:722–34. doi: 10.1182/blood-2014-10-604777
153. Majji S, Wijayalath W, Shashikumar S, Pow-Sang L, Villasante E, Brumeanu TD, et al. Differential effect of HLA class-I versus class-II transgenes on human T and B cell reconstitution and function in NRG mice. *Sci Rep.* (2016) 6:28093. doi: 10.1038/srep28093
154. Masse-Ranson G, Dusséaux M, Fiquet O, Darche S, Boussand M, Li Y, et al. Accelerated thymopoiesis and improved T-cell responses in HLA-A2/-DR2 transgenic BRGS-based human immune system mice. *Eur J Immunol.* (2019) 49:954–65. doi: 10.1002/eji.201848001
155. Karpel ME, Boutwell CL, Allen TM. BLT humanized mice as a small animal model of HIV infection. *Curr Opin Virol.* (2015) 13:75–80. doi: 10.1016/j.coviro.2015.05.002
156. Greenblatt MB, Vrbanac V, Tivey T, Tsang K, Tager AM, Aliprantis AO. Graft versus host disease in the bone marrow, liver and thymus humanized mouse model. *PLoS One.* (2012) 7:e44664. doi: 10.1371/journal.pone.0044664
157. Covassin L, Jangalwe S, Jouvet N, Laning J, Burzenski L, Shultz LD, et al. Human immune system development and survival of NOD-scid IL2rgamma

(NSG) mice engrafted with human thymus and autologous hematopoietic stem cells. *Clin Exp Immunol.* (2013) 174:372–88. doi: 10.1111/cei.12180
158. Victora GD, Nussenzweig MC. Germinal centers. *Annu Rev Immunol.* (2012) 30:429–57. doi: 10.1146/annurev-immunol-020711-075032
159. Aguzzi A, Kranich J, Krautler NJ. Follicular dendritic cells: origin, phenotype, and function in health and disease. *Trends Immunol.* (2014) 35:105–13. doi: 10.1016/j.it.2013.11.001
160. Randall TD, Carragher DM, Rangel-Moreno J. Development of secondary lymphoid organs. *Ann Rev Immunol.* (2008) 26:627–50. doi: 10.1146/annurev.immunol.26.021607.090257
161. Salguero G, Daenthanasanmak A, Münz C, Raykova A, Guzmán CA, Riese P, et al. Dendritic cell-mediated immune humanization of mice: implications for allogeneic and xenogeneic stem cell transplantation. *J Immunol.* (2014) 192:4636–47. doi: 10.4049/jimmunol.1302887
162. Theobald SJ, Kreer C, Khailaie S, Bonifacius A, Eiz-Vesper B, Figueiredo C, et al. Repertoire characterization and validation of gB-specific human IgGs directly cloned from humanized mice vaccinated with dendritic cells and protected against HCMV. *PLoS Pathog.* (2020) 16:e1008560. doi: 10.1371/journal.ppat.1008560
163. Chung YS, Son JK, Choi B, Park JB, Chang J, Kim SJ. Transplantation of human spleen into immunodeficient NOD/SCID IL2Rγ(null) mice generates humanized mice that improve functional B cell development. *Clin Immunol.* (2015) 161:308–15. doi: 10.1016/j.clim.2015.09.001
164. Chappaz S, Flueck L, Farr AG, Rolink AG, Finke D. Increased TSLP availability restores T- and B-cell compartments in adult IL-7–deficient mice. *Blood.* (2007) 110:3862–70. doi: 10.1182/blood-2007-02-074245
165. Chappaz, S. and Finke D, The IL-7 signaling pathway regulates lymph node development independent of peripheral lymphocytes. *J Immunolo.* (2010) 184:3562–9. doi: 10.4049/jimmunol.0901647
166. Yaguchi T, Kobayashi A, Inozume T, Morii K, Nagumo H, Nishio H, et al. Human PBMC-transferred murine MHC class I/II-deficient NOG mice enable long-term evaluation of human immune responses. *Cell Mol Immunol.* (2018) 15:953–62. doi: 10.1038/cmi.2017.106
167. Brehm MA, Kenney LL, Wiles MV, Low BE, Tisch RM, Burzenski L, et al. Lack of acute xenogeneic graft- versus-host disease, but retention of T-cell function following engraftment of human peripheral blood mononuclear cells in NSG mice deficient in MHC class I and II expression. *Faseb j.* (2019) 33:3137–51. doi: 10.1096/fj.201800636R
168. Kalscheuer H, Danzl N, Onoe T, Faust T, Winchester R, Goland R, et al. A model for personalized in vivo analysis of human immune responsiveness. *Sci Transl Med.* (2012) 4:125ra30. doi: 10.1126/scitranslmed.3003481
169. Kuruvilla JG, Troyer RM, Devi S, Akkina R. Dengue virus infection and immune response in humanized RAG2(-/-)gamma(c)(-/-) (RAG-hu) mice. *Virology.* (2007) 369:143–52. doi: 10.1016/j.virol.2007.06.005
170. Aspord C, Pedroza-Gonzalez A, Gallegos M, Tindle S, Burton EC, Su D, et al. Breast cancer instructs dendritic cells to prime interleukin 13-secreting CD4+ T cells that facilitate tumor development. *J Exp Med.* (2007) 204:1037–47. doi: 10.1084/jem.20061120
171. Wang M, Yao LC, Cheng M, Cai D, Martinek J, Pan CX, et al. Humanized mice in studying efficacy and mechanisms of PD-1-targeted cancer immunotherapy. *Faseb J.* (2018) 32:1537–1549. doi: 10.1096/fj.201700740R
172. Nguyen R, Patel AG, Griffiths LM, Dapper J, Stewart EA, Houston J, et al. Next-generation humanized patient-derived xenograft mouse model for pre-clinical antibody studies in neuroblastoma. *Cancer Immunol Immunother.* (2020) doi: 10.1007/s00262-020-02713-6. [Epub ahead of print].
173. Byrne AT, Alferez DG, Amant F, Annibali D, Arribas J, Biankin AV, et al. Interrogating open issues in cancer precision medicine with patient-derived xenografts. *Nat Rev Cancer.* (2017) 17:254–268. doi: 10.1038/nrc.2016.140
174. Myburgh R, Kiefer JD, Russkamp NF, Magnani CF, Nuñez N, Simonis A, et al. Anti-human CD117 CAR T-cells efficiently eliminate healthy and malignant CD117-expressing hematopoietic cells. *Leukemia.* (2020) 34:2688–703. doi: 10.1038/s41375-020-0818-9
175. Biernacki MA, Foster KA, Woodward KB, Coon ME, Cummings C, Cunningham TM, et al. CBFB-MYH11 fusion neoantigen enables T cell recognition and killing of acute myeloid leukemia. *J Clin Invest.* (2020) 130:5127–41. doi: 10.1172/JCI137723
176. Grompe M, Strom S. Mice with human livers. *Gastroenterology.* (2013) 145:1209–14. doi: 10.1053/j.gastro.2013.09.009
177. Billerbeck E, Mommersteeg MC, Shlomai A, Xiao JW, Andrus L, Bhatta A, et al. Humanized mice efficiently engrafted with fetal hepatoblasts and syngeneic immune cells develop human monocytes and NK cells. *J Hepatol.* (2016) 65:334–43. doi: 10.1016/j.jhep.2016.04.022
178. Dandri M, Burda MR, Török E, Pollok JM, Iwanska A, Sommer G, et al. Repopulation of mouse liver with human hepatocytes and in vivo infection with hepatitis B virus. *Hepatology.* (2001) 33:981–8. doi: 10.1053/jhep.2001.23314
179. Mercer DF, Schiller DE, Elliott JF, Douglas DN, Hao C, Rinfret A, et al. Hepatitis C virus replication in mice with chimeric human livers. *Nat Med.* (2001) 7:927–33. doi: 10.1038/90968
180. Azuma H, Paulk N, Ranade A, Dorrell C, Al-Dhalimy M, Ellis E, et al. Robust expansion of human hepatocytes in Fah-/-/Rag2-/-/Il2rg-/- mice. *Nat Biotechnol.* (2007) 25:903–10. doi: 10.1038/nbt1326
181. Bissig KD, Le TT, Woods NB, Verma IM. Repopulation of adult and neonatal mice with human hepatocytes: a chimeric animal model. *Proc Natl Acad Sci USA.* (2007) 104:20507–11. doi: 10.1073/pnas.0710528105
182. Bility MT, Cheng L, Zhang Z, Luan Y, Li F, Chi L, et al. Hepatitis B virus infection and immunopathogenesis in a humanized mouse model: induction of human-specific liver fibrosis and M2-like macrophages. *PLoS Pathog.* (2014) 10:e1004032. doi: 10.1371/journal.ppat.1004032
183. Dusséaux M, Masse-Ranson G, Darche S, Ahodantin J, Li Y, Fiquet O, et al. viral load affects the immune response to HBV in mice with humanized immune system and liver. *Gastroenterology.* (2017) 153:1647–61.e9. doi: 10.1053/j.gastro.2017.08.034
184. Wahl A, De C, Abad Fernandez M, Lenarcic EM, Xu Y, Cockrell AS, et al. Precision mouse models with expanded tropism for human pathogens. *Nat Biotechnol.* (2019) 37:1163–73. doi: 10.1038/s41587-019-0225-9

Conflict of Interest: The authors declare that the research was conducted in the absence of any commercial or financial relationships that could be construed as a potential conflict of interest.

Copyright © 2021 Martinov, McKenna, Tan, Collins, Kehret, Linton, Olsen, Shobaki and Rongvaux. This is an open-access article distributed under the terms of the Creative Commons Attribution License (CC BY). The use, distribution or reproduction in other forums is permitted, provided the original author(s) and the copyright owner(s) are credited and that the original publication in this journal is cited, in accordance with accepted academic practice. No use, distribution or reproduction is permitted which does not comply with these terms.

frontiers in Immunology

ORIGINAL RESEARCH
published: 22 February 2021
doi: 10.3389/fimmu.2021.618081

An Antibody-Drug Conjugate That Selectively Targets Human Monocyte Progenitors for Anti-Cancer Therapy

Yuta Izumi[1†], Masashi Kanayama[1†], Zhongchuzi Shen[2], Masayuki Kai[2], Shunsuke Kawamura[1], Megumi Akiyama[1,3], Masahide Yamamoto[3], Toshikage Nagao[3], Keigo Okada[3], Norihiko Kawamata[3], Shigeo Toyota[4] and Toshiaki Ohteki[1]*

[1] Department of Biodefense Research, Medical Research Institute, Tokyo Medical and Dental University (TMDU), Tokyo, Japan, [2] Oncology Research Laboratories, Oncology R&D Unit, R&D Division, Kyowa Kirin Co., Ltd., Tokyo, Japan, [3] Department of Hematology, Tokyo Medical and Dental University (TMDU), Tokyo, Japan, [4] Department of Hematology, Yokosuka Kyosai Hospital, Kanagawa, Japan

OPEN ACCESS

Edited by:
Alexandre P. A. Theocharides, University Hospital Zürich, Switzerland

Reviewed by:
Jan Jacob Schuringa, University Medical Center Groningen, Netherlands
Beat Bornhauser, University Children's Hospital Zurich, Switzerland

***Correspondence:**
Toshiaki Ohteki
ohteki.bre@mri.tmd.ac.jp

[†]These authors have contributed equally to this work

Specialty section:
This article was submitted to Cancer Immunity and Immunotherapy, a section of the journal Frontiers in Immunology

Received: 16 October 2020
Accepted: 05 January 2021
Published: 22 February 2021

Citation:
Izumi Y, Kanayama M, Shen Z, Kai M, Kawamura S, Akiyama M, Yamamoto M, Nagao T, Okada K, Kawamata N, Toyota S and Ohteki T (2021) An Antibody-Drug Conjugate That Selectively Targets Human Monocyte Progenitors for Anti-Cancer Therapy. Front. Immunol. 12:618081. doi: 10.3389/fimmu.2021.618081

As hematopoietic progenitors supply a large number of blood cells, therapeutic strategies targeting hematopoietic progenitors are potentially beneficial to eliminate unwanted blood cells, such as leukemic cells and immune cells causing diseases. However, due to their pluripotency, targeting those cells may impair the production of multiple cell lineages, leading to serious side effects such as anemia and increased susceptibility to infection. To minimize those side effects, it is important to identify monopotent progenitors that give rise to a particular cell lineage. Monocytes and monocyte-derived macrophages play important roles in the development of inflammatory diseases and tumors. Recently, we identified human monocyte-restricted progenitors, namely, common monocyte progenitors and pre-monocytes, both of which express high levels of CD64, a well-known monocyte marker. Here, we introduce a dimeric pyrrolobenzodiazepine (dPBD)-conjugated anti-CD64 antibody (anti-CD64-dPBD) that selectively induces the apoptosis of proliferating human monocyte-restricted progenitors but not non-proliferating mature monocytes. Treatment with anti-CD64-dPBD did not affect other types of hematopoietic cells including hematopoietic stem and progenitor cells, neutrophils, lymphocytes and platelets, suggesting that its off-target effects are negligible. In line with these findings, treatment with anti-CD64-dPBD directly killed proliferating monocytic leukemia cells and prevented monocytic leukemia cell generation from bone marrow progenitors of chronic myelomonocytic leukemia patients in a patient-derived xenograft model. Furthermore, by depleting the source of monocytes, treatment with anti-CD64-dPBD ultimately eliminated tumor-associated macrophages and significantly reduced tumor size in humanized mice bearing solid tumors. Given the selective action of anti-CD64-dPBD on proliferating monocyte progenitors and monocytic leukemia cells, it should be a promising tool to target cancers and other monocyte-related inflammatory disorders with minimal side effects on other cell lineages.

Keywords: monocyte, leukemia, tumor-associated macrophage, chronic myelomonocytic leukemia, common monocyte progenitor

INTRODUCTION

Chronic myelomonocytic leukemia (CMML), a hematopoietic malignancy characterized by the overproduction of monocytes and their progenitors, develops from genetic mutations in hematopoietic stem and progenitor cells (HSPCs) (1–3). CMML is classified as myelodysplastic syndrome/myeloproliferative neoplasm (MDS/MPN) (1, 4). Patients with CMML show excessive monopoiesis, dysplasia and inefficient hematopoiesis (1, 4), which often causes anemia, thrombocytopenia and infectious diseases (5). HSC transplantation is the only curative treatment for CMML patients (1, 2). However, HSC transplantation requires highly invasive pre-conditioning, carries risks of graft-versus-host disease (GVHD) and increased susceptibility to infection, which is not always applicable especially for elderly patients (the median age at the time of CMML diagnosis is 75 years old) (1). Instead, various agents have been used to control tumor burden and induce remission, but ineffectiveness (non-responders) and fatal myelosuppression remain as serious problems, causing a poor prognosis for CMML patients with 1–3 years of median overall survival (1, 6). Thus, to achieve an effective anti-leukemia therapy without disturbing normal hematopoiesis, agents with a high specificity against target leukemic cells are urgently required.

Recently, a class of molecular targeted agents named antibody-drug conjugates (ADCs) has been actively developed to avoid nonspecific cell elimination and to minimize collateral damage (7, 8). ADCs are composed of cytotoxic drugs (payload), linkers and a specific antibody (Ab), which enables the delivery of potent payloads to specific cells. In this context, the specificity for the killing activity of ADCs solely depends on the selection of a target molecule. To date, gemtuzumab ozogamicin (GO), an anti-CD33 ADC, was approved for treatment of acute myeloid leukemia (AML) by the Food and Drug Administration (FDA) in 2000 (2, 9), but to date no ADC has been approved for CMML therapy. However, CD33 is broadly expressed on normal myeloid progenitors as well as on leukemic cells of AML patients (10, 11), which causes severe myelosuppression, resulting in the voluntary withdrawal of GO from the US market in 2010 (12). GO was re-approved in 2017 and those adverse events revealed the importance of target molecule selection for ADC development. In this context, we recently reported that conventional granulocyte-monocyte progenitors (cGMP, Lin-$CD34^+CD38^+CD10^-CD123^{low}FLT3^+CD45RA^+$) are heterogeneous and contain common monocyte progenitors (cMoPs) that strictly give rise to monocytes (13). Based on that finding, we proposed a human monocyte differentiation pathway (13). Accordingly, targeting the human monocyte differentiation pathway including cMoPs could be beneficial for the therapy of CMML/AML because the progenitors can expand and generate large numbers of monocytic leukemia cells.

Monocytes and macrophages are harmful participants in some human solid tumors (14). For instance, TIE2-expressing monocytes (TEMs) enhance angiogenesis and tumor progression (15, 16) and macrophages in solid tumors, referred to as tumor-associated macrophages (TAMs), are a poor prognostic factor and exert multiple pro-tumorigenic effects such as the promotion of angiogenesis, extracellular matrix remodeling and immunosuppression (17–19). Based on that background, several drugs controlling TAMs have been developed (20–23). Colony stimulating factor 1 receptor (CSF1R) is a representative target for anti-TAM therapy because of its crucial roles in the generation and function of TAMs (24–26). However, comprehensive gene expression analysis revealed that a CSF1R blockade-resistant TAM subset likely exists in solid human tumors (18). Thus, TAMs have a remarkable plasticity and alter their function and surface molecule expression, which causes difficulties in therapeutically targeting them (27, 28).

In light of those considerations, we developed a unique ADC that selectively targets proliferating monocytic progenitors and monocytic leukemia progenitors but not mature monocytes and monocyte-derived macrophages. By blocking the sources of those cells, we succeeded in reducing leukemic monocytes in a patient-derived xenograft (PDX) model of CMML, in depleting TAMs and inversely inducing tumor regression in a solid tumor model. Importantly, the ADC treatment showed minimal cytotoxicity against multipotent HSPCs and other hematopoietic lineages. Consequently, the ADC targeting monocytic progenitors may serve as a therapeutic agent for monocytic leukemias, solid tumors and presumably monocyte-related inflammatory diseases.

MATERIALS AND METHODS

Mice and Human Samples

NOG (*NOD/Shi-scid, IL-2RγKO Jic*) and human interleukin-6 transgenic NOG (hIL-6 Tg NOG) mice (29) were purchased from CLEA Japan. All mice were maintained under specific pathogen-free conditions. Human umbilical cord blood (UCB) samples were provided by the Japanese Red Cross Kanto-Koshinetsu Cord Blood Bank, and bone marrow (BM) samples from patients with CMML were provided by the Department of Hematology, Tokyo Medical and Dental University and the Department of Hematology, Yokosuka Kyosai Hospital under agreement of the patients. Human blood samples were donated by healthy volunteers. All experiments with human materials were approved by the Scientific Ethics Committees of the Japanese Red Cross Kanto-Koshinetsu Cord Blood Bank, the Medical Research Institute, the Tokyo Medical and Dental University and/or the Yokosuka Kyosai Hospital. Informed consent was obtained from all subjects.

Antibodies and Reagents

LEGENDScreen Human PE Kit, mouse IgG1 isotype control antibody (MOPC-21), Brilliant Violet 711-conjugated streptavidin and anti-human antibodies against CD38 (HIT2), CD34 (581), CD10 (HI10a), CD123 (6H6), CD45RA (HI100), CD135 (BV10A4H2), CD64 (10.1), CLEC12A (50C1), CD45 (H130), CD14 (M5E2), CD16 (3G8), CD49f (GoH3), CD206 (15-2), CD19 (HIB19), CD56 (MEM-188, HCD56), CD4 (RPA-T4), CD8α (RPA-T8), CD11c (3.9), CD2 (RPA-2.10), CD3 (UCHT1), CD11b (ICRF44) and CD235ab (HIR2) were

purchased from BioLegend. Anti-human antibodies against CD90 (eBio5E10), CD3 (UCHT1), HLA-DR (L243), CD66b (G10F5), CD41a (HIP8) and CD42b (HIP1) and anti-mouse TER-119 (TER-119) were purchased from eBioscience. Anti-human CD163 (REA812), SIGLEC-7 (REA214), SIGLEC-9 (REA492) and REA control (REA293) Abs were purchased from Miltenyi Biotec. The anti-human CD14 Ab (RMO52) was purchased from Beckman Coulter. Propidium iodide (PI) and phorbol 12-myristate 13-acetate (PMA) were purchased from Sigma-Aldrich. The Diff-quik staining kit was purchased from Sysmex Corp. To purify antibodies against human CD64 [clones H22 (30), 32.2 (31) and 611 (32)] and the isotype control Ab against dinitrophenol (DNP), expression vectors encoding the genes for IgG1 and an IgG4 analogue, called the nullbody, were synthesized with the S239C mutation, a site used to conjugate the payload (33, 34) and were transfected into Expi293 cells using an ExpiFectamine 293 Transfection Kit (Gibco). Antibodies in cell culture supernatants were obtained by affinity purification.

Cell Lines

THP-1, U937 and Ramos cells were obtained from an in-house cell bank. The cells were cultured in Iscove's Modified Dulbecco's Media (IMDM) (Sigma-Aldrich) supplemented with 10% fetal bovine serum (FBS), 1% penicillin/streptomycin and 1% L-alanyl-L-glutamine (Wako) at 37°C in a 5% CO_2 atmosphere. Human HSC4 head and neck squamous cell carcinoma cells were purchased from the Japanese Collection of Research Bioresources (JCRB) Cell Bank and were cultured in RPMI-1640 (Sigma-Aldrich) containing 20% FBS, 1% penicillin/streptomycin, 1% MEM NEAA (Gibco), 1% sodium pyruvate (Gibco), and 0.1% 2-mercaptoethanol (Gibco).

Generation of ADC

The antibodies were reduced using Tris(2-carboxyethyl) phosphine hydrochloride (TCEP)-HCl and the reaction was carried out at 37°C for 1 h in PBS. Unreacted TCEP was then removed and replaced with oxidation buffer (20 mM phosphate, 150 mM NaCl, 1 mM EDTA, pH 6.5) using an Amicon Ultra-4 centrifuge device (Millipore). Next, (L)-dehydroascorbic acid (DHAA) was added to the antibodies to restore cross-linking between cysteines other than the S239C residue, and the oxidation reaction was carried out for 1 h at room temperature. After the reaction, unreacted DHAA was removed and replaced with conjugation buffer (1 mM EDTA, PBS) using an Amicon Ultra-4 centrifuge device. Propylene glycol was added to the antibodies and maleimide-va-dPBD (purchased from XDCExplorer) and the conjugation reaction was allowed to proceed by mixing them together. After the reaction, the unreacted maleimide-va-dPBD was removed and replaced with PBS using a NAP column (GE Healthcare). In addition, the resulting complexes were concentrated using an Amicon Ultra-4 centrifuge device and then filtered by an Ultrafree-centrifugal filter (Millipore).

Cell Preparation From Human Samples

BM samples were obtained from CMML patients (**Supplementary Table 1**). Human mononuclear cells (MNCs) were collected from blood, BM, and UCB samples by density gradient centrifugation using Lymphocyte Separation Solution (d = 1.077, Nacalai Tesque). Regarding MNCs isolated from BM and UCB, cells were stained with PE/Cy5-conjugated Lineage Abs (Abs against CD2, CD3, CD11b, CD16, CD19, CD56, CD235ab, and CD14). After washing, cells were reacted with anti-Cy5-MicroBeads (Miltenyi Biotech) and lineage$^+$ cells were depleted with an autoMACS Pro Separator (Miltenyi Biotech). After staining with specific antibodies and PI, cells were analyzed and/or sorted using a FACS Aria III or FACS Canto II (BD).

Humanization of Immunodeficient Mice

NOG or hIL-6 Tg NOG mice were sublethally irradiated (1-2 Gy) and 1×10^5 Lin$^-$CD34$^+$ cells from UCB were intravenously injected within 24 h after irradiation. To generate the PDX model, sublethally irradiated NOG mice received an intravenous injection of total MNCs or 2-3$\times10^5$ Lin$^-$CD34$^+$ cells isolated from BM samples of CMML patients. Two PDX mice were generated from each BM sample. To monitor their chimerism, circulating blood was collected every 4 weeks and the cells were analyzed by flow cytometry (FCM). After more than 8 weeks post-transplantation, 0.5 μg DNP-dPBD or H22-dPBD was intravenously administered once. At day 7 after the administration, the mice were sacrificed and analyzed.

Generation of Tumor-Bearing Humanized Mice

HSC4 cells (1.5×10^6 in 100 μl PBS) were subcutaneously injected into humanized hIL-6 Tg NOG mice 2–3 months after humanization. From day 7 after the transplantation, tumor sizes were measured every 4 days and treatments with 0.5 μg DNP-dPBD or H22-dPBD were performed at days 7, 14, and 21. MNCs in the blood, BM and tumors of mice were analyzed 28 days post-tumor inoculation.

FCM Analysis of Humanized Mice

BM cells were obtained from the hind limbs of humanized mice by flushing with PBS containing 0.5% bovine serum albumin. BM cells and blood cells were hemolyzed and stained with specific antibodies. For preparation of tumor-associated cells, tumor tissues were minced and digested in RPMI-1640 medium containing collagenase (0.5 mg/ml, Sigma-Aldrich) and DNase I (5 μg/ml, Roche) for 30 min at 37°C. After digestion, cells were filtered through a 100 μm cell strainer. Tumor-associated leukocytes were isolated by density centrifugation with Percoll (Cytiva) and then analyzed using a FACS Aria III or FACS Canto II (BD) after staining with antibodies and PI.

Internalization Assay

To examine internalization and colocalization of the H22 nullbody in lysosomes, sorted CD14^{hi}CD16$^-$ monocytes were stained with Alexa Fluor 647-labeled H22 nullbody. The cells were then washed with culture media and cultured at 37°C for 23 h. After culture, cells were incubated with 100 nM LysoTracker Red DND-99 (Invitrogen) for 1 h. After washing and fixation with 4% paraformaldehyde (PFA) in PBS (Nacalai tesque), cell images were obtained using a TCS SP8 confocal

microscope (Leica). For the quenching assay, U937 cells (5×10^4/well) were plated in 96-well U-bottom plates. After adding the Alexa Fluor 488-labeled H22 nullbody (50 μg/ml), cells were incubated on ice for 1 h or at 37°C for 1, 4, 8 or 24 h. After washing, cells were treated with 100 nM quenching Ab (anti-Alexa Fluor 488 Rabbit IgG, Invitrogen) on ice for 1 h. After washing with PBS containing 0.1% BSA and 0.1% NaN_3, signals from the internalized Alexa Fluor 488-labeled Ab were detected by FCM.

Competitive Inhibition Assay for Anti-CD64 Antibodies

THP-1 cells (2×10^5 per well in 96-well plates) were treated with purified IgG from human serum (Miltenyi Biotec) at 4°C for 10 min. After incubation with non-labeled nullbodies (10 μg/ml) at room temperature for 30 min, Alexa Fluor 647-labeled nullbodies (0.1 μg/ml) were added and incubated at room temperature for 30 min. After washing, cells were stained with 7-AAD and signals of Alexa Fluor 647 were detected by FCM.

In Vitro Cytotoxicity Assay

Cells were cultured with DNP-MMAE, H22-MMAE, DNP-dPBD, or H22-dPBD in the presence or absence of human serum (Sigma) for 4 or 6 days and cell viabilities were assessed using a CellTiter-Glo Luminescent Cell Viability Assay (Promega) according to the manufacturer's instructions. To test the impact of ADC-treatment on monocyte production from myeloid progenitors, $Lin^-CLEC12A^+$ cells (for CellTiter-Glo analysis, 3×10^3 cells/well in 96-well plates; for FCM analysis, 1×10^4 cells/well in 96-well plates) were cultured in IMDM supplemented with 10% FBS, 1% penicillin/streptomycin, 1% L-alanyl-L-glutamine, 100 ng/ml stem cell factor (SCF), 50 ng/ml thrombopoietin (TPO) and fms-like tyrosine kinase receptor-3 ligand (FLT3L) in the presence or absence of H22-dPBD or DNP-dPBD for 6 days. In some experiments, THP-1 cells were irradiated at 5 Gy immediately before the ADC-treatment, treated with 40 ng/ml PMA 24 h prior to the ADC-treatment or cultured with the IMDM medium containing 1% or 2% FBS during the ADC-treatment. To examine the antigen specificity of H22-dPBD, THP-1 cells were treated with H22-dPBD (0.04 μg/ml) in the presence of unconjugated H22 antibody (4 μg/ml). The viability of THP-1 cells was examined using a CellTiter-Glo Luminescent Cell Viability Assay at day 6. For the quantification of apoptotic THP-1 cells, the cells were cultured in the presence of 0.04 μg/ml DNP-dPBD or H22-dPBD for 3 days, and they were stained with PE-conjugated annexin V (BD Bioscience) and analyzed using a FACS Canto II.

THP-1 Xenografts

NOG mice were intravenously injected with 4×10^5 THP-1 cells after sublethal irradiation (1-2 Gy). The mice were intravenously treated with 0.5 μg ADCs at day 14 after xenografting and were analyzed by FCM at day 21. When the survival of mice was examined, mice received ADC-treatments at days 14 and 28 after xenografting and their survival was monitored until day 56.

Immunofluorescence Staining of Frozen Tumor Sections

HSC4 tumor tissues obtained from hIL-6 Tg NOG mice were embedded in O.C.T. Compound (Sakura Finetek Japan) by liquid nitrogen. The samples were sliced into 8 μm sections and placed on slides. After washing in PBS and fixation by 4% PFA (10 min at room temperature), the sections were blocked with a two-fold dilution of Block ACE (Bio-Rad) for 30 min. Immunostaining was performed for 1 h at room temperature with a 50-fold dilution of APC-conjugated anti-human CD163 Ab (REA812) or isotype-matched control Ab in the presence of a 10-fold dilution of Block ACE. The sections were further stained with 5 μM DAPI for 10 min and images were obtained using a BZ-X710 (Keyence).

Statistical Analysis

Statistical analyses were performed using Prism software version 7 (GraphPad). A two-tailed Student's *t*-test or multiple *t*-test was used for statistical analyses of two-group comparisons. Multigroup comparisons were performed by a one-way analysis of variance (ANOVA) followed by the Tukey–Kramer multiple comparisons test. For statistical evaluation of survival, the Gehan-Breslow-Wilcoxon test was used. The criterion of significance was set at $p < 0.05$. All results are expressed as means ± standard deviation of the mean (SD). Blinding or randomization of the groups was not performed. Data points more than two standard deviations from the mean were excluded as outliers. No statistical methods were used to estimate sample size.

RESULTS

Screening of Target Molecules Specifically Expressed on Monocyte Lineage Cells

To target monocytic progenitors, we screened 361 cell surface molecules expressed on UCB HSPCs including revised GMP (rGMP), cMoPs and pre-monocytes (**Figures 1A, B** and **Supplementary Figure 1A**) and identified three candidates (SIGLEC-7, SIGLEC-9, and CD64) as characteristic markers of monocytic progenitors (**Figure 1C** and **Supplementary Figure 1B**). Those markers were also expressed on mature $CD14^+$ monocytes (**Figure 1D** and **Supplementary Figure 1B**). However, SIGLEC-7 and SIGLEC-9 were excluded as candidates because they were also expressed on non-monocyte lineage cells, such as neutrophils, conventional dendritic cells (cDCs) and NK cells (**Supplementary Figure 1C**). On the other hand, CD64 was not expressed on most non-monocytic cells including B cells, T cells, NK cells, neutrophils and plasmacytoid dendritic cells (pDCs), although it was partially and weakly expressed on cDCs (**Figure 1E**). Importantly, CD64 expression was not observed on non-monocytic hematopoietic progenitors including hematopoietic stem cells (HSCs), multipotent progenitors (MPPs), lymphoid-primed multipotent progenitors (LMPP), multipotent lymphoid progenitors (MLPs), lymphoid progenitors, common myeloid progenitors (CMPs) and

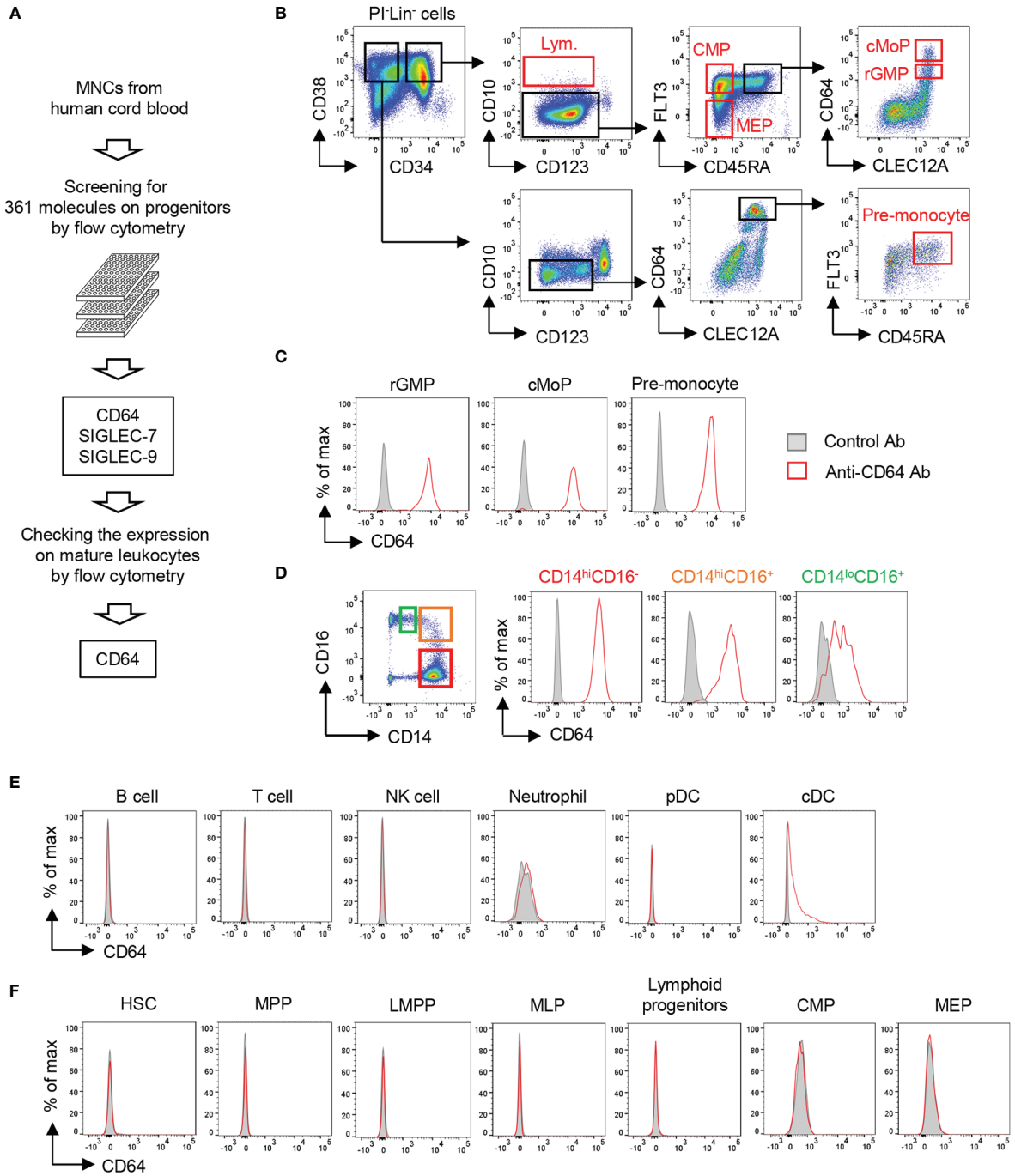

FIGURE 1 | Screening of cell surface molecules to target monocytic progenitors. **(A)** Screening scheme for molecules highly restricted in monocytic progenitors. The expression of 361 cell surface molecules on HSPCs derived from UCB were examined using FCM. Expression of candidates identified from HSPC screening was further assessed on mature hematopoietic cell lineages. **(B)** Gating strategies for hematopoietic progenitors in UCB. Lineage$^-$ cells (Lin$^-$ cells; CD2$^-$CD3$^-$CD11b$^-$CD14$^-$CD16$^-$CD19$^-$CD56$^-$CD235ab$^-$ cells) were pre-gated. Gating strategies of other HSPCs are shown in **Supplementary Figure 1A**. **(C–F)** Expression of CD64 on mature hematopoietic cells and their progenitors. CD64 expression was evaluated on monocytic progenitors **(C)**, monocytes **(D)**, non-monocytic immune cells **(E)** and the other hematopoietic stem and progenitor cells **(F)** by FCM. Each population was identified by the following gating strategies: B cell, FSC^{lo}SSC^{lo}CD3$^-$CD56$^-$CD19$^+$; T cell, FSC^{lo}SSC^{lo}CD3$^+$; NK cell, FSC^{lo}SSC^{lo}CD56$^+$CD3$^-$; Neutrophil, SSC^{hi}HLA-DR$^-$CD66b$^+$CD16$^+$; pDC, CD3$^-$CD14$^-$CD19$^-$CD56$^-$CD11c$^-$HLA-DR$^+$CD123$^+$; cDC, CD3$^-$CD14$^-$CD19$^-$CD56$^-$CD123$^-$HLA-DR$^+$CD11c$^+$. Blood monocytes (HLA-DR$^+$CD14$^+$) were subdivided into three populations based on their expression of CD14 and CD16 as shown in (**D**, left panel). The data are representative of three independent experiments.

megakaryocyte-erythrocyte progenitors (MEPs) (**Figure 1F**). It has been also known that expression of *FCGR1A* encoding CD64 is not observed in non-hematopoietic cells, such as endothelial cells, epithelial cells, adipocytes and myocytes (35). Thus, CD64 is a promising marker to specifically target monocyte lineage cells.

Generation of an ADC Targeting CD64

We next constructed an ADC against CD64 to target monocyte lineage cells, i.e., rGMP, cMoP, pre-monocytes and monocytes. To evaluate the elimination of CD64-expressing cells by the ADC, we needed another anti-CD64 Ab clone that could detect CD64 in the presence of the clone used for the ADC. We prepared three anti-CD64 Ab clones, i.e., 32.2, 611, and H22, and performed competitive inhibition assays between each clone (**Figure 2A**, upper panel). As a control, none of the clones bound CD64 after pretreatment with the same clone. Under these conditions, the recognition of CD64 by 32.2 was inhibited by pretreatment with 611 but not with H22, and 611 could not bind to CD64 when 32.2 or H22 was used as a blocking Ab. In contrast, neither 32.2 nor 611 blocked the recognition of CD64 by H22 (**Figure 2A**, upper panel). Because CD64 is an Fcγ receptor, we next tested if these clones can function in the presence of human IgG, which mimics the human serum in the body (**Figure 2A**, lower panel). Importantly, the presence of human IgG did not affect the recognition of CD64 by H22 as reported previously (36), although it somewhat decreased the CD64 recognition capacities of 32.2 and 611 (**Figure 2A**, lower panel). Based on these results, we decided to use H22 for the generation of an ADC targeting CD64 and to use 32.2 for the detection of monocytes and their progenitors.

An effective payload with cytotoxic potency and a linker are crucial components of an ADC (7). We prepared two different payloads for ADCs targeting CD64, i.e. dimeric pyrrolobenzodiazepine (dPBD), a sequence-selective DNA minor-groove binding crosslinking agent (37), and monomethyl auristatin E (MMAE), an anti-mitotic agent (38). dPBD and MMAE were linked with H22 by valine-alanine (VA) and valine-citrulline (VC), respectively, which are enzymatically cleaved in lysosomes. Cleavage of those linkers results in release of the payloads to the cytoplasm and/or the nucleus and allows them to exert their cytotoxic activities (**Supplementary Figure 2A**). We first evaluated the cytotoxic activity of H22-dPBD against THP-1 cells, a monocytic leukemia cell line expressing CD64 (**Figure 2B**). In addition to H22-dPBD humanized with IgG1 (H22(IgG1)-dPBD) and the isotype matched control ADC [DNP(IgG1)-dPBD], we also tested the nullbody H22-dPBD [H22(Null)-dPBD], in which H22 is humanized with an IgG4 analogue having three mutations that stabilize the Ab and minimize non-specific binding to Fcγ receptors (39). Compared with DNP(IgG1)-dPBD, H22(IgG1)-dPBD had a more effective level of CD64-specific cytotoxicity. For example, 0.04 μg/ml H22(IgG1)-dPBD killed most THP-1 cells, whereas the same dose of DNP(IgG1)-dPBD hardly showed any cytotoxicity against them. In addition, H22(Null)-dPBD killed THP-1 cells to the same extent as H22(IgG1)-dPBD, whereas neither H22(IgG1)-dPBD nor H22(Null)-dPBD had any cytotoxic activity against Ramos cells, a Burkitt's lymphoma cell line that does not express CD64 (**Figures 2B, C**), suggesting that H22-dPBD functions in a CD64-specific manner. The specificity was further confirmed by competitive inhibition assay, in which pre-treatment with unconjugated H22 antibody strongly decreased the killing activity of H22-dPBD (**Supplementary Figure 2B**). Compared with H22-dPBD, the cytotoxic activity of H22-MMAE against THP-1 cells was less effective (**Figure 2D**). Finally, we confirmed that the H22 nullbody was successfully internalized by U937, a monocytic human myeloid leukemia cell line expressing CD64 (**Figure 2E** and **Supplementary Figure 2C**) and by human blood monocytes (**Figure 2F**), and that the internalized ADCs were localized in lysosomes of blood monocytes (**Figure 2F**). Based on these results, we decided to use the nullbody H22-dPBD in this study (hereafter, referred to as H22-dPBD) (**Figure 2G**).

H22-dPBD Is Toxic for Monocytic Progenitors but Not for Monocytes

To observe the cytotoxic effects of ADCs, THP-1 cells were cultured for 6 days with H22-dPBD or the nullbody DNP-dPBD (hereafter DNP-dPBD) (**Figure 3A**). In this context, the viability (%) of THP-1 cells seemed to reflect cell death rather than the inhibition of cell proliferation, because the number of apoptotic THP-1 cells was significantly increased in the presence of H22-dPBD at day 3 during culture (**Figure 3B**). We next examined whether the cell cycle state affects the cytotoxic effects of H22-dPBD. THP-1 cells were treated with PMA, which induces the differentiation of THP-1 cells into macrophage-like cells with cell cycle arrest (40). Interestingly, the PMA-treatment enhanced the resistance of THP-1 cells to H22-dPBD (**Figures 3C, D**), although PMA-treated and non-treated THP-1 cells expressed CD64 at similar levels (**Supplementary Figure 2D**) and the PMA-treated THP-1 cells successfully internalized the ADC (**Supplementary Figure 2E**). Similarly, THP-1 cells that had been treated with moderate irradiation or cultured under low FBS concentrations showed less proliferation capacity (**Supplementary Figure 2F**) and inversely more resistance to the ADC treatment (**Supplementary Figure 2G**). These findings implied that H22-dPBD preferentially exerts its cytotoxic activity against proliferating cells. Thus, we further investigated the cytotoxic effects of H22-dPBD on the differentiation of primary myeloid progenitor cells into monocytes. To this end, we isolated $Lin^{-}CLEC12A^{+}$ cells from UCB, which enriched myeloid progenitor cells including CMPs, rGMPs and cMoPs (13, 41). When the cells were cultured in the presence of FLT3L, TPO and SCF for 6 days, they predominantly gave rise to $CD64^{+}$ cells, which contains monocytes and their progenitors (**Figure 3E**). Under these conditions, the addition of H22-dPBD greatly decreased the production both of $CD14^{+}$ monocytes and of $CD64^{+}CD14^{-}$ monocyte progenitors (**Figures 3F–I**). In contrast, H22-dPBD did not kill primary blood monocytes when added in culture (**Figure 3J**). Taken together, these results indicated that H22-dPBD selectively eliminated $CD64^{+}$ monocyte progenitors rather than mature monocytes *in vitro*.

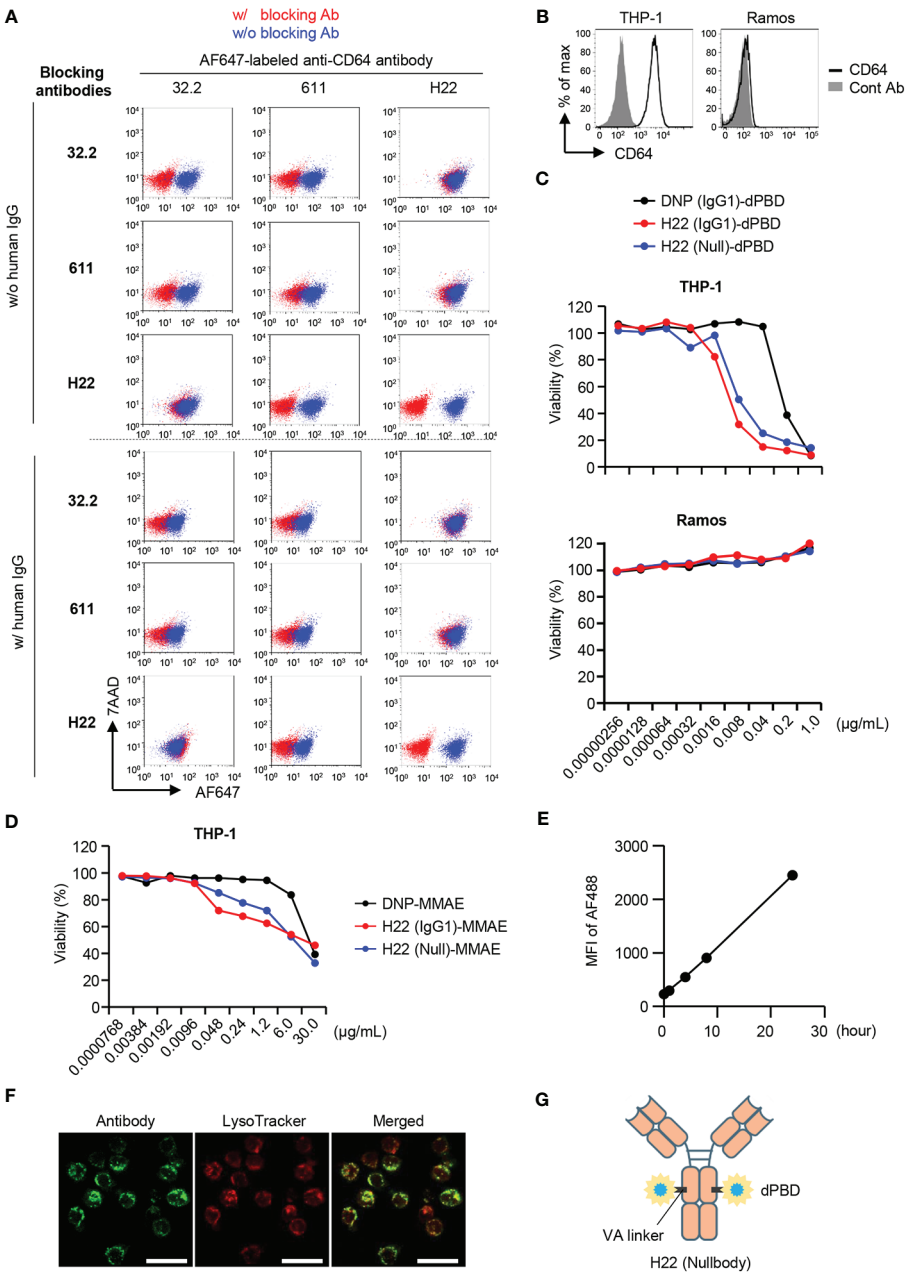

FIGURE 2 | Selection of antibodies and payloads for ADC construction. **(A)** Competitive inhibition of anti-CD64 antibodies. Three clones of anti-CD64 antibodies (32.2, 611 and H22) were assessed for their capacities of epitope recognition in the presence of other clones. THP-1 cells were pretreated with blocking antibodies and then stained with Alexa Fluor 647 (AF647)-labeled anti-CD64 antibody in the presence or absence of human IgG. To estimate binding capacity, the signal intensity in the presence of the competitors (red dots) was compared with that in the absence of competitors (blue dots). **(B)** CD64 expression on THP-1 and Ramos cells. **(C)** Cytotoxicity assays with H22-dPBD. THP-1 and Ramos cells cultured with different ADCs composed of dPBD and an antibody, such as the anti-DNP antibody humanized with IgG1 (DNP(IgG1)-dPBD), H22 humanized with IgG1 (H22(IgG1)-dPBD), or H22 humanized with nullbody, an IgG4 analogue [H22(Null)-dPBD], in the presence of 20% human serum for 4 days. The relative viability of cells was estimated based on the quantification of ATP. **(D)** Cytotoxicity assay with H22-MMAE. THP-1 cells were cultured with ADCs composed of MMAE and an antibody, such as the anti-DNP antibody humanized with IgG1 [DNP(IgG1)-MMAE], H22 humanized with IgG1 (H22(IgG1)-MMAE) or H22 humanized with IgG4 nullbody (H22(Null)-MMAE), in the presence of 20% human serum for 4 days. Relative viability was estimated based on the quantification of ATP. **(E)** Internalization of H22 nullbody by U937 cells. Cells were pre-cultured with Alexa Fluor 488-labeled H22 antibody for the indicated times. The cells were then incubated with a quenching antibody on ice for 1 h and the signal intensity of Alexa Fluor 488 (AF488) was measured by FCM. **(F)** Internalization of H22 nullbody into primary monocytes. $CD14^{hi}CD16^{-}$ monocytes sorted from peripheral blood were stained with the AF647-labeled H22 nullbody. The cells were then cultured for 23 h after reaction with the H22 nullbody and stained with LysoTracker (100 nM) for 1 h. Cell images were obtained by confocal microscopy. Scale bar, 20 μm. **(G)** A schematic illustration of the structure of H22-dPBD. Data are representative of two **(A–E)** or three **(F)** independent experiments.

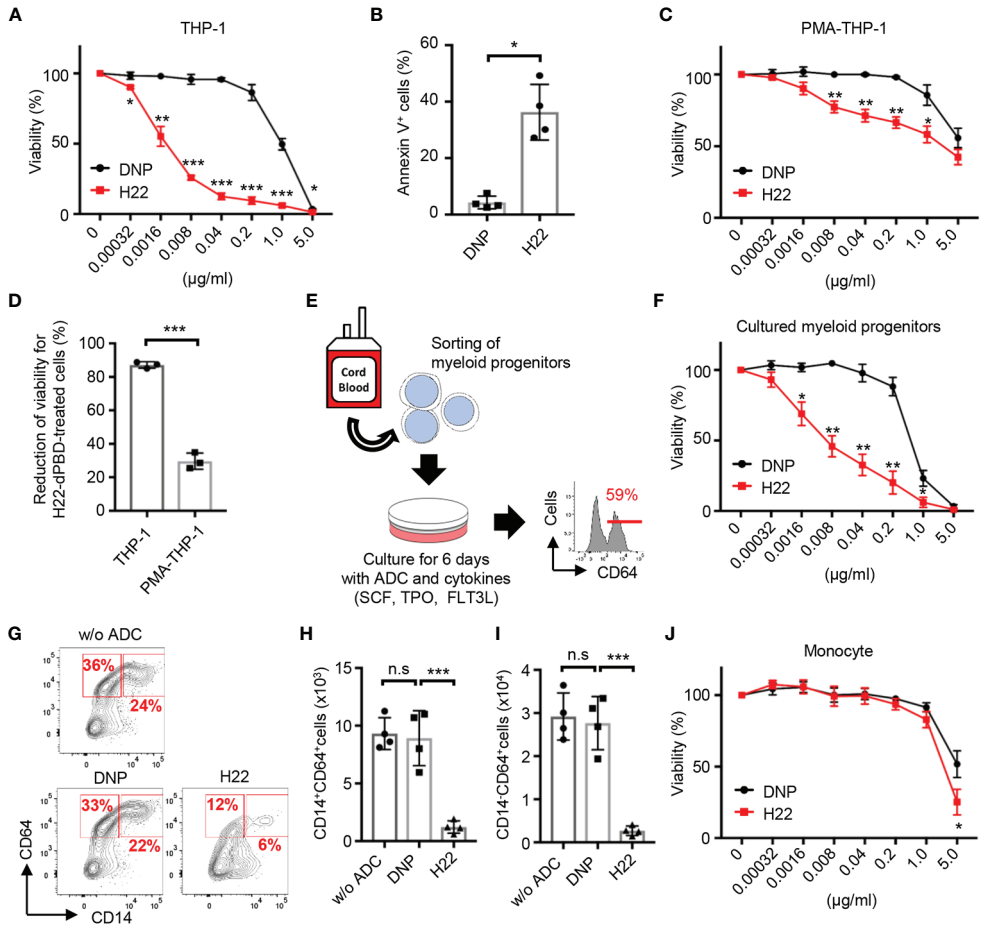

FIGURE 3 | Preferential cytotoxic activity of H22-dPBD against monocytic progenitors, but not monocytes. **(A)** Evaluation of cytotoxic activity of H22-dPBD against THP-1 cells. THP-1 cells were cultured for 6 days in the presence of DNP-dPBD or H22-dPBD and their relative viability was estimated based on the quantification of ATP (n=3). **(B)** Induction of apoptosis by H22-dPBD. THP-1 cells were cultured with ADCs (0.04 μg/ml) for 3 days and the frequency of apoptotic cells was evaluated by FCM (n=4). **(C)** Killing activity of H22-dPBD against PMA-treated THP-1 cells. THP-1 cells were stimulated with 40 ng/ml PMA for 24 h prior to culture with the ADC and the susceptibility of cells to H22-dPBD was examined as shown in **(A)** (n=3). **(D)** Killing efficacy of H22-dPBD treatment against THP-1 cells and PMA-treated THP-1 cells. Normalized reduction of cell viability was calculated from the data of treatment with 0.04 μg/ml ADCs in **(A)** and **(C)** (n=3). **(E)** Experimental scheme of the killing assay against myeloid progenitors. Lin$^-$CLEC12A$^+$ myeloid progenitors were sorted from UCB and were cultured with ADCs and cytokines (100 ng/ml SCF, 50 ng/ml TPO and FLT3L). The number on the histogram indicates the mean frequency of CD64$^+$ progenies yielded through 6-day culture (n=3). **(F)** Cytotoxic activity of H22-dPBD against cells generated from Lin$^-$CLEC12A$^+$ progenitors at day 6. Relative viability was assessed based on the quantification of ATP (n=3). **(G–I)** FCM analysis of CD64$^+$ cells from Lin$^-$CLEC12A$^+$ myeloid progenitors. Cells were cultured with cytokines and 0 or 0.008 μg/ml ADC for 6 days and the numbers of CD14$^+$ monocytes **(H)** and CD14$^-$CD64$^+$ monocytic progenitors **(I)** were determined. **(J)** Cytotoxic activity of H22-dPBD against mature monocytes. CD14^{hi}CD16$^-$ monocytes were sorted from the peripheral blood of healthy donors and were cultured for 6 days in the presence or absence of ADC (n=4). The data were pooled from three **(A, D)** or four **(B, J)** independent experiments or are representative of two **(F)** or three **(C, E, G–I)** independent experiments. Multiple *t*-test **(A, C, F, J),** Student's *t*-test **(B, D)** and one-way ANOVA **(H, I)** were used to assess statistical significance. Error bars represent standard deviation of the mean. *$p < 0.05$, **$p < 0.01$, ***$p < 0.001$; n.s, not significant.

Cytotoxic Effects of H22-dPBD in Humanized Mice

Given the selective cytotoxicity of H22-dPBD against proliferating monocytic cells *in vitro*, we further examined the effects of H22-dPBD *in vivo* using humanized mice. UCB-derived Lin$^-$CD34$^+$ HSPCs were transplanted into sublethally irradiated *NOD/Scid/IL2Rγnull* (NOG) mice (42). Two months after the transplantation, when reconstitution of the human hematopoietic system was confirmed, 0.5 μg H22-dPBD or control DNP-dPBD was intravenously injected and the impact of ADCs was evaluated 7 days later (**Supplementary Figure 3**). As expected, the injection of H22-dPBD induced drastic reductions of monocytes in the BM and blood and their progenitors, pre-monocytes, cMoPs, and rGMPs, in the BM (**Figures 4A, B**). In contrast, there were no significant decreases in the numbers of platelets, neutrophils and lymphoid cells in H22-dPBD-treated humanized mice, although the number of cDCs was partially reduced (**Figures 4C–E**). In addition, treatment with H22-dPBD did not alter the numbers of multipotent progenitors such as Lin$^-$CD34$^+$CD38$^-$

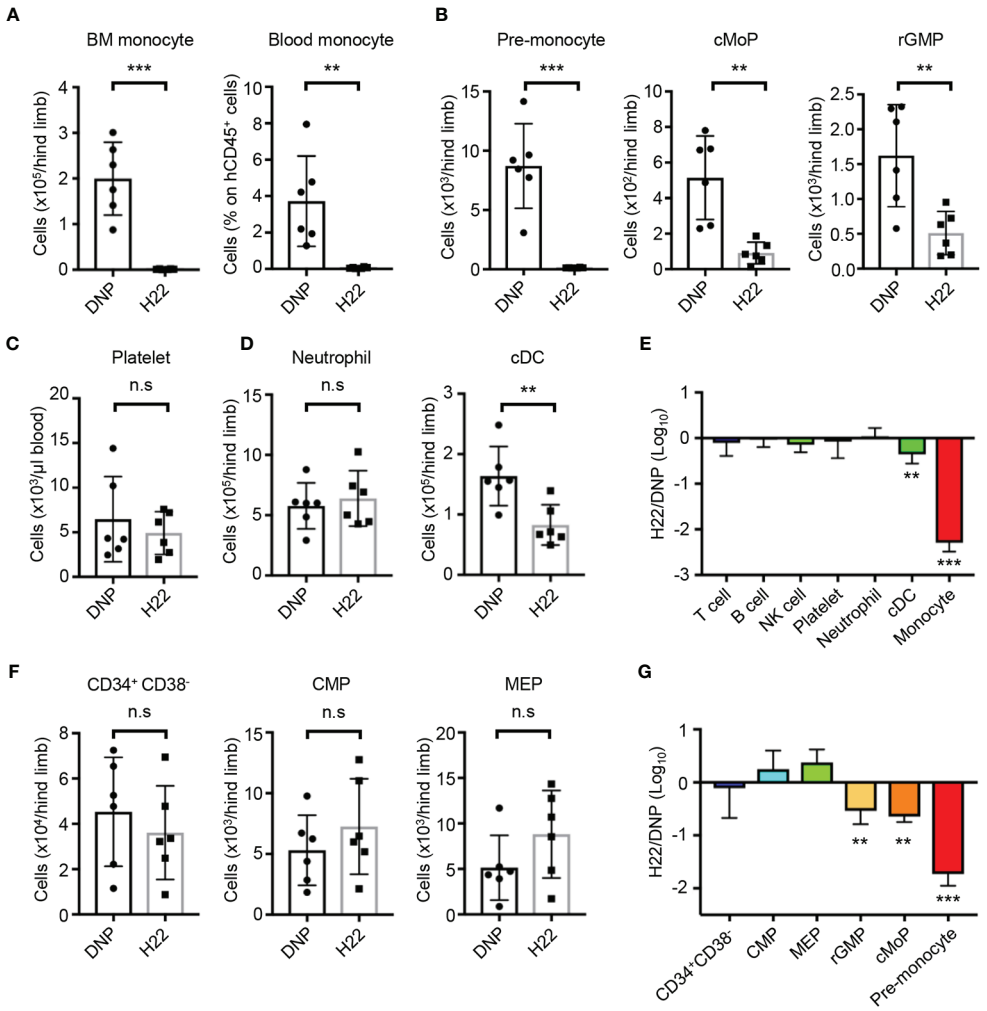

FIGURE 4 | H22-dPBD-mediated elimination of monocytes and their progenitors without severe side effects in hematopoiesis. **(A–G)** BM-humanized NOG mice were generated as shown schematically in **Supplementary Figure 3**. Seven days after intravenous administration of DNP-dPBD or H22-dPBD (0.5 μg/mouse), hematopoietic cells in the BM and blood were analyzed by FCM. The number of BM monocytes and frequency of blood monocytes **(A)**, cell numbers of monocytic progenitors in the BM **(B)**, concentration of platelets (TER119$^-$CD235ab$^-$hCD41a$^+$hCD41b$^+$) in the blood **(C)**, numbers of neutrophils and cDCs in the BM **(D)**, and numbers of Lin$^-$CD34$^+$CD38$^-$ HSPCs, CMPs, and MEPs in the BM **(F)** are shown. Ratios in cell numbers of mature immune cells in the BM and results of their statistical analyses between DNP-dPBD- and H22-dPBD-treated mice are summarized in **(E)**. Ratios in cell numbers of HSPCs and results of their statistical analyses between DNP-dPBD- and H22-dPBD-treated mice are summarized in **(G)**. Each point in the bar graphs shows the value for an individual mouse (n=6 per group). Error bars represent standard deviation of the mean. Student's *t*-test **(A–D, F)** was used to assess statistical significance. $^{**}p < 0.01$, $^{***}p < 0.001$; n.s, not significant. Data were pooled from two **(C)** or three **(A, B, D, F)** independent experiments.

cells that are enriched with HSCs, CMPs and MEPs (**Figures 4F, G**). Thus, H22-dPBD selectively depleted the monocyte lineage with minimal side effects on non-monocytic lineages and multipotent progenitors *in vivo*.

Therapeutic Effects of H22-dPBD in a PDX Model of CMML

The selective monocyte-removing effect of H22-dPBD *in vivo* was reminiscent of its application to CMML, a type of leukemia with increased numbers of monocytes and immature blood cells. To prepare PDX mice, BM cells obtained from CMML patients were transplanted into sublethally irradiated NOG mice (**Figure 5A**, **Supplementary Table 1**). Upon reconstitution, the frequency of monocytes in human CD45$^+$ cells of CMML PDX mice was much higher than that of NOG mice humanized with UCB cells (**Figure 5B**). In addition, the monocytes in the PDX mice showed the characteristic morphology of monocytic dysplasia such as round nuclei and high nuclear-cytoplasmic ratios (**Figure 5C**, lower panel), in contrast to the horseshoe-shaped nuclei of UCB-derived normal monocytes (**Figure 5C**, upper panel). Thus, the pathology of CMML was recapitulated in the PDX mice.

To test the therapeutic effects of H22-dPBD, H22-dPBD or control DNP-dPBD was administered once into the PDX mice and the efficacy of leukemic monocyte removal was evaluated on

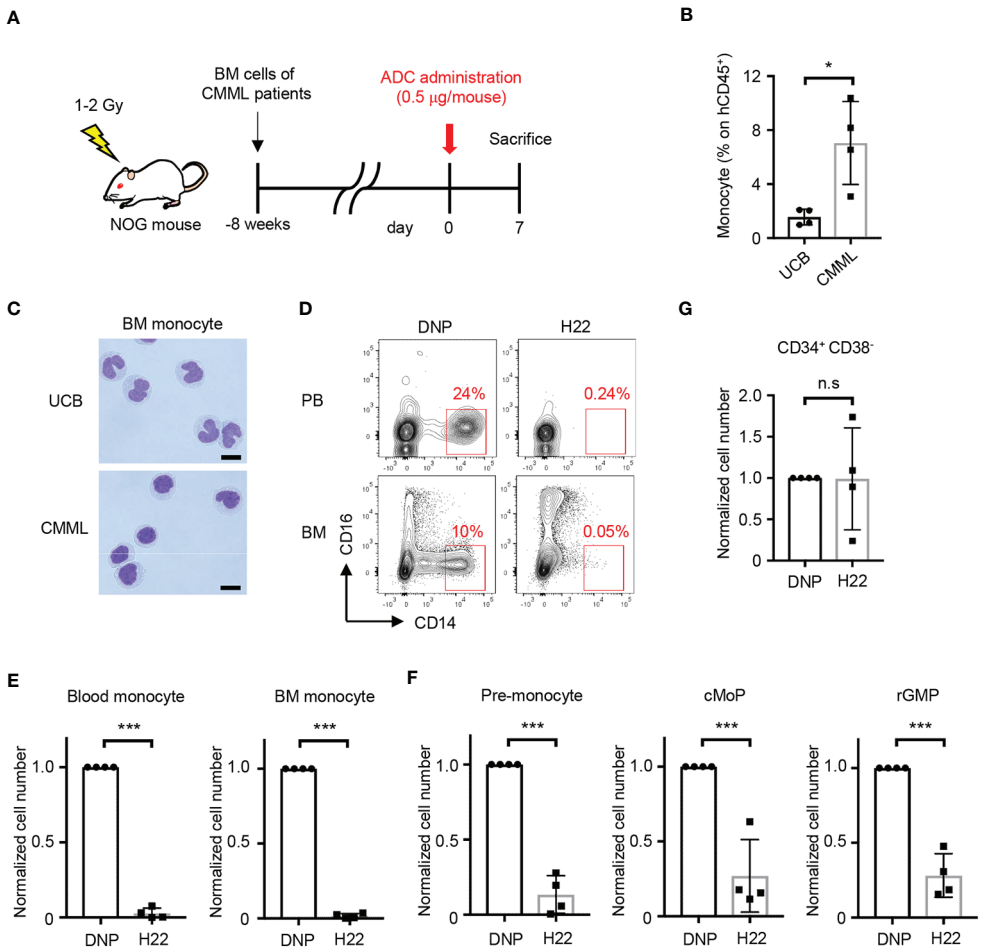

FIGURE 5 | H22-dPBD eliminates patient-derived leukemic monocytes *in vivo*. **(A)** Experimental scheme showing the treatment of PDX mice with ADCs. CMML patient-derived Lin$^-$CD34$^+$ BM cells were transferred to sublethally irradiated NOG mice 8 weeks before the administration of DNP-dPBD or H22-dPBD (0.5 μg/mouse). The mice were analyzed 7 days after the ADC treatment. **(B, C)** Frequency of hCD45$^+$ cells **(B)** and cell morphology **(C)** of BM CD14^{hi}CD16$^-$ monocytes obtained from NOG mice humanized with normal UCB or CMML patient-derived BM cells. Cells were sorted and stained with Diff-quik (scale bars, 5 μm). **(D)** Representative FCM plots of hCD45$^+$ cells in the peripheral blood (upper panels) or BM (lower panels) from DNP-dPBD- or H22-dPBD-treated PDX mice. **(E–G)** Impact of ADC-treatment in hematopoiesis of PDX mice. Cell numbers of monocytes, monocytic progenitors and Lin$^-$CD34$^+$CD38$^-$ cells are shown in **(E)**, **(F)**, and **(G)**, respectively. Each point in the bar graphs shows the value for an individual mouse (n=4 per group). Error bars represent standard deviation of the mean. Student's *t*-test was used to assess statistical significance. *$p < 0.05$, ***$p < 0.001$; n.s, not significant. Data are representative **(C, D)** or pooled **(B, E–G)** from four independent experiments.

day 7 (**Figure 5A**). Importantly, both the CD14^{hi} leukemic monocytes and the monocyte progenitors were almost completely depleted in the blood and/or BM of H22-dPBD-treated CMML PDX mice (**Figures 5D–F**, **Supplementary Figures 4A, B**). In contrast, there was no significant difference in the number of Lin$^-$CD34$^+$CD38$^-$ HSPCs between those two groups (**Figure 5G**, **Supplementary Figure 4C**). Thus, H22-dPBD could successfully remove leukemic monocytes without severe side effects on hematopoiesis.

We then attempted to evaluate the impact of H22-dPBD treatment on the overall survival of CMML PDX mice. However, those mice did not effectively support the engraftment of HSPCs derived from CMML patients, and with the low chimerism, it was impossible to test their survival. Therefore, we transplanted THP-1 cells to sublethally irradiated NOG mice and treated the mice with H22-dPBD or DNP-dPBD at 2 and at 4 weeks after the xenografting (**Supplementary Figure 5A**). Following the injection if H22-dPBD, THP-1 cells were dramatically eliminated in the BM (**Supplementary Figure 5B**) and the survival rate of xenografted mice was significantly prolonged (**Supplementary Figure 5C**). These results suggested the usefulness of H22-dPBD as a therapeutic agent for CMML patients.

H22-dPBD Prevents Solid Tumor Development by Eliminating TAMs

Because TAMs can be derived from monocytes (18, 20), it was worth investigating whether treatment with H22-dPBD can

eliminate TAMs through the depletion of their progenitors and would lead to the reduction of solid tumor size. According to a previous report, we transplanted Lin$^-$CD34$^+$ UCB cells into human IL-6-Tg NOG mice, which generates TAMs with a functionally immunosuppressive nature and show an enhanced tumor-growth (29). A few months later, we subcutaneously transplanted HSC4 human squamous carcinoma cells into those humanized mice (**Figure 6A**). In this context, HSC4 cells did not express CD64 and thus were not targeted by H22-dPBD treatment *in vitro* (**Supplementary Figure 6**). Before injecting H22-dPBD, we confirmed that the chimerism of hCD45$^+$ cells and the frequency of monocytes in hCD45$^+$ cells were similar between the H22-dPBD- and DNP-dPBD-treatment groups (data not shown). Additionally, hCD45$^+$ cells were dominant in tumor-infiltrating leukocytes in this model (**Figure 6B**). Under these conditions, treatment with H22-dPBD effectively eradicated both blood monocytes and tumor-infiltrating CD14$^+$ cells, some of which expressed CD163, a representative TAM marker (43, 44) (**Figures 6C–F**). In contrast, the numbers of total human leukocytes and non-monocytic myeloid cells in the tumor were unaffected (**Figure 6G**), suggesting there were minimal side effects in tumor-infiltrated non-monocytic cell lineages. Importantly, we found that the HSC4 tumor development was significantly suppressed in both volume and weight at 3 weeks after the initial treatment with H22-dPBD (**Figures 6H, I**). Collectively, these results demonstrate that anti-CD64 dPBD is a promising agent to directly treat monocytic leukemia and indirectly suppress solid tumor development through the depletion of TAMs.

DISCUSSION

As cytotoxic side effects caused by anti-cancer drug treatments are major challenges for the treatment of leukemias, various drug-delivery systems including ADCs have been developed to specifically target cancer cells. In this context, the H22-dPBD ADC that we generated in this study has a unique characteristic. Although the H22 nullbody binds both to monocyte progenitors and to mature monocytes, the H22-dPBD ADC selectively eliminated proliferating monocyte progenitors. This could be because the DNA-crosslinking caused by dPBD is more cytotoxic for proliferating cells, in which replication and transcription of DNA are actively occurring. Supporting this notion, the inhibition of THP-1 cell proliferation by treatment with PMA clearly decreased the sensitivity against H22-dPBD, although it did not alter the level of CD64 expression or ADC internalization. Given the difference in proliferation potential between cell lines and primary cells, at least in some cases, cell line-based studies may not reflect the true therapeutic efficacy and target cells of drugs, which can lead to misinterpretation.

Because CD64 is a well-known marker for monocytes and macrophages (36, 45), various ADCs against CD64 have been generated to eliminate leukemic monocytes and/or inflammatory macrophages (46–51). However, in most cases, the efficacy of ADCs was tested in culture and/or in a xenograft model using leukemic cell lines. Thus, it remained unclear if anti-CD64 ADCs work to remove patient-derived monocytic leukemia cells *in vivo*. In addition, the side effects of anti-CD64 ADCs on other cell lineages, especially hematopoietic progenitors, have never been evaluated to date. However, our recent findings, i.e., the identification of CD64$^+$ monocytic progenitors, such as rGMP, cMoP and pre-monocytes, provided an opportunity to reconsider and review the utility of anti-CD64 ADC for anti-cancer therapy and side effects on hematopoiesis.

Under that background, we developed a new ADC targeting human CD64 (H22-dPBD), which kills monocytic progenitors, but not monocytes or other progenitors, and demonstrated that targeting monocytic progenitors with that ADC sharply decreased the number of monocytes in the BM and blood of humanized mice. Treatment with H22-dPBD partially reduced the number of cDCs, which might reflect the presence of monocyte-derived cDCs among total cDCs. Interestingly, treatment with H22-dPBD did not alter the number of neutrophils in humanized mice. This was unexpected because treatment with H22-dPBD *in vivo* partially decreased rGMPs that have the potential to give rise to granulocytes and monocytes. Since neutrophils are short-lived cells, this result may reflect an alternative differentiation pathway of neutrophil generation through unknown progenitors. It might also be possible that H22-dPBD preferentially eliminated monocyte-committed rGMPs, but not neutrophil-committed rGMPs. Indeed, both in mice and in humans, a neutrophil-committed progenitor was identified in the GMP fraction (52, 53). Another possible explanation is the mechanism that stabilizes neutrophil production such as a neutrophil rheostat (neutrostat) (54–56). Given that neutrophils are short-lived cells that first appear in an emergency, there might be complicated regulatory mechanisms of neutrophil homeostasis *in vivo*.

It has been suggested that TAMs are resistant to anti-CD64 ADCs because of their lower expression level of CD64 and the higher degradation capacity of protein-based anti-cancer drugs than are M1 macrophages (28, 36, 37). Considering the property of H22-dPBD to effectively kill monocytic progenitors, it can eradicate any monocyte-derived cells regardless of their nature such as their proliferation state, their capacities to degrade and effuse drugs, and their expression level of CD64. Thus, anti-CD64 ADCs are suitable agents that can target highly heterogeneous monocyte-derived cells such as TAMs. Indeed, in our solid tumor-bearing humanized mouse model, tumor-infiltrating CD163$^+$ TAM-like cells were successfully removed by treatment with H22-dPBD. Importantly, the depletion of TAMs by H22-dPBD significantly attenuated solid tumor progression *in vivo*, suggesting the utility of anti-CD64 ADCs for anti-solid tumor therapy. In this study, we administered ADCs three times in the observation period, because it takes a long time for solid tumors to progress. Although those treatments did not significantly alter the numbers of hCD45$^+$ cells and non-monocytic myeloid cells that infiltrated in the tumor, we noticed that the number of BM neutrophils was reduced (data not shown). This might be due to the reduction of rGMP by three injections of H22-dPBD, which could be stronger than a single

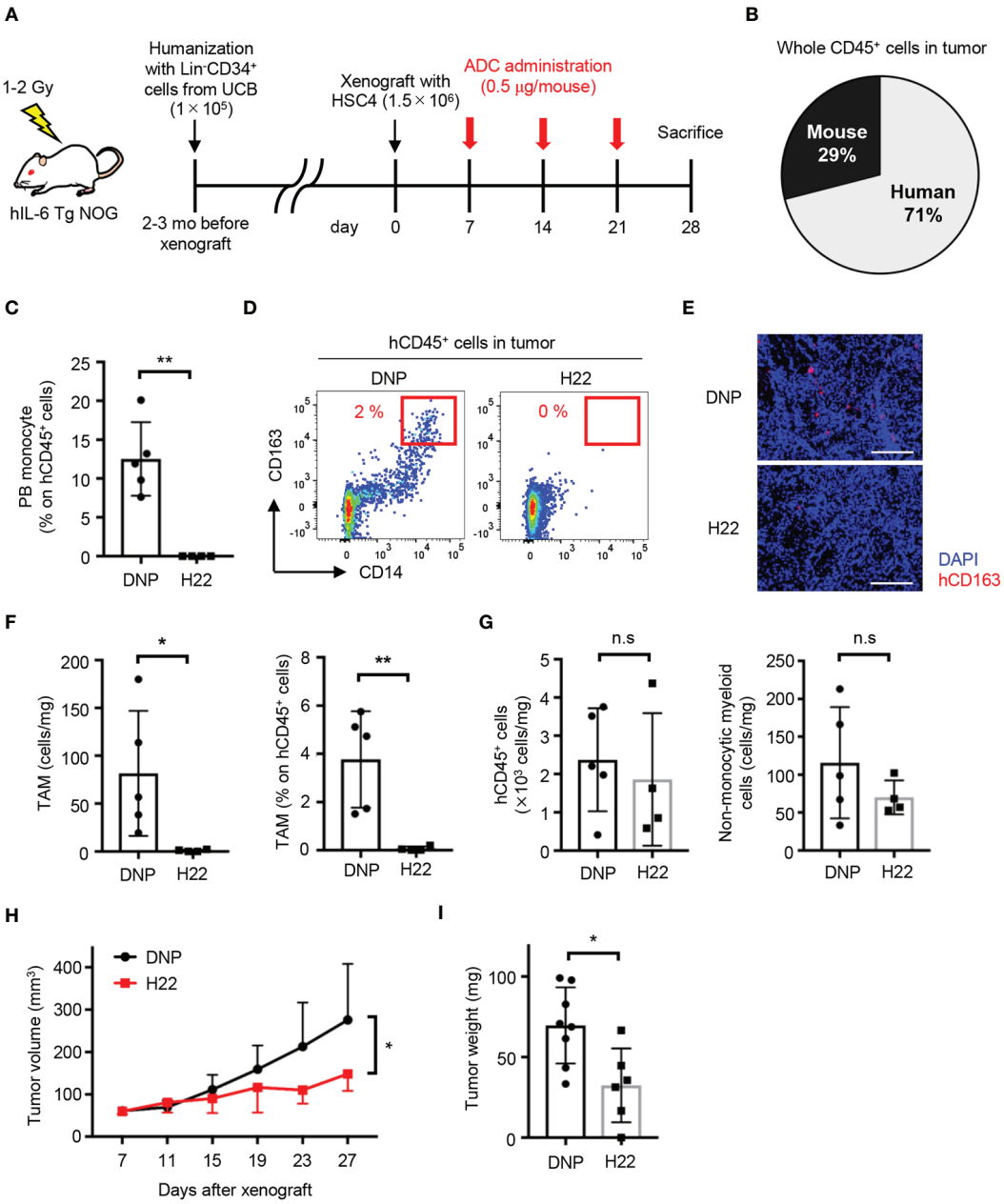

FIGURE 6 | H22-dPBD eliminates TAMs and inhibits the development of solid tumors. **(A)** Experimental scheme of the generation and therapeutic treatment of solid tumor-bearing humanized mice with ADCs. At day 0, HSC4 cells (1.5×10^6 cells/mouse) were subcutaneously transplanted in hIL-6 Tg NOG mice humanized with UCB-derived Lin$^-$CD34$^+$ cells. DNP- or H22-dPBD (0.5 μg/mouse) were intravenously injected to the mice once a week from day 7 and tumor sizes were measured every 4 days from day 7. The mice were sacrificed at day 28 and tumor weights and cells infiltrating the tumors were evaluated. mo: months. **(B)** Ratio of hCD45$^+$ and mCD45$^+$ cells in total leukocytes in the tumor. **(C)** Frequency of monocytes in circulating hCD45$^+$ cells at day 28. **(D)** Representative FCM plots of tumor-infiltrating hCD45$^+$ cells. Frequencies of CD163^{hi}CD14$^+$ TAM-like cells are shown. **(E)** Histological evaluation of tumor-infiltrating CD163$^+$ cells in DNP-dPBD- or H22-dPBD-treated mice. Scale bars: 200 μm. **(F)** Number and frequency of TAMs in DNP-dPBD- or H22-dPBD-treated mice. **(G)** Numbers of total hCD45$^+$ cells and hCD45$^+$CD3$^-$CD19$^-$CD56$^-$CD14$^-$ (non-lymphoid, non-monocytic) cells in the tumor. **(H)** Time-course analysis of tumor development. Tumor volumes were calculated according to the following formula; 0.5 × length × (width)^2. Statistical analysis was performed on data at day 27. Averages of tumor size in each group were shown. **(I)** Tumor weights of DNP-dPBD- or H22-dPBD-treated mice at day 28. Error bars represent standard deviation of the mean. Each point in the bar graphs shows the value for an individual mouse (DNP-treated group: n=8, H22-treated group: n=6). Student's *t*-test was performed to assess statistical significance. $^*p < 0.05$, $^{**}p < 0.01$; n.s, not significant. Data are representative of three independent experiments **(D, E)** or are pooled from two independent experiments **(B, C, F–I)**. Data points more than two standard deviations from the mean were excluded as outliers **(H, I)**.

injection. However, owing to the properties of the humanized mouse model, in which neutrophils poorly egress from the BM and circulate in the peripheral blood (29), the attenuation of tumor development was probably not due to the reduction of neutrophils in this model. To minimize the side effects of the three injections on BM neutrophils, further optimization of dosages and injection intervals will be required.

Tissue-resident macrophages are derived either from yolk sac progenitors during the embryonic stage or from monocytes (57). In this study, we successfully eliminated TAMs generated from human monocytes in humanized hIL-6-Tg NOG mice. On the other hand, TAMs from yolk sac-derived macrophages cannot be evaluated in tumor-bearing humanized mouse models, suggesting their limitation and a requirement for further technological innovation.

In summary, H22-dPBD is a unique ADC that selectively targets proliferating monocyte-committed progenitors and is effective in treating monocytic leukemia and TAM-targeted suppression of solid tumor development (**Supplementary Figure 7**). Since monocytes and monocyte-derived cells including macrophages, DCs and osteoclasts play key roles in the progression of various pathological conditions (28), the strategy targeting monocytic progenitors might also be applicable to treating a variety of other disorders, in particular those involving excessive inflammation and autoimmunity.

DATA AVAILABILITY STATEMENT

The raw data supporting the conclusions of this article will be made available by the authors, without undue reservation.

ETHICS STATEMENT

The studies involving human participants were reviewed and approved by the institution ethical committee of Tokyo Medical and Dental University and Yokosuka Kyosai Hospital. The patients/participants provided their written informed consent to participate in this study. The animal study was reviewed and approved by the Institutional Animal Care Committee of the Tokyo Medical and Dental University.

AUTHOR CONTRIBUTIONS

YI and MKan planned and performed the majority of experiments. MKai and ZS generated ADCs and evaluated activities with *in vitro* experiments. SK performed the screening of molecules expressed on monocytic progenitors. MA, MY, TN, KO, NK, and ST provided samples from patients and YI, MKan, and TO conceived of the project and wrote the manuscript. All authors contributed to the article and approved the submitted version.

FUNDING

This research was supported by the AMED (#JP19cm0106333, TO).

ACKNOWLEDGMENTS

We thank N. Nakamura, K. Tanaka, and F. Ouchi at the Yokosuka Kyosai Hospital and K. Watanabe and H. Akiyama for helping with the collection of human samples. We also acknowledge the Japanese Red Cross Kanto-Koshinetsu Cord Blood Bank and all donors for providing UCB, blood, or BM samples.

SUPPLEMENTARY MATERIAL

The Supplementary Material for this article can be found online at: https://www.frontiersin.org/articles/10.3389/fimmu.2021.618081/full#supplementary-material

REFERENCES

1. Arber DA, Orazi A. Update on the pathologic diagnosis of chronic myelomonocytic leukemia. *Mod Pathol* (2019) 32(6):732–40. doi: 10.1038/s41379-019-0215-y
2. Elmariah H, DeZern AE. Chronic myelomonocytic leukemia: 2018 update to prognosis and treatment. *Curr Hematol Malig Rep* (2019) 14(3):154–63. doi: 10.1007/s11899-019-00509-9
3. Patnaik MM, Tefferi A. Cytogenetic and molecular abnormalities in chronic myelomonocytic leukemia. *Blood Cancer J* (2016) 6:e393. doi: 10.1038/bcj.2016.5
4. Arber DA, Orazi A, Hasserjian R, Thiele J, Borowitz MJ, Le Beau MM, et al. The 2016 revision to the World Health Organization classification of myeloid neoplasms and acute leukemia. *Blood* (2016) 127(20):2391–405. doi: 10.1182/blood-2016-03-643544
5. Catalano L, Improta S, de Laurentiis M, Molica S, Majolino I, Musto P, et al. Prognosis of chronic myelomonocytic leukemia. *Haematologica* (1996) 81(4):324–9.
6. Patnaik MM, Wassie EA, Lasho TL, Hanson CA, Ketterling R, Tefferi A. Blast transformation in chronic myelomonocytic leukemia: Risk factors, genetic features, survival, and treatment outcome. *Am J Hematol* (2015) 90(5):411–6. doi: 10.1002/ajh.23962
7. Thomas A, Teicher BA, Hassan R. Antibody-drug conjugates for cancer therapy. *Lancet Oncol* (2016) 17(6):e254–e62. doi: 10.1016/S1470-2045(16)30030-4
8. Kim EG, Kim KM. Strategies and advancement in antibody-drug conjugate optimization for targeted cancer therapeutics. *Biomol Ther (Seoul)* (2015) 23(6):493–509. doi: 10.4062/biomolther.2015.116
9. Yu B, Liu D. Gemtuzumab ozogamicin and novel antibody-drug conjugates in clinical trials for acute myeloid leukemia. *Biomark Res* (2019) 7:24. doi: 10.1186/s40364-019-0175-x
10. Damle NK, Frost P. Antibody-targeted chemotherapy with immunoconjugates of calicheamicin. *Curr Opin Pharmacol* (2003) 3(4):386–90. doi: 10.1016/s1471-4892(03)00083-3
11. Dinndorf PA, Andrews RG, Benjamin D, Ridgway D, Wolff L, Bernstein ID. Expression of normal myeloid-associated antigens by acute leukemia cells. *Blood* (1986) 67(4):1048–53. doi: 10.1182/blood.V67.4.1048.1048

12. Bross PF, Beitz J, Chen G, Chen XH, Duffy E, Kieffer L, et al. Approval summary: Gemtuzumab ozogamicin in relapsed acute myeloid leukemia. *Clin Cancer Res* (2001) 7(6):1490–6.
13. Kawamura S, Onai N, Miya F, Sato T, Tsunoda T, Kurabayashi K, et al. Identification of a human clonogenic progenitor with strict monocyte differentiation potential: A counterpart of mouse cMoPs. *Immunity* (2017) 46(5):835–48.e4. doi: 10.1016/j.immuni.2017.04.019
14. Gentles AJ, Newman AM, Liu CL, Bratman SV, Feng W, Kim D, et al. The prognostic landscape of genes and infiltrating immune cells across human cancers. *Nat Med* (2015) 21(8):938–45. doi: 10.1038/nm.3909
15. Murdoch C, Tazzyman S, Webster S, Lewis CE. Expression of Tie-2 by human monocytes and their responses to angiopoietin-2. *J Immunol* (2007) 178 (11):7405–11. doi: 10.4049/jimmunol.178.11.7405
16. Venneri MA, De Palma M, Ponzoni M, Pucci F, Scielzo C, Zonari E, et al. Identification of proangiogenic TIE2-expressing monocytes (TEMs) in human peripheral blood and cancer. *Blood* (2007) 109(12):5276–85. doi: 10.1182/blood-2006-10-053504
17. Singhal S, Stadanlick J, Annunziata MJ, Rao AS, Bhojnagarwala PS, O'Brien S, et al. Human tumor-associated monocytes/macrophages and their regulation of T cell responses in early-stage lung cancer. *Sci Transl Med* (2019) 11(479): eaat1500. doi: 10.1126/scitranslmed.aat1500
18. Zhang L, Li Z, Skrzypczynska KM, Fang Q, Zhang W, O'Brien SA, et al. Single-cell analyses inform mechanisms of myeloid-targeted therapies in colon cancer. *Cell* (2020) 181(2):442–59.e29. doi: 10.1016/j.cell.2020.03.048
19. Gordon SR, Maute RL, Dulken BW, Hutter G, George BM, McCracken MN, et al. PD-1 expression by tumour-associated macrophages inhibits phagocytosis and tumour immunity. *Nature* (2017) 545(7655):495–9. doi: 10.1038/nature22396
20. DeNardo DG, Ruffell B. Macrophages as regulators of tumour immunity and immunotherapy. *Nat Rev Immunol* (2019) 19(6):369–82. doi: 10.1038/s41577-019-0127-6
21. Ngambenjawong C, Gustafson HH, Pun SH. Progress in tumor-associated macrophage (TAM)-targeted therapeutics. *Adv Drug Delivery Rev* (2017) 114:206–21. doi: 10.1016/j.addr.2017.04.010
22. Vinogradov S, Warren G, Wei X. Macrophages associated with tumors as potential targets and therapeutic intermediates. *Nanomed (Lond)* (2014) 9 (5):695–707. doi: 10.2217/nnm.14.13
23. Zhou J, Tang Z, Gao S, Li C, Feng Y, Zhou X. Tumor-associated macrophages: Recent insights and therapies. *Front Oncol* (2020) 10:188. doi: 10.3389/fonc.2020.00188
24. Ao JY, Zhu XD, Chai ZT, Cai H, Zhang YY, Zhang KZ, et al. Colony-stimulating factor 1 receptor blockade inhibits tumor growth by altering the polarization of tumor-associated macrophages in hepatocellular carcinoma. *Mol Cancer Ther* (2017) 16(8):1544–54. doi: 10.1158/1535-7163
25. Lamb YN. Pexidartinib: First Approval. *Drugs* (2019) 79(16):1805–12. doi: 10.1007/s40265-019-01210-0
26. Lee JH, Chen TW, Hsu CH, Yen YH, Yang JC, Cheng AL, et al. A phase I study of pexidartinib, a colony-stimulating factor 1 receptor inhibitor, in Asian patients with advanced solid tumors. *Invest New Drugs* (2020) 38(1):99–110. doi: 10.1007/s10637-019-00745-z
27. Mantovani A, Locati M. Tumor-associated macrophages as a paradigm of macrophage plasticity, diversity, and polarization: lessons and open questions. *Arterioscler Thromb Vasc Biol* (2013) 33(7):1478–83. doi: 10.1161/ATVBAHA.113.300168
28. Shapouri-Moghaddam A, Mohammadian S, Vazini H, Taghadosi M, Esmaeili SA, Mardani F, et al. Macrophage plasticity, polarization, and function in health and disease. *J Cell Physiol* (2018) 233(9):6425–40. doi: 10.1002/jcp.26429
29. Hanazawa A, Ito R, Katano I, Kawai K, Goto M, Suemizu H, et al. Generation of human immunosuppressive myeloid cell populations in human interleukin-6 transgenic NOG mice. *Front Immunol* (2018) 9:152. doi: 10.3389/fimmu.2018.00152
30. Graziano RF, Tempest PR, White P, Keler T, Deo Y, Ghebremariam H, et al. Construction and characterization of a humanized anti-gamma-Ig receptor type I (Fc gamma RI) monoclonal antibody. *J Immunol* (1995) 155(10):4996–5002.
31. Graziano RF, Fanger MW. Fc gamma RI and Fc gamma RII on monocytes and granulocytes are cytotoxic trigger molecules for tumor cells. *J Immunol* (1987) 139(10):3536–41.
32. Graziano R, Sundaxrapandiyan K. inventors/applicants (for US only); Medarex, Inc., applicant (for all designated States except US). Human Monoclonal Antibodies to Fc Gamma Receptor I (CD64). International patent WO 2006/002438 A3. (2006).
33. Sussman D, Westendorf L, Meyer DW, Leiske CI, Anderson M, Okeley NM, et al. Engineered cysteine antibodies: an improved antibody-drug conjugate platform with a novel mechanism of drug-linker stability. *Protein Eng Des Sel* (2018) 31(2):47–54. doi: 10.1093/protein/gzx067
34. Jeffrey SC, Burke PJ, Lyon RP, Meyer DW, Sussman D, Anderson M, et al. A potent anti-CD70 antibody-drug conjugate combining a dimeric pyrrolobenzodiazepine drug with site-specific conjugation technology. *Bioconjug Chem* (2013) 24(7):1256–63. doi: 10.1021/bc400217g
35. Su AI, Wiltshire T, Batalov S, Lapp H, Ching KA, Block D, et al. A gene atlas of the mouse and human protein-encoding transcriptomes. *Proc Natl Acad Sci USA* (2004) 101(16):6062–7. doi: 10.1073/pnas.0400782101
36. Akinrinmade OA, Chetty S, Daramola AK, Islam MU, Thepen T, Barth S. CD64: An attractive immunotherapeutic target for M1-type macrophage mediated chronic inflammatory diseases. *Biomedicines* (2017) 5(3):56. doi: 10.3390/biomedicines5030056
37. Hartley JA, Flynn MJ, Bingham JP, Corbett S, Reinert H, Tiberghien A, et al. Pre-clinical pharmacology and mechanism of action of SG3199, the pyrrolobenzodiazepine (PBD) dimer warhead component of antibody-drug conjugate (ADC) payload tesirine. *Sci Rep* (2018) 8(1):10479. doi: 10.1038/s41598-018-28533-4
38. Bai R, Pettit GR, Hamel E. Dolastatin 10, a powerful cytostatic peptide derived from a marine animal. Inhibition of tubulin polymerization mediated through the vinca alkaloid binding domain. *Biochem Pharmacol* (1990) 39(12):1941–9. doi: 10.1016/0006-2952(90)90613-p
39. Namisaki H, Saito S, Hiraishi K, Haba T, Tanaka Y, Yoshida H, et al. R409K mutation prevents acid-induced aggregation of human IgG4. *PloS One* (2020) 15(3):e0229027. doi: 10.1371/journal.pone.0229027
40. Spano A, Barni S, Sciola L. PMA withdrawal in PMA-treated monocytic THP-1 cells and subsequent retinoic acid stimulation, modulate induction of apoptosis and appearance of dendritic cells. *Cell Prolif* (2013) 46(3):328–47. doi: 10.1111/cpr.12030
41. Bill M, van Kooten Niekerk P B, Woll P S, Laine Herborg L, Stidsholt Roug A, Hokland P, et al. Mapping the CLEC12A expression on myeloid progenitors in normal bone marrow; implications for understanding CLEC12A-related cancer stem cell biology. *J Cell Mol Med* (2018) 22(4):2311–8. doi: 10.1111/jcmm.13519
42. Ito M, Hiramatsu H, Kobayashi K, Suzue K, Kawahata M, Hioki K, et al. NOD/SCID/gamma(c)(null) mouse: an excellent recipient mouse model for engraftment of human cells. *Blood* (2002) 100(9):3175–82. doi: 10.1182/blood-2001-12-0207
43. Van Gorp H, Delputte PL, Nauwynck HJ. Scavenger receptor CD163, a Jack-of-all-trades and potential target for cell-directed therapy. *Mol Immunol* (2010) 47(7-8):1650–60. doi: 10.1016/j.molimm.2010.02.008
44. Reinartz S, Schumann T, Finkernagel F, Wortmann A, Jansen JM, Meissner W, et al. Mixed-polarization phenotype of ascites-associated macrophages in human ovarian carcinoma: correlation of CD163 expression, cytokine levels and early relapse. *Int J Cancer* (2014) 134(1):32–42. doi: 10.1002/ijc.28335
45. Ong SM, Teng K, Newell E, Chen H, Chen J, Loy T, et al. A novel, five-marker alternative to CD16-CD14 gating to identify the three human monocyte subsets. *Front Immunol* (2019) 10:1761:1761. doi: 10.3389/fimmu.2019.01761
46. Fet NG, Fiebeler A, Klinge U, Park JK, Barth S, Thepen T, et al. Reduction of activated macrophages after ischaemia-reperfusion injury diminishes oxidative stress and ameliorates renal damage. *Nephrol Dial Transplant* (2012) 27(8):3149–55. doi: 10.1093/ndt/gfr792
47. Hristodorov D, Mladenov R, Fischer R, Barth S, Thepen T. Fully human MAP-fusion protein selectively targets and eliminates proliferating CD64(+) M1 macrophages. *Immunol Cell Biol* (2016) 94(5):470–8. doi: 10.1038/icb.2016.4
48. Mladenov R, Hristodorov D, Cremer C, Gresch G, Grieger E, Schenke L, et al. CD64-directed microtubule associated protein tau kills leukemic blasts ex vivo. *Oncotarget* (2016) 7(41):67166–74. doi: 10.18632/oncotarget.11568
49. Ribbert T, Thepen T, Tur MK, Fischer R, Huhn M, Barth S. Recombinant, ETA'-based CD64 immunotoxins: improved efficacy by increased valency, both in vitro and in vivo in a chronic cutaneous inflammation model in

human CD64 transgenic mice. *Br J Dermatol* (2010) 163(2):279–86. doi: 10.1111/j.1365-2133.2010.09824.x
50. Schiffer S, Letzian S, Jost E, Mladenov R, Hristodorov D, Huhn M, et al. Granzyme M as a novel effector molecule for human cytolytic fusion proteins: CD64-specific cytotoxicity of Gm-H22(scFv) against leukemic cells. *Cancer Lett* (2013) 341(2):178–85. doi: 10.1016/j.canlet.2013.08.005
51. Tur MK, Huhn M, Jost E, Thepen T, Brümmendorf TH, Barth S. In vivo efficacy of the recombinant anti-CD64 immunotoxin H22(scFv)-ETA' in a human acute myeloid leukemia xenograft tumor model. *Int J Cancer* (2011) 129(5):1277–82. doi: 10.1002/ijc.25766
52. Kwok I, Becht E, Xia Y, Ng M, Teh YC, Tan L, et al. Combinatorial single-cell analyses of granulocyte-monocyte progenitor heterogeneity reveals an early uni-potent neutrophil progenitor. *Immunity* (2020) 53(2):303–18.e5. doi: 10.1016/j.immuni.2020.06.005
53. Zhu YP, Padgett L, Dinh HQ, Marcovecchio P, Blatchley A, Wu R, et al. Identification of an early unipotent neutrophil progenitor with pro-tumoral activity in mouse and human bone marrow. *Cell Rep* (2018) 24(9):2329–41.e8. doi: 10.1016/j.celrep.2018.07.097
54. Moutsopoulos NM, Konkel J, Sarmadi M, Eskan MA, Wild T, Dutzan N, et al. Defective neutrophil recruitment in leukocyte adhesion deficiency type I disease causes local IL-17-driven inflammatory bone loss. *Sci Transl Med* (2014) 6(229):229ra40. doi: 10.1126/scitranslmed.3007696
55. Stark MA, Huo Y, Burcin TL, Morris MA, Olson TS, Ley K. Phagocytosis of apoptotic neutrophils regulates granulopoiesis via IL-23 and IL-17. *Immunity* (2005) 22(3):285–94. doi: 10.1016/j.immuni.2005.01.011
56. Soehnlein O, Steffens S, Hidalgo A, Weber C. Neutrophils as protagonists and targets in chronic inflammation. *Nat Rev Immunol* (2017) 17(4):248–61. doi: 10.1038/nri.2017.10
57. Zhu Y, Herndon JM, Sojka DK, Kim KW, Knolhoff BL, Zuo C, et al. Tissue-resident macrophages in pancreatic ductal adenocarcinoma originate from embryonic hematopoiesis and promote tumor progression. *Immunity* (2017) 47(3):597. doi: 10.1016/j.immuni.2017.08.018

Conflict of Interest: MKai and ZS are employees of Kyowa Kirin Co., Ltd.

The remaining authors declare that the research was conducted in the absence of any commercial or financial relationships that could be construed as a potential conflict of interest.

Copyright © 2021 Izumi, Kanayama, Shen, Kai, Kawamura, Akiyama, Yamamoto, Nagao, Okada, Kawamata, Toyota and Ohteki. This is an open-access article distributed under the terms of the Creative Commons Attribution License (CC BY). The use, distribution or reproduction in other forums is permitted, provided the original author(s) and the copyright owner(s) are credited and that the original publication in this journal is cited, in accordance with accepted academic practice. No use, distribution or reproduction is permitted which does not comply with these terms.

frontiers in Immunology

ORIGINAL RESEARCH
published: 25 March 2021
doi: 10.3389/fimmu.2021.642198

Development of LT-HSC-Reconstituted Non-Irradiated NBSGW Mice for the Study of Human Hematopoiesis *In Vivo*

George Adigbli[1†], Peng Hua[2,3†], Masateru Uchiyama[1], Irene Roberts[2,4], Joanna Hester[1‡], Suzanne M. Watt[3,5‡] and Fadi Issa[1‡]*

[1] Transplantation Research and Immunology Group, John Radcliffe Hospital, Nuffield Department of Surgical Sciences, University of Oxford, Oxford, United Kingdom, [2] MRC Molecular Haematology Unit, Weatherall Institute of Molecular Medicine, Radcliffe Department of Medicine, John Radcliffe Hospital, Oxford, United Kingdom, [3] Nuffield Division of Clinical Laboratory Medicine, Radcliffe Department of Medicine, John Radcliffe Hospital, University of Oxford, Oxford, United Kingdom, [4] Department of Paediatrics, Children's Hospital, John Radcliffe Hospital, University of Oxford, Oxford, United Kingdom, [5] Adelaide Medical School, Faculty of Health and Medical Sciences, University of Adelaide, and Precision Medicine Theme, South Australian Health and Medical Research Institute, Adelaide, SA, Australia

OPEN ACCESS

Edited by:
Tim Willinger,
Karolinska Institutet, Sweden

Reviewed by:
Dominique Bonnet,
Francis Crick Institute,
United Kingdom
Teja Celhar,
Singapore Immunology Network
(A*STAR), Singapore

***Correspondence:**
Fadi Issa
fadi.issa@nds.ox.ac.uk

[†]These authors have contributed equally to this work and share first authorship

[‡]These authors share senior authorship

Specialty section:
This article was submitted to Cancer Immunity and Immunotherapy, a section of the journal Frontiers in Immunology

Received: 15 December 2020
Accepted: 03 March 2021
Published: 25 March 2021

Citation:
Adigbli G, Hua P, Uchiyama M, Roberts I, Hester J, Watt SM and Issa F (2021) Development of LT-HSC-Reconstituted Non-Irradiated NBSGW Mice for the Study of Human Hematopoiesis In Vivo. Front. Immunol. 12:642198. doi: 10.3389/fimmu.2021.642198

Humanized immune system (HIS) mouse models are useful tools for the *in vivo* investigation of human hematopoiesis. However, the majority of HIS models currently in use are biased towards lymphocyte development and fail to support long-term multilineage leucocytes and erythrocytes. Those that achieve successful multilineage reconstitution often require preconditioning steps which are expensive, cause animal morbidity, are technically demanding, and poorly reproducible. In this study, we address this challenge by using HSPC-NBSGW mice, in which NOD,B6.SCID IL-2r$\gamma^{-/-}$Kit$^{W41/W41}$ (NBSGW) mice are engrafted with human CD133^{+} hematopoietic stem and progenitor cells (HSPCs) without the need for preconditioning by sublethal irradiation. These HSPCs are enriched in long-term hematopoietic stem cells (LT-HSCs), while NBSGW mice are permissive to human hematopoietic stem cell (HSC) engraftment, thus reducing the cell number required for successful HIS development. B cells reconstitute with the greatest efficiency, including mature B cells capable of class-switching following allogeneic stimulation and, within lymphoid organs and peripheral blood, T cells at a spectrum of stages of maturation. In the thymus, human thymocytes are identified at all major stages of development. Phenotypically distinct subsets of myeloid cells, including dendritic cells and mature monocytes, engraft to a variable degree in the bone marrow and spleen, and circulate in peripheral blood. Finally, we observe human erythrocytes which persist in the periphery at high levels following macrophage clearance. The HSPC-NBSGW model therefore provides a useful platform for the study of human hematological and immunological processes and pathologies.

Keywords: human immune system mice, human hematological reconstitution *in vivo*, immune reconstitution, red blood cell reconstitution, non-irradiation, genome editing

INTRODUCTION

The ability to conduct experiments on human cells and tissues in small animal models holds great value for immunological research. Humanized immune system (HIS) mice are produced by successful transplantation and engraftment of human hematopoietic cells into immunodeficient mice. These *in vivo* models provide a powerful tool for the study of long-term human hematopoiesis and for the preclinical investigation of transplant rejection, cancer, autoimmunity and infection.

Immunodeficient strains such as the non-obese diabetic (NOD)/severe combined immunodeficiency (SCID)/interleukin-(IL)2 receptor gamma chain null (IL2r$\gamma^{-/-}$) mouse (NSG) (1) have profound deficiencies of innate and adaptive immunity and impaired capacity to repopulate the murine bone marrow, both of which enhance engraftment of human hematopoietic stem cells (HSCs) (2). Despite this, attainment of high levels of human leucocyte chimaerism requires preconditioning and adoptive transfer of large numbers of HSCs (3, 4). To address this, the NOD,B6.SCID IL-2r$\gamma^{-/-}$ Kit$^{W41/W41}$ (NBSGW) immunodeficient mouse strain was developed by adding *Kit*$^{W41/W41}$ alleles to the NSG (5). This allele affords a competitive advantage to transplanted HSCs through a loss-of-function mutation of the tyrosine kinase motif of the stem cell factor receptor, c-Kit. A recent study demonstrated successful humanization of NBSGW mice using HSCs sourced from human umbilical cord blood (hUCB), bone marrow and mobilized peripheral blood (6). The majority of HSC-based HIS models in current use utilize human umbilical cord blood (hUCB)-derived cells, with HSC isolation based on expression of CD34. However, because HSC yields from individual hUCB units are both highly variable and expensive to procure and isolate (7), there is a need for mouse models that can support immune reconstitution following transplantation of low numbers of primitive HSCs. In NBSGW mice, successful humanization with high levels of chimaerism is achievable following transplantation of 0.25x10^6–1x10^6 CD34$^+$ HSCs (8). In contrast to CD34, CD133, a pentaspan transmembrane protein on human HSCs, is a key biomarker, expressed on the surface of human HSCs before and then with CD34 (9), and used in place of CD34 for the isolation and characterization of human HSCs (10, 11). In UCB, the CD133$^+$ subpopulation has been shown to be particularly enriched for long-term (LT)-HSCs and the CD133^{neg} fraction to lack LT-HSCs (12, 13). Additionally, the CD133$^+$ population includes a small fraction of CD34^{neg} LT-HSCs which have the capacity for self-renewal (13), are increasingly appreciated as the determinants of successful transplantation (14), and are likely discarded where transplantation is based only on CD34 selection. In NOG mice, isolation based on CD133 positivity has been shown to improve engraftment of UCB HSCs compared with CD133$^-$ HSCs (15).

For immunological research, combined reconstitution of functional human adaptive and innate immune cells is desirable to enable more accurate experimental representation of human immunity to be achieved *in vivo*. Currently available models demonstrate cellular tropism, with biased reconstitution of particular populations of cells. Peripheral blood leucocyte (PBL) HIS models are commonly used examples, which are typically T cell-biased (16). HSC-based HIS models tend to support myeloid cell engraftment but are typically skewed toward reconstitution of immature B cells (17) which fail to mature into functional mature B cells.

T cells that develop within the thymi of HIS mice include CD4$^+$ and CD8$^+$ cells with broad Vβ distribution together with regulatory T cells (Tregs) and γδ T cells (18). To date, successful intrathymic *de novo* T cell development following human HSC transplantation has required the use of irradiated newborn mice (19–21). When this has also been demonstrated in adult mice, its achievement requires irradiation and weekly injections of human Fc-IL7 fusion protein, which conferred the additional effect of diminishing the human B cell population (3).

Human erythropoiesis is not well supported in humanized mouse models. Within the NBSGW mouse, bone marrow-based erythropoiesis occurs with complete maturation, enucleation and globin gene expression (8). However, survival of mature human erythrocytes in the peripheral blood does not occur, likely as a result of murine macrophage-mediated erythrocyte phagocytosis.

In this study we harness stemness properties of CD133$^+$ hUCB LT-HSCs to achieve successful irradiation-independent human hematopoietic reconstitution in NBSGW mice using low doses of HSCs. The model is technically easy to use and achieves robust multilineage reconstitution of lymphoid and myeloid human cells which persist long-term. For decades, achieving this has challenged several of the available HIS mouse models, which are unable to support both engraftment of all lymphocytes and myeloid cells and maturation and survival into the long-term (22). Human thymocytes develop in a humanized thymic microenvironment and both naïve and memory CD4$^+$ and CD8$^+$ T cells repopulate in the periphery. Both immature and mature B cells are present, which are antibody class-switching and functional. Finally, we identify human erythropoiesis within the bone marrow.

MATERIALS AND METHODS

Cell Isolation

hUCB was collected from the John Radcliffe Hospital, Oxford, UK or provided *via* the NHS Cord Blood Bank, London and used with informed, written pre-consent and ethical approval from the South Central Oxford C and Berkshire Ethical Committees (# 15/SC/0027) and the Oxfordshire Research Ethics Committee B (#07/H0605/130), in accordance with the Helsinki Declaration of 1975, as revised in 2008.

Mononuclear cells (MNCs; density <1.077g/ml) were isolated by density gradient centrifugation no more than 24 hours after hUCB collection. Human CD133$^+$/hCD34$^+$ hematopoietic stem and progenitor cells (HSPCs) were enriched by magnetic bead selection using the human CD133/hCD34 direct microbead kits (MACS, Miltenyi Biotec GmbH) and cryopreserved until use (23, 24). Purity was routinely assessed by flow cytometry and only cell isolates with >90% hCD133$^+$ or hCD34$^+$ cell purity were used for

experiments. PBMCs were isolated from leucocyte cones obtained from healthy donors (NHS Blood and Transplant [NHSBT] UK) by LSM1077 (PAA) gradient centrifugation.

Cell Dose, Preparation and Injection Into Mice

NOD,B6.SCID Il2r$\gamma^{-/-}$ Kit$^{W41/W41}$ (NBSGW) mice were obtained from the Jackson Laboratory and then bred and housed in the Biomedical Services Unit of the John Radcliffe Hospital (Oxford, UK) in individually ventilated cages. All experiments were performed using protocols approved by the Animal Care and Ethical Review Committee at the University of Oxford, in accordance with the UK Animals (Scientific Procedures) Act 1986 and under the PPL P8869535A. Cells were quantified for injection using Countbright absolute counting beads (Molecular Probes) by flow cytometry (23). HSPCs were injected intravenously at doses of between 1,000-250,000 CD133$^+$ cells, suspended in 200µl of IMDM/1%HSA (human serum albumin) into non-irradiated adult (5-16 weeks of age) recipient male or female mice. Mice were regularly bled for human leucocyte reconstitution assessment. 20-22 weeks after HSPC injection, peripheral blood, spleen, thymus and bone marrow were harvested. Engraftment was defined as >0.1% hCD45$^+$ cell chimaerism in bone marrow at final harvest (25). A separate group of 8-10 week old male or female mice were injected intravenously with 5x10^6 human PBMCs suspended in 200µl of RPMI 1650. 4-6 weeks after PBMC injection peripheral blood, spleen and thymus were harvested.

Sample Processing

Blood, spleen, both femurs and thymus were harvested. Spleen and thymus were mashed and filtered using a 70µm nylon filter, washed with MACS buffer, and red blood cells lysed (BD Pharmlyse), followed by repeated filtering. Femurs were cleaned, crushed with the back end of a 10ml syringe plunger and filtered through a 70µm nylon filter with MACS buffer to wash out bone marrow cells. 1/50th of a femur was taken for RBC staining and remaining bone marrow was lysed with RBC lysis buffer (BD Pharmlyse). Cells were then washed and filtered again. 10µl of peripheral blood was taken for RBC staining (no RBC lysis) and 50µl of blood was taken for each of the remaining stains after undergoing RBC lysis with BD Pharmlyse buffer, followed by washing with MACS buffer.

Flow Cytometric Analysis

Bone marrow, spleen, thymus and blood single cell suspensions prepared as described above were used for flow cytometry. The antibodies against human and mouse cell surface antigens are detailed in **Supplementary Table 1**. Briefly, cells were incubated with a mixture of fluorescently labeled antibodies diluted in FACS buffer for 30 minutes on ice. Cells were washed once, resuspended in FACS buffer and acquired immediately on a BD FACSCanto flow cytometer (BD Biosciences). 7-AAD (eBioscience) was added to the antibody mix to distinguish live and dead cells. Data were analyzed using FACSDiva (BD) and FlowJo software (TreeStar Inc.).

Human Skin Transplantation

Human tissue samples were obtained with full informed written consent and with ethical approval from the Oxfordshire Research Ethics Committee (REC B), under study number 07/H0605/130. In 2 separate experiments, 14 non-irradiated adult NBSGW mice were injected with CD133$^+$ hUCB cells suspended in 200µl of IMDM/1%HSA and 11-13 weeks after humanization, received a 1cm x 1cm allogeneic split-thickness human skin graft harvested from excess abdominal tissue used for reconstructive surgery (as previously described (26)). 6 additional mice, which did not receive skin transplants were observed to 100 days to compare incidence of adverse effects. At the time of skin transplantation, multilineage leucocyte reconstitution can be observed in the peripheral blood (data not shown). Grafts were monitored for clinical features of rejection and mice were sacrificed when these were observed. In the absence of rejection grafts were harvested 100 days after transplantation. Spleens were harvested concurrently and splenocytes, processed (as above) and analyzed by FACS for the frequency of class-switched memory B cells. Additionally, blood was harvested and serum separated from cells following centrifugation at 1300rpm for 10 minutes. IgD and IgG expression was assessed by cytometric bead array (Biolegend Legendplex Human Ig Isotyping Panel (8-plex)) according to the manufacturer's instructions. Data were analyzed using FACSDiva (BD) and FlowJo software (TreeStar Inc.).

Phagocyte Depletion

For the phagocyte depletion assays, mice were injected with 50,000 CD34$^+$ hUCB HSPCs. On week 10, mice were checked for human leucocyte reconstitution and allocated to the clodronate and PBS-treated groups to provide equal distribution of human leucocyte reconstitution levels. Mice received either 200µl clodronate liposomes (at 5mg clodronate per ml; Liposoma B.V.) or 200µl PBS intraperitoneally. Five (5) days after injection, mice were analyzed for mouse macrophage depletion and human RBC levels in the peripheral blood (27). The bone marrow was then harvested at day 6 post-clodronate injection.

Data Analysis and Statistics

Statistical analyses were performed using GraphPad Prism 5 software using the Mann Whitney test and paired t-test as described in each figure legend. A p value of <0.05 was considered statistically significant. Median values are shown, unless stated otherwise.

RESULTS

Human Leucocyte Reconstitution and HSPC Engraftment in HSPC-NBSGW Mice

We first examined human hematopoietic chimaerism in the peripheral blood following transplantation of hUCB CD133$^+$ HSCs (≥1x10^3 CD133$^+$ cells injected) into non-irradiated NBSGW mice (referred to herein as HSPC-NBSGW mice). Following isolation, >96% of CD133$^+$ cells were strongly

positive for CD34, and included a small number of the rare but highly potent $CD133^+CD34^-$ LT-HSCs (**Supplementary Figure 1a**). Successful humanization was demonstrated by a dose-dependent increase in human $CD45^+$ cell chimaerism in the bone marrow, spleen and peripheral blood by 20-22 weeks (**Figures 1A, B**; **Supplementary Tables 2** and **3**, **Supplementary Figure 1B**). Engraftment was greatest in the bone marrow (mean ± SD from 35.0±36.2 to 97.4±1.9%) and spleen (from 32.0±39.4 to 98.5±0.9%) (**Supplementary Table 2**). Robust engraftment was also present in the peripheral blood (from 12.1±24.7 to 80.0±14.2%), with higher chimaerism than described in comparable irradiated HSPC mice similarly humanized intravenously with hUCB HSCs (28). At all doses administered, reconstitution in the blood demonstrated no signs of declining at 20-22 weeks (**Figure 1B**). Recipient sex did not significantly affect chimaerism in the bone marrow, spleen or peripheral blood (**Figures 1C–G**, **Supplementary Figure 1C**), however we identified a trend consistent with other immunodeficient strains including NSG mice in which lower levels of human $CD45^+$ cell engraftment are seen in the bone marrow of male recipients. Engraftment of a sizeable proportion of Lin^-CD34^+ and $Lin^-CD34^+CD38^{lo/-}$ cells in the bone marrow was seen and suggests a pool of stable, self-renewing HSPCs is maintained for at least 20 weeks (**Figures 2A–D**). Relative engraftment of these cells was greater in the bone marrow of female as compared to male recipients when 5-10x10^3 HSPCs were transplanted (**Figures 2C, D**). We previously demonstrated functional self-renewal through engraftment of human leukocytes in NBSGW mice secondarily transplanted with bone marrow cells from HSPC-NBSGW mice (29),

B Cells Dominate Multilineage Human Leucocyte Engraftment

We observed multilineage human leucocyte engraftment in the bone marrow, spleen and peripheral blood (**Figure 3**; **Supplementary Figure 2**). B cells engrafted with the greatest frequency (**Figures 3A, B**; **Supplementary Figures 2A–C**, followed by myeloid and T cells (**Supplementary Tables 2** and **3**). In mice receiving 1x10^3 hUCB HSPCs, $hCD19^+$ B cell engraftment was higher in females (**Supplementary Figure 2d**). No other sex-specific differences in leucocyte subset engraftment were observed (**Supplementary Figures 2D–F**). We also identified human natural killer cells, which were most populous in the peripheral blood. (**Supplementary Figures 2G, H**)

B cell hematopoiesis was assessed by examining the developmental stages of B cells in the bone marrow, spleen and peripheral blood 20-22 weeks after humanization (**Figure 3B**). Within the bone marrow, immature B cells expressing CD10 were most populous (30) (**Figures 3C, D**), contrasting with increasing frequencies of larger $CD10^-$ mature B cells in the spleen and blood (**Figures 3D, E**), supporting early observations of the memory phenotype being associated with greater-sized B cells (31). This correlates with human bone marrow, which contains more $CD10^+$ cells (with higher CD10 density) than both hUCB $CD34^+$ cells and G-CSF-mobilized peripheral blood (30). Next, we analyzed mature B cell phenotypes. As expected, only a small proportion of $CD10^-$ B cells populated the bone marrow and the majority were naïve, lacking CD27 expression (**Figures 3F–G**). Of these, almost half were $CD27^-IgD^-$ double-negative B cells (**Figure 3G**), a heterogenous population described as early-stage bone marrow cells (32), and more recently as memory precursor, extracellular antibody secreting cell precursor, and atypical/tissue based memory cells, with activated phenotypes in inflammatory diseases (33). As in humans, antigen-inexperienced $CD27^-IgD^+$ B cells formed the other major mature B cell population in the bone marrow (34) (**Figure 3G**). Within the spleen a greater proportion of mature B cells was observed and among them both unswitched ($CD27^+IgD^+$) and class-switched memory B cells ($CD27^+IgD^-$) (**Figures 3F–G**). This reflected the notion that class switch recombination (CSR) occurs predominantly (although not exclusively) in germinal center (secondary lymphoid organ) B cells, initiated by activation-induced cytidine deaminase (35). To assess the capacity for isotype switching to be stimulated *in vivo*, we introduced an antigen challenge by transplanting allogeneic human skin onto HSPC-NBSGW mice 11-13 weeks after humanization. At the point of skin allograft rejection (or after 100 days), we analyzed the phenotypes of human leucocytes, splenic B cells and immunoglobulin subtypes in peripheral serum (**Figures 3H–K**; **Supplementary Figures 2i–k**). We found a significantly higher frequency of $CD27^+IgD^-$ memory B cells (**Figure 3I**), together with lower serum IgD and higher IgG1 levels (**Figures 3J, K**) in mice exposed to allogeneic skin transplants compared with mice not exposed. This indicates the potential for specific human B cell responses to be mounted in response to antigen challenge within this model.

Altogether, these findings demonstrate that following transplantation of hUCB $CD133^+$ HSPCs a continuous process of human B cell development and functional maturation occurs within the primary and secondary lymphoid organs of HSPC-NBSGW mice.

Thymic Development of Human T Cells in HSPC-NBSGW Mice

Having identified long-term engraftment of T cells (**Figure 3A**; **Supplementary Figure 2**), we sought to investigate whether persistence of these cells is also supported by continuous hematopoiesis and thymic development. We first assessed T cell subset profiles within the bone marrow, spleen and blood. Transplantation of high doses (≥50x10^3) of HSPCs produced robust engraftment of both $CD8^+$ and $CD4^+$ T cells, predominantly in the spleen and peripheral blood (**Figures 4A, B**). At these doses we identified the major T cell subtypes within both $CD8^+$ and $CD4^+$ T cell populations: 1) central memory (Tcm), 2) effector memory (Tem), 3) T effector memory re-expressing CD45RA (TemRA) and 4) naïve (Tn) (**Figures 4C, D**; **Supplementary Table 4**). Tem and Tcm cells were the most populous subtypes, however a significant proportion of CD45RA-expressing cells also persisted long-term (**Figures 4C–F**; **Supplementary Figure 3D**, **Supplementary Table 4**). We found T cell reconstitution in HSPC-NBSGW mice to

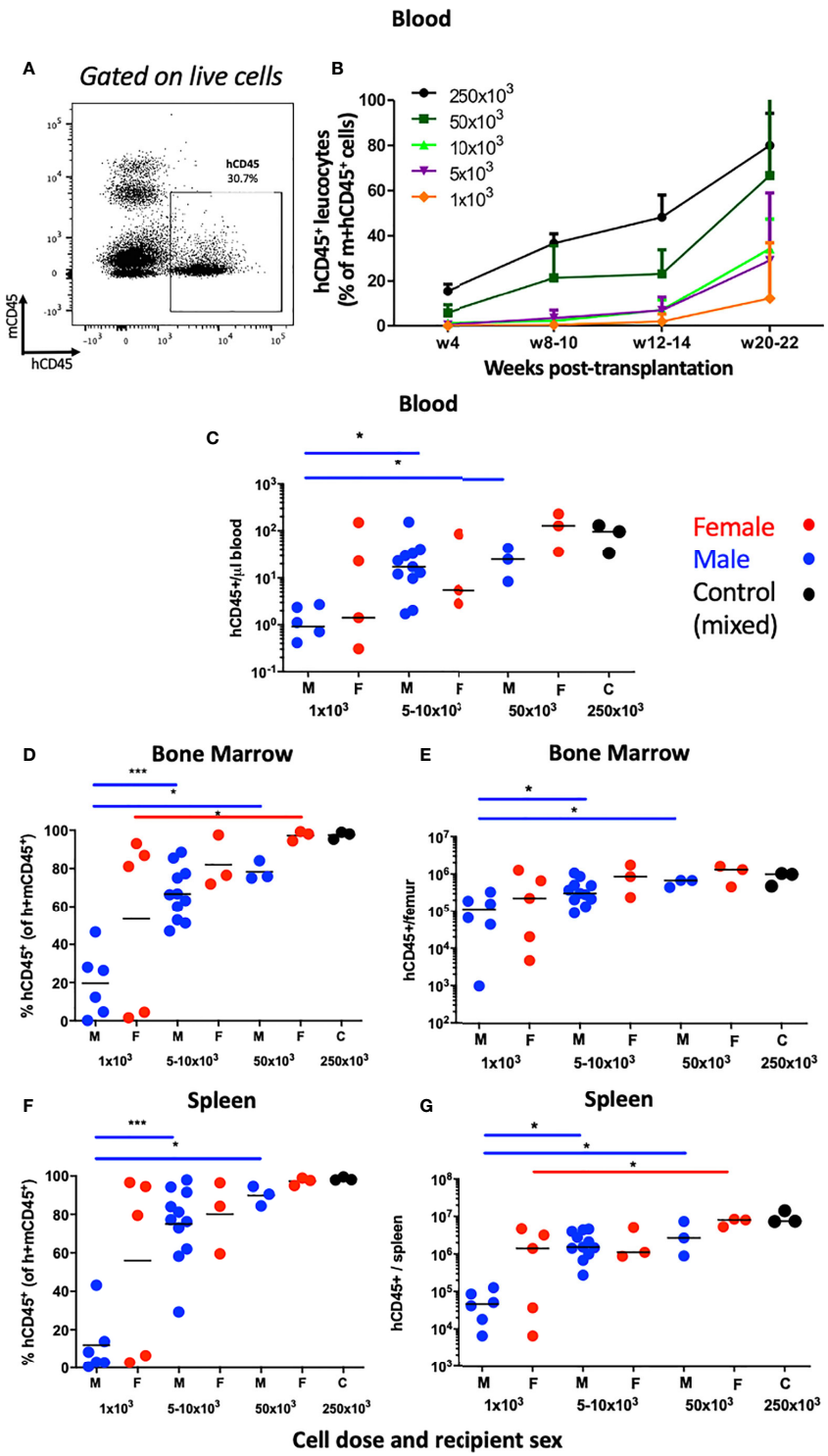

FIGURE 1 | Human leucocyte reconstitution in HSPC-NBSGW mice. **(A)** Representative flow cytometric analysis of mCD45⁺ vs hCD45⁺ cells in the peripheral blood of non-irradiated NBSGW recipients 20-22 weeks after i.v. injection with $1x10^3$ hCD133⁺ hUCB HSPCs. **(B)** Frequencies of hCD45⁺ leucocytes in the blood at indicated time points according to dose of injected HSPCs (mean and SD shown). **(C)** Absolute numbers of human CD45⁺ leucocytes per microliter of blood in male and female recipient mice, based on number of injected HSPCs. **(D–G)** Human CD45⁺ leucocyte frequencies (percentage of total mouse plus human CD45⁺ cells) and corresponding absolute numbers per, bone marrow of one femur and spleen in male and female recipient mice, based on number of injected HSPCs. M- male (blue symbols), F- female (red symbols), $250x10^3$ C – control group (mixed sex). Statistical significance was assessed using a Mann Whitney test (*$p<0.05$, ***$p<0.001$). In **(C)**, two points fall below the cut-off shown for $1x10^3$ cells infused. Non-statistical bars represent median values.

more accurately reproduce the average human peripheral blood profiles than in NBSGW mice humanized with peripheral blood mononuclear cells (PBMCs), which fail to reconstitute CD45RA-expressing T cells and are instead composed entirely of Tem and Tcm (**Supplementary Figures 3A–D**).

To identify whether *de novo* T cell development from transplanted HSPCs occurs in this model, we analyzed human and mouse leucocyte populations in the thymi of recipient mice humanized with HSPCs or PBMCs (**Figure 5**). The majority of thymic cells were human CD45$^+$ leucocytes (**Figures 5A, B**) expressing CD3, together with a small population of CD19$^+$ cells (**Supplementary Figure 4A**). The majority of CD3$^+$ cells were CD4$^+$CD8$^+$ double-positive (DP) thymocytes (**Figures 5C, D**) with an average frequency equivalent to those seen in thymus biopsies from human infants (36). In contrast, following humanization with mature PBMCs, no double-positive T cells were identified within the thymus (**Supplementary Figures 4B–C**).

Successful Engraftment and Reconstitution of Phenotypically Distinct Subsets of Innate Myeloid Cells

Developing humanized mouse models capable of reconstituting cells of the innate and adaptive immune systems and long-term survival is difficult to achieve, especially in the absence of irradiation and engineered or exogenous cytokine expression. Having identified engraftment of human CD33$^+$ myeloid cells (**Figure 3A**; **Supplementary Table 2**; **Supplementary Figure 2**), we assessed subtype reconstitution (**Figure 6**). At all doses of HSPCs transplanted, myeloid cells engrafted with the greatest

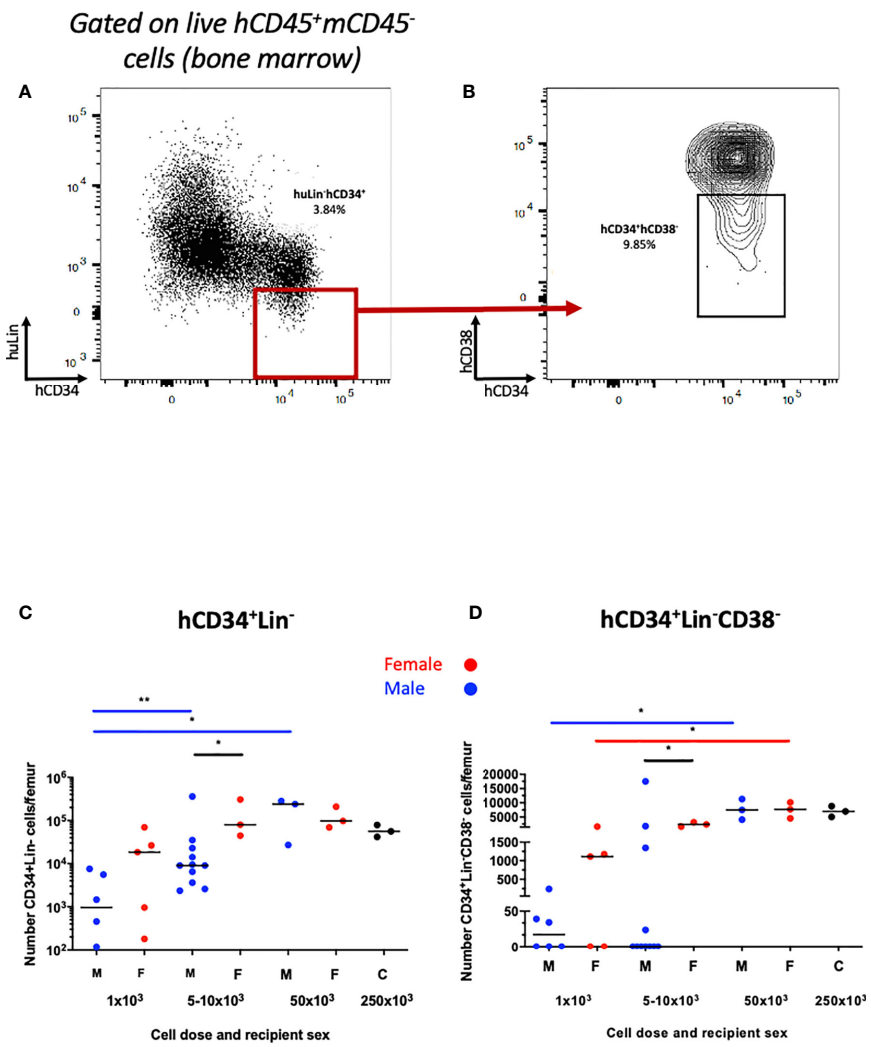

FIGURE 2 | Human HSPC engraftment in the bone marrow of HSPC-NBSGW mice. Representative dot plots of **(A)** hCD34$^+$Lin$^-$ and **(B)** hCD34$^+$Lin$^-$hCD38$^{low\backslash-}$ HSPCs in the bone marrow. Number of **(C)** hCD34$^+$Lin$^-$ and **(D)** hCD34$^+$Lin$^-$hCD38$^{low\backslash-}$ cells per femur in male and female recipients at the point of harvest (20-22 weeks). M- male (blue symbols), F- female (red symbols), 250x10^3 – control group (mixed sex). Statistical significance was assessed using a Mann Whitney test (*p<0.05, **p<0.01). Median values shown.

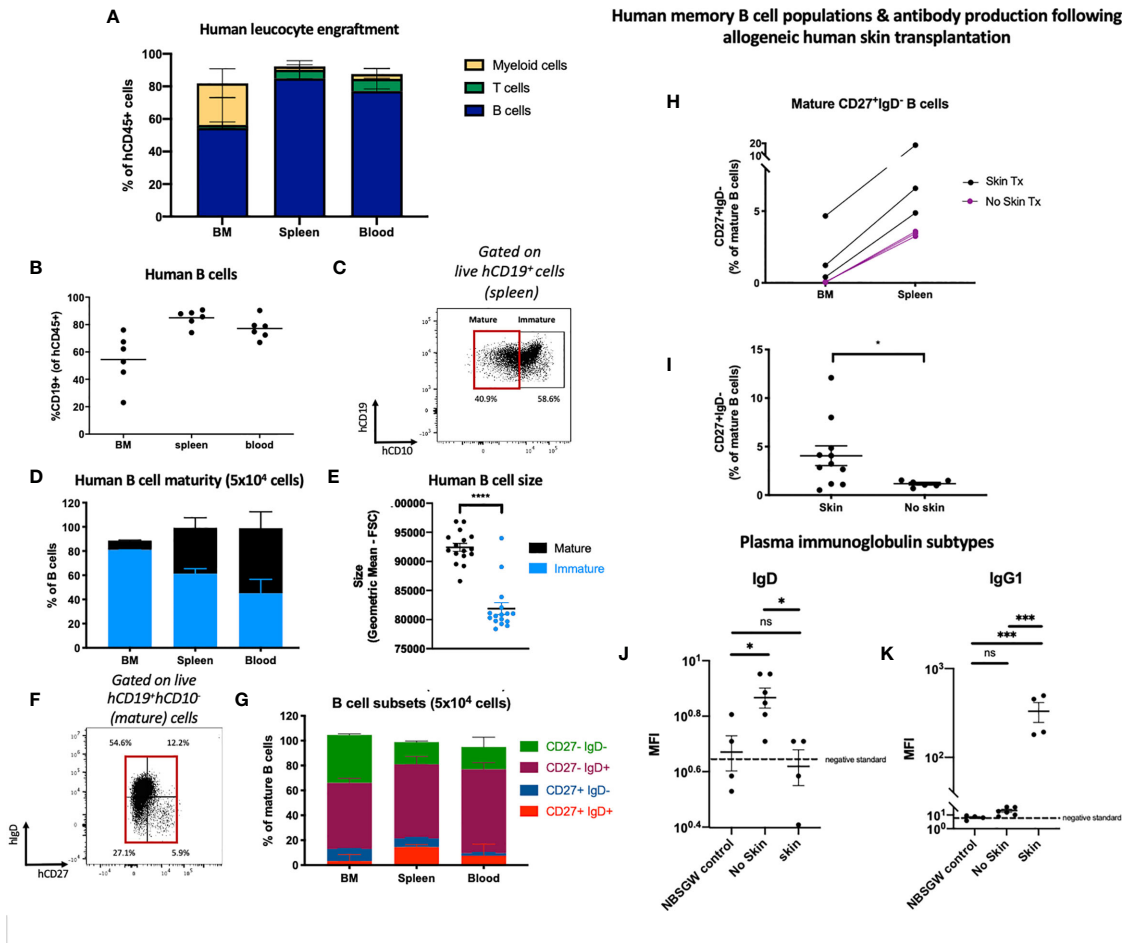

FIGURE 3 | Human B cell engraftment and development in HSPC-NBSGW mice. **(A)** Frequencies of human B cells, myeloid cells and T cells in the bone marrow, spleen and blood of HSPC-NBSGW mice 20-22 weeks after cell injection (50x10^3 cells). **(B)** Frequency of hCD19$^+$ cells in the bone marrow (BM), spleen and peripheral blood (50x10^3 cells). Bars indicate median values. **(C)** Representative flow cytometric analysis of CD10 expression on human CD45$^+$CD19$^+$ B cells in spleens harvested at 20-22 weeks. **(D)** Frequencies of mature (CD10-) and immature (CD10+) human B cells in the bone marrow, spleen and blood. **(E)** Sizes of mature vs immature human splenic B cells (determined by forward scatter (FSC). **(F)** Representative flow cytometric analysis and **(G)** corresponding frequencies of mature (CD10$^-$) B cell subsets in the bone marrow, spleen and blood, based on IgD and CD27 expression. The red box indicates mature cells [as gated in **(C)**]. **(H)** Frequencies of IgD-negative memory B cells in the femurs and spleens of HSPC-NBSGW mice which received allogeneic split-thickness human skin grafts 11 weeks after humanization and were sacrificed at the time of skin rejection (skin Tx) or 100 days after transplantation (no skin Tx). **(I)** Frequencies of class-switched memory B cells in the spleens of mice which did (skin) and did not (no skin) receive allogeneic split-thickness human skin grafts. **(J, K)** Geometric mean fluorescence intensity (MFI) of plasma **(J)** human IgD and **(K)** human IgG1 in NBSGW (control), HSPC-NBSGW (no skin) and human skin-transplanted HSPC-NBSGW (skin) mice. Dashed lines represent negative standards (background fluorescence). Bars represent median + IQR **(A, D, G)**, mean + SEM **(E, I)** and median **(H)** values. Statistical significance was assessed using the paired t test **(D)**, two-tailed Mann-Whitney test **(I)**, and ordinary one-way ANOVA with Tukey's multiple comparisons test **(J, K)** (*p<0.05; ***p<0.001; ****p<0.0001; ns p>0.05).

frequency in the bone marrow (**Figure 6A**; **Supplementary Table 2**). Within the bone marrow and spleen we identified populations of HLA-DR^{hi}, HLA-DR^{int} and HLA-DR$^-$ cells (**Figures 6B, C**). The CD33$^+$HLA-DR^{hi} subset, which includes CD11c$^+$ conventional dendritic cells (cDCs), formed the most common subtype in the bone marrow (**Figures 6B–G**; **Supplementary Figures 5A, B**). As similarly described in human bone marrow, these cDCs expressed CD33, high levels of CD11c and HLA-DR, and were CD14$^-$ (37) and CD11b$^{lo/-}$ aiding the distinction from monocyte/macrophage lineage cells (**Figures 6D–F**). The HLA-DR^{int} fraction, which includes CD14-expressing mature monocytes/macrophages is found predominantly in the blood where it forms approximately half of all myeloid cells (**Figures 6B–F** and **H**). A less mature CD14$^+$HLA-DR$^-$ population, which may include myeloid-derived suppressor cells is also present, especially in the spleen (**Figure 6C**). Together, these data demonstrate successful engraftment and reconstitution of phenotypically distinct subsets of innate myeloid cells, which express molecules of antigen presentation.

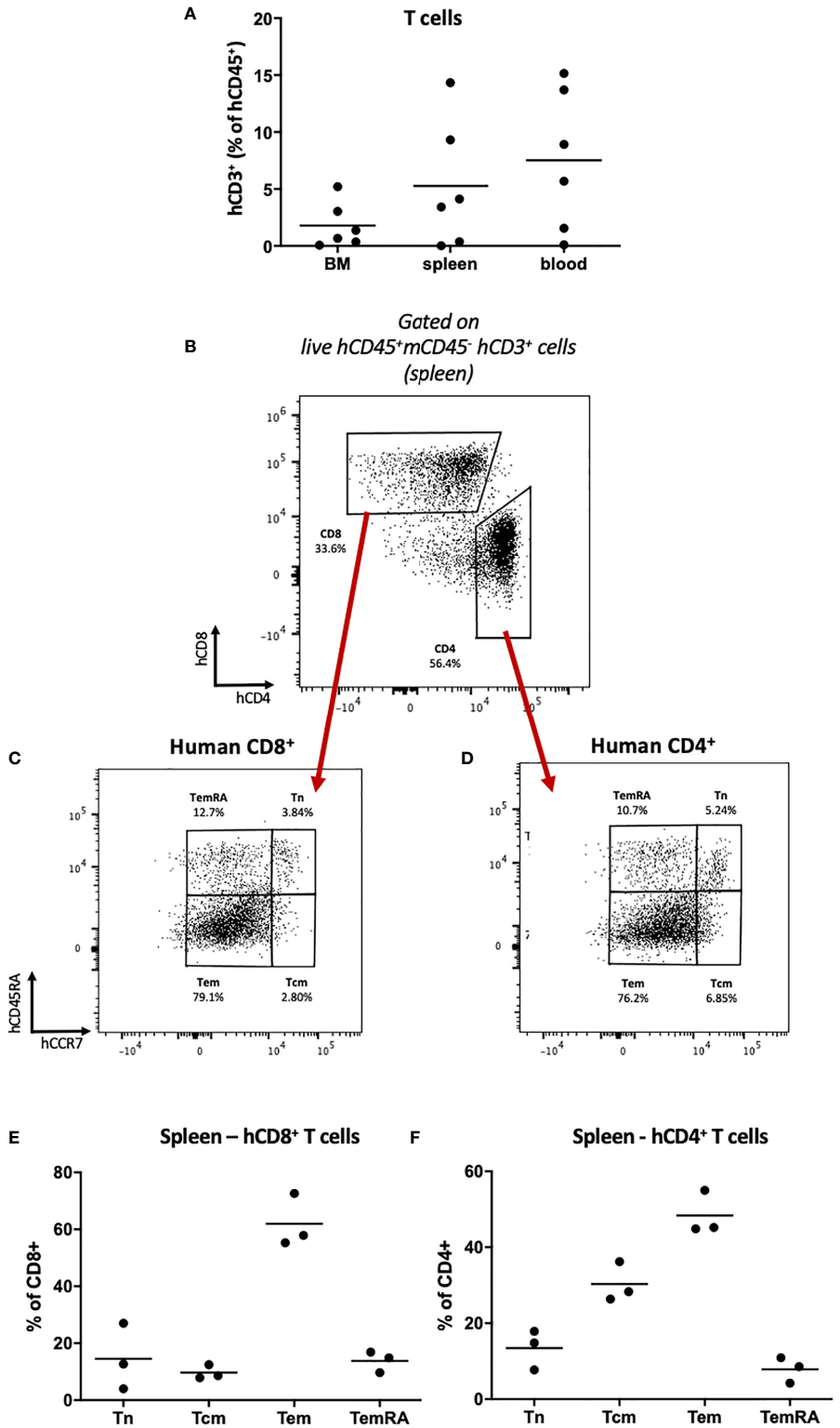

FIGURE 4 | Human T cell repopulation in HSPC-NBSGW mice **(A)** Frequencies of human CD3$^+$ T cells in the bone marrow, spleen and blood of HSPC-NBSGW mice 20-22 weeks after cell injection, as determined by flow cytometry (50x10^3 HSPC dose shown). **(B–D)** Representative flow cytometric analysis of **(B)** CD4 and CD8 expression on live human CD45$^+$CD3$^+$ splenic T cells, **(C)** CD8$^+$ and **(D)** CD4$^+$ T cell subsets, determined by surface expression of CD45RA and CCR7. **(E, F)** Frequencies of CD8$^+$ **(D)** and CD4$^+$ **(E)** splenic T cell subsets: naïve (Tn; hCD45RA$^+$hCCR7$^+$), Tcm (hCD45RA$^-$hCCR7$^+$), Tem (hCD45RA$^-$hCCR7$^-$) and TemRA (hCD45RA$^+$hCCR7$^-$) (250x10^3 HSPC dose shown). Bars indicate median values.

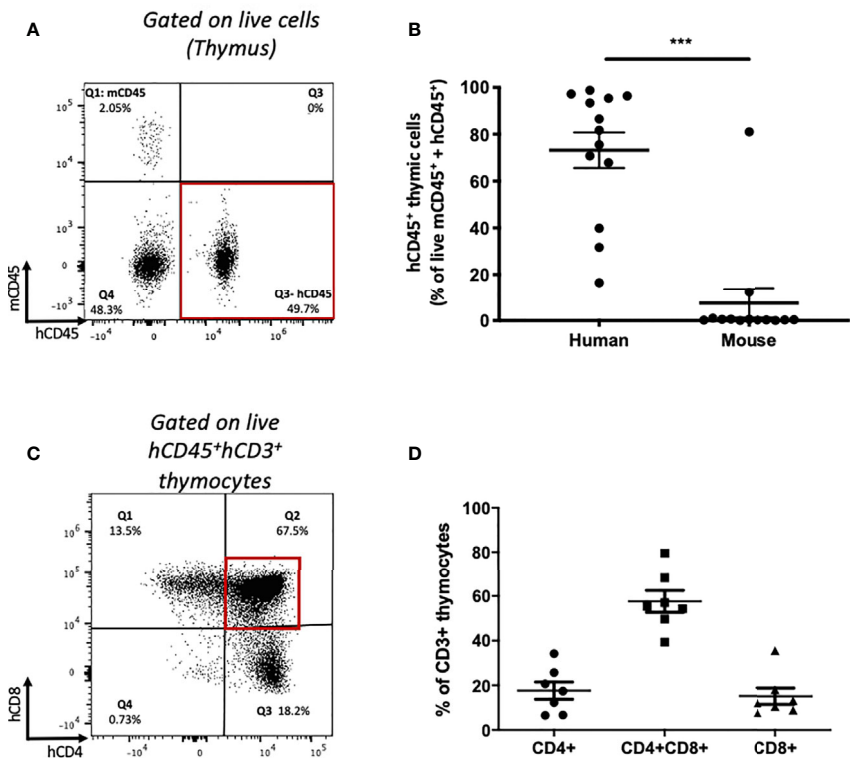

FIGURE 5 | Thymic human leucocyte engraftment and development of human thymocytes in HSPC-NBSGW mice. **(A)** Representative flow cytometric plot and **(B)** corresponding frequencies of human and mouse CD45$^+$ cells (as percentage of mCD45 + hCD45 cells) in the thymi of HSPC-NBSGW mice 20-22 weeks after cell injection (50x10^3 dose shown). **(C)** Representative flow cytometric analysis and **(D)** corresponding frequencies of single-positive CD4$^+$, CD8$^+$ and double-positive CD4$^+$CD8$^+$ human thymocytes. Bars represent the mean ± SEM. Statistical significance was assessed using paired t tests (***p<0.001).

Phagocytosis-Dependent Impairment in Peripheral Engraftment of Human Erythrocytes

Next we investigated engraftment of erythrocytes. In HSPC-NBSGW mice, Glycophorin A analysis (CD235a) demonstrated dose-dependent engraftment of erythroid cells within the bone marrow, however only a small, transient population of RBCs were found in the peripheral blood (**Figures 7A, B**, **Supplementary Figure 6A**). To determine whether absence from the periphery results from defective erythroid lineage differentiation, we assessed erythroid cell maturity in the bone marrow (**Figures 7C–F**). In addition to a small population of mature erythrocytes (**Figures 7C, D**; **Supplementary Figure 6A**), dose-dependent frequencies of erythroid precursors at various stages of development were identified, with no significant discrepancies noted between male and female mice (**Figures 7E, F**; **Supplementary Figures 6B–D**). To identify whether the lack of peripheral reconstitution results instead from phagocytosis of human erythroid cells by mouse phagocytes, we assessed survival following phagocyte depletion (**Figures 8A–G**). Using a previously reported technique (27), clodronate liposomes (CloLip) were injected intravenously 11 weeks after humanization, successfully reducing the frequencies of monocytes in the peripheral blood (**Figure 8A**). This was associated with increased numbers of mature erythrocytes in the blood (168-fold compared with control; 335 ± 237 vs 2 ± 1.6 per µl of blood) (**Figures 8B–D**), suggesting that phagocytosis contributes at least in part to the impaired reconstitution of human erythroid cells in this model. While there was no significant difference in the frequencies of early erythroid precursors in the bone marrow following phagocyte clearance, as expected, an increase in reticulocytes and mature erythrocytes was seen (19% (16-27.7%) vs 31.5% (5.2-36.9%) as median (with range), p<0.05) (**Figures 8E–G**).

DISCUSSION

Here we show robust long-term multilineage reconstitution of human hematopoeitic cells in NBSGW mice. We also show that the numbers of circulating RBCs can be increased in NBSGW mice following mouse macrophage clearance, enhancing the capacity to study disorders of human erythropoiesis in the context of complete human lymphoid development.

For optimal human HSC engraftment, there must be a permissive bone marrow niche in favor of human

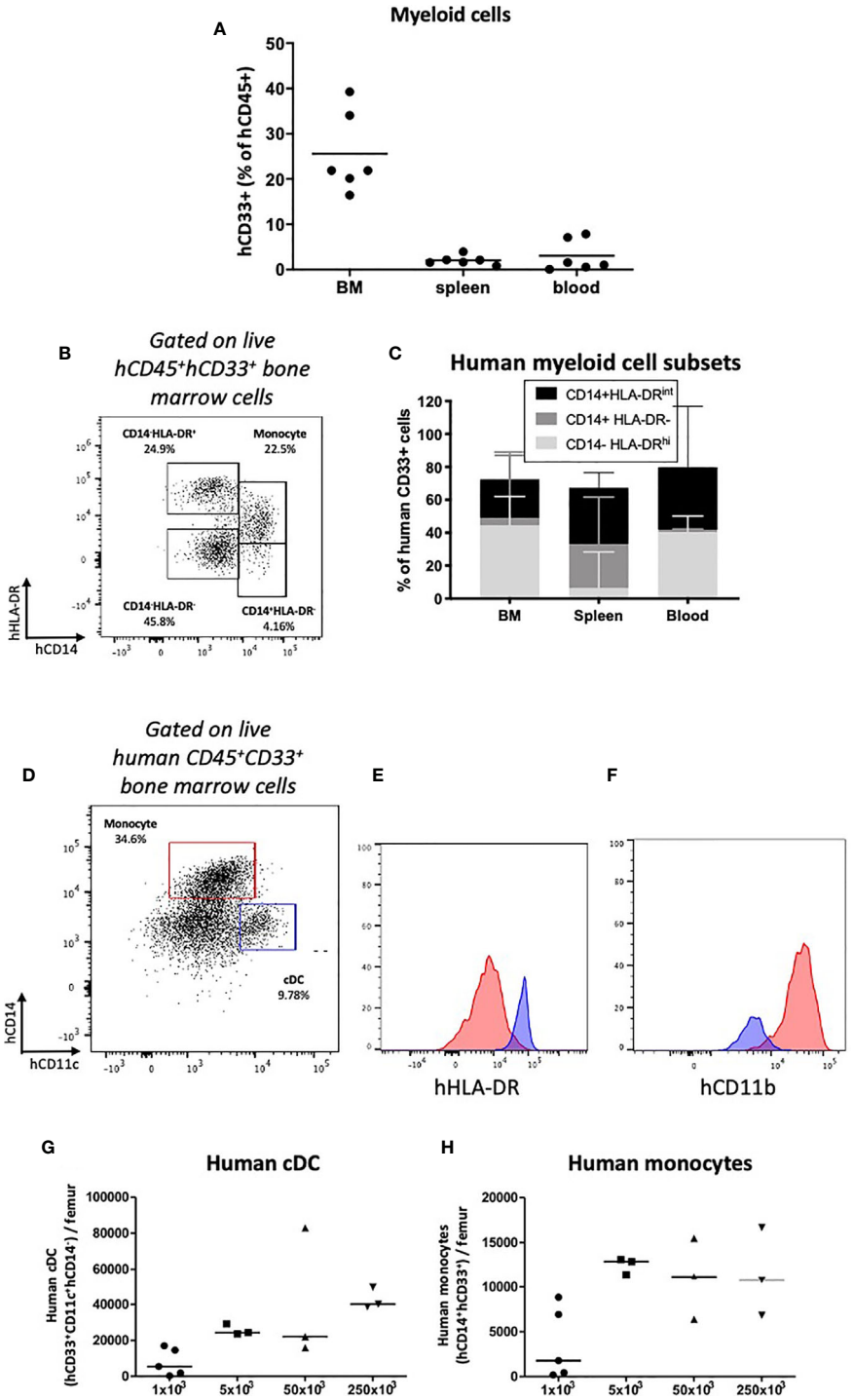

FIGURE 6 | Human myeloid cell engraftment in HSPC-NBSGW mice. **(A)** Frequencies of human CD33$^+$ myeloid cells in the bone marrow, spleen and peripheral blood of HSPC-NBSGW mice 20-22 weeks after cell injection. **(B)** Representative flow cytometric plot and **(C)** corresponding frequencies of myeloid subsets based on CD14 and HLA-DR expression. **(D)** Representative flow cytometry plot and **(E, F)** corresponding histograms demonstrating human conventional dendritic cells (cDCs) (blue; hCD11c$^+$hCD14$^-$hCD33$^+$) and human monocytes/macrophages (red; hCD14$^+$hCD33$^+$) in the bone marrow of HSPC-NBSGW mice (50x10^3 dose shown). Histograms demonstrate high HLA-DR expression and low CD11b expression in cDCs (blue histograms) as compared with monocytes (red histograms). **(G)** Numbers of human cDCs (hCD11c+hCD14-hCD33+) **(H)** and human monocytes/macrophages (hCD14$^+$hCD33$^+$) in the bone marrow of one femur in mice receiving different numbers of hUCB CD133$^+$ HSPCs. Bars indicate median values **(A, G, H)** and median + IQR **(C)**.

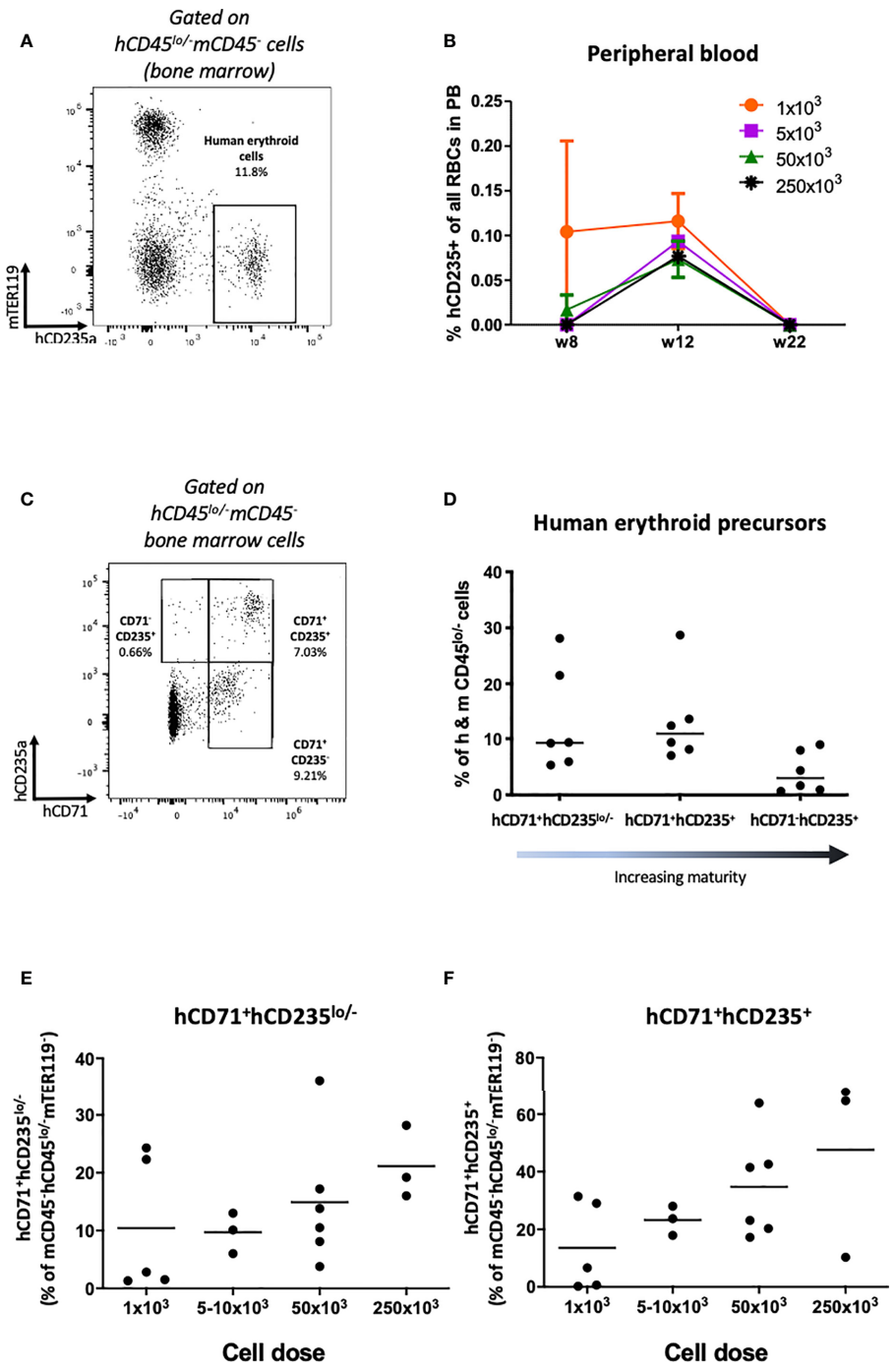

FIGURE 7 | Human erythrocyte reconstitution in HSPC-NBSGW mice. **(A)** Representative flow cytometric analysis demonstrating the identification of hCD45$^{lo/-}$mCD45^{-}hCD235a^{+}mTER119^{-} human erythroid cells in the bone marrow. **(B)** Frequency of hCD235^{+} cells in the peripheral blood at different time points following injection with increasing numbers of hUCB CD133^{+} HSPCs (mean ± SD shown). **(C)** Representative flow cytometric analysis and **(D)** corresponding frequencies of hCD71^{+}hCD235$^{lo/-}$, hCD71^{+}hCD235^{+} and hCD71^{-}hCD235^{+} erythroid precursors (in ascending order of maturity) in the bone marrow (BM) 20-22 weeks after humanization (50x10^{3} dose shown). **(E)** Frequency of hCD71^{+}hCD235$^{-/lo}$ and **(F)** hCD71^{+}hCD235^{+} erythroid precursors in the bone marrow (BM) following humanization with increasing numbers of hUCB CD133^{+} HSPCs. Red symbols – female mice, blue symbols – male mice. Bars indicate median values.

hematopoiesis. This has been achieved through 1) mutation of critical murine growth factor receptors such as the c-kit receptor (W41/Wv alleles) in NSGW41, NSGWv/+, NSGWv, NBSGW, SRG-W41 and BRgWv mice, 2) direct treatment with an anti-c-Kit receptor antibody, 3) provision of exogenous human cytokines, 4) knock-in of human cytokine genes (e.g. SCF,

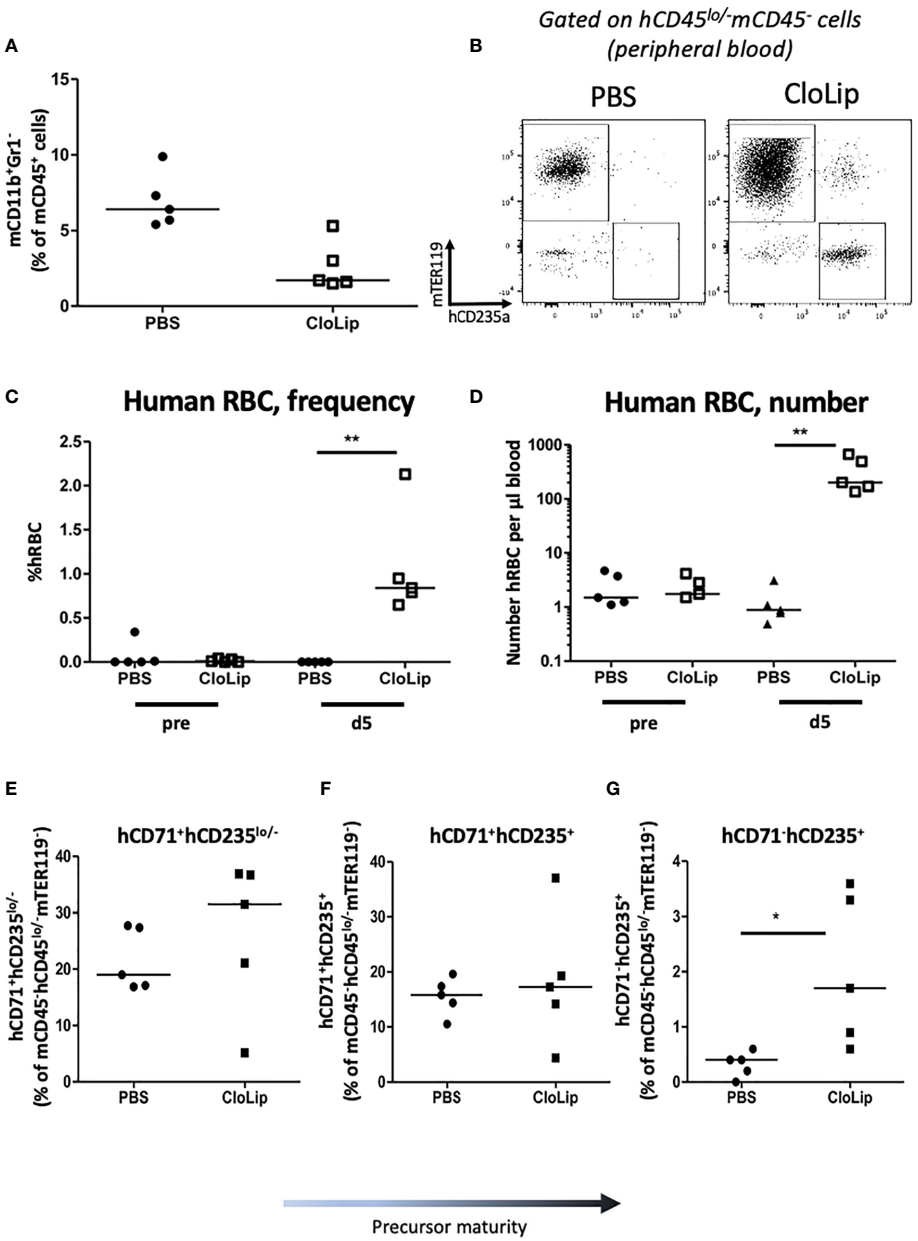

FIGURE 8 | Effect of murine phagocyte clearance on human erythrocyte reconstitution HSPC-NBSGW mice. **(A–G)** HSPC-NBSGW mice injected with $50x10^3$ hUCB $CD34^+$ cells 11 weeks earlier were injected with clodronate liposomes (CloLip) or PBS (control) and analyzed over 6 days. **(A)** Frequency of mouse $CD11b^+Gr1^-$ cells in the blood 5 days after clodronate liposome (CloLip) treatment. **(B)** Representative flow cytometric analysis of human $CD235^+$ RBCs in the blood 5 days after CloLip treatment. **(C)** frequency and **(D)** absolute number of human RBCs ($hCD235^+$) in the peripheral blood 5 days after CloLip treatment. **(E)** Frequencies of $hCD71^+hCD235^{-/lo}$, **(F)** $hCD71^+hCD235^+$ and **(G)** $hCD71^-hCD235^+$ in the bone marrow (BM) 6 days after CloLip/PBS treatment. Symbols represent individual mice. Bars represent median values **(A)**–**(C–G)**; Statistical significance was assessed using the Mann Whitney test (*$p<0.05$, **$p<0.01$).

TPO, GM-CSF, M-CSF, IL-3 in NSG-SGM3/NSGS, MSTRG and MISTRG mice) (4, 5, 8, 36, 38–43), and 5) transplant of hematopoietic niches (e.g. human mesenchymal stromal cells, or thymus) with or without expression of human cytokine transgenes [e.g. NSG-SGM3-BLT mice (44)]. NSGW41, BRgWv, NBSGW and SRG-W41 mice are reported to show robust human HSPC engraftment in the absence of irradiation and this is coupled with improved human bone marrow erythropoiesis compared to irradiated NSG mice (4, 36, 38–40, 43–45). Our results extend these and our own previous findings (29) by demonstrating consistent engraftment and human leucocyte reconstitution following intravenous transplantation of as few as $10x10^3$ $CD133^+$ HSPCs in adult nonirradiated NBSGW recipients over the extended period of 20-22 weeks,

regardless of sex and without the requirement to co-transplant other human hematopoietic niche tissues. To our knowledge this is the lowest hUCB HSPC dose reported to achieve such high BM (75.5%), splenic (73.5%) and peripheral blood (29%) engraftment at this late a time point. It is also notable, that in this model, leucocyte subset reconstitution approximated more closely to human peripheral blood populations (46) than previously described in humanized NBSGW mice (5). The capacity to achieve robust reconstitution in adult mice is particularly attractive due to the ease of intravenous injection compared with neonates and the potential simplicity of injecting fresh cells, with the flexibility of not requiring timed breeding.

Importantly, we have also demonstrated that development and maturation of human lymphocytes and myeloid cells occurs within this model, producing a humanized mouse that represents a more complete human immune system. Reconstitution of both T and B lymphocytes is important for studies of vaccination and infection immunity, enabling incorporation of humoral and cellular components of the human immune system. Additionally, as effective antibody class switching is dependent on T cell help, humanized mice supporting robust T and B cell reconstitution can allow studies on the development of protective humoral immunity in various infectious diseases.

hUCB HSPC-humanized mice typically support engraftment of human B cells at high frequencies (47). In several models, these develop quite normally in the bone marrow yet demonstrate features of developmental block (48), manifesting defective peripheral maturation and humoral responses (1, 49). We have demonstrated development of a large population of mature B cells in the spleens and peripheral blood of HSPC-NBSGW mice. Since only mature B cells are capable of carrying out effective antigen presentation and effector function, this is likely to be a distinguishing feature of this model. We further demonstrate the frequency of class-switched memory B cells to increase following exposure to allogeneic human skin transplants. This feature suggests the functional capacity for HSPC-NBSGW B cells to respond to an immune challenge and may represent an important step in fields such as transplantation research, where improvements enhanced human T- and B function may enable more accurate reflections of human alloresponses. As the detrimental effects of donor-specific antibodies and the tolerogenic effects of regulatory B cells are increasingly becoming focal points of attention in transplantation, models such as this may add functional humoral immunity to the predominantly T cell biased PBMC-based humanized models.

The re-creation of cellular immune responses is a fundamental requirement of HIS mice. Following humanization with $CD133^+$ hUCB HSPCs, we demonstrate peripheral reconstitution of the T cell subsets in proportions that more accurately reflect the human blood profile than can be achieved following humanization with PBMCs. It should be noted, that while PBMC-driven HIS models have been very useful in studying T cell-driven immune responses (50), cellular therapies (51) and biologics (52), disproportionately large T cell reconstitution in HIS mice generated using PBMCs (particularly Tem cells) risks the development of xenogeneic GvHD and underrepresentation of the global immunological complexity.

Within the thymus we identified a humanized thymic cell microenvironment with a sizeable fraction of $CD4^+CD8^+$ (Double positive, DP) human thymocytes, similar to that seen in thymus biopsies from human infants (36). Identification of T cells in the peripheral blood only after 12 weeks in the earliest instances, suggests *de novo* T cell development rather than proliferation of transplanted mature hUCB MNCs.

In our experience, engraftment of $50x10^3$ human HSPCs produces rapid, robust and reliable reconstitution, supporting utility of this dose for a broad range of *in vivo* experiments. A recognized shortcoming of utilising human cord blood in mouse experiments - which we also experienced - is the limited number of mice that can be engrafted from a single UCB unit when high numbers of HSPCs are used per mouse. It is our view that experimental biases that result from low numbers of donor replicates may be overcome if more mice can be robustly engrafted (i.e. >20% peripheral blood chimerism) using smaller UCB fractions (i.e. <50x103 HSPCs). We show that this is possible and feel that where investigators may find benefit in expanding the utility of a single UCB unit, a longer period of engraftment may be an acceptable compromise, particularly considering the reported longevity of humanized NBSGW mice (survival ≥ 36 weeks post-humanization (6)).

As efforts continue to broaden the use of humanized small animal models for the *in vivo* study of human hematopoiesis, immunology, cancer and infection, technically uncomplicated models achieving ever-closer functional human hematopoiesis such as the one reported here represent an important practical next step.

DATA AVAILABILITY STATEMENT

The raw data supporting the conclusions of this article will be made available by the authors, without undue reservation.

ETHICS STATEMENT

hUCB was collected from the John Radcliffe Hospital, Oxford, UK or provided *via* the NHS Cord Blood Bank, London and used with informed, written pre-consent and ethical approval from the South Central Oxford C and Berkshire Ethical Committees (# 15/SC/0027) and the Oxfordshire Research Ethics Committee B (#07/H0605/130), in accordance with the Helsinki Declaration of 1975, as revised in 2008. Written informed consent to participate in this study was provided by the participants' legal guardian/next of kin. All mouse experiments were performed using protocols approved by the Committee on Animal Care and Ethical Review at the University of Oxford and in accordance with the UK

Animals (Scientific Procedures) Act 1986 and under PPL number P8869535A.

AUTHOR CONTRIBUTIONS

GA: conception and design, collection and assembly of data, data analysis and interpretation, manuscript writing, and final approval of manuscript. PH: conception and design, collection and/or assembly of data, data analysis and interpretation, manuscript writing, and final approval of manuscript. MU: collection and assembly of data, manuscript writing, and final approval of manuscript. IR: conception and design, financial support, data analysis and interpretation, and final approval of manuscript. JH: conception and design, collection and assembly of data, data analysis and interpretation, financial support, manuscript writing, and final approval of manuscript. SW: conception and design, financial support, data analysis and interpretation, manuscript writing, and final approval of manuscript. FI: conception and design, financial support, collection and assembly of data, data analysis and interpretation, manuscript writing, and final approval of manuscript. All authors contributed to the article and approved the submitted version.

FUNDING

MRC Discovery Award: Weatherall Institute of Molecular Medicine grant no. MC_PC_15069 (lead investigator: Professor D. Higgs). Kidney Research UK Senior Fellowship (JH) (SF1/2014), Wellcome Trust CRCD Fellowship (FI) Clarendon Scholarship (GA).

ACKNOWLEDGMENTS

We would like to thank Professor Doug Higgs and members of the Weatherall Institute of Molecular Medicine, the Radcliffe Department of Medicine and the Nuffield Department of Surgery for their support.

SUPPLEMENTARY MATERIAL

The Supplementary Material for this article can be found online at: https://www.frontiersin.org/articles/10.3389/fimmu.2021.642198/full#supplementary-material

REFERENCES

1. Shultz LD, Ishikawa F, Greiner DL. Humanized mice in translational biomedical research. *Nat Rev Immunol* (2007) 7(2):118–30. doi: 10.1038/nri2017
2. Qing Y, Lin Y, Gerson SL. An intrinsic BM hematopoietic niche occupancy defect of HSC in scid mice facilitates exogenous HSC engraftment. *Blood* (2012) 119(7):1768–71. doi: 10.1182/blood-2011-05-350611
3. Shultz LD, Lyons BL, Burzenski LM, Gott B, Chen X, Chaleff S, et al. Human lymphoid and myeloid cell development in NOD/LtSz-scid IL2Rγnull mice engrafted with mobilized human hemopoietic stem cells. *J Immunol* (2005) 174(10):6477–89. doi: 10.4049/jimmunol.174.10.6477
4. McDermott SP, Eppert K, Lechman ER, Doedens M, Dick JE. Comparison of human cord blood engraftment between immunocompromised mouse strains. *Blood* (2010) 116(2):193–200. doi: 10.1182/blood-2010-02-271841
5. McIntosh BE, Brown ME, Duffin BM, Maufort JP, Vereide DT, Slukvin II, et al. B6.SCID Il2rgamma-/- Kit(W41/W41) (NBSGW) mice support multilineage engraftment of human hematopoietic cells. *Stem Cell Rep* (2015) 4(2):171–80. doi: 10.1016/j.stemcr.2014.12.005
6. Hess NJ, Lindner PN, Vazquez J, Grindel S, Hudson AW, Stanic AK, et al. Different Human Immune Lineage Compositions Are Generated in Non-Conditioned NBSGW Mice Depending on HSPC Source. *Front Immunol* (2020) 11(2701):1–11. doi: 10.3389/fimmu.2020.573406
7. Dessels C, Alessandrini M, Pepper MS. Factors Influencing the Umbilical Cord Blood Stem Cell Industry: An Evolving Treatment Landscape. *Stem Cells Trans Med* (2018) 7(9):643–50. doi: 10.1002/sctm.17-0244
8. Fiorini C, Abdulhay NJ, McFarland SK, Munschauer M, Ulirsch JC, Chiarle R, et al. Developmentally-faithful and effective human erythropoiesis in immunodeficient and Kit mutant mice. *Am J Hematol* (2017) 92(9):E513–e9. doi: 10.1002/ajh.24805
9. McGuckin CP, Pearce D, Forraz N, Tooze JA, Watt SM, Pettengell R. Multiparametric analysis of immature cell populations in umbilical cord blood and bone marrow. *Eur J Haematol* (2003) 71(5):341–50. doi: 10.1034/j.1600-0609.2003.00153.x
10. Miraglia S, Godfrey W, Yin AH, Atkins K, Warnke R, Holden JT, et al. A novel five-transmembrane hematopoietic stem cell antigen: isolation, characterization, and molecular cloning. *Blood* (1997) 90(12):5013–21. doi: 10.1182/blood.V90.12.5013.5013_5013_5021
11. Yin AH, Miraglia S, Zanjani ED, Almeida-Porada G, Ogawa M, Leary AG, et al. AC133, a novel marker for human hematopoietic stem and progenitor cells. *Blood* (1997) 90(12):5002–12. doi: 10.1182/blood.V90.12.5002.5002_5002_5012
12. Gallacher L, Murdoch B, Wu DM, Karanu FN, Keeney M, Bhatia M. Isolation and characterization of human CD34(-)Lin(-) and CD34(+)Lin(-) hematopoietic stem cells using cell surface markers AC133 and CD7. *Blood* (2000) 95(9):2813–20. doi: 10.1182/blood.V95.9.2813.009k20_2813_2820
13. Sumide K, Matsuoka Y, Kawamura H, Nakatsuka R, Fujioka T, Asano H, et al. A revised road map for the commitment of human cord blood CD34-negative hematopoietic stem cells. *Nat Commun* (2018) 9(1):2202. doi: 10.1038/s41467-018-04441-z
14. Matsuoka Y, Nakamura F, Hatanaka K, Fujioka T, Otani S, Kimura T, et al. The number of CD34(+)CD133(+) hematopoietic stem cells residing in umbilical cord blood (UCB) units is not correlated with the numbers of total nucleated cells and CD34(+) cells: a possible new indicator for quality evaluation of UCB units. *Int J Hematol* (2018) 108(6):571–9. doi: 10.1007/s12185-018-2502-7
15. Takahashi M, Matsuoka Y, Sumide K, Nakatsuka R, Fujioka T, Kohno H, et al. CD133 is a positive marker for a distinct class of primitive human cord blood-derived CD34-negative hematopoietic stem cells. *Leukemia* (2014) 28(6):1308–15. doi: 10.1038/leu.2013.326
16. Issa F, Hester J, Goto R, Nadig SN, Goodacre TE, Wood K. Ex vivo-expanded human regulatory T cells prevent the rejection of skin allografts in a humanized mouse model. *Transplantation* (2010) 90(12):1321–7. doi: 10.1097/TP.0b013e3181ff8772
17. Vuyyuru R, Patton J, Manser T. Human immune system mice: current potential and limitations for translational research on human antibody responses. *Immunol Res* (2011) 51(2-3):257–66. doi: 10.1007/s12026-011-8243-9
18. Manz MG. Human-hemato-lymphoid-system mice: opportunities and challenges. *Immunity* (2007) 26(5):537–41. doi: 10.1016/j.immuni.2007.05.001
19. Gimeno R, Weijer K, Voordouw A, Uittenbogaart CH, Legrand N, Alves NL, et al. Monitoring the effect of gene silencing by RNA interference in human CD34+ cells injected into newborn RAG2-/-γc-/-mice: functional inactivation of p53 in developing T cells. *Blood* (2004) 104(13):3886–93. doi: 10.1182/blood-2004-02-0656

20. Ishikawa F, Yasukawa M, Lyons B, Yoshida S, Miyamoto T, Yoshimoto G, et al. Development of functional human blood and immune systems in NOD/SCID/IL2 receptor {gamma} chain(null) mice. *Blood* (2005) 106(5):1565–73. doi: 10.1182/blood-2005-02-0516
21. Traggiai E, Chicha L, Mazzucchelli L, Bronz L, Piffaretti J-C, Lanzavecchia A, et al. Development of a human adaptive immune system in cord blood cell-transplanted mice. *Science* (2004) 304(5667):104–7. doi: 10.1126/science.1093933
22. Adigbli G, Ménoret S, Cross AR, Hester J, Issa F, Anegon I. Humanization of Immunodeficient Animals for the Modeling of Transplantation, Graft Versus Host Disease and Regenerative Medicine. *Transplantation* (2020) 104 (11):2290–306. doi: 10.1097/TP.0000000000003177
23. Tarunina M, Hernandez D, Kronsteiner-Dobramysl B, Pratt P, Watson T, Hua P, et al. A Novel High-Throughput Screening Platform Reveals an Optimized Cytokine Formulation for Human Hematopoietic Progenitor Cell Expansion. *Stem Cells Dev* (2016) 25(22):1709–20. doi: 10.1089/scd.2016.0216
24. Chang CH, Hale SJ, Cox CV, Blair A, Kronsteiner B, Grabowska R, et al. Junctional adhesion molecule-A is highly expressed on human hematopoietic repopulating cells and associates with the key hematopoietic chemokine receptor CXCR4. *Stem Cells* (2016) 34(6):1664–78. doi: 10.1002/stem.2340
25. Ito M, Hiramatsu H, Kobayashi K, Suzue K, Kawahata M, Hioki K, et al. NOD/SCID/gamma(c)(null) mouse: an excellent recipient mouse model for engraftment of human cells. *Blood* (2002) 100(9):3175–82. doi: 10.1182/blood-2001-12-0207
26. Issa F, Hester J, Milward K, Wood KJ. Homing of regulatory T cells to human skin is important for the prevention of alloimmune-mediated pathology in an in vivo cellular therapy model. *PloS One* (2012) 7(12):e53331. doi: 10.1371/journal.pone.0053331
27. Hu Z, Van Rooijen N, Yang Y-G. Macrophages prevent human red blood cell reconstitution in immunodeficient mice. *Blood* (2011) 118(22):5938–46. doi: 10.1182/blood-2010-11-321414
28. Wunderlich M, Chou F-S, Sexton C, Presicce P, Chougnet CA, Aliberti J, et al. Improved multilineage human hematopoietic reconstitution and function in NSGS mice. *PloS One* (2018) 13(12):e0209034–e. doi: 10.1371/journal.pone.0209034
29. Hua P, Hester J, Adigbli G, Li R, Psaila B, Roy A, et al. The BET inhibitor CPI203 promotes ex vivo expansion of cord blood long-term repopulating HSCs and megakaryocytes. *Blood* (2020) 136(21):2410–5. doi: 10.1182/blood.2020005357
30. Ichii M, Oritani K, Yokota T, Zhang Q, Garrett KP, Kanakura Y, et al. The density of CD10 corresponds to commitment and progression in the human B lymphoid lineage. *PloS One* (2010) 5(9):e12954. doi: 10.1371/journal.pone.0012954
31. Agematsu K, Nagumo H, Yang FC, Nakazawa T, Fukushima K, Ito S, et al. B cell subpopulations separated by CD27 and crucial collaboration of CD27+ B cells and helper T cells in immunoglobulin production. *Eur J Immunol* (1997) 27(8):2073–9. doi: 10.1002/eji.1830270835
32. Loder F, Mutschler B, Ray RJ, Paige CJ, Sideras P, Torres R, et al. B cell development in the spleen takes place in discrete steps and is determined by the quality of B cell receptor-derived signals. *J Exp Med* (1999) 190(1):75–89. doi: 10.1084/jem.190.1.75
33. Sanz I, Wei C, Jenks SA, Cashman KS, Tipton C, Woodruff MC, et al. Challenges and Opportunities for Consistent Classification of Human B Cell and Plasma Cell Populations. *Front Immunol* (2019) 10(2458):1–17. doi: 10.3389/fimmu.2019.02458
34. Wu Y-CB, Kipling D, Dunn-Walters DK. The relationship between CD27 negative and positive B cell populations in human peripheral blood. *Front Immunol* (2011) 2:81–. doi: 10.3389/fimmu.2011.00081
35. Stavnezer J, Guikema JEJ, Schrader CE. Mechanism and regulation of class switch recombination. *Annu Rev Immunol* (2008) 26:261–92. doi: 10.1146/annurev.immunol.26.021607.090248
36. Cosgun KN, Rahmig S, Mende N, Reinke S, Hauber I, Schafer C, et al. Kit regulates HSC engraftment across the human-mouse species barrier. *Cell Stem Cell* (2014) 15(2):227–38. doi: 10.1016/j.stem.2014.06.001
37. Zhang J, Supakorndej T, Krambs JR, Rao M, Abou-Ezzi G, Ye RY, et al. Bone marrow dendritic cells regulate hematopoietic stem/progenitor cell trafficking. *J Clin Invest* (2019) 129(7):2920–31. doi: 10.1172/JCI124829
38. Theocharides APA, Rongvaux A, Fritsch K, Flavell RA, Manz MG. Humanized hemato-lymphoid system mice. *Haematologica* (2016) 101 (1):5–19. doi: 10.3324/haematol.2014.115212
39. Brehm MA, Cuthbert A, Yang C, Miller DM, DiIorio P, Laning J, et al. Parameters for establishing humanized mouse models to study human immunity: analysis of human hematopoietic stem cell engraftment in three immunodeficient strains of mice bearing the IL2rgamma(null) mutation. *Clin Immunol (Orlando Fla)* (2010) 135(1):84–98. doi: 10.1016/j.clim.2009.12.008
40. Chen B, Fan W, Zou J, Zhang S, He J, Shu C, et al. Complement Depletion Improves Human Red Blood Cell Reconstitution in Immunodeficient Mice. *Stem Cell Rep* (2017) 9(4):1034–42. doi: 10.1016/j.stemcr.2017.08.018
41. Schmidt MR, Appel MC, Giassi LJ, Greiner DL, Shultz LD, Woodland RT. Human BLyS facilitates engraftment of human PBL derived B cells in immunodeficient mice. *PloS One* (2008) 3(9):e3192. doi: 10.1371/journal.pone.0003192
42. Rahmig S, Kronstein-Wiedemann R, Fohgrub J, Kronstein N, Nevmerzhitskaya A, Bornhauser M, et al. Improved Human Erythropoiesis and Platelet Formation in Humanized NSGW41 Mice. *Stem Cell Rep* (2016) 7 (4):591–601. doi: 10.1016/j.stemcr.2016.08.005
43. Miller PH, Rabu G, MacAldaz M, Knapp DJ, Cheung AM, Dhillon K, et al. Analysis of parameters that affect human hematopoietic cell outputs in mutant c-kit-immunodeficient mice. *Exp Hematol* (2017) 48:41–9. doi: 10.1016/j.exphem.2016.12.012
44. Jangalwe S, Shultz LD, Mathew A, Brehm MA. Improved B cell development in humanized NOD-scid IL2Rγ(null) mice transgenically expressing human stem cell factor, granulocyte-macrophage colony-stimulating factor and interleukin-3. *Immun Inflammation Dis* (2016) 4(4):427–40. doi: 10.1002/iid3.124
45. Lan P, Tonomura N, Shimizu A, Wang S, Yang YG. Reconstitution of a functional human immune system in immunodeficient mice through combined human fetal thymus/liver and CD34+ cell transplantation. *Blood* (2006) 108(2):487–92. doi: 10.1182/blood-2005-11-4388
46. Rongvaux A, Takizawa H, Strowig T, Willinger T, Eynon EE, Flavell RA, et al. Human hemato-lymphoid system mice: current use and future potential for medicine. *Annu Rev Immunol* (2013) 31:635–74. doi: 10.1146/annurev-immunol-032712-095921
47. Brehm MA, Shultz LD, Greiner DL. Humanized mouse models to study human diseases. *Curr Opin Endocrinol Diabetes Obes* (2010) 17(2):120–5. doi: 10.1097/MED.0b013e328337282f
48. Watanabe Y, Takahashi T, Okajima A, Shiokawa M, Ishii N, Katano I, et al. The analysis of the functions of human B and T cells in humanized NOD/shi-scid/gammac(null) (NOG) mice (hu-HSC NOG mice). *Int Immunol* (2009) 21 (7):843–58. doi: 10.1093/intimm/dxp050
49. Lang J, Ota T, Kelly M, Strauch P, Freed BM, Torres RM, et al. Receptor editing and genetic variability in human autoreactive B cells. *J Exp Med* (2016) 213(1):93–108. doi: 10.1084/jem.20151039
50. Nadig SN, Więckiewicz J, Wu DC, Warnecke G, Zhang W, Luo S, et al. In vivo prevention of transplant arteriosclerosis by ex vivo-expanded human regulatory T cells. *Nat Med* (2010) 16(7):809–13. doi: 10.1038/nm.2154
51. Issa F, Milward K, Goto R, Betts G, Wood KJ, Hester J. Transiently Activated Human Regulatory T Cells Upregulate BCL-XL Expression and Acquire a Functional Advantage in vivo. *Front Immunol* (2019) 10:889. doi: 10.3389/fimmu.2019.00889
52. Zaitsu M, Issa F, Hester J, Vanhove B, Wood KJ. Selective blockade of CD28 on human T cells facilitates regulation of alloimmune responses. *JCI Insight* (2017) 2(19). doi: 10.1172/jci.insight.89381

Conflict of Interest: The authors declare that the research was conducted in the absence of any commercial or financial relationships that could be construed as a potential conflict of interest.

Copyright © 2021 Adigbli, Hua, Uchiyama, Roberts, Hester, Watt and Issa. This is an open-access article distributed under the terms of the Creative Commons Attribution License (CC BY). The use, distribution or reproduction in other forums is permitted, provided the original author(s) and the copyright owner(s) are credited and that the original publication in this journal is cited, in accordance with accepted academic practice. No use, distribution or reproduction is permitted which does not comply with these terms.

frontiers in Immunology

METHODS
published: 29 March 2021
doi: 10.3389/fimmu.2021.607282

OPEN ACCESS

Edited by:
Alexandre P.A. Theocharides, University Hospital Zürich, Switzerland

Reviewed by:
Heinz Laubli, University Hospital of Basel, Switzerland
Sheng Guo, Crown Bioscience, China

***Correspondence:**
Julie Lang
Julie.lang@cuanschutz.edu

†Present Address:
Jing H. Wang, UPMC Hillman Cancer Center, Department of Medicine, School of Medicine, University of Pittsburgh, Pittsburgh, PA, United States

Specialty section:
This article was submitted to Cancer Immunity and Immunotherapy, a section of the journal Frontiers in Immunology

Received: 16 September 2020
Accepted: 04 March 2021
Published: 29 March 2021

Citation:
Marín-Jiménez JA, Capasso A, Lewis MS, Bagby SM, Hartman SJ, Shulman J, Navarro NM, Yu H, Rivard CJ, Wang X, Barkow JC, Geng D, Kar A, Yingst A, Tufa DM, Dolan JT, Blatchford PJ, Freed BM, Torres RM, Davila E, Slansky JE, Pelanda R, Eckhardt SG, Messersmith WA, Diamond JR, Lieu CH, Verneris MR, Wang JH, Kiseljak-Vassiliades K, Pitts TM and Lang J (2021) Testing Cancer Immunotherapy in a Human Immune System Mouse Model: Correlating Treatment Responses to Human Chimerism, Therapeutic Variables and Immune Cell Phenotypes. Front. Immunol. 12:607282. doi: 10.3389/fimmu.2021.607282

Testing Cancer Immunotherapy in a Human Immune System Mouse Model: Correlating Treatment Responses to Human Chimerism, Therapeutic Variables and Immune Cell Phenotypes

Juan A. Marín-Jiménez[1], Anna Capasso[2], Matthew S. Lewis[3], Stacey M. Bagby[4], Sarah J. Hartman[4], Jeremy Shulman[3], Natalie M. Navarro[4], Hui Yu[4,5], Chris J. Rivard[4,5], Xiaoguang Wang[3], Jessica C. Barkow[3], Degui Geng[4], Adwitiya Kar[6], Ashley Yingst[7], Dejene M. Tufa[7], James T. Dolan[8], Patrick J. Blatchford[9], Brian M. Freed[3,10], Raul M. Torres[3,5], Eduardo Davila[4,5], Jill E. Slansky[3,5], Roberta Pelanda[3,5], S. Gail Eckhardt[2], Wells A. Messersmith[4,5], Jennifer R. Diamond[4,5], Christopher H. Lieu[4], Michael R. Verneris[7], Jing H. Wang[3,5†], Katja Kiseljak-Vassiliades[5,6], Todd M. Pitts[4,5] and Julie Lang[3]*

[1] Department of Medical Oncology, Catalan Institute of Oncology (ICO-L'Hospitalet), Barcelona, Spain, [2] Department of Oncology, Livestrong Cancer Institutes, Dell Medical School, University of Texas at Austin, Austin, TX, United States, [3] Department of Immunology and Microbiology, School of Medicine, University of Colorado, Aurora, CO, United States, [4] Division of Medical Oncology, School of Medicine, University of Colorado, Aurora, CO, United States, [5] University of Colorado Cancer Center, Aurora, CO, United States, [6] Division of Endocrinology, School of Medicine, University of Colorado, Aurora, CO, United States, [7] Department of Pediatrics, School of Medicine, University of Colorado, Aurora, CO, United States, [8] Rocky Vista College of Osteopathic Medicine – OMS3, Rocky Vista University, Parker, CO, United States, [9] Department of Biostatistics and Informatics, Colorado School of Public Health, University of Colorado Denver, Aurora, CO, United States, [10] Division of Allergy and Clinical Immunology, School of Medicine, University of Colorado, Aurora, CO, United States

Over the past decade, immunotherapies have revolutionized the treatment of cancer. Although the success of immunotherapy is remarkable, it is still limited to a subset of patients. More than 1500 clinical trials are currently ongoing with a goal of improving the efficacy of immunotherapy through co-administration of other agents. Preclinical, small-animal models are strongly desired to increase the pace of scientific discovery, while reducing the cost of combination drug testing in humans. Human immune system (HIS) mice are highly immune-deficient mouse recipients rtpeconstituted with human hematopoietic stem cells. These HIS-mice are capable of growing human tumor cell lines and patient-derived tumor xenografts. This model allows rapid testing of multiple, immune-related therapeutics for tumors originating from unique clinical samples. Using a cord blood-derived HIS-BALB/c-Rag2^{null}Il2rγ^{null}SIRPα^{NOD} (BRGS) mouse model, we summarize our experiments testing immune checkpoint blockade combinations in these mice bearing a variety of human tumors, including breast, colorectal, pancreatic, lung, adrenocortical, melanoma and hematological malignancies. We present in-depth

characterization of the kinetics and subsets of the HIS in lymph and non-lymph organs and relate these to protocol development and immune-related treatment responses. Furthermore, we compare the phenotype of the HIS in lymph tissues and tumors. We show that the immunotype and amount of tumor infiltrating leukocytes are widely-variable and that this phenotype is tumor-dependent in the HIS-BRGS model. We further present flow cytometric analyses of immune cell subsets, activation state, cytokine production and inhibitory receptor expression in peripheral lymph organs and tumors. We show that responding tumors bear human infiltrating T cells with a more inflammatory signature compared to non-responding tumors, similar to reports of "responding" patients in human immunotherapy clinical trials. Collectively these data support the use of HIS mice as a preclinical model to test combination immunotherapies for human cancers, if careful attention is taken to both protocol details and data analysis.

Keywords: humanized mice, immunotherapy, checkpoint blockade, preclinical model, combination testing, immune correlates, PDX (patient derived xenograft), TME (tumor microenvironment)

INTRODUCTION

Treatments that block CTLA-4 and/or PD-1/PD-L1 immune checkpoint molecules can release strong anti-tumoral immune responses and have shown important clinical benefit for many malignancies (1–3). Beyond ICB monotherapies, combination immunotherapies, in which typically a targeted drug, chemotherapy or irradiation are co-administered to augment the immune response, have shown strong rationale and are being evaluated in pre-clinical and clinical studies (4–11). However, few are yet standard of care for cancer treatment, indicating there is an urgent need of improving preclinical testing using models that recapitulate the human tumor microenvironment (TME) heterogeneity and anti-tumor immune responses. The TME is a highly complex mixture of tumor, stromal cells and immune cells and their interconnectivity is facilitated by blood vessels, extracellular matrix and signaling molecules (12, 13). The TME is best recapitulated in an *in vivo* setting so testing combination immunotherapies requires animal models. Mouse models have provided the basic tenets for ICB treatments (14, 15). However, syngeneic mouse tumor models represent, at most, a handful of human tumors, and combination studies in these models translate poorly to the clinic (16–19).

Furthermore, the immune systems, drugs and TMEs differ among humans and mice (20–22). Human cancers are heterogeneous, both among and within patients. This cancer diversity is well-represented in clinical trials. However, these trials are very expensive, time-consuming, and wrought with insufficient patient recruitment and high patient variability due to previous treatments and health conditions. In addition, ethical considerations limit tissue accessibility to gather mechanistic data.

For these reasons, scientists have become interested in using Human Immune System (HIS) mice, often referred to as "humanized" mice, as preclinical *in vivo* models to investigate current and to develop novel combinatorial immunotherapies (18, 23–32). HIS-mice are created either by injection of human peripheral blood mononuclear cells (PBMCs), or human hematopoietic stem cells (HSC) into immunodeficient mouse hosts that lack mouse T, B and natural killer (NK) cells due to genetic deletions, including a *recombinase activating gene* (*Rag)* or *Severe-Combined Immunodeficiency (SCID)* mutation and *IL2 Receptor Common gamma Chain* (*IL2Rγc)* (33–37). The injection of human PBMCs offers the ability to genetically match the HIS with the tumor (38). However, the developed HIS consists of mostly activated T cells that ultimately mount a human anti-mouse immune response in a classic graft-versus-host reaction (39, 40). Selection of tumor-specific T cells can mitigate this effect; however, the HIS in this case is almost pure T cell lineage cells and omits other important immune cells (38). On the other hand, HIS-mice generated with the engraftment of human HSCs isolated from umbilical cord blood (CB) or fetal liver donor tissue, develop a robust multi-lineage HIS (41–43). Importantly, human tumors grow in these immunodeficient mouse hosts, even in the presence of a HIS developed from an allogeneic CB donor that is non-HLA matched to the implanted tumor (44–46). Furthermore, the HIS that develops in these mice is tolerant of the mouse host. Therefore these "basic", i.e. that is no thymic transplants or HLA/cytokine transgenes, HIS-models can be used to test human immune responses to a multitude of human cancers that grow in this small animal model. However, the T cell response is not limited to tumor-specific antigens (Ags) as it is also allogeneic.

Abbreviations: ACC, Adrenal adenocarcinoma; BRGS, BALB/c-Rag2^{null}Il2rγ^{null}SIRPα^{NOD}; CB, Cord blood; CDX, Cell line-derived xenograft; CRC, Colorectal cancer; DLBCL, Diffuse Large B Cell Lymphoma; HIS, Human Immune System; HSC, Hematopoietic Stem Cell; ICB, Immune checkpoint blockade; ILC, Innate lymphoid cell; LN, Lymph nodes; MISTRG, M-CSFh, IL-3/GM-CSFh, hSIRPAtg; TPOh; Rag2-/-; IL2RgC-/-; NK, Natural Killer; NSG, NOD/SCID/Il2rγ-null; NSGS, NOD.Cg-Prkdcscid Il2rgtm1Wjl Tg (CMV-IL3, CSF2,KITLG)1Eav/MloySzJ; PBMCs, Peripheral blood mononuclear cells; PDAC, Pancreatic ductal adenocarcinoma; PDX, Patient-derived xenograft; SCLC, Small cell lung cancer; SGR, Specific growth rate; TIL, Tumor infiltrating leukocyte; TME, Tumor microenvironment; TNBC, Triple negative breast cancer.

Since 2016, there have been several reports using the HIS-mouse model to test human immunotherapies (23, 26, 27, 47–50). These studies have provided essential evidence supporting the use of this model to test clinically-relevant treatments on human tumors. However, critical model-specific information is often lacking. HIS-mice suffer from variability in human chimerism that differs over time and among labs (51). Therefore, it is important to consider and report this variability in experimental design and analysis (51). Analyses of human immune cells in tumors alone can be misconstrued without consideration of those cells in the lymph organs of the same animal. In addition, the HIS-mouse model offers the opportunity to perform in-depth characterizations of the immune system. With the abundance of lymph and tumor tissue, one can relatively easily interrogate the activation and functional states of human immune cells, and are not limited to mere subset analyses.

Using a CB-derived HIS-BRGS mouse model (52), we summarize our experiments testing immunotherapy combinations for a variety of human tumors, including breast, colorectal, pancreatic, lung, adrenocortical, melanoma and hematological malignancies. In these experiments, we allocate HIS-mice, implanted with the same patient- or cell line-derived xenografts (PDX or CDX), into multiple treatment arms and study tumor growth and immune responses. Here, we present data from more than 30 experiments to highlight the utility of using the HIS-CB-mouse model for studying ICB-induced changes in immune responses to human tumors. We evaluate the kinetics and subsets of the HIS in lymph and non-lymph organs and consider these data in our experimental protocol for testing immunotherapies. We compare the HIS in lymph organs, which has mouse-to-mouse and time after engraftment variability, to the human immune infiltration in tumors. We show that properties and quantities of tumor infiltrating leukocytes are tumor dependent in this HIS-CB-BRGS model. We further present our flow cytometric analyses of immune cell subsets, activation state, cytokine production and inhibitory receptor expression in peripheral lymph organs and tumors as immune correlates for treatments. We show experiments in which a larger number of human infiltrating T cells are present in responding tumors and that these T cells have a stronger inflammatory phenotype compared to T cells in non-responding tumors, similar to reports of inflammatory signatures in studies of responding patients in human immunotherapy clinical trials (53–55). Collectively these data support the use of HIS mice as a preclinical model to test combination ICB treatments to human cancers, if careful attention is taken to both protocol details and data analysis. Finally, we discuss other applications, including the ability to test tumor-specific responses in HIS-mice, as well as important limitations of these models.

MATERIALS AND METHODS

Previously published materials and methods are included in **Supplementary File 1** that details the following sections: $CD34^+$ Stem Cell Isolation, Generation of HIS-BRGS Mice, Tissue Harvest and Processing, Cell Staining, Flow Cytometry and Chimerism Evaluation, and ELISA (23, 39, 48, 56).

Reagents

All reagents used in these studies are listed in **Table 1**.

PDX and CDX

For ACC, CRC, PDAC and TNBC PDXS: patients undergoing either removal of primary or metastatic cancers at the University of Colorado Hospital were consented in accordance with IRB-approved institutional protocols (IRB #s 08-439, 04-0066, 15-0516). MSI status was verified by PCR in a CLIA-CAP certified lab, where applicable. The PDX models developed at the University of Colorado Denver AMC campus were generated and passaged in athymic nude mice (purchased from Envigo, Hsd : Athymic Nude $Foxn1^{nu}$ Indianapolis, IN) prior to subcutaneous trocar injection into both flanks of HIS-BRGS mice. The SCLC PDXs were obtained through collaborations with Jeffrey A. Kern (National Jewish Health), who obtained original PDX from Dr. Rudin (MSKCC).

TNBC cell line MDA-MB-231 was kindly provided by Scott Kopeck. Melanoma (C8161) and SCLC (H187 and H82) cell lines were obtained from American Type Culture Collection (Manassas, VA). C8161 was modified to express GFP (C8G) and served as a control for C8M line. C8M was engineered to overexpress IRAK-M. DLBCL cell lines OCI-Ly7 and DHL-16 were obtained from Dr. Wing C. (John) Chan (City of Hope Medical Center, Duarte, CA). Thawed aliquots were expanded in DMEM or RPMI media supplemented with 10% FBS, 1% PenStrep and 1% non-essential amino acids. Cell lines were harvested during exponential growth phase within 6 passages, mixed 1:1 with Matrigel (BD Biosciences), and 1-5 million cells were injected subcutaneously into both flanks using a 23-gauge needle. Trocar injection procedure and other development and maintenance instructions for the PDX model are available from https://www.jove.com/v/54393/development-maintenance-preclinical-patient-derived-tumor-xenograft. The cell lines were authenticated by PCR and underwent mycoplasma testing at the Molecular Biology Service Center (Barbara Davis Center, University of Colorado Denver Anschutz Medical Campus).

Experimental details with kinetics and replicates are included in **Table 2**. ICB and combination therapies used for each experiment are included in **Table 3**.

Protocol for Testing Immunotherapies in HIS-BRGS Mice

Model-specific immune attributes have been considered in developing our protocol to study human combination immunotherapies in HIS-BRGS mice. In this protocol, two major characteristics of the model were considered: 1) the engraftment kinetics of the HIS with delayed T cell and LN development, and 2) the inherent variability of the human chimerism. Our experimental timeline is illustrated in **Figure 1A**. At approximately 10 and 15 weeks of age, blood from HIS-BRGS mice *via* retro-orbital route was collected and mixed with 50 µl of heparin. The PBMCs were purified over a Ficoll-hypaque gradient and stained with Abs to mCD45, hCD45, hCD3, hCD19 or hCD20, hCD4 or hCD8, and hPD-1 to assess human chimerism (relative to mouse) as well as

TABLE 1 | Flow cytometry antibodies and reagents.

Antibodies									
Specie	**Target**	**FC**	**Clone**	**Vendor**	**Specie**	**Target**	**FC**	**Clone**	**Vendor**
Anti-human	CD4	BUV395	RPA-T4	BD Bioscience	Anti-human	CD11c	PacB	s-hcl-3	biolegend
	CD45	BUV395	HI30	BD Bioscience		CD45	PacB	HI30	biolegend
	Granzyme B	Fitc	QA16A02	biolegend		CD11c	BV421	s-hcl-3	biolegend
	CD3	Fitc	HIT3a	biolegend		CD25	BV421	M-A251	biolegend
	CD4	Fitc	OKt4	biolegend		PDL1	BV421	29E.2A3	biolegend
	CD5	Fitc	UCHT2	biolegend		Tim3	BV421	F38-2E2	biolegend
	CD8	Fitc	RPA-T8	biolegend		HLA-DR	BV480	G48-6	BD Bioscience
	CD14	Fitc	63D3	biolegend		CD56	BV650	3G8	biolegend
	CD25	Fitc	M-A251	biolegend		CD45RA	BV650	HI100	biolegend
	CD33	Fitc	HIM3-4	biolegend		CD4	BV785	RPA-T4	biolegend
	CD148	Fitc	A3	biolegend		CD19	APC	HIB19	biolegend
	Epcam	Fitc	9C4	biolegend		FoxP3	APC	236A/E7	biolegend
	CD3	PE	HIT3a	biolegend		FoxP3	AF647	259D	biolegend
	CD8	PE	Hit8a	biolegend		Granzyme B	AF647	GB11	biolegend
	CD11b	PE	ICRF44	biolegend		PD1	APC	EH12.2H7	biolegend
	CD14	PE	63D3	biolegend		CD45RA	APC	HI100	biolegend
	CD33	PE	P67.6	biolegend		CD197/CCR7	APC	GO43H7	biolegend
	CD197/CCR7	PE	GO43H7	biolegend		TNFa	APC	Mab11	biolegend
	CD11c	PE	s-hcl-3	biolegend		HLA-DR	APC	L243	biolegend
	CD45RO	PE	UCHL1	biolegend		HLA-DR	APCFire	L243	biolegend
	TIM-3	PE	F38-2E2	biolegend		CD8	APCFire	RPA-T8	biolegend
	Eomes	PE	WD1928	Invitrogen	Anti-mouse	mCD45	APCCY7	30-F11	biolegend
	CD3	PERCP	HIT3a	biolegend		GR1 (Ly6)	PerCP	RBC-8C5	biolegend
	CD4	PERCP	Okt4	biolegend		H-2 (Class I)	PE	M1/42	biolegend
	CD20	PERCP	2H7	biolegend		I-A/I-E (class II)	Fitc	M5/ 114.15.2	
	CD45	PERCP	HI30	biolegend		MHC I-A/I-E	APCCy7	M5/ 114.15.2	biolegend
	CD197/CCR7	PERCP	GO43H7	biolegend		F4/80	AF647	BM8	biolegend
	CXCR3	PERCP	G025H7	biolegend		Ly6G	BV605	IA8	biolegend
	HLA-ABC	PERCP	W6/32	biolegend	Human	FCR Block			miltenyi
	CD3	PeCy7	HIT3a	biolegend	Mouse	CD32		2.4G2	biolegend
	CD11b	PeCy7	ICRF44	biolegend		Zombie Green			biolegend
	CD45	PeCy7	HI30	biolegend		780 Ghost Dye			Tonbo
	IFNg	PeCy7	4S.B3	biolegend					

Materials		Elisa reagents				
Name	**Vendor**	**Type**	**Specie**	**FC**	**Clone**	**Vendor**
Rec Hu IL6	R&D systems	IgM standard				Sigma
Rec Hu SCF	R&D systems	IgG standard				Sigma
Rec Hu FLT3L	R&D systems	Mouse anti-human	IgM	AP	UHB	Southern Biotech
FCS	Gibco	Mouse anti-human	IgG	AP	JDC-10	Southern Biotech
FCS	Stemcell	Mouse anti-human	IgM	Unlabeled	SA-DA4	Southern Biotech
HBSS	Gibco	Mouse anti-human	IgG	Unlabeled	H2	Southern Biotech
IMDM	Gibco	p-nitrophenly substrate				Sigma
Golgi Stop	BD Bioscience					
Cell Stim Cocktail	Invitrogen					
Saponin	Sigma					
Formaldehyde	Fisher					
Ficoll Hypaque	GE Healthcare					
DNAase	Sigma					
Liberase DL	Roche					
Pen-strep 100X	Gibco					
Glutamax	Gibco					

FC, fluorochrome.

T and B cell chimerism, as described previously (23, 57). To reduce the influence of genetic and engraftment variability on experimental outcomes, we allocated HIS-mice (~>25% hCD45^{+}) generated from the same CB (see **Table 2** for exceptions) into equivalent treatment groups based on human chimerism, including total T cell and CD8 frequencies (**Figure 1B**). Time of tumor injection was based on

TABLE 2 | Experiment nomenclature and details for HIS-BRGS mouse study.

Tumor type	Name	Date (Qtr/Yr)	Tumor take rate (%)	Age at tumor injection (weeks)	Tx start (days)	Age of harvest (weeks)	Exp. length (weeks)	Treatment groups				CB(#)
								Vehicle (n)	ICB (n)	Drug (n)	Combo (n)	
TNBC	A1	03/16	100	17	16	24-25	6-7	3	3	–	–	157
	A2	04/16	88	20-21	10	27	5-6	4	3	2	2	164
	A3	02/17	96	20-23	14-15	23-28	4-6	8	5	–	–	174
	A4	03/17	100	19	19	24	6	4	2	4	3	177
	A5	01/19	93	21-24	21	26-30	5-6	2	2	2	2	194
	A6	04/19	96	16-19	19	21-25	5-6	6	5	–	5	204
	B	01/18	95	21	35	29-32	8-11	3	5	2	4	185
CRC (MSI-H)	A	03/16	89	20	30	25	7-8	6	8	–	–	163
CRC (MSS)	B1	01/17	94	18-21	12	21-24	3	4	4	–	–	171
	C	02/17	100	18	18	22-24	4-6	3	3	2	3	172
	B2	4/2017	94	21-23	17	25-28	4-7	6	4	4	5	182
	D1(P)	03-04/ 2018	94	18-19	19-41	24-28	5-10	4	5	4	4	187
	E	04/2018	67	19-21	42-61	29-36	9-11	2	5	5	4	192
	F	01/2019	100	21	21	24-26	4-5	6	4	4	6	198
	D2(M)	2/2019	92	18-20	17	22-26	4-5	4	1	3	2	199
	G	3/2019	98	18-22	41-54	27-33	9-11	3	3	4	4	201
	D3(P)	01/2020	98	18-20	20	23-25	5-6	6	–	–	7	206
	H	01/2020	90	19-20	16	23-25	4-6	5	6	6	6	209
	I	02/2020	100	17-20	30	25-30	8-10	6	5	5	6	209
PDAC	A	04/2018	50	31-33	38	37-39	7	1	–	2	–	192
	B	04/2019	90	16-25	25	20-29	5-8	2	–	7	–	206
SCLC	A	01/2019	67	17-24	NA	22-31	5-7	2	–	–	–	198
	B	01/2019	88	18	NA	21-23	3-5	2	–	–	–	198
	C	01/2019	88	15-22	NA	20-25	3-6	4	–	–	–	198
	D	03/2019	100	21-22	19	26-27	5	1	2	2	2	202
ACC	A	03/2017	70	18-19	49-70	29-37	10-18	5	4	–	–	175
	B	02/2020	98	17-21	28-56	26-33	8-12	6	5	6	5	210/ 212
MEL	A	04/2015	56	15	8	20	6	3	3	–	–	151/ 152
	B	04/2018	83	21-22	NA	25	3	3	–	–	–	195
	C	04/2018	100	21-22	NA	25	3	3	–	–	–	195
DLBCL	A1	02/2018	100	12	NA	16	4	3	–	–	–	189
	A2	03/2018	100	21	12	25	4	3	3	–	–	194
	B	04/2018	75	26-28	56	30-35	7	3	3	3	3	194

Each row represents an independent experiment with implantation of: triple-negative breast cancer (TNBC), microsatellite stable (MSS) and instable (MSI-H) colorectal cancer (CRC), pancreatic adenocarcinoma (PDAC), small-cell lung cancer (SCLC), adrenocortical carcinoma (ACC), melanoma (MEL) and diffuse large B-cell lymphoma (DLBCL). For each tumor type, we represent different CDX/PDX by a letter, with experimental repeats indicated by a number. (P) refers to a primary tumor and (M) to metastatic origin.

human T cell populations, which can vary among cohorts produced from distinct CBs. We also considered the tumor growth kinetics, to coordinate tumor and T cell engraftment with the availability of individual tumors in donor mice. To increase experimental power, we injected tumors into both flanks of the HIS-BRGS mice typically between 19 and 21 weeks of age (**Table 2**). Mice were monitored for health, weighed, and tumors were measured twice weekly and treatments begun once the tumors reached an average volume of 100-300mm^3. Mice were euthanized in groups of 4-8 based on tumor sizes, health and timing. We attempted to harvest all mice within a reasonable timeframe to gather the most consistent data (**Table 2**). At harvest, we collected lymph nodes (LNs), spleens and tumors, and digested into single cell suspensions, as described in **Supplementary File 1**. Cell counts for LNs (combined peripheral and mesenteric) and spleens were enumerated using a hemocytometer.

Tumor Growth Calculations

The following equation was used to estimate tumor volume: (length × width^2) × 0.52 and recorded in the Study Director software package (Studylog Systems). Tumor growth curves are presented as average tumor volume ± SEM for each treatment group in study. The specific growth rate (SGR) was calculated by the following formula:

$$SGR\ (\%\ of\ volume\ growth/day) = \frac{\ln(V_2/V_1)}{(t_2 - t_1)}$$

TABLE 3 | Human tumor xenografts and treatments in the HIS-BRGS experiments.

Tumor type	Name	CDX/ PDX	Cell linename	ICB Drug	CombinationDrug	Tumor Response
TNBC	A1	CDX	MDA-MB-231	Nivolumab	–	Yes
	A2		MDA-MB-231	Nivolumab	HDACi	Yes
	A3		MDA-MB-231	Nivolumab	–	Yes
	A4		MDA-MB-231	Nivolumab	WNTi	Yes
	A5		MDA-MB-231	Nivolumab	WNTi	No
	A6		MDA-MB-231	Nivolumab ± Ipilimumab	–	Yes
	B	PDX	–	Nivolumab	WNTi	No
CRC (MSI-H)	A	PDX	–	Nivolumab	–	Yes
CRC (MSS)	B1	PDX	–	Nivolumab	–	Yes (then relapse)
	C		–	Nivolumab	HDACi	No
	B2		–	Nivolumab	Multi-TKI	Yes
	D1(P)		–	Nivolumab	WNTi	Yes
	E		–	Nivolumab	Multi-TKI	Yes
	F		–	Nivolumab	Multi-TKI	No (all slow growers)
	D2(M)		–	Nivolumab	Multi-TKI	No
	G		–	Nivolumab	WNTi	No
	D3(P)		–	Nivolumab	Multi-TKI	Yes
	H		–	Nivolumab	MEKi + VEGFi	No
	I		–	Nivolumab	MEKi + VEGFi	No
PDAC	A	PDX	–	–	Multi-TKI	No
	B		–	–	WNTi	No
SCLC	A	CDX	H187	–	–	–
	B		H82	–	–	–
	C	PDX	–	–	–	–
	D		–	Nivolumab	Chemotherapy	No
ACC	A	PDX	–	Pembrolizumab	–	Yes
	B		–	Pembrolizumab	Chemotherapy	No
MEL	A	PDX	–	Nivolumab	–	No
	B	CDX	C8G	–	–	–
	C		C8M	–	–	–
DLBCL	A1	CDX	OCI-Ly7	Nivolumab	HDACi	–
	A2		OCI-Ly7	Nivolumab	HDACi	No
	B		DHL-16	Nivolumab	HDACi	Yes

cell-line xenograft (CDX), patient-derived xenograft (PDX), histone deacetylase (HDAC), Wnt signaling pathway (WNT), tyrosine kinase inhibitor (TKI), mitogen-activated protein kinase kinase (MEK), vascular endothelial growth factor (VEGF), "i" represents inhibitor ***Materials and Methods****.*

Tumor and Lymph Organ Immune Evaluation by Flow Cytometry

The LN, spleen and tumor cell suspensions are stained with fluorescently-labeled Abs (**Table 1**) to evaluate some or all of the following: 1) mouse ($mCD45^+$) and human ($hCD45^+$) immune subsets including human T ($CD4^+$ and $CD8^+$, either through direct staining or defined as $CD3^+CD4^-$ T cells), B ($CD19^+$ or $CD20^+$), and myeloid ($CD11b^+$, $CD11c^+$, $CD14^+$, or $CD33^+$) cells; 2) T cell functional properties including populations of activated T cells ($HLA\text{-}DR^+$), T_{EM} ($CCR7^-CD45RO^+$) and T_{CM} ($CCR7^+CD45RO^+$) cells, Tregs ($CD25^+$, $FoxP3^+$), and cytotoxic (Granzyme B (GrB), IFNγ, or TNFα) T cells; 3) $CD11c^+$ B cells, 4) the expression of HLA-DR on myeloid cell populations, and 5) the immunogenic properties of tumor ($EpCAM^+$ where applicable) and human immune cells, including the expression of inhibitory receptor PD-L1 and MHC class I (HLA-ABC) and II (HLA-DR) molecules. The mCD45 population served as a negative control for human specific expression. We "counted" the number of distinct immune populations on the flow analyzer by staining and collecting a pre-defined volume of cells that we then "back-calculated" to quantitate the total relative cell number (**Figure 1C**). Low chimerism mice (lacking LN or with <1 million human T cells in the spleen at end of the study) were not considered for the analysis.

Statistics

Data were plotted using GraphPad Prism version 8.3.0 for macOS (GraphPad Software). For comparisons between two independent groups with approximately normally distributed variables, we used unpaired, parametric two-group t-tests with Welch's correction in the case of unequal variances. One way ANOVA was used to compare means of approximately normally distributed variables among three or more groups, or the Welch's ANOVA for data sets with unequal group variances. For those variables far from normally distributed, we used a non-parametric Wilcoxon for comparing the median between two groups and Kruskal-Wallis test for more than two groups. Simple

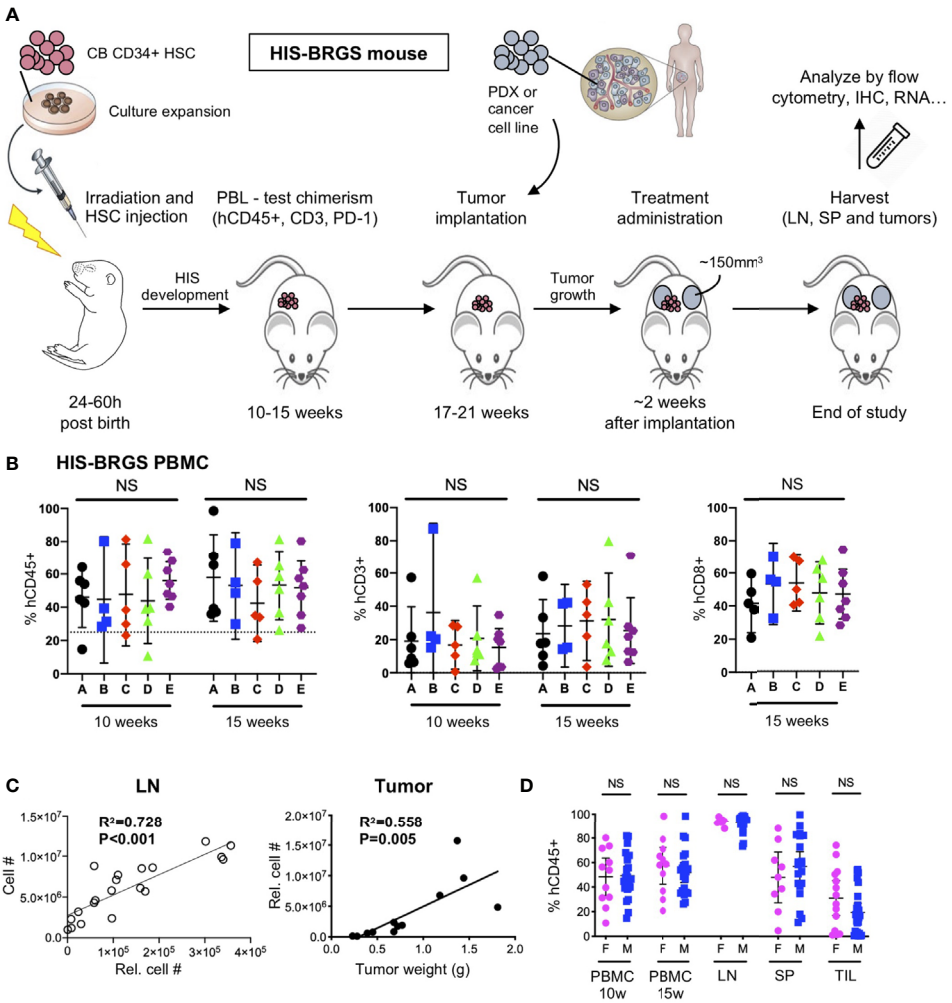

FIGURE 1 | Protocol for evaluation of immunotherapy treatments in HIS-BRGS mice. **(A)** Timeline of HIS-BRGS mouse model development. **(B)** Allocation of HIS-BRGS mice into experimental treatment groups A-E based on equivalent human (hCD45+), T (CD3+) and CD8+ T cell chimerism. NS, no significance [Welch's ANOVA test]. **(C)** Correlation of cell counts determined by flow cytometry (Relative cell count) and hemocytometer cell count in the lymph nodes (LN, left) or tumor weight (right) [linear regression analysis, R-squared score (R2) and P value (P) in bold if statistically significant ($P < 0.05$)]. **(D)** Human (hCD45+) chimerism in the blood (PBMC), LN, spleen (SP) and tumor tissue (TIL) of female (F) vs male (M) HIS-BRGS mice [two-group t-test, two tailed].

linear regression analyses were also performed to assess possible associations using Prism software.

RESULTS

HIS Characteristics and Kinetics of Reconstitution in Immunodeficient Mice

The injection of human $CD34^+$ HSCs, isolated from either human CB or fetal liver, into mice lacking T, B and NK cells, and possessing a SIRPα that binds human CD47 (NOD or human), generates robust human chimerism and a multilineage HIS (52, 58, 59). Similar to bone marrow transplantation in humans, the HIS that develops follows a consistent pattern of delayed engraftment and immune reconstitution (56, 60–62). We tested for human chimerism at least 8 weeks post engraftment by collecting blood and enumerating the proportions of mouse (m) and human (h) CD45+ cells by flow cytometry. Human chimerism is variable, with an average percentage of $hCD45^+ > 50\%$ of total hematopoietic ($mCD45^+ + hCD45^+$) cells at 10-15 weeks, consistent with other laboratories (60, 62, 63). In contrast to other reports (62), we observe no difference between chimerism in female and male recipients (55.7 ± 21.8, n=35 females, average 57.2 ± 19.0, n=41 males, p=0.74, **Figures 1D**, **2A**).

B cells are the dominant population early in reconstitution, followed gradually by T cell reconstitution (**Figure 2B**) (51, 56). This pattern is regardless of recipient strain (e.g. NSG, BRG or BRGS), a human HLA selecting element in the thymus (HLA-

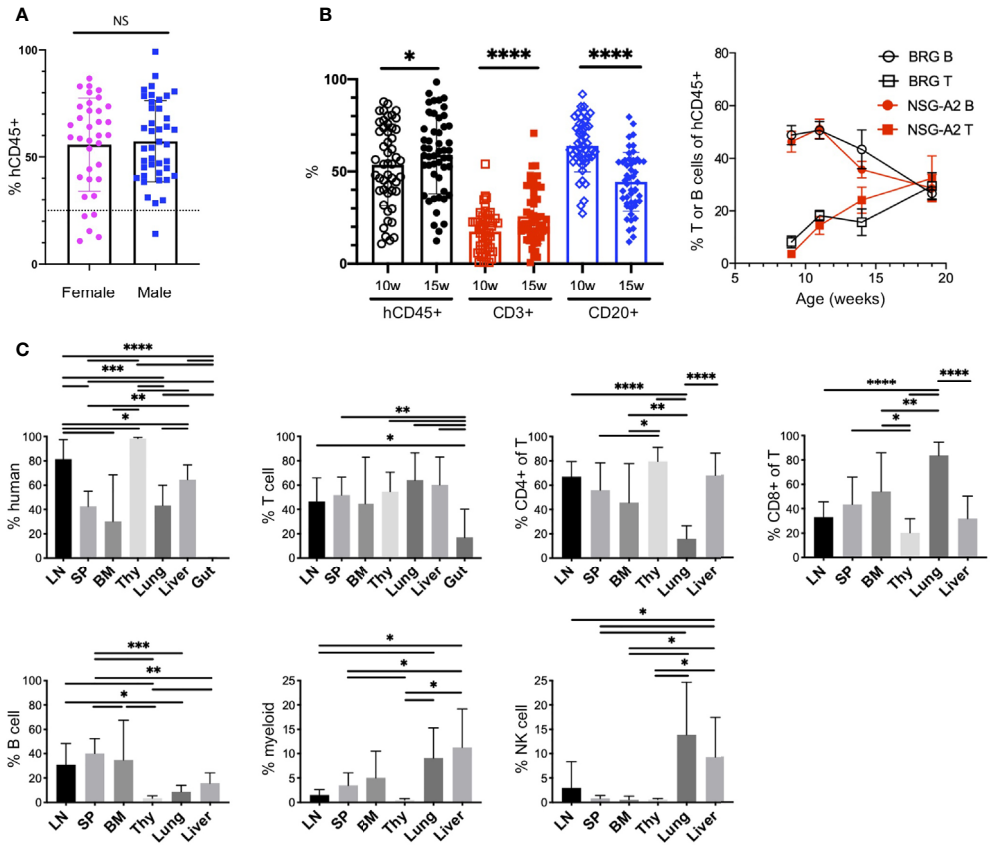

FIGURE 2 | The human immune system in HIS-BRGS-mice. **(A)** Human chimerism (%hCD45 of (h+m) CD45) among female (F) and male (M) HIS-BRGS mice at 10 weeks of age *(n=35 F, n=41 M; two-group t-test p value = 0.74)*. **(B)** Percentage of human (hCD45), T cell (CD3) and B cell (CD20) subsets in PBMCs of HIS-BRGS (left panel) and BRG or NSG-A2 mice (right panel) at indicated times post engraftment. *$p < 0.05$, ****$p < 0.0001$ [paired t-test, two-tailed]. **(C)** Chimerism by organ for multiple HIS-BRGS mice (n=7, except for BM CD4+/CD8+,n=6) from one CB. T cell (CD3+), B cell (CD19+), myeloid population (CD11b/33/14 or 11c+), NK cell (CD56+) populations. Gate: hCD45+ or hCD45+CD3+ (CD4+, CD8+ of T). *$p < 0.05$, **$p < 0.01$, ***$p < 0.001$, ****$p < 0.0001$, NS, no significance. [Welch's two-group t-test, two-tailed between organs as indicated by edges of each line]. *LN, lymph nodes; SP, spleen; BM, bone marrow; Thy, thymus*.

A2, **Figure 2B**), and even to a large extent the initial age of the recipient mouse (i.e. HSC injection into neonate or adult), although faster T cell reconstitution has been reported from neonatal injections (63). We have previously shown that T cell development is essential for the population of human cells in the LNs, which typically occurs 3-4 months following engraftment and significantly correlates with the presence of human immunoglobulins (Igs) in the sera, a feature consistent with a more functional adaptive immune system (56, 64, 65). We observe relatively high concentrations of hIgG (up to 5 mg/ml) in the sera in our facility (39, 56, 66). Importantly, systemic immune responses are expected in our model, as both T and B cell subpopulations are seen in lymph and non-lymph organs (**Figure 2C** and **Supplementary Figure 1A**).

Cells of the innate immune system, including the myeloid lineage, are important in instructing immune outcomes. HIS-mice in a "basic" NOD/SCID/Il2rγ-null (NSG), NOD/RAG-1/Il2rγ-null (NRG) or BRGS recipient are notoriously deficient in human myeloid cells relative to the lymphocyte lineage (24, 63, 64). However, the mouse myeloid lineage is intact (25, 67, 68). In our HIS-BRGS mice we detected multiple non-lymphocyte human hematopoietic populations by staining with CD11b, CD14, CD33 and CD11c myeloid lineage markers with varying levels of MHC Class II, HLA-DR expression (**Figure 2C** and **Supplementary Figure 1B**). These populations are more prominent in the bone marrow and non-lymph organs (liver and lung) than in the LNs and spleen (**Figure 2C** and **Supplementary Figure 1B**).

We have also examined other less frequent immune populations, and similar to other labs, we have found immature NK cells populations (33, 69–72). We have also observed innate lymphoid cells (ILCs) in low frequencies, mostly in the LNs, that are likely important in LN organogenesis (**Supplementary Figure 2A**) (70). Furthermore, we identified plasmacytoid dendritic cells that we identify as Lin$^-$ (CD3$^-$CD19$^-$CD11b$^-$CD11c$^-$CD14$^-$CD33$^-$), HLA-DR$^+$ cells with confirmed expression of CD123 (**Supplementary Figure 2B**). We have not observed human mucosal-associated invariant

T cells in any organ (73) (**Supplementary Figure 2C**). In our model, we have seen good reconstitution of developing human T cells in the thymus, with both clear double-positive ($CD4^+CD8^+$) and single-positive populations, yet very few human immune cells in the gut (**Figure 2C**) (70).

Overall, the HIS-CB-BRGS model demonstrated strong human chimerism with a multi-lineage immune system, with not only T cells but other essential immune populations, allowing the study of their complex and coordinated interactions during the immune response.

Human T Cells in HIS-Mice Show an Activated and "Exhausted" Phenotype

Upon Ag encounter, T cells proceed through an activation continuum in which individual cells can ultimately proliferate and produce cytokines (74–76). However, to control this destructive response, immune cells also upregulate inhibitory receptors, leading to a non-responsive state of "exhaustion". The sequential expression of inhibitory receptors has revealed subsets of exhausted T cells that correlate with the ability to reinvigorate their cytotoxic function: PD-1^+ $Tim3^-$ T cells represent a more "recoverable" population while PD-1^+TIM-3^{hi} cells are more "exhausted" (74–76). This continuum represents the central paradigm in ICB therapies that are targeting the less-exhausted T cells capable of functioning upon release of the inhibitory signal (75, 76).

Relevant to the HIS model, we find extensive T cell activation, as determined by HLA-DR expression, and populations of both effector memory (T_{EM}) (77) and central memory (T_{CM}) T cell populations (56) (**Figure 3A**, **Supplementary Figure 3A**). In addition, we observe a very large population of T cells with an exhausted phenotype, as defined by expression of both PD-1 and TIGIT inhibitory receptors that increases with time (23, 48, 78). However, these same T cells show weak co-expression of TIM-3 (**Figure 3B**). The expression of Eomes and T-bet transcription factors in T cells from lymph organs and tumor infiltrating leukocytes (TILs) of HIS-BRGS mice also support an activated and exhausted gene expression profile in these mice (**Supplementary Figure 3B**). Furthermore, we consistently observe obvious regulatory T cell (Treg) populations, which are more notable in the LNs than in the spleen (**Figure 3C**). The prevalence of this population in HIS models has been inconsistently reported, perhaps due to experimental timing or differences in anatomical location (51, 79, 80). These activated/exhausted T cell phenotypes correlate with increased frequencies of $CD11c^+$ B cells, a population associated with increased Ig production in both humans and mice (**Figure 3D** and **Supplementary Figure 3A**) (81–83).

In view of these results, we can confirm the activated phenotype of T and B cells in our model, as routinely seen in untreated cohorts of both unmanipulated and tumor-bearing HIS-BRGS mice (23, 48, 56).

Growth of Human Tumors in HIS-Mice

A major breakthrough for the HIS model was the discovery that tumors can grow in humanized mice (29, 46, 47). Indeed, our group has validated this finding using flank injection models of multiple human cancers (23, 48, 49). **Table 2** provides experimental details for each of our 33 HIS-BRGS oncology studies, including nomenclature, study time points and number of mice per treatment group. **Table 3** summarizes the origin of the 33 tumors (PDX/CDX and tumor type), study treatment for

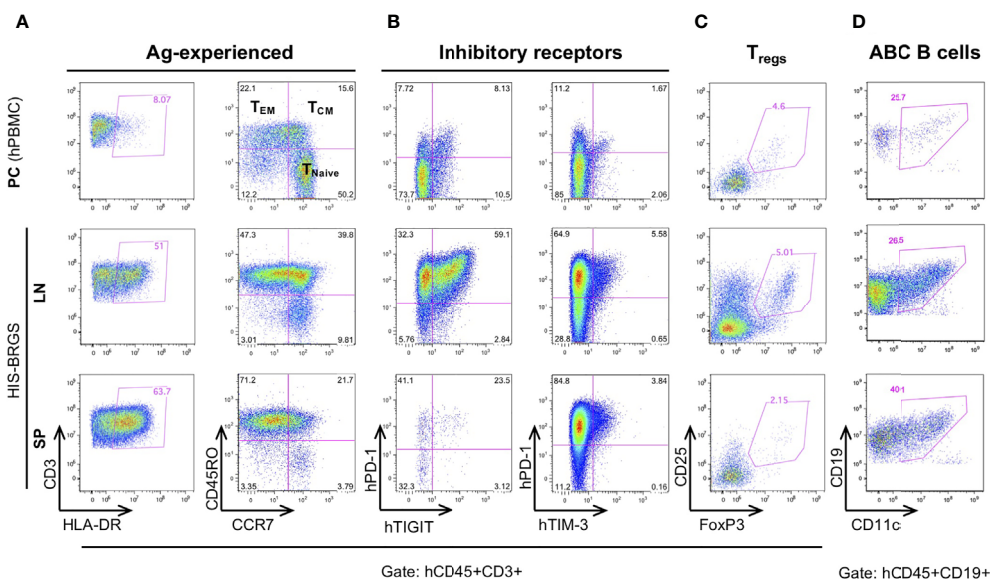

FIGURE 3 | Immunostimulatory and immunomodulating human lymphocyte subsets in the lymph nodes (LN) and spleen (SP) of HIS-BRGS mice. T cell expression of **(A)** activation marker, HLA-DR, and memory cell markers, CD45RO/CCR7, **(B)** inhibitory receptors, PD-1, TIGIT, TIM-3, and **(C)** regulatory T cell markers, $CD25^+FoxP3^+$. **(D)** $CD11c^+$ B cells. Human PBMC served as a technical staining control ("PC", top row).

each experiment, usually ICB +/- combinational drug, and whether significant tumor growth inhibition was measured.

As an indication of reproducibility of the system, we injected the same MDA-MB-231 TNBC CDX in six independent HIS-BRGS experiments, with six distinct CBs (**Table 2**, A1-A6). In all of these experiments the tumors grew quickly, and similar to rates observed in nude mice or non-humanized BRGS recipients (23). Of note, tumor take rate for all 33 experiments was high, with a mean of 89.4% (95%CI 84.6 – 94.1) and did not significantly differ across tumor types (P=0.18) or xenograft class (CDX vs PDX, P=0.53). As illustrated by CRC experiments, tumor take rate was also similar between primary tumor and metastatic tissue derived PDXs (**Table 2**, CRC D1-D3).

Although we typically use a flank-injection model for ease of measurement and consistency, the model is well-suited for orthotopic injections, which has been shown to yield results consistent to the flank injection model in a similar HIS-mouse model (44). We have observed metastatic spread to the liver and lungs in some tumors, and also in EBV-induced lymphomas that developed *de novo* following viral infection (66). Indeed, we have recently observed metastatic liver burden from i.v. injection of a CDX, in which we could observe tumor growth using the *in vivo* imaging system (IVIS, data not shown).

In summary, we provide ample evidence that human xenografts grow in the multi-lineage HIS models generated from human HSCs. As similarly observed by other groups (50, 84), we achieved high and reproducible tumor take rates in our HIS-BRGS mice.

Infiltration of Human Immune Cells in HIS-BRGS Mice Varies by Tumor Type

The TME governs the immune response against malignant cells. "Cold" tumors have reduced immune infiltration and an immune-suppressive TME while "hot" tumors are characterized by cytotoxic T cell infiltration (12, 85). To ascertain if the degree of infiltration was determined by differences in the chimerism among HIS-BRGS mice or was rather influenced by the tumor itself, we measured the infiltration of immune cells into the tumors in these thirty-three independent experiments in which a human CDX/PDX was implanted into the flanks of HIS-BRGS mice (**Table 2**). We found different patterns of immune infiltration, as shown in the variable mCD45$^+$ and hCD45$^+$ proportion across different experiment examples (**Figure 4A**). In order to achieve a general overview, we then plotted cumulative hCD45$^+$ and hCD3$^+$ percentages for all vehicle, i.e. untreated, HIS-BRGS mice in each of these experiments (**Figure 4B**). We observed variable infiltration of human immune cells within single experiments (e.g. TNBC A1), but larger differences in average infiltration were observed across tumor types (**Figures 4A, B**). For instance, the infiltration into the TNBC CDXs A1-6 was variable (range 0.16-76.6, p=0.0032 Welch's ANOVA) but the average infiltration was consistently higher than our low-infiltration tumor "cut-off" of 0.1% cell, which in our experience represents samples with too few human cells to perform further analyses (<100 hCD45+ cells). In comparison, the CRC MSS PDXs had relatively low infiltration of hCD45$^+$ cells with similar variability among tumors (range 0.015-5.38, p=0.0028 Welch's ANOVA) compared to the TNBC data sets. However, the average infiltration for all TNBC CDXs (A1-A6) versus all CRC MSS tumors (B1-I) showed a significant difference (p =0.0015, two-group t-test with Welch's correction). The conclusion holds, with even more significance, after removing the two highest TNBC outliers (>70%) with p<0.0001 using the same test. The experiments with implanted tumors of shared xenograft origin showed similar hCD45$^+$ infiltration, as illustrated by CRC-MSS PDXs "B1/B2" (p=0.31, two-group t-test) and "D1p/D2m/D3p" (p=0.10, Welch's ANOVA test) although D1p and D3p did show variable infiltration of hCD45+ cells (p=0.04, two-group Welch's t-test). These differences among PDXs of same origin are small relative to differences measured across all CRC MSS tumor types. The percentage of hCD45$^+$ also mirrored the expected infiltration for other tumors. For example, the MSI-H Lynch syndrome-associated ACC tumor "A" showed higher hCD45$^+$ infiltration relative to the sporadic ACC "B" counterpart. Indeed, SCLC tumors "A-D" had almost no hCD45$^+$ infiltration as expected for this well-known "cold" tumor (86, 87). We also compared right versus left flank tumors and observed quite consistent hCD45$^+$ infiltration within an individual HIS-mouse, although the tumors were often quite different in size (**Supplementary Figure 4**) (44, 84).

As a further indicator of TME phenotype, we measured the frequency of human T cells in these same tumors (**Figure 4B**). We observed much greater variability in T cell frequencies, among and within tumors of different origins. Even among the few hCD45$^+$ cells detected in the SCLC tumors, there were different amounts of T cell infiltration. On the other hand, melanoma tumors had consistently high T cell infiltrates. Similar to reports by other groups (50), we found very few infiltrating B cells, although this lineage is prevalent in the spleens and LNs of HIS-BRGS mice (23). The majority of the non-T cells in tumors of our HIS-BRGS mice was of the myeloid lineage (23). Altogether, and consistent with other studies in HIS-mice (44, 84), these data suggest the tumors in our HIS-BRGS model generally recapitulate their unique TME in regard to immune infiltration.

Parameters Influencing Human Infiltration

Human immune cells clearly infiltrated human tumors implanted into HIS-mice. To better understand the factors that could influence tumor infiltration in our model, we analyzed the data with respect to protocol parameters.

Influence of Human Chimerism on Tumor Immune Infiltration

Given the variable nature of human chimerism in HIS-mouse models, we sought to determine the influence of this feature on infiltration into the tumors. First, we correlated tumor hCD45+ infiltration with the amount of hCD45$^+$ and hCD3$^+$ cells measured in 1) PBMCs of the HIS-mice prior to tumor injection (we allocated mice into equivalent "chimerism"

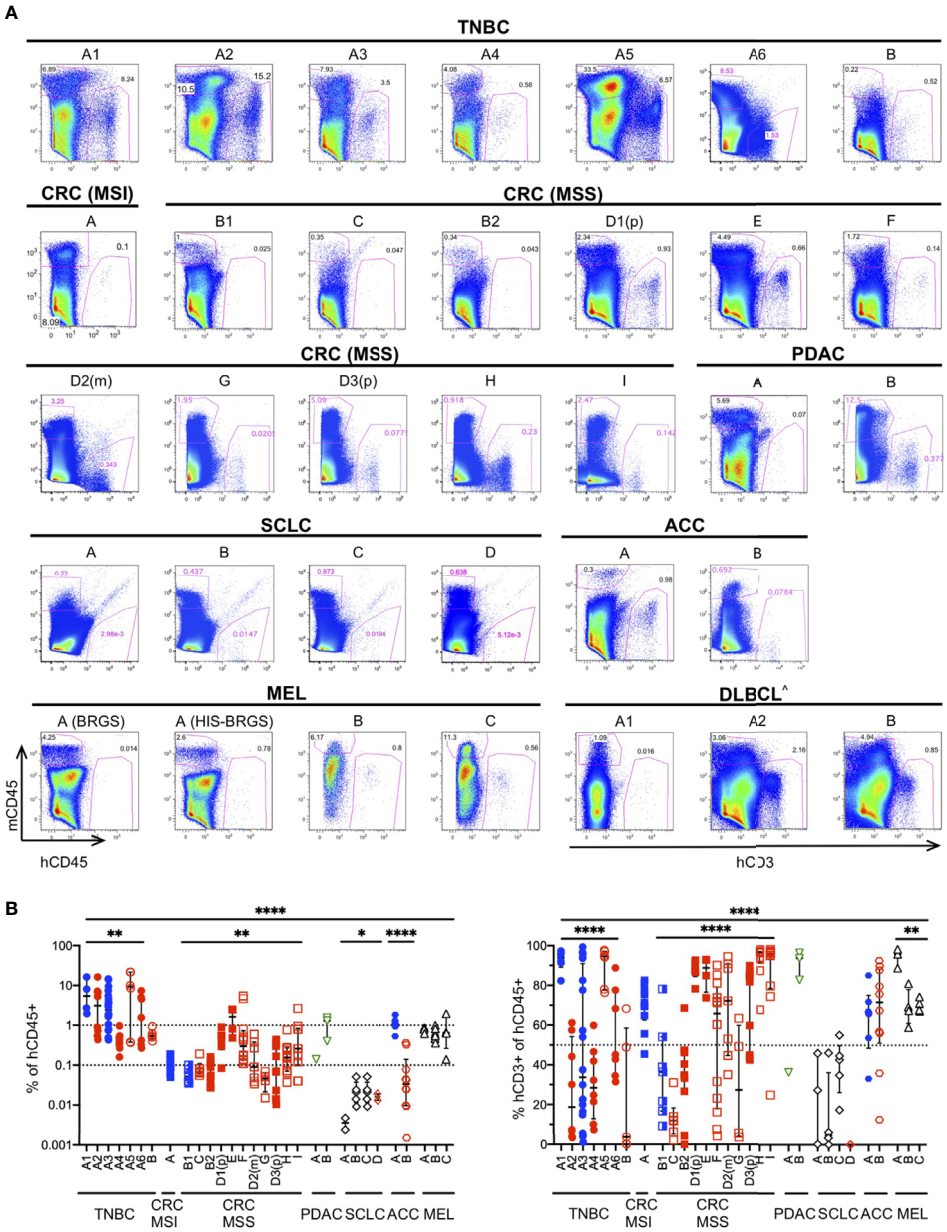

FIGURE 4 | Infiltration of human immune cells into different human tumors in **untreated** HIS-BRGS mice. **(A)** Representative flow cytometry plots showing mouse (mCD45$^+$, y-axis) and human (hCD45$^+$ or (^) hCD3$^+$ for hematological malignancy, x-axis) leukocyte infiltration into tumors in HIS-BRGS mice: TNBC MDA-MB-231 (A1-6) and PDX **(B)**; CRC PDX: MSI-H **(A)** and MSS (B-I); PDAC PDX (A, B); SCLC CDX **(A, B)** and PDX (C, D); ACC PDX (A, B); melanoma PDX **(A)** and CDX (B,C); and DLBCL CDX (A,B). Different experiments with the same tumor have the same letter but different numbers; (p) refers to a primary tumor and (m) to metastatic origin. Background staining represented by melanoma PDX A injected into non-humanized BRGS mouse (lower left). **(B)** Percentage of hCD45$^+$ (of singlet gate, left) and CD3$^+$ T cells (hCD45+ gate, right) in tumors of untreated HIS-BRGS mice. Filled symbols represent experiments in which tumors in treated HIS-BRGS mice responded to treatment and open symbols represent non-responding experiments. The data are log-transformed to approximate normal distributions. The colors represent experiments testing nothing (black), ICB monotherapy (blue), targeted therapies alone (green) or immunotherapy combinations (red). *$p < 0.05$, **$p < 0.01$, ****$p < 0.0001$ [The lower lines in B reflect analyses of differences in means across experiments of the same tumor type using Welch's ANOVA (TNBC, CRC, SCLC, MEL) or two-group t-test (ACC). The upper line shows Welch's ANOVA analysis for differences in means across all tumors, regardless of type].

groups based on this parameter) and 2) the spleen at end of study. We analyzed combined data from six TNBC CDX (A1-6) and five CRC PDX (B2, D2, D3, E, F) independent experiments (**Figure 5A**). Tumor immune infiltration did not appear significantly influenced by human chimerism or human T cell percentage, as determined in the blood of the HIS-mice prior to tumor injection. However, tumor hCD45$^+$ infiltration showed a positive correlation with human chimerism at the end of study,

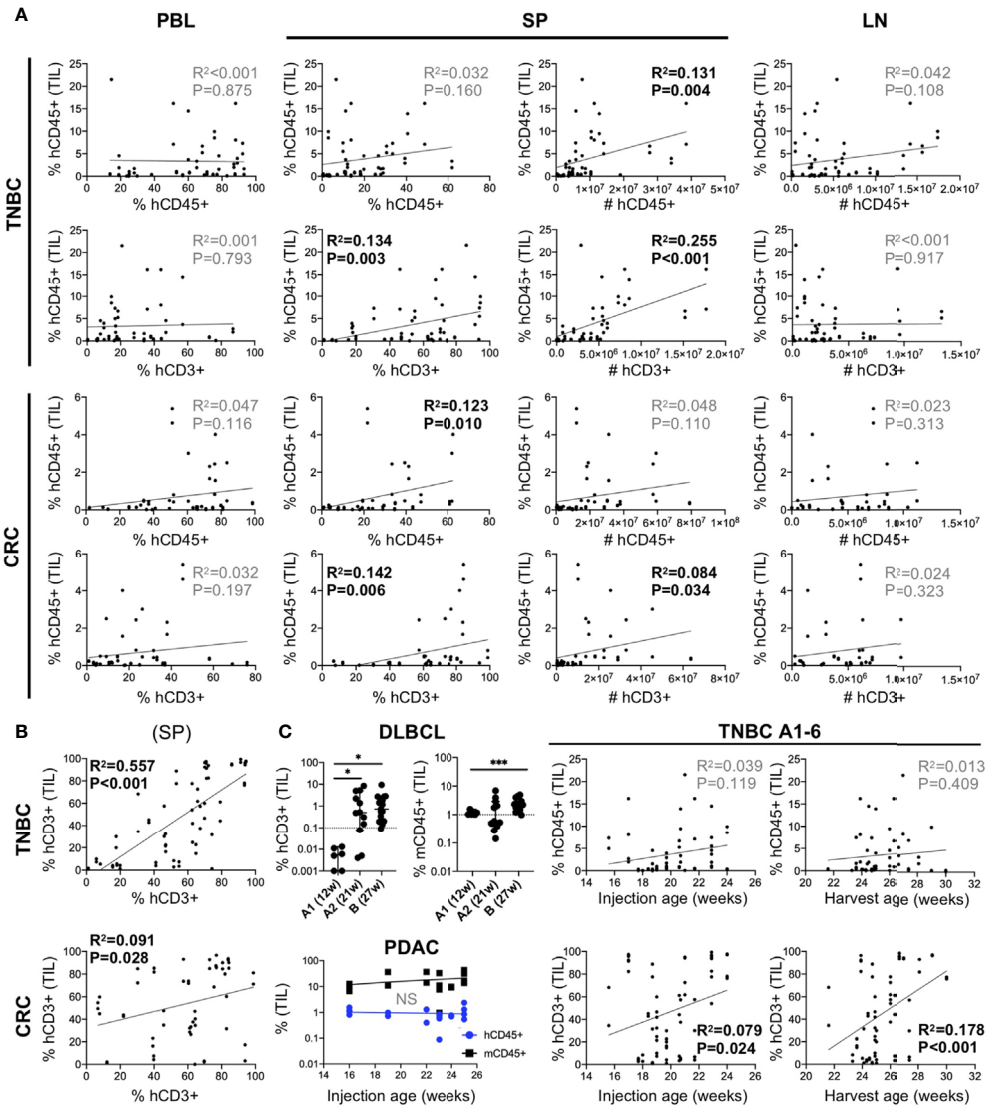

FIGURE 5 | Influence of human chimerism and timing of tumor injection on human immune infiltration in human tumors in untreated HIS-BRGS-mice. **(A)** Correlation of hCD45$^+$ infiltration in HIS-BRGS tumors with human chimerism in lymph organs. Data from six TNBC CDX (top, A1-A6) and five CRC (bottom, CRC B2, D2, D3, E, F) independent experiments. hCD45 and hCD3 chimerism (percentage and absolute number, #) in PBMC prior to tumor injection (PBL at 15 weeks), and in the spleen (SP) and lymph nodes (LN) at end of study. **(B)** Positive correlation between T cell infiltration in TNBC A1-A6 and CRC tumors (B2, D2, D3, E, F) and T cell chimerism in spleens of HIS-BRGS mice. **(C)** Influence of timing of tumor injection on human immune cell infiltration into tumors. Human (hCD45+) or T (hCD3$^+$) and mouse (mCD45$^+$) immune cell infiltration into DLBCL CDXs (*upper left*) or PDAC PDX (lower left) with different tumor injection timepoints. Correlation of hCD45+ and hCD3$^+$ infiltration into untreated TNBC CDXs (A1-A6) and the age of HIS-BRGS mice at time of tumor injection or end of study (*right*). *$p < 0.05$, ***$p < 0.001$ [**A, B**: Linear regression analysis, R-squared score (R^2) and P value (P) in bold if statistically significant ($P < 0.05$); **(C)**: Welch's two-group t-test, two-tailed between organs as indicated by edges of each line].

in terms of total number (TNBC) or percentage (CRC) of hCD45$^+$ cells in the spleen of HIS-mice. In contrast, the number of human cells in the LNs, which are consistently >85% hCD45+ cells, showed no correlation with hCD45$^+$ tumor infiltrates in the either models. Notably, we observed a stronger correlation of hCD45$^+$ tumor infiltration with the percentage and number of T cells in the spleen, most notable in TNBC A1-A6 tumors (% T cells p=0.003, T cell #s p<0.001), but also among the CRC MSS PDX models (% T cells p=0.006, T cell #s p=0.034). Similarly, the proportion of T cells in the spleen correlated with those in the tumors with a higher correlation in the TNBC than CRC MSS datasets (**Figure 5B**). In our studies, hCD3$^+$ rather than hCD45$^+$ percentage in the blood prior to tumor injection appeared as a better indicator of respective chimerism in the spleen (and thus T cell infiltrates in tumor) at end of study (**Supplementary Figure 5**). Overall, we did not detect a clear impact of baseline chimerism on tumor immune infiltration, but our data suggests that the systemic response seen in the spleen, which correlates with

T cell chimerism in the blood, may be influencing tumor infiltration.

Timing of Tumor Injection

T cells take months to appear in immune organs in HIS-mice, and yet they influence human immune cell infiltration into the tumors. Therefore, we evaluated the influence of timing of tumor injection on human infiltration into tumors. In a series of experiments using a DLBCL CDX, the tumors were injected at 12 ("A1") or 21 ("A2") weeks (**Table 2**). The DLBCL is of hematopoietic origin and express hCD45 and hCD19, thus we evaluated the infiltration of human T cells ($CD3^+$) as the readout for human immune infiltration. In the case of early tumor injections, we observed very few tumor-infiltrating T cells, although $mCD45^+$ (myeloid lineage) cells clearly infiltrated the tumors. However, in mice injected at 21 weeks of age, we observed increased frequencies of $hCD3^+$ T cells in the tumors, confirming the need for later tumor injections. DLBCL CDX "B", that was injected at a much later timepoint (27 weeks), showed similarly high frequencies of $CD3^+$ T cells (**Figure 5C**). In another experiment, PDAC tumors were injected into a cohort of HIS-BRGS mice of different ages (16-25 weeks). In this case the human infiltration remained consistently low, likely influenced more by a suppressive TME even in the presence of sufficient human T cells (**Figure 5C**). Consistent with the correlation of increased splenic $hCD3^+$ T cells with $hCD45^+$ infiltration into tumors in the MDA-MB-231-bearing HIS-mice (see section 5.1), a similar analysis showed increased human T cell infiltration in these tumors with either age of tumor injection and age of mice at end of study (**Figure 5C**). Thus, we conclude that, in addition to a basic human chimerism cutoff, it is also important to: 1) have sufficient T cells in the HIS-mice for the tumor studies (i.e. timing of tumor injections is crucial) and 2) treatment cohorts must be allocated by human and more importantly, T cell PBMC chimerism, to reduce potential effects of chimerism on experimental outcomes.

Cord Blood

The generation of HIS-mice from distinct CB units is another source of variability that should be considered. Our TNBC and CRC studies testing the same tumor with different CBs suggest the CB plays a relatively minor role in determining human infiltration (**Figures 4A, B**, TNBC A1-A6, CRC B1-B2, and CRC D1-D3). In addition, we provide two examples below (see section 7) to show differences in immune responses to two unique CRC PDX or DLBCL CDX HIS-BRGS models that were treated with the same therapies in mice generated from the same CB.

Immune Response to Tumor Allograft in HIS-BRGS Mice

Despite high and reproducible tumor take rates in our HIS-BRGS mice (50, 84), tumor sizes varied greatly (**Supplementary Figure 4**), a feature that is also common in mouse syngeneic studies (88). We wondered if the HIS anti-tumoral response contributes to this variability. Since time points differed between experiments, tumor weight or volumes measured at a specific time do not accurately reflect tumor growth in our study. Therefore, we calculated the specific growth rate (SGR, see material and methods section) for each tumor, which represents the growth of the tumor considering initial and ending times and volumes.

We first analyzed the effects of the HIS on the SGR in individual vehicle (untreated) mice from five CRC experiments (B2, D2, D3, E, F) (**Figure 6A**). We observed no difference in the growth of tumors relative to the $hCD45^+$ or T cell chimerism in the blood prior to tumor injection or number of human cells in the LNs or spleen at end of study. However, we did notice a negative correlation between SGR and percentage of $hCD45^+$ cells in the spleen and number of T cells in secondary lymph organs. Indeed, the number of CD8+ T cells in the LNs and CD4+ T cells in the spleen were the strongest predictors of slower-growing tumors in our analysis. Thus, we speculate that a T cell-driven response may be influencing tumor growth in HIS-BRGS mice; however, this effect is relatively marginal as the tumors continue to grow, albeit at different rates.

In this same series of CRC experiments, we secondly analyzed HIS-BRGS mice that had been treated with an ICB combination therapy for at least two weeks (**Figure 6B**). In this case, we found that the frequency of T cells in the PBMCs prior to tumor injection correlated with tumor growth rates. In these treated mice, the tumors were overall smaller in size, with lower SGRs, supporting a successful combination ICB therapy response (manuscript in preparation). In this ICB-treated cohort, the human chimerism in the immune organs at end of study had no significant influence on the tumor growth rates. Thus, the effect of T cell responses on tumor growth in untreated HIS-BRGS mice is not that obvious in ICB-treated HIS-BRGS tumor-bearing mice, where an overwhelming immune response might be masking its influence.

Correlates of Immune Response

A major objective in cancer immunotherapy studies is to understand why some patients respond and others do not, in an effort to define predictive biomarkers of response and prognosis. Many recent high-impact studies have focused on determining immune properties that correlate with therapeutic response (53–55, 89–94). These studies have been performed in mouse models and/or clinical trials using PBMCs and rarely tumor tissue following treatments. With our tissue availability, we designed multiple flow cytometry panels, to evaluate 1) the immune subsets in the HIS-mice (**Supplementary Figure 1**), 2) the activation state of the T cells including the upregulation of HLA-DR and PD-1 or TIM-3 inhibitory receptors, as well as the frequency of Treg, naïve, T_{EM} and T_{CM} populations (**Figure 3**), 3) the cytotoxic T cell effector function as determined by production of GrB, TNFα and IFNγ (**Figure 7A**), and 4) Ag presentation molecules and inhibitory receptors on the tumors (see section 8) (23).Using these flow panels, we have analyzed immune correlates in two ways: 1) by treatment groups or 2) by tumor response (SGR).

In previous studies we used the first approach to establish immunotypes among anti-PD-1 treated HIS-BRGS mice (23, 48, 49). Here we apply this strategy to immune responses following

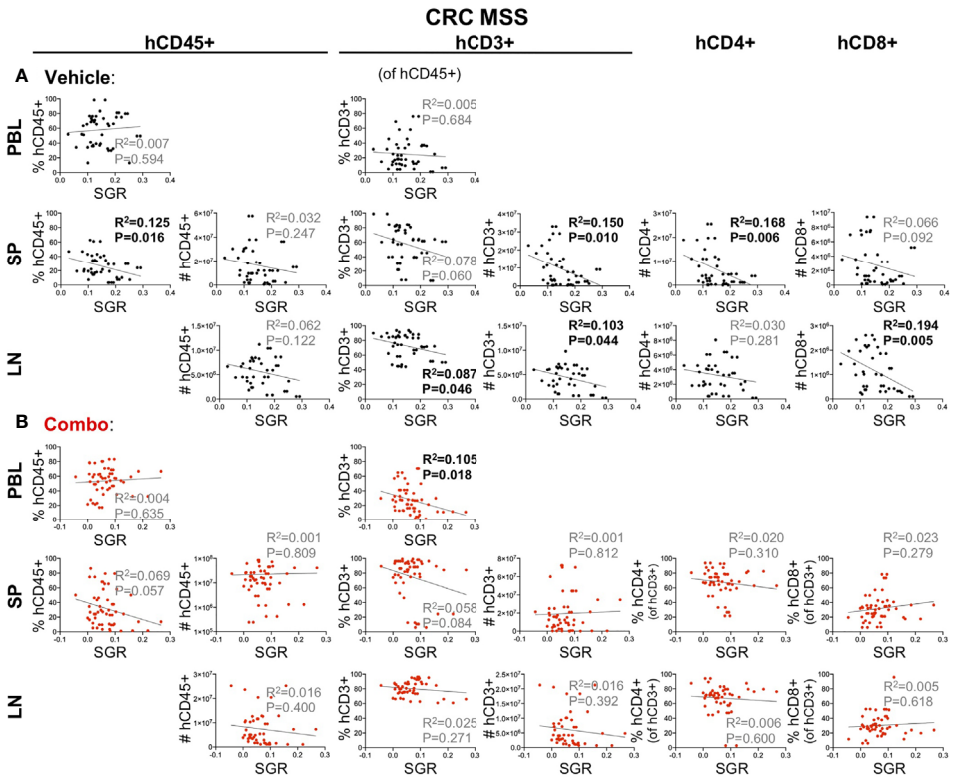

FIGURE 6 | Correlation of tumor growth and human chimerism in lymph organs for 5 CRC MSS PDX models (B2, D2, D3, E, F) in HIS-BRGS mice receiving either no treatment **(A)** or a combination immunotherapy **(B)**. Linear regression analysis was performed between tumor specific growth rate (SGR) and immune cell populations in the blood prior to tumor injection (PBL at 15 weeks) or in the spleen (SP) and lymph nodes (LN) at end of study. [Linear regression analysis, R-squared score (R^2) and P value (P) in bold if statistically significant ($P < 0.05$)].

combination immunotherapies. We observed increased frequencies of $hCD3^+$ T cells in the tumors of DLBCL B CDX from mice in the combination-treated group. Furthermore, we observed trends of increased CD8+ T cells, GrB^+CD4^+ and $IFN\gamma^+CD8^+$ among the T cells infiltrating the combo-treated tumors, although the data were not statistically significant in all cases among this small sample with variable responses among the combination-treated group (**Figure 7B**). As stated earlier, another likely source of variability in our system is the CB. Human HSCs harbor genetic variation and we have found that the human chimerism, both the kinetics and amounts, can differ by CB batch. We have generated >60 mice from some CB HSCs, and in these cases, we have used HSCs from the same CB for different experiments. Two distinct CRC MSS PDXs ("H" and "I") were implanted in mice generated from the same CB, and then treated with the same drugs. We observed similar human infiltrations (see H and I in **Figures 2A, B**), yet distinct immune responses (**Figure 7C**). Using the first approach, only "H" CRC model showed increased human infiltration upon combination immunotherapy. In contrast, we observed a significant decrease in Treg frequencies in both PDXs after treatment. Remarkably, PDX "I" showed increased $TNF\alpha^+$ $CD4^+$ T cells whereas PDX "H" had enriched GrB^+ $CD4^+$ and T_{EM} $CD8^+$ populations.

Using the second (SGR) approach, we sought to elucidate whether an immunotype, as opposed to the human chimerism (see section 6 and **Figure 3**), was associated with lower tumor growth rates. This approach is more akin to studying immune correlates of responders versus non-responders in clinical trials. We used the series of five CRC PDXs (B2, D2, D3, E, F) treated with the same combination immunotherapy for this analysis. We established that activated HLA-DR^+ $CD4^+$ T cells in the tumors were the best predictors of tumor growth inhibition, in line with the analyses by treatment groups (**Figure 7D** and manuscript in preparation). Interestingly, using this same approach to evaluate an innate response to the tumors by the HIS in untreated mice in this model, revealed that a lower SGR correlated with increased $IFN\gamma^+$ $CD4^+$ T cell and decreased myeloid and $TNF\alpha^+$ $CD8^+$ immunotype (**Supplementary Figure 6**). We further assessed the CB effect by studying two DLBCL CDXs ("A2" and "B") implanted into HIS-BRGS mice generated from the same CB. We found that CDX "B" had tumor growth inhibition upon combination immunotherapy (**Figure 7B**) while CDX "A2" did not (**Figure 7E**). By analyzing the T cell infiltration and frequency of $IFN\gamma^+$ CD4 and CD8 T cells for model "A2", we found that increased T cells in the tumors, most notably the $IFN\gamma^+$ CD8 T cells, correlated with slow-growing tumors (**Figure 7E**). In this experiment, one of the three untreated mice

appeared to have robust tumor growth inhibition in both flanks, illustrating the need for sufficient number of mice per treatment group.

Thus, we demonstrated that we can observe immunotypes that correlate with drug regimens and tumor responses in our HIS-BRGS tumor-bearing mice. Notably, these immunotypes can be unique to different tumors or combination treatments, even with the same CB.

Evaluation of Tumor Immunogenicity

The TME plays an active role in suppressing the immune system, oftentimes by decreased Ag presentation. To evaluate the effect of

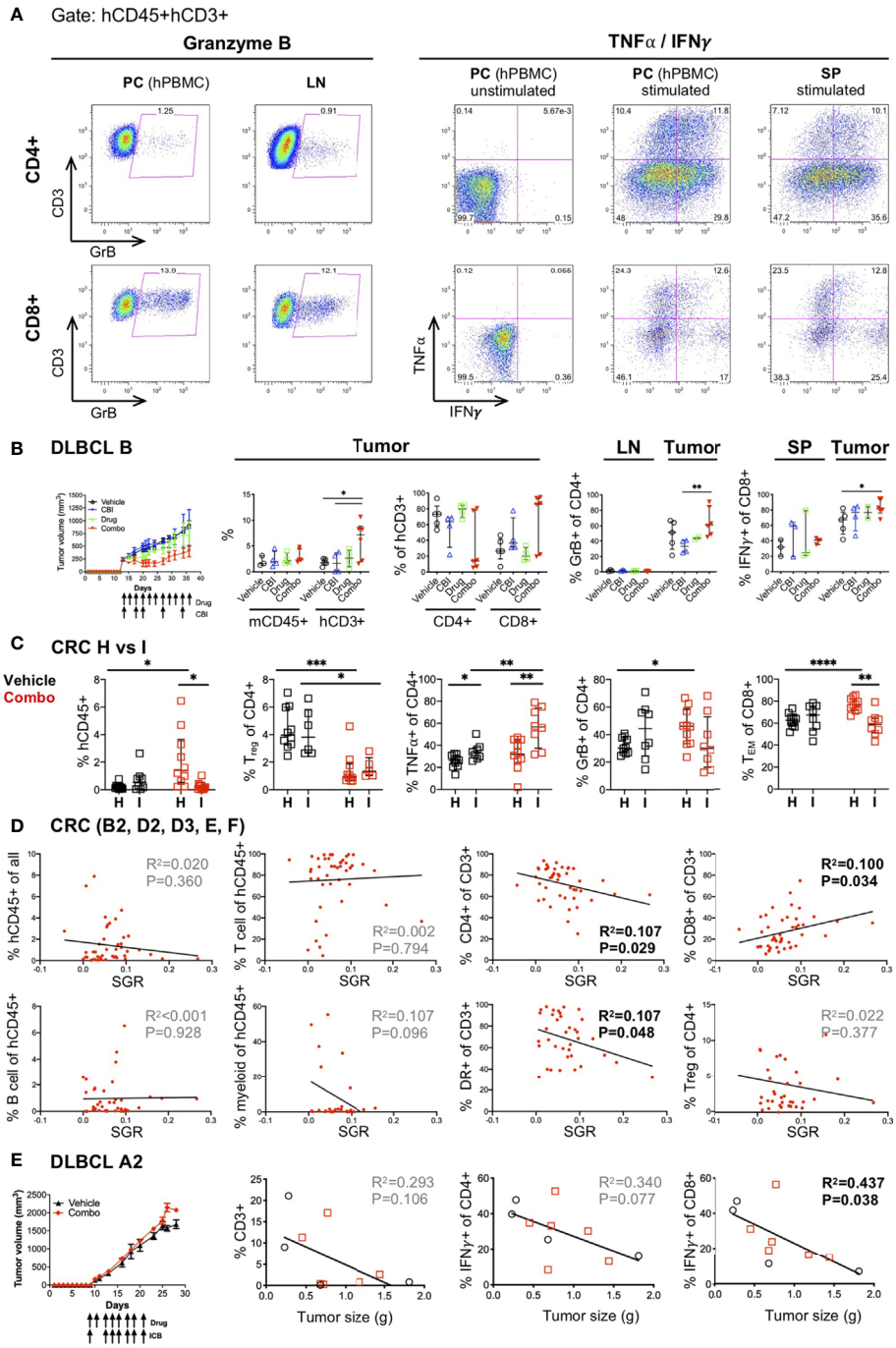

FIGURE 7 | Continued

FIGURE 7 | Correlates of immune response to human tumors following combination immunotherapy treatments in HIS-BRGS mice. **(A)** Representative flow cytometry plots showing expression of Granzyme B (left) and TNFα and IFNγ cytokines (right) in CD4$^+$ (top row) and CD8$^+$ T cells (bottom row). Cells are cultured overnight with cell stimulation and blocked with Golgi Plug for final four hours to detect TNFα and IFNγ. Human PBMCs serve as technical staining control, and as stimulation controls for TNFα/IFNγ. **(B)** Tumor growth and immune response in HIS-BRGS mice with DLBCL CDX B tumors treated with monotherapies and combination ICI therapies. Tumor growth curves over time (left panel) and frequencies of mCD45$^+$, hCD3$^+$, CD4$^+$ T, and CD8$^+$T cell populations (left graphs), and GrB$^+$CD4$^+$ T cells and IFNγ$^+$CD8$^+$ T cells (right graphs) in indicated tissues. **(C)** Immune correlates of combination immunotherapy response to two CRC MSS PDXs in HIS-BRGS mice, generated from same CB. Infiltration of hCD45$^+$ cells (left), and frequencies of Tregs, TNFα$^+$CD4$^+$ T, GrB$^+$CD8$^+$ and T_{EM} CD8$^+$ cells in CRC (H, I) PDXs in HIS-BRGS mice. **(D)** Correlation of immunotypes and tumor growth (SGR) in a series of five independent experiments of HIS-BRGS mice bearing CRC MSS PDXs (B2, D2, D3, E, F) and treated with the same combination immunotherapy. The frequency of human (hCD45$^+$), T (CD3$^+$), CD4$^+$ T, CD8$^+$ T, B (CD19$^+$), and myeloid (CD11b$^+$, CD11c$^+$, CD14$^+$ or CD33$^+$) cells (top rows), and the frequency of activated (HLA-DR$^+$) T cells (2nd row, 3rd panel) and Tregs (2nd row, 4th panel) in CRC PDX relative to the specific growth rate (SGR) for that tumor. **(E)** Tumor growth and immune correlates in HIS-BRGS mice with DLBCL CDX A2 tumors and treated with same combination ICI therapy as in **(B)**. Tumor growth curves over time (left panel) and correlations of tumor size with frequency of CD3, IFNγ CD4$^+$ and IFNγ CD8$^+$ in DLCBL A in HIS-BRGS mice. Symbols represent data from an individual tissue from tumor-bearing HIS-BRGS mouse that are untreated (black), treated with ICB (blue) alone, drug alone (green), or combination ICB (red). $^*p < 0.05$, $^{**}p < 0.01$, $^{***}p < 0.001$, $^{****}p < 0.0001$ reflects significance test between two groups at edge of line. [**(B,C)**: Two-group t-test with Welch's correction, two-tailed; with the exception of % mCD45 and % of hCD3+ (CD4+ and CD8+) in the tumor, which was evaluated with non-parametric test due to confirmed non-normal distribution in the "combo" group. **(D, E)**: linear regression analysis, R-squared score (R^2) and P value (P) in bold if statistically significant (P<0.05)].

treatments on the TME in our HIS-BRGS mice, we measured the expression of both class I (HLA-ABC) and II (HLA-DR) MHC molecules on the tumor cells by flow cytometry. We consistently observed low MHC I and II expression on human cells in tumors, and even more so on the tumor cells themselves (**Figure 8A**) (23, 48). However, we have previously reported upregulation of HLA-ABC and HLA-DR on tumors following immunotherapy treatment (23). We observed both increased MHC class II expression in slow-growing CRC MSS models (**Figure 8B**) and increased MHC class I expression in smaller and T cell-enriched DLBCL "A2" tumors (**Figure 8C**). In these DLBCL tumors, increased IFNγ expression by CD8 T cells similarly correlated with slow-growing lymphomas, consistent with reports showing upregulation of MHC genes by IFNγ responsive genes and increased tumor response (**Figure 7E**) (95–97). Furthermore, ICB success has been related to PD-L1 expression in the tumor for some tumor types (98), so we measured the relative MFI expression of PD-L1 inhibitory receptor on the tumor cells and found no significance in the CRC MSS models (**Figures 8A, B**).

Mouse Immune Myeloid Subsets in Tumors of HIS-BRGS Mice

Mouse immune cells, which are strictly of the myeloid lineage due to the absence of T, B, NK and ILC lymphocyte populations, have been often ignored in HIS-mouse studies, with few exceptions (99). However, they represent the dominant

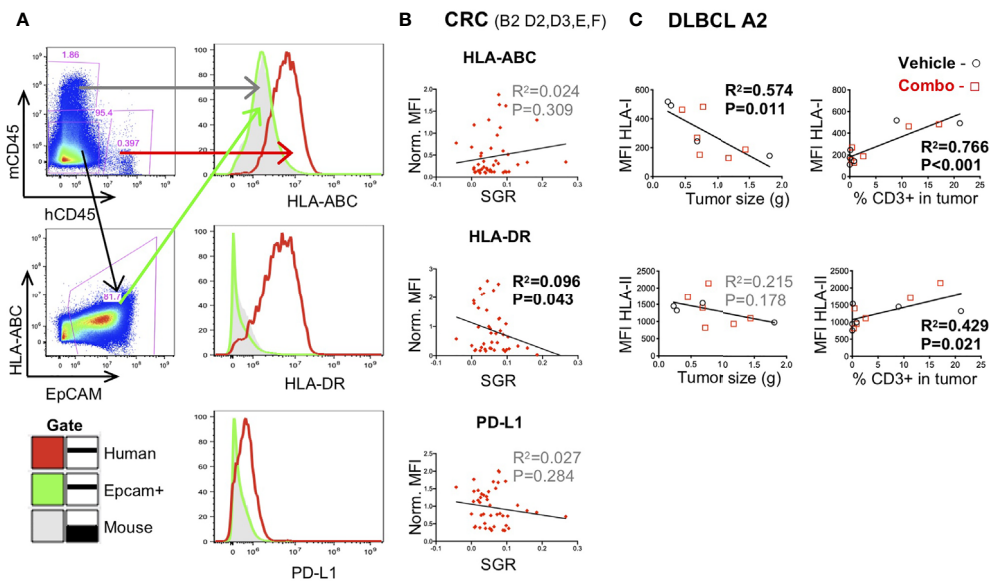

FIGURE 8 | Expression of immune-related molecules on human tumors in HIS-BRGS mice. **(A)** Representative flow cytometry plots illustrating gating for expression on the tumors: mCD45$^-$ hCD45$^-$ cells are gated in the tumor cell suspension and when possible, a tumor-specific Ag (e.g. EpCAM) is included, **(B)** Correlation of tumor growth rates with expression of human HLA-ABC (MHC Class I), HLA-DR (MHC Class II) and PD-L1 on hCD45$^-$mCD45$^-$EpCAM$^+$ CRC MSS PDX (B2, D2, D3, E, F) in HIS-BRGS mice. **(C)** Correlation of tumor weight (grams) and human T (hCD3) cell infiltration with expression of human HLA-ABC (Class I) and HLA-DR (Class II) on DLBCL CDX A2 in HIS-BRGS mice. Expression of HLA-ABC, HLA-DR and PD-L1 on hCD45$^+$ and mCD45$^+$ populations serve as positive and negative controls, respectively. [Linear regression analysis, R-squared score (R^2) and P value (P) in bold if statistically significant (P < 0.05)].

myeloid population and therefore likely play a role in Ag presentation to the HIS and in TME immunomodulation. As with other immune cell types, myeloid cells are composed of multiple sub-types, with immunostimulatory or inhibitory functions (100, 101). We enumerated the frequency of mCD45$^+$ cells in tumors excised from HIS-BRGS mice with flow cytometry. We observed more mCD45$^+$ cells than hCD45$^+$ cells, indicating a predominant myeloid rather than lymphocytic infiltration in tumors. In addition, we observed a narrower range of mCD45$^+$ infiltrating cells than hCD45$^+$ cells across all tumor types (**Figure 9A** compared to **Figure 4B**, mCD45+ range 0.1-100, hCD45+ range 0.001-100). The variability was similar for both hCD45+ and mCD45+ cell infiltrations into the TNBC A1-A6 experiments (p=0.022, Welch's ANOVA) but higher variability was observed among the CRC MSS PDX models (p=0.0028 for hCD45+, p<0.0001 for mCD45+, Welch's ANOVA), suggesting differences among PDX TMEs. We found much higher infiltration of mCD45$^+$ cells in the PDAC and some CRC models, tumors that are resistant to immunotherapy and may contain a dominant myeloid immunosuppressive population, represented by mCD45$^+$ cells in our model. On the other hand, the Lynch syndrome-associated ACC PDX "A2" had a higher ratio of hCD45$^+$/mCD45$^+$ cells relative to other tumors (**Figure 9A**). The decreased mCD45$^+$ presence may be relevant to the positive ICB immunotherapy response in this model (48).

In our experience, we routinely notice two distinct populations of mouse cells: a mCD45^{hi} and a mCD45^{lo}. We stained the mouse cells with GR1, F4/80 and Ly6G to distinguish granulocytes (polymorphonuclear, PMNs), defined as mCD45 (hi)GR1$^+$F4/80$^-$or Ly6G$^+$ from macrophage lineage, mCD45(int) GR1$^-$F4/80$^+$Ly6G$^-$ (**Figure 9B**). We found that neutrophils were a minor population in the LNs, intermediate in the spleen but dominant in the bone marrow, consistent with physiological distribution in mice or humans. However, the frequency of mouse neutrophils in the tumors were tumor-dependent, with very high populations in a non-responsive CRC and low frequencies in ICB-responsive TNBC. We next queried whether the expression of mouse MHC molecules was altered in tumors of these mice, as is common for myeloid TILs. We stained the mCD45+ cells for expression of mouse MHC Class I (anti-H-2) and MHC Class II (anti-I-A/I-E) (**Figures 9C, D**). We found that the expression of mouse MHC molecules was highest in the LNs and was actually downregulated in the spleens and, even more so, in the bone marrow of HIS mice. In all cases the expression was lower (ratio <1.0) than that from a wild-type

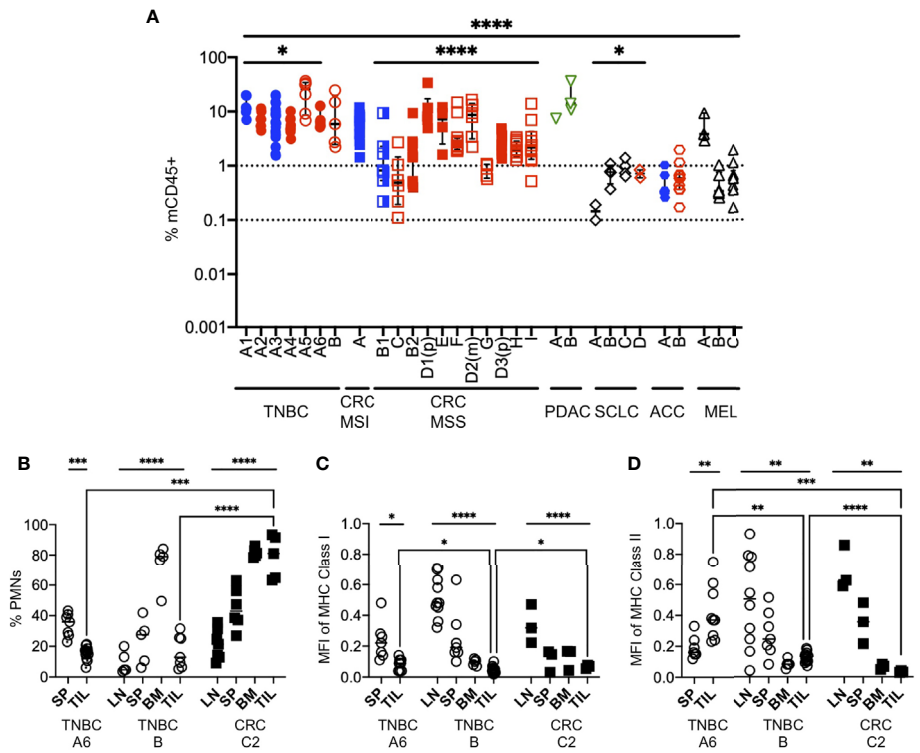

FIGURE 9 | Mouse myeloid cells in human tumors of HIS-BRGS mice. **(A)** Infiltration of mCD45$^+$ cells into human PDX or CDX in HIS-BRGS mice, same tumors as for **Figure 4B**. *$p < 0.05$, ****$p < 0.0001$ [Welch's ANOVA among means within experiments with same tumor type or across tumor types, lines indicated the tumors included in the analysis] **(B)** Frequencies of mouse neutrophils (PMNs) in lymph tissues and human tumors (TNBC, CRC). Normalized expression (geometric mean fluorescence intensity) of mouse MHC Class I **(C)** and MHC Class II **(D)** expression in total mCD45$^+$ cells. Expression was normalized to mCD45$^+$ positive control cells for each day for comparison. *$p < 0.05$, **$p < 0.01$, ***$p < 0.001$, ****$p < 0.0001$ [(**B–D**: Upper lines show two-group t test or Welch's ANOVA among means of different organs in the same experiment. Two-group t-test with Welch's correction were performed between the means of TILs (brackets)].

mouse, which we used as normalization control. Furthermore, the expression of MHC class I was lowest in the TILs of the mouse, regardless of tumor type (TNBC or CRC, **Figure 9C**). Similar to MHC Class I, MHC Class II expression was lower in TILs of both the TNBC PDX and CRC PDX mice; however, it was higher in the TNBC CDX tumor relative to the spleen (**Figure 9D**). Together, these data support a likely immunosuppressive role of the mouse $CD45^+$ cells in the TME of the implanted tumors.

DISCUSSION

Here we present our studies testing human immune responses to human tumors, in our HIS-BRGS mouse model. The model is powerful in its ability to test a variety of tumors (either CDX or PDX), each harboring their own individual genotypes and corresponding mechanisms of immune evasion. The acceptance of these tumor allografts in the presence of a HIS with both innate and adaptive arms of the immune system represents a central paradox of this model. These tumors are immunologically allogeneic to the HIS that has developed in the murine host from a non-HLA matched HSC donor (CB or fetal liver in most cases, as adult tissues yield few $CD34^+$ cells) (61). We consider this the beauty (the coveted ability to study human tumors in the presence of a HIS in a small animal model) and the beast (the lack of rejection of the allogeneic tumors) of the system. Thus, a significant question remains to be solved: why does the human immune system in these mice not reject the human tumors? In our preliminary data, we found that tumors can grow if implanted early or late after engraftment, i.e. in the presence of human T cells. The tumor acceptance suggests that the HIS in these mice is impaired and incapable of mounting an adaptive immune response to reject the tumor. This response could be explained by 1) an immature, uncoordinated immune system that lacks proper human-specific cytokines, chemokines and receptor interactions, or 2) a highly activated and immunosuppressed immune system. Several publications reveal the lack of robust T cell dependent immune responses to immunological challenges in HIS mice (36, 51). B cells are also reported to not fully develop (43, 102), although in older HIS-mice, mature B cells are found in the spleen, and are abundant in the LNs (56). Histological analyses show suboptimal TB coordination, typically associated with poorly formed germinal centers (43, 56). However, in our studies of HIS-mice spanning more than a decade, we find signs of robust, yet admittedly still incomplete, HIS responses if evaluated months after engraftment (56).

We present data supporting that this lack of allograft rejection is due in part to the immunosuppressed nature of the HIS in these mouse models, and not merely an immature immune system. Many T cells in HIS-mice are of the memory phenotype, more like a human adult than a newborn (56, 103). This activation appears to be Ag-driven and not merely the result of lymphopenia-induced activation as 1) it occurs months after engraftment, and 2) the presence of many $CD28^-$ T cells, which are the result of late-stage Ag-activation (data not shown) (103). Notably, both $CD4^+$ and $CD8^+$ T cells are highly activated and express abundant inhibitory receptors such as PD-1 and TIGIT, yet less TIM-3. We have observed an increase of exhausted T cells over time with increased PD-1 expression with age (23). Importantly, the ability of the T cells to recover from exhaustion has been shown through administration of anti-PD-1 Abs that have correlated with reduced tumor burden for certain human tumors and even EBV-induced lymphomas (23, 48, 50, 104, 105). This feature suggests that a mature HIS can develop in these mice with the ability to mount adaptive immune responses; however, exhaustion must first be overcome. The exact nature of this immunosuppression in HIS mice is still unknown, although it likely relates to the xenogeneic nature of thymic selection.

We conclude that tumor immunotherapy studies in these HIS-mouse models are best suited to test the ability of a treatment to inflame a tumor. The treatment must also release the inherent immunosuppression in the HIS-mouse. Tumor growth inhibition and changes in immune responses in the tumors represent the experimental readouts. However, the validation of this model relies on its' ability to distinguish the release of immunosuppression among therapies and individual human tumors, i.e. if all tumors respond equivalently the model is not useful.

Immune Responses to Individual Human Tumors Are Unique in HIS-BRGS Mice

Tumors evolve distinct mechanisms of immune evasion, including limited access of the immune system to the tumor, accumulation of immunomodulating cells, or increase in immunosuppressive molecules (12). A valid representation of a TME is essential to an immunotherapy-based preclinical model and is the appeal of any *in vivo* setting, as the TME is very difficult to truly replicate *in vitro* (16, 17, 31). Here, we present flow cytometry data showing human cell infiltration varies by tumor type. This is similar to studies evaluating HIS infiltration by IHC or flow cytometry in the same (44) or a similar (84) model. In all cases, the infiltration of the human lymphocytes is lower than that of the $mCD45^+$ myeloid cells, a situation similar to the accumulation of myeloid lineage cells in human tumors. However, in most cases the relative patterns of mCD45+ infiltration into individual tumors mirrored that of the $hCD45^+$ cells, supporting a tumor-dependent influence of immune infiltration *in vivo*. We have observed a few examples supporting that some ICB-responsive tumors have increased infiltration in our model (TNBC A1-6 and Lynch syndrome-associated ACC A) (23, 48). Furthermore, three SCLC tumors appeared "cold" with very little infiltration, even mCD45+ cells, a phenotype consistent with their limited response to ICB treatments in clinical trials (106). We also demonstrated more reproducible $hCD45^+$ and mCD45+ infiltration in tumors from the same origin (e.g., TNBC A1-6) compared to tumors from distinct PDXs (e.g. CRC MSS), that showed higher variability in immune cell infiltrations, reflecting the unique phenotype of each tumor. The differences in immune infiltration observed in repeat experiments (e.g. TNBC A1-A6, CRC D1P/D3P) are small

compared to differences in average infiltrations across all tumors ($p<0.0001$); however, these differences do reflect the limitations of the model. We suggest that differences in human chimerism, CB donor genetics or changes in the tumor characteristics with passages in culture or mice are contributing factors to this variability. More replicates with different batches of HIS-mice are necessary for confirmation. Collectively these data support the ability of HIS-mouse models to represent the unique properties of individual human tumors.

The results of our study suggest monitoring the immune response may be more informative, or at least complementary, than the actual tumor growth in HIS-BRGS oncology models. Although we achieved high tumor take rates for most models, we observed an effect of chimerism on the growth of individual tumors, even in the absence of treatments. The presence at end of study of cytotoxic T cells in the lymph organs of mice with slow-growing tumors supports a role of the HIS in controlling the allogeneic tumor growth. Thus, tumor growth curves might be influenced by HIS responses in the untreated group.

On the other hand, we consistently detect changes in individual immune parameters among treatment cohorts, even with similar average growth rates. The differences among groups show statistical significance even in experiments with as few as 3 or 4 HIS-mice per group (i.e. typically>5 tumors). Furthermore, when the immune parameters were correlated to the SGR, we did observe the tumor size as a function of the immune response, e.g. smaller tumors appeared to be enriched in $CD4^+HLA\text{-}DR^+$ T cells in HIS-CRC-BRGS mice treated with combination immunotherapy. This correlation held up over 5 independent CRC PDXs treated with the same drug combination, although to varying degrees. Our studies testing another combination immunotherapy for CRC MSS highlight the influence of individual tumors on immune responses, as seen in distinct GrB^+ T_{EM} $CD8^+$ versus $CD4^+TNF\alpha^+$ driven responses to another tumor (CRC H,I; **Figure 7C**). These mice were generated from the same CB, and injected one week apart, leaving the PDX as the largest experimental variable in this case. To further illustrate this point, we have previously reported an increased $CD8^+IFN\gamma^+$ signature upon treatment with anti-PD-1 Ab (nivolumab) to both a TNBC CDX and CRC MSI-H PDX, similar to reports from studies in mouse models or human trials (23, 73, 91, 95, 107). In another study, increased $CD8^+GrB^+TIM\text{-}3^+CD28^-$ cells correlated with smaller ACC tumors that had been treated with pembrolizumab, also an anti-PD-1 Ab (48). It is interesting to note that we can observe either or both $CD4^+$ or $CD8^+$ T cell responses in different scenarios. The importance of $CD4^+$ T cells in a tumor immune response is gaining acceptance (108), and clinical trials and syngeneic mouse model studies have similarly identified distinct immune correlates (53, 54, 94, 109, 110). As in clinical trial studies, these data are strictly correlative. In our studies, the immune correlates are most significant among human T cells in the TILs, with a few exceptions in which we have observed systemic treatment effects in either the LN or spleen. The ability to test the responses in secondary lymph organs, and even more importantly in the tumors, is a major advantage of this model. In clinical trials, the amount of tumor tissue is often limited to less-quantitative IHC analyses while the systemic immune system is limited to the blood.

A further advantage of the HIS-model for immunotherapy studies is the ability to evaluate the cancer cells themselves. We have detected increases in human HLA molecules and changes in inhibitory receptors such as PD-L1, that are consistent with increased IFNγ responses. Integrating these data with spatial information from IHC (or other techniques) can provide valuable information on cell interactions within the TME, as we have previously reported (23, 48).

All-in-all, this study supports the use of HIS-BRGS model to evaluate immune responses to distinct therapies for a wide repertoire of individual tumors. In this model, the activation of the T cells requires release of the inherent immunosuppression, a condition that may mirror the suppressed immune system in a tumor.

Considerations for Experimental Design Using HIS-CB-Mouse Models

We acknowledge the limitations of the model and strongly advise consideration of engraftment and reconstitution details, particularly the late appearance of human T cells and LNs. In our hands, the model has an optimal experimental window, typically between 18 and 30 weeks of age, to test T-cell directed immunotherapies. Therefore, timing of tumor injections is critical and should be designed to insure 1) adequate T cells (typically >18 weeks in our lab) at time of treatment, and 2) a multi-lineage immune system, as B cell and myeloid populations are less frequent in older mice (typically >30 weeks). Each laboratory should test their own kinetics and long-term engraftment, as they may differ due to model and experimental protocols. For xenografts with slow growth rates, we suggest implanting early so they establish at around 18 weeks of age. This often requires testing growth rates in immunodeficient mice prior to use in HIS-mice. We have also shown that the human T cell chimerism affects the degree of human immune infiltration into tumors, and even limited control of tumor growth by the HIS in the absence of therapies. Thus, it is important to control for this variability in experimental design: our approach is to allocate mice into equivalent groups based on human, T cell, and CD8 frequencies. More recently, we have used the matched animal analysis (MANILA) software for random group allocation and treatment assignment, guaranteeing balanced interventions according to these parameters (111). The generation of HIS-mice from distinct CB units is another source of variability that should be considered. As in humans, but not syngeneic mouse models, the immune system in HIS-mice is genetically unique. However, unlike humans, the environment of these mice is well controlled in terms of age and immune exposures. Wang et al. analyzed studies in HIS-mice prepared from different CBs, but injected with the same tumors (50). They concluded that CB genetics were responsible for differences in tumor growth outcomes in these studies, although they did not test the influence of human chimerism. They also determined that the HLA match of the CB to the

tumor had little contribution, not surprising since there was a maximum of 4 HLA matches, leaving a large alloreactive T cell repertoire (50). Although we have not formally addressed this parameter, we provided examples illustrating differences in immune responses to unique CRC or DLBCL tumors in our HIS-BRGS models that were treated with the same therapies in mice generated from the same CB. In conclusion, our numerous studies testing immunotherapy treatments on human tumors in HIS-BRGS-mice highlight the inherent variability in the system that includes: 1) age of mice and corresponding immune system (T cells develop late), 2) human chimerism, 3) CB donor and 4) the human tumor. Our experimental approach strives to minimize these variables, stressing the differences in human tumors.

Another important consideration in any study of immune correlates to an immunological challenge (tumor, pathogen, vaccine) is the kinetics of the response. Each data point represents a snapshot in time of the immune response. It is well appreciated that this response is a dynamic and complex process that includes a typical early activation event. The fate of individual cells is unique, as some will become non-functional or die, some will become memory, and some will proliferate and become effector cells, secreting a variety of cytokines. On a single-cell level, changes in activating and inhibitory receptors ensue along with transcriptional and epigenetic reprogramming. Analyses of immune correlates at a single point in time, whether on a single cell or a population level, provide an "aerial" view of the immune system. In our model, the difference in tumor growth rates and the work required on harvest day, limits our analyses to typically 4-8 mice on a single day. We have the added challenge that the immune system in the mice changes over time. Therefore, it is likely that our observed immune responses may be impacted by different timepoints: for example, more TIM-3 expression may represent a more exhausted response (i.e. TIM-3 is upregulated after PD-1 in an activated T cell). We do attempt to analyze similar numbers of mice from each experimental cohort on each day.

Flexibility of HIS-Mouse Models

Immunotherapy research and technology advance at a brisk rate and preclinical models must follow the pace. This HIS-mouse model offers the opportunity for in-depth mechanistic study of the kinetics of anti-tumor immune responses. Given that we can generate 60 HIS-mice from the same CB, implant the same tumor, and evaluate both lymph tissues and tumors from the same mouse, experiments can be designed to evaluate the response in cohorts from various interventions, at defined time points. We have done this in a limited fashion with a nivolumab treatment of MDA-MB-231 CDXs and found that the response is indeed distinct over a 10-day period, with a significant increase of $CD8^{+}IFN\gamma^{+}$ T cells observed only after 21 days of treatment (23). The model offers the flexibility to similarly test dosing regimens. Single cell flow, mass cytometry, RNAseq, and ATACseq techniques can be utilized for in-depth immune and tumor characterization as well. Depletions of immune cell populations, such as $CD8^{+}$ T cells, have also been performed in these HIS-models, to garner mechanistic information concerning the roles of distinct immune populations (50). An additional approach with the HIS-mouse model is the ability to genetically manipulate the HSC prior to "humanization," and thus track a tumor-specific T cell receptor (112) or test the role of distinct genes in a response (e.g. knock-out IFNγ). Likewise, a human CDX can be genetically manipulated to test the role of a cancer gene. In addition to ICB studies, HIS-mice have been used to test CAR T cells (113). We propose this model should support testing a range of immune-related therapies.

Thus, the HIS-models offer robust flexibility to study human immune responses to human tumors in a preclinical *in vivo* setting. It is important to note that a small animal model in a controlled facility will always have much less variability than a human trial. Furthermore, experimental replicates between treated and untreated animals are possible and provide increased experimental power. These studies in the HIS-model are limited mainly by their relative expense and technical challenge. In comparison to syngeneic mouse models, these mice are labor-intensive and require expertise in their use and evaluation. However, they are a fraction of the cost of a clinical trial. On the other hand, organoids represent an improved 3-D *in vitro* model for testing combination immunotherapies (114). As with any model, this model has advantages and disadvantages in its representation of the TME (115, 116). The ultimate validation as preclinical models for the testing of immunotherapy regimens is correlation to the success in the clinic. We have presented limited data showing clinical correlation: 1) a case study of a patient with ACC responding to pembrolizumab in the clinic and an immune response in a matched PDX in our HIS-BRGS mice (48), and 2) correlation of increased immune response and reduced tumor growth in nivolumab-treated CRC MSI-H PDX compared to CRC MSS PDXs, consistent with clinical trial data. We are currently testing an immunotherapy combination in our model on PDXs derived from patients in a clinical trial testing the same drug regimen. These correlations with clinical trials are necessary for true validation of the HIS mouse model for these studies.

Immune-related adverse events represent significant ICB-associated toxicities in the clinic (117). Indeed, HIS-mice have been reported to show indications of these toxicities upon administration of human ICB-drugs (118, 119). We are currently also testing the efficacy of the HIS-BRGS mice as a preclinical model for testing ICB-related toxicities in the presence or absence of a human tumor. In all experiments, we measure animal weights along with tumors and do observe significant loss of weight in very few mice and this does not correlate with treatment. We have observed occasional instances of ICB-related colitis/diarrhea and salivary gland changes in our experiments with this model; however, these are not in the majority of animals. The model offers the ability to analyze a wide array of tissues, to evaluate human immune infiltration by IHC, as an indication of autoimmune-infiltration. In our model, the HIS system is tolerant of mouse tissues due to its development and selection in the mouse thymus. Thus, the allo-response should be directed specifically to the allogeneic tumor upon release of immunosuppression. Immune reactivity to the mouse tissues would represent autoimmune responses.

Improvements to HIS-Mouse Models

As with all experimental models, HIS-mice harbor unique limitations that must be considered in the data interpretation. Specifically, the myeloid population is more variable in its chimerism than either the T or B lymphocyte populations in "basic" HIS-mouse models (67, 68, 120). We have found that their presence is more pronounced in tissues and indeed we have observed a much higher frequency of myeloid cells in tumor than in either LN or spleen (23, 48). To address this relative human myeloid deficiency in HIS-mice, several groups have generated immunodeficient recipients with transgenic human myeloid specific cytokines, including the NOD-scid IL2Rγnull-3/GM/SF (NSGS) (121) and MISTRG (68) models. Human tumors grow in NSGS mice and therefore this model has also been used for immunotherapy preclinical studies (122). The MISTRG model is best equipped to grow myeloid marker specific tumors such as Acute Myeloid Leukemia (123). However, there have been reports of short experimental windows and anemia associated with these models (69, 124). Alternative models to improve human myeloid reconstitution are immunodeficient mice harboring a mutation in the c-kit gene (NSGW41 or NBSGW) (125, 126). This mutation interferes with mouse myeloid production and allows increased human myelopoiesis due to lack of competition. Additional advantages to these models are the lack of irradiation required for engraftment, increased human erythropoiesis and increased HSC longevity in the mouse (99, 103, 124). We are in the process of testing the HIS-NBSGW strain for immunotherapy studies in an effort to develop a more representative HIS-mouse model with reduced myeloid mouse-to-mouse variability.

An additional and important limitation is the allogeneic nature of the implanted tumor. In the "basic" HIS-models T cell selection occurs typically on mouse MHC molecules (103, 127). Significant efforts have been made to include human MHC molecules in HIS-mice, in order to study Ag-specific responses. One approach has been incorporating human HLA transgenes in the recipient. The HLA-A2 NSG mouse recipient has been the most widely used of these models, due to the high representation of this allele in the general population (127, 128). One can thus select HLA-A2$^+$ CB or fetal liver samples to generate the HIS-mouse, and HLA-A2$^+$ tumors. Although this approach includes some tumor specific reactivities, there is still overwhelming alloreactivity to other HLA molecules, since T cells will also be selected on other mouse MHC molecules and react to the non-HLA-A2 human alleles. Another approach is to "knock-out" the mouse MHC genes and force selection exclusively on the human HLA (129). Hu et al. also transfected the HSC with a tumor-specific T cell receptor transgene prior to humanization. This system enabled studies of a human T cell response to a MART tumor-specific Ag (112). Although very relevant information can be garnered from this approach, tumor responses include multiple Ags of varying affinities (130). Furthermore, both CD4$^+$ and CD8$^+$ T cells influence the TME. Indeed, HIS-mice with both human MHC Class I and Class II transgenes showed greatly improved immune responses over either transgenic alone (131, 132).

Other groups have solved the T cell selection problem with the transplant of a thymus of fetal origin matched to the donor liver in the liver-thymus model (133). This system allows a complete histocompatibility match of the immune system and the thymus, especially if the mouse MHC is also absent. However, matching a tumor to this system has the same odds as a bone marrow transplantation, i.e. realistically improbable. Therefore, the tumor will still be allogeneic to the immune system. One must also keep in mind that a more functional HIS, as in both the liver-thymus and human HLA-transgenic mouse models, should react better to a human tumor that is not completely HLA-matched. Thus, the essential feature of growing a human tumor in a HIS-model may be compromised in these models. There are few reports of immunotherapy studies in either of these models, which may be indicative of compromised multi-lineage tumor growth, a concept that needs to be formally assessed (122, 134). In the end, a practical HIS-model may require balancing the most representative HIS with reduced natural immunity (rejection) of the tumor.

The ultimate goal for a preclinical small animal model is to make a true "avatar"- a mouse with a HIS generated from the same patient as the tumor (45). This would also require a matched thymus or some source of T cell selection. Practically speaking we are years away from this goal: 1) adult HSCs in unmanipulated blood do not generate human chimerism in immunodeficient mice (57) and therefore the HSCs from the patient, who often harbor inferior stem cells due to the disease, must be acquired from bone marrow stem cells, a population that generates inferior HIS-mice in both quantity and quality (45, 61, 135); 2) a matched thymus is required for proper selection of the T cells - the surgical acquisition of a matched thymus, which in adults is not present due to involution, is an obvious barrier, leaving the technologically-challenging induction of a thymic organ using induced pluripotent stem cells as the best option; and finally 3) the timing of generating these chimeras with matched tumors/thymus/HIS takes many months (minimum 6), a period that is too long for a practical personalized-medicine approach. In the meantime, the HIS-mouse immediately offers a model capable of testing combination immunotherapies and interrogating the immune responses to unique human tumors. This work suggests caution in experimental design to achieve optimal data.

DATA AVAILABILITY STATEMENT

The original contributions presented in the study are included in the article/**Supplementary Material**. Further inquiries can be directed to the corresponding author.

ETHICS STATEMENT

The animal studies were reviewed and approved by University of Colorado AMC Institutional Animal Care and Use Committee. All acquisition of human tumor samples were consented under IRB approvals as indicated in Materials and Methods.

AUTHOR CONTRIBUTIONS

JM-J, AC, and JL are responsible for the paper concept and overall experimental designs. JM-J, ML, and JL analyzed the data, wrote the manuscript, and prepared the figures. BF contributed acquisition of cord bloods. HY, CR, RT, ED, JES, RP, SGE, WM, MV, CL, JW, JRD, KK-V, and TP all contributed funding, experimental design and/or intellectual discussions. AC, ML, SB, SH, JS, NN, HY, CR, XW, JB, DG, AK, AY, DT, and JL all helped perform experiments in the HIS-BRGS mice. JS, JB, NN, ML, and JL generated and managed the humanized mouse colony. JES, RP, RT, TP, MV, JRD, and KK-V helped with editing of the manuscript. JM-J, JTD, and PB provided help with data analysis and statistics. All authors contributed to the article and approved the submitted version.

FUNDING

This work was supported by NIH NAIAD RO1 (I124474 and AI124474S, RP/JL), NCI RO1 (R01CA229259-01, CL), CPRIT Scholar in Cancer Research grant (RR160093, SE), DOD Career Development Award (CA191245, AC), NIH-NCI K08 (K08CA222620, KK-V) and Cancer League of Colorado, Golfers Against Cancer Award (KK-V).

ACKNOWLEDGMENTS

We are grateful to Christine Childs, Kristine Terrell, and Dana Davis at the University of Colorado Cancer Center Flow Cytometry Shared Resource for their tireless commitment to the flow cytometry instruments. We also would similarly like to acknowledge all of the Office of Laboratory Sciences staff at the University of Colorado Denver Anschutz Medical Campus vivarium who care for our mice. We thank the staff at Clinimmune for their professional communication and efforts to provide us with cord blood samples. We are grateful to Dexiang Gao, PhD Biostatistian, for help with statistical analyses advice. Finally, we thank John Reilly, Dean of the medical school, and John Cambier, Terry Frye, Aimee Bernard, and Lanette Schwarz for funding and directing the Human Immunology and Immunotherapy Initiative (HI3) that has supported the establishment of our humanized mouse core. We would like to thank James Di Santo and Helene Strick-Marshand for kindly providing the BRGS mouse strain.

SUPPLEMENTARY MATERIAL

The Supplementary Material for this article can be found online at: https://www.frontiersin.org/articles/10.3389/fimmu.2021.607282/full#supplementary-material

REFERENCES

1. Cancer Research Institute. *FDA Approval Timeline of Active Immunotherapies*. (2020) Available at: https://www.cancerresearch.org/scientists/immuno-oncology-landscape/fda-approval-timeline-of-active-immunotherapies.
2. Le DT, Durham JN, Smith KN, Wang H, Bartlett BR, Aulakh LK, et al. Mismatch repair deficiency predicts response of solid tumors to PD-1 blockade. *Science* (2017) 357(6349):409–13. doi: 10.1126/science.aan6733
3. Andre T, Shiu K-K, Kim TW, Jensen BV, Jensen LH, Punt CJA, et al. Pembrolizumab versus chemotherapy for microsatellite instability-high/mismatch repair deficient metastatic colorectal cancer: The phase 3 KEYNOTE-177 Study. *J Clin Oncol* (2020) 38(18_suppl):LBA4–4. doi: 10.1200/JCO.2020.38.18_suppl.LBA4
4. Rotte A, Jin JY, Lemaire V. Mechanistic overview of immune checkpoints to support the rational design of their combinations in cancer immunotherapy. *Ann Oncol* (2018) 29(1):71–83. doi: 10.1093/annonc/mdx686
5. Bommareddy PK, Shettigar M, Kaufman HL. Integrating oncolytic viruses in combination cancer immunotherapy. *Nat Rev Immunol* (2018) 18 (8):498–513. doi: 10.1038/s41577-018-0014-6
6. Chowdhury PS, Chamoto K, Honjo T. Combination therapy strategies for improving PD-1 blockade efficacy: a new era in cancer immunotherapy. *J Intern Med* (2018) 283(2):110–20. doi: 10.1111/joim.12708
7. Grosser R, Cherkassky L, Chintala N, Adusumilli PS. Combination Immunotherapy with CAR T Cells and Checkpoint Blockade for the Treatment of Solid Tumors. *Cancer Cell* (2019) 36(5):471–82. doi: 10.1016/j.ccell.2019.09.006
8. Joo SY, Chung YS, Choi B, Kim M, Kim JH, Jun TG, et al. Systemic human T cell developmental processes in humanized mice cotransplanted with human fetal thymus/liver tissue and hematopoietic stem cells. *Transplantation* (2012) 94 (11):1095–102. doi: 10.1097/TP.0b013e318270f392
9. Khalil DN, Smith EL, Brentjens RJ, Wolchok JD. The future of cancer treatment: immunomodulation, CARs and combination immunotherapy. *Nat Rev Clin Oncol* (2016) 13(6):394. doi: 10.1038/nrclinonc.2016.65
10. Melero I, Gaudernack G, Gerritsen W, Huber C, Parmiani G, Scholl S, et al. Therapeutic vaccines for cancer: an overview of clinical trials. *Nat Rev Clin Oncol* (2014) 11(9):509–24. doi: 10.1038/nrclinonc.2014.111
11. Raja J, Ludwig JM, Gettinger SN, Schalper KA, Kim HS. Oncolytic virus immunotherapy: future prospects for oncology. *J Immunother Cancer* (2018) 6(1):140. doi: 10.1186/s40425-018-0458-z
12. Murciano-Goroff YR, Warner AB, Wolchok JD. The future of cancer immunotherapy: microenvironment-targeting combinations. *Cell Res* (2020) 30(6):507–19. doi: 10.1038/s41422-020-0337-2
13. Sanmamed MF, Chen L. A Paradigm Shift in Cancer Immunotherapy: From Enhancement to Normalization. *Cell* (2019) 176(3):677. doi: 10.1016/j.cell.2019.01.008
14. Chambers CA, Kuhns MS, Egen JG, Allison JP. CTLA-4-mediated inhibition in regulation of T cell responses: mechanisms and manipulation in tumor immunotherapy. *Annu Rev Immunol* (2001) 19:565–94. doi: 10.1146/annurev.immunol.19.1.565
15. Okazaki T, Honjo T. PD-1 and PD-1 ligands: from discovery to clinical application. *Int Immunol* (2007) 19(7):813–24. doi: 10.1093/intimm/dxm057
16. Chulpanova DS, Kitaeva KV, Rutland CS, Rizvanov AA, Solovyeva VV. Mouse Tumor Models for Advanced Cancer Immunotherapy. *Int J Mol Sci* (2020) 21(11):1–15. doi: 10.3390/ijms21114118
17. Olson B, Li Y, Lin Y, Liu ET, Patnaik A. Mouse Models for Cancer Immunotherapy Research. *Cancer Discovery* (2018) 8(11):1358–65. doi: 10.1158/2159-8290.CD-18-0044
18. Sobczuk P, Brodziak A, Khan MI, Chhabra S, Fiedorowicz M, Welniak-Kaminska M, et al. Choosing The Right Animal Model for Renal Cancer Research. *Transl Oncol* (2020) 13(3):100745. doi: 10.1016/j.tranon.2020.100745
19. Ireson CR, Alavijeh MS, Palmer AM, Fowler ER, Jones HJ. The role of mouse tumour models in the discovery and development of anticancer drugs. *Br J Cancer* (2019) 121(2):101–8. doi: 10.1038/s41416-019-0495-5
20. Bjornson-Hooper Z, Fragiadakis G, Spitzer M, Madhireddy D, McIlwain D, Nolan G. A comprehensive atlas of immunological differences between

humans, mice and non-human primates. *bioRxiv* (2019) 1–13. doi: 10.1101/574160
21. Mestas J, Hughes CC. Of mice and not men: differences between mouse and human immunology. *J Immunol* (2004) 172(5):2731–8. doi: 10.4049/jimmunol.172.5.2731
22. Shay T, Jojic V, Zuk O, Rothamel K, Puyraimond-Zemmour D, Feng T, et al. Conservation and divergence in the transcriptional programs of the human and mouse immune systems. *Proc Natl Acad Sci U.S.A.* (2013) 110(8):2946–51. doi: 10.1073/pnas.1222738110
23. Capasso A, Lang J, Pitts TM, Jordan KR, Lieu CH, Davis SL, et al. Characterization of immune responses to anti-PD-1 mono and combination immunotherapy in hematopoietic humanized mice implanted with tumor xenografts. *J Immunother Cancer* (2019) 7(1):37. doi: 10.1186/s40425-019-0518-z
24. Carrillo MA, Zhen A, Kitchen SG. The Use of the Humanized Mouse Model in Gene Therapy and Immunotherapy for HIV and Cancer. *Front Immunol* (2018) 9:746. doi: 10.3389/fimmu.2018.00746
25. Kahkonen TE, Halleen JM, Bernoulli J. Immunotherapies and Metastatic Cancers: Understanding Utility and Predictivity of Human Immune Cell Engrafted Mice in Preclinical Drug Development. *Cancers (Basel)* (2020) 12(6):1–17. doi: 10.3390/cancers12061615
26. Morton JJ, Bird G, Refaeli Y, Jimeno A. Humanized Mouse Xenograft Models: Narrowing the Tumor-Microenvironment Gap. *Cancer Res* (2016) 76(21):6153–8. doi: 10.1158/0008-5472.CAN-16-1260
27. Politi K. Leveraging Patient-Derived Models for Immunotherapy Research. *Am Soc Clin Oncol Educ Book* (2020) 40:e344–50. doi: 10.1200/EDBK_280579
28. Tyagi RK, Li J, Jacobse J, Snapper SB, Shouval DS, Goettel JA. Humanized mouse models of genetic immune disorders and hematological malignancies. *Biochem Pharmacol* (2020) 174:113671. doi: 10.1016/j.bcp.2019.113671
29. Wege AK, Schmidt M, Ueberham E, Ponnath M, Ortmann O, Brockhoff G, et al. Co-transplantation of human hematopoietic stem cells and human breast cancer cells in NSG mice: a novel approach to generate tumor cell specific human antibodies. *MAbs* (2014) 6(4):968–77. doi: 10.4161/mabs.29111
30. Zumwalde NA, Gumperz JE. Modeling Human Antitumor Responses In Vivo Using Umbilical Cord Blood-Engrafted Mice. *Front Immunol* (2018) 9:54. doi: 10.3389/fimmu.2018.00054
31. Sanmamed MF, Chester C, Melero I, Kohrt H. Defining the optimal murine models to investigate immune checkpoint blockers and their combination with other immunotherapies. *Ann Oncol* (2016) 27(7):1190–8. doi: 10.1093/annonc/mdw041
32. Yip H, Haupt C, Maresh G, Zhang X, Li L. Humanized mice for immune checkpoint blockade in human solid tumors. *Am J Clin Exp Urol* (2019) 7(5):313–20.
33. Li Y, Di Santo JP. Modeling Infectious Diseases in Mice with a "Humanized" Immune System. *Microbiol Spectr* (2019) 7(2):1. doi: 10.1128/microbiolspec.BAI-0019-2019
34. Shultz LD, Lyons BL, Burzenski LM, Gott B, Chen X, Chaleff S, et al. Human lymphoid and myeloid cell development in NOD/LtSz-scid IL2R gamma null mice engrafted with mobilized human hemopoietic stem cells. *J Immunol* (2005) 174(10):6477–89. doi: 10.4049/jimmunol.174.10.6477
35. Theocharides AP, Rongvaux A, Fritsch K, Flavell RA, Manz MG. Humanized hemato-lymphoid system mice. *Haematologica* (2016) 101(1):5–19. doi: 10.3324/haematol.2014.115212
36. Tsuji M, Akkina R. Editorial: Development of Humanized Mouse Models for Infectious Diseases and Cancer. *Front Immunol* (2019) 10:3051. doi: 10.3389/fimmu.2019.03051
37. Walsh NC, Kenney LL, Jangalwe S, Aryee KE, Greiner DL, Brehm MA, et al. Humanized Mouse Models of Clinical Disease. *Annu Rev Pathol* (2017) 12:187–215. doi: 10.1146/annurev-pathol-052016-100332
38. Jespersen H, Lindberg MF, Donia M, Soderberg EMV, Andersen R, Keller U, et al. Clinical responses to adoptive T-cell transfer can be modeled in an autologous immune-humanized mouse model. *Nat Commun* (2017) 8(1):707. doi: 10.1038/s41467-017-00786-z
39. Lang J, Zhang B, Kelly M, Peterson JN, Barbee J, Freed BM, et al. Replacing mouse BAFF with human BAFF does not improve B-cell maturation in hematopoietic humanized mice. *Blood Adv* (2017) 1(27):2729–41. doi: 10.1182/bloodadvances.2017010090
40. van Rijn RS, Simonetti ER, Hagenbeek A, Hogenes MC, de Weger RA, Canninga-van Dijk MR, et al. A new xenograft model for graft-versus-host disease by intravenous transfer of human peripheral blood mononuclear cells in RAG2-/- gammac-/- double-mutant mice. *Blood* (2003) 102(7):2522–31. doi: 10.1182/blood-2002-10-3241
41. Ito M, Hiramatsu H, Kobayashi K, Suzue K, Kawahata M, Hioki K, et al. NOD/SCID/gamma(c)(null) mouse: an excellent recipient mouse model for engraftment of human cells. *Blood* (2002) 100(9):3175–82. doi: 10.1182/blood-2001-12-0207
42. Pearson T, Shultz LD, Miller D, King M, Laning J, Fodor W, et al. Non-obese diabetic-recombination activating gene-1 (NOD-Rag1 null) interleukin (IL)-2 receptor common gamma chain (IL2r gamma null) null mice: a radioresistant model for human lymphohaematopoietic engraftment. *Clin Exp Immunol* (2008) 154(2):270–84. doi: 10.1111/j.1365-2249.2008.03753.x
43. Traggiai E, Chicha L, Mazzucchelli L, Bronz L, Piffaretti JC, Lanzavecchia A, et al. Development of a human adaptive immune system in cord blood cell-transplanted mice. *Sci 2004* (5667) 304:104–7. doi: 10.1126/science.aan6733
44. Gammelgaard OL, Terp MG, Preiss B, Ditzel HJ. Human cancer evolution in the context of a human immune system in mice. *Mol Oncol* (2018) 12(10):1797–810. doi: 10.1002/1878-0261.12374
45. Morton JJ, Bird G, Keysar SB, Astling DP, Lyons TR, Anderson RT, et al. XactMice: humanizing mouse bone marrow enables microenvironment reconstitution in a patient-derived xenograft model of head and neck cancer. *Oncogene* (2016) 35(3):290–300. doi: 10.1038/onc.2015.94
46. Seitz G, Pfeiffer M, Fuchs J, Warmann SW, Leuschner I, Vokuhl C, et al. Establishment of a rhabdomyosarcoma xenograft model in human-adapted mice. *Oncol Rep* (2010) 24(4):1067–72. doi: 10.3892/or.2010.1067
47. Choi Y, Lee S, Kim K, Kim SH, Chung YJ, Lee C. Studying cancer immunotherapy using patient-derived xenografts (PDXs) in humanized mice. *Exp Mol Med* (2018) 50(8):99. doi: 10.1038/s12276-018-0115-0
48. Lang J, Capasso A, Jordan KR, French JD, Kar A, Bagby SM, et al. Development of an Adrenocortical Cancer Humanized Mouse Model to Characterize Anti-PD1 Effects on Tumor Microenvironment. *J Clin Endocrinol Metab* (2020) 105(1):26–42. doi: 10.1210/clinem/dgz014
49. Tentler JJ, Lang J, Capasso A, Kim DJ, Benaim E, Lee YB, et al. RX-5902, a Novel beta-catenin Modulator, Potentiates the Efficacy of Immune Checkpoint Inhibitors in Preclnical Models of Triple-negative Breast Cancer. *BMC Cancer* (2020) 20:1063. doi: 10.1186/s12885-020-07500-1
50. Wang M, Yao LC, Cheng M, Cai D, Martinek J, Pan CX, et al. Humanized mice in studying efficacy and mechanisms of PD-1-targeted cancer immunotherapy. *FASEB J* (2018) 32(3):1537–49. doi: 10.1096/fj.201700740R
51. Stripecke R, Munz C, Schuringa JJ, Bissig KD, Soper B, Meeham T, et al. Innovations, challenges, and minimal information for standardization of humanized mice. *EMBO Mol Med* (2020) 12(7):e8662. doi: 10.15252/emmm.201708662
52. Legrand N, Huntington ND, Nagasawa M, Bakker AQ, Schotte R, Strick-Marchand H, et al. Functional CD47/signal regulatory protein alpha (SIRP (alpha)) interaction is required for optimal human T- and natural killer-(NK) cell homeostasis *in vivo*. *Proc Natl Acad Sci U S A* (2011) 108(32):13224–9. doi: 10.1073/pnas.1101398108
53. Keenan TE, Burke KP, Van Allen EM. Genomic correlates of response to immune checkpoint blockade. *Nat Med* (2019) 25(3):389–402. doi: 10.1038/s41591-019-0382-x
54. Reuben A, Spencer CN, Prieto PA, Gopalakrishnan V, Reddy SM, Miller JP, et al. Genomic and immune heterogeneity are associated with differential responses to therapy in melanoma. *NPJ Genom Med* (2017) 2:1–11. doi: 10.1038/s41525-017-0013-8
55. Yamaguchi K, Mishima K, Ohmura H, Hanamura F, Ito M, Nakano M, et al. Activation of central/effector memory T cells and T-helper 1 polarization in malignant melanoma patients treated with anti-programmed death-1 antibody. *Cancer Sci* (2018) 109(10):3032–42. doi: 10.1111/cas.13758
56. Lang J, Kelly M, Freed BM, McCarter MD, Kedl RM, Torres RM, et al. Studies of lymphocyte reconstitution in a humanized mouse model reveal a requirement of T cells for human B cell maturation. *J Immunol* (2013) 190(5):2090–101. doi: 10.4049/jimmunol.1202810

57. Lang J, Weiss N, Freed BM, Torres RM, Pelanda R. Generation of hematopoietic humanized mice in the newborn BALB/c-Rag2null Il2rgammanull mouse model: a multivariable optimization approach. *Clin Immunol* (2011) 140(1):102–16. doi: 10.1016/j.clim.2011.04.002
58. Shultz LD, Keck J, Burzenski L, Jangalwe S, Vaidya S, Greiner DL, et al. Humanized mouse models of immunological diseases and precision medicine. *Mamm Genome* (2019) 30(5-6):123–42. doi: 10.1007/s00335-019-09796-2
59. Yamauchi T, Takenaka K, Urata S, Shima T, Kikushige Y, Tokuyama T, et al. Polymorphic Sirpa is the genetic determinant for NOD-based mouse lines to achieve efficient human cell engraftment. *Blood* (2013) 121(8):1316–25. doi: 10.1182/blood-2012-06-440354
60. Audige A, Rochat MA, Li D, Ivic S, Fahrny A, Muller CKS, et al. Long-term leukocyte reconstitution in NSG mice transplanted with human cord blood hematopoietic stem and progenitor cells. *BMC Immunol* (2017) 18(1):28. doi: 10.1186/s12865-017-0209-9
61. Lepus CM, Gibson TF, Gerber SA, Kawikova I, Szczepanik M, Hossain J, et al. Comparison of human fetal liver, umbilical cord blood, and adult blood hematopoietic stem cell engraftment in NOD-scid/gammac-/-, Balb/c-Rag1-/-gammac-/-, and C.B-17-scid/bg immunodeficient mice. *Hum Immunol* (2009) 70(10):790–802. doi: 10.1016/j.humimm.2009.06.005
62. Volk V, Reppas AI, Robert PA, Spineli LM, Sundarasetty BS, Theobald SJ, et al. Multidimensional Analysis Integrating Human T-Cell Signatures in Lymphatic Tissues with Sex of Humanized Mice for Prediction of Responses after Dendritic Cell Immunization. *Front Immunol* (2017) 8:1709. doi: 10.3389/fimmu.2017.01709
63. Brehm MA, Cuthbert A, Yang C, Miller DM, DiIorio P, Laning J, et al. Parameters for establishing humanized mouse models to study human immunity: analysis of human hematopoietic stem cell engraftment in three immunodeficient strains of mice bearing the IL2rgamma(null) mutation. *Clin Immunol* (2010) 135(1):84–98. doi: 10.1016/j.clim.2009.12.008
64. Li Y, Masse-Ranson G, Garcia Z, Bruel T, Kok A, Strick-Marchand H, et al. A human immune system mouse model with robust lymph node development. *Nat Methods* (2018) 15(8):623–30. doi: 10.1038/s41592-018-0071-6
65. Seung E, Tager AM. Humoral immunity in humanized mice: a work in progress. *J Infect Dis* (2013) 208 Suppl 2:S155–159. doi: 10.1093/infdis/jit448
66. Coleman CB, Lang J, Sweet LA, Smith NA, Freed BM, Pan Z, et al. Epstein-Barr Virus Type 2 Infects T Cells and Induces B Cell Lymphomagenesis in Humanized Mice. *J Virol* (2018) 92(21):1–22. doi: 10.1128/JVI.00813-18
67. Douam F, Ziegler CGK, Hrebikova G, Fant B, Leach R, Parsons L, et al. Selective expansion of myeloid and NK cells in humanized mice yields human-like vaccine responses. *Nat Commun* (2018) 9(1):5031. doi: 10.1038/s41467-018-07478-2
68. Rongvaux A, Takizawa H, Strowig T, Willinger T, Eynon EE, Flavell RA, et al. Human hemato-lymphoid system mice: current use and future potential for medicine. *Annu Rev Immunol* (2013) 31:635–74. doi: 10.1146/annurev-immunol-032712-095921
69. Herndler-Brandstetter D, Shan L, Yao Y, Stecher C, Plajer V, Lietzenmayer M, et al. Humanized mouse model supports development, function, and tissue residency of human natural killer cells. *Proc Natl Acad Sci U S A* (2017) 114(45):E9626–34. doi: 10.1073/pnas.1705301114
70. Lopez-Lastra S, Masse-Ranson G, Fiquet O, Darche S, Serafini N, Li Y, et al. A functional DC cross talk promotes human ILC homeostasis in humanized mice. *Blood Adv* (2017) 1(10):601–14. doi: 10.1182/bloodadvances.2017004358
71. Matsuda M, Ono R, Iyoda T, Endo T, Iwasaki M, Tomizawa-Murasawa M, et al. Human NK cell development in hIL-7 and hIL-15 knockin NOD/SCID/IL2rgKO mice. *Life Sci Alliance* (2019) 2(2):1–13. doi: 10.26508/lsa.201800195
72. Strowig T, Chijioke O, Carrega P, Arrey F, Meixlsperger S, Ramer PC, et al. Human NK cells of mice with reconstituted human immune system components require preactivation to acquire functional competence. *Blood* (2010) 116(20):4158–67. doi: 10.1182/blood-2010-02-270678
73. Benci JL, Xu B, Qiu Y, Wu TJ, Dada H, Twyman-Saint Victor C, et al. Tumor Interferon Signaling Regulates a Multigenic Resistance Program to Immune Checkpoint Blockade. *Cell* (2016) 167(6):1540–1554 e1512. doi: 10.1016/j.cell.2016.11.022
74. Huang AC, Postow MA, Orlowski RJ, Mick R, Bengsch B, Manne S, et al. T-cell invigoration to tumour burden ratio associated with anti-PD-1 response. *Nature* (2017) 545(7652):60–5. doi: 10.1038/nature22079
75. McLane LM, Abdel-Hakeem MS, Wherry EJ. CD8 T Cell Exhaustion During Chronic Viral Infection and Cancer. *Annu Rev Immunol* (2019) 37:457–95. doi: 10.1146/annurev-immunol-041015-055318
76. Schnell A, Bod L, Madi A, Kuchroo VK. The yin and yang of co-inhibitory receptors: toward anti-tumor immunity without autoimmunity. *Cell Res* (2020) 30(4):285–99. doi: 10.1038/s41422-020-0277-x
77. Jenkins RW, Aref AR, Lizotte PH, Ivanova E, Stinson S, Zhou CW, et al. Ex Vivo Profiling of PD-1 Blockade Using Organotypic Tumor Spheroids. *Cancer Discovery* (2018) 8(2):196–215. doi: 10.1158/2159-8290.CD-17-0833
78. Manieri NA, Chiang EY, Grogan JL. TIGIT: A Key Inhibitor of the Cancer Immunity Cycle. *Trends Immunol* (2017) 38(1):20–8. doi: 10.1016/j.it.2016.10.002
79. Billerbeck E, Barry WT, Mu K, Dorner M, Rice CM, Ploss A. Development of human CD4+FoxP3+ regulatory T cells in human stem cell factor-, granulocyte-macrophage colony-stimulating factor-, and interleukin-3-expressing NOD-SCID IL2Rgamma(null) humanized mice. *Blood* (2011) 117(11):3076–86. doi: 10.1182/blood-2010-08-301507
80. Onoe T, Kalscheuer H, Danzl N, Chittenden M, Zhao G, Yang YG, et al. Human natural regulatory T cell development, suppressive function, and postthymic maturation in a humanized mouse model. *J Immunol* (2011) 187(7):3895–903. doi: 10.4049/jimmunol.1100394
81. Naradikian MS, Hao Y, Cancro MP. Age-associated B cells: key mediators of both protective and autoreactive humoral responses. *Immunol Rev* (2016) 269(1):118–29. doi: 10.1111/imr.12380
82. Rubtsova K, Rubtsov AV, Thurman JM, Mennona JM, Kappler JW, Marrack P. B cells expressing the transcription factor T-bet drive lupus-like autoimmunity. *J Clin Invest* (2017) 127(4):1392–404. doi: 10.1172/JCI91250
83. Winslow GM, Papillion AM, Kenderes KJ, Levack RC. CD11c+ T-bet+ memory B cells: Immune maintenance during chronic infection and inflammation? *Cell Immunol* (2017) 321:8–17. doi: 10.1016/j.cellimm.2017.07.006
84. Rios-Doria J, Stevens C, Maddage C, Lasky K, Koblish HK. Characterization of human cancer xenografts in humanized mice. *J Immunother Cancer* (2020) 8(1):1–8. doi: 10.1136/jitc-2019-000416
85. Ochoa de Olza M, Navarro Rodrigo B, Zimmermann S, Coukos G. Turning up the heat on non-immunoreactive tumours: opportunities for clinical development. *Lancet Oncol* (2020) 21(9):e419–30. doi: 10.1016/S1470-2045(20)30234-5
86. Pavan A, Attili I, Pasello G, Guarneri V, Conte PF, Bonanno L. Immunotherapy in small-cell lung cancer: from molecular promises to clinical challenges. *J Immunother Cancer* (2019) 7(1):205. doi: 10.1186/s40425-019-0690-1
87. Wang W, Hodkinson P, McLaren F, Mackean MJ, Williams L, Howie SEM, et al. Histologic assessment of tumor-associated CD45(+) cell numbers is an independent predictor of prognosis in small cell lung cancer. *Chest* (2013) 143(1):146–51. doi: 10.1378/chest.12-0681
88. Yu JW, Bhattacharya S, Yanamandra N, Kilian D, Shi H, Yadavilli S, et al. Tumor-immune profiling of murine syngeneic tumor models as a framework to guide mechanistic studies and predict therapy response in distinct tumor microenvironments. *PloS One* (2018) 13(11):e0206223. doi: 10.1371/journal.pone.0206223
89. Joseph RW, Elassaiss-Schaap J, Kefford R, Hwu WJ, Wolchok JD, Joshua AM, et al. Baseline Tumor Size Is an Independent Prognostic Factor for Overall Survival in Patients with Melanoma Treated with Pembrolizumab. *Clin Cancer Res* (2018) 24(20):4960–7. doi: 10.1158/1078-0432.CCR-17-2386
90. Plesca I, Tunger A, Muller L, Wehner R, Lai X, Grimm MO, et al. Characteristics of Tumor-Infiltrating Lymphocytes Prior to and During Immune Checkpoint Inhibitor Therapy. *Front Immunol* (2020) 11:364. doi: 10.3389/fimmu.2020.00364
91. Ribas A, Wolchok JD. Cancer immunotherapy using checkpoint blockade. *Science* (2018) 359(6382):1350–5. doi: 10.1126/science.aar4060
92. Rossi G, Russo A, Tagliamento M, Tuzi A, Nigro O, Vallome G, et al. Precision Medicine for NSCLC in the Era of Immunotherapy: New Biomarkers to Select the Most Suitable Treatment or the Most Suitable Patient. *Cancers (Basel)* (2020) 12(5):1125–55. doi: 10.3390/cancers12051125
93. Tsai AK, Khan AY, Worgo CE, Wang LL, Liang Y, Davila E. A Multikinase and DNA-PK Inhibitor Combination Immunomodulates Melanomas, Suppresses Tumor Progression, and Enhances Immunotherapies. *Cancer Immunol Res* (2017) 5(9):790–803. doi: 10.1158/2326-6066.CIR-17-0009

94. Wei SC, Levine JH, Cogdill AP, Zhao Y, Anang NAS, Andrews MC, et al. Distinct Cellular Mechanisms Underlie Anti-CTLA-4 and Anti-PD-1 Checkpoint Blockade. *Cell* (2017) 170(6):1120–1133 e1117. doi: 10.1016/j.cell.2017.07.024
95. Castro F, Cardoso AP, Goncalves RM, Serre K, Oliveira MJ. Interferon-Gamma at the Crossroads of Tumor Immune Surveillance or Evasion. *Front Immunol* (2018) 9:847. doi: 10.3389/fimmu.2018.00847
96. Wang X, Waschke BC, Woolaver RA, Chen Z, Zhang G, Piscopio AD, et al. Histone Deacetylase Inhibition Sensitizes PD1 Blockade-Resistant B-cell Lymphomas. *Cancer Immunol Res* (2019) 7(8):1318–31. doi: 10.1158/2326-6066.CIR-18-0875
97. Zhang S, Kohli K, Black RG, Yao L, Spadinger SM, He Q, et al. Systemic Interferon-gamma Increases MHC Class I Expression and T-cell Infiltration in Cold Tumors: Results of a Phase 0 Clinical Trial. *Cancer Immunol Res* (2019) 7(8):1237–43. doi: 10.1158/2326-6066.CIR-18-0940
98. Davis AA, Patel VG. The role of PD-L1 expression as a predictive biomarker: an analysis of all US Food and Drug Administration (FDA) approvals of immune checkpoint inhibitors. *J Immunother Cancer* (2019) 7(1):278. doi: 10.1186/s40425-019-0768-9
99. Knibbe-Hollinger JS, Fields NR, Chaudoin TR, Epstein AA, Makarov E, Akhter SP, et al. Influence of age, irradiation and humanization on NSG mouse phenotypes. *Biol Open* (2015) 4(10):1243–52. doi: 10.1242/bio.013201
100. Elliott LA, Doherty GA, Sheahan K, Ryan EJ. Human Tumor-Infiltrating Myeloid Cells: Phenotypic and Functional Diversity. *Front Immunol* (2017) 8:86. doi: 10.3389/fimmu.2017.00086
101. Gabrilovich DI. Myeloid-Derived Suppressor Cells. *Cancer Immunol Res* (2017) 5(1):3–8. doi: 10.1158/2326-6066.CIR-16-0297
102. Watanabe Y, Takahashi T, Okajima A, Shiokawa M, Ishii N, Katano I, et al. The analysis of the functions of human B and T cells in humanized NOD/shi-scid/gammac(null) (NOG) mice (hu-HSC NOG mice). *Int Immunol* (2009) 21(7):843–58. doi: 10.1093/intimm/dxp050
103. Harris DT, Badowski M. Long term human reconstitution and immune aging in NOD-Rag (-)-gamma chain (-) mice. *Immunobiology* (2014) 219 (2):131–7. doi: 10.1016/j.imbio.2013.08.013
104. Ma SD, Xu X, Jones R, Delecluse HJ, Zumwalde NA, Sharma A, et al. PD-1/CTLA-4 Blockade Inhibits Epstein-Barr Virus-Induced Lymphoma Growth in a Cord Blood Humanized-Mouse Model. *PloS Pathog* (2016) 12(5): e1005642. doi: 10.1371/journal.ppat.1005642
105. Rosato RR, Davila-Gonzalez D, Choi DS, Qian W, Chen W, Kozielski AJ, et al. Evaluation of anti-PD-1-based therapy against triple-negative breast cancer patient-derived xenograft tumors engrafted in humanized mouse models. *Breast Cancer Res* (2018) 20(1):108. doi: 10.1186/s13058-018-1037-4
106. Horn L, Mansfield AS, Szczesna A, Havel L, Krzakowski M, Hochmair MJ, et al. First-Line Atezolizumab plus Chemotherapy in Extensive-Stage Small-Cell Lung Cancer. *N Engl J Med* (2018) 379(23):2220–9. doi: 10.1056/NEJMoa1809064
107. Ni L, Lu J. Interferon gamma in cancer immunotherapy. *Cancer Med* (2018) 7(9):4509–16. doi: 10.1002/cam4.1700
108. Marty Pyke R, Thompson WK, Salem RM, Font-Burgada J, Zanetti M, Carter H. Evolutionary Pressure against MHC Class II Binding Cancer Mutations. *Cell* (2018) 175(2):416–428 e413. doi: 10.1016/j.cell.2018.08.048
109. Barry KC, Hsu J, Broz ML, Cueto FJ, Binnewies M, Combes AJ, et al. A natural killer-dendritic cell axis defines checkpoint therapy-responsive tumor microenvironments. *Nat Med* (2018) 24(8):1178–91. doi: 10.1038/s41591-018-0085-8
110. Chuah S, Chew V. High-dimensional immune-profiling in cancer: implications for immunotherapy. *J Immunother Cancer* (2020) 8(1):1–10. doi: 10.1136/jitc-2019-000363
111. Laajala TD, Jumppanen M, Huhtaniemi R, Fey V, Kaur A, Knuuttila M, et al. Optimized design and analysis of preclinical intervention studies. *vivo Sci Rep* (2016) 6:30723. doi: 10.1038/srep30723
112. Hu Z, Xia J, Fan W, Wargo J, Yang YG. Human melanoma immunotherapy using tumor antigen-specific T cells generated in humanized mice. *Oncotarget* (2016) 7(6):6448–59. doi: 10.18632/oncotarget.7044
113. Mhaidly R, Verhoeyen E. Humanized Mice Are Precious Tools for Preclinical Evaluation of CAR T and CAR NK Cell Therapies. *Cancers (Basel)* (2020) 12(7):1915–38. doi: 10.3390/cancers12071915
114. Yuki K, Cheng N, Nakano M, Kuo CJ. Organoid Models of Tumor Immunology. *Trends Immunol* (2020) 41(8):652–64. doi: 10.1016/j.it.2020.06.010
115. Cattaneo CM, Dijkstra KK, Fanchi LF, Kelderman S, Kaing S, van Rooij N, et al. Tumor organoid-T-cell coculture systems. *Nat Protoc* (2020) 15(1):15–39. doi: 10.1038/s41596-019-0232-9
116. Dijkstra KK, Monkhorst K, Schipper LJ, Hartemink KJ, Smit EF, Kaing S, et al. Challenges in Establishing Pure Lung Cancer Organoids Limit Their Utility for Personalized Medicine. *Cell Rep* (2020) 31(5):107588. doi: 10.1016/j.celrep.2020.107588
117. Young A, Quandt Z, Bluestone JA. The Balancing Act between Cancer Immunity and Autoimmunity in Response to Immunotherapy. *Cancer Immunol Res* (2018) 6(12):1445–52. doi: 10.1158/2326-6066.CIR-18-0487
118. Vudattu NK, Waldron-Lynch F, Truman LA, Deng S, Preston-Hurlburt P, Torres R, et al. Humanized mice as a model for aberrant responses in human T cell immunotherapy. *J Immunol* (2014) 193(2):587–96. doi: 10.4049/jimmunol.1302455
119. Weaver JL, Zadrozny LM, Gabrielson K, Semple KM, Shea KI, Howard KE. BLT-Immune Humanized Mice as a Model for Nivolumab-Induced Immune-Mediated Adverse Events: Comparison of the NOG and NOG-EXL Strains. *Toxicol Sci* (2019) 169(1):194–208. doi: 10.1093/toxsci/kfz045
120. Skelton JK, Ortega-Prieto AM, Dorner M. A Hitchhiker's guide to humanized mice: new pathways to studying viral infections. *Immunology* (2018) 154(1):50–61. doi: 10.1111/imm.12906
121. Wunderlich M, Chou FS, Link KA, Mizukawa B, Perry RL, Carroll M, et al. AML xenograft efficiency is significantly improved in NOD/SCID-IL2RG mice constitutively expressing human SCF, GM-CSF and IL-3. *Leukemia* (2010) 24(10):1785–8. doi: 10.1038/leu.2010.158
122. Zhai L, Ladomersky E, Lauing KL, Wu M, Genet M, Gritsina G, et al. Infiltrating T Cells Increase IDO1 Expression in Glioblastoma and Contribute to Decreased Patient Survival. *Clin Cancer Res* (2017) 23 (21):6650–60. doi: 10.1158/1078-0432.CCR-17-0120
123. Song Y, Rongvaux A, Taylor A, Jiang T, Tebaldi T, Balasubramanian K, et al. A highly efficient and faithful MDS patient-derived xenotransplantation model for pre-clinical studies. *Nat Commun* (2019) 10(1):366. doi: 10.1038/s41467-018-08166-x
124. Wunderlich M, Sexton C, Mizukawa B, Mulloy JC. NSGS Mice Develop a Progressive, Myeloid Cell Dependent Aplastic Anemia and Bone Marrow Failure Upon Engraftment With Human Umbilical Cord Blood CD34+ Cells. In: *ASH: 2013. Blood*. American Society of Hematology (US) (2013) 3716.
125. McIntosh BE, Brown ME, Duffin BM, Maufort JP, Vereide DT, Slukvin II, et al. B6.SCID Il2rgamma-/- Kit(W41/W41) (NBSGW) mice support multilineage engraftment of human hematopoietic cells. *Stem Cell Rep* (2015) 4(2):171–80. doi: 10.1016/j.stemcr.2014.12.005
126. Rahmig S, Kronstein-Wiedemann R, Fohgrub J, Kronstein N, Nevmerzhitskaya A, Bornhauser M, et al. Improved Human Erythropoiesis and Platelet Formation in Humanized NSGW41 Mice. *Stem Cell Rep* (2016) 7(4):591–601. doi: 10.1016/j.stemcr.2016.08.005
127. Halkias J, Yen B, Taylor KT, Reinhartz O, Winoto A, Robey EA, et al. Conserved and divergent aspects of human T-cell development and migration in humanized mice. *Immunol Cell Biol* (2015) 93(8):716–26. doi: 10.1038/icb.2015.38
128. Strowig T, Gurer C, Ploss A, Liu YF, Arrey F, Sashihara J, et al. Priming of protective T cell responses against virus-induced tumors in mice with human immune system components. *J Exp Med* (2009) 206(6):1423–34. doi: 10.1084/jem.20081720
129. Ashizawa T, Iizuka A, Nonomura C, Kondou R, Maeda C, Miyata H, et al. Antitumor Effect of Programmed Death-1 (PD-1) Blockade in Humanized the NOG-MHC Double Knockout Mouse. *Clin Cancer Res* (2017) 23(1):149–58. doi: 10.1158/1078-0432.CCR-16-0122
130. Hoffmann MM, Slansky JE. T-cell receptor affinity in the age of cancer immunotherapy. *Mol Carcinog* (2020) 59(7):862–70. doi: 10.1002/mc.23212
131. Majji S, Wijayalath W, Shashikumar S, Pow-Sang L, Villasante E, Brumeanu TD, et al. Differential effect of HLA class-I versus class-II transgenes on human T and B cell reconstitution and function in NRG mice. *Sci Rep* (2016) 6:28093. doi: 10.1038/srep28093
132. Masse-Ranson G, Dusseaux M, Fiquet O, Darche S, Boussand M, Li Y, et al. Accelerated thymopoiesis and improved T-cell responses in HLA-A2/-DR2 transgenic BRGS-based human immune system mice. *Eur J Immunol* (2019) 49(6):954–65. doi: 10.1002/eji.201848001
133. Victor Garcia J. Humanized mice for HIV and AIDS research. *Curr Opin Virol* (2016) 19:56–64. doi: 10.1016/j.coviro.2016.06.010
134. Jewett A, Kos J, Kaur K, Safaei T, Sutanto C, Chen W, et al. Natural Killer Cells: Diverse Functions in Tumor Immunity and Defects in Pre-neoplastic

and Neoplastic Stages of Tumorigenesis. *Mol Ther Oncol* (2020) 16:41–52. doi: 10.1016/j.omto.2019.11.002

135. Kalscheuer H, Danzl N, Onoe T, Faust T, Winchester R, Goland R, et al. A model for personalized *in vivo* analysis of human immune responsiveness. *Sci Transl Med* (2012) 4(125):125ra130. doi: 10.1126/scitranslmed.3003481

Conflict of Interest: The authors declare that the research was conducted in the absence of any commercial or financial relationships that could be construed as a potential conflict of interest.

Copyright © 2021 Marín-Jiménez, Capasso, Lewis, Bagby, Hartman, Shulman, Navarro, Yu, Rivard, Wang, Barkow, Geng, Kar, Yingst, Tufa, Dolan, Blatchford, Freed, Torres, Davila, Slansky, Pelanda, Eckhardt, Messersmith, Diamond, Lieu, Verneris, Wang, Kiseljak-Vassiliades, Pitts and Lang. This is an open-access article distributed under the terms of the Creative Commons Attribution License (CC BY). The use, distribution or reproduction in other forums is permitted, provided the original author(s) and the copyright owner(s) are credited and that the original publication in this journal is cited, in accordance with accepted academic practice. No use, distribution or reproduction is permitted which does not comply with these terms.

frontiers in Oncology

ORIGINAL RESEARCH
published: 30 March 2021
doi: 10.3389/fonc.2021.632364

Inhibition of LDH-A by Oxamate Enhances the Efficacy of Anti-PD-1 Treatment in an NSCLC Humanized Mouse Model

Tianyun Qiao[1], Yanlu Xiong[1], Yangbo Feng[1], Wenwen Guo[2], Yongsheng Zhou[1], Jinbo Zhao[1], Tao Jiang[1], Changhong Shi[3] and Yong Han[1,4]**

[1] Department of Thoracic Surgery, Tangdu Hospital, The Fourth Military Medical University, Xi'an, China, [2] School of Basic Medical Sciences, Medical College of Yan'an University, Yanan, China, [3] Laboratory Animal Center, The Fourth Military Medical University, Xi'an, China, [4] Department of Thoracic Surgery, Air Force Medical Center, Beijing, China

OPEN ACCESS

Edited by:
Yasuyuki Saito,
Kobe University, Japan

Reviewed by:
Hongbin Deng,
Chinese Academy of Medical Sciences and Peking Union Medical College, China
Ana Paula Lepique,
University of São Paulo, Brazil

***Correspondence:**
Yong Han
hanyong_td@163.com
Changhong Shi
changhong@fmmu.edu.cn

Specialty section:
This article was submitted to Cancer Immunity and Immunotherapy, a section of the journal Frontiers in Oncology

Received: 23 November 2020
Accepted: 15 March 2021
Published: 30 March 2021

Citation:
Qiao T, Xiong Y, Feng Y, Guo W, Zhou Y, Zhao J, Jiang T, Shi C and Han Y (2021) Inhibition of LDH-A by Oxamate Enhances the Efficacy of Anti-PD-1 Treatment in an NSCLC Humanized Mouse Model. Front. Oncol. 11:632364. doi: 10.3389/fonc.2021.632364

Immunotherapy is a curable treatment for certain cancers, but it is still only effective in a small subset of patients, partly because of the lack of sufficient immune cells in the tumor. It is reported that targeted lactate dehydrogenase (LDH) to reduce lactic acid production can promote the infiltration and activity of immune cells and turn tumors into hot tumors. Therefore, we constructed a humanized mouse model to evaluate the efficacy of using classical LDH inhibitor oxamate and pembrolizumab alone or in combination in non-small cell lung cancer (NSCLC). We found that both oxamate and pembrolizumab monotherapy significantly delayed tumor growth; moreover, combination therapy showed better results. Immunofluorescence analysis showed that oxamate treatment increased the infiltration of activated CD8+ T cells in the tumor, which might have enhanced the therapeutic effects of pembrolizumab. Treatment of the humanized mice with anti-CD8 abrogated the therapeutic effects of oxamate, indicating CD8+ T cells as the main force mediating the effect of oxamate. In conclusion, Our preclinical findings position that oxamate not only inhibits tumor growth at a high safe dose but also enhances the efficacy of pembrolizumab in Hu-PBMC-CDX mice. Our study also provides a preclinical model for exploring the efficacy of other immune-based combination therapies for NSCLC.

Keywords: non-small cell lung cancer, NSCLC, immunotherapy, anti-PD-1, oxamate, LDH, humanized mice model

INTRODUCTION

Lung cancer is a malignant tumor with the highest cancer fatality rate worldwide (1). Non-small cell lung cancer (NSCLC) accounts for 85% of all lung cancers, and most patients are found to be in advanced stages, have lost treatment opportunities, and have a low 5-year survival rate (2). In recent years, immunotherapy has brought new hope to patients. Several immune checkpoint inhibitors, such as nivolumab, pembrolizumab, atezolizumab, and durvalumab, have yielded excellent benefits in prolonging progression-free survival and overall survival for both second-line and first-line NSCLC patients, and have received US Food and Drug Administration approval (3). However, only a subgroup of patients benefits from such therapy. This is because immunotherapy is only applicable

to patients with high programmed death ligand 1 (PD-L1) expression (tumor proportion score [TPS] > 50%), which is found in only a small number of patients (15%) (4). Therefore, combination therapy based on immunotherapy has become a new research direction. The purpose of combination therapy is to increase the number and activity of tumor-infiltrating lymphocytes through other treatments, thereby enhancing the effect of immunotherapy (5). Clinically, the most widely used combination therapy is chemotherapy combined with immunotherapy. In 2016, the FDA approved pembrolizumab/carboplatin/pemetrexed for first-line treatment of non-squamous NSCLC, regardless of the expression level of PD-L1. Additional treatment options include atezolizumab/carboplatin/paclitaxel/bevacizumab or atezolizumab/carboplatin/nab-paclitaxel. These combination treatments require less strict conditions than immune monotherapy (TPS > 50%). Moreover, there is no need to detect the expression level of PD-L1 and tumor mutational burden (TMB), which enables more patients to receive the treatment (4). However, in view of the strong side effects of chemotherapy both in monotherapy and combination therapy, more combination therapies with high efficacy and low toxicity need to be developed.

The Warburg effect is ubiquitous in all types of tumors, and its characteristic is that the energy metabolism of tumor cells is still dominated by glycolysis under conditions of sufficient oxygen (6, 7). Tumor cells absorb a large amount of glucose, convert pyruvate to lactic acid through lactate dehydrogenase A (LDH-A), a key enzyme in glycolysis; and oxidize nicotinamide adenine dinucleotide hydride (NADH) to nicotinamide adenine dinucleotide (NAD^+) at the same time (8). Glycolytic metabolism in tumor cells leads to competition for limited nutrition in the tumor microenvironment and makes stromal and immune cells nutrition deficient (9, 10). Its main metabolites also affect the tumor microenvironment. A large amount of lactic acid produced by glycolysis is transported out of tumor cells through the monocarboxylate transporter (MCT), which acidifies the tumor microenvironment and promotes the secretion of vascular endothelial growth factor (VEGF) and of angiogenesis (11, 12). A large amount of lactic acid released by tumor cells can also increase the concentration of lactic acid in the tumor microenvironment and inhibit the efflux of lactic acid produced by glycolysis of T lymphocytes, resulting in acidification of the intracellular environment of T lymphocytes and inhibition of T activation, thus promoting tumor immune escape (13, 14). Therefore, as a product of glycolysis, lactic acid can not only promote tumor cell invasion, metastasis, and angiogenesis but also immune escape by acidifying the tumor microenvironment. In view of its important role in cancer metabolism, targeting lactic acid metabolism and its key enzymes is considered a potential target for cancer therapy (15). In addition, because LDH-A is not a key enzyme in normal cell metabolism, targeting it does not cause obvious symptoms, indicating that selective LDH-A inhibitors have minimal side effects. Therefore, LDH-A is considered an attractive target for the development of new anticancer drugs.

In recent years, as an inhibitor of LDH, oxamate has been proven to be a promising anticancer drug; however, its specific action mechanism is still unclear (16, 17). In previous studies, oxamate was shown to inhibit the growth and metastasis of cervical (18), gastric (19), and liver cancer cells *in vitro* (20). Furthermore, it significantly inhibited the level of LDH in mouse tumors (21). However, the traditional preclinical model is to transplant tumor cell lines or patient-derived xenografts (PDXs) into immunodeficient mice to evaluate the therapeutic effect of a drug (22). Because of the lacking human immune system, this model cannot be applied to evaluate the effect of oxamate on the immune system.

Therefore, a humanized mouse model has emerged as a promising translational platform for evaluating the efficacies of new immunotherapeutics. The human peripheral blood mononuclear cell (Hu-PBMC) mouse model or human-hematopoietic stem cell (Hu-HSC) mouse model was established by transplanting fresh PBMCs or umbilical cord blood-derived CD34+ hematopoietic stem cells into severe combined immunodeficiency mice. Then, a tumor cell line or PDX was transplanted into the mice so that the model had both the human immune system and tumor (23, 24). To date, the application of humanized mouse models has focused mainly on the evaluation of the preclinical efficacy and mechanism of new immune antibodies and is rarely used in the preclinical evaluation of combination therapy. Therefore, we believe that this is a research direction worthy of attention.

The present study aimed to investigate the potential anticancer effect of oxamate in an NSCLC humanized model and to clarify the mechanisms involved. Furthermore, this study investigated the effectiveness of oxamate in terms of potentiating the antitumor action of pembrolizumab to ascertain whether the latter can be used as an adjuvant therapy in cancer treatment.

MATERIALS AND METHODS

Cell Lines

H460 and H1299 cells (human non-small cell lung cancer cell lines) and HBE cells (normal lung epithelial cell line) were purchased from the Cell Bank of the Chinese Academy of Sciences (Shanghai, China). All cell lines were cultured in RPMI-1640 (Gibco) medium, supplemented with 10% heat-inactivated fetal bovine serum (FBS; Gibco) and 1% penicillin-streptomycin (Thermo Fisher Scientific, Waltham, MA, USA) at 37°C with 5% CO_2.

Mice

NOD-prkdc^{scid}IL2rg^{tm1}/Bcgen (B-NDG) mice were purchased from Biocytogen (Beijing, China) and maintained at specific pathogen-free conditions in the Laboratory Animal Center of the Air Force Military Medical University. All procedures were approved by the Institutional Animal Care and Use Committee of Air Force Military Medical University (IACUC-20200602). Mice used in these studies were provided autoclaved food and water. Mice were humanely euthanized by CO2 inhalation if a solitary subcutaneous tumor exceeded 1500 mm^3 in area.

Reagents

Oxamate sodium was purchased from Sigma-Aldrich Corp (St. Louis, MO, USA). Three fresh peripheral blood samples were

collected from the Blood Transfusion Department of Xijing Hospital (Xi'an, Shaanxi Province, China) and approved by the Medical Ethics Committee (KY20193035).

Establishment of Hu-PBMC Models

Human whole peripheral blood mononuclear cells were isolated using Lymphoprep (StemCell Technologies, Vancouver, BC, Canada) according to the manufacturer's instructions. A total of 1×10^7 human PBMCs were transplanted (ip) into 6-week-old B-NDG mice. Peripheral blood from all mice was monitored for human T cell (hCD45+hCD3+) reconstitution at the 2nd, 3rd, 4th, and 5th week. Mice that had over 25% hCD45+hCD3+ cells in the peripheral blood were considered to constitute the Hu-PBMC model. Humanized mice from different PBMC donors with different levels of hCD45+hCD3+ cells were randomly assigned to each experimental group in all experiments.

Establishment of Immune-CDX Models

To optimally use the treatment window of humanized mice, we subcutaneously injected H1299 cells into the mice 1 week after PBMC transplantation. A total of 5×10^6 H1299 cells in the logarithmic growth phase were collected, suspended in serum-free medium mixed with matrigel (Corning Life Sciences, Bedford, MA, USA), and injected into right flank of Hu-PBMC mice. This way, the mice were successfully constructed in the 3rd week and at the same time, the tumor reached the volume of the initial treatment (50–120 mm^3). Body weight and tumor growth were recorded every 4 to 5 days. Tumor volume was calculated by the following formula: [length×$width^2$]/2. Vehicle control saline was injected intraperitoneally every day until the study end point. In the monotherapy group, pembrolizumab (anti-PD-1; Merck, Whitehouse Station, NJ, USA) was injected intraperitoneally at a high dose (10 mg/kg) twice-weekly until the study end point. Oxamate (Sigma-Aldrich Corp) was injected intraperitoneally at 300 mg/kg every day until the study end point. The combined treatment group was simultaneously treated with pembrolizumab and oxamate until the study end point. Mice were sacrificed on day 15, and organs were removed, weighed, and processed for IHC and IFC analyses.

To deplete hCD8+ T cells in Hu-PBMC-B-NDG mice, 200 mg anti-CD8 depletion mAb (clone RPA-T8; BioLegend, San Diego, CA, USA) was injected into mice (ip) 2 days before the Oxamate treatment and then followed by weekly intraperitoneal injections of anti-CD8 mAb for 2 weeks.

Flow Cytometry

At the completion of the study, 15 days after the start of treatment or when the total tumor burden reached 1500mm^3 in volume, the animals were euthanized with carbon dioxide, and tissues were collected under sterile conditions. Blood was collected from the heart soon after euthanasia. The spleen and bone marrow were collected and digested into single-cell suspensions. Single-cell suspensions were incubated with fluorescently-labeled antibodies to evaluate anti-human CD45-FITC (clone HI30) and anti-human CD3-phycoerythrin (clone UCHT1). All antibodies were purchased from BD Biosciences (San Jose, CA, USA). FC500 (Beckman Coulter, Miami, FL. USA) was used for cell acquisition, and data analysis was carried out using the FlowJo software (TreeStar, San Carlos, CA, USA).

Histology and Immunohistochemistry

Tissues harvested from humanized and non-humanized B-NDG mice were fixed with 4% paraformaldehyde for 24 h and then paraffin-embedded. The paraffin-embedded tissues were cut in 4-μm sections and were subjected to standard hematoxylin and eosin staining or immunohistochemistry (IHC). The IHC was performed with the indicated antibodies: anti-human PD-L1 (ab205921, Abcam, Cambridge, MA, USA), anti-human CD45 (ab8216, Abcam), anti-human CD4 (ab183685, Abcam), anti-human CD8 (ab108343, Abcam), and anti-human Foxp3 (ab20034, Abcam). Anti-human CD4 (EP204) antibodies were provided by Cell Signaling Technology (Danvers, MA, USA). Histology slides were scanned with the Aperio imaging system (Leica Biosystems, USA) and analyzed using the ImageScope software (Leica Biosystems).

Immunofluorescence Microscopy

Resected tumor tissues and the spleen were fixed in 4% paraformaldehyde and embedded either in paraffin or in optimal cutting temperature (Sakura Finetek, Torrance, CA, USA) compound and frozen. Sections were deparaffinized, rehydrated, and boiled in a microwave for 20 min in 10 mM citrate buffer for antigen retrieval. Immunohistochemistry was performed using anti-human CD45 (ab40763; Abcam), anti-human CD8 (ab108343; Abcam), anti-human Granzyme B (ab208586; Abcam), anti-human PD-1 (ab234444; Abcam) and anti-human TNF-alpha (ab215188; Abcam). The secondary antibody included goat anti-rabbit IgG AF488 (ab150077, Abcam) and goat anti-mouse IgG AF647 (ab150115, Abcam). Sections were incubated overnight at 4°C before being incubated with the appropriate Alexa Fluor-conjugated secondary antibodies. Slides were washed between staining steps with Bond Wash (Leica) and stripped between each round of staining with heat treatment in antigen retrieval buffer. Nuclei were counterstained with DAPI (ab104139, Abcam). For acquisition, data were acquired by sequential acquisition, and tile-scan imaging was performed on an SP8 confocal microscope (Leica Microsystems, Wetzlar, Germany).

Detection of Cell Viability and LDH Activity

The cell counting kit-8 (CCK-8) assay kit (Dojindo, Shanghai, China) was used to test the effects of oxamate sodium on cell viability at different concentrations or times. Cells were seeded at 5×10^3/well and treated with different concentrations of oxamate sodium (0-100 mmol/l) for 12, 24 and 48 h, respectively. Ten microliters of CCK-8 solution was added into each well, then incubated in the dark for another 3 h. Optical density was measured using a microplate reader (Bio-Tek Instruments, Inc., Winooski, VT, USA) at 450 nm.

Intracellular LDH activity was determined using an LDH activity assay kit (Solarbio, Beijing, China). Cells treated with different concentrations of oxamate were harvested and lysed for protein to measure the LDH activity. As for glycolysis stress test,

Seahorse Bioscience cell energy metabolism analysis system was used. Cells were plated on Cell-Tak-coated Seahorse culture plates (50,000 cells per well) in medium consisting of minimal, unbuffered DMEM supplemented with 2 mM glutamine. Basal rates were taken for about 25 min. Cells were stimulated with 10 mM glucose, 2 μM oligomycin and 10 mM 2-DG.

Statistical Analysis

All data are expressed as the mean ± standard error (SE). Statistical analyses of all data were performed by GraphPad Prism (Version 7.0, GraphPad Software, Inc, San Diego, CA, USA). Differences between groups were tested with analysis of variance, and $p < 0.05$ was considered significant.

RESULTS

Inhibition of LDH by Oxamate Suppresses Cell Viability in NSCLC Cells

First, to explore the effect of oxamate on cell proliferation in NSCLC cells, CCK-8 (cell counting kit-8) assay were conducted. H1299, A549 cancer cells, and normal lung human bronchial epithelial (HBE) cells were treated with different doses of oxamate for 24 h. We observed that oxamate significantly inhibited the viability of H1299 and A549 cells in a dose-dependent manner, while it had little effect on HBE cells (**Figure 1A**). The IC_{50} (50% inhibitory concentration) values of oxamate for H1299 and A549 cells were 32.13 ± 2.50 and 19.67 ± 1.53 mmol/L, respectively, but for HBE cells, the value was very high at 96.73 ± 7.60 mmol/L (**Figure 1B**). Next, given its high sensitivity to oxamate, we selected H1299 cells and treated them with different doses of oxamate for 12, 24, and 48 h, and found that the inhibition of H1299 by oxamate was also time-dependent (**Figure 1C**). These results indicate that oxamate has an obvious killing effect on tumor cells but has low cytotoxicity on normal human cells. This provides a basis for the application of oxamate for inhibiting the production of lactic acid *in vivo*.

In order to further determine the previously reported inhibitory effect of oxamate on LDH, we used commercial kits to detect the activity of LDH in cells treated with different doses of oxamate. Oxamate could reduce the LDH activity of H1299 in a dose-dependent manner, thus reducing the production of lactic acid (**Figure 1D**). Furthermore, we also examined the effects of different concentrations of Oxamate on glycolysis of H1299 and HBE cells. The results showed that 24-hour Oxamate treatment could significantly inhibit the glycolysis activity of tumor cells in a dose-dependent manner while have limited effect on HBE cells (**Figure 1E**). The result demonstrated that LDH inhibition by oxamate disturbed glycolysis and decreased lactic acid production in the NSCLC cells.

Establishment and Identification of a Humanized Mouse Model

The construction strategy of the humanized mouse model is shown in **Figure 2A**. The isolated PBMCs were injected into adult mice, and the reconstitution level of human T (hCD45+ CD3+) cells in the peripheral blood of the mice was dynamically monitored using flow cytometry (**Figure 2B**). With the extension of reconstruction time, human T (CD45+CD3+) cells increased significantly. We also observed that there were differences in the level of human T cells among different donors. As shown in **Figure 2C**, at the 5th week, the reconstruction levels of donor 1 and donor 2 were better than that of donor 3; therefore, in the follow-up experiment, we used the frozen PBMCs of donor 1 and donor 2 to construct the humanized mouse model. After successful reconstruction, the humanized mice reconstructed from two donor sources were randomly assigned to four experimental groups. Humanized mice generally undergo graft-versus-host reaction (GVHD) at the 5-6th week of reconstruction, including weight loss, arched back, hair removal, and other GVHD reactions.

In addition, the reconstruction levels of different organs in humanized mice are different, and we focused on immune organs such as the spleen and bone marrow. The results showed that the level of human T cells in the peripheral blood was similar to that in the spleen but significantly higher than that in the bone marrow (**Figure 2D**). We also observed that the spleen of humanized mice was larger than that of normal mice, which may be caused by an infiltration of a large number of human immune cells (**Figure 2E**). To further determine the immune subpopulations in spleen, we performed an immunohistochemical analysis and found that CD45+ cells showed high infiltration in the spleen, along with high infiltration of CD4+ and CD8+T cells (**Figures 2F, G**). These results indicated that the humanized mice were reconstructed successfully, and all organs were infiltrated with immune cells.

Hu-PBMC-B-NDG Mice Support Tumor Growth of NSCLC Cell Line

We analyzed the expression of PD-L1 in the H1299 cell line and found that its PD-L1 was moderately expressed. To confirm that high PD-L1 expression continues after tumor formation, we transplanted the H1299 cell line into B-NDG mice to construct a CDX (cell-line-derived xenograft) model, and found medium PD-L1 expression in the tumors (**Figure 3A**). In order to determine whether the human immune system has an effect on tumor growth, we transplanted H1299 cell lines on non-humanized mice and compared the tumor growth rate between non-humanized and humanized mice. The growth of tumor cell lines in humanized mice was slower than that in non-humanized mice, indicating that the immune system had a certain retarding effect on tumor growth (**Figure 3B**). Moreover, we performed hematoxylin and eosin staining and histochemical analysis of the tumors and found CD45+, CD8+, CD4+, and Treg immune cell infiltrations in the tumors grown in humanized mice. These results suggest that the NSCLC cell line can grow in humanized mice and have immune infiltration (**Figure 3C**).

For understanding the characteristics of immune infiltration in tumor tissue, we further analyzed the infiltration of CD45+ immune cells and CD8+ T cells in the tumor using immunofluorescence. We observed that CD45+ immune cells mainly gathered at the edge of the tumor, while the immune

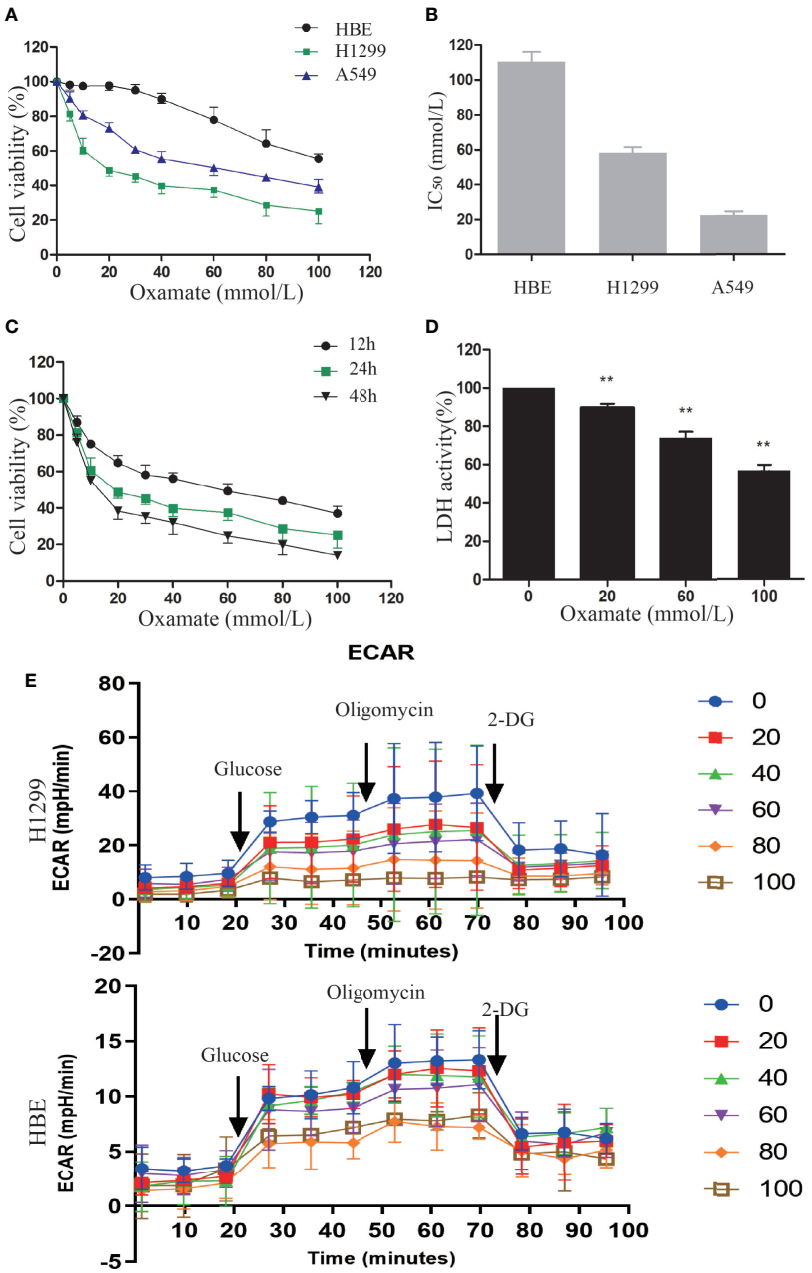

FIGURE 1 | Different effects of oxamate on the cell viability and LDH enzyme activity in NSCLC cells and normal lung epithelial cells. **(A)** A549, H1299 and HBE cells were exposed to varying doses of oxamate for 24 h, and tested by CCK-8 assay. Cell viability was calculated as a percentage of untreated cells (100%); values are represented as means ± SD; n=4. **(B)** IC_{50} of different cells at 24h were calculated by the growth curves. **(C)** The effect of oxamate on H1299 cells was determined at different time points. **(D)** Cells were treated with 0, 20, 60 and 100 mM oxamate for 24 h and using a commercially available kit to determine the intracellular LDH enzyme activity. Values are represented as means ± SD; n=6. **P<0.01 vs. the untreated control. **(E)** Cells were treated with 0, 20, 40, 60, 80 and 100 mM oxamate for 24 h and using a glycolysis stress test to determine the glycolysis ability. 2-DG, 2-deoxy-d-glucose; oligo, oligomycin; Values are represented as means ± SD; n=4.

infiltration in the center of the tumor was very low, which was similar to the tumor immune cell infiltration in clinical patients (**Figure 3D**). We believe that the low immune infiltration in the center of the tumor in CDX and clinical specimens may be the main reason for the limitation of tumor immunotherapy. These results signify that the Hu-PBMC-CDX model can simulate clinical tumor infiltration to a certain extent and is an ideal preclinical model for immunotherapy.

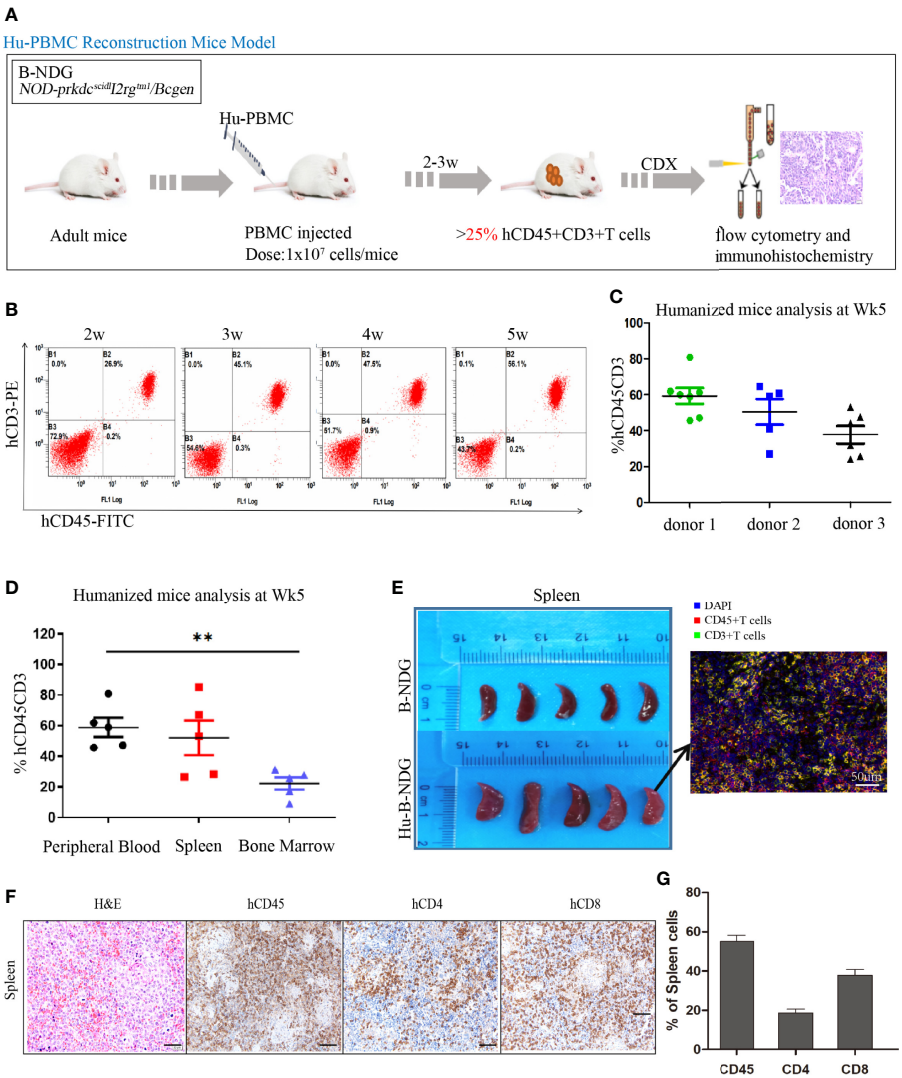

FIGURE 2 | Construction and identification of humanized mouse model of immune system. **(A)** Adult B-NDG mice were injected with 1 × 10^7 PBMC (iv), followed by subcutaneous injection of 5 × 10^6 tumor cell lines. 2-3 weeks later, the peripheral blood of mice was collected from the tail vein to detect the content of hCD45+CD8+T cells, which marked the successful construction of the Hu-PBMC-CDX mouse model when it was more than 25%. **(B)** Dynamic flow detection of hCD45+CD3+T cell level in peripheral blood of a representative Hu-PBMC mouse model. **(C)** Reconstruction level of humanized mice constructed by PBMC from three different donors at the fifth week, n=5. **(D)** Reconstruction levels of hCD45+CD3+ T cells in peripheral blood, spleen and bone marrow of humanized mice at the 5th week, n=5. **P<0.01. **(E)** The spleen of normal B-NDG mice was compared with that of Hu-PBMC mouse model mice, n=5. **(F, G)** Immunohistochemistry for CD45, CD8, CD4, and H&E stains in spleen are shown. Representative images were taken at 20x magnification and the scale bar denotes 50 mm.

Evaluating the Antitumor Effect of Oxamate and Anti-PD-1 Monoclonal Antibody in Hu-PBMCs-CDX Mouse Model

When the volume of Hu-PBMCs-CDX tumor reached 50–120 mm^3, the treatment was commenced and the treatment scheme is illustrated in **Figure 4A**. Daily oxamate treatment can significantly slow down tumor growth; moreover, pembrolizumab monotherapy also inhibits tumor growth. Notably, the effect of the combination therapy was better than that of the two separate monotherapies, indicating that oxamate enhances the therapeutic effect of pembrolizumab (**Figure 4B**). For evaluating the safety of drug treatment, we dynamically monitored the body weight of mice in each treatment group. The results indicate that despite the daily high dose, there was no abnormal weight loss in the oxamate monotherapy group compared with the control group, which corresponds to the aforementioned low toxicity of oxamate to human HBE cells, indicating that it has a large safety range. At the same time, no significant weight loss was observed in the mice in the combined treatment group, indicating that the combined treatment did not increase toxicity (**Figure 4C**). Fifteen days after the start of treatment, the mice were euthanized, and the tumor tissues were collected. As shown in **Figures 4D, E**, the

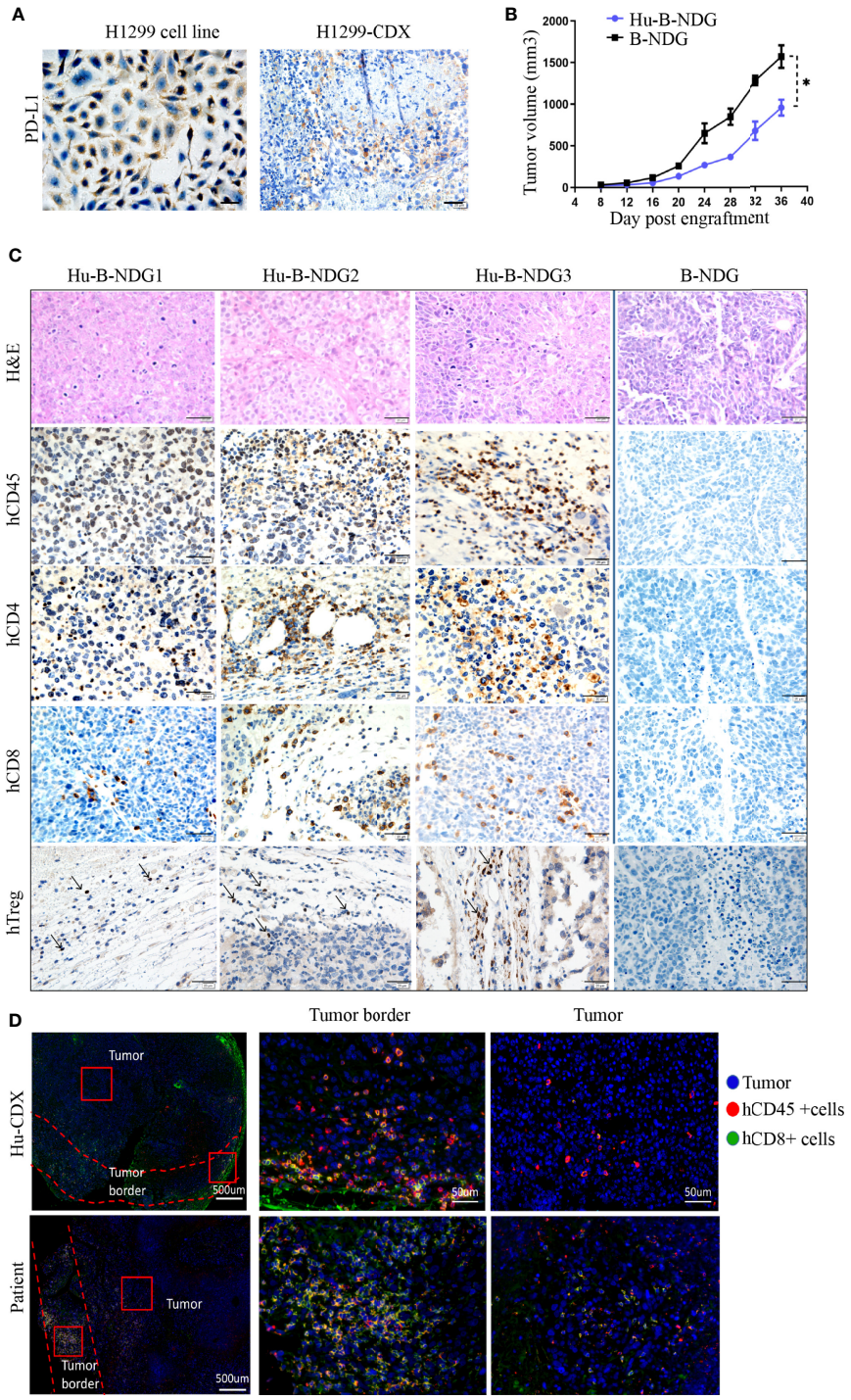

FIGURE 3 | Growth of NSCLC CDX in Hu-PBMC-B-NDG mice. **(A)** Immunohistochemical analysis of PD-L1 expression in H1299 cell line and CDX. **(B)** Growth curve of H1299 cell line on B-NDG and Hu-PBMC-B-NDG mice.Data are presented as the mean ± SD of the volume of CDX (mm^3); n = 5. *P<0.05. **(C)** Immunohistochemistry for CD45, CD8, CD4,Treg(Foxp3) and H&E stains in three tumours from humanzied B-NDG mice and one tumour from B-NDG mice are shown. Representative images were taken at 40x magnification and the scale bar denotes 20 mm. **(D)** Immunofluorescence was used to analyze the immunocyte infiltration in the center and border of tumors from Hu-PBMC-CDX and clinical patients. Representative images were taken at 40x magnification and the scale bar denotes 50 mm.

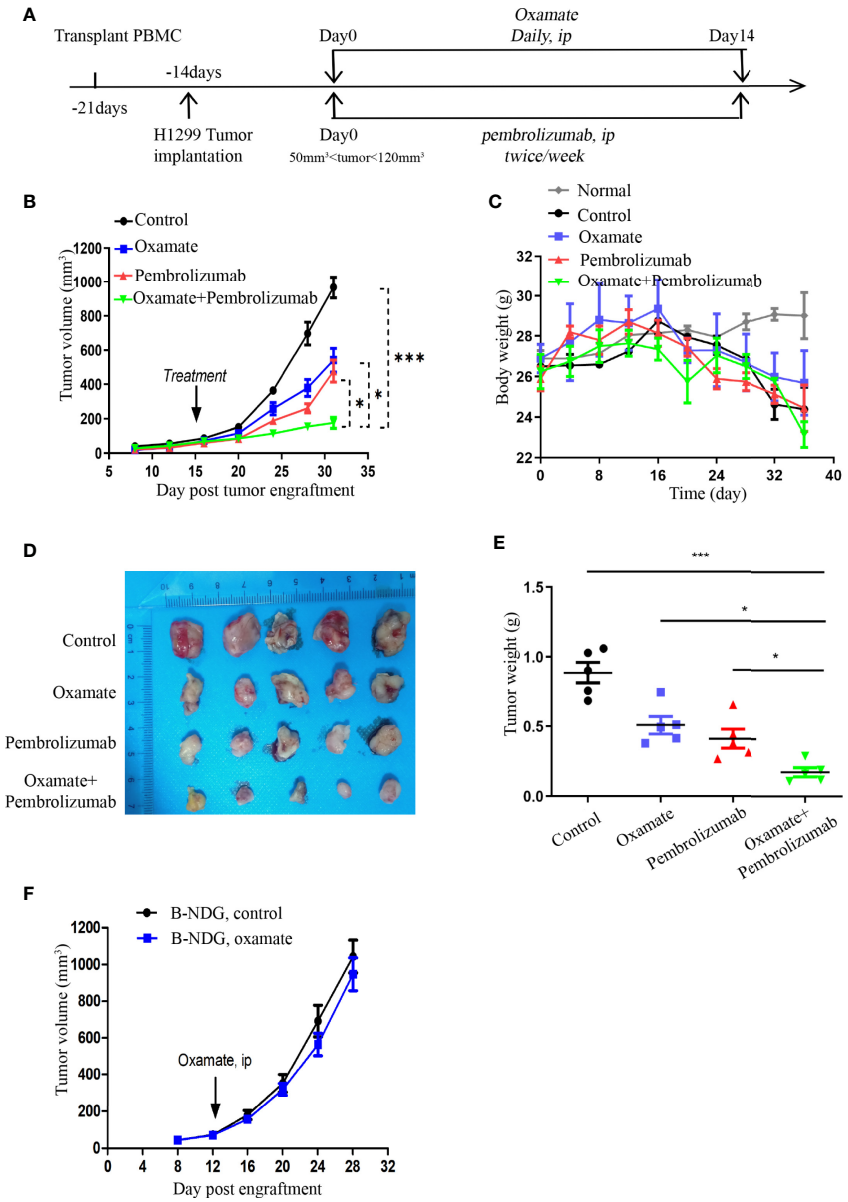

FIGURE 4 | Effects of Oxamate alone or in Combinations with Pembrolizumab on NSCLC Hu-PBMC-CDX. **(A)** Experimental timeline for treatment NSCLC CDX with Oxamate and pembrolizumab in Hu-PBMC-B-NDG mice. **(B)** Tumor growth curve of control group, Oxamate monotherapy group, Pembrolizumab monotherapy group and combination treatment group. Data are presented as the mean ± SD of the volume of CDX (mm^3); n = 5. *P<0.05, ***P<0.001. **(C)** The body weight of mice in each treatment group and normal mice without PBMCs transplantation was monitored every four days from the beginning of PBMCs transplantation to the end of treatment; n=5. **(D, E)** At the end of treatment, the tumors of each treatment group were collected, photographed and weighed; n = 5. *P<0.05, ***P<0.001 **(F)** Tumour growth after treated with Oxamate or PBS in B-NDG mice bearing NSCLC cell line. Group mean differences between Oxamate vs. controls were not significant; n = 5.

tumor volume and weight of the combined treatment group were significantly reduced, showing a good therapeutic effect.

In addition, to investigate whether the underlying mechanism of tumor growth inhibition by oxamate is mediated by the immune system, we treated the unreconstructed tumor-bearing mice with oxamate and found that the tumor growth was only slightly delayed compared to that in the control mice, but the results were not statistically significant (**Figure 4F**). This indicates that the inhibition of tumor growth by oxamate is mediated by the immune system, which inspired us to explore the underlying mechanism of oxamate promoting immunotherapy.

Evaluating the TIL After Treatment in Hu-PBMCs-CDX Mouse Model

For studying the underlying mechanism of immunotherapy, we performed immunofluorescence analysis on the tumor tissues of

each treatment group to observe the changes in immune cell infiltration after treatment. Previous studies have reported that CD8+ cytotoxic T cells mainly mediate the effect of tumor immunotherapy, so we analyzed the number of CD8+ cells in different parts of the tumor. In the periphery of tumors, oxamate alone increased CD8+ immune cells, whereas the combination with pembrolizumab resulted in a significantly higher proportion compared with that of either treatment alone or control. In the center of tumors, CD8+ immune cells increased with the combined regimen compared with that of either pembrolizumab or oxamate. No statistical difference was found between oxamate and pembrolizumab, both in the center and periphery of tumors (**Figures 5A, B**). This finding suggests that increased infiltration of CD8+T cells both in the periphery and center might have caused the therapeutic effect of oxamate. We also compared the immune infiltration of the spleen in each treatment group, and found no significant difference among the groups, indicating that the effect of each treatment group on immune cells was limited to the tumor site. As shown in **Figure 5C**, CD8+ T cell infiltration in the center of the tumor increased after combined therapy. Furthermore, in order to analyze the activation state of increased CD8+ T cells in the combined treatment group, we performed immunofluorescence staining of CD8+ Granzyme B + and CD8+ PD-1+ in the control group and the combined treatment group. The results showed that the proportion of activated CD8+ cells in the combined treatment group increased significantly. This shows that combined therapy can not only increase the infiltration of CD8+ cells, but also change its immunosuppressive state (**Figures 5D, E**).

Further, to verify the role of CD8+T cells in oxamate treatment, we used CD8+ antibodies in the reconstructed humanized mice to remove CD8+ immune cells from the mice, followed by oxamate treatment to observe the effect (**Figure 5F**). Compared with normal humanized mice, oxamate had no inhibitory effect on tumor growth in Hu-PBMCs-CDX mice treated with the CD8 antibody. This shows that the effect of oxamate is mainly mediated by CD8+T cells. One of the possible mechanisms by which oxamate could enhance the effect of immunotherapy is by increasing the infiltration of CD8+T cells in the center of the tumor by reducing the production of lactic acid.

DISCUSSION

In this study, we found that oxamate effectively inhibited the activity of LDH at the cellular level, thus reducing the production of lactic acid. In fact, in view of the inhibitory effect of a highly acidic environment on the immune system, researchers have been investigating ways to inhibit the tumor glycolysis pathway, such as targeting key enzymes of glycolysis [FX-11 (25) and oxamate (26)], lactic acid excretion [MCT-1/MCT-2 inhibitor like diclofenac (27)], and proton pump inhibitors [esomeprazole (28)], to combine them with immunotherapy. In one study, esomeprazole combined with adoptive cell transfer (ACT), a therapy based on the transfer of tumor reactive immune cells, increased the survival of mice loaded with B16 melanoma (29). Previous studies have reported that oxamate can inhibit LDH-A activity and CDX growth in nasopharyngeal carcinoma (30), and breast cancer (21) meanwhile enhances their sensitivity to radiotherapy or chemotherapy. However, the combined application of oxamate and immunotherapy has not been explored. Our study showed that oxamate can be effectively combined with immunotherapy to enhance its anti-tumor effect, and it has minor side effects on normal cells and tissues despite its high dose. In addition, unlike proton pump inhibitors (31), LDH-A is not a necessary enzyme for normal cell metabolism, so the overall effect of its inhibition by oxamate on the human body is very small, which is also conducive for its future clinical application.

In this study, we constructed the Hu-PBMC-B-NDG model and conducted the first preclinical combined therapy trial for NSCLC, which proved that the therapeutic effect of oxamate combined with pembrolizumab was better than that of a single drug. Previous studies have reported that in immune-intact mouse models, oral alkaline buffer or transplantation of LDH-A-deficient tumors to inhibit the acidic microenvironment of tumors can enhance the therapeutic effect of anti-PD-1 and improve the immunosuppressive state of the tumor microenvironment (32, 33). These studies show that it is feasible to target lactic acid metabolism to enhance the effect of immunotherapy. However, these anti-PD-1 antibodies are mouse antibodies rather than clinical antibodies, such as pembrolizumab and nivolumab. Therefore, the main purpose of our study was to observe whether drugs targeting lactic acid metabolism can enhance the efficacy of anti-PD-1 antibodies that have been used clinically. With the development of immunotherapy, humanized mouse models with both the human immune system and tumor cells have become an indispensable preclinical research model for immunotherapy research. At present, most studies only evaluate the anti-tumor effect and the mechanism of antibody monotherapy in humanized mice, and there are only few preclinical trials of combined therapy (34, 35). Therefore, our study provides a good basis for the combined application of drugs targeting metabolism and the immune system in clinical practice. The humanized mouse model could also be used to study additional immune-based combination therapies, such as the combination of angiogenic factor inhibitor (VEGF Inhibitor) and anti-PD-1.

Our study showed that the increase in the immunotherapy effect of combined treatment with oxamate is mediated by increased CD8+T cell infiltration in tumor tissues. Jerome Galon and Daniela Bruni categorized the tumors into hot, altered (excluded and immunosuppressed), and cold tumors, according to the distribution of cytotoxic CD3+T cells and CD8 +T cells in the tumor tissue. They proposed that the immunoscore of the tumor tissue is positively related to the effect of immunotherapy (36). Our study showed that NSCLC CDX constructed in humanized mouse models belongs to altered-excluded tumors, in which CD3+ and CD8+ T cell infiltrates are low at the tumor center and high at the margin, resulting overall in an intermediate immunoscore. Therefore, in

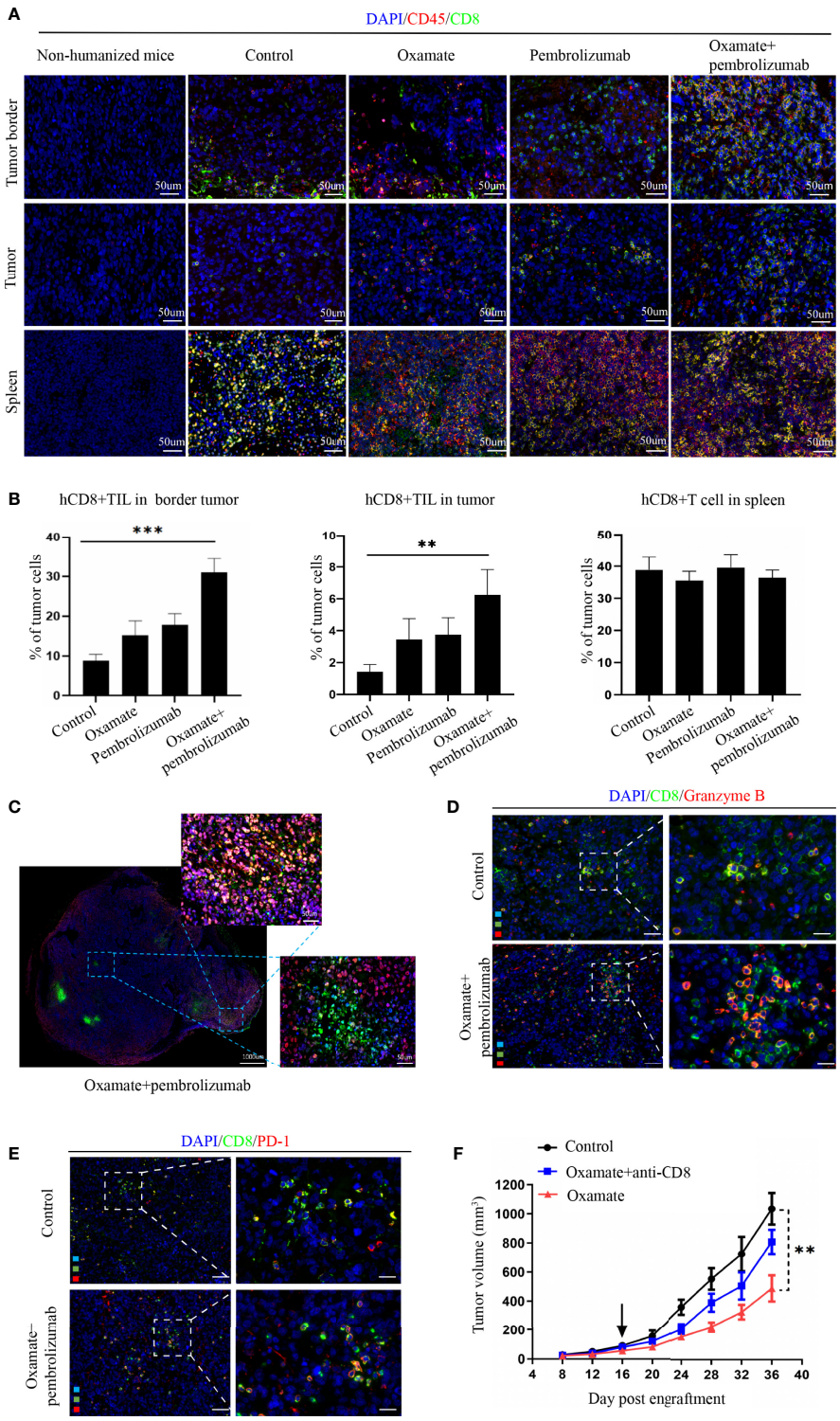

FIGURE 5 | Analysis of tumor immune cell infiltration in NSCLC Hu-PBMC-B-NDG mice after treatment. **(A)** The infiltration of CD45+ and CD8+ immuno cells in the spleen and tumours in each treatment group was analyzed by immunofluorescence. CD45+(Red) CD8+(Green). **(B)** Immunofluorescence quantitative analysis of CD8+T cells in tumor and spleen of each treatment group. **P<0.01, ***P<0.001. **(C)** Immunofluorescence of a representative CDX after treated with oxamate + pembrolizumab. **(D)(E)** Immunofluorescence was used to analyze the activation of CD8+ cells in the control group and the combined treatment group, and CD8+ Granzyme B + T cells and CD8+ PD-1+ T cells were labeled respectively. **(F)** Tumour growth curve of Hu-PBMC-CDX treated with oxamate alone or oxamate plus anti-CD8 depletion mAb. Data are presented as the mean ± SD of the volume of CDX (mm^3); n = 6. **P<0.01.

NSCLC, the key to the success of immunotherapy-based combination therapy is to transform altered tumors into hot tumors (37, 38). In a previous study, Brand et al. injected a $Ldha^{low}$ cell line into C57BL/6 mice and found that the number of CD8+T cells in the $Ldha^{low}$ tumor was higher than that in the control group and was accompanied by functional activation, which may be achieved *via* the upregulation of nuclear factor of activated T cells (NFAT) (39). In our study, we found that this increase mainly took place at the center of the tumor and that the removal of CD8+T cells can eliminate the effect of immunotherapy. As for the reason why oxamate increases tumor immune infiltration, a previous study suggested that the decrease of lactic acid level in tumors can downregulate the expression of PD-L1, thus strongly blocking the PD-1/PD-L1 pathway. Leading to elevation of pro-inflammatory anti-tumor responses such as higher infiltration and activity of CD8+ cytotoxic cells and a diminished frequency of Treg cells (33). In addition, it has been reported that targeted lactic acid metabolism can reduce the production of angiogenic factor (VEGF) by downregulating hypoxia-inducible factor 1a (HIF1a), which contributes to the normalization of tumor blood vessels and increases the infiltration of immune cells (40). We believe that the immune-promoting effect of oxamate may be more complicated and go beyond mere interference with the VEGF and PD-1/PD-L1 signaling pathways. This aspect is worth exploring in-depth in future studies.

The immune system of a humanized mouse model constructed by PBMCs is mainly composed of human T cells and lacks immune subpopulations such as B cells and NK cells, so the limitation of our study is that we could not study the effect of oxamate on these subpopulations and the role of these subpopulations in immunotherapy. In a follow-up experiment, we will use the Hu-HSC-B-NDG mouse model constructed by CD34+ hematopoietic stem cells to further study the effects of oxamate on B cells, NK cells and others. In general, this study successfully created a humanized mouse model of NSCLC to study the effect of combined therapy and its mechanism. We proved that oxamate can both inhibit tumor growth and enhance the efficacy of pembrolizumab by increasing the number of immune infiltrating cells. This provides a preclinical model and a basis for follow-up experiments on combined therapy of drugs targeting metabolic pathways and immune drugs.

DATA AVAILABILITY STATEMENT

The raw data supporting the conclusions of this article will be made available by the authors, without undue reservation.

ETHICS STATEMENT

The animal study was reviewed and approved by Institutional Animal Care and Use Committee of Air Force Military Medical University.

AUTHOR CONTRIBUTIONS

Q-TY contributed to the conception, design, data acquisition, and analysis and drafted and critically revised the manuscript. Y-LX, Y-BF, W-WG, Y-SZ, J-BZ, and TJ contributed to data acquisition and critically revised the manuscript. C-HS and YH contributed to conception, data analysis, and interpretation and drafted and critically revised the manuscript. All authors contributed to the article and approved the submitted version.

FUNDING

The National Natural Science Foundation of China (81772462) and (81001041) provided funding support for the design, analysis, and publication of this study.

ACKNOWLEDGMENTS

We would like to thank Editage (www.editage.cn) for English language editing.

REFERENCES

1. Bray F, Ferlay J, Soerjomataram I, Siegel RL, Torre LA, Jemal A. Global cancer statistics 2018: GLOBOCAN estimates of incidence and mortality worldwide for 36 cancers in 185 countries. *CA Cancer J Clin* (2018) 68:394–424. doi: 10.3322/caac.21492
2. Miller KD, Nogueira L, Mariotto AB, Rowland JH, Yabroff KR, Alfano CM, et al. Cancer treatment and survivorship statistics, 2019. *CA Cancer J Clin* (2019) 69:363–85. doi: 10.3322/caac.21565
3. Carlisle JW, Steuer CE, Owonikoko TK, Saba NF. An update on the immune landscape in lung and head and neck cancers. *CA Cancer J Clin* (2020) 0:1–13. doi: 10.3322/caac.21630
4. Hanna NH, Schneider BJ, Temin S, Baker S, Brahmer J, Ellis PM, et al. Therapy for stage IV non-small-cell lung cancer without driver alterations: ASCO and OH (CCO) Joint Guideline Update. *J Clin Oncol* (2020) 38:1608–32. doi: 10.1200/JCO.19.03022
5. Galluzzi L, Humeau J, Buqué A, Zitvogel L, Kroemer G. Immunostimulation with chemotherapy in the era of immune checkpoint inhibitors. *Nat Rev Clin Oncol* (2020) 17(12):725–41. doi: 10.1038/s41571-020-0413-z
6. Sanderson SM, Locasale JW. Revisiting the Warburg effect: Some tumors hold their breath. *Cell Metab* (2018) 28:669–70. doi: 10.1016/j.cmet.2018.10.011
7. Burgess DJ. Metabolism: Warburg behind the butyrate paradox? *Nat Rev Cancer* (2012) 12:798–9. doi: 10.1038/nrc3401
8. Flores A, Sandoval-Gonzalez S, Takahashi R, Krall A, Sathe L, Wei L, et al. Increased lactate dehydrogenase activity is dispensable in squamous carcinoma cells of origin. *Nat Commun* (2019) 10:91. doi: 10.1038/s41467-018-07857-9
9. Polyzos AA, Lee DY, Datta R, Hauser M, Budworth H, Holt A, et al. Metabolic reprogramming in astrocytes distinguishes region-specific neuronal susceptibility in Huntington mice. *Cell Metab* (2019) 29:1258–73.e11. doi: 10.1016/j.cmet.2019.03.004
10. Lundø K, Trauelsen M, Pedersen SF, Schwartz TW. Why Warburg works: Lactate controls immune evasion through GPR81. *Cell Metab* (2020) 31:666–8. doi: 10.1016/j.cmet.2020.03.001
11. Lee DC, Sohn HA, Park ZY, Oh S, Kang YK, Lee KM, et al. A lactate-induced response to hypoxia. *Cell* (2015) 161:595–609. doi: 10.1016/j.cell.2015.03.011
12. Zhang Y, Wang J. Targeting uptake transporters for cancer imaging and treatment. *Acta Pharm Sin B* (2020) 10:79–90. doi: 10.1016/j.apsb.2019.12.005

13. Ganapathy-Kanniappan S. Linking tumor glycolysis and immune evasion in cancer: Emerging concepts and therapeutic opportunities. *Biochim Biophys Acta Rev Cancer* (2017) 1868:212–20. doi: 10.1016/j.bbcan.2017.04.002
14. Vinasco K, Mitchell HM, Kaakoush NO, Castaño-Rodríguez N. Microbial carcinogenesis: Lactic acid bacteria in gastric cancer. *Biochim Biophys Acta Rev Cancer* (2019) 1872:188309. doi: 10.1016/j.bbcan.2019.07.004
15. Martinez-Outschoorn UE, Peiris-Pagés M, Pestell RG, Sotgia F, Lisanti MP. Cancer metabolism: a therapeutic perspective. *Nat Rev Clin Oncol* (2017) 14:11–31. doi: 10.1038/nrclinonc.2016.60
16. Zhao Z, Han F, Yang S, Wu J, Zhan W. Oxamate-mediated inhibition of lactate dehydrogenase induces protective autophagy in gastric cancer cells: involvement of the Akt-mTOR signaling pathway. *Cancer Lett* (2015) 358:17–26. doi: 10.1016/j.canlet.2014.11.046
17. Liu J, Pan C, Guo L, Wu M, Guo J, Peng S, et al. A new mechanism of trastuzumab resistance in gastric cancer: MACC1 promotes the Warburg effect via activation of the PI3K/AKT signaling pathway. *J Hematol Oncol* (2016) 9:76. doi: 10.1186/s13045-016-0302-1
18. Stone SC, Rossetti RAM, Alvarez KLF, Carvalho JP, Margarido PFR, Baracat EC, et al. Lactate secreted by cervical cancer cells modulates macrophage phenotype. *J Leukoc Biol* (2019) 105:1041–54. doi: 10.1002/JLB.3A0718-274RR
19. Liu X, Yang Z, Chen Z, Chen R, Zhao D, Zhou Y, et al. Effects of the suppression of lactate dehydrogenase A on the growth and invasion of human gastric cancer cells. *Oncol Rep* (2015) 33:157–62. doi: 10.3892/or.2014.3600
20. Cassim S, Raymond VA, Dehbidi-Assadzadeh L, Lapierre P, Bilodeau M. Metabolic reprogramming enables hepatocarcinoma cells to efficiently adapt and survive to a nutrient-restricted microenvironment. *Cell Cycle* (2018) 17:903–16. doi: 10.1080/15384101.2018.1460023
21. El-Sisi AE, Sokar SS, Abu-Risha SE, El-Mahrouk SR. Oxamate potentiates taxol chemotherapeutic efficacy in experimentally-induced solid ehrlich carcinoma (SEC) in mice. *BioMed Pharmacother* (2017) 95:1565–73. doi: 10.1016/j.biopha.2017.09.090
22. Wu P, Xu R, Chen X, Zhao Y, Tan D, Zhao Y, et al. Establishment and characterization of patient-derived xenografts for hormone-naïve and castrate-resistant prostate cancers to improve treatment modality evaluation. *Aging (Albany NY)* (2020) 12:3848–61. doi: 10.18632/aging.102854
23. De La Rochere P, Guil-Luna S, Decaudin D, Azar G, Sidhu SS, Piaggio E. Humanized mice for the study of immuno-oncology. *Trends Immunol* (2018) 39:748–63. doi: 10.1016/j.it.2018.07.001
24. Meraz IM, Majidi M, Meng F, Shao R, Ha MJ, Neri S, et al. An improved patient-derived xenograft humanized mouse model for evaluation of lung cancer immune responses. *Cancer Immunol Res* (2019) 7:1267–79. doi: 10.1158/2326-6066.CIR-18-0874
25. Scroggins BT, Matsuo M, White AO, Saito K, Munasinghe JP, Sourbier C, et al. Hyperpolarized [1-^{13}C]-pyruvate magnetic resonance spectroscopic imaging of prostate cancer *in vivo* predicts efficacy of targeting the Warburg effect. *Clin Cancer Res* (2018) 24:3137–48. doi: 10.1158/1078-0432.CCR-17-1957
26. Chen YJ, Mahieu NG, Huang X, Singh M, Crawford PA, Johnson SL, et al. Lactate metabolism is associated with mammalian mitochondria. *Nat Chem Biol* (2016) 12:937–43. doi: 10.1038/nchembio.2172
27. Renner K, Bruss C, Schnell A, Koehl G, Becker HM, Fante M, et al. Restricting glycolysis preserves T cell effector functions and augments checkpoint therapy. *Cell Rep* (2019) 29:135–50.e9. doi: 10.1016/j.celrep.2019.08.068
28. Lindner K, Borchardt C, Schöpp M, Bürgers A, Stock C, Hussey DJ, et al. Proton pump inhibitors (PPIs) impact on tumor cell survival, metastatic potential and chemotherapy resistance, and affect expression of resistance-relevant miRNAs in esophageal cancer. *J Exp Clin Cancer Res* (2014) 33:73. doi: 10.1186/s13046-014-0073-x
29. Pilon-Thomas S, Kodumudi KN, El-Kenawi AE, Russell S, Weber AM, Luddy K, et al. Neutralization of tumor acidity improves antitumor responses to immunotherapy. *Cancer Res* (2016) 76:1381–90. doi: 10.1158/0008-5472.CAN-15-1743
30. Zhai X, Yang Y, Wan J, Zhu R, Wu Y. Inhibition of LDH-A by oxamate induces G2/M arrest, apoptosis and increases radiosensitivity in nasopharyngeal carcinoma cells. *Oncol Rep* (2013) 30:2983–91. doi: 10.3892/or.2013.2735
31. Spugnini EP, Fais S. Drug repurposing for anticancer therapies. A lesson from proton pump inhibitors. *Expert Opin Ther Pat* (2020) 30:15–25. doi: 10.1080/13543776.2020.1704733
32. Azzarito T, Lugini L, Spugnini EP, Canese R, Gugliotta A, Fidanza S, et al. Effect of modified alkaline supplementation on syngenic melanoma growth in CB57/BL mice. *PloS One* (2016) 11:e0159763. doi: 10.1371/journal.pone.0159763
33. Daneshmandi S, Wegiel B, Seth P. Blockade of lactate dehydrogenase-A (LDH-A) improves efficacy of anti-programmed cell death-1 (PD-1) therapy in melanoma. *Cancers (Basel)* (2019) 11:450. doi: 10.3390/cancers11040450
34. Lin S, Huang G, Cheng L, Li Z, Xiao Y, Deng Q, et al. Establishment of peripheral blood mononuclear cell-derived humanized lung cancer mouse models for studying efficacy of PD-L1/PD-1 targeted immunotherapy. *MAbs* (2018) 10:1301–11. doi: 10.1080/19420862.2018.1518948
35. Rosato RR, Dávila-González D, Choi DS, Qian W, Chen W, Kozielski AJ, et al. Evaluation of anti-PD-1-based therapy against triple-negative breast cancer patient-derived xenograft tumors engrafted in humanized mouse models. *Breast Cancer Res* (2018) 20:108. doi: 10.1186/s13058-018-1037-4
36. Galon J, Bruni D. Approaches to treat immune hot, altered and cold tumours with combination immunotherapies. *Nat Rev Drug Discov* (2019) 18:197–218. doi: 10.1038/s41573-018-0007-y
37. AbdulJabbar K, Raza SEA, Rosenthal R, Jamal-Hanjani M, Veeriah S, Akarca A, et al. Geospatial immune variability illuminates differential evolution of lung adenocarcinoma. *Nat Med* (2020) 26:1054–62. doi: 10.1038/s41591-020-0900-x
38. Liu Y, Zugazagoitia J, Ahmed FS, Henick BS, Gettinger SN, Herbst RS, et al. Immune cell PD-L1 colocalizes with macrophages and is associated with outcome in PD-1 pathway blockade therapy. *Clin Cancer Res* (2020) 26:970–7. doi: 10.1158/1078-0432.CCR-19-1040
39. Brand A, Singer K, Koehl GE, Kolitzus M, Schoenhammer G, Thiel A, et al. LDHA-associated lactic acid production blunts tumor immunosurveillance by T and NK cells. *Cell Metab* (2016) 24:657–71. doi: 10.1016/j.cmet.2016.08.011
40. Colegio OR, Chu NQ, Szabo AL, Chu T, Rhebergen AM, Jairam V, et al. Functional polarization of tumour-associated macrophages by tumour-derived lactic acid. *Nature* (2014) 513:559–63. doi: 10.1038/nature13490

Conflict of Interest: The authors declare that the research was conducted in the absence of any commercial or financial relationships that could be construed as a potential conflict of interest.

Copyright © 2021 Qiao, Xiong, Feng, Guo, Zhou, Zhao, Jiang, Shi and Han. This is an open-access article distributed under the terms of the Creative Commons Attribution License (CC BY). The use, distribution or reproduction in other forums is permitted, provided the original author(s) and the copyright owner(s) are credited and that the original publication in this journal is cited, in accordance with accepted academic practice. No use, distribution or reproduction is permitted which does not comply with these terms.

frontiers in Immunology

REVIEW
published: 02 April 2021
doi: 10.3389/fimmu.2021.662360

Fit-For-All iPSC-Derived Cell Therapies and Their Evaluation in Humanized Mice With NK Cell Immunity

Charlotte Flahou[1], *Tatsuya Morishima*[2,3], *Hitoshi Takizawa*[2] *and Naoshi Sugimoto*[1*]

[1] Department of Clinical Application, Center for iPS Cell Research and Application (CiRA), Kyoto University, Kyoto, Japan, [2] Laboratory of Stem Cell Stress, International Research Center for Medical Sciences (IRCMS), Kumamoto University, Kumamoto, Japan, [3] Laboratory of Hematopoietic Stem Cell Engineering, International Research Center for Medical Sciences (IRCMS), Kumamoto University, Kumamoto, Japan

OPEN ACCESS

Edited by:
Tim Willinger,
Karolinska Institutet, Sweden

Reviewed by:
Christian Beausejour,
Université de Montréal, Canada
Nico Lachmann,
Hannover Medical School, Germany
Igor Slukvin,
University of Wisconsin-Madison,
United States

***Correspondence:**
Naoshi Sugimoto
sugimoto.naoshi.4v@kyoto-u.jp

Specialty section:
This article was submitted to
Cancer Immunity
and Immunotherapy,
a section of the journal
Frontiers in Immunology

Received: 01 February 2021
Accepted: 17 March 2021
Published: 02 April 2021

Citation:
Flahou C, Morishima T, Takizawa H and Sugimoto N (2021) Fit-For-All iPSC-Derived Cell Therapies and Their Evaluation in Humanized Mice With NK Cell Immunity. Front. Immunol. 12:662360. doi: 10.3389/fimmu.2021.662360

Human induced pluripotent stem cells (iPSCs) can be limitlessly expanded and differentiated into almost all cell types. Moreover, they are amenable to gene manipulation and, because they are established from somatic cells, can be established from essentially any person. Based on these characteristics, iPSCs have been extensively studied as cell sources for tissue grafts, blood transfusions and cancer immunotherapies, and related clinical trials have started. From an immune-matching perspective, autologous iPSCs are perfectly compatible in principle, but also require a prolonged time for reaching the final products, have high cost, and person-to-person variation hindering their common use. Therefore, certified iPSCs with reduced immunogenicity are expected to become off-the-shelf sources, such as those made from human leukocyte antigen (HLA)-homozygous individuals or genetically modified for HLA depletion. Preclinical tests using immunodeficient mice reconstituted with a human immune system (HIS) serve as an important tool to assess the human alloresponse against iPSC-derived cells. Especially, HIS mice reconstituted with not only human T cells but also human natural killer (NK) cells are considered crucial. NK cells attack so-called "missing self" cells that do not express self HLA class I, which include HLA-homozygous cells that express only one allele type and HLA-depleted cells. However, conventional HIS mice lack enough reconstituted human NK cells for these tests. Several measures have been developed to overcome this issue including the administration of cytokines that enhance NK cell expansion, such as IL-2 and IL-15, the administration of vectors that express those cytokines, and genetic manipulation to express the cytokines or to enhance the reconstitution of human myeloid cells that express IL15R-alpha. Using such HIS mice with enhanced human NK cell reconstitution, alloresponses against HLA-homozygous and HLA-depleted cells have been studied. However, most studies used HLA-downregulated tumor cells as the target cells and tested *in vitro* after purifying human cells from HIS mice. In this review, we give an overview of the current state of iPSCs in cell therapies, strategies to lessen their immunogenic potential, and then expound on the development of HIS mice with

reconstituted NK cells, followed by their utilization in evaluating future universal HLA-engineered iPSC-derived cells.

Keywords: humanized mice, human induced pluripotent stem cells, regenerative medicine, natural killer cells, human leukocyte antigen

INTRODUCTION

The ability to reprogram adult cells into induced pluripotent stem cells (iPSCs) has changed regenerative medicine. The original reprogramming to induce pluripotency in somatic cells was done by the ectopic co-expression of four transcriptions factors, c-MYC, OCT3/4, SOX2 and KLF4, or similar combinations (1–4). iPSCs (re-)acquire the ability to develop the three embryonic germ layers and propagate in culture indefinitely. Their cell fate can then be further directed to differentiate iPSCs into various types of differentiated human cells (5). In addition, iPSCs can be established from essentially anyone and genetically manipulated. iPSCs are therefore regarded as a suitable platform to develop regenerative cell therapies.

As iPSC-derived cells make their way to clinical applications, allogeneic cells as off-the-shelf products are being preferentially considered (6, 7). Thus, a critical challenge is making iPSCs immunologically tolerable by the receiving individual. To circumvent the most significant alloimmune barriers to allotransplantation, namely the mismatch of HLA, a number of strategies are being explored. iPSCs can be established from people with homozygous HLA haplotypes, which would increase the number of matching recipients to a single donor, and are available through iPSC stocks (8–10). In addition, engineering the HLA expression of the cells to be transplanted, specifically downregulating HLA, could also be immunologically tolerable for the recipient. However, even supposing that the T cell-based primary rejection mechanism is avoided by HLA downregulation, natural killer (NK) cells possess complementary recognition pathways which can promote graft rejection (11–13).

Accurately recapitulating NK cell rejection mechanisms *in vivo* is therefore crucial for successful HLA-homozygous and HLA-engineered iPSC-based transplantation therapies. To this end, notable efforts have allowed for mice with a humanized immune system (HIS) to acquire an increasingly comprehensive representation of human immune cell populations (14). From interventions aiming to entirely mute the mouse immune system to sophisticated genetic engineering to switch mouse immune factors to their human version, strategies have yielded mouse models that can recapitulate specific parts of human immunity. Notably, the reconstitution of the innate immune compartment, such as myeloid cells and NK cells, has recently gathered a fair amount of attention.

This review aims to provide the reader with an overview of the therapeutic potential of iPSCs with strategies to overcome HLA barriers in regenerative medicine, along with their evaluation in HIS mice sufficiently reconstituted with human NK cells.

CURRENT STATUS OF THE CLINICAL APPLICATION OF IPSCS IN REGENERATIVE MEDICINE

Cell replacement therapy and regenerative medicine advances are excitingly multiplying as research explores their great proliferation potential and high versatility of iPSC application. Contrary to the relatively controversial embryonic stem cells (ESCs), iPSCs do not involve the handling of embryonic material and therefore provide a more acceptable platform to develop regenerative therapies. Nevertheless, norms and expectations surrounding the ethical implications of iPSCs have been accounted for since the early times of their development (15) and regularly discussed since then (16, 17). In addition to their minimal ethical hurdle, iPSCs – like ESCs – can be produced off-the shelf in clinically relevant quantities in bioreactors or culture dishes, which enables a stable supply and use for emergency situations, given the right logistics. They can also be differentiated into various types of adult human cells (5) as well as qualified for safety (pathogens and contamination) and consistency (genotyping, phenotype characterization). iPSCs are also relatively receptive to genetic engineering, which opens endless possibilities for clinical applications. Reports from pre-clinical and *in vitro* studies, reviews (6, 18, 19), as well as two clinical trials for age-related macular degeneration (AMD) (20, 21) and, more recently, mesenchymal stromal cells (MSCs) for graft versus host disease (GVHD) (22) have so far indicated that iPSC-based therapies are safe.

Although iPSCs are only a little over a decade old, as of December 2020, about twenty clinical trials have been publicly announced as either completed or ongoing, including one targeting COVID-19 using iPSC-derived MSCs (23) (**Table 1**). AMD was the first pathology to be given approval for human transplantation of iPSCs-derived cells (20, 21). To date degenerative eye disorders are of the most commonly targeted diseases in iPSC-based clinical trials (24–27), along with cardiac syndromes such as heart failure and myocardial ischemia (28–32), followed by neuropathies - Parkinson's disease and spinal cord injury (33, 34) -, and thrombocytopenia from aplastic anemia (35). In contrast to the replacement of defective cells illustrated by those studies mentioned previously, iPSCs-based development of immunotherapies, namely iPSC-derived MSCs and iPSC-derived NK cells, have been conducted more proactively by the private sector for GVHD (36) and hematologic malignancies (37–40), respectively. Of note, within all the trial mentioned, three used autologous patient-derived iPSCs as the source of the cell for transplantation (two trials for AMD and the trial for thrombocytopenia from aplastic anemia), while the other trials transplanted cells differentiated from banked iPSCs.

TABLE 1 | Registered clinical trials using iPSCs.

Affiliation	Disease target	Cell therapy	ID	Date	Cell source
Help Therapeutics	Heart failure	iPSC-CMs	NCT03763136	(estimated) May 1, 2019	Allogeneic
University Medical Center Goettingen	Heart failure	iPSC-CMs and stromal cells in hydrogel	NCT04396899	(estimated) December, 2020	Allogeneic
Osaka University	Myocardial ischemia	iPSC-CMs	NCT04696328	2-Dec-19	Allogeneic
National Eye Institute	AMD	iPSC-RPE on PLGA scaffold	NCT04339764	23-Sep-20	Autologous
Cynata Therapeutics	Steroid-resistant GVHD	iPSC-MSCs	NCT02923375	1-Mar-17	Allogeneic
Fate Therapeutics	Various cancers	iPSC-NK cells	NCT03841110	15-Feb-19	Allogeneic
Fate Therapeutics	AML, B-cell lymphoma	iPSC-NK cells	NCT04023071	4-Oct-19	Allogeneic
Fate Therapeutics	B-cell lymphoma or CLL	iPSC-NK cells	NCT04245722	19-Mar-20	Allogeneic
Fate Therapeutics	AML, multiple myeloma	iPSC-NK cells	NCT04614636	(estimated) November, 2020	Allogeneic
Cynata Therapeutics	COVID-19, ARDS	iPSC-MSCs	NCT04537351	24-Aug-20	Allogeneic
Keio University School of Medicine	Heart failure	iPSC-CMs	jRCTa032200189	9-Nov-20	Allogeneic
Kobe City Eye Hospital	Retinitis Pigmentosa	iPSC-RPE	jRCTa050200027	5-Oct-20	Allogeneic
Kyoto University Hospital	Thrombocytopenia	iPSC-platelets	jRCTa050190117	14-May-19	Autologous
Keio University School of Medicine	Spinal cord injury	iPSC-neural stem/progenitor cells	jRCTa031190228	1-Dec-20	Allogeneic
Kyoto University Hospital	Parkinson's disease	iPSC-dopaminergic progenitors	JMA-IIA00384	12-Sep-18	Allogeneic
RIKEN	AMD	iPSC-RPE	UMIN000011929	2-Oct-13	Autologous
Kobe City Eye Hospital	AMD	iPSC-RPE	UMIN000026003	6-Feb-17	Allogeneic (HLA-matched)

AMD, age-related macular degeneration; GVHD, graft versus host disease; AML, acute myeloid leukemia; CLL, chronic lymphocytic leukemia; ARDS, acute respiratory distress syndrome; CMs, cardiomyocytes; MSCs, mesenchymal stromal cells; RPE, Retinal Pigment Epithelium.

STRATEGIES TO CIRCUMVENT IMMUNE REJECTION AGAINST IPSC-DERIVED GRAFTS

Graft rejection is a major issue in allogeneic transplantations. The general mechanism of an allograft rejection is the dominant activation of the recipient's T cells by recognizing non-self alloantigens on the donor major histocompatibility complex (MHC) antigens, which are HLAs in the case of humans. Jean Dausset described the first HLA, HLA-A2, in 1958 (41) after his observations in 1952 of donor-recipient leukocyte incompatibilities, which were then extended to tissues. Today we know that the two classes of HLA, class I, HLA-A, -B, and –C, and class II, HLA-DR, -DP, and -DQ, are encoded within chromosome 6p21 (**Figure 1**) (42). Humans carry a pair of HLA haplotypes, which are specifically distributed relative to

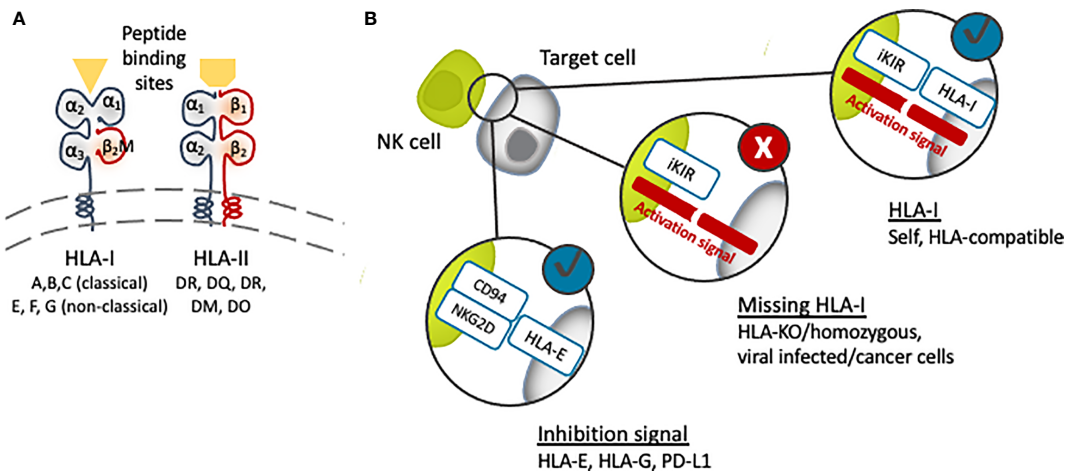

FIGURE 1 | **(A)** Schematic structure of human leukocyte antigen (HLA). Targeting the β2M subunit of HLA-I will cause disruption of all HLA-I expression [major (A–C) and minor (E–G)]. **(B)** The presence of HLA-I matching with the recipient NK cells' inhibitory KIR receptor (iKIR) will induce tolerance, while the lack or downregulation of HLA-I will trigger NK cell immunity.

ethnicities and geographic regions. To minimize the rejection caused by an alloimmune response, matching for the HLA haplotype between the donor and recipient is necessary, and comprehensive guidelines are applied for best practices to ensure clinical benefits to the patients (43–45).

HLA class I are cell surface proteins built up with a polymorphic heavy chain and a conserved light chain, called β-2-microglobulin (β2M), forming together a functional heterodimer (**Figure 1**). They are found in all nucleated cells and platelets, although their expression in iPSCs is lower compared to somatic cells (46). The main function of HLA class I molecules is to display peptide antigens to T cell receptors (TCRs) on CD8+ T cells. In contrast, CD4+ T cells receive antigenic cues from peptides mounted on HLA class II, which are expressed only in dendritic cells (DCs), macrophages, B cells and other antigen-presenting cells (APCs). When the HLA on transplanted cells is different from the host, T cells will initiate cytotoxic and other immune responses leading to graft destruction.

iPSCs offer a unique opportunity to circumvent the immunological barriers to transplantation, and, as reviewed elsewhere (47, 48), a number of strategies are being explored to reduce the potential immunogenicity of the iPSC (or ESC)-derived biological transplantation material. The three main strategies, autologous, HLA homozygous and HLA depleted, are discussed here (**Figure 2**).

AUTOLOGOUS IPSC-DERIVED GRAFTS

The history of allotransplantation has revealed HLA as the major driver of an immune response, but minor histocompatibility antigens and ABO antigens can be crucial alloantigens as well. Therefore, immunosuppressive agents with non-negligible side effects are usually used. However, rejection still cannot be controlled in some cases. Autologous iPSCs can be established from essentially any patient so long a small portion of skin or blood is available and provide differentiated cells that, in principle, cause no alloimmune-mediated rejection. However, there are some reports stating the immunogenicity of autologous iPSC-derived grafts, which may be due to epigenetically dysregulated expression of immunogenic proteins, somatic mutations and other alterations due to genetic instabilities and genetic manipulations (49–56).

Based on less concern of rejection and donor-derived infection, autologous iPSCs were chosen in the first clinical trial for AMD, which reported no adverse events two years after the transplantation (20). In the case of the trial for thrombocytopenia due to aplastic anemia, the person receiving iPSC-derived platelets suffers from platelet transfusion refractoriness due to an anti-platelet alloantibody, justifying the transplantation of autologous cells (35, 57).

Autologous iPSC-derived cells are often not practical, however, because as mentioned above, establishing iPSCs from patients and differentiating them to a final cell product each time requires labor- and cost-intensive logistics and the quality would vary each time (17). Indeed, not only could the therapy be prohibitively expensive, it may also not even be available in time to benefit the patient. Moreover, in the case the pathology is caused by a mutation, the generated cells will possess the same mutation if not corrected by genetic engineering.

HLA-HOMOZYGOUS IPSC STOCKS AS SOURCE CELLS OF ALLOGRAFTS

As an alternative, iPSCs established from people with homozygous HLA haplotypes are available through iPSC stock projects. Currently, there is momentum to build biobanks of iPSCs with enough HLA haplotypes to supply HLA-matched cells to a wide population (8–10). iPSCs with homozygous HLA haplotypes are stocked, and good manufacturing practice (GMP) grade lines have been distributed for regenerative medicine. Homozygous haplotypes are advantageous, since they have wide compatibility potential due to the need to only match one of the two HLA haplotypes of the recipient to avoid the intense rejection mediated by T cell-HLA interactions. Thus, the mass production of uniform allogeneic off-the-shelf donor-derived material would greatly expand the number of patients who would benefit from these regenerative therapies. Accordingly,

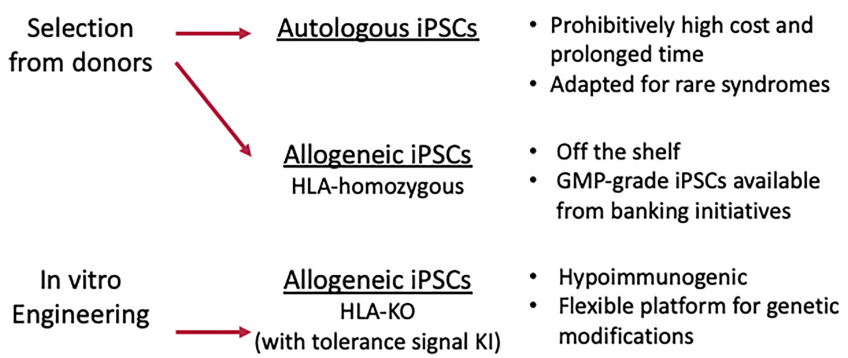

FIGURE 2 | Capability of iPSCs to provide immune-compatible products.

allogeneic iPSCs are predominantly preferred in clinical trials using iPSC products (**Table 1**).

However, limitations still exist, because HLA are highly polymorphic, and, as mentioned earlier, epitope heterogeneity greatly varies between geographic regions and ethnicities. Building stocks for a heterogeneous population is a greater logistic and financial challenge than for a relatively homogeneous population. For example, the required size of the Japanese HLA-homozygous iPS cell bank is relatively small compared with other regions (17). Moreover, banks must take in account alleles of rare frequencies, which adds to the number of cells to stock. Indeed, it becomes increasing difficult to cover a higher rate of the population. For Japan, the 10 most frequent HLA haplotypes can cover 50% of the population, but the 75 most frequent haplotypes are needed to reach 80%, and 140 to reach 90% (9, 17). Considering that each iPSC cell line needs to undergo careful characterization and regulatory safety evaluation, the workload, although feasible, is costly and time-consuming.

HLA DEPLETION

Another option is to leverage the property of iPSCs to be amenable to genetic manipulation, specifically, eliminate or downregulate the HLA expression, to avoid T cell recognition (**Figure 3**). For most cases, the reduction of HLA class I expression have been achieved by targeting the conserved β2M chain. Researchers have access to several molecular tools to disrupt β2M expression, and the choice depends on the outcome needed. Post-transcriptional manipulation by RNA interference (RNAi), either using small interfering RNA (siRNA) or short hairpin RNA (shRNA), stably downregulated or silenced the expression of HLA proteins in B-lymphocyte cell lines (58) in conjunction with human ESCs (59), iPSCs (60), primary human hepatocytes (61), endothelial cells (62, 63) and in a perfusion system at the whole organ level in rat kidney (64). Silencing with RNAi proved to be stable even after the iPSCs were differentiated to megakaryocytes and even platelets (60). TALENs (65), CRISPR/Cas9 (66–71) and vector-mediated gene targeting technology (72–74), on the other hand, are used to achieve complete depletion of HLA-I through β2M-targeting. The simultaneous knockout of HLA-A/B/C by multiplex CRISPR/Cas9 has also been reported (75).

Notably, in those studies, the complete knockout of HLA was found stable after the ESC/iPSCs were differentiated, and no off-target integration or non-specific cleavage events were observed (66, 74). However, current technology cannot rule out off-target events and potential unwanted cell behavior. Introducing modalities such as suicide genes or other safeguards to eliminate the possibility of grafts with uncontrolled growth is recommended (76). Two major suicide genes studied are thymidine kinase gene of the herpes simplex virus (HSV-TK), which can be switched on with ganciclovir treatment, and inducible caspase-9 (iCas9), which can be activated with a synthetic chemical inducer of dimerization (CID) treatment. To overcome its inactivation in proliferating cells, HSV-TK gene was transcriptionally linked to a cell-division gene CDK1 (77). Further, the combination of HSV-TK and iCas9 can kill all cell types or specifically undifferentiated ESCs/iPSCs (78). New technologies such as synthetic microRNA switches can also be applied to eliminate unwanted cells safely (79, 80).

Both knockdown and knockout have distinct advantages. Because CD8+T cell immunity can be triggered by even a very low number of HLA-I-peptide complexes (81), complete knockout of HLA class I can enable total invisibility from

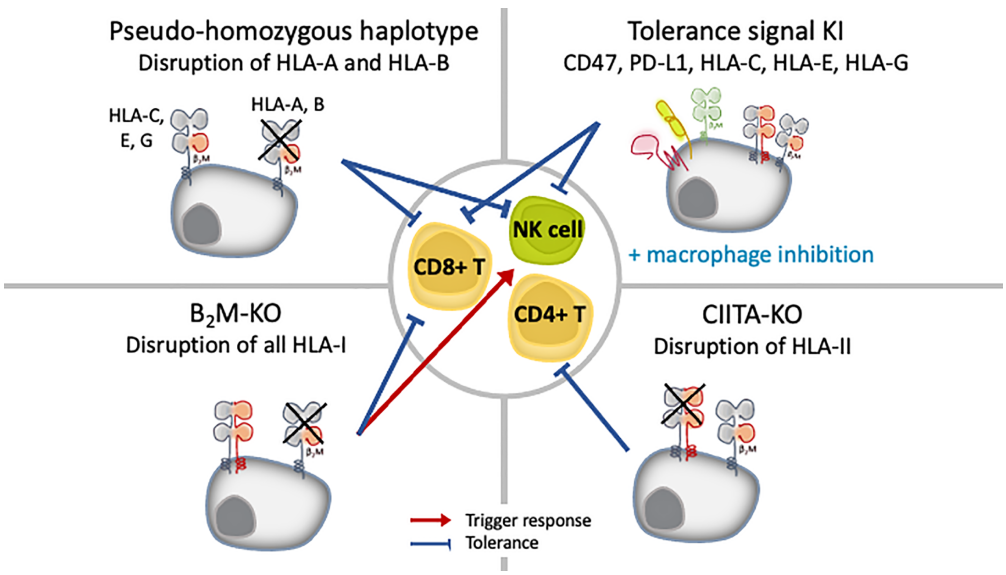

FIGURE 3 | iPSC engineering strategies to inhibit allogeneic immunity and promote tolerance.

T cell cytotoxicity. This approach is also applicable for CD4+ T cells and HLA class II-mediated antigen presentation, for which disruption is achieved by targeting class II MHC transactivator (CIITA) genes (66–69). Additionally, neither approach seems to be detrimental to cell function after differentiation to megakaryocytes and platelets (70, 71), cardiomyocytes (67, 68) or RPE cells (66). However, because HLA class I molecules are also ligands that negatively regulate the activation of NK cells, the complete loss of HLA class I risks triggering a response by NK cells through "missing self" immunity, thus, residual expression instead of complete removal of HLA class I might be preferential to prevent graft rejection by NK cells.

EVADING NK CELL RESPONSE AGAINST HLA-HOMOZYGOUS OR HLA-DEPLETED CELLS

NK cells are the innate counterpart of cytotoxic CD8+ T cells, presenting cytotoxic activities and releasing cytokines such as interferon-γ (IFNγ) upon target cell recognition. NK cells recognize "missing self" cells that have downregulated the expression of HLA class I (11–13), such as virus-infected cells, tumor cells and experimentally HLA-mismatch allografts. The balance between activation and inhibitory signals regulates NK cell activity, and HLA class I molecules act as ligands that inhibit NK cell activation through killer immunoglobulin-like receptors (KIR) and CD94/NKG2A heterodimer (**Figure 1**). Among HLA class I molecules, all HLA-C molecules and some HLA-A and HLA-B are ligands for inhibitory KIRs. HLA-C molecules are divided into C1 and C2 groups based on the group of KIR they bind. Accordingly, one study showed that endothelial cells generated from HLA-C1/C1 iPSCs were killed by NK cells from an HLA-C1/C2 individual *in vitro*, as they were regarded as missing C2 (82). This "missing self HLA-C" immune response demonstrates the importance of considering the rejection of HLA-homozygous and HLA-depleted iPSC-derived allografts by host NK cells.

Attempts to promote tolerance against NK cells for transplanted iPSC-derived cells have come from a deeper understanding of the involvement of HLA-C, non-classical HLA class I (HLA-E, -F and -G) and self-signal (CD47 and PD-L1) pathways in cancer evasion as well as in physiological immune privileged sites, particularly the maternal-placenta interface (**Figure 3**) (83–86). In early studies, isoforms of HLA-G, a quasi-monomorphic HLA, were expressed in HLA class I-deficient or HLA class I-expressing cell lines and proved to be protective against NK cell cytotoxic activity in both cases (87, 88). *In vitro*, the forced expression of HLA-G induced an immunosuppressive phenotype in human ESCs expressing moderate levels of HLA-A, -B, -C, and low levels of HLA class II as well as in their epidermal precursor derivatives, which expressed lower levels of HLA-I overall (89). Riteau et al. showed that HLA-E was also a potent inhibitor of NK cell cytotoxicity (86). In an *in vivo* monkey model, iPSC-derived RPE cells were shown to repress NK cell cytotoxicity by a mechanism dependent on HLA-E, which was naturally expressed on these cells (90). Recently, human ESCs with knock-in of only HLA-E in conjunction with the depletion of whole HLA class I by targeting β2M did not elicit an immune response from either CD8+T cells or NK cells *in vitro* and *in vivo* (72).

Another strategy exploits immune checkpoint molecules such as PD-L1 and CD47. Both are immunomodulatory molecules involved in mechanisms of self-protection or "don't eat me" signaling. CD47 is a ubiquitous receptor whose function is to inhibit phagocytosis (91). Its overexpression in MHC class I knockout murine iPSCs was protective in a mouse model (68). Finally, the selective targeting of classical HLA class I has been proposed as a strategy to create hypo-immune cells that are "invisible" to NK cells. Indeed, the specific targeting of HLA-A in B-lymphocyte cell lines *in vitro* and the disruption of both HLA-A and -B alleles in iPSCs *in vitro* and *in vivo* reduced lysis by T cells and NK cells (58, 69, 92).

MODELLING HUMAN IMMUNITY IN HIS MOUSE MODELS

Transplantation tolerance and rejection mechanisms operate through several interconnected pathways involving both the adaptive and innate immune systems (93). Animal models should therefore recapitulate as many human immune system components as possible. In the human immune system, these cellular and molecular components work as an overall horizontal system that allows redundant and complementary processes to efficiently protect against internal and external threats to the body's homeostasis. The mouse immune system mirrors the general paradigms of these complementary processes in humans, but differs in finer but significant aspects (94, 95). Although not perfect models (94, 95), mice are nonetheless instrumental pre-clinical assets for testing new therapies before moving on to human trials. In order to improve the predictive value of rodent-based studies so that mechanistic insights into immune responses are not "lost in translation" but highly relevant for transplantation studies, immune-deficient mice can be engrafted with a functional human immune system (**Figure 4**). These models will hereafter be referred to as HIS mice.

Three sources of human hemato-lymphoid cells or tissues are commonly transplanted into immunodeficient mice to stably reconstitute the human immune system. 1) In the hu-PBL model, peripheral blood leukocytes (PBL) are isolated from human blood and then transplanted into mice. 2) In the hu-SRC model, the cells transplanted are human severe combined immunodeficiency (SCID) repopulating cells (SRC), that is to say: CD34+ hematopoietic stem cells (HSCs) from umbilical cord blood (UCB), fetal liver, bone marrow (BM) or granulocyte colony-stimulating factor (G-CSF) mobilized peripheral blood. 3) In the last model, hu-BLT (BM/liver/thymus), a combination of fetal liver and thymus fragments is injected under the kidney capsule with fetal liver HSCs. Choosing one model over the other will lead to varying outcomes in the engraftment level or

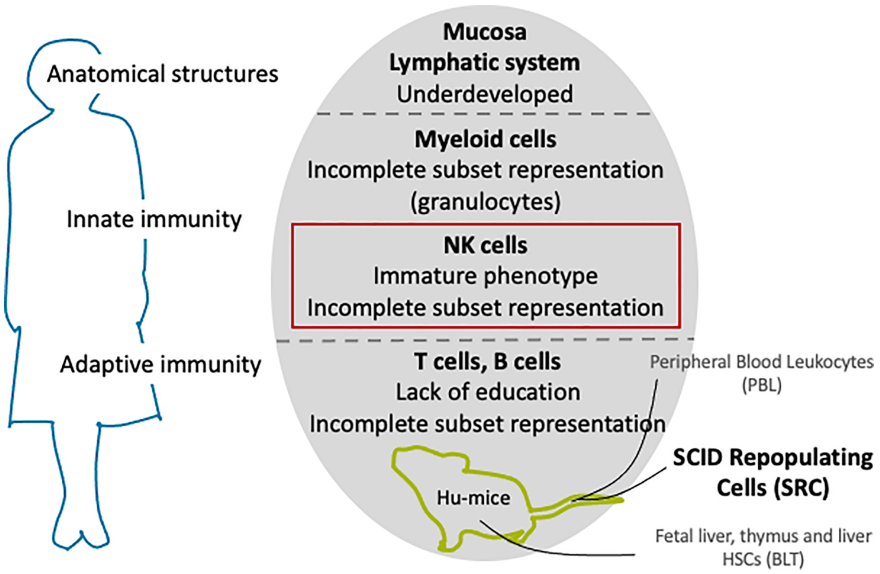

FIGURE 4 | Current challenges in recounstituting a human immune system in immundeficient mice.

repopulation allotment (96). Briefly, the hu-PBL model has the advantage of grafting readily mature lymphoid cells and has a high reconstitution of CD3+ T cells, while the hu-SRC and hu-BLT models employ more primitive stem cells. As a consequence, the hu-PBL model provides a relatively easy and straightforward recapitulation of the mature immune system, but also the least physiological. Furthermore, it easily develops xeno-GVHD, which limits the experimental window period. The hu-SRC model takes a comparatively longer time to achieve reconstitution but provides the multilineage development of hematopoietic cells and can recapitulate the development of the endogenous human immune system. However, innate immune cells such as myeloid lineages and NK cells as well as T cells are less developed. In addition, xeno-GVHD could still develop, but this can be overcome by the depletion of mouse MHC molecules (97). The hu-BLT model is reputed to have the highest level of human cell reconstitution and allows the robust reconstitution of educated T cells. However, it requires high technical skills to produce as well as fetal human tissue, thus, its availability is very limited.

The development of an HIS following the xenotransplantation of human cells is not tolerated unless the mice are severely immunocompromised first. Humanization of the mouse immune system is built on three main steps of genetic manipulation and breeding. Historically, the first genetic mutant immunodeficient mice was CB17-*scid* mice discovered in 1983, in which severe combined immunodeficiency (scid) affecting T and B cells resulted from the spontaneous homozygous loss of a functional mutation in the *PRKDC* gene (protein kinase, DNA-activated, catalytic polypeptide) (98). However, the mutation did not mute the innate immune system, and murine adaptive cells progressively reconstituted as the mice aged, which resulted in the low engraftment of human cells. In a subsequent manipulation, the scid mutation was crossed in non-obese diabetic (NOD) mice (NOD-*scid*), which resulted in lower innate immune system function and resolved the diabetes from the NOD background, which was T-cell mediated (99, 100). NOD-*scid* mice have been extensively used in xenotransplantation studies, but they are impeded by a characteristically short lifespan and predisposition to lymphoma, a still relatively low level of chimerism, and the progressive "leaking" of T and B cells. Recombination-activating gene (Rag)-1 and Rag-2 knockout mice helped to reduce the reappearance of the adaptive immune system but resolved neither the tendency of the NOD-*scid* to develop lymphomas nor the engraftment issues. The last major genetic manipulation, namely the disruption of murine cytokine signaling by targeting the interleukin-2 (IL-2) receptor γ chain locus, resulted in higher chimerism levels and more silencing of both adaptive and innate cells. The resulting immunodeficient $IL2rg^{null}$ mice were then crossed with various stains such as NOD-*scid* to produce the NOD-*scid* gamma strain (NSG) and in the same manner the NOD-*Rag1* gamma (NRG) and BALB/c- *Rag2* gamma (BRG) strains.

ENHANCING NK CELL RECONSTITUTION IN HIS MOUSE MODELS

NSG-, NOG-, and BRG-based HIS mice have had an important beneficial impact in biomedical research but are more inclined toward modelling T and B cells and do not adequately reconstituted innate effectors, particularly myeloid cells and NK cells. Human NK cells constitute 10% to 15% of human peripheral lymphocytes, but were found to be around 1% to 3% in HIS mice (101). Despite their poor representation, NK cells

have been identified in various organs, their phenotype described, and their function (cytotoxicity and cytokine production) assessed in hu-SRC (102–105) and hu-BLT (106) models. Additionally, several approaches have been studied over the decade to successfully reconstitute more mature human NK cells with cytotoxic function *in vivo* or *ex vivo*.

EXOGENOUS SUPPLY OF HUMAN CYTOKINES

Human cytokine supplementation has quickly proven to be useful for NK cell proliferation and differentiation in HIS mice (101, 104, 105, 107). Human cytokines can be either repeatedly administered or their expression introduced by cytokine-encoding virus vectors or plasmids. One such cytokine considered crucial for NK cell development is IL-15, which, along with IL-2 and IL-7, belongs to the family of cytokines that shares common γ chain (γc) as their receptor subunit to convey activation signals (108). The binding of IL-15 to the β and γ heterodimer complex of IL-15 receptor (IL-15Rβγ) requires trans-presentation in complex with IL-15Rα, which is expressed on myeloid-lineage cells such as monocytes and dendritic cells and also stromal cells (108). Indeed, the injection of human IL-15/IL-15Rα complex induced extensive human NK cell expansion and differentiation toward the late stage $CD56^{lo}$CD16+ and KIR+ phenotypes in BRG mice receiving human CD34+ fetal liver cells, although the organ reconstitution was low in lymphoid organs (101). Reconstitution in mice was enhanced also by IL-15 supplementation *via* plasmids that express IL-15 and FLT3 ligand in mice (107). or by adenovirus vectors that express human IL-15 (101). The introduction of human FLT3 ligand in adenovirus vector alone can also expand human myeloid and NK cells in HIS mice (109). In this case, human FLT3 ligand primarily expands the myeloid cells, which in turn provide human IL-15/IL-15Rα to expand the human NK cells.

TRANSGENIC EXPRESSION OF HUMAN CYTOKINE GENES

The genetic engineering of interleukins in HIS mice models can increase the number of NK cells in lymphoid and non-lymphoid organs (110–112) as well as the number of CXCR6+ tissue-resident NK cells in the spleen, liver and BM (111, 112). The knock-in of human IL-15 (SRG-15 (111)) or double knock-in of IL-7 and IL-15 (hIL-7xhIL-15 KI (112)) on the other brought a significant increase in the number of human NK cells in peripheral blood compared with conventional NOG or NSG mice, achieving the physiological NK cell numbers observed in human blood in SRG-15 mice.

IL-2 and IL-7 are also two cytokines regarded fundamental to NK physiology and supplementation candidates to improve NK reconstitution. Accordingly, the transgenic expression of human IL-2 gene in a NOG mouse substrain (Hu-HSCs NOG–IL-2 Tg (110)) was able to increase the human NK cell number, but supplementation with IL-7 alone proved to be insufficient (113). The same insufficiency was found after knocking in just IL-7 in the lymphoid and non-lymphoid organs of NSG mice (112).

While researchers have increased the number of human NK cells in SRG-15 mice, the cells did not have the high degree of similarity with the NK cell repertoire of humans after stimulation (111). NK cells from SRG-15 lacked licensed (or "educated") NK cell subsets and showed a hypo-responsiveness when challenged with K562 cells (111). The hIL-7xhIL-15 KI model also could not reflect the normal frequency of mature human NK cells, on par with hIL-15 or hIL-15-hIL/15Rα complex injection studies (112). Finally, Hu-HSCs NOG–IL-2 Tg NK cells showed a bias toward IL-2 chronic activation phenotypes, and their receptor expression did not always correspond to their natural human NK counterparts, although the KIR diversity range did (110).

NEXT GENERATION OF HIS MICE

Constitutive exposure to specific sets of human interleukins through genetic engineering seems to improve the number of NK cells in HIS mice and achieves a high reconstitution of NK cells that is superior to simple injections. However, intravenous and hydrodynamic injections of the expression plasmids as well as transgenic modifications induce systemic supra-physiological levels of human cytokines, which do not recapitulate the typical spatial and temporal expression in humans. While the replacement of mouse genes with their human counterparts allows for physiological regulation to take place, the replacement of interleukins involved in NK cell development has proven to be insufficient for mirroring human NK immunity (111, 112).

Accordingly, there seems to be more biological layers that still need to be introduced in HIS mice in order to improve the precision of human NK cell immunity reconstitution. One such path is the reconstitution of the immune cell niche in the mouse microenvironment, since NK cells typically mature through exposition to human myeloid - such as monocytes macrophages and dendritic cells- and epithelial/stromal cells, which are likely to be sources of IL-15/IL-15Rα (114). However, the mouse microenvironment-human cells cross-reactivity is limited (94, 101). Moreover, improving myeloid cell lineage representation might improve cell engraftment, as observed after the co-injection of T cell-depleted "support" cells (115). An exception is the maintenance of *ex vivo* expanded UCB-derived NK cells in HIS mice, in which autologous UCB was used for the humanized cell source (116).

Several strategies that use gene knock-in and knock-out to produce the human microenvironment and signal networks have shown optimized myelopoiesis in HIS mice: NSG-SGM3 mice, also designated NSGS, express the human cytokines stem cell factor (SCF), granulocyte-macrophage colony-stimulating factor (GM-CSF), and IL-3 (117, 118); NSGW41 mice show an inactivated mutant mouse Kit gene (119, 120); NOG-EXL mice expresses human IL-3 and GM-CSF (121); and MISTRG mice express human macrophage colony-stimulating factor (M-CSF),

IL-3, GM-CSF, and thrombopoietin (TPO) (114). In the NSGS, NSGW41 and NOG-EX models, more comprehensive NK cell development is required. However, when engrafted with UCB CD34+ cells, NSGS recently showed better engraftment of CD3-CD56+ NK cells in the BM and spleen compared to NSG mice (122, 123). In contrast, abundant human myeloid cells and monocytes were found to be source of IL-15 and IL-15Rα in MISTRG mice, and a significant increase in NK cell numbers was observed in various organs of this model with effectual cytotoxic and IFNγ production (114).

While these models provide a new ground to explore NK reconstitution, no model has achieved all-inclusive human immunity. Therefore, each model should be carefully considered depending on its specific advantages and shortcomings to fit the intended research purposes and further adjustments are required. For example, NK cells need education through inhibitory receptors and, notably, HLA-I molecules, to acquire their effector function. Since mice express their own set of MHC-I, it is likely that the reconstituted NK cells are less responsive than they should be. Supporting human NK cell reconstitution in mice could be achieved with more genetic modifications, such as mouse strains modified to express human MHC-I, which have already been developed (124), and exogenously supplying NK-specific cytokines, as shown recently using injections of IL15/IL-15Rα in MSTRG mice (70). However, because immunity is an intricate and refined system, tentative tampering often comes with a price to the mice's health. Cytokines are known to have systemic toxicity, and recent mouse strains develop life-shortening syndromes (118, 125, 126). This effect, coupled with the development of xeno-GVHD, potentially worsens in the case of IL-15 injection, since T cells also benefit from IL-15 supplementation, limiting long-term graft studies. However, as mentioned above, this may be overcome by depleting mouse MHC molecules (97).

EVALUATION OF HLA-DEFICIENT CELLS IN HIS MICE WITH NK CELLS

The evaluation in HIS mice of HLA-homozygous or HLA-engineered iPSC-derived cells for regenerative therapy should be done in the presence of human NK cells in order to model the full range of NK functions. In particular, whether "missing self" grafts are rejected *in vivo* by human NK cells reconstituted in HIS mice models needs to be examined. In these experiments, components of the graft survival and tolerance response are comparatively evaluated against rejection controls, and evidences of rejection capability is essential to validate the response of the host mouse. An adequate rejection control will depend on the work outline, such the tolerance-induced condition vs. non-induced condition, autologous vs. allogeneic, wild-type vs. HLA engineered cells. It can also depend on the intrinsic properties of the graft. In the case of blood cell transfusions, the control and target populations can be mixed, administered and assessed for the ration thereafter. In the case of solid organs, two different fragments can be compared in different sites or different individuals.

The intra-graft presence of immune cells, when relevant, is the most common feature assessed in PSC-derived cell transplantation studies (72, 125–133), although its use as an estimation of actual rejection is controversial (127, 128, 133). Commonly, the assessment of immune cell infiltration is complemented by other measures of rejection, such as (but not limited to) tracking graft survival *in vivo* with fluorescence or bioluminescence imaging (BLI) (68, 69, 72, 125, 126), tissue damage analysis with staining for cell death markers (126, 127), or, when possible, by assays of the loss or gain of graft function such as blood glucose regulation by human ESC-derived islet like cells grafts (128).

As mentioned above, *in vitro* responses of NK cells from HLA-C1/C2 donors against HLA-C1/C1 homozygous iPSC-derived endothelial cells have been observed (82), raising concern of NK cells rejecting HLA-homozygous grafts. Meanwhile, an *in vivo* study that transplanted MHC homozygous monkey iPSC-derived neurons into monkey brain did not observe the infiltration of NK cells in the engrafted tissue (129) and a later preclinical study confirmed the survival of human HLA-homozygous iPSC-derived dopaminergic progenitors in mouse brain (19). In a clinical trial setting, the graft survival of HLA-homozygous RPE cells following local steroid administration was reported (21). However, *in vivo* studies are still few, and since the brain and eyes are regarded as immune privileged sites, whether HLA-homozygous cells could be rejected by NK cells should be differently assessed for other transplantation sites.

HLA-depleted or other genetically modified ESC/iPSC-derived cells have not reached clinical trials, but many have been investigated and assessed for immunogenicity against NK cells. For instance, the adoptive transfer of NK-92, an IL-2-dependant NK cell line, in immunodeficient NSG-B2m, a mouse model for beta-2 microglobulin deficiency and therefore expresses no mouse MHC class I, showed that human ESCs-derived CD45+ hematopoietic cells lacking polymorphic HLA class I was subject to NK-92-mediated lysis, but not if HLA-E was overexpressed (72). Similarly, tolerance against NK cells was reported for cells derived from HLA-A/B-knockout, HLA-C-retaining iPSCs (also preserving non-canonical HLA-E, -F, and -G, if expressed at all), or for human ESCs with HLA-ABC-KO and overexpressed HLA-G, PD-L1 and CD47 (69, 130). The studies found a functional activity by the reconstituted phenotypically human NK cells.

The rejection of HLA-depleted cells should be evaluated in SRC-transplanted HIS mice, which better recapitulate the *in vivo* response in humans. Various HLA class I-deficient cells are used to assess the immunity of HIS mice with enhanced human NKF cell development (**Table 2**). EB virus-immortalized lymphoblastoid cell lines, LCLs, and its mutant subclone deficient for endogenous HLA class I were used (105, 114). These LCLs were injected into HIS NSG mice infused with human fetal liver CD34+ cells. The rate of the HLA class I-deficient subset was smaller in the spleen, especially when the mice were pretreated with poly I:C, which had likely induced IL-15 and IL15Rα expression on myeloid cells (105). In a similar

TABLE 2 | Rejection of HLA-deficient cells in HIS Hu-SRC mice *in vivo*.

Mouse strain	Human cytokine supply	HSC source	Target cells	Analysis	Reference
NSG	Indirect via poly I:C injection	UCB	LCL721.221, LCL721.45	12 h spleen FCM [vs. poly I:C(-)]	Strowig et al. (105)
MITRG /MISTRG	M-CSF/ IL-3/ GM-CSF/ TPO overexpression	UCB	LCL721.221, LCL721.45	12 h spleen FCM [vs. hu-NSG]	Rongvaux et al. (114)
NSG	IL15/IL15Rα, poly I:C injection	Parent-derived BM (KIR mismatch)	Patient-derived B-ALL cells	20 h BM	Kübler et al. (132)
NOG-IL-2-Tg	IL-2 overexpression	UCB	K562 leukemia cells	Tumor size [vs. non-Tg]	Katano et al. (110)
SRG-15	IL-15 overexpression	Fetal liver	K562 leukemia cells	24 h, FCM	Herndler-Brandstetter et al. (111)
MITRG /MISTRG	M-CSF/ IL-3/GM-CSF/ TPO overexpression + IL15/IL15Rα injection	UCB	iPSC-derived B2M-/- HPCs and platelets	6h Blood, FCM	Suzuki et al. (70)

UCB, umbilical cord blood; BM, bone marrow; HPCs, hematopoietic progenitor cells; WT, wild type; FCM, flow cytometry.

experimental design, the rate of the HLA class I-deficient subset was less in the spleen of HIS MISTRG mice compared with HIS NSG mice (114). These results indicate that human NK cells in HIS mice can specifically reject HLA class I-deficient cells if they are quantitatively and/or functionally sufficient. However, caution is required, as it later became clear that the defect of HLA expression was not confirmable in the deposited cells (134). Alternatively, cell lines that lack the expression of HLA class I, such as the leukemia-derived K562 cells, have been explored (110, 111). The growth of subcutaneously inoculated K562 cells was suppressed in HIS NOG-IL-15 Tg mice transferred with human peripheral blood NK cells compared with non-transferred mice (110). Another study co-injected K562 cells together with HLA class I-expressing Raji cells to reveal that the growth rate of K562 cells was lower in HIS SRG-15 mice than in HIS NSG or SRG mice (111). Meanwhile, one study grafted B cell acute lymphoblastic leukemia patient cells into HIS NSG mice reconstituted with parent-derived BM HSCs primed with IL-15 and poly I:C. There were fewer KIR mismatched leukemia cells in the BM of these mice than non-humanized NSG mice, indicating reconstituted NK cell-dependent tumor lysis (135).

While these models successfully rejected "missing self-HLA" cells by human NK cells in HIS mice, all cells used were malignant and thus may not be applicable to regenerative medicine settings, in which non-tumor allografts would be administered. In this regard, we recently showed that HIS MSTRG mice treated with IL-15/IL-15Rα to enhance human NK cell reconstitution significantly rejected HLA class-I knockout iPSC-derived hematopoietic progenitor cells (70). Interestingly, this model also showed that HLA class I-knockout iPSC-derived platelets were not rejected by NK cells *in vivo*. These findings show the importance of assaying each cell type *in vivo* for NK cell immunogenicity.

Besides evaluating the "missing self" response, NK cells could target allogeneic and autologous contaminating undifferentiated human iPSCs that are downregulated for HLA class I (132). The proper reconstitution of NK cells is therefore indispensable for assessing the risk of teratomas formation in HIS mice. This targeting also argues for caution in the potential use of immune-suppressants in iPSC-derived regenerative therapies, since host NK cells can mitigate the development of teratomas if not managed by other strategies such as irradiation in anucleate cell products (136) and introducing suicide genes (76–78) or drug-resistant miRNA switches (79, 80).

CONCLUSION

The proper modeling of NK cell immunity is fundamental to assessing the complete immunogenicity profile of new allotransplantable materials with HLA-homozygous or HLA-depleted phenotypes derived from iPSCs. In this regard, HIS mice using SRC as the source cells are a generally available system that represent a chimeric system inhabited by an endogenous human immune system. Thus, they could provide pre-clinical models to recapitulate the allograft rejection in human transplantation therapies for pre-clinical application. Since the development of HIS mice with human NK cells has only developed recently, most of these mice have been used to generally evaluate the rejection of malignant cells lacking HLA class I. However, but as the field of iPSC-based regenerative medicine progress, it is expected that their application against non-malignant iPSC-derived allografts will be extensively studied. There are still issues to overcome such as a long lifespan with stable engraftment to assess chronic allograft rejection and also reproducibility of the reconstitution, as the most common SRCs, UCB HSCs, are abundantly available without invasive procedure but will vary between donors. While further optimization is required to completely and reproducibly reconstitute the human immune system, the general availability and sophisticated engineering of HIS mice should advance experimental cell replacement therapies and regenerative medicine.

AUTHOR CONTRIBUTIONS

All authors wrote and reviewed the manuscript. All authors contributed to the article and approved the submitted version.

FUNDING

This work was supported in part by Core Center for iPS Cell Research (JP20bm0104001, NS), Projects for Technological Development (JP20bm0404037, NS) and The Program for Technological Innovation of Regenerative Medicine (JP20bm0704051, NS) from the Japan Agency for Medical Research and Development (AMED) and by Monbukagakusho (MEXT) scholarship from the Japanese Government (CF). Laboratory of Hematopoietic Stem Cell Engineering is supported with an unrestricted grant from the Chemo-Sero-Therapeutic Research Institute (KAKETSUKEN) (TM). The funder was not involved in the study design, collection, analysis, interpretation of data, the writing of this article or the decision to submit it for publication.

ACKNOWLEDGMENTS

The authors thank Peter Karagiannis and Koji Eto of CiRA for critical reading of the manuscript.

REFERENCES

1. Takahashi K, Yamanaka S. Induction of Pluripotent Stem Cells from Mouse Embryonic and Adult Fibroblast Cultures by Defined Factors. *Cell* (2006) 126(4):663–76. doi: 10.1016/j.cell.2006.07.024
2. Takahashi K, Tanabe K, Ohnuki M, Narita M, Ichisaka T, Tomoda K, et al. Induction of Pluripotent Stem Cells from Adult Human Fibroblasts by Defined Factors. *Cell* (2007) 131(5):861–72. doi: 10.1016/j.cell.2007.11.019
3. Yu J, Vodyanik MA, Smuga-Otto K, Antosiewicz-Bourget J, Frane JL, Tian S, et al. Induced Pluripotent Stem Cell Lines Derived from Human Somatic Cells. *Science* (2007) 318(5858):1917–20. doi: 10.1126/science.1151526
4. Park I-H, Zhao R, West JA, Yabuuchi A, Huo H, Ince TA, et al. Reprogramming of human somatic cells to pluripotency with defined factors. *Nature* (2008) 451(7175):141–6. doi: 10.1038/nature06534
5. Williams LA, Davis-Dusenbery BN, Eggan KC. SnapShot: Directed Differentiation of Pluripotent Stem Cells. *Cell* (2012) 149(5):1174–1174.e1. doi: 10.1016/j.cell.2012.05.015
6. Blau HM, Daley GQ. Stem Cells in the Treatment of Disease. *N Engl J Med* (2019) 380(18):1748–60. doi: 10.1056/NEJMra1716145
7. Yamanaka S. Pluripotent Stem Cell-Based Cell Therapy—Promise and Challenges. *Cell Stem Cell* (2020) 27(4):523–31. doi: 10.1016/j.stem.2020.09.014
8. Turner M, Leslie S, Martin NG, Peschanski M, Rao M, Taylor CJ, et al. Toward the Development of a Global Induced Pluripotent Stem Cell Library. *Cell Stem Cell* (2013) 13(4):382–4. doi: 10.1016/j.stem.2013.08.003
9. Umekage M, Sato Y, Takasu N. Overview: an iPS cell stock at CiRA. *Inflamm Regen* (2019) 39:17. doi: 10.1186/s41232-019-0106-0
10. Sullivan S, Ginty P, McMahon S, May M, Solomon SL, Kurtz A, et al. The Global Alliance for iPSC Therapies (GAiT). *Stem Cell Res* (2020) 49:102036. doi: 10.1016/j.scr.2020.102036
11. Lanier LL. Up on the tightrope: natural killer cell activation and inhibition. *Nat Immunol* (2008) 9(5):495–502. doi: 10.1038/ni1581
12. Vivier E, Raulet DH, Moretta A, Caligiuri MA, Zitvogel L, Lanier LL, et al. Innate or Adaptive Immunity? The Example of Natural Killer Cells. *Science* (2011) 331(6013):44–9. doi: 10.1126/science.1198687
13. Long EO, Kim HS, Liu D, Peterson ME, Rajagopalan S. Controlling natural killer cell responses: integration of signals for activation and inhibition. *Annu Rev Immunol* (2013) 31:227–58. doi: 10.1146/annurev-immunol-020711-075005
14. Allen TM, Brehm MA, Bridges S, Ferguson S, Kumar P, Mirochnitchenko O, et al. Humanized immune system mouse models: progress, challenges and opportunities. *Nat Immunol* (2019) 20(7):770–4. doi: 10.1038/s41590-019-0416-z
15. Zarzeczny A, Scott C, Hyun I, Bennett J, Chandler J, Chargé S, et al. iPS Cells: Mapping the Policy Issues. *Cell* (2009) 139(6):1032–7. doi: 10.1016/j.cell.2009.11.039
16. Lowenthal J, Lipnick SL, Rao M, Hull SC. Specimen collection for induced pluripotent stem cell research: harmonizing the approach to informed consent. *Stem Cells Transl Med* (2012) 1(5):409–21. doi: 10.5966/sctm.2012-0029
17. Saito MK, Matsunaga A, Takasu N, Yamanaka S. Donor Recruitment and Eligibility Criteria for HLA-Homozygous iPS Cell Bank in Japan. In: D Ilic, editor. *Stem Cell Banking*. New York, NY: Springer New York: Stem Cell Biology and Regenerative Medicine (2014). p. 67–76. Available at: http://link.springer.com/10.1007/978-1-4939-0585-0_7.
18. Trounson A, McDonald C. Stem Cell Therapies in Clinical Trials: Progress and Challenges. *Cell Stem Cell* (2015) 17(1):11–22. doi: 10.1016/j.stem.2015.06.007
19. Doi D, Magotani H, Kikuchi T, Ikeda M, Hiramatsu S, Yoshida K, et al. Pre-clinical study of induced pluripotent stem cell-derived dopaminergic progenitor cells for Parkinson's disease. *Nat Commun* (2020) 11(1):3369. doi: 10.1038/s41467-020-17165-w
20. Mandai M, Watanabe A, Kurimoto Y, Hirami Y, Morinaga C, Daimon T, et al. Autologous Induced Stem-Cell–Derived Retinal Cells for Macular Degeneration. *N Engl J Med* (2017) 376(11):1038–46. doi: 10.1056/NEJMoa1608368
21. Sugita S, Mandai M, Hirami Y, Takagi S, Maeda T, Fujihara M, et al. HLA-Matched Allogeneic iPS Cells-Derived RPE Transplantation for Macular Degeneration. *J Clin Med* (2020) 9(7):2217. doi: 10.3390/jcm9072217
22. Bloor AJC, Patel A, Griffin JE, Gilleece MH, Radia R, Yeung DT, et al. Production, safety and efficacy of iPSC-derived mesenchymal stromal cells in acute steroid-resistant graft versus host disease: a phase I, multicenter, open-label, dose-escalation study. *Nat Med* (2020) 26(11):1720–5. doi: 10.1038/s41591-020-1050-x
23. *Pilot, Open-label, Randomised Controlled Clinical Trial to Investigate Early Efficacy of CYP-001 in Adults Admitted to Intensive Care With COVID-19*. Australia: Cynata Therapeutics Limited (2020). Available at: https://clinicaltrials.gov/ct2/show/NCT04537351. Report No.: NCT04537351.
24. *A Study of transplantation of autologous induced pluripotent stem cell (iPSC) derived retinal pigment epithelium (RPE) cell sheet in subjects with exudative age related macular degeneration*. Japan: RIKEN, Laboratory for Retinal Regeneration (2013). Available at: https://upload.umin.ac.jp/cgi-open-bin/ctr_e/ctr_view.cgi?recptno=R000013279. Report No.: UMIN000011929.
25. UMIN Clinical Trials Registry. *A Study of transplantation of allogenic induced pluripotent stem cell (iPSC) derived retinal pigment epithelium (RPE) cell suspension in subjects with neovascular age related macular degeneration*. Japan: Kobe City Eye Hospital (2017). Available at: https://upload.umin.ac.jp/cgi-open-bin/ctr_e/ctr_view.cgi?recptno=R000029894. Report No.: UMIN000026003.
26. Japan Registry of Clinical Trials (jRCT). *Safety study using allogenic iPSC-retinal sheets for patients with retinitis pigmentosa (iRERP)*. Japan: Kobe City Eye Hospital (2020). Available at: https://jrct.niph.go.jp/en-latest-detail/jRCTa050200027. Report No.: jRCTa050200027.
27. *A Phase I/IIa Trial for Autologous Transplantation of Induced Pluripotent Stem Cell-Derived Retinal Pigment Epithelium for Geographic Atrophy Associated With Age-Related Macular Degeneration*. United States: National Eye Institute (NEI (2020). Available at: https://clinicaltrials.gov/ct2/show/NCT04339764. Report No.: NCT04339764.
28. Japan Registry of Clinical Trials (jRCT). *Safety study of regenerative therapy with allogeneic induced pluripotent stem cell-derived cardiac spheres for severe heart failure (Regenerative cardiac spheres)*. Japan: Keio University School of Medicine (2020). Available at: https://jrct.niph.go.jp/en-latest-detail/jRCTa032200189. Report No.: jRCTa032200189.
29. *The Study of Human Epicardial Injection With Allogenic Induced Pluripotent Stem Cell-derived Cardiomyocytes in Ischemic Heart Failure*. China, Jiangsu: Help Therapeutics (2019). Available at: https://clinicaltrials.gov/ct2/show/NCT03763136. Report No.: NCT03763136.

30. Clinical Trial of Human (Allogeneic). *iPS Cell-derived Cardiomyocytes Sheet for Ischemic*. Osaka: Osaka University (2021). Available at: https://clinicaltrials.gov/ct2/show/NCT04696328. Report No.: NCT04696328.
31. *Safety and Efficacy of Induced Pluripotent Stem Cell-derived Engineered Human Myocardium as Biological Ventricular Assist Tissue in Terminal Heart Failure*. Germany: University Medical Center Goettingen (2020). Available at: https://clinicaltrials.gov/ct2/show/NCT04396899. Report No.: NCT04396899.
32. Mallapaty S. Revealed: two men in China were first to receive pioneering stem-cell treatment for heart-disease. *Nature* (2020) 581(7808):249–50. doi: 10.1038/d41586-020-01285-w
33. *Kyoto Trial to Evaluate the Safety and Efficacy of iPSC-derived dopaminergic progenitors in the treatment of Parkinson"s Disease*. Japan: Kyoto University Hospital (2018). Available at: https://rctportal.niph.go.jp/en/detail?trial_id=JMA-IIA00384. Report No.: JMA-IIA00384.
34. *Regenerative medicine for spinal cord injury at subacute stage using human induced pluripotent stem cell-derived neural stem/progenitor cells*. Japan: Keio University School of Medicine (2020). Available at: https://jrct.niph.go.jp/en-latest-detail/jRCTa031190228. Report No.: jRCTa031190228.
35. *Clinical study of autologous transfusion of iPS cell-derived platelets for thrombocytopenia (iPLAT1)*. Japan: Kyoto University Hospital (2020). Available at: https://jrct.niph.go.jp/en-latest-detail/jRCTa050190117. Report No.: jRCTa050190117.
36. *An Open-Label Phase 1 Study to Investigate the Safety and Efficacy of CYP-001 for the Treatment of Adults With Steroid-Resistant Acute Graft Versus Host Disease*. Australia, United Kingdom: Cynata Therapeutics Limited (2020). Available at: https://clinicaltrials.gov/ct2/show/NCT02923375. Report No.: NCT02923375.
37. *A Phase I, Open-Label, Multicenter Study of FT538 as Monotherapy in Relapsed/Refractory Acute Myelogenous Leukemia and in Combination With Monoclonal Antibodies in Relapsed/Refractory Multiple Myeloma*. United States: Fate Therapeutics (2020). Available at: https://clinicaltrials.gov/ct2/show/NCT04614636. Report No.: NCT04614636.
38. *A Phase I, Open-Label, Multicenter Study of FT596 as a Monotherapy and in Combination With Rituximab or Obinutuzumab in Subjects With Relapsed/Refractory B-cell Lymphoma and Chronic Lymphocytic Leukemia [Internet]*. United States: Fate Therapeutics (2020). Available at: https://clinicaltrials.gov/ct2/show/NCT04245722. Report No.: NCT04245722.
39. *A Phase I Study of FT516 as Monotherapy in Relapsed/Refractory Acute Myelogenous Leukemia and in Combination With Monoclonal Antibodies in Relapsed/Refractory B-Cell Lymphoma*. United States: Fate Therapeutics (2020). Available at: https://clinicaltrials.gov/ct2/show/NCT04023071. Report No.: NCT04023071.
40. *FT500 as Monotherapy and in Combination With Immune Checkpoint Inhibitors in Subjects With Advanced Solid Tumors (Phase 1)*. United States: Fate Therapeutics (2020). Available at: https://clinicaltrials.gov/ct2/show/NCT03841110. Report No.: NCT03841110.
41. Dausset J. Iso-leuco-anticorps. *Acta Haematol* (1958) 20(1–4):156–66. doi: 10.1159/000205478
42. The MHC sequencing consortium. Complete sequence and gene map of a human major histocompatibility complex. *Nature* (1999) 401(6756):921–3. doi: 10.1038/44853
43. Zachary AA, Leffell MS. HLA Mismatching Strategies for Solid Organ Transplantation – A Balancing Act. *Front Immunol* (2016) 7:575. doi: 10.3389/fimmu.2016.00575
44. Wiebe C, Nickerson P. Strategic Use of Epitope Matching to Improve Outcomes. *Transplantation* (2016) 100(10):2048–52. doi: 10.1097/TP.0000000000001284
45. Sypek M, Kausman J, Holt S, Hughes P. HLA Epitope Matching in Kidney Transplantation: An Overview for the General Nephrologist. *Am J Kidney Dis* (2018) 71(5):720–31. doi: 10.1053/j.ajkd.2017.09.021
46. Kim E-M, Manzar G, Zavazava N. Human iPS cell-derived hematopoietic progenitor cells induce T-cell anergy in in vitro-generated alloreactive CD8(+) T cells. *Blood* (2013) 121(26):5167–75. doi: 10.1182/blood-2012-11-467753
47. Lanza R, Russell DW, Nagy A. Engineering universal cells that evade immune detection. *Nat Rev Immunol* (2019) 19(12):723–33. doi: 10.1038/s41577-019-0200-1
48. Zhao W, Lei A, Tian L, Wang X, Correia C, Weiskittel T, et al. Strategies for Genetically Engineering Hypoimmunogenic Universal Pluripotent Stem Cells. *iScience* (2020) 23(6):101162. doi: 10.1016/j.isci.2020.101162
49. Zhao T, Zhang Z-N, Rong Z, Xu Y. Immunogenicity of induced pluripotent stem cells. *Nature* (2011) 474(7350):212–5. doi: 10.1038/nature10135
50. Araki R, Uda M, Hoki Y, Sunayama M, Nakamura M, Ando S, et al. Negligible immunogenicity of terminally differentiated cells derived from induced pluripotent or embryonic stem cells. *Nature* (2013) 494(7435):100–4. doi: 10.1038/nature11807
51. de Almeida PE, Meyer EH, Kooreman NG, Diecke S, Dey D, Sanchez-Freire V, et al. Transplanted terminally differentiated induced pluripotent stem cells are accepted by immune mechanisms similar to self-tolerance. *Nat Commun* (2014) 5(1):1–12. doi: 10.1038/ncomms4903
52. Zhao T, Zhang Z, Westenskow PD, Todorova D, Hu Z, Lin T, et al. Humanized Mice Reveal Differential Immunogenicity of Cells Derived from Autologous Induced Pluripotent Stem Cells. *Cell Stem Cell* (2015) 17(3):353–9. doi: 10.1016/j.stem.2015.07.021
53. Todorova D, Kim J, Hamzeinejad S, He J, Xu Y. Brief Report: Immune Microenvironment Determines the Immunogenicity of Induced Pluripotent Stem Cell Derivatives. *Stem Cells* (2016) 34(2):510–5. doi: 10.1002/stem.2227
54. Liu X, Li W, Fu X, Xu Y. The Immunogenicity and Immune Tolerance of Pluripotent Stem Cell Derivatives. *Front Immunol* (2017) 8:645. doi: 10.3389/fimmu.2017.00645
55. Deuse T, Hu X, Agbor-Enoh S, Koch M, Spitzer MH, Gravina A, et al. De novo mutations in mitochondrial DNA of iPSCs produce immunogenic neoepitopes in mice and humans. *Nat Biotechnol* (2019) 37(10):1137–44. doi: 10.1038/s41587-019-0227-7
56. Wagner DL, Amini L, Wendering DJ, Burkhardt L-M, Akyüz L, Reinke P, et al. High prevalence of Streptococcus pyogenes Cas9-reactive T cells within the adult human population. *Nat Med* (2019) 25(2):242–8. doi: 10.1038/s41591-018-0204-6
57. Akabayashi A, Nakazawa E, Jecker NS. The world's first clinical trial for an aplastic anemia patient with thrombocytopenia administering platelets generated from autologous iPS cells. *Int J Hematol* (2018) 109(2):239–40. doi: 10.1007/s12185-018-02565-y
58. Figueiredo C, Seltsam A, Blasczyk R. Class-, gene-, and group-specific HLA silencing by lentiviral shRNA delivery. *J Mol Med* (2005) 84(5):425–37. doi: 10.1007/s00109-005-0024-2
59. Deuse T, Seifert M, Tsao PS, Hua X, Velden J, Eiermann T, et al. Immunobiology of naive and genetically modified HLA-class-I-knockdown human embryonic stem cells. *J Cell Sci* (2011) 124(23):4127–8. doi: 10.1242/jcs.104125
60. Börger A-K, Eicke D, Wolf C, Gras C, Aufderbeck S, Schulze K, et al. Generation of HLA-Universal iPSC-Derived Megakaryocytes and Platelets for Survival Under Refractoriness Conditions. *Mol Med* (2016) 22(1):274–85. doi: 10.2119/molmed.2015.00235
61. Figueiredo C, Oldhafer F, Wittauer E, Carvalho-Oliveira M, Akhdar A, Beetz O, et al. Silencing of HLA class I on primary human hepatocytes as a novel strategy for reduction in alloreactivity. *J Cell Mol Med* (2019) 23(8):5705–14. doi: 10.1111/jcmm.14484
62. Figueiredo C, Eicke D, Yuzefovych Y, Avsar M, Hanke JS, Pflaum M, et al. Low immunogenic endothelial cells endothelialize the Left Ventricular Assist Device. *Sci Rep* (2019) 9(1):11318. doi: 10.1038/s41598-019-47780-7
63. Wiegmann B, Figueiredo C, Gras C, Pflaum M, Schmeckebier S, Korossis S, et al. Prevention of rejection of allogeneic endothelial cells in a biohybrid lung by silencing HLA-class I expression. *Biomaterials* (2014) 35(28):8123–33. doi: 10.1016/j.biomaterials.2014.06.007
64. Yuzefovych Y, Valdivia E, Rong S, Hack F, Rother T, Schmitz J, et al. Genetic Engineering of the Kidney to Permanently Silence MHC Transcripts During ex vivo Organ Perfusion. *Front Immunol* (2020) 11:265. doi: 10.3389/fimmu.2020.00265
65. Lu P, Chen J, He L, Ren J, Chen H, Rao L, et al. Generating Hypoimmunogenic Human Embryonic Stem Cells by the Disruption of Beta 2-Microglobulin. *Stem Cell Rev Rep* (2013) 9(6):806–13. doi: 10.1007/s12015-013-9457-0
66. Petrus-Reurer S, Winblad N, Kumar P, Gorchs L, Chrobok M, Wagner AK, et al. Generation of Retinal Pigment Epithelial Cells Derived from Human Embryonic Stem Cells Lacking Human Leukocyte Antigen Class I and II. *Stem Cell Rep* (2020) 14(4):648–62. doi: 10.1016/j.stemcr.2020.02.006
67. Mattapally S, Pawlik KM, Fast VG, Zumaquero E, Lund FE, Randall TD, et al. Human Leukocyte Antigen Class I and II Knockout Human Induced Pluripotent Stem Cell–Derived Cells: Universal Donor for Cell Therapy. *J Am Heart Assoc* (2018) 7(23):e010239. doi: 10.1161/JAHA.118.010239

68. Deuse T, Hu X, Gravina A, Wang D, Tediashvili G, De C, et al. Hypoimmunogenic derivatives of induced pluripotent stem cells evade immune rejection in fully immunocompetent allogeneic recipients. *Nat Biotechnol* (2019) 37(3):252–8. doi: 10.1055/s-0040-1705474
69. Xu H, Wang B, Ono M, Kagita A, Fujii K, Sasakawa N, et al. Targeted Disruption of HLA Genes via CRISPR-Cas9 Generates iPSCs with Enhanced Immune Compatibility. *Cell Stem Cell* (2019) 24(4):566–78.e7. doi: 10.1016/j.stem.2019.02.005
70. Suzuki D, Flahou C, Yoshikawa N, Stirblyte I, Hayashi Y, Sawaguchi A, et al. iPSC-Derived Platelets Depleted of HLA Class I Are Inert to Anti-HLA Class I and Natural Killer Cell Immunity. *Stem Cell Rep* (2020) 14(1):49–59. doi: 10.1016/j.stemcr.2019.11.011
71. Norbnop P, Ingrungruanglert P, Israsena N, Suphapeetiporn K, Shotelersuk V. Generation and characterization of HLA-universal platelets derived from induced pluripotent stem cells. *Sci Rep* (2020) 10(1):8472. doi: 10.1038/s41598-020-65577-x
72. Gornalusse GG, Hirata RK, Funk SE, Riolobos L, Lopes VS, Manske G, et al. HLA-E-expressing pluripotent stem cells escape allogeneic responses and lysis by NK cells. *Nat Biotechnol* (2017) 35(8):765–72. doi: 10.1038/nbt.3860
73. Riolobos L, Hirata RK, Turtle CJ, Wang P-R, Gornalusse GG, Zavajlevski M, et al. HLA Engineering of Human Pluripotent Stem Cells. *Mol Ther* (2013) 21(6):1232–41. doi: 10.1038/mt.2013.59
74. Wang D, Quan Y, Yan Q, Morales JE, Wetsel RA. Targeted Disruption of the β_2-Microglobulin Gene Minimizes the Immunogenicity of Human Embryonic Stem Cells: Disruption of B2M Reduces Immunogenicity of hESCs. *Stem Cells Transl Med* (2015) 4(10):1234–45. doi: 10.5966/sctm.2015-0049
75. Hong CH. Antigen Presentation by Individually Transferred HLA Class I Genes in HLA-A, HLA-B, HLA-C Null Human Cell Line Generated Using the Multiplex CRISPR-Cas9 System. *J Immunother* (2017) 40(6):201–10. doi: 10.1097/CJI.0000000000000176
76. Jeong HC, Cho SJ, Lee MO, Cha HJ. Technical approaches to induce selective cell death of pluripotent stem cells. *Cell Mol Life Sci* (2017) 74 (14):2601–11. doi: 10.1007/s00018-017-2486-0
77. Liang Q, Monetti C, Shutova MV, Neely EJ, Hacibekiroglu S, Yang H, et al. Linking a cell-division gene and a suicide gene to define and improve cell therapy safety. *Nature* (2018) 563(7733):701–4. doi: 10.1038/s41586-018-0733-7
78. Martin RM, Fowler JL, Cromer MK, Lesch BJ, Ponce E, Uchida N, et al. Improving the safety of human pluripotent stem cell therapies using genome-edited orthogonal safeguards. *Nat Commun* (2020) 11(1):2713. doi: 10.1038/s41467-020-16455-7
79. Miki K, Endo K, Takahashi S, Funakoshi S, Takei I, Katayama S, et al. Efficient detection and purification of cell populations using syn- thetic MicroRNA switches. *Cell Stem Cell* (2015) 16(6):699–711. doi: 10.1016/j.stem.2015.04.005
80. Parr CJC, Katayama S, Miki K, Kuang Y, Yoshida Y, Morizane A, et al. MicroRNA-302 switch to identify and eliminate undifferentiated human pluripotent stem cells. *Sci Rep* (2016) 6:32532. doi: 10.1038/Srep32532
81. Brower RC, England R, Takeshita T, Kozlowski S, Margulies DH, Berzofsky JA, et al. Minimal requirements for peptide mediated activation of CD8+ CTL. *Mol Immunol* (1994) 31(16):1285–93. doi: 10.1016/0161-5890(94)90079-5
82. Ichise H, Nagano S, Maeda T, Miyazaki M, Miyazaki Y, Kojima H, et al. NK Cell Alloreactivity against KIR-Ligand-Mismatched HLA-Haploidentical Tissue Derived from HLA Haplotype-Homozygous iPSCs. *Stem Cell Rep* (2017) 9(3):853–67. doi: 10.1016/j.stemcr.2017.07.020
83. Borrego FRR, Ulbrecht M, Weiss EH, Coligan JE, Brooks AG. Recognition of Human Histocompatibility Leukocyte Antigen (HLA)-E Complexed with HLA Class I Signal Sequence–derived Peptides by CD94/NKG2 Confers Protection from Natural Killer Cell–mediated Lysis. *J Exp Med* (1998) 87 (5):813–8. doi: 10.1084/jem.187.5.813
84. Braud VM, Allan DSJ, O'Callaghan CA, Söderström K, D'Andrea AD, Ogg GS, et al. HLA-E binds to natural killer cell receptors CD94/NKG2A, B and C. *Nature* (1998) 391(6669):795–9. doi: 10.1038/35869
85. Dulberger CL, McMurtrey CP, Hölzemer A, Neu KE, Liu V, Steinbach AM, et al. Human Leukocyte Antigen F Presents Peptides and Regulates Immunity through Interactions with NK Cell Receptors. *Immunity* (2017) 46(6):1018–29.e7. doi: 10.1016/j.immuni.2017.06.002
86. Rouas-Freiss N, Gonçalves RM, Menier C, Dausset JC, Carosella ED. Direct evidence to support the role of HLA-G in protecting the fetus from maternal uterine natural killer cytolysis. *Proc Natl Acad Sci U S A* (1997) 94 (21):11520–5. doi: 10.1073/pnas.94.21.11520
87. Riteau B, Menier C, Khalil-Daher I, Martinozzi S, Pla M, Dausset JC, et al. HLA-G1 co-expression boosts the HLA class I-mediated NK lysis inhibition. *Int Immunol* (2001) 13(2):193–201. doi: 10.1093/intimm/13.2.193
88. Rouas-Freiss N, Marchal R, Kirszenbaum M, Dausset JC, Carosella ED. The alpha1 domain of HLA-G1 and HLA-G2 inhibits cytotoxicity induced by natural killer cells: is HLA-G the public ligand for natural killer cell inhibitory receptors? *Proc Natl Acad Sci U S A* (1997) 94(10):5249–54. doi: 10.1073/pnas.94.10.5249
89. Zhao L, Teklemariam T, Hantash BM. Heterelogous expression of mutated HLA-G decreases immunogenicity of human embryonic stem cells and their epidermal derivatives. *Stem Cell Res* (2014) 13(2):342–54. doi: 10.1016/j.scr.2014.08.004
90. Sugita S, Makabe K, Iwasaki Y, Fujii S, Takahashi M. Natural Killer Cell Inhibition by HLA-E Molecules on Induced Pluripotent Stem Cell–Derived Retinal Pigment Epithelial Cells. *Invest Ophthalmol Vis Sci* (2018) 59 (5):1719–31. doi: 10.1167/iovs.17-22703
91. Jaiswal S, Jamieson CHM, Pang WW, Park CY, Chao MP, Majeti R, et al. CD47 Is Upregulated on Circulating Hematopoietic Stem Cells and Leukemia Cells to Avoid Phagocytosis Siddhartha. *Cell* (2009) 138(2):271–85. doi: 10.1016/j.cell.2009.05.046
92. Torikai H, Reik A, Soldner F, Warren EH, Yuen C, Zhou Y, et al. Toward eliminating HLA class I expression to generate universal cells from allogeneic donors. *Blood* (2013) 122(8):1341–9. doi: 10.1182/blood-2013-03-478255
93. Dijke IE. Immunobiology of Transplantation. In: RP Michel, B GJ, editors. *Pathology of Transplantation*. Cham: Springer International Publishing (2016). p. 7–51. Available at: http://link.springer.com/10.1007/978-3-319-29683-8_2.
94. Mestas J, Hughes CCW. Of Mice and Not Men: Differences between Mouse and Human Immunology. *J Immunol* (2004) 172(5):2731–8. doi: 10.4049/jimmunol.172.5.2731
95. Shay T, Jojic V, Zuk O, Rothamel K, Puyraimond-Zemmour D, Feng T, et al. Conservation and divergence in the transcriptional programs of the human and mouse immune systems. *Proc Natl Acad Sci U S A* (2013) 110(8):2946–51. doi: 10.1073/pnas.1222738110
96. Walsh NC, Kenney LL, Jangalwe S, Aryee K-E, Greiner DL, Brehm MA, et al. Humanized Mouse Models of Clinical Disease. *Annu Rev Pathol Mech Dis* (2017) 12(1):187–215. doi: 10.1146/annurev-pathol-052016-100332
97. Brehm MA, Kenney LL, Wiles MV, Low BE, Tisch RM, Burzenski L, et al. Lack of acute xenogeneic graft- versus-host disease, but retention of T-cell function following engraftment of human peripheral blood mononuclear cells in NSG mice deficient in MHC class I and II expression. *FASEB J* (2019) 33(3):3137–51. doi: 10.1096/fj.201800636R
98. Bosma GC, Custer RP, Bosma MJ. A severe combined immunodeficiency mutation in the mouse. *Nature* (1983) 301(5900):527–30. doi: 10.1038/301527a0
99. Shultz LD, Schweitzer PA, Christianson SW, Gott B, Schweitzer IB, Tennent B, et al. Multiple defects in innate and adaptive immunologic function in NOD/LtSz- scid mice. *J Immunol* (1995) 154(1):180–91.
100. Van der Loo J. Nonobese Diabetic/Severe Combined Immunodeficiency (NOD/SCID) Mouse as a Model System to Study the Engraftment and Mobilization of Human Peripheral Blood Stem Cells. *Blood* (1998) 92 (7):2556–70. doi: 10.1182/blood.V92.7.2556.2556_2556_2570
101. Huntington ND, Legrand N, Alves NL, Jaron B, Weijer K, Plet A, et al. IL-15 trans-presentation promotes human NK cell development and differentiation in vivo. *J Exp Med* (2009) 206(1):25–34. doi: 10.1084/jem.20082013.
102. Hiramatsu H, Nishikomori R, Heike T, Ito M, Kobayashi K, Katamura K, et al. Complete reconstitution of human lymphocytes from cord blood CD34+ cells using the NOD/SCID/γcnull mice model. *Blood* (2003) 102(3):873–80. doi: 10.1182/blood-2002-09-2755
103. Kwant-Mitchell A, Pek EA, Rosenthal KL, Ashkar AA. Development of Functional Human NK Cells in an Immunodeficient Mouse Model with the Ability to Provide Protection against Tumor Challenge. Sandberg JK, editor. *PLoS One* (2009) 4(12):e8379. doi: 10.1371/journal.pone.0008379
104. Pek EA, Chan T, Reid S, Ashkar AA. Characterization and IL-15 dependence of NK cells in humanized mice. *Immunobiology* (2011) 216(1–2):218–24. doi: 10.1016/j.imbio.2010.04.008

105. Strowig T, Chijioke O, Carrega P, Arrey F, Meixlsperger S, Rä PC, et al. Human NK cells of mice with reconstituted human immune system components require preactivation to acquire functional competence. *Blood* (2010) 116(20):4158–67. doi: 10.1182/blood-2010-02-270678
106. Calderon VE, Valbuena G, Goez Y, Judy BM, Huante MB, Sutjita P, et al. A Humanized Mouse Model of Tuberculosis. Cardona P-J, editor. *PLoS One* (2013) 8(5):e63331. doi: 10.1371/journal.pone.0063331
107. Chen Q, Khoury M, Chen J. Expression of human cytokines dramatically improves reconstitution of specific human-blood lineage cells in humanized mice. *Proc Natl Acad Sci U S A* (2009) 106(51):21783–8. doi: 10.1073/pnas.0912274106
108. Waldmann TA. The biology of interleukin-2 and interleukin-15: implications for cancer therapy and vaccine design. *Nat Rev Immunol* (2006) 6(8):595–601. doi: 10.1038/nri1901
109. Douam F, Ziegler CGK, Hrebikova G, Fant B, Leach R, Parsons L, et al. Selective expansion of myeloid and NK cells in humanized mice yields human-like vaccine responses. *Nat Commun* (2018) 9(1):5031. doi: 10.1038/s41467-018-07478-2
110. Katano I, Takahashi T, Ito R, Kamisako T, Mizusawa T, Ka Y, et al. Predominant development of mature and functional human NK cells in a novel human IL-2-producing transgenic NOG mouse. *J Immunol* (2015) 194 (7):3513–25. doi: 10.4049/jimmunol.1401323
111. Herndler-Brandstetter D, Shan L, Yao Y, Stecher C, Plajer V, Lietzenmayer M, et al. Humanized mouse model supports development, function, and tissue residency of human natural killer cells. *Proc Natl Acad Sci U S A* (2017) 114(45):E9626–34. doi: 10.1073/pnas.1705301114
112. Matsuda M, Ono R, Iyoda T, Endo T, Iwasaki M, Tomizawa-Murasawa M, et al. Human NK cell development in hIL-7 and hIL-15 knockin NOD/SCID/IL2rgKO mice. *Life Sci Alliance* (2019) 2(2):e201800195. doi: 10.26508/lsa.201800195
113. André MC, Erbacher A, Gille C, Schmauke V, Goecke B, Hohberger A, et al. Long-term human CD34+ stem cell-engrafted nonobese diabetic/SCID/IL-2R gamma(null) mice show impaired CD8+ T cell maintenance and a functional arrest of immature NK cells. *J Immunol Baltim Md 1950* (2010) 185(5):2710–20. doi: 10.4049/jimmunol.1000583
114. Rongvaux A, Willinger T, Martinek J, Strowig T, Gearty SV, Teichmann LL, et al. Development and function of human innate immune cells in a humanized mouse model. *Nat Biotechnol* (2014) 32(4):364–72. doi: 10.1038/nbt.2858
115. Lang J, Weiss NA, Freed BM, Torres RM, Pelanda R. Generation of hematopoietic humanized mice in the newborn BALB/c-Rag2null Il2rγnull mouse model: a multivariable optimization approach. *Clin Immunol* (2011) 140(1):102–16. doi: 10.1016/j.clim.2011.04.002
116. Vahedi F, Nham T, Poznanski SM, Chew MV, Shenouda MM, Lee D, et al. Ex Vivo Expanded Human NK Cells Survive and Proliferate in Humanized Mice with Autologous Human Immune Cells. *Sci Rep* (2017) 7(1):12083. doi: 10.1038/s41598-017-12223-8
117. Billerbeck E, Barry WT, Mu K, Dorner M, Rice CM, Ploss A. Development of human CD4+FoxP3+ regulatory T cells in human stem cell factor-, granulocyte-macrophage colony-stimulating factor-, and interleukin-3-expressing NOD-SCID IL2Rγ(null) humanized mice. *Blood* (2011) 117 (11):3076–86. doi: 10.1182/blood-2010-08-301507
118. Nicolini FE, Cashman JD, Hogge DE, Humphries RK, Eaves CJ. NOD/SCID mice engineered to express human IL-3, GM-CSF and Steel factor constitutively mobilize engrafted human progenitors and compromise human stem cell regeneration. *Leukemia* (2004) 18(2):341–7. doi: 10.1038/sj.leu.2403222
119. Cosgun KN, Rahmig S, Mende N, Reinke S, Hauber I, Schäfer C, et al. Kit regulates HSC engraftment across the human-mouse species barrier. *Cell Stem Cell* (2014) 15(2):227–38. doi: 10.1016/j.stem.2014.06.001
120. Rahmig S, Kronstein-Wiedemann R, Fohgrub J, Kronstein N, Nevmerzhitskaya A, Bornhäuser M, et al. Improved Human Erythropoiesis and Platelet Formation in Humanized NSGW41 Mice. *Stem Cell Rep* (2016) 7(4):591–601. doi: 10.1016/j.stemcr.2016.08.005
121. Ito R, Takahashi T, Katano I, Kawai K, Kamisako T, Ogura T, et al. Establishment of a Human Allergy Model Using Human IL-3/GM-CSF–Transgenic NOG Mice. *J Immunol* (2013) 191(6):2890–9. doi: 10.4049/jimmunol.1203543
122. Beyer AI, Muench MO. Comparison of Human Hematopoietic Reconstitution in Different Strains of Immunodeficient Mice. *Stem Cells Dev* (2017) 26(2):102–12. doi: 10.1089/scd.2016.0083
123. Wunderlich M, Chou F-S, Sexton C, Presicce P, Chougnet CA, Aliberti J, et al. Improved multilineage human hematopoietic reconstitution and function in NSGS mice. *PLoS One* (2018) 13(12):e0209034. doi: 10.1371/journal.pone.0209034
124. Shultz LD, Saito Y, Najima Y, Tanaka S, Ochi T, Tomizawa M, et al. Generation of functional human T-cell subsets with HLA-restricted immune responses in HLA class I expressing NOD/SCID/IL2rγnull humanized mice. *Proc Natl Acad Sci* (2010) 107(29):13022–7.
125. Kooreman NG, de Almeida PE, Stack JP, Nelakanti RV, Diecke S, Shao N-Y, et al. Alloimmune Responses of Humanized Mice to Human Pluripotent Stem Cell Therapeutics. *Cell Rep* (2017) 20(8):1978–90. doi: 10.1016/j.celrep.2017.08.003
126. Li J, Li X, Liang C, Ling L, Chen Z, Wong CK, et al. Coreceptor blockade targeting CD4 and CD8 allows acceptance of allogeneic human pluripotent stem cell grafts in humanized mice. *Biomaterials* (2020) 248:120013. doi: 10.1016/j.biomaterials.2020.120013
127. Rong Z, Wang M, Hu Z, Stradner M, Zhu S, Kong H, et al. An Effective Approach to Prevent Immune Rejection of Human ESC-Derived Allografts. *Cell Stem Cell* (2014) 14(1):121–30. doi: 10.1016/j.stem.2013.11.014
128. Szot GL, Yadav M, Lang J, Kroon E, Kerr J, Kadoya K, et al. Tolerance Induction and Reversal of Diabetes in Mice Transplanted with Human Embryonic Stem Cell-Derived Pancreatic Endoderm. *Cell Stem Cell* (2015) 16(2):148–57. doi: 10.1016/j.stem.2014.12.001
129. Morizane A, Kikuchi T, Hayashi T, Mizuma H, Takara S, Doi H, et al. MHC matching improves engraftment of iPSC-derived neurons in non-human primates. *Nat Commun* (2017) 8(1):385. doi: 10.1038/s41467-017-00926-5
130. Han X, Wang M, Duan S, Franco PJ, Kenty JH-R, Hedrick P, et al. Generation of hypoimmunogenic human pluripotent stem cells. *Proc Natl Acad Sci* (2019) 116(21):10441–6. doi: 10.1073/pnas.1902566116
131. Perrier-Groult E, Pérès E, Pasdeloup M, Gazzolo L, Duc Dodon M, Mallein-Gerin F. Evaluation of the biocompatibility and stability of allogeneic tissue-engineered cartilage in humanized mice. *PLoS One* (2019) 14(5):e0217183. doi: 10.1371/journal.pone.0217183
132. Benabdallah B, Désaulniers-Langevin C, Colas C, Li Y, Rousseau G, Guimond JV, et al. Natural Killer Cells Prevent the Formation of Teratomas Derived From Human Induced Pluripotent Stem Cells. *Front Immunol* (2019) 10:2580. doi: 10.3389/fimmu.2019.02580
133. Benabdallah B, Désaulniers-Langevin C, Goyer M-L, Colas C, Maltais C, Li Y, et al. Myogenic progenitor cells derived from human induced pluripotent stem cell are immune-tolerated in humanized mice. *Stem Cells Transl Med* (2021) 10(2):267–77. doi: 10.1002/sctm.19-0452
134. ATCC. *LCL 721221 ATCC CRL1855-1077*. Available at: https://www.atcc.org/support/faqs/11472/LCL%20721221%20ATCC%20CRL1855-1077.aspx. (Accessed March 27, 2021)
135. Kübler A, Woiterski J, Witte K-E, Bühring H-J, Hartwig UF, Ebinger M, et al. Both mature KIR+ and immature KIR– NK cells control pediatric acute B-cell precursor leukemia in NOD.Cg-Prkdcscid IL2rgtmWjl/Sz mice. *Blood* (2014) 124(26):3914–23. doi: 10.1182/blood-2014-05-572743
136. Ito Y, Nakamura S, Sugimoto N, Arai F, Nishimura S, Correspondence KE, et al. Turbulence Activates Platelet Biogenesis to Enable Clinical Scale Ex Vivo Production Article Turbulence Activates Platelet Biogenesis to Enable Clinical Scale Ex Vivo Production. *Cell* (2018) 174:636–48.e18. doi: 10.1016/j.cell.2018.06.011

Conflict of Interest: NS has applied for patents related to this manuscript.

The remaining authors declare that the research was conducted in the absence of any commercial or financial relationships that could be construed as a potential conflict of interest.

Copyright © 2021 Flahou, Morishima, Takizawa and Sugimoto. This is an open-access article distributed under the terms of the Creative Commons Attribution License (CC BY). The use, distribution or reproduction in other forums is permitted, provided the original author(s) and the copyright owner(s) are credited and that the original publication in this journal is cited, in accordance with accepted academic practice. No use, distribution or reproduction is permitted which does not comply with these terms.

frontiers in Oncology

ORIGINAL RESEARCH
published: 13 April 2021
doi: 10.3389/fonc.2021.642466

PD-1 Inhibition Enhances Blinatumomab Response in a UCB/PDX Model of Relapsed Pediatric B-Cell Acute Lymphoblastic Leukemia

Mark Wunderlich[1], Nicole Manning[1], Christina Sexton[1], Eric O'Brien[2], Luke Byerly[2], Cody Stillwell[1], John P. Perentesis[2,3], James C. Mulloy[1,3] and Benjamin Mizukawa[2,3]**

[1] Experimental Hematology and Cancer Biology, Cancer and Blood Disease Institute, Cincinnati Children's Hospital Medical Center, Cincinnati, OH, United States, [2] Oncology, Cancer and Blood Disease Institute, Cincinnati Children's Hospital Medical Center, Cincinnati, OH, United States, [3] Department of Pediatrics, University of Cincinnati College of Medicine, Cincinnati, OH, United States

OPEN ACCESS

Edited by:
Alexandre P. A. Theocharides, University Hospital Zürich, Switzerland

Reviewed by:
Carsten Riether, University of Bern, Switzerland
Sinisa Dovat, Penn State University, United States
Chunhua Song, Pennsylvania State University, United States

***Correspondence:**
Mark Wunderlich
mark.wunderlich@cchmc.org
Benjamin Mizukawa
benjamin.mizukawa@cchmc.org

Specialty section:
This article was submitted to Cancer Immunity and Immunotherapy, a section of the journal Frontiers in Oncology

Received: 16 December 2020
Accepted: 22 March 2021
Published: 13 April 2021

Citation:
Wunderlich M, Manning N, Sexton C, O'Brien E, Byerly L, Stillwell C, Perentesis JP, Mulloy JC and Mizukawa B (2021) PD-1 Inhibition Enhances Blinatumomab Response in a UCB/PDX Model of Relapsed Pediatric B-Cell Acute Lymphoblastic Leukemia. Front. Oncol. 11:642466. doi: 10.3389/fonc.2021.642466

Immune therapies such as blinatumomab, CD19-directed bispecific CD3 T-cell Engager (BiTE), have resulted in significant improvements in outcomes for relapsed B-cell acute lymphoblastic leukemia (B-ALL). However, up to half of blinatumomab treated patients do not respond completely or relapse after therapy. As a result, there is a need to identify potential strategies to improve the efficacy of BiTE therapy. The anti-PD-1 antibody pembrolizumab has been shown to successfully activate T cells against a wide range of cancer types. Here, we tested the ability of umbilical cord blood (UCB) reconstituted mice to respond to blinatumomab therapy with or without concurrent pembrolizumab treatment. Humanized mice were engrafted with patient-derived xenograft (PDX) cells derived from pediatric and adolescent/young adult (AYA) B-ALL patients who had either failed to achieve remission with negative minimum residual disease (MRD negative) or experienced a relapse. Mock-treated humanized mice engrafted with PDX cells efficiently developed overt disease within 30 days of engraftment of B-ALL. However, single agent therapy with either blinatumomab or pembrolizumab reduced disease burden in engrafted mice, with some mice observed to be MRD negative after the 28-day treatment course. Combination therapy significantly improved the percentage of MRD negative mice and improved long-term survival and cure rates as compared to mice that were given blinatumomab alone. Importantly, no benefits were observed in treated mice that lacked human immune cell reconstitution. These results indicate that UCB-humanized NRGS mice develop activatable immune function, and UCB-humanized PDX leukemia models can be used in preclinical studies to evaluate specificity, efficacy, and cooperativity of immune therapies in B-ALL.

Keywords: patient derived xenograft, blinatumomab, pembrolizumab, B-ALL, humanized mice, immune checkpoint inhibition, PD-1, bispecific T-cell engager

INTRODUCTION

IL-2Ry immune deficient mice engrafted with human umbilical cord blood (UCB) develop human immune systems with mixed B, T, NK, and myeloid populations. We have previously generated modified NOD/SCID/Gamma (NSG) and NOD/RAG/Gamma (NRG) mouse strains that include transgenic expression of human cytokines SCF, GM-CSF, and IL-3 (NSGS/NRGS) (1, 2). Relative to NSG/NRG, the NSGS/NRGS mice have increased myeloid and NK fractions, more complete B cell differentiation, and faster T cell reconstitution (3, 4). Additionally, both innate and adaptive immune function is also improved as measured by DTH assay and human antigen specific antibody production in response to immunization. NSGS and NRGS mice are also more permissive to human hematopoietic engraftment, particularly in the absence of conditioning (1–3).

B-ALL is the most common hematopoietic malignancy among the pediatric population. While responses to therapy are generally good with survival rates approaching 90% in the pediatric population, a significant number of patients will relapse or be refractory to standard therapy (5). MRD status during and after therapy correlates strongly with relapse free survival and overall survival (6). Recently, new effective therapies for patients in relapse have further improved survival, including the CD19-directed Bi-specific T cell Engager (BiTE), blinatumomab. As a treatment for therapy resistant disease, blinatumomab has been shown to lead to longer relapse free survival compared to historical data using standard chemotherapy approaches in adult patients (7). A group of 20 such patients who received blinatumomab achieved a long-term relapse free survival of 60-65% at 3 years, regardless of HSCT (8). A larger phase 3 trial found that while blinatumomab was more effective than standard chemotherapy for relapsed adult B-ALL in terms of induction of remission and length of overall survival, it was still only effective for fewer than half of patients (9). In a large multi-center trial, blinatumomab therapy lead to increased likelihood of remission and longer survival compared to standard chemotherapy for relapsed adult B-ALL, while the final long-term survival rate was virtually identical (9). This finding suggests that blinatumomab can successfully eliminate leukemia-initiating cells (LICs). In addition, a phase 2 clinical trial showed blinatumomab therapy was effective in adult patients with low level MRD+ disease with significant improvements in EFS, RFS, and OS (10).

Immune checkpoint inhibitors (CPI) targeting ligand-receptor interactions that suppress immune effector cell activation have entered wide use in cancer therapy. Pembrolizumab, an anti-PD-1 blocking antibody, is one such CPI that stimulates immune activity against a wide range of malignancies. It prevents ligation to PD-L1, a surface ligand which is frequently found upregulated on cancer cells and provides inhibitory signaling to the T cell as an immune escape mechanism. BM samples from B-ALL patients at both diagnosis and relapse contain T cells with increased PD-1 expression, relative to healthy controls or patients in remission (11–13). Additionally, increased PD-L1 expression has been noted on relapsed B-ALL with increased levels on blinatumomab non-responder blasts, compared to responders (12, 14). Addition of blinatumomab to an ex vivo co-culture of patient blasts and a B-ALL cell line resulted in a further upregulation of PD-1, but not when healthy donor lymphocytes were used in place of leukemic blasts, indicating that this phenomenon was mediated by the leukemia cells. Combination of pembrolizumab with blinatumomab resulted in a temporary response in one patient that was previously blinatumomab resistant, although it is unclear whether this result could have been realized with pembrolizumab alone since donor T lymphocytes were also infused at the same time (12).

Recently, several models have been developed to study immune therapy in a xenograft setting. NSG mice engrafted with PBMNCs demonstrated efficacy of a novel dual CD3XPDL1 BiTE against a xenografted melanoma cell line (15). However, PBMNC models are problematic due to the rapid onset of GVHD. Double knockout of MHC class I and II in the NOG strain allowed GVHD-free engraftment of PBMNCs which responded to a lab made PD-1 antibody and slowed the growth of two partially MHC matched human cell lines *in vivo* (16). Also, NSG mice engrafted with fetal liver HSCs generated a more complete human immune system which was able to slow tumor growth of HCC PDX tumors upon either pembrolizumab or ipilimumab treatment (17). Finally, UCB reconstituted NSG mice also generated pembrolizumab-responsive human immune systems that successfully slowed the growth of a variety of solid tumor PDX and CDX models (18). UCB based models have the benefits of relying on a cheap and readily available source of HSCs that is not labor intensive and has limited risk of acute GVHD.

Here, we developed a tractable system to test immunotherapy in UCB-reconstituted NSGS and NRGS mice engrafted with B-ALL PDX models. Mice treated with either blinatumomab or pembrolizumab were partially protected from disease at day 30 by flow MRD analysis. The combination of blinatumomab and pembrolizumab resulted in fewer mice with detectable MRD and improved survival. These results demonstrate the utility of dual UCB/PDX models for examining novel combinations of immune therapies *in vivo* that may improve response rates of relapsed and refractory pediatric B-ALL.

METHODS

UCB Humanization

UCB was obtained from the Translational Trials Development Support Laboratory of CCHMC. Units were RBC depleted by hetastarch sedimentation and unselected WBCs were viably frozen in IMDM/50%Hespan/25%BSA/5%DMSO until needed. At thaw, cells were mixed with OKT3 and intravenously (IV) injected into busulfan conditioned mice (2). PB was monitored for the appearance of human CD45+CD3+ T cells by flow cytometry.

PDX Models

Previously generated PDX models were obtained from the Pediatric Leukemia Avatar Program of the Cancer & Blood Diseases Institute (CBDI) at Cincinnati Children's Hospital

Medical Center (CCHMC). Original patient material was collected under IRB approved protocols. Viably frozen primary and secondary spleen preparations were used to initiate B-ALL in the cohorts described here.

Antibody Treatments

Discarded residual aliquots of blinatumomab and pembrolizumab were obtained from the CCHMC pharmacy. Blinatumomab (Blincyto, 12.5ug/mL) was diluted to 0.25ug/mL in sterile PBS/3% FBS with antibiotics. Each dose consisted of a 250uL ip injection (approximately 2.0-2.5ug/kg). Pembrolizumab (Keytruda, 25mg/mL) was diluted to 1mg/mL with PBS/3% FBS and antibiotics. Each dose was a 300uL ip injection (approximately 10mg/kg). Antibody treatments started the day of B-ALL engraftment. Blinatumomab injections were repeated daily for up to 4 weeks and pembrolizumab was given once or twice on days 1 and 15 (see **Table 1** for specific details).

Transfusion

Some mice were given transfusions to relieve anemia that has been described to occur in NSGS and NRGS mice with human immune reconstitution (19). Donor mice were bled from the tail into a 1.5mL tube containing 100uL heparin (Sigma Aldrich #2106 - dissolved in 1mL PBS). 400uL PB was added to each tube. This sample was immediately iv injected into 2 recipient mice (250uL each).

Statistics

Mann-Whitney and paired tTests were performed with Prism 8 software (GraphPad). Log rank test was performed online at http://bioinf.wehi.edu.au/software/russell/logrank/. Significance was set to $p<0.05$.

RESULTS

Pembrolizumab in Combination With Blinatumomab Improves Clearance of B-ALL in PDX Mice

To test the suitability of humanized mice to respond to immune modulatory therapies for B-ALL, we first generated UCB engrafted mice with detectable T cells in circulation (**Figure 1A**). After approximately 4 months, the majority of human CD45+ cells were found to be human CD3+ T cells. One of several B-ALL PDX models (**Table 1**) was then engrafted prior to treatment with blinatumomab with or without pembrolizumab.

We began by testing if blinatumomab would have any direct effects on engraftment or expansion of B-ALL in mice without human immune reconstitution. Mouse macrophages could potentially eliminate or reduce leukemic burden if they successfully recognize blinatumomab-labeled cells. Also, some antibodies may directly affect the target cells. Importantly, we observed no delay in development or reduction of established human B-ALL in the PB of engrafted mice that received blinatumomab in absence of human immune reconstitution (**Figure 1B**).

Next, we engrafted humanized mice with a B-ALL PDX sample and initiated treatment with either blinatumomab, pembrolizumab, or the combination (**Figure 1C**). Non-humanized control (Non-hu CNTL) mice developed robust disease within 30 days as measured by bone marrow aspiration and disease specific flow cytometry. In humanized mice that did not receive either specific antibody, a small but inconsistent decrease in disease levels was seen. Blinatumomab treated mice had a significantly lower disease level in the BM while pembrolizumab treatment also led to a significant reduction in disease, although to a lesser degree. Combination therapy resulted in the greatest reduction in detectable disease and more mice with MRD negative bone marrow (fewer than 0.01% leukemic blasts, the clinical cutoff for flow cytometry based MRD assessment). These results were consistent for 4 separate PDX samples derived from relapsed B-ALL (**Figure 1C** and **Table 1**) with combination treatment leading to a significantly higher proportion of MRD negative mice (paired tTest, $p=0.0128$, **Figure 1D** and **Table 2**).

Pembrolizumab Reverses T Cell Lymphopenia Induced by Blinatumomab

A significant drop in peripheral B cells was observed when we measured CD19+ B cells in the PB of humanized mice with B-ALL engraftment after treatment with blinatumomab, reminiscent of the B cell aplasia observed in patients (**Figure 1E**). This decrease was more dramatic in the combination cohort, possibly indicating increased killing of both normal and malignant B cells. Analysis of CD3+ T cell

TABLE 1 | PDX model summary.

Experiment	PDX ID	Patient History	Cytogenetics	Blina Response	Mouse Strain	UCB Transplant	PDX Cell#	PDX Treatments
Expt#1	ALL #1	Infant bi-lineage leukemia; relapse w/B-ALL post-HSCT	t(6;11)	PD; CD19+	NSGS	8.0M WBCs w/ OKT3, IV	3.0M	Blina 2X per day ip (4 weeks), Pembro 1st and 3rd Monday
Expt#2	ALL #2	B-ALL; early marrow relapse	t(1;19)	PD; CD19+	NSGS	7.0M WBCs w/ OKT3, IV	2.5M	Blina 2X per day ip (2 weeks), Pembro 1st Monday
Expt#3	ALL #3	Ph+(T315I) B-ALL, MRD negative post-Blina; relapse post-HSCT	t(9;22)	CR; later CD19+ relapse post-HSCT	NRGS	8.0M WBCs w/ OKT3, IV	1.0M	Blina 1X per day ip (4 weeks), Pembro 1st and 3rd Monday
Expt#4	ALL #4	Infant B-ALL; primary refractory disease	t(4;11)	PD; CD19-	NRGS	6.3M WBCs w/ OKT3, IV	3.0M	Blina 1X per day ip (4 weeks), Pembro 1st and 3rd Monday

PDX, patient-derived xenograft; ALL, acute lymphoblastic leukemia; HSCT, hematopoietic stem cell transplant; Ph, Philadelphia chromosome; Blina, blinatumomab; PD, progressive disease; CR, complete remission; WBC, white blood cell; UCB, umbilical cord blood; Pembro, pembrolizumab.

numbers in the PB before and after therapy showed peripheral T cells increased slightly in control untreated mice over time, which is expected since T cells gradually increase as a percentage of WBCs in xenograft PB over time (**Figure 1F**). In contrast, peripheral T cells dropped in most blinatumomab treated mice. However, the addition of pembrolizumab reversed this effect and combination treated mice had increased T cells after treatment, which might indicate a mechanism for increased efficacy.

Combination Therapy Increases Survival of UCB-Humanized Mice With B-ALL Engraftment

Following MRD assessment, we monitored mice for long term survival. Untreated humanized mice succumbed to B-ALL between 40 and 60 days after engraftment (**Figure 1G**). Most of the blinatumomab treated mice developed fatal leukemia with delayed kinetics, however there were 2 long-term survivors. A significantly higher proportion of combination treated mice survived until the end of the experiment. As a functional test for residual leukemia initiating cells (LICs), we harvested BM from these surviving mice and transplanted whole marrow into busulfan conditioned secondary hosts. None of the flow cytometry-based MRD negative samples generated leukemia indicating a lack of transfer of undetected residual disease from the primary mouse. All mice remained disease free in the secondary graft at 120 days suggesting the survival benefit seen in the primary cohort is durable and represents clearance of leukemia-initiating cells.

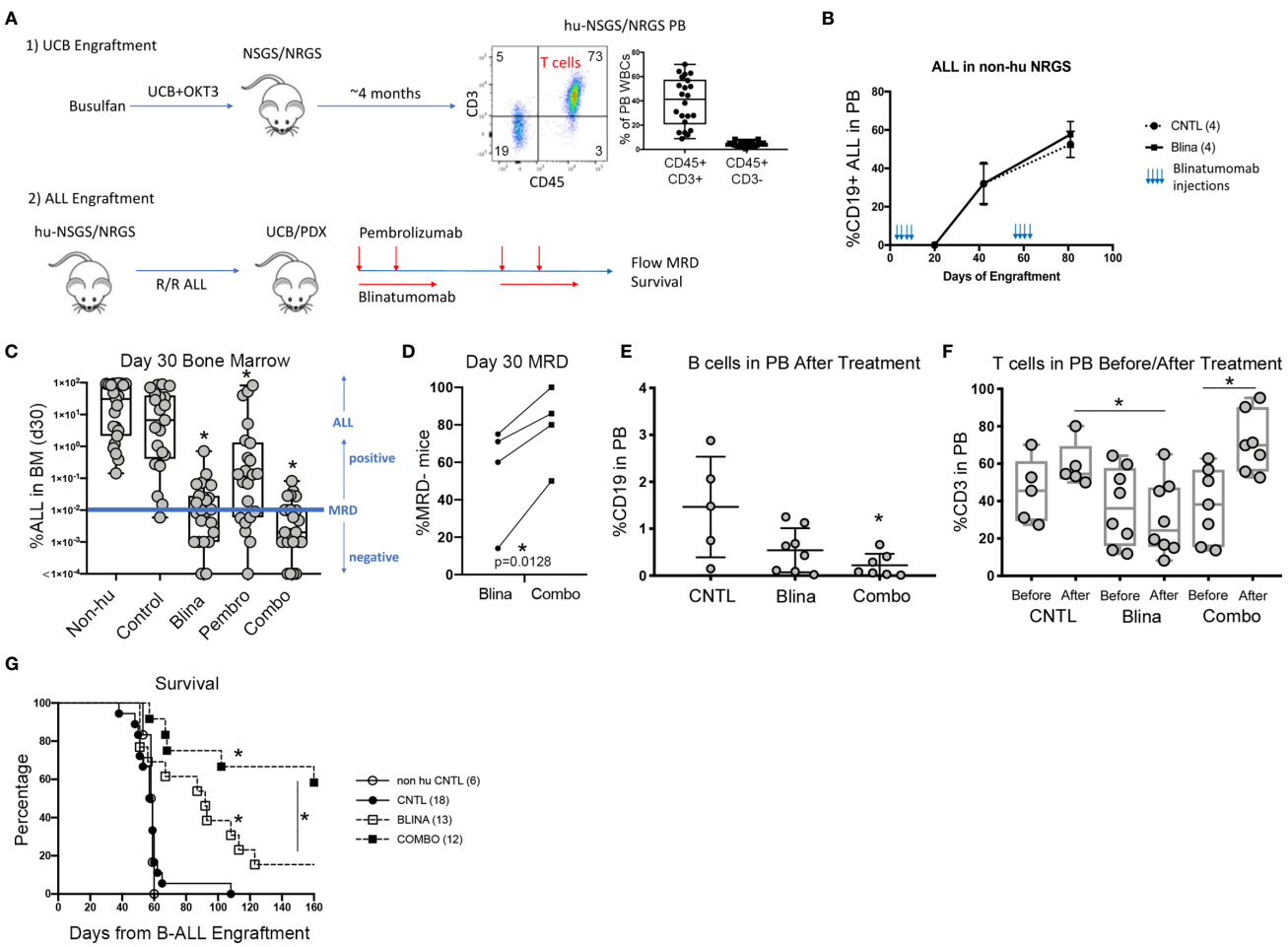

FIGURE 1 | Modeling combined blinatumomab (Blina) and PD-1 inhibition with pembrolizumab (Pembro) in humanized mice. **(A)** Schematic outlining the experimental setup. **(B)** Non-humanized mice were treated with Blina or control (CNTL) immediately after engraftment (2 weeks, beginning on day 1) with B-ALL and were re-treated after disease was readily detectable in PB (beginning on day 48). **(C)** B-ALL engraftment (from 4 unique PDX models) was detected in the bone marrow of mice 30 days after therapy was initiated. Treatment was started on day 1 of B-ALL injection according to the schedules in **Table 1**. *$p < 0.05$ by Mann-Whitney test. **(D)** Proportion of mice with lower than 0.01% B-ALL in the marrow (MRD-) at day 30 for each of the 4 samples in Blina or combo groups. *$p = 0.0128$ by paired tTest. **(E)** Flow cytometry measurement of B cells in the PB of mice after therapy. *$p < 0.05$ by Mann-Whitney test. **(F)** Flow cytometry measurement of T cells in the PB of mice before and after therapy. *$p < 0.05$ by Mann-Whitney test. **(G)** Survival of treated mice correlates with MRD flow detection. *$p < 0.05$ by log rank test.

TABLE 2 | Fraction of MRD- mice at day 30.

Treatment Group	Expt #1	Expt #2	Expt #3	Expt #4	Total	Percentage
Non-hu CNTL	0 of 6	0 of 7	0 of 5	0 of 5	0 of 23	0%
CNTL	1 of 14	1 of 6	0 of 5	0 of 6	2 of 31	6%
Blinatumomab	5 of 7	3 of 4	3 of 5	1 of 7	12 of 23	52%
Pembrolizumab	1 of 6	3 of 4	3 of 5	0 of 7	7 of 22	32%
Combination	6 of 7	5 of 5	4 of 5	3 of 6	18 of 23	78%*

Paired tTest, Blinatumomab vs. Combination = 0.0128.

DISCUSSION

Here we have established a model system to examine immune therapies in the context of a humanized mouse reconstituted with UCB hematopoietic stem cells. The method relies on a readily available source of stem cells and avoids GVHD and labor-intensive steps of other models. Our model of early treatment with blinatumomab after engraftment mimics several completed and ongoing clinical trials in which blinatumomab has been used against residual post chemotherapy MRD (7, 10, 20). One question that remains unanswered is if blinatumomab could be used concurrently or consecutively with conventional chemotherapy, and how the lymphotoxic effects of chemotherapy impact efficacy of blinatumomab (21). We have recently optimized conditions for modeling standard 4-drug ALL induction protocols in xenografts which could be used to investigate this possibility (22).

One common toxicity with blinatumomab therapy in cases of overt disease is the development of cytokine release syndrome (CRS) which appears to progress to hemophagocytic lymphohistiocytosis or macrophage activation syndrome (MAS) (23, 24). One case report reported on the use of tocilizumab to target the IL-6R in a patient experiencing severe CRS-induced MAS (25). While there was a rapid clinical improvement of CRS symptoms, it remains unclear if targeting IL-6 signaling interferes with the activity of blinatumomab or whether the two therapies can be delivered simultaneously without affecting the anti-leukemic effect. The UCB reconstituted NSGS/NRGS mice we used in this study do in fact develop a progressive, myeloid driven MAS over time that responds to either gemtuzumab ozogamicin or tocilizumab (19). It would be interesting to test whether blinatumomab therapy would induce CRS and exacerbate MAS in mice with higher initial levels of B-ALL. If so, our model could evaluate the effects of tocilizumab and other potential therapies that might treat CRS/MAS while preserving the efficacy of blinatumomab.

The drop in PB B and T cells after blinatumomab treatment is consistent with long term elimination of B cells and a transient drop in PB T cells observed in patients (26). However, in patients, T cell levels reached a nadir after 1-2 days and recovered to normal levels within 8-10 days before expansion over baseline (particularly for CD8+ T cells) (20) which was observed for the duration of the 28-day cycle. A drop in T cells was observed in the beginning of each cycle. Levels of T cell expansion during blinatumomab treatment has been shown to correlate with long term survival in patients that achieve MRD negative status (27). We are unable to replicate the slow constant infusion of blinatumomab and instead must rely on repeated bolus injections which may result in increased elimination of T cells and explain the lack of expansion. We did however observe T cell expansion after combination therapy, indicating that immune checkpoint inhibition may serve to counteract the T cell lymphopenia associated with blinatumomab. It remains unclear whether this quantitative increase in PB T cell numbers is directly related to improved efficacy.

The B-ALL PDX models used in these experiments represent cases of relapsed or persistent residual disease for which blinatumomab has established clinical indication. Two of our PDX ALL models (#1 and #2) were derived from patient samples representing relapsed disease that was unsuccessfully salvaged with blinatumomab. In both cases, the disease that progressed during blinatumomab treatment remained CD19+, suggesting immune escape or anergy. PDX model ALL#3 was derived from a patient who achieved an MRD negative remission after blinatumomab and subsequently underwent allogeneic stem cell transplant, only to relapse post-transplant with CD19+ disease. This illustrates the great need for strategies to enhance the efficacy of immunotherapies. B-ALL PDX models in human immune cell-reconstituted mice provide a valuable resource for development and validation of those strategies.

In these experiments, samples from patients that were refractory to blinatumomab in the clinical setting nevertheless showed some response in the PDX experiments. This may be due to the use of a healthy UCB-derived immune cell repertoire, as opposed to the endogenous immune cells that may be compromised in number or function in patients heavily pretreated with cytotoxic chemotherapy. This PDX system provides one avenue to investigate whether CPI failure results from leukemia-intrinsic factors, or from defects in the immune milieu.

A number of clinical trials have been initiated to assess the efficacy of combined blinatumomab with CPI, such as pembrolizumab or nivolumab, in the treatment of B-ALL. Preliminary findings in a phase I clinical trial of blinatumomab and nivolumab in adults with relapsed/refractory (R/R) CD19 positive B-ALL demonstrated favorable safety profile and clearance of MRD in this heavily pretreated cohort (28). A similar study will examine this approach in pediatric and adolescent/young adult (AYA) patients with R/R CD19 positive B-ALL (NCT04546399). Combinations of immune therapies may have dramatically different efficacies depending on timing and sequence as has been shown in a mouse model of

breast cancer combining anti-PD-1 with anti-OX40 antibodies (29). Similarly, the combination of blinatumomab and nivolumab is being investigated in clinical trials to determine whether CTLA-4 inhibition with ipilimumab can further augment the immune response to eliminate CD19 positive B-ALL (NCT02879695). The humanized models of immune therapy in leukemia PDX mice presented here could provide an important preclinical testing platform for examining the efficacy of such combinations and their mechanisms of response, resistance, and toxicity.

DATA AVAILABILITY STATEMENT

The raw data supporting the conclusions of this article will be made available by the authors, without undue reservation.

ETHICS STATEMENT

The studies involving human participants were reviewed and approved by Cincinnati Children's Hospital Medical Center Institutional Review Board. Written informed consent from the participants' legal guardian/next of kin was not required to participate in this study in accordance with the national legislation and the institutional requirements. The animal study was reviewed and approved by Cincinnati Children's Hospital Medical Center Institutional Animal Care and Use Committee.

AUTHOR CONTRIBUTIONS

Study Design: MW, JM, and BM. Experimentation and Data Collection: MW, NM, CSe, EO'B, LB, and CSt. Data Interpretation: MW, JM, and BM. Drafting Manuscript: MW. Editing and Revision: JM and BM. Samples and Reagents: EO'B, LB, JP, and BM. Funding: MW, JP, and JM. All authors contributed to the article and approved the submitted version.

FUNDING

This work was supported by NIH/NCI R50 CA211404 (MW), NIH/NCI R01 CA204895 (JM) NIH/NCI R01 CA215504 (JM), and a CCHMC ARC award (JP and JM). Flow cytometry was supported in part by NIH grant P30AR070549.

ACKNOWLEDGMENTS

The authors thank the CCHMC Comprehensive Mouse and Cancer Core for providing some of the mice used, the CCHMC Research Flow Cytometry Core for access to cytometers, and the CCHMC Translational Trial Development and Support Laboratory for providing UCB units.

REFERENCES

1. Wunderlich M, Chou FS, Link KA, Mizukawa B, Perry RL, Carroll M, et al. AML xenograft efficiency is significantly improved in NOD/SCID-IL2RG mice constitutively expressing human SCF, GM-CSF and IL-3. *Leukemia* (2010) 24(10):1785–8. doi: 10.1038/leu.2010.158
2. Wunderlich M, Brooks RA, Panchal R, Rhyasen GW, Danet-Desnoyers G, Mulloy JC. OKT3 prevents xenogeneic GVHD and allows reliable xenograft initiation from unfractionated human hematopoietic tissues. *Blood* (2014) 123(24):e134–44. doi: 10.1182/blood-2014-02-556340
3. Wunderlich M, Chou FS, Sexton C, Presicce P, Chougnet CA, Aliberti J, et al. Improved multilineage human hematopoietic reconstitution and function in NSGS mice. *PloS One* (2018) 13(12):e0209034. doi: 10.1371/journal.pone.0209034
4. Billerbeck E, Barry WT, Mu K, Dorner M, Rice CM, Ploss A. Development of human CD4+FoxP3+ regulatory T cells in human stem cell factor-, granulocyte-macrophage colony-stimulating factor-, and interleukin-3-expressing NOD-SCID IL2Rgamma(null) humanized mice. *Blood* (2011) 117(11):3076–86. doi: 10.1182/blood-2010-08-301507
5. Jeha S, Pei D, Choi J, Cheng C, Sandlund JT, Coustan-Smith E, et al. Improved CNS Control of Childhood Acute Lymphoblastic Leukemia Without Cranial Irradiation: St Jude Total Therapy Study 16. *J Clin Oncol* (2019) 37(35):3377–91. doi: 10.1200/JCO.19.01692
6. Brüggemann M, Raff T, Flohr T, Gökbuget N, Nakao M, Droese J, et al. Clinical significance of minimal residual disease quantification in adult patients with standard-risk acute lymphoblastic leukemia. *Blood* (2006) 107 (3):1116–23. doi: 10.1182/blood-2005-07-2708
7. Gökbuget N, Dombret H, Giebel S, Brüggemann M, Doubek M, Foa R, et al. Blinatumomab vs historic standard-of-care treatment for minimal residual disease in adults with B-cell precursor acute lymphoblastic leukaemia. *Eur J Haematol* (2020) 104(4):299–309. doi: 10.1111/ejh.13375
8. Topp MS, Gökbuget N, Zugmaier G, Degenhard E, Goebeler ME, Klinger M, et al. Long-term follow-up of hematologic relapse-free survival in a phase 2 study of blinatumomab in patients with MRD in B-lineage ALL. *Blood* (2012) 120(26):5185–7. doi: 10.1182/blood-2012-07-441030
9. Kantarjian H, Stein A, Gokbuget N, Fielding AK, Schuh AC, Ribera JM, et al. Blinatumomab versus Chemotherapy for Advanced Acute Lymphoblastic Leukemia. *N Engl J Med* (2017) 376(9):836–47. doi: 10.1056/NEJMoa1609783
10. Gokbuget N, Dombret H, Bonifacio M, Reichle A, Graux C, Faul C, et al. Blinatumomab for minimal residual disease in adults with B-precursor acute lymphoblastic leukemia. *Blood* (2018) 131(14):1522–31. doi: 10.1182/blood-2017-08-798322
11. Park SH, You E, Park CJ, Cho YU, Jang S, Im HJ, et al. Increased expression of immune checkpoint programmed cell death protein-1 (PD-1) on T cell subsets of bone marrow aspirates in patients with B-Lymphoblastic leukemia, especially in relapse and at diagnosis. *Cytom B Clin Cytom* (2020) 98(4):336–47. doi: 10.1002/cyto.b.21879
12. Feucht J, Kayser S, Gorodezki D, Hamieh M, Doring M, Blaeschke F, et al. T-cell responses against CD19+ pediatric acute lymphoblastic leukemia mediated by bispecific T-cell engager (BiTE) are regulated contrarily by PD-L1 and CD80/CD86 on leukemic blasts. *Oncotarget* (2016) 7(47):76902–19. doi: 10.18632/oncotarget.12357
13. Liu L, Chang YJ, Xu LP, Zhang XH, Wang Y, Liu KY, et al. T cell exhaustion characterized by compromised MHC class I and II restricted cytotoxic activity associates with acute B lymphoblastic leukemia relapse after allogeneic hematopoietic stem cell transplantation. *Clin Immunol* (2018) 190:32–40. doi: 10.1016/j.clim.2018.02.009
14. Kohnke T, Krupka C, Tischer J, Knosel T, Subklewe M. Increase of PD-L1 expressing B-precursor ALL cells in a patient resistant to the CD19/CD3-bispecific T cell engager antibody blinatumomab. *J Hematol Oncol* (2015) 8:111. doi: 10.1186/s13045-015-0213-6
15. Horn LA, Ciavattone NG, Atkinson R, Woldergerima N, Wolf J, Clements VK, et al. CD3xPDL1 bi-specific T cell engager (BiTE) simultaneously activates T cells and NKT cells, kills PDL1(+) tumor cells, and extends the

survival of tumor-bearing humanized mice. *Oncotarget* (2017) 8(35):57964–80. doi: 10.18632/oncotarget.19865
16. Ashizawa T, Iizuka A, Nonomura C, Kondou R, Maeda C, Miyata H, et al. Antitumor Effect of Programmed Death-1 (PD-1) Blockade in Humanized the NOG-MHC Double Knockout Mouse. *Clin Cancer Res* (2017) 23(1):149–58. doi: 10.1158/1078-0432.CCR-16-0122
17. Zhao Y, Shuen TWH, Toh TB, Chan XY, Liu M, Tan SY, et al. Development of a new patient-derived xenograft humanised mouse model to study human-specific tumour microenvironment and immunotherapy. *Gut* (2018) 67 (10):1845–54. doi: 10.1136/gutjnl-2017-315201
18. Wang M, Yao LC, Cheng M, Cai D, Martinek J, Pan CX, et al. Humanized mice in studying efficacy and mechanisms of PD-1-targeted cancer immunotherapy. *FASEB J* (2018) 32(3):1537–49. doi: 10.1096/fj.201700740R
19. Wunderlich M, Stockman C, Devarajan M, Ravishankar N, Sexton C, Kumar AR, et al. A xenograft model of macrophage activation syndrome amenable to anti-CD33 and anti-IL-6R treatment. *JCI Insight* (2016) 1(15):e88181. doi: 10.1172/jci.insight.88181
20. Topp MS, Kufer P, Gökbuget N, Goebeler M, Klinger M, Neumann S, et al. Targeted therapy with the T-cell-engaging antibody blinatumomab of chemotherapy-refractory minimal residual disease in B-lineage acute lymphoblastic leukemia patients results in high response rate and prolonged leukemia-free survival. *J Clin Oncol* (2011) 29(18):2493–8. doi: 10.1200/JCO.2010.32.7270
21. Curran E, Stock W. Taking a "BiTE out of ALL": blinatumomab approval for MRD-positive ALL. *Blood* (2019) 133(16):1715–9. doi: 10.1182/blood-2018-12-852376
22. Wunderlich M, Manning N, Sexton C, Sabulski A, Byerly L, O'Brien E, et al. Improved chemotherapy modeling with RAG-based immune deficient mice. *PloS One* (2019) 14(11):e0225532. doi: 10.1371/journal.pone.0225532
23. Frey N. Cytokine release syndrome: Who is at risk and how to treat. *Best Pract Res Clin Haematol* (2017) 30(4):336–40. doi: 10.1016/j.beha.2017.09.002
24. Barrett DM, Teachey DT, Grupp SA. Toxicity management for patients receiving novel T-cell engaging therapies. *Curr Opin Pediatr* (2014) 26 (1):43–9. doi: 10.1097/MOP.0000000000000043
25. Teachey DT, Rheingold SR, Maude SL, Zugmaier G, Barrett DM, Seif AE, et al. Cytokine release syndrome after blinatumomab treatment related to abnormal macrophage activation and ameliorated with cytokine-directed therapy. *Blood* (2013) 121(26):5154–7. doi: 10.1182/blood-2013-02-485623
26. Klinger M, Brandl C, Zugmaier G, Hijazi Y, Bargou RC, Topp MS, et al. Immunopharmacologic response of patients with B-lineage acute lymphoblastic leukemia to continuous infusion of T cell-engaging CD19/CD3-bispecific BiTE antibody blinatumomab. *Blood* (2012) 119(26):6226–33. doi: 10.1182/blood-2012-01-400515
27. Zugmaier G, Gökbuget N, Klinger M, Viardot A, Stelljes M, Neumann S, et al. Long-term survival and T-cell kinetics in relapsed/refractory ALL patients who achieved MRD response after blinatumomab treatment. *Blood* (2015) 126 (24):2578–84. doi: 10.1182/blood-2015-06-649111
28. Webster J, Luskin MR, Prince GT, DeZern AE, DeAngelo DJ, Levis MJ, et al. Blinatumomab in Combination with Immune Checkpoint Inhibitors of PD-1 and CTLA-4 in Adult Patients with Relapsed/Refractory (R/R) CD19 Positive B-Cell Acute Lymphoblastic Leukemia (ALL): Preliminary Results of a Phase I Study. *Blood* (2018) 132(Supplement 1):557–7. doi: 10.1182/blood-2018-99-111845
29. Messenheimer DJ, Jensen SM, Afentoulis ME, Wegmann KW, Feng Z, Friedman DJ, et al. Timing of PD-1 Blockade Is Critical to Effective Combination Immunotherapy with Anti-OX40. *Clin Cancer Res* (2017) 23 (20):6165–77. doi: 10.1158/1078-0432.CCR-16-2677

Conflict of Interest: The authors declare that the research was conducted in the absence of any commercial or financial relationships that could be construed as a potential conflict of interest.

Copyright © 2021 Wunderlich, Manning, Sexton, O'Brien, Byerly, Stillwell, Perentesis, Mulloy and Mizukawa. This is an open-access article distributed under the terms of the Creative Commons Attribution License (CC BY). The use, distribution or reproduction in other forums is permitted, provided the original author(s) and the copyright owner(s) are credited and that the original publication in this journal is cited, in accordance with accepted academic practice. No use, distribution or reproduction is permitted which does not comply with these terms.

frontiers in Immunology

REVIEW
published: 22 April 2021
doi: 10.3389/fimmu.2021.648580

Humanized Mouse Models for the Advancement of Innate Lymphoid Cell-Based Cancer Immunotherapies

*Nina B. Horowitz[1,2], Imran Mohammad[1], Uriel Y. Moreno-Nieves[1], Ievgen Koliesnik[1], Quan Tran[1] and John B. Sunwoo[1]**

[1] Department of Otolaryngology-Head and Neck Surgery, Stanford Cancer Institute and Institute for Stem Cell Biology and Regenerative Medicine, Stanford University School of Medicine, Stanford, CA, United States, [2] Department of Bioengineering, Stanford University School of Medicine and School of Engineering, Stanford, CA, United States

Innate lymphoid cells (ILCs) are a branch of the immune system that consists of diverse circulating and tissue-resident cells, which carry out functions including homeostasis and antitumor immunity. The development and behavior of human natural killer (NK) cells and other ILCs in the context of cancer is still incompletely understood. Since NK cells and Group 1 and 2 ILCs are known to be important for mediating antitumor immune responses, a clearer understanding of these processes is critical for improving cancer treatments and understanding tumor immunology as a whole. Unfortunately, there are some major differences in ILC differentiation and effector function pathways between humans and mice. To this end, mice bearing patient-derived xenografts or human cell line-derived tumors alongside human genes or human immune cells represent an excellent tool for studying these pathways *in vivo*. Recent advancements in humanized mice enable unparalleled insights into complex tumor-ILC interactions. In this review, we discuss ILC behavior in the context of cancer, the humanized mouse models that are most commonly employed in cancer research and their optimization for studying ILCs, current approaches to manipulating human ILCs for antitumor activity, and the relative utility of various mouse models for the development and assessment of these ILC-related immunotherapies.

Keywords: humanized mice, innate lymphocyte cells, natural killer cell, cancer immunotherapy, oncoimmunology, PDX models

OPEN ACCESS

Edited by:
Yasuyuki Saito, Kobe University, Japan

Reviewed by:
Dietmar Herndler-Brandstetter, University of Vienna, Austria
Paola Vacca, Bambino Gesù Children Hospital (IRCCS), Italy

***Correspondence:**
John B. Sunwoo
sunwoo@stanford.edu

Specialty section:
This article was submitted to Cancer Immunity and Immunotherapy, a section of the journal Frontiers in Immunology

Received: *31 December 2020*
Accepted: *11 March 2021*
Published: *22 April 2021*

Citation:
Horowitz NB, Mohammad I, Moreno-Nieves UY, Koliesnik I, Tran Q and Sunwoo JB (2021) Humanized Mouse Models for the Advancement of Innate Lymphoid Cell-Based Cancer Immunotherapies. Front. Immunol. 12:648580. doi: 10.3389/fimmu.2021.648580

INTRODUCTION

Natural killer (NK) cells are lymphocytes of the innate immune system capable of killing cancerous or precancerous cells as well as virally infected cells. NK cell functions are tightly regulated by the balance of signals from activating receptors and inhibitory receptors (1, 2). It was first observed in the 1970s that these "naturally occurring killer lymphocytes" can kill tumor cell lines without the need for prior sensitization (3, 4). Later studies in mice showed an increase in tumor growth and metastasis after NK cells were depleted genetically or therapeutically, supporting the crucial role of NK cells in cancer immunosurveillance (5, 6).

NK cells belong to a family of immune cells called innate lymphoid cells (ILCs) (7). The ILC family is a heterogeneous class of immune cells that are increasingly studied for their emerging roles

in cancer. ILC family members have differential effects on tumors; some ILC subgroups inhibit tumor growth while others promote it (8). Numerous studies have contributed to the understanding of mouse ILC biology (9). It is important to note, however, that there are species-specific markers and potential developmental differences between mouse and human ILC subsets (10–12).

Human ILCs, especially NK cells, have been leveraged to treat cancer through a variety of modalities including antibody-based therapies, cell-based therapies and bioengineered immunomodulatory therapies. While some of these therapies have shown remarkable success, especially with hematopoietic cancers, many are limited in their efficacy against solid tumors (13–15). This highlights the need for solid tumor mouse models that allow for more accurate studies of human ILCs and their related therapies.

Many murine models have been developed to study cancer development and treatment. While these mouse models are valuable tools, some have limitations due to species differences between mice and humans. In contrast to most human cells, mouse cells have a higher basal metabolic rate, shorter lifespan and active telomerase (16), all resulting in differential susceptibility to cancer between the two species. Xenograft models, in which cancer cell lines derived from patients are injected into immunodeficient mice, are often used for preclinical drug testing (17, 18). However, tumors produced by cell line xenograft models lack the heterogeneity and tumor microenvironment (TME) seen in human tumors.

Given the significant influence of the tumor microenvironment on immune cells, a better model is needed to study cancer immunology and immunotherapy. Patient-derived tumor xenograft (PDX) models preserve the genetic and cellular heterogeneity of the tumor, as well as some aspects of the tumor microenvironment (19). For this reason, PDX models are increasingly used in cancer research. Yet unfortunately, PDX models similarly lack crucial components of the human immune system such as circulating T and B cells. To study the biology and efficacy of cancer treatments, a more accurate recapitulation of both the TME and the human immune system is needed. To this end, humanized mouse models have been developed in which immunodeficient mice are reconstituted with representative subsets of human immune cells (20–22).

To study human ILCs and their role in cancer, humanized mouse models can serve as useful tools. In this review, we will discuss the role of ILCs in cancer, existing humanized mouse models that can be leveraged for more precise studies of ILCs, and therapeutics that employ ILCs against cancer along with mouse model considerations for accurate assessment of those therapies.

INNATE LYMPHOID CELLS

The origins of innate lymphoid cells (ILCs) in humans were elucidated from reconstitution of ILC groups in patients with hematopoietic stem cell transplantations (23) and in humanized mouse models engrafted with human CD34+ stem cells (24). Human ILCs are derived from Lin− CD34+ CD45RA+ CD117+ IL-1R1+ RORγt+ hematopoietic progenitors (25, 26) and represent a family of developmentally-related cells involved in immunity and in tissue development and homeostasis. ILC subgroups can remain circulating in the body or become tissue-resident (24). In 2013, Spits et al. proposed a classification for ILCs (27). According to this classification, these largely tissue-resident cells (28) are divided into three groups, based on similarities to adaptive T helper (Th) cell subsets. ILCs are distinguished by the reliance on transcription factors that dictate their development and maintenance and by their ability to produce signature Th cytokines mirroring those of the Th cell subsets (27). This section provides an overview of the different human and murine ILC lineages and their complex roles in cancer; following sections will elaborate on the humanized mouse models available to study ILC-based immunotherapies and drugs that influence ILC activation directly or indirectly.

Group 1 ILCs

Group 1 ILCs are characterized by their capacity to produce IFN-γ and their dependence on transcription factor T-BET (27, 29). Group I ILCs include conventional NK cells and subsets of innate lymphocytes, termed ILC1s, which differ from NK cells in their phenotypes, locations, functions, or transcription factor dependence (30). One important difference between both human and murine NK cells and ILC1s is that NK cells express the transcription factor Eomesodermin (EOMES), which is important for their differentiation and function (27, 29, 31).

In contrast to ILC1s, which are mainly tissue-resident cells, NK cells are found in both peripheral blood and tissues (30). Human peripheral blood NK cells were originally divided into two subsets, $CD56^{bright}$ and $CD56^{dim}$ NK cells. More recently, additional distinct populations of tissue-resident NK cells have been described in human and murine tissues such as the gut, kidney, and liver, each displaying tissue-specific phenotypes and functions (32–35). Some NK cells in mice and humans express Fc receptors, which are functional surface molecules that bind to the conserved regions of antibodies and can induce killing of antibody-coated target cells (36).

The phenotypes and functions of ILC1s depend on the tissue microenvironment, and ILCs with a mixed NK cell and ILC1 phenotype have been observed in humans (29, 30, 37). For instance, human intra-epithelial ILC1 (ieILC1) cells possess features shared by conventional NK cells and helper ILC1; they produce IFN-γ and express both transcription factors EOMES and T-BET (30). Both NK cells and ILC1s represent a first line of defense for humans and mice against infections with viruses and certain bacteria, and are essential for the clearance of intracellular microbial infections (38–40). NK cells appear to be more potent in mediating cytotoxicity, while the primary role of ILC1s is the production of pro-inflammatory cytokines (30, 40).

Group 2 ILCs

Human and murine ILC2s require the transcription factor GATA-binding protein 3 (GATA-3) for their differentiation and maintenance, similar to Th2 cells, and produce cytokines such as IL-5 and IL-13 in response to activation by IL-25 and IL-33 (27, 41, 42). Human ILC2s express CRTH2 and high levels of CD161, whereas most mouse ILC2s express ST2 (29). ILC2s in both mice and humans are important in the immune defense against helminth infections and in the pathogenesis of asthma (41, 43–45).

Group 3 ILCs

Group 3 ILC3s in humans and mice produce IL-17 and IL-22, similarly to Th17 cells, and are dependent on the transcription factor retinoic acid receptor-related orphan receptor-γt (RORγt; encoded by *RORC*) for their development and function (27). Group 3 ILCs are abundant at mucosal sites and are involved in immune responses to extracellular bacteria and the containment of intestinal commensals. Human ILC3s produce IL-22, by which they promote intestinal homeostasis (46). Both human and mouse ILC3s can also produce granulocyte–macrophage colony-stimulating factor (GM-CSF) (7). Two subsets of ILC3s can be distinguished on the basis of cell surface expression of NKp44 (also known as NCR2) in humans and NKp46 (also known as NCR1) in mice, termed NCR+ or NCR- (41).

ILCs and Cancer

As the scientific community continues to unravel the biology of ILCs in cancer, many studies have investigated the efficacy of targeting or employing ILCs as a cancer therapy. Among ILC1s, NK cells are heavily studied for their potential in cancer immunotherapy (47). However, the role of ILCs in tumor immunity is yet to be fully elucidated. ILCs are enriched in many human cancers (48, 49) and there is increasing evidence showing that they exhibit phenotypic and functional plasticity. For instance, after TGF-β exposure, both murine and human NK cells can convert to an ILC1-like phenotype (50–52). ILC lineage plasticity has also been observed; human ILC2s can convert to an ILC3 phenotype with IL-1β, IL-23, and TGF-β stimulation (53). Additionally, Gury-BenAri et al. found that upon perturbation of the mouse microbiome by administration of broad spectrum antibiotics, the transcriptional profiles of mouse intestinal ILC1s and ILC2s became more similar to that of ILC3s (54). ILC plasticity has potential consequences on tumor growth and behavior. For example, a decrease in mouse ILC1s and transdifferentiation within ILC2 subtypes correlated with colorectal cancer progression (55, 56).

Recent investigations into the complex biology of ILCs have revealed the strong influence of the tumor microenvironment (TME) on ILC responses (57). For example, human tumor cells under stressful TME conditions upregulate MICA, MICB, and ULBP1-6, which are ligands for the NK activating receptor NKG2D (58). Chronic engagement of NKG2D can result in NK cell tolerance (59). Furthermore, the TME can adopt an immunosuppressive environment by exploiting cytotoxic T lymphocyte associated protein 4 (CTLA-4), programmed cell death protein 1 (PD-1), and other immune cell reprogramming pathways (60). These pathways are further discussed in the ILC Immunotherapeutics section.

The hypoxic, immunosuppressive milieu of the TME has been shown to cause immune cell dysfunction, leading to treatment failure (61, 62). Certain cytokines within the TME can also prevent antitumor activity by ILCs. IL-33, a cytokine that activates ILC2s, has been shown to be pro-tumorigenic in humans and mice by promoting tumor growth, metastasis, and angiogenesis (63, 64). Its presence in the TME causes ILC2s to produce IL-13, which recruits myeloid-derived suppressor cells (MDSCs) to induce tumor tolerance (65, 66). Similarly, IL-23 can induce ILC3s to express immunosuppressive IL-17 and IL-22 in colon cancer models (67). It is critical to account for the role of the TME when studying the effects of ILCs and ILC treatments on cancer, and strategies to target and specifically block these inhibitory pathways may represent potential new immunotherapies.

HUMANIZED MOUSE MODELS

Mouse Models for Improved Human Immune System Engraftment

Humanized mice were originally defined as mice bearing functional human genes, cells, or tissues. In more recent years, the term humanized mice has generally been used for genetically modified immunodeficient mice that are permissive to the development of human immune cells (**Figure 1** and **Table 1**). In this review, we briefly discuss immunocompetent mice carrying functional human genes, but our primary focus is on immunodeficient mice bearing human immune cells, as these are significantly more useful for cancer immunotherapy research. Early humanized mouse models were generated by transferring human peripheral blood mononuclear cells (PBMCs), hematopoietic stem and progenitor cells (HSPCs), or fetal hematopoietic tissues into the severe combined immunodeficient mouse strain, CB17-*scid* (75–77). CB17-*scid* mice are deficient in the *Prkdc* gene, which encodes the catalytic subunit of the DNA-dependent protein kinase. The *Prkdc* gene product is crucial for V(D)J recombination to generate functional T and B cells. The absence of T and B cells in *Prkdc*-deficient mice promotes host acceptance of xenografts. However, CB17-*scid* mice have NK cells and other innate immune cells that can restrict efficient engraftment of human immune cells.

The development of a non-obese diabetic-*scid* (NOD-*scid*) mouse model led to increased human immune cell engraftment levels, compared to CB17-*scid* mice (78). Later, it was reported that the better engraftment in NOD-*scid* vs. CB17-*scid* is due a polymorphism in the signal-regulatory protein α (*SIRPa*) gene (79, 80). The polymorphism allows for engagement of SIRPα on mouse myeloid cells to CD47 on human cells. This gives the "do not eat me" signal and inhibits phagocytosis of human cells by mouse myeloid cells. Thus, in NOD-*scid* mice, the SIRPα polymorphism supported better development of human

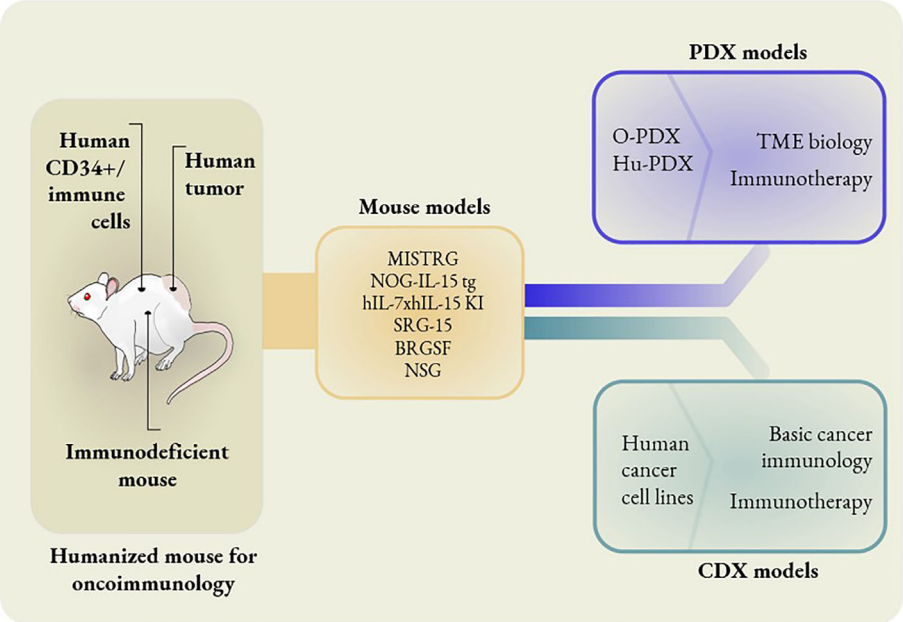

FIGURE 1 | Different mouse models to study oncoimmunology. In knock-in models, mouse genes are replaced with human counterparts. MISTRG mice have human genes replaced that encode M-CSF, IL-3, GM-CSF, TPO and SIRPα. NOG-IL-15 tg mice have human IL-15 transgene expression. hIL-7xhIL-15 double knock-in mice express human IL-7 and IL-15. SRG-15 mice have the mouse IL-15 gene replaced with the human IL-15 gene. BRGSF mice are Flt3-deficient mice in a BRGS background with exogenous administration of human Flt3L. The O-PDX model consists of orthotopic patient-derived xenografts placed in MISTRG mice. The Hu-PDX mouse model consists of patient-derived xenografts placed in NSG mice with reconstituted human immune systems. Human cancer cell lines can be used in place of PDX in basic cancer immunology and immunotherapy studies. However, PDX models are ideal for the studies of TME biology and certain immunotherapies, e.g. combination immunotherapies.

hematopoiesis (79). However, the residual activity of NK cells and other innate cells in the NOD-*scid* mice prevented optimal engraftment of human cells. This was overcome with the usage of mice with germline mutations in the interleukin 2 receptor subunit gamma (*Il2rg*) gene, which encodes a receptor component called the common gamma chain. This mouse strain, termed NOD-*scid* Il2rg$^{-/-}$ (NSG), is hospitable to transplanted human immune cells because the host mice completely lack NK cells (81).

Humanized Knock-in Models to Study Cancer

Mouse strains harboring human gene knock-ins have also been developed to allow for the robust development of human immune cells in the mouse microenvironment. As previously described, the NOD-*scid* mouse strain contains a polymorphism in SIRPα, which reduces phagocytosis of engrafted human cells. With this knowledge, researchers attempted to improve the engraftment of human cells with

TABLE 1 | Humanized mice to study ILC-cancer interactions.

Mouse Model	Human Tumor Cells Administered	Human Cells Engrafted	Human Lineage Reconstitution (*lineages with improved reconstitution compared to NSG mice)	References
MISTRG	Me275 melanoma cells	CD34+ HSPCs	*monocytes, *macrophages, *DCs, T, B and *NK cells	(21)
SRG-15	Raji tumor cells and K562 tumor cells	CD34+ HSPCs	myeloid cells, *T, B *NK cells and *ILCs	(68)
NOG-IL-15 Tg	NCI-N87 human gastric cancer cell	Peripheral blood NK cells and *in vitro*-expanded NK cells	*NK cells	(69)
hIL-7xhIL-15 KI	-	CD34+ HSPCs	T and *NK cells	(70)
BRGSF	-	CD34+ HSPCs	*myeloid cells, T, B, DC, *NK cells and *ILCs	(71)
O-PDX (MISTRG)	Neuroblastoma	CD34+ HSPCs	*NK cells	(72)
Hu-PDX (NSG)	Lung adenocarcinoma	CD34+ HSPCs	T, B and NK cells	(73)
HTM (NSG)	Breast cancer	CD34+ HSPCs	T, B, NK cells and macrophages	(74)

transgenic expression of human SIRPα in the mice (82). Continued genetic manipulations of mouse strains led to an advanced mouse model called MISTRG which exhibits enhanced engraftment of human immune cells by replacing several mouse cytokines genes with corresponding human genes (21). In the MISTRG strain, mouse genes are replaced with human genes encoding M-CSF, IL-3, GM-CSF, thrombopoietin and SIRPα. These cytokines support the survival of myeloid and lymphoid cells in mouse peripheral blood and tissues.

IL-15 is an essential cytokine for the development and differentiation of NK cells. Human NK cells show poor engraftment or impaired development in mice, as mouse IL-15 is not sufficient for the development of fully functional human NK cells (83, 84). Although there is no expression of human IL-15 by mouse cells in MISTRG mice, the engrafted human monocytes and macrophages produce human IL-15 to support the endogenous development of human NK cells. Rongvaux et al. used the MISTRG mouse model for the *in vivo* investigation of NK cell activity against melanoma tumor xenografts (21).

Because of the importance of IL-15 in NK cell development and survival, routine injections of recombinant human IL-15 have also been used to promote survival of human NK cells after adoptive transfer (85). In one study, researchers differentiated NK cells *in vitro* from CD34+ HSPCs obtained from human cord blood. With subcutaneous injections of recombinant human IL-15 every 48 hours, they then demonstrated that adoptive transfer of human NK cells can control the growth of ovarian cancer xenografts in NSG mice and promote survival of the mice (85). However, recombinant human IL-15 is expensive and routine injections every 2-3 days can be laborious. Consequently, transgenic and knock-in mice expressing human IL-15 have been developed such as NOG-IL-15 Tg, hIL-7xhIL-15 KI NSG mice, and SRG-15 mice (68, 70).

The NOG-IL-15 Tg mouse model is generated from the NOD/Shi-*scid*-IL-2Rγ^{null} mouse background with the addition of human IL-15 transgene expression (69). This enables long term maintenance of transferred human NK cells isolated from peripheral blood. Using this model, Katano et al. showed that the transfer of *in vitro*-cultured NK cells in the presence of anti-Her2 antibody can suppress Her2-positive gastric cancer (69). To refine the murine host for human NK cell development *in vivo*, double gene knock-in of human IL-7 and IL-15 was done in NSG mice, which were termed hIL-7xhIL-15 KI NSG mice (70). These IL-15 producing mice are useful tools for the assessment of tumor models and combination immunotherapies involving NK cells.

A particularly attractive HIS model is called SRG-15 and involves two human gene replacements to encode human IL-15 and SIRPα. Upon injection of human CD34+ HSPCs, the SRG-15 mice can develop human T cells, B cells, NK cells and myeloid cells. Importantly, the SRG-15 mouse model allows for study of human tissue-resident immune cells, including the development of tissue-resident CD8+ T cells (IELs) and tissue-resident ILC subsets (68). The secretion of human IL-15 from mouse stromal and epithelial cells in the SRG-15 mice was sufficient to produce functional human NK cells following CD34+ HSPC engraftment (68). Furthermore, the NK cells from the reconstituted human immune system in SRG-15 mice (following CD34+ HSPC engraftment) were shown to successfully hinder CD20+ Raji tumor growth with co-administration of rituximab (68). This demonstrates that the SRG-15 mice model can be used to establish and evaluate novel combination therapy protocols.

Di Santo et al. developed another HIS mouse model to study human ILC, called Flt3-deficient BALB/c *Rag2*$^{-/-}$*Il2rg*$^{-/-}$*Sirpa*^{NOD} (BRGSF). Flt3, the FMS-related tyrosine kinase 3, is a cytokine crucial for dendritic cell (DC) homeostasis. In mice lacking Flt3, the endogenous mouse DCs will no longer compete with CD34+ HSPC derived human DCs for Flt3 ligand (Flt3L) signaling. Upon exogenous administration of Flt3L, the expanded human DCs in this mouse strain provide the cytokine environment for the development of NK cells and other ILCs (71). Specifically, the researchers engrafted human CD34+ HSPCs in BRGSF mice and were able to isolate phenotypically and functionally mature human NK cells and other ILC subsets (71).

Notably, out of the many HIS mouse models described in this section, the endogenous development of human NK cells from CD34+ HSPC has only been shown in hIL-7xhIL-15 KI NSG, MISTRG, SRG-15, and BRGSF mice. This is important to consider when selecting a humanized mouse model for the study of any immunotherapy that may rely on modulation of NK cell or ILC behavior, or the survival of adoptively transferred NK cells or ILCs. In conclusion, the mouse models discussed here serve as useful tools for the study of NK cell development and cytotoxicity, and some can even be used to study the development and behavior of other ILC subsets.

Cancer Cell Line Derived Xenograft (CDX) Models for ILC Studies

In cancer cell line derived xenograft (CDX) models, established human cancer cell lines are subcutaneously transplanted into mice to form tumors. During the injection, tumor cells can be mixed with effector cells such as NK cells to evaluate the impact of the human immune cells on tumors *in vivo*. Alternatively, instead of co-injection of effector immune cells and tumor cells, effector cells can be injected after successful engraftment of tumor cells. One such study demonstrated the effective elimination of B-cell Non-Hodgkin lymphoma tumors with anti-CD20 chimeric antigen receptor (CAR) NK cells. To establish the CDX, Raji-Luc cells, a human Non-Hodgkin lymphoma cell line expressing luciferase, were injected into NSG mice and allowed to grow for several weeks. NK cells were expanded from peripheral blood NK cells, engineered to express the anti-CD20 CAR construct, and injected into the NSG mice bearing Raji-Luc cell line xenografts. Treatment with anti-CD20 CAR NK cells showed significant reduction in tumor size, as demonstrated by the decrease in luciferase signal from the tumors. The study also demonstrated that CAR NK cells could inhibit dissemination of the tumor into other organs (86). Cany et al. established an acute myeloid leukemia (AML) xenograft model by injecting GFP and luciferase expressing K562 leukemia cells (K562.LucGFP) intrafemorally in NSG mice. They showed

that NK cells, derived from umbilical cord blood, could target the leukemia cells residing in the bone marrow (87).

Cancer cell lines are advantageous for their ease in genetic manipulations and for establishing early proof of concept studies, but continuous passage of cell lines in 2D culture could result in the loss of epithelial to mesenchymal transition (EMT) potential (88). The tumors generated from cell lines also fail to reflect tumor vascularization and tumor microenvironment observed in human cancers (89). Fortunately, patient-derived xenograft models can overcome some of these drawbacks (90).

PDX Humanized Models to Study ILCs

Patient-derived tumor xenografts are becoming an increasingly popular tool to dissect the intrinsic properties of cancer initiating cells and the interaction between tumor and immune cells *in vivo* (91). Cancers are heterogenous mixtures of cells containing malignant cells, nonmalignant stromal cells, vascular endothelial cells and immune cells. Initial cancer drug development studies did not consider the involvement of the immune system, as most of the studies were performed in immunodeficient mice with tumor explants (92). The emerging improved PDX models involve the transplantation of both tumor explants from patients and human immune cells to establish a human immune system in the mouse host.

Several studies have attempted co-transplantation of human HSPCs and tumors in mice. One such model is orthotopic patient-derived xenograft (O-PDX) for neuroblastoma, in which MISTRG mice undergo double transplantation of CD34 + HSPCs and neuroblastoma xenografts. This allows for long-term hematopoiesis and PDX engraftment simultaneously (72). The NK cells in this model exhibit antibody-dependent cell-mediated cytotoxicity (ADCC), which shows potential for preclinical testing of different monoclonal antibodies in neuroblastoma (72). In a separate study, Meraz et al. also co-transplanted cord blood derived CD34+ HSPCs and lung cancer PDX to form a NSG mouse model with a humanized immune system and PDX, which they named Hu-PDX (73). The reconstituted humanized immune system showed an antitumor response of T cells but not NK cells after administration of the checkpoint inhibitor antibody pembrolizumab (73). Thus, such a model can be used for studying immune responses to cancer and developing immunotherapy treatments against cancer.

Another category of PDX models are immunoavatar cancer models, which are highly suited for preclinical trials of immunotherapy and can also be used to develop personalized treatment strategies. In this model, human immune cells (such as PBMCs) and tumor tissue (e.g. melanoma) are taken from the same patients or individuals in autologous fashion. This model more accurately recapitulates the unique immune responses against tumors originally occurring in the patient, as they are from the same source of origin (93, 94). One issue with this model, however, is that it suffers from GVHD responses in which human T cells from the engrafted PBMCs mount immune responses against mouse cells after several weeks (92, 94).

Overall, these mouse models aid in proof-of-concept studies to better understand immune cell interactions with tumors *in vivo*. Engrafted PDX tissues demonstrate pathohistological and genetic resemblance to the original tumor, in addition to preserving parental solid tumor architecture (95). These properties make them an attractive model for personalized therapy testing, pre-clinical drug screening and basic cancer research (96).

Limitations of Humanized Mouse Models for Cancer Research

Although humanized mouse models act as excellent models to study solid tumors, there are a few shortcomings that still need to be addressed. Many PDX transplant methods are subcutaneous, even if the original tumor was not located in that type of tissue. As a result, the environment around the tumor lacks organ-specific factors and the chronic inflammatory milieu. Developing solid tumors in the abdomen or by orthotopic transplantation into organs can also make it challenging to measure tumor size or assess tumor growth *via in vivo* imaging analysis. A potential utility of humanized cancer models is to interrogate simultaneous development of immune cells and cancer cells *in vivo*. Yet even though tumor cells and HSPCs can be co-transplanted intrahepatically into newborn humanized mice at same time, the development of the tumor sometimes precedes the reconstitution of multilineage human immune cells (74).

Mice bearing PDX could be a useful tool to dissect the role of human ILCs in cancer. However, these studies must reconcile the differences between mouse and human biology. While the original human cancer cells survive and proliferate within a PDX, over time the human stromal cells within the tumor are replaced by mouse stromal cells; this can affect the maintenance and behavior of tumor-infiltrating human immune cells (97). Hence, humanized mouse models reconstituted with multiple human immune cell lineages and engrafted with tumors are being developed to facilitate their application in designing better immunotherapy strategies.

ILC IMMUNOTHERAPEUTICS STUDIES IN MURINE HOSTS

Mouse Model Development and Considerations for Antibody-Based Therapies

Antibody-based immunotherapies are less expensive than cell-based therapies and represent a promising area to explore as combination therapeutics, since they can be administered alongside another therapeutic agent that stimulates the adaptive or innate immune system for a synergistic effect (98). A treatment that activated both ILCs and adaptive immune cells in a safe and specific manner could potentially avoid the possibility of antigen escape, be more likely to succeed in controlling metastases, and induce a systemic immune response and immune memory. However, these treatments are difficult to study in immunocompetent mice as most clinically relevant antibodies are highly specific for their human targets and thus do not exhibit cross-reactivity to their murine

counterparts (99). For these reasons, researchers use humanized mice as a more accurate tool to study complex immune responses during antibody treatments. Antibodies being studied for their ability to modulate NK cell and ILC behavior include checkpoint inhibitors, Bispecific Killer cell Engagers (BiKEs), Trispecific Killer cell Engagers (TriKEs), NK Cell Engagers (NKCEs), and other novel recombinant antibodies such as drug-conjugated antibodies (**Figure 2**).

Checkpoint inhibitors block an inhibitory ligand on a tumor cell or the cognate receptor on a tumor-targeting immune cell to prevent the inhibitory signal from impacting the immune cell (100). Checkpoint molecules such as PD-1 and CTLA-4 can modulate the functionality of both adaptive and innate immune cells (101). For example, secretion of cytokines such as IL-5 and IL-13 by human ILC2s (102) or degranulation and secretion of IFN-γ by human NK cells (103) can be inhibited. NK cells express inhibitory receptors that recognize MHC class I molecules (KIRs in humans and Ly49s in mice). Human NK cells also express CD94/NKG2A, PD-1, TIM3, TIGIT, and LAG3 in certain contexts (104, 105). Other human ILCs also express inhibitory receptors in both normal and pathological conditions (106). ILC1s express TIM-3, LAG-3, CD96, and TIGIT; ILC2s express PD-1 and KLRG1; and ILC3s express TIGIT and CD96 (65). Blockade of these pathways *in vivo* can result in the reactivation of NK cells and ILCs, which may generate a strong antitumor response (105). Human inhibitory receptors such as KIRs are difficult to study in immunocompetent mouse models, since they diverge structurally between human and mouse NK cells and do not exhibit cross-reactivity - murine Ly49s would not bind to human MHC and human KIRs would not bind to murine MHC (107). As a result, early work surrounding NK/ILC checkpoint inhibitors relied on the use of immunodeficient mice with transplanted human tumor cells and single human immune cell types - a time consuming and limited approach.

A major advance towards targeting immune checkpoints was the generation of humanized CTLA-4 or PD-1 knock-in mouse models. Murine cells are modified to express the human form of the protein of interest under the same genetic regulation as its murine counterpart; the mice retain an intact functional murine immune system with the exception of the single altered protein and intracellular signaling through these molecules is largely preserved (108, 109). These models recapitulate immune modulation by tumor cells because human CTLA-4 is capable of interacting with mouse B7-1 and B7-2 (108) and human PD-1 is capable of interacting with mouse PD-L1 (110). Since human PD-1 interacts in subtly different ways with human PD-L1 compared to murine PD-L1 (111), a further improvement to the accuracy of these models is a mouse that expresses both human PD-1 and human PD-L1.

These mice are not considered human immune system (HIS) mice as they do not possess human immune cells, but they represent a robust model system that can be utilized to validate the binding and antitumor efficacy of antibodies against individual human checkpoint molecules. Mice expressing

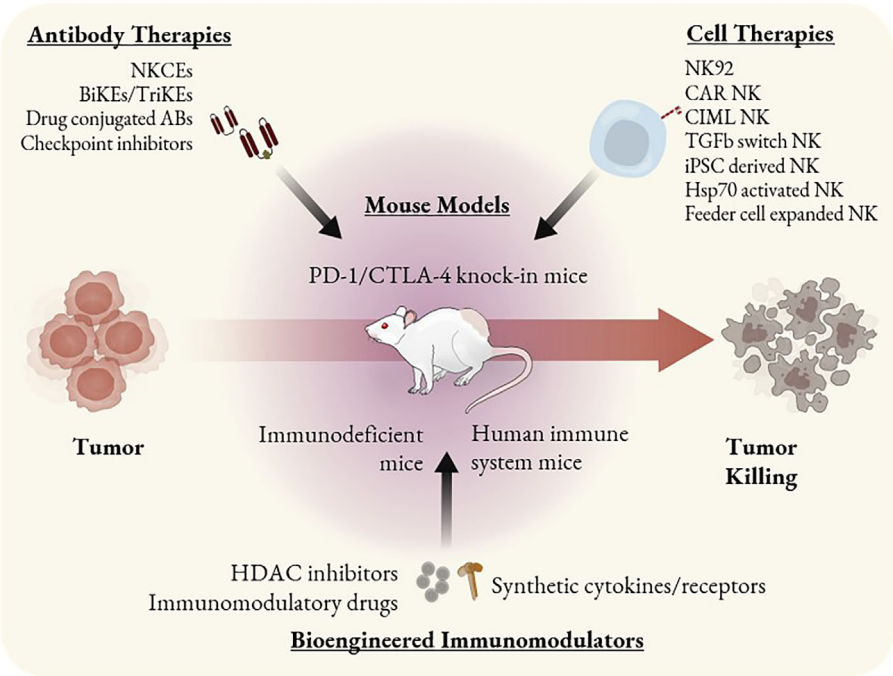

FIGURE 2 | ILC based immunotherapeutics and mouse models as tools to study them. Immunotherapies that involve ILC antitumor activity can be categorized as antibody-based, cell-based, or other bioengineered immunomodulators. Mouse models such as PD-1 and CTLA-4 knock-in can be used to study checkpoint inhibitors. SCID mice bearing PDX or CDX can be used to study the efficacy of single agent cell therapies such as CAR NK cells or NK92 cells. HIS mice are the most optimal tool to study combination therapies or immunomodulators that may alter the behavior of multiple immune cell types.

human CTLA-4 and dual humanized mice expressing human PD-1 and CTLA-4 or both human PD-L1 and PD-1 without expression of murine PD-L1 or PD-1 are now commercially available (112). Knock-in models are a useful tool for studying direct and secondary effects of targeted antibody therapies on tumor growth *in vivo*, minimizing off-target toxicities, and optimizing antibody binding kinetics to decrease the frequency of severe immunotherapy-related adverse events.

To study the effects of checkpoint inhibitors on human immune cells, immunodeficient mice are required. Marasco et al. used NSG mice with transplanted human T and NK cells to study the efficacy of CAR T cells that secrete anti-PD-L1 antibodies, so they could observe the effects of the antibodies on NK cells alongside T cells and tumor cells (113). However, NSG mice are not optimized to ensure NK cell engraftment. Models such as the MISTRG, SRG-15, and NOG-IL-15 Tg mice will further enable longer-term study of NK cell responses to antibody therapies as they can provide a constant cytokine signal to ensure NK cell survival (69). Future research using humanized mice should include the screening and optimization of a wide variety of Fc regions, receptor targets, and drug conjugates to strongly induce ILCs to kill tumor cells.

In addition to checkpoint inhibitors, other antibodies are in development that directly activate NK cells. BiKEs induce NK cell killing by binding to CD16 on the surface of NK cells and a tumor antigen simultaneously, while TriKEs target CD16, a tumor antigen, and an IL-15 molecule to activate the NK cells (114). By binding to CD16 and colocalizing tumor cells with NK cells, the antibodies trigger ADCC pathways and induce target cell killing. These antibodies show promise *in vitro* and *in vivo*, but most clinical research has been restricted to hematologic malignancies (115). To study the antibodies in mice, researchers have used xenogenic models such as NSG mice injected with human ovarian cancer cells and NK cells (116). Another novel NK cell stimulating antibody is a trifunctional NKCE that binds to NKp46 and CD16 on NK cells and a tumor antigen on target cells. Anti-CD20 NKCEs targeting NKp46 exhibited strong efficacy against solid tumors and intravenously injected Raji B cells in SCID mice (117). Drug-conjugated antibodies can also be used for immunotherapy, such as brentuximab vedotin which contains a microtubule depolymerizing agent and a variable fragment targeting CD30 on tumor cells (118). Microtubule inhibitors have cytotoxic effects on cancer cells and also induce maturation in some innate immune cells; these drug-conjugated antibodies were first tested for *in vivo* efficacy in SCID mouse xenograft models (119).

While antibody therapies have proven to be successful in clinical trials and data shows they are able to improve the activity of NK cells that enter a tumor, antibodies are unable to directly increase recruitment of immune cells to the tumor (105). Rather, they rely on activation of tumor infiltrating immune cells to generate chemotactic signals that will recruit and activate additional immune cells (120). However, this strategy is not always successful, as the immunosuppressive TME is capable of dampening the activation induced by the antibodies and preventing a strong immune response (121). Much more work needs to be done in order to improve the homing of ILCs to tumors and their activation within the TME, and mice with human immune systems are a necessary tool for these studies.

NSG or SCID mice transplanted with NK cells are sufficient to test the direct activation of NK cells by antibodies and the resulting tumor cell killing. However, they do not enable researchers to study whether these NK cells could induce the activation or recruitment of other tumor-resident or circulating immune cells through cytokine secretion or other mechanisms. This is because they do not contain diverse human immune cell subsets and therefore do not accurately represent the immune milieu present in a human tumor. For a more thorough assessment of broad immune activation after administration of these recombinant antibodies, HIS mice optimized for NK/ILC survival and proliferation would be required.

ILC-Based Cell Therapies and Mouse Model Considerations

Adoptive cell therapies for cancer, while at first dominated by adaptive immune cells, are beginning to show promise using NK cells. Unfortunately, it is difficult to accurately model the long term influence of adoptive cell therapies on tumor progression in immunodeficient mice. Many ILCs require cytokine stimulation to survive in the absence of other immune cells, and administering those cytokines frequently can be costly and time consuming (70). For example, NK cells will survive and proliferate in NOD Rag gamma (NRG) immunodeficient mice without exogenous cytokine administration only if the mice are also transplanted with autologous human cord blood immune cells (122). Additionally, tumors grown in immunodeficient mice lack human intratumoral immune cells. Thus, it is impossible to determine whether adoptively transferred cells will activate other innate or adaptive immune cells in the TME - a critical factor for developing a systemic immune response and immune memory (34). Many cell therapies are also difficult to test in a precise manner using the murine immune system because their human cell homologs are different in ways that range from subtle to potentially significant, or artificial receptors such as CARs must be modified to function within murine signaling pathways.

The most ideal models to study the potential success or failure of adoptively transferred ILCs are humanized mice that have been optimized to ensure the survival and expansion of ILCs in the murine host, such as NOG-IL-15 Tg mice with transplanted human PBMCs or MISTRG, SRG-15, or BRGSF mice reconstituted with CD34+ stem cells. These transplant models enable long term studies of cell survival, differentiation, and proliferation without the added cost of cytokine injections or the need to engineer cells to produce their own cytokines (70). They also enable researchers to study a broad range of ILCs in parallel in the context of their therapy, as multiple populations can be induced from a single injection of fetal pluripotent stem cells rather than having to transplant them individually. For example, Ishikawa et al. used IL-6 knock-in mice engrafted with human CD34+ stem cells to study the effects of IL-6 on co-activation of macrophages and T cells (123). However, it is worth noting that

mouse models endogenously expressing human cytokines can contain supra-physiological concentrations of those cytokines, which may alter the results of the studies and make results more complex to interpret (124).

ILC-based cell therapies currently in development rely on phenotypically modulated NK cells and ILCs, CAR NK cells, or NK cell lines (**Figure 2**). Phenotypic modulation of these cells is possible because NK cells and ILCs respond to cytokines, growth factors, pathogens, and other external stimuli in varied manners, and this can be exploited to enhance the efficacy of cell therapies or enable production of clinically relevant doses of cells. For example, briefly activating NK cells with IL-12, IL-15, and IL-18 can improve their long-term cytotoxicity. These cells, known as cytokine-induced memory-like (CIML) NK cells, exhibit increased proliferation, persistence, memory-like functionality, and IFN-γ production (125, 126) and show increased cytotoxicity towards many cancer cell types including ovarian cancer cells, leukemia cell lines, and primary human AML blasts (127, 128).

Cytokine-induced phenotype modulation can also be leveraged alongside growth factors to differentiate NK cells from induced pluripotent stem cells (iPSCs) (129). iPSC-derived NK cells are capable of ADCC, and CAR NK cells from this source are currently in preclinical or phase I/II testing (130). However, since there are large numbers of developmental pathways involved in these pipelines, it is difficult to perfectly replicate them using murine cells. It is equally difficult to study the interactions of human iPSC-derived NK cells with other immune cells accurately in immunodeficient mice. HIS mice enable more rigorous studies of the effects of adoptive cell therapies on other immune subsets.

Several unique subsets of NK cells are also of great interest for cancer therapies. These include NK cells, which lack expression of the intracellular signaling protein FcεRγ, called gNK cells. gNK cells appear to be induced by CMV infection (131) and exhibit increased ADCC function; they are being studied for their ability to enhance antibody therapies in B cell leukemia and lymphoma (132). Researchers are also developing methods for *ex vivo* NK cell activation to improve cell therapies. These strategies include culture with heat shock protein 70 (Hsp70), TKD peptide, and IL-2, which has been studied using both murine and human NK cells (133), and co-culture with feeder cells such as K562 that can be altered to express stimulatory molecules such as OX40 ligand (134) or IL-21 (135).

The most striking successes of ILC-based cell immunotherapies have involved CAR NK cells. CAR NK cells target surface molecules on tumor cells and exhibit a more favorable safety profile than CAR T cells (136). An anti-CD19 CAR NK cell that produces IL-15 achieved a 73% response rate in HLA mismatched patients with non-Hodgkin's lymphoma or chronic lymphocytic leukemia. These cord blood derived CAR NK cells could show promise as a standardizable off-the-shelf therapeutic (137). Additional CAR NK cell therapies currently in clinical trials include cells targeting mesothelin, CD22, PSMA, and NKG2D ligands on tumor cells, and others currently in development include variations in cytokine production, intracellular signaling domains, and costimulatory molecules (138). CAR NK cells producing IL-15 were tested for early *in vivo* efficacy in a Raji lymphoma NSG xenograft model (138), but this model did not enable researchers to assess whether other immune cells were activated by the CAR NK cells. Another type of CAR used with NK cells is a TGF-β chimeric switch receptor which uses TGF-β to activate, rather than inhibit, NK cells in the TME (139). This receptor was studied in NSG mice with transplanted neuroblastoma cells, CAR NK cells, and intraperitoneal administration of IL-2. Future work should incorporate HIS mice to determine whether CAR NKs/ILCs can activate other immune subsets circulating in the bloodstream or residing within the TME.

NK cell lines are another area of interest for cell therapies. NK92 is an immortal cell line that was isolated from a patient with a rare NK cell lymphoma (140). CAR NK92 cells represent a potential cell therapeutic that is simple to standardize and produce in bulk. NK92s were assessed against malignant melanoma in SCID mice and showed significant potential (141). The first in human trial involving irradiated NK92 cells used anti-CD33 CAR NK92s for patients with relapsed and refractory acute myeloid leukemia, and no significant adverse events were observed (142). However, it is not yet clear whether these cells will function well against solid tumors. Due to the short lifetime of irradiated cells, it also remains to be seen whether they are capable of initiating an antitumor response that could generate long-term immunological memory. This is difficult to model in mice without humanized immune systems, since the effect of the irradiated cells on tumor size or survival might be brief or insignificant but their impact on other immune cells could be what drives tumor eradication.

Non-irradiated NK92 cells could be given to patients if they were transduced with suicide genes to ensure they could be killed if they began proliferating too rapidly (143). Researchers are studying non-irradiated Smad3-silenced NK92 cells (NK-92-S3KD) in xenograft mouse models to assess their efficacy against hepatoma and melanoma (144). Other cell lines that mimic human NK/ILC1 behavior include NK101 (145), NK3.3, YTS, and NKL (146). However, it will be difficult to assess their efficacy against solid tumors without a robust *in vivo* model that includes other immune cells due to the drastic impacts of the TME on suppression of immune cytotoxicity and the highly interactive nature of cell therapies when considering tumor-resident immune cells. Complex tumor-immune and immune-immune interactions are difficult to model using immunodeficient mice, but are critical in predicting the success or failure of cell therapies. For these reasons, HIS mice represent a more optimal tool for studying NK cell therapy *in vivo*.

DISCUSSION: BIOENGINEERED IMMUNOMODULATORS AND TARGETED DRUG DELIVERY AS NEW FRONTIERS

Modeling potential therapeutics using standard immunodeficient mice with one or two transplanted human

immune cell types is not a sufficiently rigorous approach. These mice inhibit the ability of researchers to broadly identify indirect effects of their drugs on other immune cells as a result of the primary effects on their target cell of interest, and tumors grown in them from cell lines or transplanted tissue do not contain representative tumor-resident immune cell populations. For both combination and single agent therapies involving precise modulation of ILCs, HIS mice optimized to support the engraftment and development of multiple immune cell types represent a significant improvement for modeling possible responses from tumor cells and immune cells. Here we discuss the next generation of ILC-related immunotherapies and the mouse models required to study them.

Several new immunotherapies in development could enhance ILC antitumor functionality (**Figure 2**) but require humanized mice for accurate modeling of their effects. Histone deacetylases (HDACs) and HDAC inhibitors are able to alter transcription of genes related to tumor growth or suppression (147) and induce cell cycle arrest in cancer cells (148). HDACs have been shown to enhance ADCC of NK cells against tumor cells (149), but some HDAC inhibitors can diminish NK cell longevity and cytotoxicity (150) while others enhance NK cell functions (151). These treatments are difficult to study accurately since they impact both tumor cells and tumor-resident immune cells in different ways—not all of which are replicated by murine cells. Further studies in mice optimized for NK cell survival will enable determination of the effects of HDACs on tumor and NK cells simultaneously.

Synthetic cytokines can also enhance NK/ILC immunotherapies, since the broad mechanisms of action of endogenous cytokines limit the doses that can be safely administered (152). Artificial cytokines can be engineered to exhibit modified binding profiles, enhanced stability and specificity, increased activation of immune cells, multifunctional capacity, and lower induction of autoimmunity (153). For example, synthetic IL-2 and IL-2R pairs enable specific activation of only the engineered immune cells in a patient (154). Synthetic cytokines can also be targeted to tumor cells to improve activation of immune cells only within the TME (155). Artificially tethered membrane-bound IL-15 can improve longevity and cytotoxicity of NK cells (156), and membrane-bound IL-21 on feeder cells can modulate NK cell phenotype when expanding them for autologous therapy (135). In the future, synthetic cytokine and receptor pairs could be used to specifically activate CAR NK cells or ILCs only when they are adjacent to tumor cells. Since a major advantage of bioengineered cytokines is their ability to activate multiple types of immune cells simultaneously and synergistically, HIS mice represent an optimal tool for studying their effects on NK cells and ILCs in addition to other immune cells.

Non-cytokine immunomodulatory drugs (IMiDs) ranging from snake venom (157) to antimicrobial peptides (AMPs) such as cathelicidin (158) have been tested for their ability to improve NK cell antitumor functions. Drugs such as lenalidomide and pomalidomide can enhance antitumor ILC behavior as well (159, 160). Bryostatins are protein kinase C modulators that are currently being engineered to improve CAR NK functionality (161). These and many other drugs have the potential to broadly or specifically activate NK cells or ILCs in addition to other immune cells within the TME. However, only small numbers of murine studies have been carried out thus far to determine their ability to activate tumor-resident ILCs and influence tumor eradication *in vivo*. To accurately assess them, HIS mice optimized for NK/ILC proliferation such as NOG-IL-15 Tg mice transplanted with human PBMCs should be used.

Finally, almost all of the therapies discussed in this review can be further enhanced through targeted drug delivery. This enables researchers to consider thousands of drugs for cancer therapy that were previously considered too toxic to administer systemically. These drugs can be targeted to cancer cells or activated only within the TME using delivery mechanisms such as oncolytic viruses (162), coated nanoparticles (163), and ultrasound activation (164). This also increases the quantity of drugs to which the tumor can be exposed, potentially increasing their efficacy. Oncolytic viruses can be used as checkpoint inhibitor delivery vehicles, limiting autoimmunity and other disorders that might originate from systemic delivery (165). NK/ILC therapies can also be strengthened by using transplanted cells as a delivery vehicle or enhancing their function through separately targeted drugs. This could improve their killing capacity, localization to tumors, or activation within the TME. Researchers have used NK92 cells to bring drug-loaded nanoparticles to a solid tumor and block inhibitory signals in the TME (166), and local delivery of chemoattractants such as CCL20 or CXCL16 can increase tumor infiltration by ILCs (167). There is a great deal of future work that should be done in the drug delivery space to enhance ILC-related therapies, and HIS mice are the most ideal tool for early stage optimization and assessment because these mice can facilitate the survival and proliferation of ILC/NK cell therapies and their tumors will contain diverse immune cell populations.

CONCLUDING REMARKS

In order to solve critical unanswered questions surrounding the dynamic interactions between ILCs, solid tumors, and other tumor-resident immune cells, researchers should leverage humanized mouse models to increase the accuracy and utility of their studies. New generations of mice have been optimized to ensure ILC survival and enable development of multiple immune cell types simultaneously, both of which are critical for accurately studying the direct effects of immunotherapies as well as their indirect effects on other immune cells. Topics related to ILC-cancer biology that are in need of further investigation include: determining why current immunotherapies show limited efficacy in solid tumors, identifying methods to subvert the signals in the TME that are suppressing ILCs, assessing the unknown roles and plasticity of ILCs in cancer both endogenously and after adoptive transfer, and understanding the signals communicated between ILCs and other immune or tumor cells and how those correlate with tumor growth or eradication. For all of these endeavors, humanized mice represent a useful tool to study these complex questions.

The broad range of biotechnology that is being invented at breakneck speed is inspiring but also daunting. It seems virtually impossible to test all of these potential immunotherapy-enhancing agents in an accurate manner - especially in combination with each other - using standard immunodeficient mouse models. The potential utilities of combination therapies are much broader than those of single agent therapies, so it is important to study them accurately. While the primary effects of these therapies can be assessed on single types of immune or cancer cells by transplanting them into immunodeficient mice, that approach misses a large portion of information that is critical to predicting their efficacy against solid or liquid tumors: the secondary effects these cells will have on other cells in the TME or bloodstream. Improved *in vivo* modeling using humanized mice would drastically increase our ability to determine which of these technologies should be translated to a clinical setting for human trials and potentially save the lives of many patients, along with the costly sums of money required to test individual drugs. HIS mice expressing molecules such as IL-15 that improve ILC survival and proliferation will further enable researchers to design and optimize cellular and molecular immunotherapies.

AUTHOR CONTRIBUTIONS

NH, IM, and JS conceived and organized the outline of the review. NH, IM, UM-N, IK, QT, and JS contributed to the writing. IM created the figures. All authors contributed to the article and approved the submitted version.

FUNDING

This work was supported by grants from the National Institutes of Health (R35DE030054; R01DE027750), which is funding the JBS laboratory for research on cancer immunotherapy.

REFERENCES

1. Lanier LL. NK cell recognition. *Annu Rev Immunol* (2005) 23:225–74. doi: 10.1146/annurev.immunol.23.021704.115526
2. Pegram HJ, Andrews DM, Smyth MJ, Darcy PK, Kershaw MH. Activating and inhibitory receptors of natural killer cells. *Immunol Cell Biol* (2011) 89) 2:216–24. doi: 10.1038/icb.2010.78
3. Herberman RB, Nunn ME, Lavrin DH. Natural cytotoxic reactivity of mouse lymphoid cells against syngeneic and allogeneic tumors. I. Distribution of reactivity and specificity. *Int J Cancer* (1975) 16(2):216–29. doi: 10.1002/ijc.2910160204
4. Kiessling R, Klein E, Wigzell H. "Natural" killer cells in the mouse. I. Cytotoxic cells with specificity for mouse Moloney leukemia cells. Specificity and distribution according to genotype. *Eur J Immunol* (1975) 5(2):112–7. doi: 10.1002/eji.1830050208
5. Kim S, Iizuka K, Aguila HL, Weissman IL, Yokoyama WM. In vivo natural killer cell activities revealed by natural killer cell-deficient mice. *Proc Natl Acad Sci U S A* (2000) 97(6):2731–6. doi: 10.1073/pnas.050588297
6. Smyth MJ, Crowe NY, Godfrey DI. NK cells and NKT cells collaborate in host protection from methylcholanthrene-induced fibrosarcoma. *Int Immunol* (2001) 13(4):459–63. doi: 10.1093/intimm/13.4.459
7. Artis D, Spits H. The biology of innate lymphoid cells. *Nature* (2015) 151 (4):10–7. doi: 10.1038/nature14189
8. Jacquelot N, Luong K, Luong K, Seillet C. Physiological regulation of innate lymphoid cells. *Front Immunol* (2019) 10:405. doi: 10.3389/fimmu.2019.00405
9. Vivier E, Artis D, Colonna M, Diefenbach A, Di Santo JP, Eberl G, et al. Innate Lymphoid Cells: 10 Years On. *Cell* (2018) 174(5):1054–66. doi: 10.1016/j.cell.2018.07.017
10. Mjösberg J, Mazzurana L. ILC-poiesis: Making Tissue ILCs from Blood. *Immunity* (2017) 46(3):344–6. doi: 10.1016/j.immuni.2017.03.002
11. Scoville SD, Freud AG, Caligiuri MA. Modeling human natural killer cell development in the era of innate lymphoid cells. *Front Immunol* (2017) 8:360. doi: 10.3389/fimmu.2017.00360
12. Scoville SD, Freud AG, Caligiuri MA. Cellular pathways in the development of human and murine innate lymphoid cells. *Curr Opin Immunol* (2019) 56:100–6. doi: 10.1016/j.coi.2018.11.003
13. Bonaventura P, Shekarian T, Alcazer V, Valladeau-Guilemond J, Valsesia-Wittmann S, Amigorena S, et al. Cold tumors: A therapeutic challenge for immunotherapy. *Front Immunol* (2019) 10:168. doi: 10.3389/fimmu.2019.00168
14. Stern LA, Jonsson VD, Priceman SJ. CAR T Cell Therapy Progress and Challenges for Solid Tumors. *Cancer Treat Res* (2020) 180:297–326. doi: 10.1007/978-3-030-38862-1_11
15. Zhang H, Ye ZL, Yuan ZG, Luo ZQ, Jin HJ, Qian QJ. New strategies for the treatment of solid tumors with CAR-T cells. *Int J Biol Sci* (2016) 12(6):718–29. doi: 10.7150/ijbs.14405
16. Rangarajan A, Weinberg RA. Comparative biology of mouse versus human cells: Modelling human cancer in mice. *Nat Rev Cancer* (2003) 3)12:952–9. doi: 10.1038/nrc1235
17. Mattern J, Bak M, Hahn EW, Volm M. Human tumor xenografts as model for drug testing. *Cancer Metastasis Rev* (1988) 7(3):263–84. doi: 10.1007/BF00047755
18. Voskoglou-Nomikos T, Pater JL, Seymour L. Clinical Predictive Value of the in Vitro Cell Line, Human Xenograft, and Mouse Allograft Preclinical Cancer Models. *Clin Cancer Res* (2003) 9(11):4227–39.
19. Hidalgo M, Amant F, Biankin AV, Budinská E, Byrne AT, Caldas C, et al. Patient-derived Xenograft models: An emerging platform for translational cancer research. *Cancer Discov* (2014) 4(9):998–1013. doi: 10.1158/2159-8290.CD-14-0001
20. Abate-Daga D, Lagisetty KH, Tran E, Zheng Z, Gattinoni L, Yu Z, et al. A novel chimeric antigen receptor against prostate stem cell antigen mediates tumor destruction in a humanized mouse model of pancreatic cancer. *Hum Gene Ther* (2014) 25(12):1003–12. doi: 10.1089/hum.2013.209
21. Rongvaux A, Willinger T, Martinek J, Strowig T, Gearty SV, Teichmann LL, et al. Development and function of human innate immune cells in a humanized mouse model. *Nat Biotechnol* (2014) 32(4):364–72. doi: 10.1038/nbt.2858
22. Zhao Y, Shuen TWH, Toh TB, Chan XY, Liu M, Tan SY, et al. Development of a new patient-derived xenograft humanised mouse model to study human-specific tumour microenvironment and immunotherapy. *Gut* (2018) 67(10):1845–54. doi: 10.1136/gutjnl-2017-315201
23. Marius Munneke J, Björklund AT, Mjösberg JM, Garming-Legert K, Bernink JH, Blom B, et al. Activated innate lymphoid cells are associated with a reduced susceptibility to graft-versus-host disease. *Blood* (2014) 124(5):812–21. doi: 10.1182/blood-2013-11-536888
24. Lim AI, Li Y, Lopez-Lastra S, Stadhouders R, Paul F, Casrouge A, et al. Systemic Human ILC Precursors Provide a Substrate for Tissue ILC Differentiation. *Cell* (2017) 168(6):1086–1100.e10. doi: 10.1016/j.cell.2017.02.021
25. Moretta L, Locatelli F. Innate lymphoid cells in normal and disease: An introductory overview. *Immunol Lett* (2016) 179:1. doi: 10.1016/j.imlet.2016.07.008
26. Scoville SD, Mundy-Bosse BL, Zhang MH, Chen L, Zhang X, Keller KA, et al. A Progenitor Cell Expressing Transcription Factor RORγt Generates All Human Innate Lymphoid Cell Subsets. *Immunity* (2016) 44(5):1140–50. doi: 10.1016/j.immuni.2016.04.007

27. Spits H, Artis D, Colonna M, Diefenbach A, Di Santo JP, Eberl G, et al. Innate lymphoid cells-a proposal for uniform nomenclature. *Nat Rev Immunol* (2013) 13(2):145–9. doi: 10.1038/nri3365
28. Gasteiger G, Fan X, Dikiy S, Lee SY, Rudensky AY. Tissue residency of innate lymphoid cells in lymphoid and nonlymphoid organs. *Science (80-)* (2015) 350(6263):981–5. doi: 10.1126/science.aac9593
29. Bal SM, Golebski K, Spits H. Plasticity of innate lymphoid cell subsets. *Nat Rev Immunol* (2020) 20(9):552–65. doi: 10.1038/s41577-020-0282-9
30. Riggan L, Freud AG, O'Sullivan TE. True Detective: Unraveling Group 1 Innate Lymphocyte Heterogeneity. *Trends Immunol* (2019) 40(10):909–21. doi: 10.1016/j.it.2019.08.005
31. Gordon SM, Chaix J, Rupp LJ, Wu J, Madera S, Sun JC, et al. The Transcription Factors T-bet and Eomes Control Key Checkpoints of Natural Killer Cell Maturation. *Immunity* (2012) 36(1):55–67. doi: 10.1016/j.immuni.2011.11.016
32. Freud AG, Mundy-Bosse BL, Yu J, Caligiuri MA. The Broad Spectrum of Human Natural Killer Cell Diversity. *Immunity* (2017) 47(5):820–33. doi: 10.1016/j.immuni.2017.10.008
33. Melsen JE, Lugthart G, Lankester AC, Schilham MW. Human Circulating and Tissue-Resident CD56bright Natural Killer Cell Populations. *Front Immunol* (2016) 7:262. doi: 10.3389/fimmu.2016.00262
34. Schmidt L, Eskiocak B, Kohn R, Dang C, Joshi NS, DuPage M, et al. Enhanced adaptive immune responses in lung adenocarcinoma through natural killer cell stimulation. *Proc Natl Acad Sci U S A* (2019) 116(35):17460–9. doi: 10.1073/pnas.1904253116
35. Michel T, Poli A, Cuapio A, Briquemont B, Iserentant G, Ollert M, et al. Human CD56 bright NK Cells: An Update. *J Immunol* (2016) 196(7):2923–31. doi: 10.4049/jimmunol.1502570
36. Yeap WH, Wong KL, Shimasaki N, Teo ECY, Quek JKS, Yong HX, et al. CD16 is indispensable for antibodydependent cellular cytotoxicity by human monocytes. *Sci Rep* (2016) 6:34310. doi: 10.1038/srep34310
37. Spits H, Bernink JH, Lanier L. NK cells and type 1 innate lymphoid cells: Partners in host defense. *Nat Immunol* (2016) 17(7):758–64. doi: 10.1038/ni.3482
38. Bernink JH, Peters CP, Munneke M, Te Velde AA, Meijer SL, Weijer K, et al. Human type 1 innate lymphoid cells accumulate in inflamed mucosal tissues. *Nat Immunol* (2013) 14(3):221–9. doi: 10.1038/ni.2534
39. Fuchs A, Vermi W, Lee JS, Lonardi S, Gilfillan S, Newberry RD, et al. Intraepithelial type 1 innate lymphoid cells are a unique subset of il-12- and il-15-responsive ifn-γ-producing cells. *Immunity* (2013) 38(4):769–81. doi: 10.1016/j.immuni.2013.02.010
40. Fuchs A. ILC1s in tissue inflammation and infection. *Front Immunol* (2016) 7:104. doi: 10.3389/fimmu.2016.00104
41. Colonna M. Innate Lymphoid Cells: Diversity, Plasticity, and Unique Functions in Immunity. *Immunity* (2018) 48(6):1104–17. doi: 10.1016/j.immuni.2018.05.013
42. Salimi M, Barlow JL, Saunders SP, Xue L, Gutowska-Owsiak D, Wang X, et al. A role for IL-25 and IL-33-driven type-2 innate lymphoid cells in atopic dermatitis. *J Exp Med* (2013) 210(13):2939–50. doi: 10.1084/jem.20130351
43. Ebbo M, Crinier A, Vély F, Vivier E. Innate lymphoid cells: Major players in inflammatory diseases. *Nat Rev Immunol* (2017) 17(11):665–78. doi: 10.1038/nri.2017.86
44. Helfrich S, Mindt BC, Fritz JH, Duerr CU. Group 2 innate lymphoid cells in respiratory allergic inflammation. *Front Immunol* (2019) 10:930. doi: 10.3389/fimmu.2019.00930
45. Herbert DR, Douglas B, Zullo K. Group 2 innate lymphoid cells (ILC2): Type 2 immunity and helminth immunity. *Int J Mol Sci* (2019) 20(9):2276. doi: 10.3390/ijms20092276
46. Cella M, Fuchs A, Vermi W, Facchetti F, Otero K, Lennerz JKM, et al. A human natural killer cell subset provides an innate source of IL-22 for mucosal immunity. *Nature* (2009) 457(7230):722–5. doi: 10.1038/nature07537
47. Hodgings. Killers 2.0: NK cell therapies at the forefront of cancer control. *J Clin Invest* (2019) 129(9):3499–510. doi: 10.1172/JCI129338
48. Bruchard M, Ghiringhelli F. Deciphering the roles of innate lymphoid cells in cancer. *Front Immunol* (2019) 10:656. doi: 10.3389/fimmu.2019.00656
49. Salimi M, Wang R, Yao X, Li X, Wang X, Hu Y, et al. Activated innate lymphoid cell populations accumulate in human tumour tissues. *BMC Cancer* (2018) 18(1):341. doi: 10.1186/s12885-018-4262-4
50. Cortez VS, Ulland TK, Cervantes-Barragan L, Bando JK, Robinette ML, Wang Q, et al. SMAD4 impedes the conversion of NK cells into ILC1-like cells by curtailing non-canonical TGF-β signaling. *Nat Immunol* (2017) 18(9):995–1003. doi: 10.1038/ni.3809
51. Gao Y, Souza-Fonseca-Guimaraes F, Bald T, Ng SS, Young A, Ngiow SF, et al. Tumor immunoevasion by the conversion of effector NK cells into type 1 innate lymphoid cells. *Nat Immunol* (2017) 18(9):1004–15. doi: 10.1038/ni.3800
52. Hawke LG, Mitchell BZ, Ormiston ML. TGF-β and IL-15 Synergize through MAPK Pathways to Drive the Conversion of Human NK Cells to an Innate Lymphoid Cell 1–like Phenotype. *J Immunol* (2020) 204(12):3171–81. doi: 10.4049/jimmunol.1900866
53. Golebski K, Ros XR, Nagasawa M, van Tol S, Heesters BA, Aglmous H, et al. IL-1β, IL-23, and TGF-β drive plasticity of human ILC2s towards IL-17-producing ILCs in nasal inflammation. *Nat Commun* (2019) 10(1):2162. doi: 10.1038/s41467-019-09883-7
54. Gury-BenAri M, Thaiss CA, Serafini N, Winter DR, Giladi A, Lara-Astiaso D, et al. The Spectrum and Regulatory Landscape of Intestinal Innate Lymphoid Cells Are Shaped by the Microbiome. *Cell* (2016) 166(5):1231–1246.e13. doi: 10.1016/j.cell.2016.07.043
55. Ghaedi M, Ohashi PS. ILC transdifferentiation: roles in cancer progression. *Cell Res* (2020) 30(7):562–3. doi: 10.1038/s41422-020-0326-5
56. Wang S, Qu Y, Xia P, Chen Y, Zhu X, Zhang J, et al. Transdifferentiation of tumor infiltrating innate lymphoid cells during progression of colorectal cancer. *Cell Res* (2020) 30(7):610–22. doi: 10.1038/s41422-020-0312-y
57. Jacquelot N, Hall E, Freud A, Amedei A, Tugues S, Ducimetière L, et al. The Interplay Between Innate Lymphoid Cells and the Tumor Microenvironment. *Front Immunol* (2019) 10:2895. doi: 10.3389/fimmu.2019.02895
58. Schmiedel D, Mandelboim O. NKG2D ligands-critical targets for cancer immune escape and therapy. *Front Immunol* (2018) 9:2040. doi: 10.3389/fimmu.2018.02040
59. Coudert JD, Scarpellino L, Gros F, Vivier E, Held W. Sustained NKG2D engagement induces cross-tolerance of multiple distinct NK cell activation pathways. *Blood* (2008) 111(7):3571–8. doi: 10.1182/blood-2007-07-100057
60. Munn DH, Bronte V. Immune suppressive mechanisms in the tumor microenvironment. *Curr Opin Immunol* (2016) 39:1–6. doi: 10.1016/j.coi.2015.10.009
61. Baginska J, Viry E, Paggetti J, Medves S, Berchem G, Moussay E, et al. The critical role of the tumor microenvironment in shaping natural killer cell-mediated anti-tumor immunity. *Front Immunol* (2013) 4:490. doi: 10.3389/fimmu.2013.00490
62. Hasmim M, Messai Y, Ziani L, Thiery J, Bouhris JH, Noman MZ, et al. Critical role of tumor microenvironment in shaping NK cell functions: Implication of hypoxic stress. *Front Immunol* (2015) 6:482. doi: 10.3389/fimmu.2015.00482
63. Fournié JJ, Poupot M. The pro-tumorigenic IL-33 involved in antitumor immunity: A yin and yang cytokine. *Front Immunol* (2018) 9:2506. doi: 10.3389/fimmu.2018.02506
64. Jovanovic IP, Pejnovic NN, Radosavljevic GD, Pantic JM, Milovanovic MZ, Arsenijevic NN, et al. Interleukin-33/ST2 axis promotes breast cancer growth and metastases by facilitating intratumoral accumulation of immunosuppressive and innate lymphoid cells. *Int J Cancer* (2014) 134(7):1669–82. doi: 10.1002/ijc.28481
65. Crinier A, Vivier E, Bléry M. Helper-like innate lymphoid cells and cancer immunotherapy. *Semin Immunol* (2019) 41:101274. doi: 10.1016/j.smim.2019.04.002
66. Wasmer MH, Krebs P. The role of IL-33-dependent inflammation in the tumor microenvironment. *Front Immunol* (2017) 7:682:1. doi: 10.3389/fimmu.2016.00682
67. Liu Y, Song Y, Lin D, Lei L, Mei Y, Jin Z, et al. NCR – group 3 innate lymphoid cells orchestrate IL-23/IL-17 axis to promote hepatocellular carcinoma development. *EBioMedicine* (2019) 41:333–44. doi: 10.1016/j.ebiom.2019.02.050

68. Herndler-Brandstetter D, Shan L, Yao Y, Stecher C, Plajer V, Lietzenmayer M, et al. Humanized mouse model supports development, function, and tissue residency of human natural killer cells. *Proc Natl Acad Sci U S A* (2017) 114(45):E9626–34. doi: 10.1073/pnas.1705301114
69. Katano I, Nishime C, Ito R, Kamisako T, Mizusawa T, Ka Y, et al. Long-term maintenance of peripheral blood derived human NK cells in a novel human IL-15- transgenic NOG mouse. *Sci Rep* (2017) 7:17230. doi: 10.1038/s41598-017-17442-7
70. Matsuda M, Ono R, Iyoda T, Endo T, Iwasaki M, Tomizawa-Murasawa M, et al. Human NK cell development in hIL-7 and hIL-15 knockin NOD/SCID/IL2rgKO mice. *Life Sci Alliance* (2019) 2(2):e201800195. doi: 10.26508/lsa.201800195
71. Lopez-Lastra S, Masse-Ranson G, Fiquet O, Darche S, Serafini N, Li Y, et al. A functional DC cross talk promotes human ILC homeostasis in humanized mice. *Blood Adv* (2017) 1(10):601–14. doi: 10.1182/bloodadvances.2017004358
72. Nguyen R, Patel AG, Griffiths LM, Dapper J, Stewart EA, Houston J, et al. Next-generation humanized patient-derived xenograft mouse model for pre-clinical antibody studies in neuroblastoma. *Cancer Immunol Immunother* (2020) 70:721–32. doi: 10.1007/s00262-020-02713-6
73. Meraz IM, Majidi M, Meng F, Shao RP, Ha MJ, Neri S, et al. An improved patient-derived xenograft humanized mouse model for evaluation of lung cancer immune responses. *Cancer Immunol Res* (2019) 7(8):1267–79. doi: 10.1158/2326-6066.CIR-18-0874
74. Wege AK, Ernst W, Eckl J, Frankenberger B, Vollmann-Zwerenz A, Männel DN, et al. Humanized tumor mice-A new model to study and manipulate the immune response in advanced cancer therapy. *Int J Cancer* (2011) 129 (9):2194–206. doi: 10.1002/ijc.26159
75. Lapidot T, Pflumio F, Doedens M, Murdoch B, Williams DE, Dick JE. Cytokine stimulation of multilineage hematopoiesis from immature human cells engrafted in SCID Mice. *Science (80-)* (1992) 255(5048):1137–41. doi: 10.1126/science.1372131
76. McCune JM, Namikawa R, Kaneshima H, Shultz LD, Lieberman M, Weissman IL. The SCID-hu mouse: Murine model for the analysis of human hematolymphoid differentiation and function. *Science (80-)* (1988) 241(4873):1632–9. doi: 10.1126/science.2971269
77. Mosier DE, Gulizia RJ, Baird SM, Wilson DB. Transfer of a functional human immune system to mice with severe combined immunodeficiency. *Nature* (1988) 335(6187):256–9. doi: 10.1038/335256a0
78. Hesselton RAM, Greiner DL, Mordes JP, Rajan TV, Sullivan JL, Shultz LD. High levels of human peripheral blood mononuclear cell engraftment and enhanced susceptibility to human immunodeficiency virus type 1 infection in NOD/LtSz-scid/scid mice. *J Infect Dis* (1995) 172(4):974–82. doi: 10.1093/infdis/172.4.974
79. Takenaka K, Prasolava TK, Wang JCY, Mortin-Toth SM, Khalouei S, Gan OI, et al. Polymorphism in Sirpa modulates engraftment of human hematopoietic stem cells. *Nat Immunol* (2007) 8:1313–23. doi: 10.1038/ni1527
80. Yamauchi T, Takenaka K, Urata S, Shima T, Kikushige Y, Tokuyama T, et al. Polymorphic Sirpa is the genetic determinant for NOD-based mouse lines to achieve efficient human cell engraftment. *Blood* (2013) 121(8):1316–25. doi: 10.1182/blood-2012-06-440354
81. Shultz LD, Lyons BL, Burzenski LM, Gott B, Chen X, Chaleff S, et al. Human Lymphoid and Myeloid Cell Development in NOD/LtSz- scid IL2R γ null Mice Engrafted with Mobilized Human Hemopoietic Stem Cells. *J Immunol* (2005) 174(10):6477–89. doi: 10.4049/jimmunol.174.10.6477
82. Strowig T, Rongvaux A, Rathinam C, Takizawa H, Borsotti C, Philbrick W, et al. Transgenic expression of human signal regulatory protein alpha in Rag2 -/-γ c-/- mice improves engraftment of human hematopoietic cells in humanized mice. *Proc Natl Acad Sci U S A* (2011) 108(32):13218–23. doi: 10.1073/pnas.1109769108
83. Huntington ND, Legrand N, Alves NL, Jaron B, Weijer K, Plet A, et al. IL-15 trans-presentation promotes human NK cell development and differentiation in vivo. *J Exp Med* (2009) 206(1):25–34. doi: 10.1084/jem.20082013
84. Strowig T, Chijioke O, Carrega P, Arrey F, Meixlsperger S, Rämer PC, et al. Human NK cells of mice with reconstituted human immune system components require preactivation to acquire functional competence. *Blood* (2010) 116(20):4158–67. doi: 10.1182/blood-2010-02-270678
85. Hoogstad-van Evert JS, Cany J, van den Brand D, Oudenampsen M, Brock R, Torensma R, et al. Umbilical cord blood CD34+ progenitor-derived NK cells efficiently kill ovarian cancer spheroids and intraperitoneal tumors in NOD/SCID/IL2Rgnull mice. *Oncoimmunology* (2017) 6(8):e1320630. doi: 10.1080/2162402X.2017.1320630
86. Chu Y, Hochberg J, Yahr A, Ayello J, Van De Ven C, Barth M, et al. Targeting CD20+ aggressive B-cell non-hodgkin lymphoma by Anti-CD20 CAR mRNA-modified expanded natural killer cells in vitro and in NSG Mice. *Cancer Immunol Res* (2015) 3(4):333–44. doi: 10.1158/2326-6066.CIR-14-0114
87. Cany J, van der Waart AB, Tordoir M, Franssen GM, Hangalapura BN, de Vries J, et al. Natural Killer Cells Generated from Cord Blood Hematopoietic Progenitor Cells Efficiently Target Bone Marrow-Residing Human Leukemia Cells in NOD/SCID/IL2Rgnull Mice. *PloS One* (2013) 8(6):e64384. doi: 10.1371/journal.pone.0064384
88. Guerin MV, Finisguerra V, Van den Eynde BJ, Bercovici N, Trautmann A. Preclinical murine tumor models: A structural and functional perspective. *eLife* (2020) 9:e50740. doi: 10.7554/eLife.50740
89. Olson B, Li Y, Lin Y, Liu ET, Patnaik A. Mouse models for cancer immunotherapy research. *Cancer Discov* (2018) 8(11):1358–65. doi: 10.1158/2159-8290.CD-18-0044
90. Peng S, Creighton CJ, Zhang Y, Sen B, Mazumdar T, Myers JN, et al. Tumor grafts derived from patients with head and neck squamous carcinoma authentically maintain the molecular and histologic characteristics of human cancers. *J Transl Med* (2013) 11(1):198. doi: 10.1186/1479-5876-11-198
91. Yoshida GJ. Applications of patient-derived tumor xenograft models and tumor organoids. *J Hematol Oncol* (2020) 13(1):1–16. doi: 10.1186/s13045-019-0829-z
92. Sanmamed MF, Chester C, Melero I, Kohrt H. Defining the optimal murine models to investigate immune checkpoint blockers and their combination with other immunotherapies. *Ann Oncol* (2016) 27(7):1190–8. doi: 10.1093/annonc/mdw041
93. Jespersen H, Lindberg MF, Donia M, Söderberg EMV, Andersen R, Keller U, et al. Clinical responses to adoptive T-cell transfer can be modeled in an autologous immune-humanized mouse model. *Nat Commun* (2017) 8 (1):707. doi: 10.1038/s41467-017-00786-z
94. Zitvogel L, Pitt JM, Daillère R, Smyth MJ, Kroemer G. Mouse models in oncoimmunology. *Nat Rev Cancer* (2016) 16(12):759–73. doi: 10.1038/nrc.2016.91
95. Gao H, Korn JM, Ferretti S, Monahan JE, Wang Y, Singh M, et al. High-throughput screening using patient-derived tumor xenografts to predict clinical trial drug response. *Nat Med* (2015) 21(11):1318–25. doi: 10.1038/nm.3954
96. Byrne AT, Alférez DG, Amant F, Annibali D, Arribas J, Biankin AV, et al. Interrogating open issues in cancer precision medicine with patient-derived xenografts. *Nat Rev Cancer* (2017) 17:254–68. doi: 10.1038/nrc.2016.140
97. Chao C, Widen SG, Wood TG, Zatarain JR, Johnson P, Gajjar A, et al. Patient-derived xenografts from colorectal carcinoma: A temporal and hierarchical study of murine stromal cell replacement. *Anticancer Res* (2017) 37(7):3405–12. doi: 10.21873/anticanreS.11707
98. Moynihan KD, Opel CF, Szeto GL, Tzeng A, Zhu EF, Engreitz JM, et al. Eradication of large established tumors in mice by combination immunotherapy that engages innate and adaptive immune responses. *Nat Med* (2016) 22:1402–10. doi: 10.1038/nm.4200
99. Li D, Li J, Chu H, Wang Z. A functional antibody cross-reactive to both human and murine cytotoxic T-lymphocyte-associated protein 4 via binding to an N-glycosylation epitope A functional antibody cross-reactive to both human and murine cytotoxic T-lymphocyte-associated protein 4 via binding to an N-glycosylation epitope. *mAbs* (2020) 12(1):1725365. doi: 10.1080/19420862.2020.1725365
100. Darvin P, Toor SM, Sasidharan Nair V, Elkord E. Immune checkpoint inhibitors: recent progress and potential biomarkers. *Exp Mol Med* (2018) 50:1–11. doi: 10.1038/s12276-018-0191-1
101. Beldi-Ferchiou A, Lambert M, Dogniaux S, Vély F, Vivier E, Olive D, et al. PD-1 mediates functional exhaustion of activated NK cells in patients with Kaposi sarcoma. *Oncotarget* (2016) 7:72961–77. doi: 10.18632/oncotarget.12150
102. Petrova T, Pesic J, Pardali K, Gaestel M, Arthur JSC. p38 MAPK signalling regulates cytokine production in IL-33 stimulated Type 2 Innate Lymphoid cells. *Sci Rep* (2020) 10:3479. doi: 10.1038/s41598-020-60089-0

103. Guo Y, Feng X, Jiang Y, Shi X, Xing X, Liu X, et al. PD1 blockade enhances cytotoxicity of in vitro expanded natural killer cells towards myeloma cells. *Oncotarget* (2016) 7:48360–74. doi: 10.18632/oncotarget.10235
104. Abel AM, Yang C, Thakar MS, Malarkannan S. Natural killer cells: Development, maturation, and clinical utilization. *Front Immunol* (2018) 9:1869. doi: 10.3389/fimmu.2018.01869
105. Hsu J, Hodgins JJ, Marathe M, Nicolai CJ, Bourgeois-Daigneault MC, Trevino TN, et al. Contribution of NK cells to immunotherapy mediated by PD-1/PD-L1 blockade. *J Clin Invest* (2018) 128(10):4654–68. doi: 10.1172/JCI99317
106. Caligiuri MA, Gasteiger G, Solana R, Moretta L, Mariotti FR, Quatrini L, et al. Innate Lymphoid Cells: Expression of PD-1 and Other Checkpoints in Normal and Pathological Conditions. *Front Immunol* (2019) 1:910:910. doi: 10.3389/fimmu.2019.00910
107. Sternberg-Simon M, Brodin P, Pickman Y, Önfelt B, Kärre K, Malmberg K-J, et al. Natural Killer Cell Inhibitory Receptor Expression in Humans and Mice: A Closer Look. *Front Immunol* (2013) 4:65(MAR):65. doi: 10.3389/fimmu.2013.00065
108. Du X, Liu M, Su J, Zhang P, Tang F, Ye P, et al. Uncoupling therapeutic from immunotherapy-related adverse effects for safer and effective anti-CTLA-4 antibodies in CTLA4 humanized mice. *Cell Res* (2018) 28:433–47. doi: 10.1038/s41422-018-0012-z
109. Lute KD, May KF, Lu P, Zhang H, Kocak E, Mosinger B, et al. Human CTLA4 knock-in mice unravel the quantitative link between tumor immunity and autoimmunity induced by anti-CTLA-4 antibodies. *Blood* (2005) 106(9):3127–33. doi: 10.1182/blood-2005-06-2298
110. Burova E, Hermann A, Waite J, Potocky T, Lai V, Hong S, et al. Characterization of the Anti-PD-1 Antibody REGN2810 and Its Antitumor Activity in Human PD-1 Knock-In Mice. *Mol Cancer Ther* (2017) 16(5):861–70. doi: 10.1158/1535-7163.MCT-16-0665
111. Viricel C, Ahmed M, Ahmed M, Barakat K. Human PD-1 binds differently to its human ligands: A comprehensive modeling study. *J Mol Graph Model* (2015) 57:131–42. doi: 10.1016/j.jmgm.2015.01.015
112. Immune Checkpoint Humanized Mouse Models, in: Applied StemCell. Available at: https://www.appliedstemcell.com/research/animal-models/mouse-repository/immune-checkpoint-mouse-models (Accessed Mar. 20, 2021).
113. Suarez ER, Chang DK, Sun J, Sui J, Freeman GJ, Signoretti S, et al. Chimeric antigen receptor T cells secreting anti-PD-L1 antibodies more effectively regress renal cell carcinoma in a humanized mouse model. *Oncotarget* (2016) 7:34341–55. doi: 10.18632/oncotarget.9114
114. Tay SS, Carol H, Biro M. TriKEs and BiKEs join CARs on the cancer immunotherapy highway. *Hum Vaccines Immunother* (2016) 12(11):2790–6. doi: 10.1080/21645515.2016.1198455
115. Gleason MK, Ross JA, Warlick ED, Lund TC, Verneris MR, Wiernik A, et al. CD16xCD33 bispecific killer cell engager (BiKE) activates NK cells against primary MDS and MDSC CD33+ targets. *Blood* (2014) 123(19):3016–26. doi: 10.1182/blood-2013-10-533398
116. Vallera DA, Ferrone S, Kodal B, Hinderlie P, Bendzick L, Ettestad B, et al. NK-cell-mediated targeting of various solid tumors using a B7-H3 tri-specific killer engager in vitro and in vivo. *Cancers (Basel)* (2020) 12 (9):2659. doi: 10.3390/cancers12092659
117. Gauthier L, Morel A, Anceriz N, Rossi B, Blanchard-Alvarez A, Grondin G, et al. Multifunctional Natural Killer Cell Engagers Targeting NKp46 Trigger Protective Tumor Immunity. *Cell* (2019) 177(7):1701–13. doi: 10.1016/j.cell.2019.04.041
118. Müller P, Martin K, Theurich S, Schreiner J, Savic S, Terszowski G, et al. Microtubule-depolymerizing agents used in antibody-drug conjugates induce antitumor immunity by stimulation of dendritic cells. *Cancer Immunol Res* (2014) 2(8):741–55. doi: 10.1158/2326-6066.CIR-13-0198
119. Francisco JA, Cerveny CG, Meyer DL, Mixan BJ, Klussman K, Chace DF, et al. cAC10-vcMMAE, an anti-CD30-monomethyl auristatin E conjugate with potent and selective antitumor activity. *Blood* (2003) 102(4):1458–65. doi: 10.1182/blood-2003-01-0039
120. Moral JA, Leung J, Rojas LA, Ruan J, Zhao J, Sethna Z, et al. ILC2s amplify PD-1 blockade by activating tissue-specific cancer immunity. *Nature* (2020) 579:130–5. doi: 10.1038/s41586-020-2015-4
121. Tang H, Qiao J, Fu YX. Immunotherapy and tumor microenvironment. *Cancer Lett* (2016) 370(1):85–90. doi: 10.1016/j.canlet.2015.10.009
122. Vahedi F, Nham T, Poznanski SM, Chew MV, Shenouda MM, Lee D, et al. Ex Vivo Expanded Human NK Cells Survive and Proliferate in Humanized Mice with Autologous Human Immune Cells. *Sci Rep* (2017) 7:12083. doi: 10.1038/s41598-017-12223-8
123. Ono R, Watanabe T, Kawakami E, Iwasaki M, Tomizawa-Murasawa M, Matsuda M, et al. Co-activation of macrophages and T cells contribute to chronic GVHD in human IL-6 transgenic humanised mouse model. *EBioMedicine* (2019) 41:584–96. doi: 10.1016/j.ebiom.2019.02.001
124. Lopez-Lastra S, Di Santo JP. Modeling natural killer cell targeted immunotherapies. *Front Immunol* (2017) 8:370. doi: 10.3389/fimmu.2017.00370
125. Cooper MA, Elliott JM, Keyel PA, Yang L, Carrero JA, Yokoyama WM. Cytokine-induced memory-like natural killer cells. *Proc Natl Acad Sci U S A* (2009) 106(6):1915–9. doi: 10.1073/pnas.0813192106
126. Pahl JHW, Cerwenka A, Ni J. Memory-Like NK cells: Remembering a previous activation by cytokines and NK cell receptors. *Front Immunol* (2018) 9:2796. doi: 10.3389/fimmu.2018.02796
127. Romee R, Rosario M, Berrien-Elliott MM, Wagner JA, Jewell BA, Schappe T, et al. Cytokine-induced memory-like natural killer cells exhibit enhanced responses against myeloid leukemia. *Sci Transl Med* (2016) 8(357):357ra123–357ra123. doi: 10.1126/scitranslmed.aaf2341
128. Uppendahl LD, Felices M, Bendzick L, Ryan C, Kodal B, Hinderlie P, et al. Cytokine-induced memory-like natural killer cells have enhanced function, proliferation, and in vivo expansion against ovarian cancer cells. *Gynecol Oncol* (2019) 153(1):149–57. doi: 10.1016/j.ygyno.2019.01.006
129. Hermanson DL, Bendzick L, Pribyl L, McCullar V, Vogel RI, Miller JS, et al. Induced Pluripotent Stem Cell-Derived Natural Killer Cells for Treatment of Ovarian Cancer. *Stem Cells* (2016) 34(1):93–101. doi: 10.1002/stem.2230
130. Shankar K, Capitini CM, Saha K. Genome engineering of induced pluripotent stem cells to manufacture natural killer cell therapies. *Stem Cell Res Ther* (2020) 11(1):234. doi: 10.1186/s13287-020-01741-4
131. Bigley AB, Baker FL, Simpson RJ. Cytomegalovirus: an unlikely ally in the fight against blood cancers? *Clin Exp Immunol* (2018) 193(3):265–74. doi: 10.1111/cei.13152
132. C. G. identifier: NCT03417414. *Does CMV Induced Changes in NK Lymphocyte Biology Influence the Effectiveness of Antibody Therapy Used to Treat B Cell Lymphoproliferative Diseases?* Available at: https://clinicaltrials.gov/ct2/show/NCT03417414 (Accessed Dec. 30, 2020). Full Text View - ClinicalTrials.gov.
133. Shevtsov M, Pitkin E, Ischenko A, Stangl S, Khachatryan W, Galibin O, et al. Ex vivo Hsp70-activated NK cells in combination with PD-1 inhibition significantly increase overall survival in preclinical models of glioblastoma and lung cancer. *Front Immunol* (2019) 10:454. doi: 10.3389/fimmu.2019.00454
134. Kweon S, Phan MTT, Chun S, Yu HB, Kim J, Kim S, et al. Expansion of human NK cells using K562 cells expressing OX40 ligand and short exposure to IL-21. *Front Immunol* (2019) 10:879. doi: 10.3389/fimmu.2019.00879
135. Ojo EO, Sharma AA, Liu R, Moreton S, Checkley-Luttge MA, Gupta K, et al. Membrane bound IL-21 based NK cell feeder cells drive robust expansion and metabolic activation of NK cells. *Sci Rep* (2019) 9:14916. doi: 10.1038/s41598-019-51287-6
136. Li Y, Hermanson DL, Moriarity BS, Kaufman DS. Human iPSC-Derived Natural Killer Cells Engineered with Chimeric Antigen Receptors Enhance Anti-tumor Activity. *Cell Stem Cell* (2018) 23(12):181–92. doi: 10.1016/j.stem.2018.06.002
137. Liu E, Marin D, Banerjee P, Macapinlac HA, Thompson P, Basar R, et al. Use of CAR-Transduced Natural Killer Cells in CD19-Positive Lymphoid Tumors. *N Engl J Med* (2020) 382(6):545–53. doi: 10.1056/nejmoa1910607
138. Liu E, Tong Y, Dotti G, Shaim H, Savoldo B, Mukherjee M, et al. Cord blood NK cells engineered to express IL-15 and a CD19-targeted CAR show long-term persistence and potent antitumor activity. *Leukemia* (2018) 32(2):520–31. doi: 10.1038/leu.2017.226
139. Burga RA, Yvon E, Chorvinsky E, Fernandes R, Russell C, Cruz Y, et al. Engineering the TGFβ receptor to Enhance the Therapeutic Potential of Natural Killer Cells as an Immunotherapy for Neuroblastoma. *Clin Cancer Res* (2019) 25(14):4400–12. doi: 10.1158/1078-0432.CCR-18-3183
140. Gong JH, Maki G, Klingemann HG. Characterization of a human cell line (NK-92) with phenotypical and functional characteristics of activated natural killer cells. *Leukemia* (1994) 8(4):652–8.
141. Tam YK, Miyagawa B, Ho VC, Klingemann HG. Immunotherapy of malignant melanoma in a SCID mouse model using the highly cytotoxic

natural killer cell line NK-92. *J Hematother* (1999) 8(3):281–90. doi: 10.1089/106161299320316
142. Tang X, Yang L, Li Z, Nalin AP, Dai H, Xu T, et al. First-in-man clinical trial of CAR NK-92 cells: safety test of CD33-CAR NK-92 cells in patients with relapsed and refractory acute myeloid leukemia, in: (2018). e-Century Publishing Corporation. Available at: www.ajcr.us/ (Accessed Dec. 30, 2020).
143. Zhou X, Dotti G, Krance RA, Martinez CA, Naik S, Kamble RT, et al. Inducible caspase-9 suicide gene controls adverse effects from alloreplete T cells after haploidentical stem cell transplantation. *Blood* (2015) 125 (26):4103–13. doi: 10.1182/blood-2015-02-628354
144. Wang QM, Tang PMK, Lian GY, Li C, Li J, Huang XR, et al. Enhanced cancer immunotherapy with Smad3-silenced NK-92 cells. *Cancer Immunol Res* (2018) 6(8):965–77. doi: 10.1158/2326-6066.CIR-17-0491
145. Yang HG, Kang MC, Kim TY, Hwang I, Jin HT, Sung YC, et al. Discovery of a novel natural killer cell line with distinct immunostimulatory and proliferative potential as an alternative platform for cancer immunotherapy. *J Immunother Cancer* (2019) 7(1):138. doi: 10.1186/s40425-019-0612-2
146. Gunesch JT, Angelo LS, Mahapatra S, Deering RP, Kowalko JE, Sleiman P, et al. Genome-wide analyses and functional profiling of human NK cell lines. *Mol Immunol* (2019) 11:64–75. doi: 10.1016/j.molimm.2018.07.015
147. Eckschlager T, Plch J, Stiborova M, Hrabeta J. Histone deacetylase inhibitors as anticancer drugs. *Int J Mol Sci* (2017) 18(7):1414. doi: 10.3390/ijms18071414
148. Johnstone RW, Licht JD. Histone deacetylase inhibitors in cancer therapy: Is transcription the primary target? *Cancer Cell* (2003) 4(1):13–8. doi: 10.1016/S1535-6108(03)00165-X
149. Hicks KC, Fantini M, Donahue RN, Schwab A, Knudson KM, Tritsch SR, et al. Epigenetic priming of both tumor and NK cells augments antibody-dependent cellular cytotoxicity elicited by the anti-PD-L1 antibody avelumab against multiple carcinoma cell types. *Oncoimmunology* (2018) 7(11): e1466018. doi: 10.1080/2162402X.2018.1466018
150. Rossi LE, Avila DE, Spallanzani RG, Ziblat A, Fuertes MB, Lapyckyj L, et al. Histone deacetylase inhibitors impair NK cell viability and effector functions through inhibition of activation and receptor expression. *J Leukoc Biol* (2012) 91:321–31. doi: 10.1189/jlb.0711339
151. Idso JM, Lao S, Schloemer NJ, Knipstein J, Burns R, Thakar MS, et al. Entinostat augments NK cell functions via epigenetic upregulation of IFIT1-STING-STAT4 pathway. *Oncotarget* (2020) 11(20):1799–815. doi: 10.18632/oncotarget.27546
152. García-Martínez E, Smith M, Buqué A, Aranda F, de la Peña FA, Ivars A, et al. Trial Watch: Immunostimulation with recombinant cytokines for cancer therapy. *OncoImmunolog* (2018) 7(6):e1433982. doi: 10.1080/2162402X.2018.1433982
153. Scheller J, Engelowski E, Moll JM, Floss DM. Immunoreceptor Engineering and Synthetic Cytokine Signaling for Therapeutics. *Trends Immunol* (2019) 40(3):258–72. doi: 10.1016/j.it.2019.01.001
154. Kelly PN. Engineering cytokine-receptor pairs. *Science* (2018) 359 (6379):1006B. doi: 10.1126/science.359.6379.1004-p
155. Brehs M, Pötgens AJG, Steitz J, Thewes K, Schwarz J, Conibear AC, et al. Synthetic integrin-binding immune stimulators target cancer cells and prevent tumor formation. *Sci Rep* (2017) 7:17592. doi: 10.1038/s41598-017-17627-0
156. Imamura M, Shook D, Kamiya T, Shimasaki N, Chai SMH, Coustan-Smith E, et al. Autonomous growth and increased cytotoxicity of natural killer cells expressing membrane-bound interleukin-15. *Blood* (2014) 124(7):10818–8. doi: 10.1182/blood-2014-02-556837
157. Kollipara PS, Won DH, Hwang CJ, Jung YY, Yoon HS, Park MH, et al. Enhanced Anti-Cancer Effect of Snake Venom Activated NK Cells on Lung Cancer Cells by Inactivation of NF-κB. *Biomol Ther (Seoul)* (2014) 22 (24):106–13. doi: 10.4062/biomolther.2013.103
158. Yang B, Good D, Mosaiab T, Liu W, Ni G, Kaur J, et al. Significance of LL-37 on Immunomodulation and Disease Outcome. *BioMed Res Int* (2020) 2020:8349712. doi: 10.1155/2020/8349712
159. Bailur JK, Mehta S, Zhang L, Neparidze N, Parker T, Bar N, et al. Changes in bone marrow innate lymphoid cell subsets in monoclonal gammopathy: Target for IMiD therapy. *Blood Adv* (2017) 1(25):2343–7. doi: 10.1182/bloodadvances.2017012732
160. Ocio EM, Fernández-Lázaro D, San-Segundo L, López-Corral L, Corchete LA, Gutiérrez NC, et al. In vivo murine model of acquired resistance in myeloma reveals differential mechanisms for lenalidomide and pomalidomide in combination with dexamethasone. *Leukemia* (2015) 29:705–14. doi: 10.1038/leu.2014.238
161. Hardman C, Ho S, Shimizu A, Luu-Nguyen Q, Sloane JL, Soliman MSA, et al. Synthesis and evaluation of designed PKC modulators for enhanced cancer immunotherapy. *Nat Commun* (2020) 11:1879. doi: 10.1038/s41467-020-15742-7
162. Yokoda R, Nagalo B, Vernon B, Oklu R, Albadawi H, DeLeon T, et al. Oncolytic virus delivery: from nano-pharmacodynamics to enhanced oncolytic effect. *Oncolytic Virother* (2017) 6:39–49. doi: 10.2147/ov.s145262
163. Gong C, Yu X, You B, Wu Y, Wang R, Han L, et al. Macrophage-cancer hybrid membrane-coated nanoparticles for targeting lung metastasis in breast cancer therapy. *J Nanobiotechnology* (2020) 18:92. doi: 10.1186/s12951-020-00649-8
164. Yang C, Li Y, Yang Y, Chen Z. Overview of Strategies to Improve Therapy against Tumors Using Natural Killer Cell. *J Immunol Res* (2020) 2020:8459496. doi: 10.1155/2020/8459496
165. Engeland CE, Grossardt C, Veinalde R, Bossow S, Lutz D, Kaufmann JK, et al. CTLA-4 and PD-L1 checkpoint blockade enhances oncolytic measles virus therapy. *Mol Ther* (2014) 22(11):1949–59. doi: 10.1038/mt.2014.160
166. Siegler EL, Kim YJ, Chen X, Siriwon N, Mac J, Rohrs JA, et al. Combination Cancer Therapy Using Chimeric Antigen Receptor-Engineered Natural Killer Cells as Drug Carriers. *Mol Ther* (2017) 25(12):2507–19. doi: 10.1016/j.ymthe.2017.08.010
167. Vilgelm AE, Richmond A. Chemokins modulate immune surveillance in tumorignesis, metastatsis, and response to immunotherapy. *Front Immunol* (2019) 10:333. doi: 10.3389/fimmu.2019.00333

Conflict of Interest: JS is the scientific co-founder and member of the scientific advisory board of Indapta Therapeutics; however the science presented here is not related to the focus of the company. UM-N is the founder of Conference Fund; however, the science presented here is not related to the focus of the company.

The remaining authors declare that the research was conducted in the absence of any commercial or financial relationships that could be construed as a potential conflict of interest.

Copyright © 2021 Horowitz, Mohammad, Moreno-Nieves, Koliesnik, Tran and Sunwoo. This is an open-access article distributed under the terms of the Creative Commons Attribution License (CC BY). The use, distribution or reproduction in other forums is permitted, provided the original author(s) and the copyright owner(s) are credited and that the original publication in this journal is cited, in accordance with accepted academic practice. No use, distribution or reproduction is permitted which does not comply with these terms.

frontiers in Immunology

PERSPECTIVE
published: 13 May 2021
doi: 10.3389/fimmu.2021.661900

Current Perspectives on the Role of TNF in Hematopoiesis Using Mice With Humanization of TNF/LT System

Violetta S. Gogoleva[1,2]*, *Kamar-Sulu N. Atretkhany*[1], *Arina P. Dygay*[2,3,4], *Taisiya R. Yurakova*[2,3,4], *Marina S. Drutskaya*[1,2] *and Sergei A. Nedospasov*[1,2,4]

[1] Center for Precision Genome Editing and Genetic Technologies for Biomedicine, Engelhardt Institute of Molecular Biology, Russian Academy of Sciences, Moscow, Russia, [2] Department of Immunobiology and Biomedicine, Sirius University of Science and Technology, Sirius, Russia, [3] Engelhardt Institute of Molecular Biology, Russian Academy of Sciences, Moscow, Russia, [4] Department of Immunology, Faculty of Biology, Lomonosov Moscow State University, Moscow, Russia

OPEN ACCESS

Edited by:
Yasuyuki Saito,
Kobe University, Japan

Reviewed by:
Masayuki Yamashita,
The University of Tokyo, Japan
George Kalliolias,
Hospital for Special Surgery,
United States

***Correspondence:**
Violetta S. Gogoleva
violette.gogoleva@gmail.com

Specialty section:
This article was submitted to Cancer Immunity and Immunotherapy, a section of the journal Frontiers in Immunology

Received: 31 January 2021
Accepted: 19 April 2021
Published: 13 May 2021

Citation:
Gogoleva VS, Atretkhany KN, Dygay AP, Yurakova TR, Drutskaya MS and Nedospasov SA (2021) Current Perspectives on the Role of TNF in Hematopoiesis Using Mice With Humanization of TNF/LT System. Front. Immunol. 12:661900. doi: 10.3389/fimmu.2021.661900

TNF is a multifunctional cytokine with its key functions attributed to inflammation, secondary lymphoid tissue organogenesis and immune regulation. However, it is also a physiological regulator of hematopoiesis and is involved in development and homeostatic maintenance of various organs and tissues. Somewhat unexpectedly, the most important practical application of TNF biology in medicine is anti-TNF therapy in several autoimmune diseases. With increased number of patients undergoing treatment with TNF inhibitors and concerns regarding possible adverse effects of systemic cytokine blockade, the interest in using humanized mouse models to study the efficacy and safety of TNF-targeting biologics *in vivo* is justified. This Perspective discusses the main functions of TNF and its two receptors, TNFR1 and TNFR2, in steady state, as well as in emergency hematopoiesis. It also provides a comparative overview of existing mouse lines with humanization of TNF/TNFR system. These genetically engineered mice allow us to study TNF signaling cascades in the hematopoietic compartment in the context of various experimental disease models and for evaluating the effects of various human TNF inhibitors on hematopoiesis and other physiological processes.

Keywords: cytokines, cytokine blockade, steady-state hematopoiesis, emergency hematopoiesis, humanized mouse models

INTRODUCTION TO HEMATOPOIESIS

Hematopoiesis is the process of blood cell development that in vertebrates is initiated early during embryogenesis and may be divided into 3 phases or so-called distinct waves of hematopoiesis.

The first (or **primitive**) wave takes place in the yolk sac starting in mice at embryonic day 7.5 (E7.5) and generates unipotent blood cell types (1). **The second** (or **pro-definitive**) wave occurs in

the yolk sac, embryo proper and allantois of the mouse embryo and gives rise to multipotent progenitors (2). **The third wave** of hematopoiesis represents **definitive** hematopoiesis and is dependent on the activity of hematopoietic stem cells (HSCs), which are the basic units of the adult hematopoietic system. HSCs generated in the embryonic aorta-gonad-mesonephros region first colonize the fetal liver (E10.5) and then shortly before birth (E16) migrate to the bone marrow (BM), where the majority of HSCs reside to sustain steady state hematopoiesis (3).

HSCs are multipotent, self-renewing cells capable of differentiating into all mature blood cell lineages over the lifespan of the animal. Lineage choice may be directed both intrinsically and extrinsically *via* activation of transcription factors or extrinsically by cytokines (4). The majority of HSCs are quiescent under steady-state conditions, and few HSCs cycle to sustain hematopoiesis (5). In order to maintain hematopoietic homeostasis and to prevent development of malignancies, the self-renewal and differentiation capacities of HSCs are tightly regulated. This is, at least partly, achieved by the specialized network of interactions between distinct cell types (6, 7) and secreted factors (8, 9) in the BM niche that maintains HSC activity in steady-state conditions.

However, in the case of systemic infections and pathological conditions, such as myeloablation after chemo- or radiotherapy, some HSCs may respond and exit their quiescent state. These 'activated' HSCs contribute to the pool of hematopoietic progenitor cells, which will undergo further differentiation in order to replenish the population of immune cells being in high demand at the sites of inflammation in the process of so-called **emergency hematopoiesis**. This is possible because hematopoietic stem and progenitor cells (HSPCs) express Toll-like receptors (10) and cytokine receptors (11) and, thus, can respond to inflammatory signals. Activation of TLR signaling in HSPCs not only drives myeloid cell differentiation (10), but also leads to production of cytokines, which regulate myeloid differentiation and HSPC proliferation (12). HSPCs may respond to cytokines released during inflammation either systemically or locally by cells in the hematopoietic microenvironment or BM niche. Indeed, it was shown that HSPCs express various cytokine receptors, including IL-1R (13), IL-6Rα, as well as both TNF receptors, TNFR1 and TNFR2 (12).

As mentioned above, proinflammatory cytokines are critical components of inflammation-induced myelopoiesis. However, inflammatory signals may also be implicated in the maintenance of homeostatic hematopoiesis. During embryonic development proinflammatory cytokines control HSPC specification in the pro-definitive wave of hematopoiesis (14). Moreover, proinflammatory cytokines may regulate adult hematopoiesis and maintain the balance between HSC dormancy and lineage commitment (15). This question is important because systemic and long-term anti-cytokine therapy is being applied to treat an increasing number of conditions, including autoimmune disorders. One of the proinflammatory cytokines implicated in hematopoiesis is TNF, which we discuss in the context of humanized mouse models in this Perspective.

TNF IN STEADY-STATE HEMATOPOIESIS

TNF is a pleiotropic cytokine involved in inflammation, development of secondary lymphoid organs and immune regulation. TNF is produced as a transmembrane protein and can be proteolytically cleaved into a soluble form. TNF exerts its functions *via* two distinct receptors – TNFR1 and TNFR2 (16). Both receptors also may interact with soluble ($LT\alpha_3$) and membrane-bound ($LT\alpha_2\beta_1$) lymphotoxins, respectively (17). Interestingly, TNF may play a role both in embryonic and in adult hematopoiesis (**Figure 1**).

The role of TNF during fetal hematopoiesis was mostly studied in zebrafish. These studies revealed that TNF derived from primitive neutrophils binds to TNFR2 on endothelial cells resulting in the upregulation of Notch ligand Jagged1a, which in turn binds to Notch1a receptor on the neighboring hemogenic endothelium triggering HSC fate specification. Moreover, TNF/TNFR2 axis also activates canonical NF-κB pathway in hemogenic endothelium, which triggers a transcriptional program to establish HSC generation (18). Of note, not only TNF but also other inflammatory stimuli such as TLR4-MyD88 signaling or G-CSF may lead to NF-κB activation required for HSC development (29). Interestingly, inflammatory signaling represents a highly conserved pathway regulating the HSC development. Studies in E9.5 mouse embryos revealed that hematopoietic cluster cells and endothelial cells respond to IFNγ and to a lesser extent to TNF stimulation. The most likely source of TNF in the mouse embryo is the population of primitive $F4/80^+$ macrophages, similar to the situation in zebrafish embryo (30). However, the precise contribution of TNF to mammalian HSC development is not completely understood. Taken together, TNF signaling may be required for HSC emergence in the developing embryo *via* activation of evolutionarily conserved signaling pathways, but it might be partially redundant with other inflammatory stimuli.

Many studies have been performed to examine the role of TNF in the adult hematopoiesis; however, most of these have relied on cell culture and/or bone marrow chimeras, which could indirectly affect HSPC phenotype and functions. Another challenge in understanding the role of TNF in steady-state conditions is due to its capacity to induce systemic inflammation when administered *in vivo* which in turn may activate stress-induced hematopoiesis thus obscuring TNF contribution to hematopoiesis. Therefore, in this section we will focus on *in vivo* studies using gene-deficient mice. TNF deficiency did not alter the number of $Lin^-Sca\text{-}1^+c\text{-}kit^+$ (LSK) in the BM, consisting mostly of lineage-biased multipotent progenitors (19). In early studies TNFR1-deficient bone marrow was characterized by increased number of LSK (22). However, examination of purified $LSKFLT3^-$ HSPCs revealed no differences in the numbers of HSPC isolated from the adult BM of TNFR1/TNFR2 double knockout mice (31). Hence, it is likely that TNF does not affect HSPC compartment under steady-state conditions *in vivo*.

Regarding the differentiation of HSCs to more committed progenitors, TNFR1-deficient mice showed a decrease in pre-B cell compartment and an increase in myeloid progenitors (32).

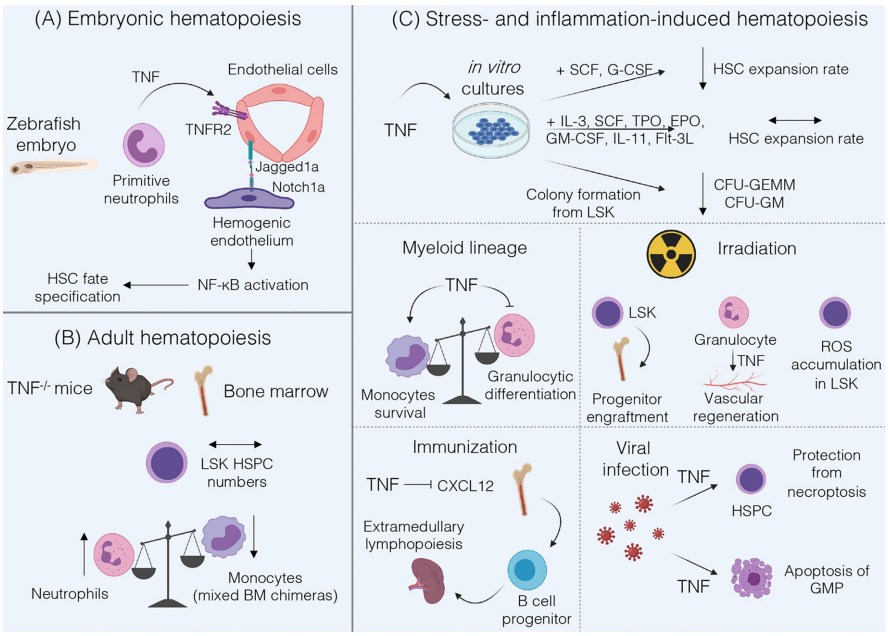

FIGURE 1 | Summary of TNF functions in hematopoiesis. **(A)** During fetal hematopoiesis in zebrafish TNF/TNFR2 signaling is required to establish HSC fate *via* activation of Notch and NF-kB signaling (18). **(B)** Bone marrow of adult TNF-deficient mice is characterized by normal LSK HSPC numbers and by an increase in Gr-1$^+$ neutrophils (19). Mixed *Tnf*$^{-/-}$ and *Tnf*$^{+/+}$ BM chimeras underrepresent TNF-deficient monocytes (20). **(C)** TNF may inhibit HSC expansion when cultured with SCF and G-CSF, but not in cytokine-rich medium (21). Addition of TNF to LSK cultures inhibits formation of CFU-GEMM and CFU-GM (22). TNF promotes monocytes survival (20) and inhibits proliferation and differentiation of granulocyte progenitors (19, 23, 24). Under inflammatory conditions induced by irradiation TNF may be beneficial for progenitor engraftment (25) but stromal cell-derived TNF induces ROS accumulation in HSPCs (26), and granulocyte-derived TNF is involved in vascular regeneration (27). Following immunization, TNF may suppress CXCL12-dependent retention of B cell progenitors in the bone marrow leading to their migration (28). In the case of viral infections TNF protects HSPCs from necroptosis, enhances myelopoiesis and induces apoptosis of GMP (21).

Accordingly, TNF-deficient mice demonstrated an increase in the number of Gr-1$^+$ neutrophils both in the BM and in peripheral blood (19). Transcriptome analysis of monocytes and their BM precursors revealed an increase in TNF expression upon differentiation of Ly6C^{hi}/Ly6C^{int} monocytes into Ly6C^{lo} monocytes (20). Therefore, TNF may control granulocyte number in the blood and BM and support monocytic differentiation *in vivo*.

TNF IN STRESS- AND INFLAMMATION-INDUCED HEMATOPOIESIS

Numerous studies on the role of TNF in HSPC functions relied on *in vitro* and *in vivo* colony formation assays together with the assessment of reconstitution potential, engraftment and survival abilities of multipotent progenitors upon transplantation into irradiated recipient mice. However, results obtained from these studies should be carefully interpreted since these setups may affect HSPC proliferation, survival, self-renewal and differentiation. We will discuss some experiments and their possible applicability to hematopoietic compartment.

Studies with competitive co-transplantation of TNFR1$^{-/-}$ TNFR2$^{-/-}$ CD45.2$^+$ and wild-type (WT) CD45.1$^+$ BM cells into lethally irradiated congenic CD45.1$^+$CD45.2$^+$ WT recipients showed enhanced activity of TNFR1$^{-/-}$TNFR2$^{-/-}$ HSCs as determined by long-term reconstitution by TNFR-deficient HSCs following transplantation. Moreover, *in vivo* administration of TNF to WT mice led to a decrease in BM cellularity and to reduction in HSC cycling activity in a competitive transplantation assay (31). These data suggest that TNF blockade may be beneficial for post-transplantation reconstitution and also supports the idea that TNF may suppress HSC activity. In contrast, transplantation of bone marrow cells from 6 months old TNFR1-deficient mice into lethally irradiated recipients showed reduced repopulating ability of TNFR1$^{-/-}$ BM cells as compared to WT cells (32). However, this effect was shown on non-purified HSPCs and under long-term transplantation conditions that may affect the outcome of the experiment. TNF does not inhibit expansion of highly purified Lin$^-$Sca-1$^+$c-kit$^+$Flk2$^-$CD150$^+$CD48$^-$ HSCs in medium supplemented with IL-3, SCF, TPO, EPO, GM-CSF, IL-11 and Flt3-L, or so-called cytokine-rich medium, regardless of TNF concentration. Under cytokine-poor conditions (medium supplemented with SCF and G-CSF only) HSC expansion rate upon addition of TNF was significantly decreased (21). Similar findings were reported by Pronk et al. when TNF was added to the culture of LSK cells (31). Importantly, studies by Yamashita et al. revealed that this effect was due to the inhibition of autophagy by TNF, which sensitized HSCs to cell death in

cytokine-deprived environment (21). Taken together, HSCs appear to be resistant to TNF cytotoxicity but this resistance may be changed by the environmental stress.

Addition of exogenous TNF to bone marrow cultures of LSK resulted in reduced numbers of large-sized colonies, such as CFU-GEMMs (colony-forming unit – granulocyte, erythroid, macrophage, megakaryocyte) and CFU-GMs (granulocyte/macrophage colony forming units), in methylcellulose assay (22). LSK isolated from TNF-deficient mice gave rise to an increased number of splenic colony-forming units in lethally irradiated recipient mice (19). Experiments with TNFR1 and TNFR2 agonists demonstrated that TNFR2 is essential for TNF-mediated inhibition of colony formation of early $Lin^{-}Sca\text{-}1^{+}$ progenitors, while addition of TNFR1 agonist had no significant effect on the number of $Lin^{-}Sca\text{-}1^{+}$ proliferative clones (23). Thus, TNF may inhibit formation of CFU-GEMM and CFU-GM colonies and differentiation potential of multipotent progenitors, presumably *via* TNFR2.

Evaluation of TNF effects on myeloid lineage commitment revealed that addition of TNF or TNFR1 agonists resulted in a decrease in G-CSF-induced colony formation and in inhibition of G-CSF expression by BM cultures (23). This was further supported *in vitro* in TNF-deficient long-term bone marrow cultures, which were characterized by increased proliferative potential of granulocytic progenitors and increased numbers of CFU-GMs within sorted LSK population, as compared to WT BM cultures (19). Consistent with *in vitro* data, CFU-GM formation was reduced in WT-recipient mice reconstituted with TNF-deficient BM, suggesting a possible role of TNF, expressed by hematopoietic and not by stromal cells, in inducing cell death at the GMP stage (33). This is also in agreement with data showing elimination of GMPs by TNF in a dose-dependent manner (21). Next, TNF was demonstrated to block granulocytic differentiation and IL-3-dependent proliferation of granulocyte-committed cells (24). At the same time, an autonomous effect of TNF on monocytes was proposed. Specifically, TNF is required for monocyte survival *in vivo* (20). Thus, TNF stands at the crossroad of myeloid lineage commitment *via* negatively affecting granulocytic cell differentiation and driving the survival of monocytes. Interestingly, these findings suggest possibilities to control the differentiation of myeloid progenitors. For example, TNF was shown to directly upregulate a central transcription factor for myeloid lineage commitment, PU.1, in HSPC *in vivo* during acute inflammation (34). Moreover, in some abnormal hematopoiesis conditions, such as clonal hematopoiesis associated with aging, TNF blockade may help to overcome TET2-mutant HSPC skewing toward myeloid lineage and the formation of CFU-GMs (35).

Other studies revealed that addition of TNF to the LSK cultures negatively regulated both long-term and short-term reconstituting activity after transplantation of LSK into lethally irradiated recipient mice (36). However, TNF produced by BM microenvironment is required for long-term engraftment and survival of purified LSK in allogeneic and syngeneic recipients (37). This is in line with the fact that the engraftment of Lin^{-} BM cells from TNFR1- and TNFRs-deficient donors in wild-type recipients was defective suggesting a stimulatory role of TNF in successful progenitor engraftment. Interestingly, homing of the engrafted progenitors to the BM was primarily mediated by TNFR1 (25). On the other hand, total body irradiation and inflammation within BM was associated with elevated levels of TNF. Subsequently, TNF induced ROS accumulation in LSK leading to impairment of their reconstitution ability. Addition of TNFR1 antagonistic peptide to LSK cultures inhibited ROS accumulation suggesting that TNFR1 blockade prior to transplantation may lead to improved reconstitution capability (26). Altogether, more precise *in vivo* studies with defined protocols of total body irradiation and transplantation are needed to identify the role of TNF in the engraftment and survival of HSPCs. For example, TNF may contribute to regeneration of BM niche after HSC transplantation, since TNF-deficient mice displayed reduced number of BM endothelial cells upon myeloablation with a single injection of 5-fluorouracil. Furthermore, $Gr1^{+}CD115^{-}$ granulocyte-derived TNF promoted vascular regeneration following transplantation (27). In the context of hematological malignancies, such as myeloproliferation, inflammation may be implicated in the disruption of BM microenvironment. $Flt3^{ITD/ITD}$ mice, harboring the most common somatic mutation in patients with acute myeloid leukemia, were shown to upregulate TNF production by endothelial cells in the BM niche, which subsequently may lead to suppression of HSC activity. Treatment of $Flt3^{+/+}$ and $Flt3^{ITD/ITD}$ mice with Etanercept resulted in partial rescue of $LSKCD150^{+}CD48^{-}$ engraftment capacities (38).

As a consequence of inflammation, TNF may mobilize B cell progenitors from BM to peripheral tissues by suppressing their CXCL12-induced retention in the BM. This mobilization establishes extramedullary lymphopoiesis possibly needed for resolution of inflammation (28). Contribution of TNF to emergency myelopoiesis was clearly demonstrated by Yamashita et al. (21). In a model of poly(I:C)-induced inflammation, TNF, on one hand, induced NF-kB activity, which protected HSPCs from inflammation-induced necroptosis and, on the other hand, promoted myelopoiesis and induced apoptosis of GMPs (21). This effect may be protective in pathogenesis of some viral infections, in which case GMPs may act as the latent reservoirs for viruses in the BM and should be eliminated (39).

Defects in hematopoiesis may lead to the development of hematologic disorders. Although the exact role of TNF in different hematological diseases remains incompletely understood, elevated levels of TNF were found in patients suffering from myeloid leukemia (40) and myelodysplastic syndromes (41, 42), Fanconi anemia (43), Hodgkin's disease (44) and Non-Hodgkin lymphoma (45).

Moreover, since TNF inhibitors are widely used to treat autoimmune disorders, it is important to address possible side effects of anti-TNF therapy. Indeed, hematological complications were reported in patients on TNF blockade (**Table 1**). For example, a case report was published showing pancytopenia

TABLE 1 | Hematological complications from systemic TNF blockade.

Adverse effect	Diagnosis	Treatment	Brief report	Onset upon anti-TNF treatment	Reference
Pancytopenia	Juvenile idiopathic arthritis	Etanercept	2/61 cases	After 0,5-12 months	(46)
	Scleroderma	Infliximab	45F case Previously diagnosed with anemia, ANA positive	After 2 weeks	(47)
	RA	Infliximab + MTX (Previously leflunomide)	66M case BM hypoplasia	After 10 days	(48)
	Indeterminate colitis	Infliximab + antibiotics	32F case	After 6 days	(49)
	RA	Etanercept	1/1073 case	NR	(50)
	RA	Etanercept + MTX	68F case	After 3 weeks	(51)
Aplastic anemia	RA	Etanercept	78M case	After 16 weeks	(52)
Thrombocytopenia	Psoriatic arthritis	Infliximab	1/16 case	After 12 weeks	(53)
	Crohn's disease	Infliximab	15M case Platelet associated autoantibodies positive	After 6 days	(54)
	RA	Etanercept	2/1073 cases	NR	(50)
	RA	Etanercept	44F case Autoantibodies negative	After 1,5 weeks	(55)
	RA	Infliximab + MTX	56F case ANA positive dsDNA autoantibodies positive	After 28 months	
	Scleroderma overlap/rheumatoid arthritis	MTX + Prednisone + Infliximab	44F case Anticardiolipin antibodies positive ANA positive Anticentromere antibodies positive	After 13 months	(56)
	Crohn's disease	Infliximab then Adalimumab (Previously metronidazole and azathioprine)	42F case Platelet associated antibodies positive Increased BM megakaryocytes Anticardiolipin antibodies negative	30 weeks after Infliximab treatment 1 week after Adalimumab treatment	(57)
	Psoriatic arthritis	Etanercept	61M case Autoantibodies negative	After 2 months	(58)
	Psoriasis	Etanercept	1/39 case ANA positive	After 9 weeks	(59)
	Psoriatic arthritis	Infliximab	1/26 case Autoantibodies negative	After 29 weeks	
	Psoriasis	Infliximab	2/26 cases ANA positive Antiplatelet antibodies positive	After 30 weeks	
	Crohn's disease	Infliximab	75M case	After 14 weeks	(60)
	Ulcerative colitis	Adalimumab + azathioprine + mesalazine	54F case Anemia Autoantibodies negative	After 4 years	(61)
Thrombocytopenia and leucopenia	Juvenile idiopathic arthritis	Etanercept	2/95 cases	NR	(62)
Thrombocytopenia and neutropenia	RA	MTX + Infliximab	60F case BM hypoplasia Autoantibodies negative	After 7 weeks	(63)
Bone marrow aplasia with pancytopenia	RA	Etanercept (Previously MTX + folic acid + Hydroxychloroquine; Leflunomide and Adalimumab discontinued months before Etanercept)	62F case Autoantibodies negative	After 23 days	(64)

(Continued)

TABLE 1 | Continued

Adverse effect	Diagnosis	Treatment	Brief report	Onset upon anti-TNF treatment	Reference
Neutropenia	RA	Etanercept	1/208 case	NR	(53)
	RA	Etanercept	2/207 cases		
	Spondyloathropathy/ Crohn's disease	Infliximab	20M case Neutrophil-associated antibodies	After 4 weeks	(65)
	RA	Adalimumab Etanercept Infliximab	3/21 cases Adalimumab 13/75 cases Etanercept 3/23 cases Infliximab 7/65 cases ANA positive	After 1 week – 26 months	(66)
	RA	Adalimumab + MTX	53F case T-cell lymphocytosis (large granular lymphocytes)	After 13 months	(67)
	Sacroiliitis	Salazopyrine + MTX + Etanercept	37F case	After 6 months	(68)
	RA	Etanercept (Previously MTX)	57F case Asymptomatic neutropenia during MTX Increased BM immature granulocyte production ANA positive Neutrophil-associated antibodies negative	After 7 weeks	(69)
	Psoriatic arthritis	Etanercept (Previously MTX)	61M case Persistent leucopenia Neutropenia during MTX Normal BM hematopoiesis ANA positive Neutrophil-associated antibodies negative	NR	
	RA	Etanercept	50F case Previous asymptomatic neutropenia Normal BM hematopoiesis ANA positive Neutrophil-associated antibodies negative	After 17 days	
	RA	Adalimumab + MTX + Prednisone	55F case ANA negative dsDNA antibodies negative	After 1 month	(70)
	RA Psoriatic arthritis Ankylosing spondylitis	Adalimumab 6/31 Etanercept 49/267 Infliximab 14/69	56/298 cases 7/31 case 6/38 cases	NR	(71)
	RA Ankylosing spondylitis	Etanercept + MTX Etanercept	64F case 36M case	After 2 weeks After 2 months	(72)
	RA	Etanercept then Etanercept re-challenge then Adalimumab	65M case	3 months after Etanercept onset 2nd neutrophil drop after Etanercept re-challenge Modest neutrophil drop after Adalimumab treatment	
	RA	Etanercept then Etanercept re-challenge then 2nd Etanercept re-challenge	71F case	6 months after Etanercept treatment 16 months after Etanercept re-challenge 8 weeks after 2nd Etanercept re-challenge	
	RA	Etanercept (Previously hydroxychloroquine + prednisolone)	42F case	After 4 injections	

(Continued)

TABLE 1 | Continued

Adverse effect		Diagnosis	Treatment	Brief report	Onset upon anti-TNF treatment	Reference
		75/235 Crohn's disease 21/46 Ulcerative colitis	Adalimumab Certolizumab Infliximab Golimumab + MTX/azathioprine/5-ASA	58/157 cases Adalimumab 2/6 cases Certolizumab 36/117 cases Infliximab 0/1 Galimumab 1/5 + MTX 77/188 + azathioprine 37/65 + 5-ASA	After 1 day – 6 years Median 1 year	(73)
Neutropenia and leucopenia		Ankylosing spondylitis	Etanercept + butazolidine then Etanercept re-challenge then Infliximab	50M case	3 weeks after Etanercept treatment 3 weeks after Etanercept re-challenge After 2nd Infliximab infusion	(74)
Leucopenia		RA	Etanercept	4/1073 cases	NR	(50)
Myelodysplastic syndrome		RA	Etanercept	1/1073 case	NR	(50)
Lymphoma	NR	RA	Etanercept	3/1073 cases	NR	(50)
	Cutaneous T-cell lymphoma	Psoriatic arthritis	Etanercept	69M case	Erythroderma after 18 months	(75)
	Systemic anaplastic large cell lymphoma (ALCL)	Crohn's disease	Infliximab	81F case	After 5 months	
	Chronic myeloid leukaemia (CML)	RA	Infliximab + MTX	56F case	After 6 months	(76)
	16 non-Hodgkin's lymphomas 1 Hodgkin's disease 1 Type B1 thymoma	15/18 RA 2/18 Psoriatic arthritis 1/18 NS	Etanercept 9/18 +MTX 4/18 prior MTX 4/18 prior other immunosuppressive drugs	18 cases Median age 64 years 2 cases non-Hodgkin's lymphoma recursion 1 case nodular sclerosing Hodgkin's disease recursion	After 2-52 weeks	(77)
	5 non-Hodgkin's lymphomas 3 Hodgkin's lymphomas	3/8 RA 5/8 Crohn's disease	Infliximab 2/8 +MTX 1/8 + 6-mercaptopurine	8 cases Median age 62 years	After 2-44 weeks	
	Non-Hodgkin's lymphomas Hodgkin's lymphomas	RA RA	Infliximab Etanercept	6/5233 cases 5/2149 cases	NR	(78)
	Hodgkin-like lymphoproliferative disorder	Ulcerative colitis	Infliximab	74M case	After 3 months	(79)
	4 Hodgkin lymphomas 4 B-cell lymphomas 1 metastatic lymphoma	Crohn's disease	Infliximab	9/1541 cases	NR	(80)

'+' treatments were taken concomitantly. ANA, anti-nuclear antibody; BM, bone marrow; MTX, methotrexate; NR, not reported; NS, not specified; RA, rheumatoid arthritis.

after treatment with Infliximab (47). Furthermore, side effects of Etanercept [which also neutralizes both $LT\alpha_3$ and $LT\alpha_2\beta_1$ (17)] treatment on hematopoietic cells have been reported including aplastic anemia (52), thrombocytopenia (55), and bone marrow aplasia with pancytopenia (64). Interestingly, a common phenomenon in patients receiving anti-TNF therapy is the development of neutropenia (81). Apart from that, some lymphoproliferative disorders were reported. For example, treatment of rheumatoid arthritis and inflammatory bowel disease (IBD) patients with Etanercept or Infliximab, respectively, led to formation of cutaneous and systemic T-cell lymphomas (75). A case of Hodgkin-type lymphoproliferative lesions was reported for an IBD patient treated with Infliximab for a 6-month period (79).

Altogether, TNF may play a crucial role in inflammation-induced hematopoiesis and may be implicated in the pathogenesis of some hematologic disorders. Anti-TNF therapy may lead to rare but severe side effects affecting hematopoietic compartment and resulting in the development of hematological complications and even malignancies. The exact mechanisms of these side effects are not well understood and should be addressed in the future using humanized mouse models.

HUMANIZED MICE AS THE TOOLS TO STUDY HEMATOPOIESIS AND TO EVALUATE THE CONSEQUENCES OF SYSTEMIC CYTOKINE ABLATION

To identify the effects and to evaluate the efficacy and safety of clinically available or novel human TNF (hTNF) inhibitors proper animal models should be generated and validated. Importantly, in spite of a conservative nature of TNF family of cytokines and their corresponding genes, most hTNF inhibitors do not block mouse TNF (82). Therefore, various panels of humanized mice that express hTNF and/or TNFRs are required to facilitate the research (**Table 2**). Such preclinical models were first generated in 1991 by G. Kollias group, when the first mice with overexpression of human TNF were reported (83).

Mice With the Overexpression of Human TNF

The very first TNF humanized model was a transgenic mouse with the overexpression of TNF due to intentional dysregulation of TNF mRNA half-life (83). In general, overexpression of cytokines in animal models is a powerful tool to study molecular mechanisms associated with increased cytokine production (98). It is well established that dysregulated TNF production is detrimental in various autoimmune diseases including rheumatoid arthritis, psoriasis and IBD (99). Mice with human TNF overexpression (hTNF Tg mice with a high transgene copy number and dysregulated control) start to develop severe polyarthritis as early as 3-4 weeks after birth with similar characteristics observed in rheumatoid arthritis patients. Administration of antibodies to hTNF Tg mice led to the suppression of arthritis (83). Moreover, TNF overexpression in hTNF Tg mice led to increased incidence of spontaneous spinal disc herniation, which is involved in the development of acute radicular pain (84). These hTNF Tg mice displayed a decrease in hemoglobin associated with mild microcytic hypochromic anemia at the age of 9 weeks. Furthermore, TNF overexpression was associated with a decrease in the frequency of Sca-1$^+$ progenitor cells and granulocytes with concurrent increase in the frequency of cells of both lymphoid and monocytic origin in the bone marrow (85). In summary, constitutive TNF overexpression is associated with the development of spontaneous autoimmune conditions. hTNF Tg mice served as an excellent model for associated disorders, such as progressive rheumatoid arthritis, although physiological relevance of using these mice in order to delineate the *in vivo* effects of systemic TNF inhibition on other functions was limited. To overcome the limitations of non-physiological levels of systemic TNF overproduction, other mouse models, such as tissue-specific, inducible and low copy number hTNF transgenic mice were developed.

Approaches to investigate tissue-restricted overexpression of human TNF in mice were also pioneered by G. Kollias group (88). For example, hTNF overexpression by T cells led to severe systemic effects, for example, CD2-hTNF Tg mice developed lethal progressive weight loss but no arthritis. hTNF overexpression by T cells also resulted in vascular thrombosis, tissue necrosis and lymphoid tissue abnormalities. Particularly, mice were characterized by reduced thymic cellularity and enlarged mesenteric lymph nodes that contained almost no lymphocytes. Overexpression of hTNF in astrocytes or neurons resulted in severe neurologic disease characterized by ataxia, seizures and relapsing hind limb paralysis (89). To delineate the contribution of soluble versus transmembrane TNF, mice that overexpress transmembrane human TNF in astrocytes (GFAP-tmTNF) or neurons (NFL-tmTNF) were engineered. Surprisingly, only astrocyte-specific overexpression of tmTNF was sufficient to trigger the development of neurologic disease (89). Thus, astrocytes appeared to be the source of pathogenic hTNF in a model of neuroinflammation.

TABLE 2 | Humanization of TNF/LT system in mice as a tool to study human hematopoiesis.

Humanized mouse line		Expression specificity	Hematopoiesis-unrelated phenotype	Hematopoiesis-related phenotype	References
hTNF Tg (Tg197)	High copy number	Systemic	Severe polyarthritis as early as 3-4 weeks after birth Spontaneous spanial disc herniation	Mild microcytic hypochromic anemia Decrease in frequency of Sca1$^+$ progenitor cells and granulocytes Increased frequency of lymphoid and monocytic origin in the bone marrow	(83–85)
	Low copy number	Systemic	Progressive arthritis at a later age Reduced body weight Increased metabolic rate Restricted motor activity		(86)
ihTNFtg	Doxycycline-inducible	Systemic	Psoriatic arthritis Keratinocyte activation Joint and skin inflammation		(87)
CD2-TNF		T cell	Progressive weight loss Vascular thrombosis Tissue necrosis Lymphoid tissue abnormalities Reduced thymic cellularity		(88)

(Continued)

TABLE 2 | Continued

Humanized mouse line	Expression specificity	Hematopoiesis-unrelated phenotype	Hematopoiesis-related phenotype	References
		Enlarged mesenteric lymph nodes almost without lymphocytes		
GFAP-wtTNF	Astrocytes	Lethal neuroinflammation Ataxia, imbalances, seizures, relapsing hind limb paralysis Diminished weight gain		(89)
GFAP-tmTNF		Severe neuroinflammation Complete hind limb paralysis Normal weight gain		
NFL-wtTNF	Neurons	Severe neuroinflammation Hind leg paralysis		
NFL-tmTNF		No abnormalities		
hTNF/LT Tg	Systemic	Thymic atrophy Impaired transition of DN1 thymocytes to the DN2		(90)
hTNFR1 Tg	Systemic	Prophylactic administration of TNFR1 antagonist leads to EAE amelioration and delayed disease onset		(91)
hTNFKI	Systemic	Pharmacological TNF inhibition with Etanercept, Infliximab and Adalimumab inhibits germinal center formation upon SRBC immunization Pharmacological TNF neutralization with Infliximab results in loss of mycobacterial infection resistance in *M. tuberculosis* infection Pharmacological TNF inhibition with Etanercept or Infliximab reduces transplantable tumor growth of MCA205 fibrosarcoma and MDSC accumulation Pharmacological TNF neutralization with Infliximab protects mice from collagen antibody-induced arthritis Exacerbated disease and decreased Treg numbers in EAE	Pharmacological TNF inhibition decreases differentiation of $CD11b^+$ cells into $Ly6C^+$ monocytes and expression of genes encoding anti-apoptotic proteins *in vitro*	(82, 92–95)
hTNF x hTNFR2KI	Systemic (with the option of Cre-mediated hTNFR2 deletion in specific cell type)	Disease score and Treg numbers comparable to wild type mice in experimental autoimmune encephalomyelitis hTNFR2 deletion in $FoxP3^+$ Tregs results in EAE exacerbation and malfunction of Tregs		(95)
hu/mTNFR1-k/i	Systemic	Treatment with TNFR1 antagonist protects cholinergic neurons against cell death and improves memory performance in a model of NMDA-induced neurodegeneration Treatment with TNFR1 antagonist inhibits EAE development and demyelination		(96, 97)
hu/mTNFR2-k/i	Systemic	Treatment with TNFR2 agonist protects cholinergic neurons against cell death and improves memory performance in a model of NMDA-induced neurodegeneration		(96)

The next step in the generation of hTNF transgenic mice was a low transgene copy number model characterized by low circulating levels of hTNF (86). In this case mice developed progressive arthritis at an older age, however, increased TNF production was also associated with reduced body weight, increased metabolic rate and restricted motor activity. This is similar to symptoms of rheumatoid cachexia in humans; therefore, these mice also represent a useful model to study conditions associated with elevated TNF production (100).

To overcome limitations of constitutive TNF overexpression, mice with reversible, doxycycline-inducible hTNF overexpression were generated. Two weeks after doxycycline administration, hTNF Tg mice developed psoriatic arthritis characterized by keratinocyte activation, joint and skin inflammation (87). Interestingly, signs of inflammation in this model were observed exclusively in the digits and, to a lesser extent, in the skin and ankles, unlike in mice with systemic TNF overexpression.

Another approach to generate mice with TNF overexpression was used by Liepinsh et al. (90). In this study mice with a large human genomic segment comprising hTNF and its two closest homologues, lymphotoxin α and β, were generated. Natural genomic context allowed hTNF/hLT genes to be expressed in response to physiological stimuli under the control of intrinsic

regulatory elements. These mice demonstrated thymic atrophy and affected thymic T cell development with impaired thymocytes differentiation. Taken together, TNF humanized mouse models that partially mimic inflammatory conditions in patients with autoimmune disorders, such as rheumatoid arthritis and psoriasis, were generated and evaluated. Furthermore, to address the efficacy and possible side effects of TNF/TNFRs inhibitors in other disease models, humanized mice with regulated and cell type-specific hTNF expression were also established.

Mice With Humanization of TNF and TNFR2

Humanized TNF knock-in (hTNFKI) mice, in which case the mouse *Tnf* gene was substituted by its human ortholog, were generated using embryonic stem cell technology. They were used as a platform to study the effects of hTNF blockade in various disease models, including infectious, autoimmune, toxicity and transplantable tumor models (92, 93, 101, 102). Also, the efficacy of a novel myeloid-specific TNF inhibitor MYSTI in blocking hTNF and its effects in mouse models of LPS/D-galactosamine-induced hepatoxicity and collagen antibody-induced arthritis were demonstrated using these hTNFKI mice (93, 102). Additionally, these engineered mice allowed investigators to compare clinically available hTNF inhibitors such as Infliximab, Etanercept and Adalimumab (82). Furthermore, TNF ablation by pharmacological neutralization in hTNFKI mice led to the loss of the resistance to mycobacterial infection and to increased bacterial burden in the lungs (92). hTNF inhibition decreased tumor growth and MDSC accumulation in transplantable MCA 205 fibrosarcoma model, indicating a pro-tumorigenic function of TNF (94). Overall, hTNFKI mice are a useful tool to assess multiple effects of human TNF inhibition in various disease models, including adverse effects of TNF neutralization on hematopoietic compartment. To delineate the role of TNF inhibition with clinically approved blockers in myeloid cell differentiation, we isolated BM cells from hTNFKI mice, cultured them in the medium supplemented with GM-CSF and IL-4 with the addition of Infliximab and analyzed immature myeloid cell differentiation after 5 days of culturing (**Figure 2A**). We observed that TNF inhibition with Infliximab shifted differentiation of immature myeloid cells *in vitro*. Thus, TNF neutralization led to an increase in the frequency of $Ly6G^{+}Ly6C^{low}$ granulocytes and to a decrease in the frequency of $Ly6G^{-}Ly6C^{high}$ monocytes (**Figure 2B**). Since TNF is important for survival of monocytes (20), we hypothesized that decreased frequency of monocytes upon anti-TNF treatment was due to induction of apoptosis. To verify that, we analyzed expression of genes encoding anti-apoptotic proteins in purified $Ly6G^{-}Ly6C^{high}$ monocytes and found down-regulation of *Bcl2*, *Bcl2a1a* and *Bcl2l1* upon treatment with Infliximab (**Figure 2C**). Altogether, TNF blockade with Infliximab in BM cultures from hTNFKI mice inhibited the differentiation of immature myeloid cells into monocytes probably due to the induction of apoptosis.

Earlier biochemical studies indicated that hTNF can efficiently bind to TNFR1, but not to TNFR2 (103, 104). Indeed, inefficiency of hTNF interaction with murine TNFR2 led to disease exacerbation and decrease in Treg numbers in the periphery and CNS in a mouse model of multiple sclerosis (EAE), in which case TNFR2 signaling is protective (95). Therefore, it was desirable to generate a mouse with humanization of TNFR2 to provide efficient TNF-TNFR2 signaling. Mice were genetically designed to include two LoxP sites into human *TNFR2* locus, which allowed conditional Cre-mediated deletion of TNFR2 extracellular part in the desired cell type. These doubly humanized hTNF x hTNFR2KI mice showed EAE disease severity and Treg numbers comparable to wild-type mice, confirming the restoration of protective TNF/TNFR2 signaling. Cre-mediated genetic deletion of TNFR2 gene in Treg cells resulted in EAE exacerbation and malfunction of Treg cells. Intrinsic TNFR2 signaling was important for the maintenance of suppressive functions of Tregs by sustaining expression of Treg signature molecules, such as FoxP3, CD25, CTLA-4 and GITR (95). Further, hTNFR2 agonists applied to Treg cells from doubly humanized mice induced increased Treg cells proliferation (95).

Dong et al. also generated useful TNF receptor humanized mouse models, namely hTNFR1 knock-in and hTNFR2 knock-in mice, and demonstrated decreased neuroinflammation in response to TNFR1 antagonist ATROSAB or TNFR2 agonist EHD2-scTNFR2 (TNF hexamer oligomerized using the CH2 domain of IgE) in a model of NMDA-induced neurodegeneration (96). Additionally, ATROSAB administration inhibited development of EAE, decreased CNS infiltration and demyelination in hTNFR1KI mice (97). Yet another transgenic hTNFR1 mouse strain was used for studying the efficacy of VHH (antigen binding fragment of heavy chain only camelid antibody)-based nanobody against human TNFR1 (TNFR one silencer, TROS) in EAE, in which case a prophylactic administration of TROS resulted in disease amelioration (91).

In summary, there is a growing panel of useful humanized mouse models for evaluation of biologics that affect TNF/TNFR1/TNFR2 systems, including their effects on hematopoiesis. Furthermore, restoration of affected signaling by humanization of both TNF and its receptor, TNFR2, makes it possible to comparatively evaluate not only anti-TNF drugs, but also hTNFR2 agonists and antagonists. Taken together, humanized mouse models will allow investigators to study efficacy of various TNF/TNFRs-targeting biologics and assess possible side effects on other systems for further clinical translation.

CONCLUDING REMARKS

For many years TNF was mainly considered a proinflammatory cytokine with its role in host defense, but also with detrimental effects on autoimmunity. However, basic studies on TNF biology, as well as reported side effects in patients receiving anti-TNF therapy, highlighted its homeostatic functions in many physiological processes, including hematopoiesis. Regulation of

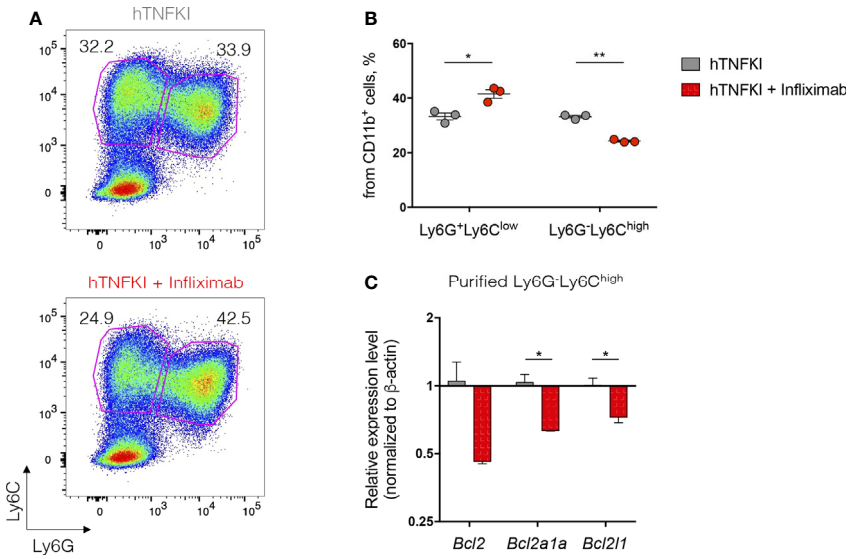

FIGURE 2 | TNF inhibition affects immature myeloid cell development *in vitro*. Bone marrow cells were isolated from femurs of hTNFKI mice and cultured for 5 days in RPMI 1640 medium supplemented with L-Glutamine (2 mM), penicillin (100 U/ml), streptomycin (100 µg/ml), HEPES (10 mM), β-mercaptoethanol (50 µM), 10% FBS, GM-CSF (20 ng/ml) and IL-4 (10 ng/ml). Infliximab was added in the final concentration of 100 ng/ml. After 5 days in culture cells were stained with Fixable Viability Dye, CD11b (M1/70), Ly6C (HK1.4), Ly6G (RB6-8C5) and acquired with BD FACSCanto II flow cytometer. Data were analyzed using FlowJo software. **(A)** Representative FACS plots of $Ly6G^{+}Ly6C^{low}$ and $Ly6G^{-}Ly6C^{high}$ cells gated on $VD^{-}CD11b^{+}$ cells. **(B)** Frequencies of $Ly6G^{+}Ly6C^{low}$ and $Ly6G^{-}Ly6C^{high}$ cells gated on $VD^{-}CD11b^{+}$ cells. **(C)** $Ly6G^{-}Ly6C^{high}$ cells were purified using Myeloid-Derived Suppressor Cell Isolation Kit (Miltenyi Biotec) according to the manufacturer's protocol. RNA was isolated from purified cells using TRIzol Reagent (Invitrogen) according to the manufacturer's instructions. RNA (1 µg) was treated with DNase I and reverse transcribed to cDNA with M-MuLV reverse transcriptase (RevertAid first strand cDNA synthesis kit, Thermo Scientific). Real-time quantitative PCR was performed using qPCRmix-HS SYBR+LowROX (Evrogen) and the following primer set: *Actb*, Forward: CTCCTGAGCGCAAGTACTCTGTG, Reverse: TAAAACGCAGCTCAGTAACAGTCC, *Bcl2*, Forward: GAGTTCGGTGGGGTCATGTG, Reverse: TATAGTTCCACAAAGGCATCCCAG, *Bcl2a1a*, Forward: GGCAGAATGGAGGTTGGGAAG, Reverse: ATTCTCGTGGGAGCCAAGGT, *Bcl2l1*, Forward: AGAGAGGCAGGCGATGAGTT, Reverse: TCCACAAAAGTGTCCCAGCC. Reactions were run using the following program on the Applied Biosystems 7500: 95°C for 10 min, 40 cycles of 95°C for 15 sec, 61°C for 30 sec and 72°C for 20 sec. Each point in a diagram represents a single mouse; mean ± SEM. $^{*}P < 0{,}05$; $^{**}P < 0{,}01$. Two-tailed unpaired Student's t-test was used.

TNF/TNFRs expression in various tissues modulates the cross-talk between immune and non-immune cells, which subsequently determines the outcome of TNF action.

Future investigation of pathological versus regulatory functions of TNF and deciphering its systemic and local effects in tissues may help to improve current therapeutic approaches. Therefore, mouse models with humanized TNF/TNFRs system represent a powerful tool to study side effects of anti-TNF therapy on hematopoiesis.

AUTHOR CONTRIBUTIONS

VG, KA, MD, and SAN designed research. VG and KA. performed research and analyzed data. VG, KA, AD, TY, MSD, and SN discussed the concept and wrote the manuscript. All authors contributed to the article and approved the submitted version.

FUNDING

Reverse genetics studies were supported by the grant 075-15-2019-1660 from the Ministry of Science and Higher Education of the Russian Federation, myelopoiesis studies were supported by RFBR grant 19-34-51030.

ACKNOWLEDGMENTS

We are greatly indebted to Dr. J.R. Keller (NCI Frederick) for useful comments on the manuscript. BioRender (https://biorender.com/) was used to make the figure.

REFERENCES

1. Yamane T. Mouse Yolk Sac Hematopoiesis. *Front Cell Dev Biol* (2018) 6:80. doi: 10.3389/fcell.2018.00080
2. Dzierzak E, Bigas A. Blood Development: Hematopoietic Stem Cell Dependence and Independence. *Cell Stem Cell* (2018) 22(5):639–51. doi: 10.1016/j.stem.2018.04.015
3. Muller AM, Medvinsky A, Strouboulis J, Grosveld F, Dzierzak E. Development of Hematopoietic Stem Cell Activity in the Mouse Embryo. *Immunity* (1994) 1(4):291–301. doi: 10.1016/1074-7613(94)90081-7
4. Rieger MA, Hoppe PS, Smejkal BM, Eitelhuber AC, Schroeder T. Hematopoietic Cytokines can Instruct Lineage Choice. *Science* (2009) 325(5937):217–8. doi: 10.1126/science.1171461

5. Wilson A, Laurenti E, Oser G, van der Wath RC, Blanco-Bose W, Jaworski M, et al. Hematopoietic Stem Cells Reversibly Switch From Dormancy to Self-Renewal During Homeostasis and Repair. *Cell* (2008) 135(6):1118–29. doi: 10.1016/j.cell.2008.10.048
6. Kunisaki Y, Bruns I, Scheiermann C, Ahmed J, Pinho S, Zhang D, et al. Arteriolar Niches Maintain Haematopoietic Stem Cell Quiescence. *Nature* (2013) 502(7473):637–43. doi: 10.1038/nature12612
7. Itkin T, Gur-Cohen S, Spencer JA, Schajnovitz A, Ramasamy SK, Kusumbe AP, et al. Distinct Bone Marrow Blood Vessels Differentially Regulate Haematopoiesis. *Nature* (2016) 532(7599):323–8. doi: 10.1038/nature17624
8. Sugiyama T, Kohara H, Noda M, Nagasawa T. Maintenance of the Hematopoietic Stem Cell Pool by CXCL12-CXCR4 Chemokine Signaling in Bone Marrow Stromal Cell Niches. *Immunity* (2006) 25(6):977–88. doi: 10.1016/j.immuni.2006.10.016
9. Ogawa M, Matsuzaki Y, Nishikawa S, Hayashi S, Kunisada T, Sudo T, et al. Expression and Function of C-Kit in Hemopoietic Progenitor Cells. *J Exp Med* (1991) 174(1):63–71. doi: 10.1084/jem.174.1.63
10. Nagai Y, Garrett KP, Ohta S, Bahrun U, Kouro T, Akira S, et al. Toll-Like Receptors on Hematopoietic Progenitor Cells Stimulate Innate Immune System Replenishment. *Immunity* (2006) 24(6):801–12. doi: 10.1016/j.immuni.2006.04.008
11. Takizawa H, Boettcher S, Manz MG. Demand-Adapted Regulation of Early Hematopoiesis in Infection and Inflammation. *Blood* (2012) 119(13):2991–3002. doi: 10.1182/blood-2011-12-380113
12. Zhao JL, Ma C, O'Connell RM, Mehta A, DiLoreto R, Heath JR, et al. Conversion of Danger Signals Into Cytokine Signals by Hematopoietic Stem and Progenitor Cells for Regulation of Stress-Induced Hematopoiesis. *Cell Stem Cell* (2014) 14(4):445–59. doi: 10.1016/j.stem.2014.01.007
13. Pietras EM, Mirantes-Barbeito C, Fong S, Loeffler D, Kovtonyuk LV, Zhang S, et al. Chronic Interleukin-1 Exposure Drives Haematopoietic Stem Cells Towards Precocious Myeloid Differentiation At the Expense of Self-Renewal. *Nat Cell Biol* (2016) 18(6):607–18. doi: 10.1038/ncb3346
14. Sawamiphak S, Kontarakis Z, Stainier DY. Interferon Gamma Signaling Positively Regulates Hematopoietic Stem Cell Emergence. *Dev Cell* (2014) 31(5):640–53. doi: 10.1016/j.devcel.2014.11.007
15. Pietras EM. Inflammation: A Key Regulator of Hematopoietic Stem Cell Fate in Health and Disease. *Blood* (2017) 130(15):1693–8. doi: 10.1182/blood-2017-06-780882
16. Atretkhany KN, Gogoleva VS, Drutskaya MS, Nedospasov SA. Distinct Modes of TNF Signaling Through its Two Receptors in Health and Disease. *J Leukoc Biol* (2020) 107(6):893–905. doi: 10.1002/JLB.2MR0120-510R
17. Kucka K, Lang I, Zhang T, Siegmund D, Medler J, Wajant H. Membrane lymphotoxin-alpha2beta is a Novel Tumor Necrosis Factor (TNF) Receptor 2 (TNFR2) Agonist. *Cell Death Dis* (2021) 12(4):360. doi: 10.1038/s41419-021-03633-8
18. Espín-Palazón R, Stachura DL, Campbell CA, García-Moreno D, Del Cid N, Kim AD, et al. Proinflammatory Signaling Regulates Hematopoietic Stem Cell Emergence. *Cell* (2014) 159(5):1070–85. doi: 10.1016/j.cell.2014.10.031
19. Drutskaya MS, Ortiz M, Liepinsh DJ, Kuprash DV, Nedospasov SA, Keller JR. Inhibitory Effects of Tumor Necrosis Factor on Hematopoiesis Seen In Vitro are Translated to Increased Numbers of Both Committed and Multipotent Progenitors in TNF-deficient Mice. *Exp Hematol* (2005) 33(11):1348–56. doi: 10.1016/j.exphem.2005.08.001
20. Wolf Y, Shemer A, Polonsky M, Gross M, Mildner A, Yona S, et al. Autonomous TNF is Critical for In Vivo Monocyte Survival in Steady State and Inflammation. *J Exp Med* (2017) 214(4):905–17. doi: 10.1084/jem.20160499
21. Yamashita M, Passegue E. TNF-Alpha Coordinates Hematopoietic Stem Cell Survival and Myeloid Regeneration. *Cell Stem Cell* (2019) 25(3):357–72e357. doi: 10.1016/j.stem.2019.05.019
22. Zhang Y, Harada A, Bluethmann H, Wang JB, Nakao S, Mukaida N, et al. Tumor Necrosis Factor (TNF) is a Physiologic Regulator of Hematopoietic Progenitor Cells: Increase of Early Hematopoietic Progenitor Cells in TNF Receptor p55-deficient Mice In Vivo and Potent Inhibition of Progenitor Cell Proliferation by TNF Alpha In Vitro. *Blood* (1995) 86(8):2930–7. doi: 10.1182/blood.V86.8.2930.bloodjournal8682930
23. Jacobsen FW, Rothe M, Rusten L, Goeddel DV, Smeland EB, Veiby OP, et al. Role of the 75-kDa Tumor Necrosis Factor Receptor: Inhibition of Early Hematopoiesis. *Proc Natl Acad Sci USA* (1994) 91(22):10695–9. doi: 10.1073/pnas.91.22.10695
24. Caux C, Favre C, Saeland S, Duvert V, Durand I, Mannoni P, et al. Potentiation of Early Hematopoiesis by Tumor Necrosis Factor-Alpha is Followed by Inhibition of Granulopoietic Differentiation and Proliferation. *Blood* (1991) 78(3):635–44. doi: 10.1182/blood.V78.3.635.635
25. Pearl-Yafe M, Mizrahi K, Stein J, Yolcu ES, Kaplan O, Shirwan H, et al. Tumor Necrosis Factor Receptors Support Murine Hematopoietic Progenitor Function in the Early Stages of Engraftment. *Stem Cells* (2010) 28(7):1270–80. doi: 10.1002/stem.448
26. Ishida T, Suzuki S, Lai CY, Yamazaki S, Kakuta S, Iwakura Y, et al. Pre-Transplantation Blockade of TNF-alpha-Mediated Oxygen Species Accumulation Protects Hematopoietic Stem Cells. *Stem Cells* (2017) 35(4):989–1002. doi: 10.1002/stem.2524
27. Bowers E, Slaughter A, Frenette PS, Kuick R, Pello OM, Lucas D. Granulocyte-Derived TNFalpha Promotes Vascular and Hematopoietic Regeneration in the Bone Marrow. *Nat Med* (2018) 24(1):95–102. doi: 10.1038/nm.4448
28. Ueda Y, Yang K, Foster SJ, Kondo M, Kelsoe G. Inflammation Controls B Lymphopoiesis by Regulating Chemokine CXCL12 Expression. *J Exp Med* (2004) 199(1):47–58. doi: 10.1084/jem.20031104
29. He Q, Zhang C, Wang L, Zhang P, Ma D, Lv J, et al. Inflammatory Signaling Regulates Hematopoietic Stem and Progenitor Cell Emergence in Vertebrates. *Blood* (2015) 125(7):1098–106. doi: 10.1182/blood-2014-09-601542
30. Li Y, Esain V, Teng L, Xu J, Kwan W, Frost IM, et al. Inflammatory Signaling Regulates Embryonic Hematopoietic Stem and Progenitor Cell Production. *Genes Dev* (2014) 28(23):2597–612. doi: 10.1101/gad.253302.114
31. Pronk CJ, Veiby OP, Bryder D, Jacobsen SE. Tumor Necrosis Factor Restricts Hematopoietic Stem Cell Activity in Mice: Involvement of Two Distinct Receptors. *J Exp Med* (2011) 208(8):1563–70. doi: 10.1084/jem.20110752
32. Rebel VI, Hartnett S, Hill GR, Lazo-Kallanian SB, Ferrara JL, Sieff CA. Essential Role for the p55 Tumor Necrosis Factor Receptor in Regulating Hematopoiesis At a Stem Cell Level. *J Exp Med* (1999) 190(10):1493–504. doi: 10.1084/jem.190.10.1493
33. Drize NI, Drutskaya MS, Gerasimova LP, Manakova TE, Chertkov IL, Turetskaya RL, et al. Changes in the Hemopoietic System of Mice Deficient for Tumor Necrosis Factor or Lymphotoxin-Alpha. *Bull Exp Biol Med* (2000) 130(7):676–8. doi: 10.1007/BF02682103
34. Etzrodt M, Ahmed N, Hoppe PS, Loeffler D, Skylaki S, Hilsenbeck O, et al. Inflammatory Signals Directly Instruct PU.1 in HSCs Via TNF. *Blood* (2019) 133(8):816–9. doi: 10.1182/blood-2018-02-832998
35. Abegunde SO, Buckstein R, Wells RA, Rauh MJ. An Inflammatory Environment Containing TNFalpha Favors Tet2-mutant Clonal Hematopoiesis. *Exp Hematol* (2018) 59:60–5. doi: 10.1016/j.exphem.2017.11.002
36. Bryder D, Ramsfjell V, Dybedal I, Theilgaard-Mönch K, Högerkorp CM, Adolfsson J, et al. Self-Renewal of Multipotent Long-Term Repopulating Hematopoietic Stem Cells is Negatively Regulated by Fas and Tumor Necrosis Factor Receptor Activation. *J Exp Med* (2001) 194(7):941–52. doi: 10.1084/jem.194.7.941
37. Rezzoug F, Huang Y, Tanner MK, Wysoczynski M, Schanie CL, Chilton PM, et al. TNF-Alpha is Critical to Facilitate Hemopoietic Stem Cell Engraftment and Function. *J Immunol* (2008) 180(1):49–57. doi: 10.4049/jimmunol.180.1.49
38. Mead AJ, Neo WH, Barkas N, Matsuoka S, Giustacchini A, Facchini R, et al. Niche-Mediated Depletion of the Normal Hematopoietic Stem Cell Reservoir by Flt3-ITD-induced Myeloproliferation. *J Exp Med* (2017) 214(7):2005–21. doi: 10.1084/jem.20161418
39. Kondo K, Kaneshima H, Mocarski ES. Human Cytomegalovirus Latent Infection of Granulocyte-Macrophage Progenitors. *Proc Natl Acad Sci USA* (1994) 91(25):11879–83. doi: 10.1073/pnas.91.25.11879
40. Sanchez-Correa B, Bergua JM, Campos C, Gayoso I, Arcos MJ, Bañas H, et al. Cytokine Profiles in Acute Myeloid Leukemia Patients At Diagnosis: Survival is Inversely Correlated With IL-6 and Directly Correlated With IL-10 Levels. *Cytokine* (2013) 61(3):885–91. doi: 10.1016/j.cyto.2012.12.023

41. Gersuk GM, Beckham C, Loken MR, Kiener P, Anderson JE, Farrand A, et al. A Role for Tumour Necrosis Factor-Alpha, Fas and Fas-Ligand in Marrow Failure Associated With Myelodysplastic Syndrome. *Br J Haematol* (1998) 103(1):176–88. doi: 10.1046/j.1365-2141.1998.00933.x
42. Dar S, Mundle S, Andric T, Qawi H, Shetty V, Reza S, et al. Biological Characteristics of Myelodysplastic Syndrome Patients Who Demonstrated High Versus No Intramedullary Apoptosis. *Eur J Haematol* (1999) 62(2):90–4. doi: 10.1111/j.1600-0609.1999.tb01727.x
43. Dufour C, Corcione A, Svahn J, Haupt R, Poggi V, Béka'ssy AN, et al. TNF-Alpha and IFN-gamma are Overexpressed in the Bone Marrow of Fanconi Anemia Patients and TNF-alpha Suppresses Erythropoiesis In Vitro. *Blood* (2003) 102(6):2053–9. doi: 10.1182/blood-2003-01-0114
44. Warzocha K, Bienvenu J, Ribeiro P, Moullet I, Dumontet C, Neidhardt-Berard EM, et al. Plasma Levels of Tumour Necrosis Factor and its Soluble Receptors Correlate With Clinical Features and Outcome of Hodgkin's Disease Patients. *Br J Cancer* (1998) 77(12):2357–62. doi: 10.1038/bjc.1998.391
45. Salles G, Bienvenu J, Bastion Y, Barbier Y, Doche C, Warzocha K, et al. Elevated Circulating Levels of TNFalpha and its p55 Soluble Receptor are Associated With an Adverse Prognosis in Lymphoma Patients. *Br J Haematol* (1996) 93(2):352–9. doi: 10.1046/j.1365-2141.1996.5181059.x
46. Quartier P, Taupin P, Bourdeaut F, Lemelle I, Pillet P, Bost M, et al. Efficacy of Etanercept for the Treatment of Juvenile Idiopathic Arthritis According to the Onset Type. *Arthritis Rheum* (2003) 48(4):1093–101. doi: 10.1002/art.10885
47. Menon Y, Cucurull E, Espinoza LR. Pancytopenia in a Patient With Scleroderma Treated With Infliximab. *Rheumatol (Oxford)* (2003) 42(10):1273–4; author reply 1274. doi: 10.1093/rheumatology/keg341
48. Marchesoni A, Arreghini M, Panni B, Battafarano N, Uziel L. Life-Threatening Reversible Bone Marrow Toxicity in a Rheumatoid Arthritis Patient Switched From Leflunomide to Infliximab. *Rheumatol (Oxford)* (2003) 42(1):193–4. doi: 10.1093/rheumatology/key051
49. Seiderer J, Goke B, Ochsenkuhn T. Safety Aspects of Infliximab in Inflammatory Bowel Disease Patients. A Retrospective Cohort Study in 100 Patients of a German University Hospital. *Digestion* (2004) 70(1):3–9. doi: 10.1159/000080075
50. Feltelius N, Fored CM, Blomqvist P, Bertilsson L, Geborek P, Jacobsson LT, et al. Results From a Nationwide Postmarketing Cohort Study of Patients in Sweden Treated With Etanercept. *Ann Rheum Dis* (2005) 64(2):246–52. doi: 10.1136/ard.2004.023473
51. Szalay B, Acs L, Vasarhelyi B, Kovacs L, Balog A. Successful Use of Tocilizumab in a Patient With Rheumatoid Arthritis Following Severe Pancytopenia During Etanercept Therapy. *J Clin Rheumatol* (2011) 17(7):377–9. doi: 10.1097/RHU.0b013e318231fd99
52. Kuruvilla J, Leitch HA, Vickars LM, Galbraith PF, Li CH, Al-Saab S, et al. Aplastic Anemia Following Administration of a Tumor Necrosis Factor-Alpha Inhibitor. *Eur J Haematol* (2003) 71(5):396–8. doi: 10.1034/j.1600-0609.2003.00115.x
53. Feletar M, Brockbank JE, Schentag CT, Lapp V, Gladman DD. Treatment of Refractory Psoriatic Arthritis With Infliximab: A 12 Month Observational Study of 16 Patients. *Ann Rheum Dis* (2004) 63(2):156–61. doi: 10.1136/ard.2003.006775
54. Selby LA, Hess D, Shashidar H, de Villiers WJ, Selby LA. Crohn's Disease, Infliximab and Idiopathic Thrombocytopenic Purpura. *Inflammation Bowel Dis* (2004) 10(5):698–700. doi: 10.1097/00054725-200409000-00033
55. Pathare SK, Heycock C, Hamilton J. Tnfalpha Blocker-Induced Thrombocytopenia. *Rheumatol (Oxford)* (2006) 45(10):1313–4. doi: 10.1093/rheumatology/kel204
56. Hamaguchi M, Kawahito Y, Ishino H, Yoshida M, Yoshikawa T. A Case Report of Tumor Necrosis Factor-Alpha Antibody-Induced Thrombocytopenia Associated With Emerging IgM Anticardiolipin Antibody in Patients With Scleroderma Overlap/Rheumatoid Arthritis. *Clin Rheumatol* (2007) 26(6):988–90. doi: 10.1007/s10067-006-0229-y
57. Salar A, Bessa X, Muñiz E, Monfort D, Besses C, Andreu M. Infliximab and Adalimumab-Induced Thrombocytopenia in a Woman With Colonic Crohn's Disease. *Gut* (2007) 56(8):1169–70. doi: 10.1136/gut.2007.123547
58. Stinco G, Piccirillo F, Patrone P. Transient and Slight Thrombocytopaenia Induced by Etanercept During Treatment of Psoriatic Arthritis. *Acta Derm Venereol* (2008) 88(3):281–2. doi: 10.2340/00015555-0400
59. Brunasso AM, Massone C. Thrombocytopenia Associated With the Use of Anti-Tumor Necrosis Factor-Alpha Agents for Psoriasis. *J Am Acad Dermatol* (2009) 60(5):781–5. doi: 10.1016/j.jaad.2008.12.001
60. Mocciaro F, Russo G, Di Mitri R, Marino A. Infliximab-Induced Thrombocytopenia in an Elderly Patient With Ileocolonic Crohn's Disease. *Inflammation Bowel Dis* (2013) 19(4):E52–53. doi: 10.1002/ibd.22989
61. Velayos Jimenez B, Cuello Garcia R, Del Olmo Martinez L, Macho Conesa A, Fernandez Salazar L. Immune Thrombocytopenic Purpura Associated With Inactive Ulcerative Colitis in Chronic Treatment With Adalimumab. *Gastroenterol Hepatol* (2020) 43(1):28–9. doi: 10.1016/j.gastre.2019.07.006
62. Gerloni V, Pontikaki I, Gattinara M, Fantini F. Focus on Adverse Events of Tumour Necrosis Factor Alpha Blockade in Juvenile Idiopathic Arthritis in an Open Monocentric Long-Term Prospective Study of 163 Patients. *Ann Rheum Dis* (2008) 67(8):1145–52. doi: 10.1136/ard.2007.069484
63. Vidal F, Fontova R, Richart C. Severe Neutropenia and Thrombocytopenia Associated With Infliximab. *Ann Intern Med* (2003) 139(3):W–W63. doi: 10.7326/0003-4819-139-3-200308050-00021-w4
64. Kozak N, Friedman J, Schattner A. Etanercept-Associated Transient Bone Marrow Aplasia: A Review of the Literature and Pathogenetic Mechanisms. *Drugs R D* (2014) 14(2):155–8. doi: 10.1007/s40268-014-0050-z
65. Favalli EG, Varenna M, Sinigaglia L. Drug-Induced Agranulocytosis During Treatment With Infliximab in Enteropathic Spondyloarthropathy. *Clin Exp Rheumatol* (2005) 23(2):247–50.
66. Rajakulendran S, Gadsby K, Allen D, O'Reilly S, Deighton C. Neutropenia While Receiving Anti-Tumour Necrosis Factor Treatment for Rheumatoid Arthritis. *Ann Rheum Dis* (2006) 65(12):1678–9. doi: 10.1136/ard.2006.056176
67. Theodoridou A, Kartsios C, Yiannaki E, Markala D, Settas L. Reversible T-large Granular Lymphocyte Expansion and Neutropenia Associated With Adalimumab Therapy. *Rheumatol Int* (2006) 27(2):201–2. doi: 10.1007/s00296-006-0187-3
68. Levalampi T, Korpela M, Vuolteenaho K, Moilanen E. Etanercept and Adalimumab Treatment in Patients With Rheumatoid Arthritis and Spondyloarthropathies in Clinical Practice: Adverse Events and Other Reasons Leading to Discontinuation of the Treatment. *Rheumatol Int* (2008) 28(3):261–9. doi: 10.1007/s00296-007-0436-0
69. Wenham C, Gadsby K, Deighton C. Three Significant Cases of Neutropenia With Etanercept. *Rheumatol (Oxford)* (2008) 47(3):376–7. doi: 10.1093/rheumatology/kem332
70. Ottaviani S, Cerf-Payrastre I, Kemiche F, Pertuiset E. Adalimumab-Induced Neutropenia in a Patient With Rheumatoid Arthritis. *Joint Bone Spine* (2009) 76(3):312–3. doi: 10.1016/j.jbspin.2008.09.017
71. Hastings R, Ding T, Butt S, Gadsby K, Zhang W, Moots RJ, et al. Neutropenia in Patients Receiving Anti-Tumor Necrosis Factor Therapy. *Arthritis Care Res (Hoboken)* (2010) 62(6):764–9. doi: 10.1002/acr.20037
72. Haroon M, Daly M, Harney S. Re-Challenge With Etanercept in Patients With Etanercept-Induced Neutropenia. *Clin Rheumatol* (2012) 31(1):151–5. doi: 10.1007/s10067-011-1822-2
73. AlAskar D, AlSardi M, Al Sulais E, Mosli M, AlAmeel T. Risk of Neutropenia in Inflammatory Bowel Disease Patients Treated With TNF Inhibitors: A Single-Center, Retrospective Cohort Study. *Saudi J Gastroenterol* (2020) 76(4):210–5. doi: 10.1093/ecco-jcc/jjz203.794
74. Montané E, Sallés M, Barriocanal A, Riera E, Costa J, Tena X. Antitumor Necrosis Factor-Induced Neutropenia: A Case Report With Double Positive Rechallenges. *Clin Rheumatol* (2007) 26(9):1527–9. doi: 10.1007/s10067-006-0415-y
75. Adams AE, Zwicker J, Curiel C, Kadin ME, Falchuk KR, Drews R, et al. Aggressive Cutaneous T-cell Lymphomas After TNFalpha Blockade. *J Am Acad Dermatol* (2004) 51(4):660–2. doi: 10.1016/j.jaad.2004.03.047
76. Broussais F, Kawashima M, Marotte H, Miossec P. Chronic Myeloid Leukaemia and Tuberculosis in a Patient With Rheumatoid Arthritis Treated With Infliximab. *Ann Rheum Dis* (2005) 64(3):509–10. doi: 10.1136/ard.2004.021378

77. Brown SL, Greene MH, Gershon SK, Edwards ET, Braun MM. Tumor Necrosis Factor Antagonist Therapy and Lymphoma Development: Twenty-Six Cases Reported to the Food and Drug Administration. *Arthritis Rheum* (2002) 46(12):3151–8. doi: 10.1002/art.10679
78. Wolfe F, Michaud K. Lymphoma in Rheumatoid Arthritis: The Effect of Methotrexate and Anti-Tumor Necrosis Factor Therapy in 18,572 Patients. *Arthritis Rheum* (2004) 50(6):1740–51. doi: 10.1002/art.20311
79. Vieites B, Avila R, Biscuola M, Carvajo F. Cutaneous Hodgkin-type Lymphoproliferative Lesion Associated With Immunomodulatory Therapy for Ulcerative Colitis. *J Cutan Pathol* (2011) 38(5):443–7. doi: 10.1111/j.1600-0560.2010.01663.x
80. D'Haens G, Reinisch W, Colombel JF, Panes J, Ghosh S, Prantera C, et al. Five-Year Safety Data From ENCORE, a European Observational Safety Registry for Adults With Crohn's Disease Treated With Infliximab [Remicade(R)] or Conventional Therapy. *J Crohns Colitis* (2017) 11 (6):680–9. doi: 10.1093/ecco-jcc/jjw221
81. Bessissow T, Renard M, Hoffman I, Vermeire S, Rutgeerts P, Van Assche G. Review Article: non-Malignant Haematological Complications of Anti-Tumour Necrosis Factor Alpha Therapy. *Aliment Pharmacol Ther* (2012) 36(4):312–23. doi: 10.1111/j.1365-2036.2012.05189.x
82. Winsauer C, Kruglov AA, Chashchina AA, Drutskaya MS, Nedospasov SA. Cellular Sources of Pathogenic and Protective TNF and Experimental Strategies Based on Utilization of TNF Humanized Mice. *Cytokine Growth Factor Rev* (2014) 25(2):115–23. doi: 10.1016/j.cytogfr.2013.12.005
83. Keffer J, Probert L, Cazlaris H, Georgopoulos S, Kaslaris E, Kioussis D, et al. Transgenic Mice Expressing Human Tumour Necrosis Factor: A Predictive Genetic Model of Arthritis. *EMBO J* (1991) 10(13):4025–31. doi: 10.1002/j.1460-2075.1991.tb04978.x
84. Gorth DJ, Shapiro IM, Risbud MV. Transgenic Mice Overexpressing Human TNF-alpha Experience Early Onset Spontaneous Intervertebral Disc Herniation in the Absence of Overt Degeneration. *Cell Death Dis* (2018) 10(1):7. doi: 10.1038/s41419-018-1246-x
85. Capocasale RJ, Makropoulos DA, Achuthanandam R, Stowell N, Quinn J, Rafferty PA, et al. Myelodysplasia and Anemia of Chronic Disease in Human Tumor Necrosis Factor-Alpha Transgenic Mice. *Cytometry A* (2008) 73 (2):148–59. doi: 10.1002/cyto.a.20512
86. Hayward MD, Jones BK, Saparov A, Hain HS, Trillat AC, Bunzel MM, et al. An Extensive Phenotypic Characterization of the hTNFalpha Transgenic Mice. *BMC Physiol* (2007) 7:13. doi: 10.1186/1472-6793-7-13
87. Retser E, Schied T, Skryabin BV, Vogl T, Kanczler JM, Hamann N, et al. Doxycycline-Induced Expression of Transgenic Human Tumor Necrosis Factor Alpha in Adult Mice Results in Psoriasis-Like Arthritis. *Arthritis Rheum* (2013) 65(9):2290–300. doi: 10.1002/art.38026
88. Probert L, Keffer J, Corbella P, Cazlaris H, Patsavoudi E, Stephens S, et al. Wasting, Ischemia, and Lymphoid Abnormalities in Mice Expressing T Cell-Targeted Human Tumor Necrosis Factor Transgenes. *J Immunol* (1993) 151 (4):1894–906.
89. Akassoglou K, Probert L, Kontogeorgos G, Kollias G. Astrocyte-Specific But Not Neuron-Specific Transmembrane TNF Triggers Inflammation and Degeneration in the Central Nervous System of Transgenic Mice. *J Immunol* (1997) 158(1):438–45.
90. Liepinsh DJ, Kruglov AA, Galimov AR, Shakhov AN, Shebzukhov YV, Kuchmiy AA, et al. Accelerated Thymic Atrophy as a Result of Elevated Homeostatic Expression of the Genes Encoded by the TNF/lymphotoxin Cytokine Locus. *Eur J Immunol* (2009) 39(10):2906–15. doi: 10.1002/eji.200839191
91. Steeland S, Van Ryckeghem S, Van Imschoot G, De Rycke R, Toussaint W, Vanhoutte L, et al. TNFR1 Inhibition With a Nanobody Protects Against EAE Development in Mice. *Sci Rep* (2017) 7(1):13646. doi: 10.1038/s41598-017-13984-y
92. Olleros ML, Chavez-Galan L, Segueni N, Bourigault ML, Vesin D, Kruglov AA, et al. Control of Mycobacterial Infections in Mice Expressing Human Tumor Necrosis Factor (TNF) But Not Mouse Tnf. *Infect Immun* (2015) 83 (9):3612–23. doi: 10.1128/IAI.00743-15
93. Drutskaya MS, Nosenko MA, Gorshkova EA, Mokhonov VV, Zvartsev RV, Polinova AI, et al. Effects of Myeloid Cell-Restricted TNF Inhibitors In Vitro and In Vivo. *J Leukoc Biol* (2020) 107(6):933–9. doi: 10.1002/JLB.3AB0120-532R
94. Atretkhany KS, Nosenko MA, Gogoleva VS, Zvartsev RV, Qin Z, Nedospasov SA, et al. Tnf Neutralization Results in the Delay of Transplantable Tumor Growth and Reduced Mdsc Accumulation. *Front Immunol* (2016) 7:147. doi: 10.3389/fimmu.2016.00147
95. Atretkhany KN, Mufazalov IA, Dunst J, Kuchmiy A, Gogoleva VS, Andruszewski D, et al. Intrinsic TNFR2 Signaling in T Regulatory Cells Provides Protection in CNS Autoimmunity. *Proc Natl Acad Sci USA* (2018) 115(51):13051–6. doi: 10.1073/pnas.1807499115
96. Dong Y, Fischer R, Naudé PJ, Maier O, Nyakas C, Duffey M, et al. Essential Protective Role of Tumor Necrosis Factor Receptor 2 in Neurodegeneration. *Proc Natl Acad Sci USA* (2016) 113(43):12304–9. doi: 10.1073/pnas.1605195113
97. Williams SK, Fairless R, Maier O, Liermann PC, Pichi K, Fischer R, et al. Anti-TNFR1 Targeting in Humanized Mice Ameliorates Disease in a Model of Multiple Sclerosis. *Sci Rep* (2018) 8(1):13628. doi: 10.1038/s41598-018-31957-7
98. Gorshkova EA, Zvartsev RV, Drutskaya MS, Gubernatorova EO. [Humanized Mouse Models as a Tool to Study Proinflammatory Cytokine Overexpression]. *Mol Biol (Mosk)* (2019) 53(5):755–73. doi: 10.1134/S0026893319050078
99. Kalliolias GD, Ivashkiv LB. TNF Biology, Pathogenic Mechanisms and Emerging Therapeutic Strategies. *Nat Rev Rheumatol* (2016) 12(1):49–62. doi: 10.1038/nrrheum.2015.169
100. Roubenoff R, Roubenoff RA, Cannon JG, Kehayias JJ, Zhuang H, Dawson-Hughes B, et al. Rheumatoid Cachexia: Cytokine-Driven Hypermetabolism Accompanying Reduced Body Cell Mass in Chronic Inflammation. *J Clin Invest* (1994) 93(6):2379–86. doi: 10.1172/JCI117244
101. Kruglov AA, Tumanov AV, Grivennikov SI, Shebzukhov YV, Kuchmiy AA, Efimov GA, et al. Modalities of Experimental TNF Blockade In Vivo: Mouse Models. *Adv Exp Med Biol* (2011) 691:421–31. doi: 10.1007/978-1-4419-6612-4_44
102. Efimov GA, Kruglov AA, Khlopchatnikova ZV, Rozov FN, Mokhonov VV, Rose-John S, et al. Cell-type-restricted Anti-Cytokine Therapy: TNF Inhibition From One Pathogenic Source. *Proc Natl Acad Sci USA* (2016) 113(11):3006–11. doi: 10.1073/pnas.1520175113
103. Ameloot P, Fiers W, De Bleser P, Ware CF, Vandenabeele P, Brouckaert P. Identification of Tumor Necrosis Factor (TNF) Amino Acids Crucial for Binding to the Murine P75 TNF Receptor and Construction of Receptor-Selective Mutants. *J Biol Chem* (2001) 276(40):37426–30. doi: 10.1074/jbc.M102020200
104. Bossen C, Ingold K, Tardivel A, Bodmer JL, Gaide O, Hertig S, et al. Interactions of Tumor Necrosis Factor (TNF) and TNF Receptor Family Members in the Mouse and Human. *J Biol Chem* (2006) 281(20):13964–71. doi: 10.1074/jbc.M601553200

Conflict of Interest: The authors declare that the research was conducted in the absence of any commercial or financial relationships that could be construed as a potential conflict of interest.

Copyright © 2021 Gogoleva, Atretkhany, Dygay, Yurakova, Drutskaya and Nedospasov. This is an open-access article distributed under the terms of the Creative Commons Attribution License (CC BY). The use, distribution or reproduction in other forums is permitted, provided the original author(s) and the copyright owner(s) are credited and that the original publication in this journal is cited, in accordance with accepted academic practice. No use, distribution or reproduction is permitted which does not comply with these terms.

Advantages of publishing in Frontiers

OPEN ACCESS
Articles are free to read for greatest visibility and readership

FAST PUBLICATION
Around 90 days from submission to decision

HIGH QUALITY PEER-REVIEW
Rigorous, collaborative, and constructive peer-review

TRANSPARENT PEER-REVIEW
Editors and reviewers acknowledged by name on published articles

Frontiers
Avenue du Tribunal-Fédéral 34
1005 Lausanne | Switzerland

Visit us: www.frontiersin.org
Contact us: frontiersin.org/about/contact

REPRODUCIBILITY OF RESEARCH
Support open data and methods to enhance research reproducibility

DIGITAL PUBLISHING
Articles designed for optimal readership across devices

FOLLOW US
@frontiersin

IMPACT METRICS
Advanced article metrics track visibility across digital media

EXTENSIVE PROMOTION
Marketing and promotion of impactful research

LOOP RESEARCH NETWORK
Our network increases your article's readership